SEQUENCE STRATIGRAPHIC INTERPRETATION OF CRETACEOUS THROUGH MIOCENE, BARCOO SUB-BASIN, BROWSE BASIN, NORTHWEST SHELF OF AUSTRALIA

by

KASIRA LAITRAKULL

B.A., Chulalongkorn University, 2004

A thesis submitted to the

Faculty of the Graduate School of the

University of Colorado in partial fulfillment

of the requirements for the degree of

Master of Sciences

Department of Geological Sciences

2012

This thesis entitled:

Sequence Stratigraphic Interpretation of Cretaceous through Miocene,

Barcoo Sub-basin, Browse Basin, Northwest Shelf of Australia

written by Kasira Laitrakull

has been approved for the Department of Geological Sciences

By

_____

(Paul Weimer)

_____

(Renaud Bouroullec)

Date _____

The final copy of this thesis examined by the signatories, and we find that both the content and the form meet acceptable presentation standards of scholarly work in the above mentioned discipline.

Laitrakull, Kasira (M.S., Geology)

Sequence stratigraphic interpretation of Cretaceous through Miocene, Barcoo sub-basin, Browse basin, Northwest Shelf of Australia

Thesis directed by Professor Paul Weimer.

ABSTRACT

The petroleum exploration in Australia started in the nineteenth century. However, due to little exploration activity only one well has been drilled for every 1300 km^2 of sedimentary basins. In fact Australia (apart from Antarctica) is the least explored continent on earth (Longley, 2001).

The Northwest Shelf of Australia is composed of Mesozoic intracratonic basins, including four major basins: the (Northern) Carnarvon, offshore Canning, Browse and Bonaparte Basins. Browse Basin is the significant essential unexplored petroleum-bearing sedimentary basin of the Northwest Shelf. The study area is located in the Barcoo Sub-basin, which is a major depocenter of the Browse Basin. During the Cretaceous through Miocene Ages, sediments of the Barcoo sub-basin were deposited and thicken seaward to the northwest.

The main purpose of this study is to analyze the sequence stratigraphic framework of Cretaceous through middle Miocene strata. The analysis of 2D seismic and well log data allows constructing a depositional and chronostratigraphic framework of the study area. The data were integrated to identify and correlate 7 major sequence

boundaries or major surfaces. Each sequence was subdivided into separate seismic descriptions characterized by specific internal reflection configuration, reflection amplitude and reflection continuity. Six depositional sequences were recognized (145.5-112.0, 112.0-89.3, 89.3-65.5, 65.5-23.0, 23.0-19.0 and 19.0-14.2 Ma) and summarized in detail with structural, isochron, seismic facies, and geologic facies maps.

Potential reservoir sands can be found in delta fronts, lower shorefaces, upper shorefaces, foreshores and mouth bars as well as in basin-floor fans, and prograding wedges. However, no field has been discovered or developed within the study area. The failures of the exploration wells are due to the relationship between hydrocarbon generations and timing of source rock in relation to the formation of the structures.

The future study of the deep targeted seismic, stratigraphic plays, and basin analysis is recommended. The exploration activity is necessary to make the Northwest Shelf to be a major petroleum province of the world in the future.

ACKNOWLEDGEMENTS

I would like to take this opportunity to gratefully thank individuals and the company who have helped make this thesis possible. The completion of this thesis, the accomplishment of my degree, and the valuable time spent in the USA would not be possible without their help and support.

First and foremost, thank to Dr. Paul Weimer, my advisor, for guidance and help during the completion of this thesis research. Thank you for your support during my career at University of Colorado at Boulder. I also thank my committee members, Dr. Renaud Bouroullec and Dr. Edmund Gustason for suggestions and constructive reviews to improve this thesis.

I wish to thank the Petroleum Authority of Thailand Exploration and Production Company Limited (PTTEP) who provided the financial support for my degree, as well as the management and colleagues at PTTEP who have always helped me during this study.

I am also grateful to the faculty of the Department of Geological Sciences at University of Colorado at Boulder Dr. Matthew Pranter, Dr. Mary Kraus and Dr. David Budd, who have always inspired and introduced me with something new. Furthermore, thank to the office staff in the Department of Geological Sciences at University of Colorado at Boulder who always have the answers to all my questions.

Moreover, I would like to thank my fellow graduate students, Humberto Torres-sastre, Dawn Tschanz, Andrew Fuhrmann, Nathan Rogers, Joseph Nicolette, Benjamin

Herber and Suyoung Choi who help me throughout my studies and gave me an unforgettable experience. We have learned and grown together. Your friendship will never be forgotten. Wish you all the best for the future to come.

Special thank are also given to Thai students at University of Colorado at Boulder and other schools for their great friendship and making my life here feel more like my real home.

Most important at all, I can’t thank my family enough for the unconditional love, never-ending support and encouragement throughout my life. I would like to dedicate this work to you all. I have been blessed with all your love and support.

CONTENTS

ABSTRACT iii

ACKNOWLEDGEMENTS v

CONTENTS vii

LIST OF TABLES ix

LIST OF FIGURES xi

CHAPTER

I. INTRODUCTION 1

II. DATA SET 6

III. REGIONAL GEOLOGIC SETTING 9

Tectonic Evolution 9

Stratigraphy 42

IV. SEQUENCE STRATIGRAPHY 59

Methodology and Interpretation Procedure 59

Time-Depth Conversion and Synthetic Seismogram 61

Interval Descriptions 62

Megasequence 1: 145.5-112.0 Ma 63

Megasequence 2: 112.0-89.3 Ma 117

Megasequence 3: 89.3-65.5 Ma 211

Megasequence 4: 65.5-23.0 Ma 248

Megasequence 5: 23.0-19.0 Ma 266

Megasequence 6: 19.0-14.2 Ma..... 284

V. DISCUSSION 303

Petroleum Systems 303

VI. CONCLUSIONS 305

VII. REFERENCES 307

LIST OF TABLES

TABLE

1. Data Set used in this study 7

2. Seismic facies codes used 60

3. Seismic facies and geologic interpretation of Subsequence I of Megasequence 1 interval 73

4. Seismic facies and geologic interpretation of Subsequence II of Megasequence 1interval 84

5. Seismic facies and geologic interpretation of Subsequence III of Megasequence 1 interval 88

6. Seismic facies and geologic interpretation of Subsequence I of Megasequence 2 interval 125

7. Seismic facies and geologic interpretation of Subsequence II of Megasequence 2 interval 145

8. Seismic facies and geologic interpretation of Subsequence III of Megasequence 2 interval 157

9. Seismic facies and geologic interpretation of Subsequence IV of Megasequence 2 interval 161

10. Seismic facies and geologic interpretation of Subsequence V of Megasequence 2 interval 165

11. Seismic facies and geologic interpretation of Subsequence VI of Megasequence 2 interval 186

12. Seismic facies and geologic interpretation of Subsequence VII of Megasequence 2 interval 190

13. Seismic facies and geologic interpretation of Subsequence I of Megasequence 3 interval 219

14. Seismic facies and geologic interpretation of Subsequence II of Megasequence 3 interval 244

15. Seismic facies and geologic interpretation of Megasequence 4 interval..... 255

16. Seismic facies and geologic interpretation of Megasequence 5 interval..... 273

17. Seismic facies and geologic interpretation of Megasequence 6 interval..... 284

LIST OF FIGURES

FIGURE

1. Map showing the location of four basins in the Northwest Shelf of Australia, and location of the study area in the Barcoo Sub-basin, southern Browse Basin 2

2. Map of the Browse Basin, Northwest Shelf of Australia showing Caswell and Barcoo Sub-basins, geographic provinces, gas fields and exploration wells 3

3. Map showing location of the study area in Barcoo Sub-basin, Browse Basin, Northwestern Shelf of Australia 5

4. Map of regional seismic profiles and wells location in the study area 8

5. Map of the Browse Basin showing location of structural evolution cross section 10

6. Tectonic evolution of the Browse Basin 12

7. Tectonic setting map showing major faults and structural features throughout the study area 14

8. a. Uninterpreted regional dip-oriented seismic profile(br-98:br98-001) 16

   b. Interpreted regional dip-oriented seismic profile (br-98:br98-001) 17

9. a. Uninterpreted regional dip-oriented seismic profile (br-98:br98-010) 18

   b. Interpreted regional dip-oriented seismic profile (br-98:br98-010) 19

10. a. Uninterpreted regional dip-oriented seismic profile (br-98:br98-019) 20

    b. Interpreted regional strike-oriented seismic profile (br-98:br98-019) 21

11. a. Uninterpreted regional dip-oriented seismic profile (br-98:br98-020) 22

b. Interpreted regional dip-oriented seismic profile (br-98:br98-020) 23

12. a. Uninterpreted regional strike-oriented seismic profile (br-98:br98-071) 24

b. Interpreted regional strike-oriented seismic profile (br-98:br98-071) 25

13. a. Uninterpreted regional strike-oriented seismic profile (br-98:br98-065) 26

b. Interpreted regional strike-oriented seismic profile (br-98:br98-065) 27

14. a. Uninterpreted regional dip-oriented seismic profile (br-98:br98-025a) 28

b. Interpreted regional dip-oriented seismic profile (br-98:br98-025a) 29

15. a. Uninterpreted regional dip-oriented seismic profile (br-98:br98-029) 30

b. Interpreted regional dip-oriented seismic profile (br-98:br98-029) 31

16. a. Uninterpreted regional dip-oriented seismic profile (br-98:br98-035) 32

b. Interpreted regional dip-oriented seismic profile (br-98:br98-035) 33

17. a. Uninterpreted regional dip-oriented seismic profile (br-98:br98-048) 34

b. Interpreted regional dip-oriented seismic profile (br-98:br98-048) 35

18. a. Uninterpreted regional dip-oriented seismic profile (br-98:br98-057) 36

b. Interpreted regional dip-oriented seismic profile (br-98:br98-057) 37

19. a. Uninterpreted regional strike-oriented seismic profile (br-98:br98-082) 38

b. Interpreted regional strike-oriented seismic profile (br-98:br98-082) 39

20. a. Uninterpreted regional strike-oriented seismic profile (br-98:br98-089) 40

b. Interpreted regional strike-oriented seismic profile (br-98:br98-089) 41

21. Tectonostratigraphic summary for the Browse Basin 43

22. Interpreted wireline response of well Barcoo-1 47

23. Interpreted wireline response of Lombardina-1 well 48

24. Interpreted wireline response of Arquebus-1ST1 well 49

25. Interpreted wireline response of Sheherazade-1 well 50

26. Time-depth curve of Barcoo-1 well 51

27. Time-depth curve of Lombardina-1 well 52

28. Time-depth curve of Arquebus-1ST1 well 53

29. Time-depth curve of Sheherazade-1 well 54

30. Well-to-seismic tie of Barcoo-1 well 55

31. Well-to-seismic tie of Lombardina-1 well 56

32. Well-to-seismic tie of Arquebus-1ST1 well 57

33. Well-to-seismic tie of Sheherazade-1 well. 58

34. Time structural contour map of top Megasequence 1 64

35. Isochron map of Megasequence 1 65

36. Dip-oriented seismic profile br-98:br98-009 illustrating seismic facies in Megasequence 1 67

37. Dip-oriented seismic profile br-98:br98-019 illustrating seismic facies in Megasequence 1 68

38. Dip oriented seismic profile br-98:br98-057 illustrating seismic facies in Megasequence 1 69

39. Strike-oriented seismic profile br-98:br98-081 illustrating seismic facies in Megasequence 1 70

40. Isochron map of Subsequence I of Megasequence 1 72

41. Seismic facies map of Subsequence I of Megasequence 1 74

42. Geologic facies map of Subsequence I of Megasequence 1 75

43. a. Uninterpreted regional dip-oriented seismic profile (br-98:br98-033) 76

b. Interpreted regional dip-oriented seismic profile illustrating a play potential in Subsequence I of Megasequence 1 77

44. a. Uninterpreted regional dip-oriented seismic profile (br-98:br98-033)..... 78

b. Interpreted regional dip-oriented seismic profile illustrating a play potential in Subsequence I of Megasequence 1 79

45. a. Uninterpreted regional strike-oriented seismic profile (br-98:br98-082)..... 80

b. Interpreted regional strike-oriented seismic profile illustrating a play potential in Subsequence I of Megasequence 1 81

46. a. Uninterpreted regional strike-oriented seismic profile (br-98:br98-082)..... 82

b. Interpreted regional strike-oriented seismic profile illustrating a play potential in Subsequence I of Megasequence 1 83

47. Isochron map of Subsequence II of Megasequence 1..... 85

48. Seismic facies map of Subsequence II of Megasequence 1 86

49. Geologic facies map of Subsequence II of Megasequence 1..... 87

50. Isochron map of Subsequence III of Megasequence 1..... 89

51. Seismic facies map of Subsequence III of Megasequence 1 90

52. Geologic facies map of Subsequence III of Megasequence 1..... 92

53. a. Uninterpreted regional dip-oriented seismic profile (br-98:br98-033)..... 93

b. Interpreted regional dip-oriented seismic profile illustrating a play potential in Subsequence II of Megasequence 1 94

54. a. Uninterpreted regional dip-oriented seismic profile (br-98:br98-033)..... 95

b. Interpreted regional dip-oriented seismic profile illustrating a play potential in Subsequence II of Megasequence 1 96

55. a. Uninterpreted regional strike-oriented seismic profile (br-98:br98-082)..... 97

b. Interpreted regional strike-oriented seismic profile illustrating a play potential in Subsequence II of Megasequence I 98

56. a. Uninterpreted regional strike-oriented seismic profile (br-98:br98-082)..... 99

b. Interpreted regional strike-oriented seismic profile illustrating a play potential in Subsequence II of Megasequence I 100

57. a. Uninterpreted regional dip-oriented seismic profile (br-98:br98-057)..... 101

b. Interpreted regional dip-oriented seismic profile illustrating a play potential in Subsequence III of Megasequence 1 102

58. a. Uninterpreted regional dip-oriented seismic profile (br-98:br98-057)..... 103

b. Interpreted regional dip-oriented seismic profile illustrating a play potential in Subsequence III of Megasequence 1 104

59. a. Uninterpreted regional strike-oriented seismic profile (br-98:br98-080)..... 105

b. Interpreted regional strike-oriented seismic profile illustrating a play potential in Subsequence III of Megasequence 1 106

60. a. Uninterpreted regional strike-oriented seismic profile (br-98:br98-080)..... 107

b. Interpreted regional strike-oriented seismic profile illustrating a play potential in Subsequence III of Megasequence 1 108

61. a. Uninterpreted regional dip-oriented seismic profile (br-98:br98-035)..... 109

b. Interpreted regional dip-oriented seismic profile illustrating a play potential in Subsequence III of Megasequence 1 110

62. a. Uninterpreted regional dip-oriented seismic profile (br-98:br98-035)..... 111

b. Interpreted regional dip-oriented seismic profile illustrating a play potential in

Subsequence III of Megasequence 1 112

63. a. Uninterpreted regional strike-oriented seismic profile (br-98:br98-085)..... 113

b. Interpreted regional strike-oriented seismic profile illustrating a play potential in Subsequence III of Megasequence 1 114

64. a. Uninterpreted regional strike-oriented seismic profile (br-98:br98-085)..... 115

b. Interpreted regional strike-oriented seismic profile illustrating a play potential in Subsequence III of Megasequence 1 116

65. Time structural contour map of top Megasequence 2..... 118

66. Isochron map of Megasequence 2 119

67. Dip-oriented seismic profile br-98:br98-005 illustrating seismic facies in Megasequence 2 120

68. Dip-oriented seismic profile br-98:br98-013 illustrating seismic facies in Megasequence 2 121

69. Dip oriented seismic profile br-98:br98-048 illustrating seismic facies in Megasequence 2 122

70. Strike-oriented seismic profile br-98:br98-088 illustrating seismic facies in Megasequence 2 123

71. Isochron map of Subsequence I of Megasequence 2..... 126

72. Seismic facies map of Subsequence I of Megasequence 2 127

73. Geologic facies map of Subsequence I of Megasequence 2..... 128

74. a. Uninterpreted regional dip-oriented seismic profile (br-98:br98-001)..... 129

b. Interpreted regional dip-oriented seismic profile illustrating a play potential in Subsequence I of Megasequence 2 130

75. a. Uninterpreted regional dip-oriented seismic profile (br-98:br98-001)..... 131

b. Interpreted regional dip-oriented seismic profile illustrating a play potential in Subsequence I of Megasequence 2 132

76. a. Uninterpreted regional strike-oriented seismic profile (br-98:br98-078a)..... 133

b. Interpreted regional strike-oriented seismic profile illustrating a play potential in Subsequence I of Megasequence 2 134

77. a. Uninterpreted regional strike-oriented seismic profile (br-98:br98-078a)..... 135

b. Interpreted regional strike-oriented seismic profile illustrating a play potential in Subsequence I of Megasequence 2 136

78. a. Uninterpreted regional dip-oriented seismic profile (br-98:br98-010)..... 137

b. Interpreted regional dip-oriented seismic profile illustrating a play potential in Subsequence I of Megasequence 2 138

79. a. Uninterpreted regional dip-oriented seismic profile (br-98:br98-010)..... 139

b. Interpreted regional dip-oriented seismic profile illustrating a play potential in Subsequence I of Megasequence 2 140

80. a. Uninterpreted regional strike-oriented seismic profile (br-98:br98-080)..... 141

b. Interpreted regional strike-oriented seismic profile illustrating a play potential in Subsequence I of Megasequence 2 142

81. a. Uninterpreted regional strike-oriented seismic profile (br-98:br98-080)..... 143

b. Interpreted regional strike-oriented seismic profile illustrating a play potential in Subsequence I of Megasequence 2 144

82. Isochron map of Subsequence II of Megasequence 2..... 146

83. Seismic facies map of Subsequence II of Megasequence 2 147

84. Geologic facies map of Subsequence II of Megasequence 2 148

85. a. Uninterpreted regional dip-oriented seismic profile (br-98:br98-010)..... 149

b. Interpreted regional dip-oriented seismic profile illustrating a play potential in Subsequence II of Megasequence 2 150

86. a. Uninterpreted regional dip-oriented seismic profile (br-98:br98-010)..... 151

b. Interpreted regional dip-oriented seismic profile illustrating a play potential in Subsequence II of Megasequence 2 152

87. a. Uninterpreted regional strike-oriented seismic profile (br-98:br98-075b)..... 153

b. Interpreted regional strike-oriented seismic profile illustrating a play potential in Subsequence II of Megasequence 2 154

88. a. Uninterpreted regional strike-oriented seismic profile (br-98:br98-075b)..... 155

b. Interpreted regional strike-oriented seismic profile illustrating a play potential in Subsequence II of Megasequence 2 156

89. Isochron map of Subsequence III of Megasequence 2..... 158

90. Seismic facies map of Subsequence III of Megasequence 2 159

91. Geologic facies map of Subsequence III of Megasequence 2..... 160

92. Isochron map of Subsequence IV of Megasequence 2 162

93. Seismic facies map of Subsequence IV of Megasequence 2 163

94. Geologic facies map of Subsequence IV of Megasequence 2 164

95. Isochron map of Subsequence V of Megasequence 2 166

96. Seismic facies map of Subsequence V of Megasequence 2 167

97. Geologic facies map of Subsequence V of Megasequence 2 169

98. a. Uninterpreted regional dip-oriented seismic profile (br-98:br98-001)..... 170

b. Interpreted regional dip-oriented seismic profile illustrating a play potential in Subsequence V of Megasequence 2 171

99. a. Uninterpreted regional dip-oriented seismic profile (br-98:br98-001)..... 172

b. Interpreted regional dip-oriented seismic profile illustrating a play potential in Subsequence V of Megasequence 2 173

100. a. Uninterpreted regional strike-oriented seismic profile (br-98:br98-083)..... 174

b. Interpreted regional strike-oriented seismic profile illustrating a play potential in Subsequence V of Megasequence 2 175

101. a. Uninterpreted regional strike-oriented seismic profile (br-98:br98-083)..... 176

b. Interpreted regional strike-oriented seismic profile illustrating a play potential in Subsequence V of Megasequence 2 177

102. a. Uninterpreted regional dip-oriented seismic profile (br-98:br98-039)..... 178

b. Interpreted regional dip-oriented seismic profile illustrating a play potential in Subsequence V of Megasequence 2 179

103. a. Uninterpreted regional dip-oriented seismic profile (br-98:br98-039)..... 180

b. Interpreted regional dip-oriented seismic profile illustrating a play potential in Subsequence V of Megasequence 2 181

104. a. Uninterpreted regional strike-oriented seismic profile (br-98:br98-085)..... 182

b. Interpreted regional strike-oriented seismic profile illustrating a play potential in Subsequence V of Megasequence 2 183

105. a. Uninterpreted regional strike-oriented seismic profile (br-98:br98-085)..... 184

b. Interpreted regional strike-oriented seismic profile illustrating a play potential in Subsequence V of Megasequence 2 185

106. Isochron map of Subsequence VI of Megasequence 2 187

107. Seismic facies map of Subsequence VI of Megasequence 2 188

108. Geologic facies map of Subsequence VI of Megasequence 2 189

109. Isochron map of Subsequence VII of Megasequence 2 191

110. Seismic facies map of Subsequence VII of Megasequence 2 192

111. Geologic facies map of Subsequence VII of Megasequence 2 194

112. a. Uninterpreted regional dip-oriented seismic profile (br-98:br98-029)..... 195

b. Interpreted regional dip-oriented seismic profile illustrating a play potential in Subsequence VII of Megasequence 2..... 196

113. a. Uninterpreted regional dip-oriented seismic profile (br-98:br98-029)..... 197

b. Interpreted regional dip-oriented seismic profile illustrating a play potential in Subsequence VII of Megasequence 2..... 198

114. a. Uninterpreted regional strike-oriented seismic profile (br-98:br98-087)..... 199

b. Interpreted regional strike-oriented seismic profile illustrating a play potential in Subsequence VII of Megasequence 2..... 200

115. a. Uninterpreted regional strike-oriented seismic profile (br-98:br98-087)..... 201

b. Interpreted regional strike-oriented seismic profile illustrating a play potential in Subsequence VII of Megasequence 2..... 202

116. a. Uninterpreted regional dip-oriented seismic profile (br-98:br98-057)..... 203

b. Interpreted regional dip-oriented seismic profile illustrating a play potential in Subsequence VII of Megasequence 2..... 204

117. a. Uninterpreted regional dip-oriented seismic profile (br-98:br98-057)..... 205

b. Interpreted regional dip-oriented seismic profile illustrating a play potential in

Subsequence VII of Megasequence 2 206

118. a. Uninterpreted regional strike-oriented seismic profile (br-98:br98-080) 207

b. Interpreted regional strike-oriented seismic profile illustrating a play potential in Subsequence VII of Megasequence 2 208

119. a. Uninterpreted regional strike-oriented seismic profile (br-98:br98-080) 209

b. Interpreted regional strike-oriented seismic profile illustrating a play potential in Subsequence VII of Megasequence 2 210

120. Time structural contour map of top Megasequence 3 212

121. Isochron map of Megasequence 3 213

122. Dip-oriented seismic profile br-98:br98-017 illustrating seismic facies in Megasequence 3 215

123. Dip-oriented seismic profile br-98:br98-002 illustrating seismic facies in Megasequence 3 216

124. Dip-oriented seismic profile br-98:br98-058 illustrating seismic facies in Megasequence 3 217

125. Strike-oriented seismic profile br-98:br98-087 illustrating seismic facies in Megasequence 3 218

126. Isochron map of Subsequence I of Megasequence 3 220

127. Seismic facies map of Subsequence I of Megasequence 3 221

128. Geologic facies map of Subsequence I of Megasequence 3 223

129. a. Uninterpreted regional dip-oriented seismic profile (br-98:br98-001) 224

b. Interpreted regional dip-oriented seismic profile illustrating a play potential in Subsequence I of Megasequence 3 225

130. a. Uninterpreted regional dip-oriented seismic profile (br-98:br98-001)..... 226

b. Interpreted regional dip-oriented seismic profile illustrating a play potential in Subsequence I of Megasequence 3 227

131. a. Uninterpreted regional dip-oriented seismic profile (br-98:br98-048)..... 228

b. Interpreted regional dip-oriented seismic profile illustrating a play potential in Subsequence I of Megasequence 3 229

132. a. Uninterpreted regional dip-oriented seismic profile (br-98:br98-048)..... 230

b. Interpreted regional dip-oriented seismic profile illustrating a play potential in Subsequence I of Megasequence 3 231

133. a. Uninterpreted regional strike-oriented seismic profile (br-98:br98-084)..... 232

b. Interpreted regional strike-oriented seismic profile illustrating a play potential in Subsequence I of Megasequence 3 233

134. a. Uninterpreted regional strike-oriented seismic profile (br-98:br98-084)..... 234

b. Interpreted regional strike-oriented seismic profile illustrating a play potential in Subsequence I of Megasequence 3 235

135. a. Uninterpreted regional dip-oriented seismic profile (br-98:br98-057)..... 236

b. Interpreted regional dip-oriented seismic profile illustrating a play potential in Subsequence I of Megasequence 3 237

136. a. Uninterpreted regional dip-oriented seismic profile (br-98:br98-057)..... 238

b. Interpreted regional dip-oriented seismic profile illustrating a play potential in Subsequence I of Megasequence 3 239

137. a. Uninterpreted regional strike-oriented seismic profile (br-98:br98-080)..... 240

b. Interpreted regional strike-oriented seismic profile illustrating a play potential in

Subsequence I of Megasequence 3 241

138. a. Uninterpreted regional strike-oriented seismic profile (br-98:br98-080)..... 242

b. Interpreted regional strike-oriented seismic profile illustrating a play potential in Subsequence I of Megasequence 3 243

139. Isochron map of Subsequence II of Megasequence 3..... 245

140. Seismic facies map of Subsequence II of Megasequence 3 246

141. Geologic facies map of Subsequence II of Megasequence 3..... 247

142. Time structural contour map of top Megasequence 4..... 249

143. Isochron map of Megasequence 4: 65.5-23.0 Ma interval..... 250

144. Dip-oriented seismic profile br-98:br98-009 illustrating seismic facies in Megasequence 4 251

145. Dip-oriented seismic profile br-98:br98-023 illustrating seismic facies in Megasequence 4 252

146. Dip-oriented seismic profile br-98:br98-056a illustrating seismic facies in Megasequence 4 253

147. Strike-oriented seismic profile br-98:br98-082 illustrating seismic facies in Megasequence 4 254

148. Seismic facies map of Megasequence 4: 65.5-23.0 Ma interval..... 256

149. Geologic facies map of Megasequence 4: 65.5-23.0 Ma interval 257

150. a. Uninterpreted regional dip-oriented seismic profile (br-98:br98-057)..... 258

b. Interpreted regional dip-oriented seismic profile illustrating a play potential in Megasequence 4 259

151. a. Uninterpreted regional dip-oriented seismic profile (br-98:br98-057)..... 260

b. Interpreted regional dip-oriented seismic profile illustrating a play potential in Megasequence 4 261

152. a. Uninterpreted regional strike-oriented seismic profile (br-98:br98-083) 262

b. Interpreted regional strike-oriented seismic profile illustrating a play potential in Megasequence 4 263

153. a. Uninterpreted regional strike-oriented seismic profile (br-98:br98-083) 264

b. Interpreted regional strike-oriented seismic profile illustrating a play potential in Megasequence 4 265

154. Time structural contour map of top Megasequence 5 267

155. Isochron map of Megasequence 5: 23.0-19.0 Ma interval 268

156. Dip-oriented seismic profile br-98:br98-005 illustrating seismic facies in Megasequence 5 269

157. Dip-oriented seismic profile br-98:br98-029 illustrating seismic facies in Megasequence 5 270

158. Dip-oriented seismic profile br-98:br98-009 illustrating seismic facies in Megasequence 5 271

159. Strike-oriented seismic profile br-98:br98-082 illustrating seismic facies in Megasequence 5 272

160. Seismic facies map of Megasequence 5: 23.0-19.0 Ma interval 274

161. Geologic facies map of Megasequence 5: 23.0-19.0 Ma interval 275

162. a. Uninterpreted regional dip-oriented seismic profile (br-98:br98-057) 276

b. Interpreted regional dip-oriented seismic profile illustrating a play potential in Megasequence 5 277

163. a. Uninterpreted regional dip-oriented seismic profile (br-98:br98-057)..... 278

b. Interpreted regional dip-oriented seismic profile illustrating a play potential in Megasequence 5 279

164. a. Uninterpreted regional strike-oriented seismic profile (br-98:br98-080)..... 280

b. Interpreted regional strike-oriented seismic profile illustrating a play potential in Megasequence 5 281

165. a. Uninterpreted regional strike-oriented seismic profile (br-98:br98-080)..... 282

b. Interpreted regional strike-oriented seismic profile illustrating a play potential in Megasequence 5 283

166. Time structural contour map of top Megasequence 6..... 285

167. Isochron map of Megasequence 6: 19.0-14.2 Ma interval..... 286

168. Dip-oriented seismic profile br-98:br98-008 illustrating seismic facies in Megasequence 6 288

169. Dip-oriented seismic profile br-98:br98-011 illustrating seismic facies in Megasequence 6 289

170. Dip-oriented seismic profile br-98:br98-037 illustrating seismic facies i84 Megasequence 6 290

171. Strike-oriented seismic profile br-98:br98-080 illustrating seismic facies in Megasequence 6 291

172. Seismic facies map of Megasequence 6: 19.0-14.2 Ma interval..... 292

173. Geologic facies map of Megasequence 6: 19.0-14.2 Ma interval 293

174. a. Uninterpreted regional dip-oriented seismic profile (br-98:br98-017)..... 294

b. Interpreted regional dip-oriented seismic profile illustrating a play potential in

Megasequence 6 295

175. a. Uninterpreted regional dip-oriented seismic profile (br-98:br98-017)..... 296

b. Interpreted regional dip-oriented seismic profile illustrating a play potential in Megasequence 6 297

176. a. Uninterpreted regional strike-oriented seismic profile (br-98:br98-075b)..... 298

b. Interpreted regional strike-oriented seismic profile illustrating a play potential in Megasequence 6 299

177. a. Uninterpreted regional strike-oriented seismic profile (br-98:br98-075b)..... 300

b. Interpreted regional strike-oriented seismic profile illustrating a play potential in Megasequence 6 301

178. Figure showing the lateral migrated channel 302

I. INTRODUCTION

The offshore region of Northwest Australia is a divergent continental margin that formed initially during the Mesozoic as an intracratonic basin within the Gondwana breakup. The Northwest Shelf comprises four northeast-trending basins; (Northern) Carnarvon, offshore Canning, Browse, and Bonaparte (Figures 1, 2). These basins include a thick Upper Paleozoic, Mesozoic and Cenozoic sedimentary successions. The margin includes the world-class gas fields with a significant potential oil province.

First exploration in the Browse basin was in 1967, when Burmah Oil Company Australia Ltd (BOCAL), which later became Woodside, acquired 1,600 kilometers of regional seismic. To date, more than 170,000 kilometers of 2D and 28,000 square kilometers of 3D seismic data have been acquired. Torosa (Scot Reef), Brecknock, Brecknock South (Calliance), Ichthys and Crux are the main gas fields in the Caswell Sub-basin of the Browse Basin (Figure 2). As of 2009, 94 exploration wells have been drilled and 17 gas discoveries have been made. However, due to the economics of the area: (1) their isolation, and being almost 300 kilometers from the mainland; (2) discoveries are in 300-500 meter of water depth and not close to major development which requires relatively expensive development drilling; and (3) no existing petroleum infrastructure in the area. Although the Browse Basin has had limited exploration, the discovery rate is favorable, 12-23% discovery success.

The study area is located in the Barcoo Sub-basin, which is one of the major depocenters of the Browse Basin on the present-day continental shelf and slope setting (Figure 3). It is covered approximately 35,000 square kilometers. About 12 kilometers of Paleozoic to Cenozoic strata were deposited in this area.

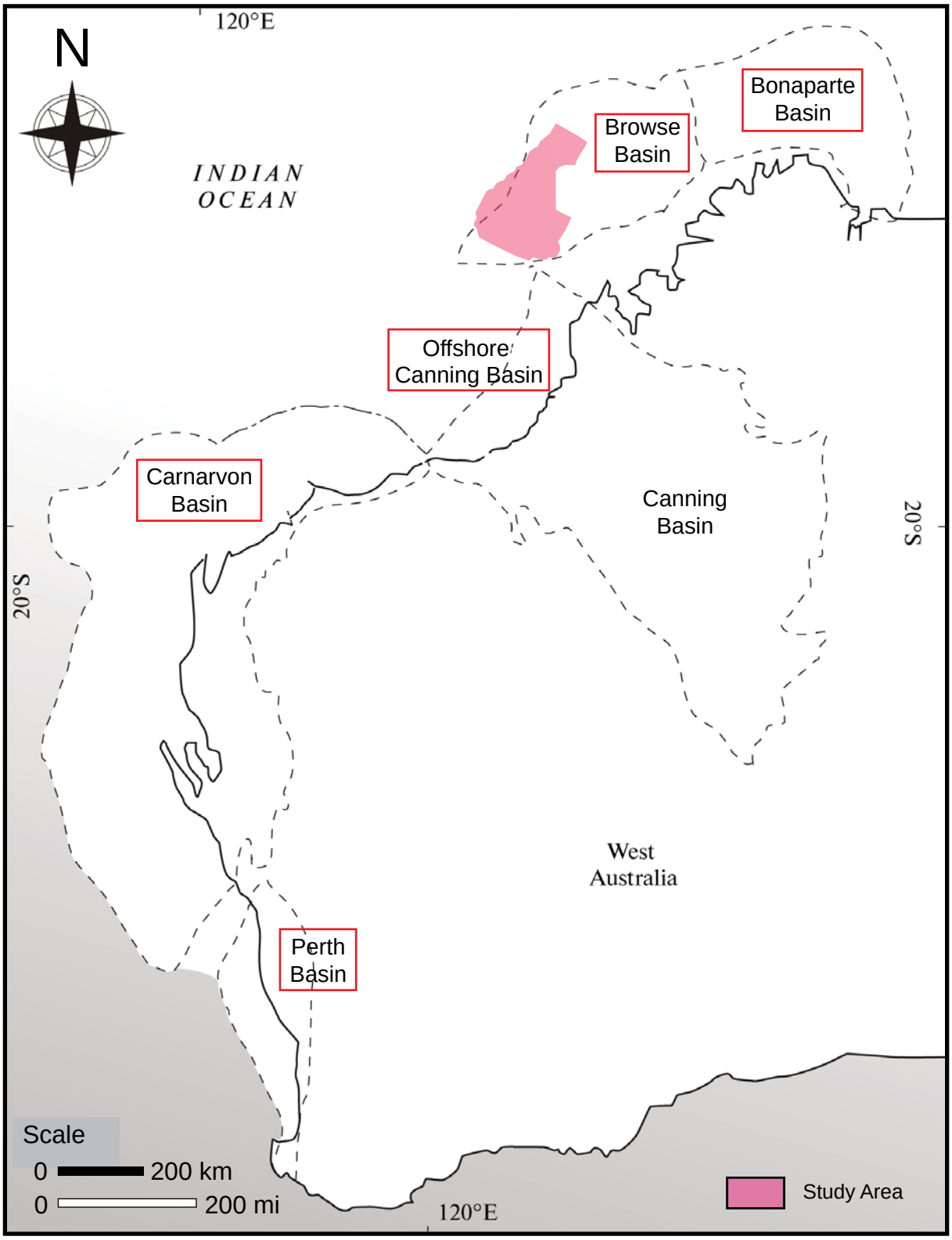

Figure 1. Map showing the location of four basins in the Northwest Shelf of Australia, and location of the study area in the Barcoo Sub-basin, southern Browse Basin (Zabanbark, 2010)

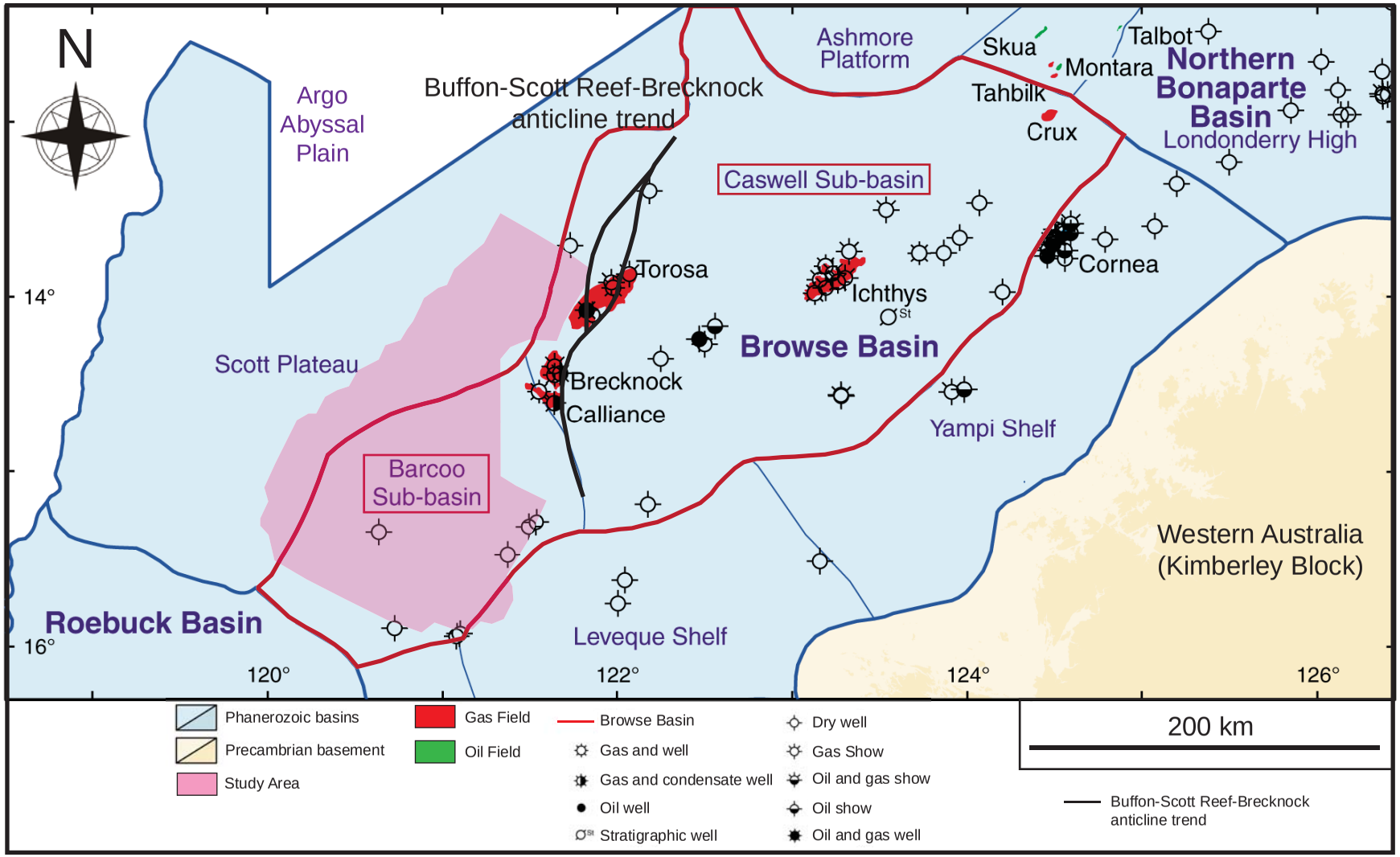

Figure 2. Map of the Browse Basin (red line), Northwest Shelf of Australia. Caswell and Barcoo Sub-basins, geographic provinces, gas fields and exploration wells are shown (Geological Survey of Western Australia, 2009).

This study focuses on describing and characterizing the Cretaceous through Miocene strata. Sequence stratigraphic analysis was done using a regional high-resolution two-dimensional seismic data. The purpose of this research is to study a seismic sequence stratigraphy of the Jurassic through the middle Miocene strata to: (1) define and describe the sequence stratigraphic framework of Lower Cretaceous through middle Miocene sedimentary units by using an integrated database of 2D and well data; (2) analyze the 2D seismic facies within a chronostratigraphic framework of each megasequence; (3) integrate seismic facies and seismic sequence stratigraphy to infer paleo-depositional environments, and (4) evaluate the potential plays for successful future exploration.

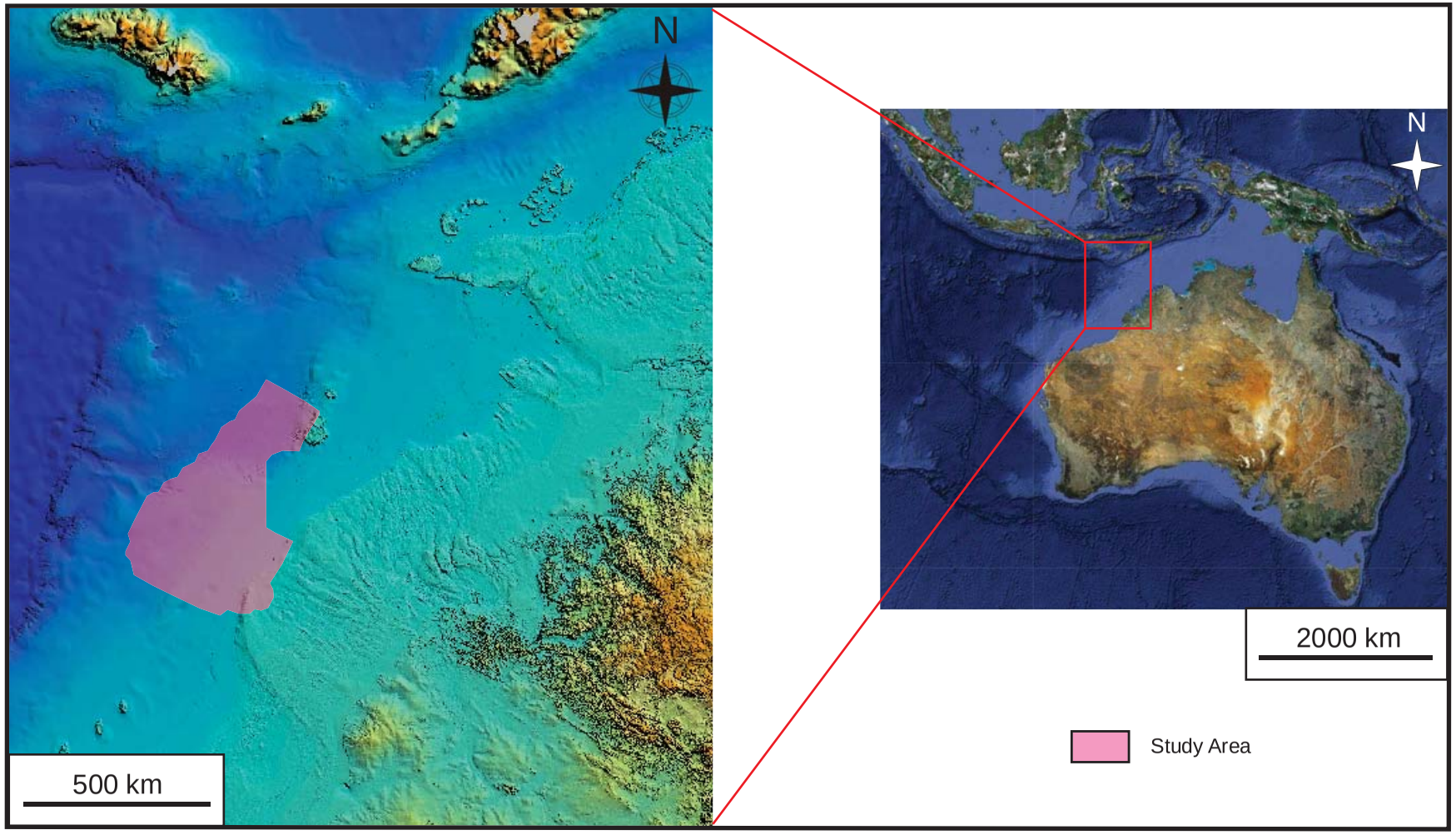

Figure 3. Map showing location of the study area in the Barcoo Sub-basin, Browse Basin, Northwest Shelf of Australia

II. DATA SET

Sub-regional 2D multifold seismic data and four conventional well logs data were used for this study. A summary of the data set available is given in Table 1. The seismic data were acquired during 2001 in WNW-ESE and NEN-SWS directions corresponding to dip and strike lines, respectively (Figure 4).

Four exploration wells have been drilled in the study area; Lombardina-1 (1974), Barcoo-1 (1979), Arquebus-1ST1 (1991) and Sheherazade-1 (1993). Each well contains a set of digital wireline logs that include gamma ray, resistivity, spontaneous potential, density and sonic. Time-depth information was used for generation of synthetic seismograms. SMT 2D/3D seismic interpretation package were used for 2D seismic interpretation and well-to-seismic correlation whereas PETRA was used to demonstrate well data.

Table 1. Data set used in this study

Seismic Data		
Donated by AGA, acquired in 2001		
Total Area:	35,000	km^2
Depositional Dip Lines		
Total:	54	
Average Spacing:	5	km
Average Length:	115	km
Depositional Strike Lines		
Total:	20	
Average Spacing:	10	km
Average Length:	280	km
Well Data		
Donated by PTTEP		
Total Number of Wells drilled in Study Area (as of August 2010):	4	
Number of wells with logs:	4	
Number of wells time-depth info:	4	
Types of wireline logs:	GR, SP, LLD, DT, RHOB	

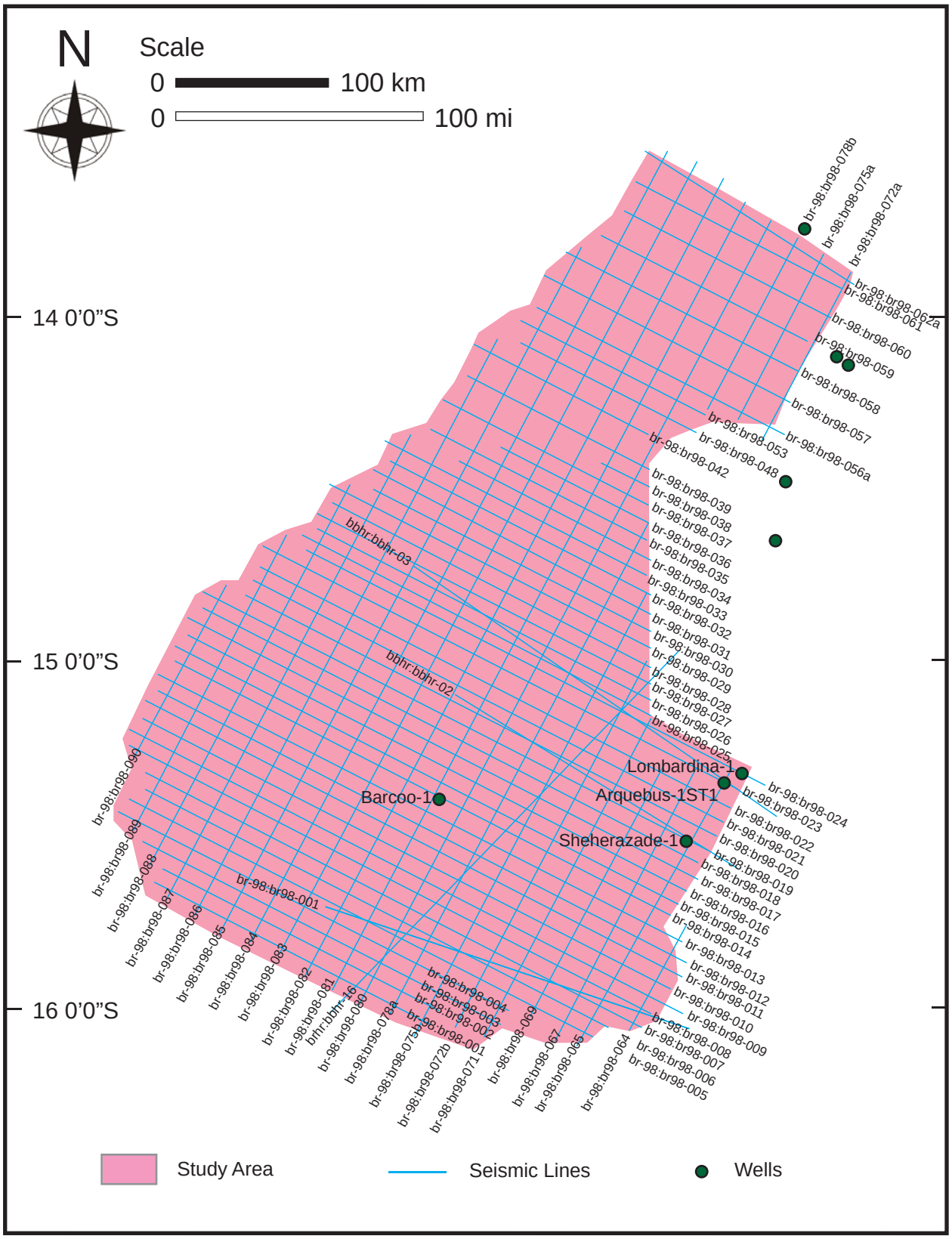

Figure 4. Map of regional seismic profiles and wells location in the study area

III. REGIONAL GEOLOGIC SETTING

The study area is located in the Barcoo Sub-basin, the present-day continental shelf of the northwestern shelf of Australia that covers 140,000 square kilometer with approximately 200 kilometer long (northeast-southwest) by 130 kilometer wide (northwest-southeast).

The Barcoo Sub-basin is separated from the Caswell Sub-basin to the northeast by a major north-northeast trending structural zone, the Buffon-Scott Reef-Brecknock anticline trend (Figure 2). The sub-basin is bounded to the southeast by the Leveque Shelf which is a highly eroded shallow basement area. Moreover, the Scott Plateau sits at the western margin of the sub-basin whereas the Roebuck Basin bounds the sub-basin in the southwest edge.

Tectonic Evolution

Browse Basin can be subdivided into two major depocenters: the Caswell and the Barcoo Sub-basins (Figures 2, 5). They were formed separates half-grabens during Upper Carboniferous to Lower Permian extension. The initial phase of Paleozoic rifting significantly influenced the development and infill of the Barcoo Sub-basin, especially the major displacement on the Barcoo fault trend and the active of extensional faults on the western margin of the Leveque Shelf. The Permian through Late Jurassic evolution of the Browse Basin is shown in Figure 6.

The structural evolution of the Browse basin developed in six tectonic phases (Struckmeyer et al, 1998):

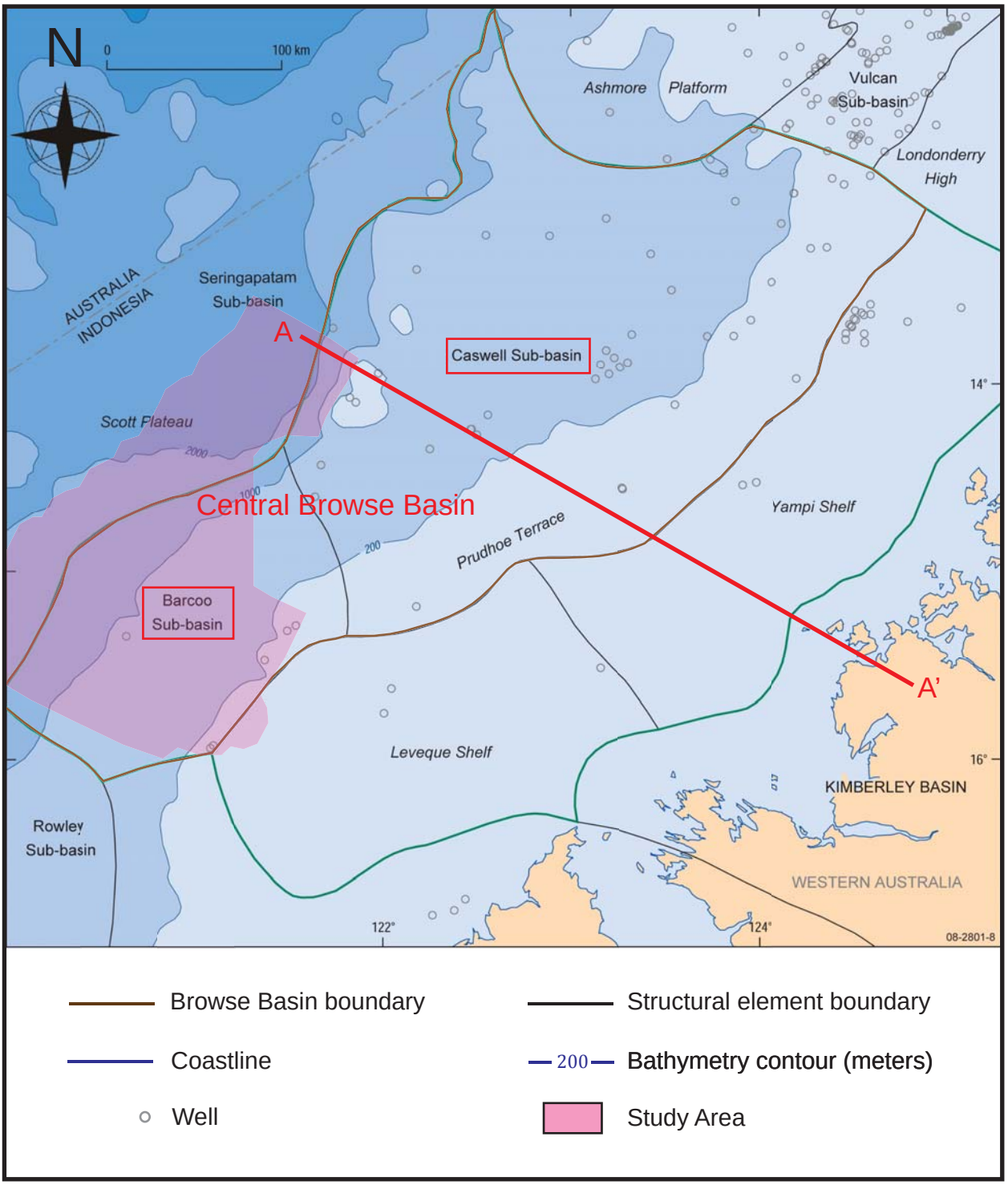

Figure 5. Map of the Browse Basin (brown line), Northwest Shelf of Australia. Location of structural evolution cross section A-A' is shown in Figure 6, modified after Nicoll et. al (2009).

(1) Extension (Upper Carboniferous to Lower Permian): The basin was initiated as a series of intracratonic extensional grabens and half-grabens (Figure 6A). The Permian sediments directly overlie eroded Precambrian basement and deposited into the central of the sub-basin. The extensional at the end of Permian led to an episode of block faulting, uplifting of the Scott Plateau and the basin subsiding. Additionally, structures formed during this extensional event were late reactivated, and played a critical role in controlling the distribution and nature of the sedimentary fill.

(2) Thermal subsidence (Upper Permian to Triassic): The sag phase of the Upper Carboniferous to Lower Permian rifting event took place during the Upper Permian to Triassic period. A passive margin environment was developed, with transgressive to shallow marine conditions. The erosional wedge of Permian and some of Triassic sediments are found overlying Precambrian basement (Figure 6B). Most of Triassic sedimentation is largely confined to the center of the basin between the Scott Plateau to the west and the Leveque Shelf to the east.

(3) Inversion (Upper Triassic to Lower Jurassic): The Permo-Triassic sag phase was terminated by compressional reactivation in the Upper Triassic to Lower Jurassic. This event resulted in reactivation and the partial inversion of Paleozoic half-grabens and Permian faults (Figure 6C), with the formation of large scale anticlines, the Buffon-Scott Reef-Brecknock Anticline Trend.

(4) Extension (Lower to Middle Jurassic): This second extension phase during Lower to Middle Jurassic resulted in the development of widespread small scale faults. During the upper Middle Jurassic continental break-up produced a major regional unconformity (Callovian Unconformity), consisting of widespread erosion across the

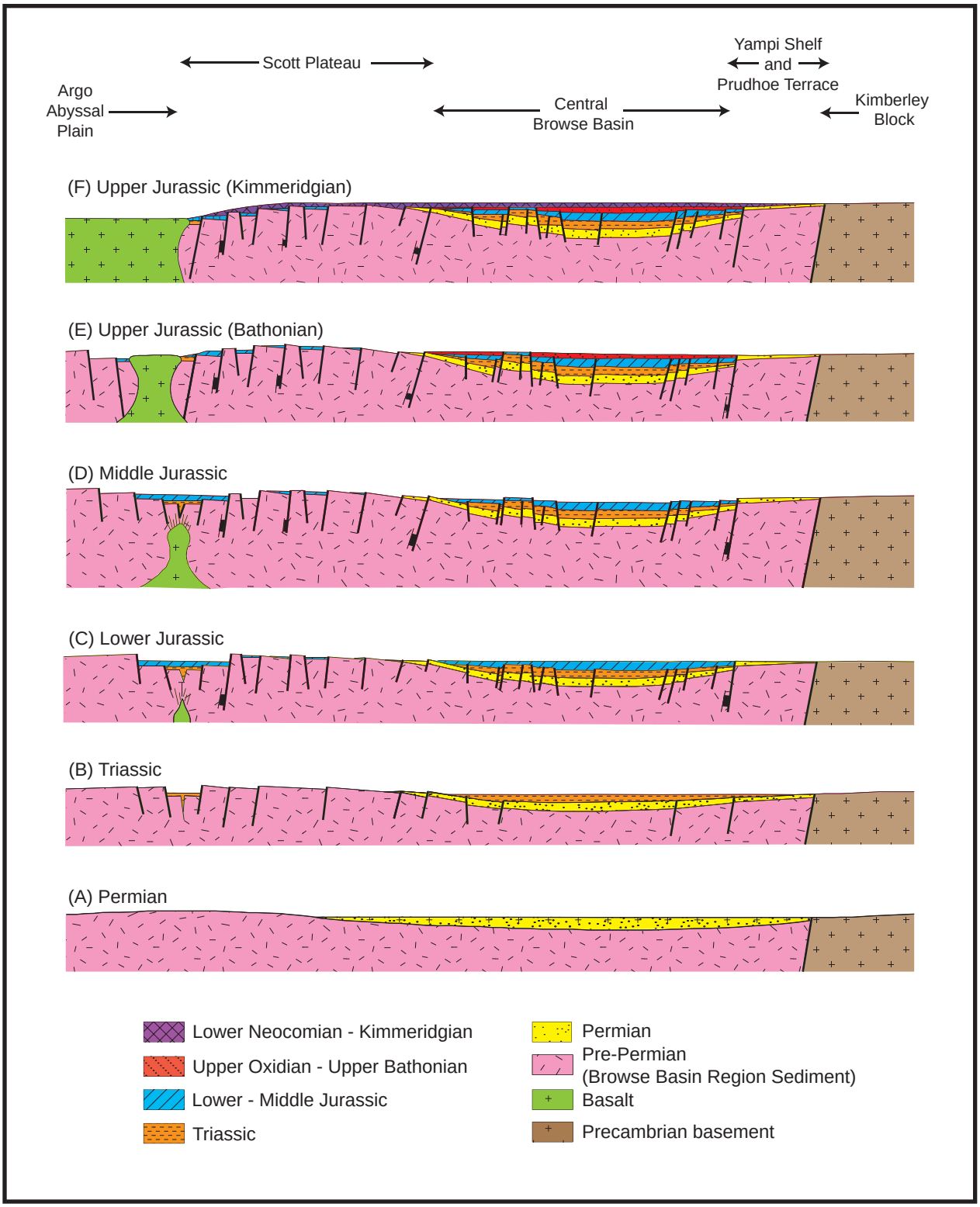

Figure 6. Tectonic evolution of the Browse Basin (modified from Allen et al., 1978; Cadman et al., 1991; Stephenson et al., 1994). Location of cross section A-A' is shown in Figure 5.

Northwest Shelf. The new oceanic crust was created at the western edge of the Scott Plateau (Figures 6D, 6E).

(5) Thermal subsidence (Upper Jurassic to Lower Miocene): A second phase of thermal subsidence combined with higher sea levels created greater accommodation, allowing for large volumes of transgressive sediments deposited in the central of the basin and on the high topographic areas. Throughout Turonian to Tertiary, a major progradational cycle was developed. The continental shelf edge migrates westwards as thick sequences of carbonates were deposited on the rapidly subsiding western shelf margin. During Upper Jurassic period, sea-floor spreading of Argo Abyssal plain continued creating (Figure 6F).

(6) Inversion (Middle to Upper Miocene): Compression took place during this period as a result of the convergence of the Australia-India and Eurasia Plates. This compression resulted in fault activation and structural shape changes, which in many cases forced leakage and onward migration of hydrocarbons.

The tectonic setting map of the Barcoo Sub-basin is shown in Figure 7. The regional structural and stratigraphic setting is illustrated in a series of regional dip and strike-oriented seismic profiles (Figures 8-20). The most prominent features of the study area are characterized by the Barcoo Platform anticline, prograding clinoform packages of Barcoo Platform, Barcoo Anticline, Barcoo Fault Trend, Barcoo Terrace, Scott Plateau and Scott Plateau Graben (Figures 7-20).

At the eastern edge of the sub-basin, the main tectonic feature is the Barcoo Platform (Figures 7- 13), which is located next to the Leveque Shelf (Figures 5, 7). The Barcoo Platform was a shelf platform during the Jurassic through Miocene. Prominent

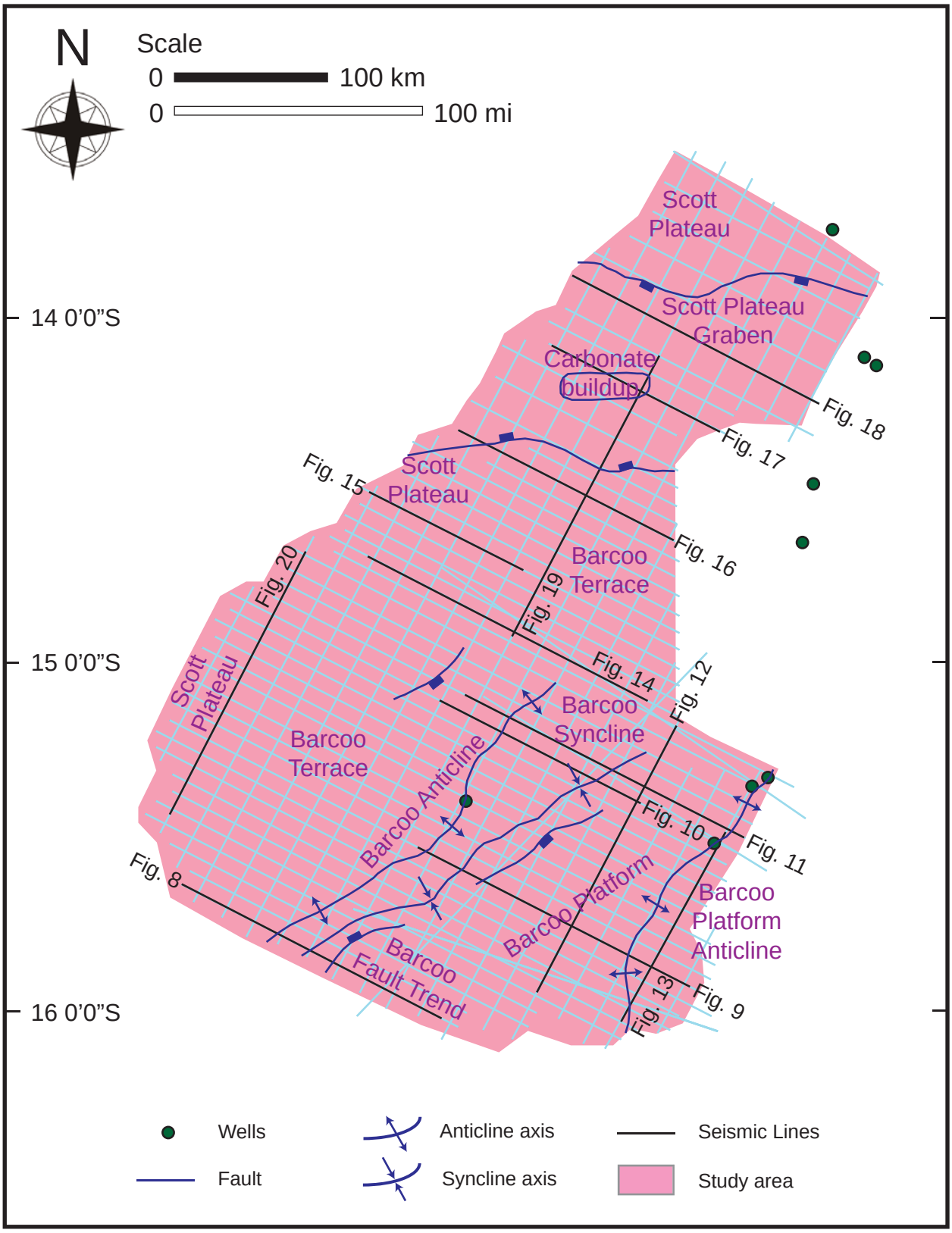

Figure 7. Tectonic setting map showing major faults and structural features throughout the study area. The regional seismic profiles (black lines) are shown in Figures 8-20.

prograding clinoform packages developed as the sediments were transported from the southeast to northwest. The Barcoo Platform Anticline is an important structure that developed associated with the transpressional deformation and Miocene inversion of the area. The anticline axis trends NNE-SSW (Figure 7). Series of small faults of Barcoo Fault Trend developed in the underlying Jurassic strata (Figures 7-14). These faults developed initially during Mesozoic rifting and were also reactivated during the Miocene forming small structure.

In the southern portion of the study area, the regional dip-oriented seismic profile illustrates the Barcoo Anticline and the graben structure of Barcoo Syncline (Figures 7, 8). The Scott Plateau is located at the western margin of the sub-basin (Figures 5, 7, 20). The central part of the study area consists of the Barcoo Terrace which located between the Scott Plateau and the Barcoo Syncline (Figures 7, 8, 11, 12). In the central portion of the study area, the Barcoo Terrace is the major tectonic feature (Figures 7, 14, 15). Farther north, an apparent carbonate buildup feature is present (Figure 17), as well as the series of fault-related structure (Figures 7, 17, 18). The Scott Plateau Graben is a prominent east-west trending graben in the northern portion of the study area (Figures 7, 16-19).

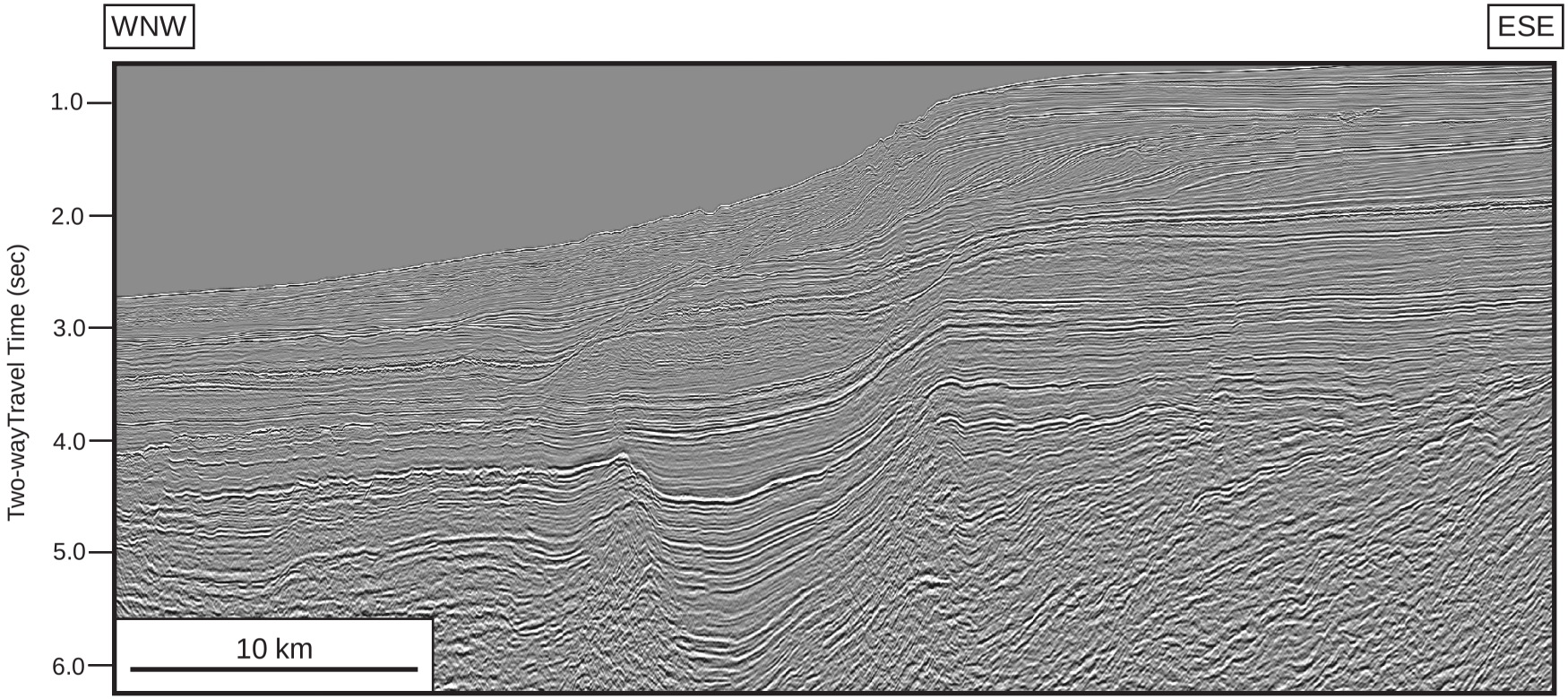

Figure 8a. Uninterpreted regional dip-oriented seismic profile (br-98:br98-001). Location of the profile is shown in Figure 7.

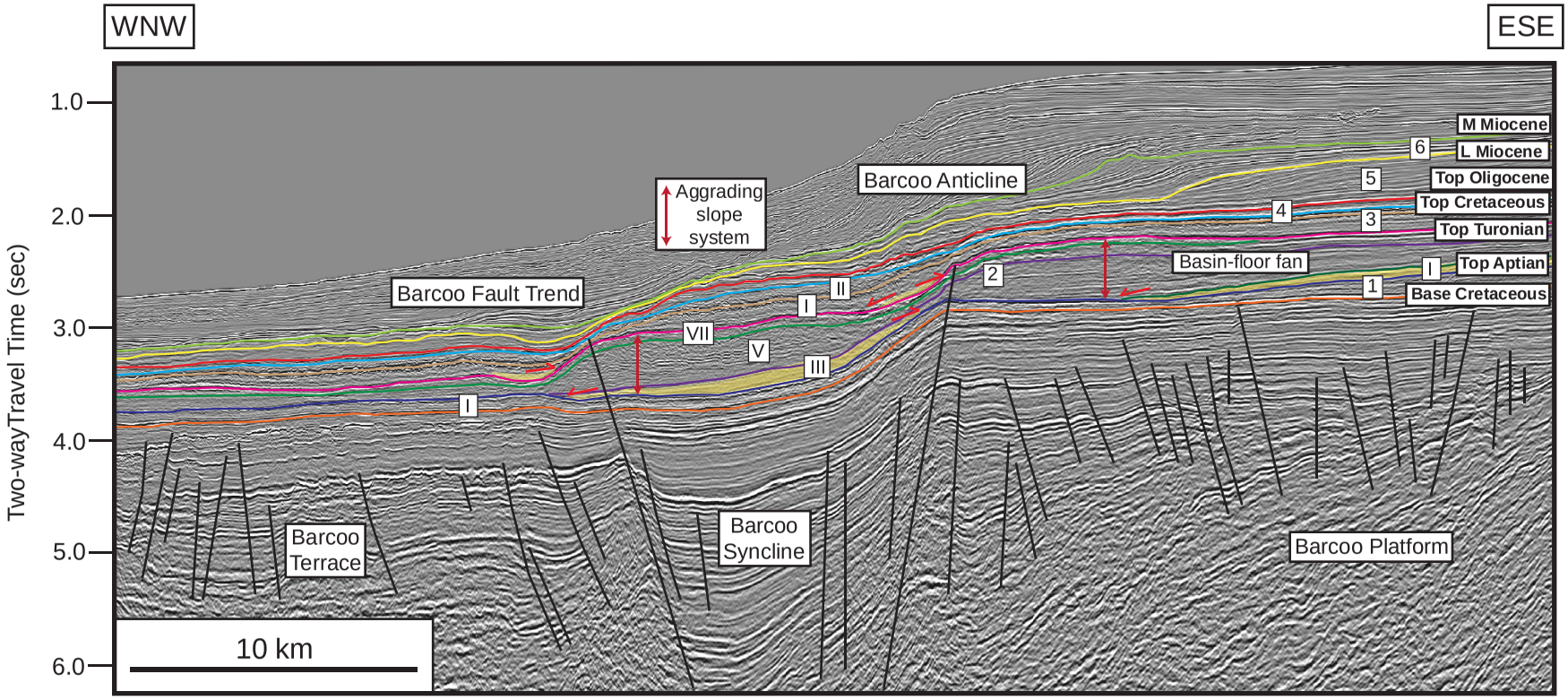

Figure 8b. Regional dip-oriented seismic profile showing all interpreted sequence boundaries from base Cretaceous to middle Miocene. The major graben structure of the Barcoo Syncline was overlain by the Upper Jurassic and younger strata. The external wedges of low angle clinoform indicate a balance between the rates of subsudence and sediment supply. The deepwater deposits are observed in Megasequences 2 and 3 (yellow shades). Moreover, Mega-sequence 2 shows the aggrading slope system whereas the distinct pragrading clinoforms are observed in Megasequences 5 and 6. Location of the profile is shown in Figure 7.

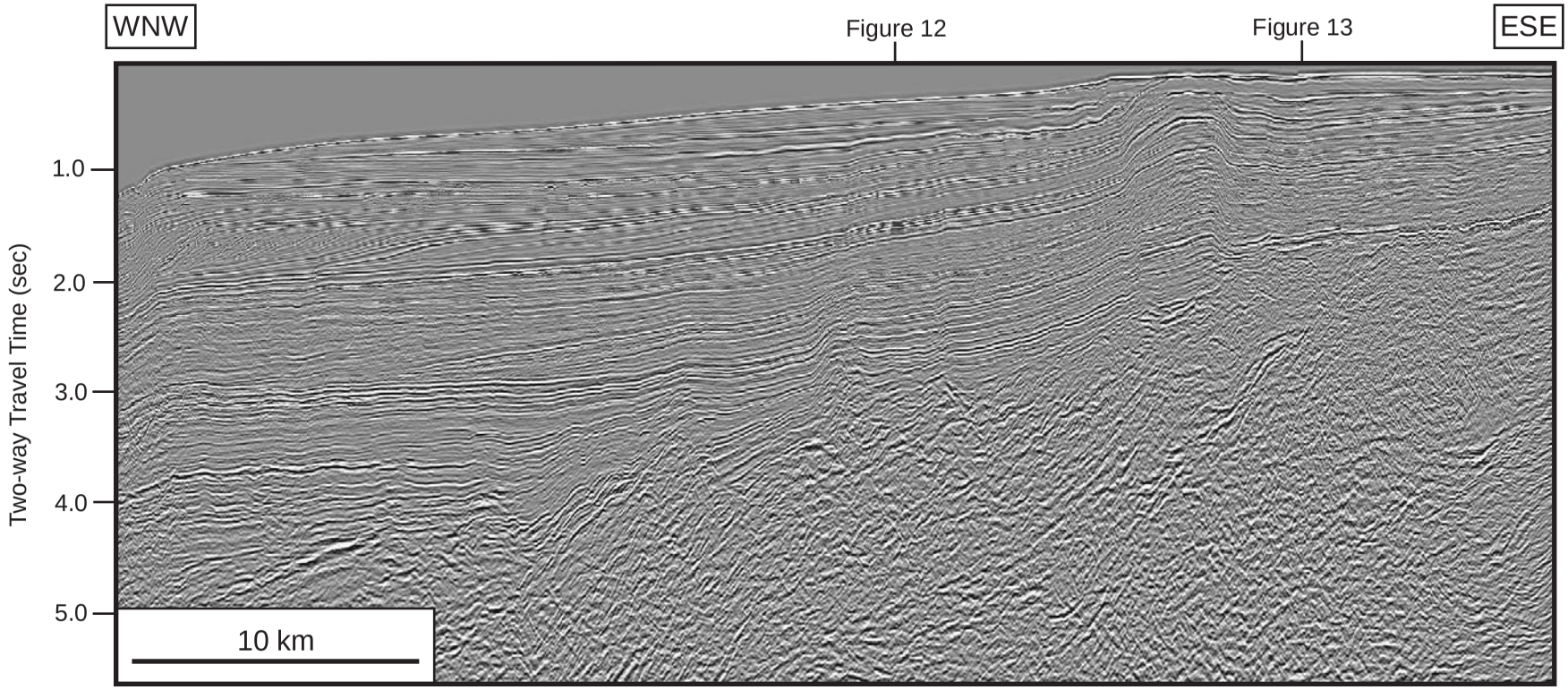

Figure 9a. Uninterpreted regional dip-oriented seismic profile (br-98:br98-010). Location of the profile is shown in Figure 7 and locations of where Figures 12, 13 cross the profile.

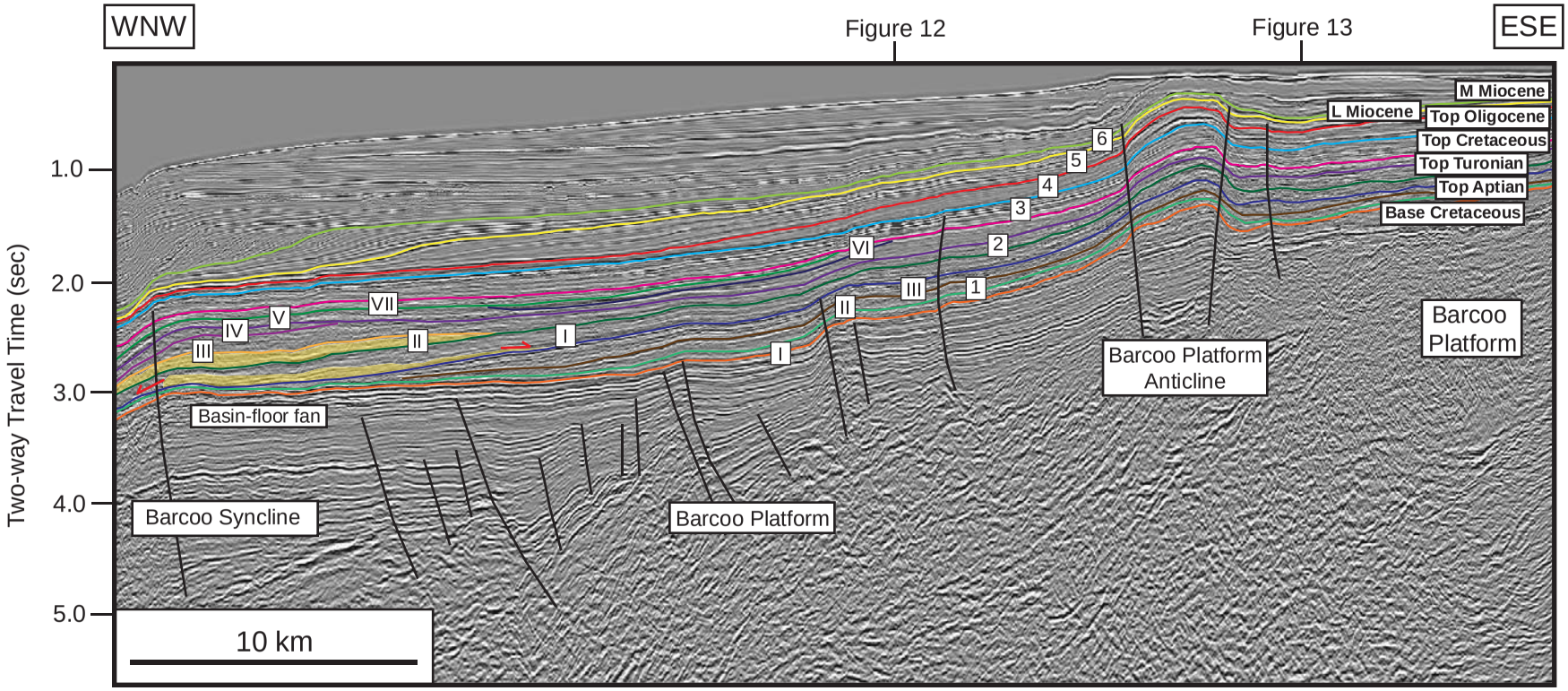

Figure 9b. Regional dip-oriented seismic profile showing all interpreted sequence boundaries from base Cretaceous to middle Miocene. The Barcoo Anticline and small faults of Barcoo fault system in the underlying Jurassic strata are observed. The Barcoo Platform anticline, which formed at the eastern margin of the Barcoo Sub-basin next to the Leveque Shelf, is associated with the fault reactivation during the late Miocene. The prograding wedge in Megasequence 1 is the basinal wedge of strata onlap onto the top Aptian sequence boundary (yellow shade). The basin-floor fan is recognized in Megasequence 2. whereas Megasequence 6 shows the distinct prograding clinoform. Location of the profile is shown in Figure 7 and locations of where Figures 12, 13 cross the profile.

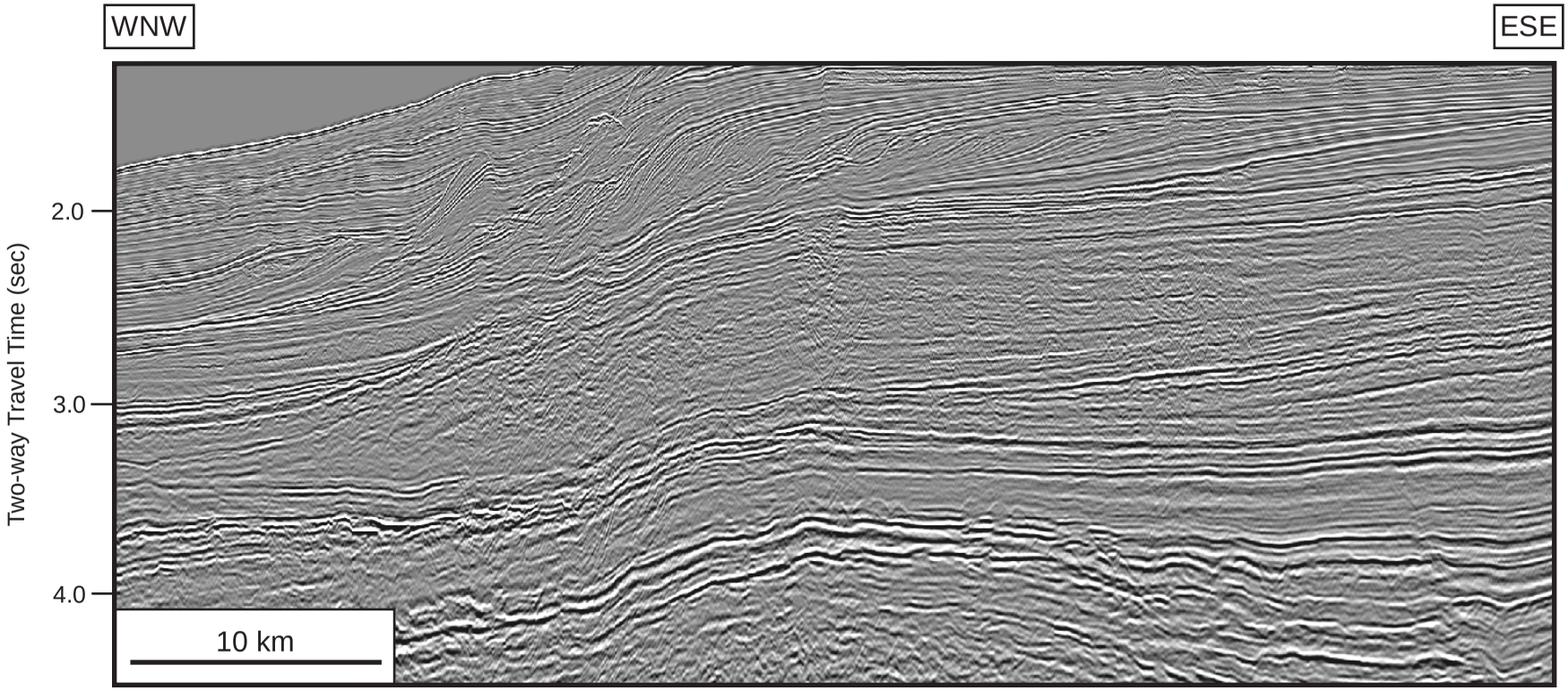

Figure 10a. Uninterpreted regional dip-oriented seismic profile (br-98:br98-019). Location of the profile is shown in Figure 7.

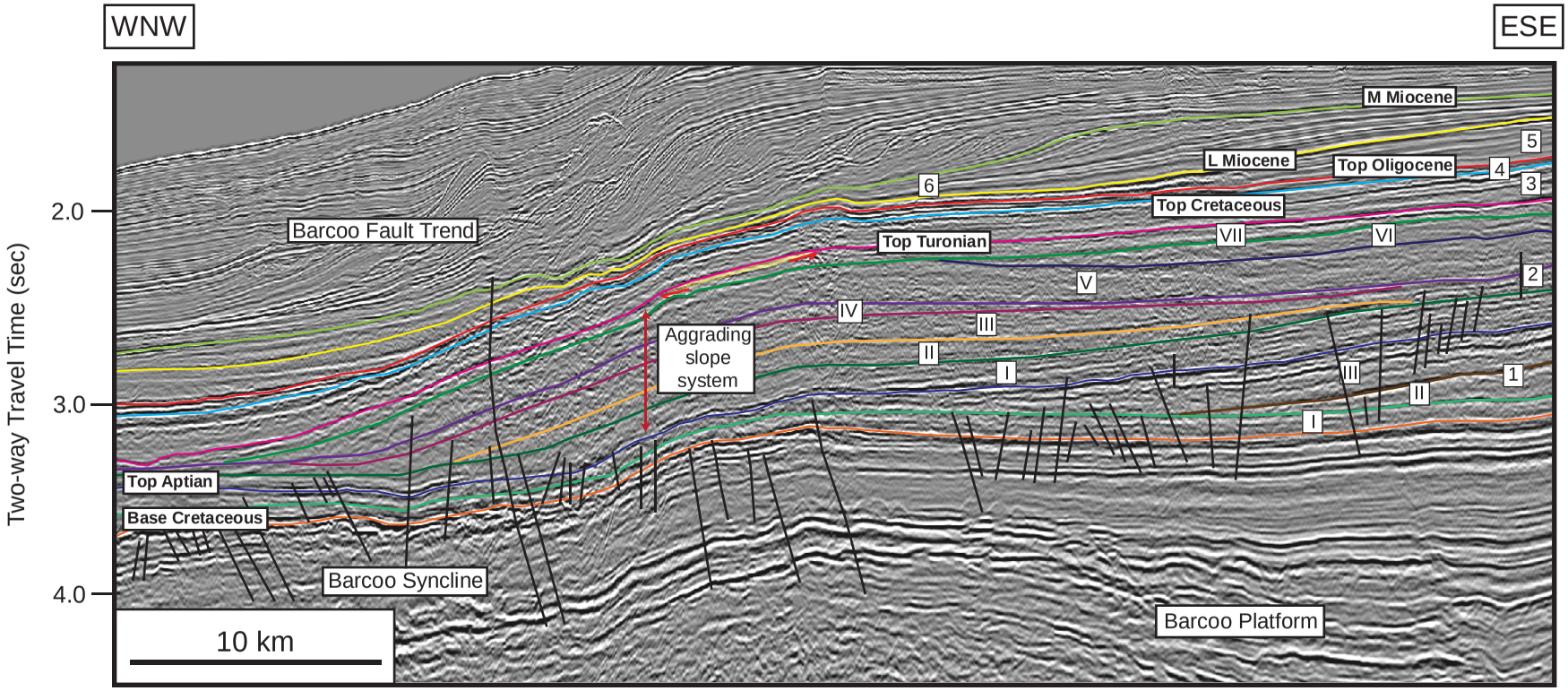

Figure 10b. Regional dip-oriented seismic profile showing all interpreted sequence boundaries from base Cretaceous to middle Miocene. Megasequence 1 consists at less three sequences whereas Megasequence 2 consists at less seven sequences. Sediment wedges and deepwater deposits are recognized (yellow shades). Megasequence 2 illustrates the aggrading slope system whereas Megasequence 6 show the distinct progradaing clinoform. Location of the profile is shown in Figure 7.

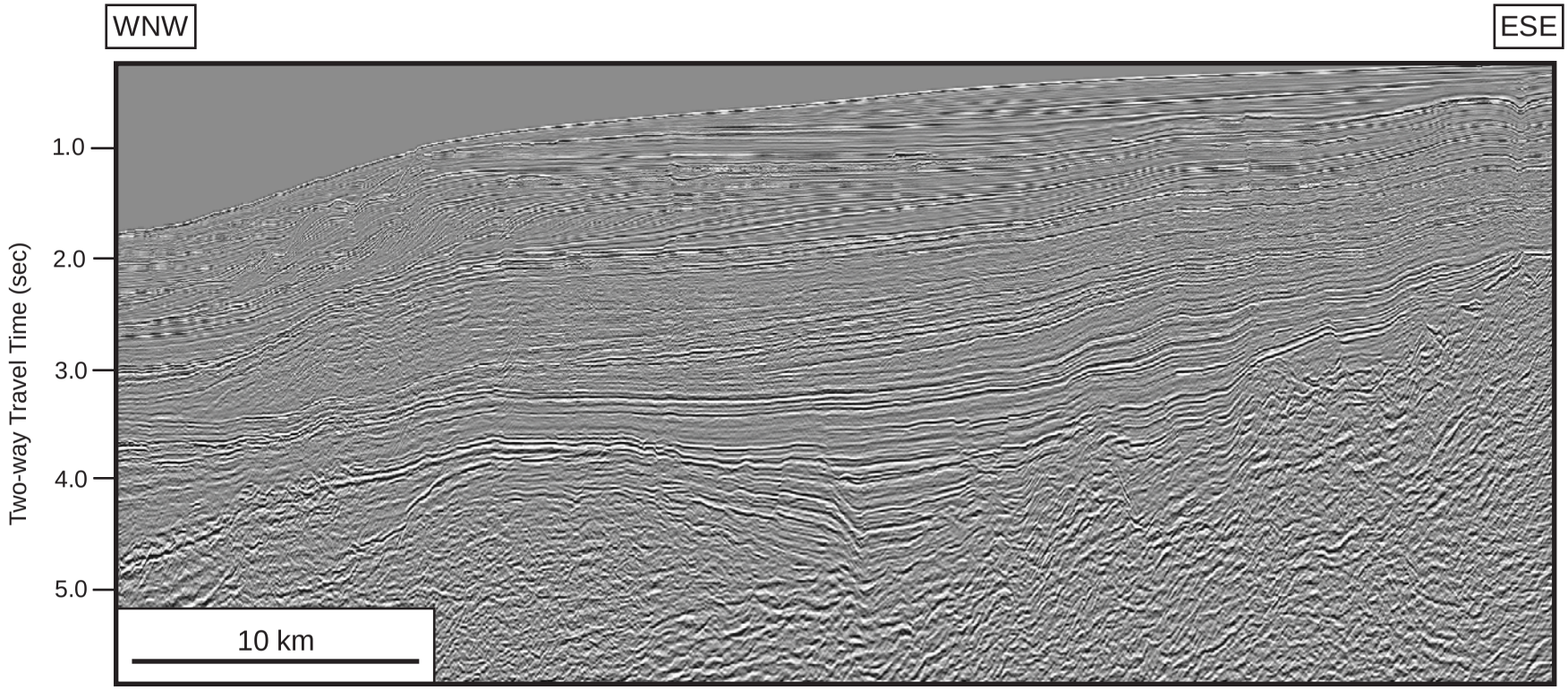

Figure 11a. Uninterpreted regional dip-oriented seismic profile (br-98:br98-020). Location of the profile is shown in Figure 7 and location of where Figure 12 crosses the profile.

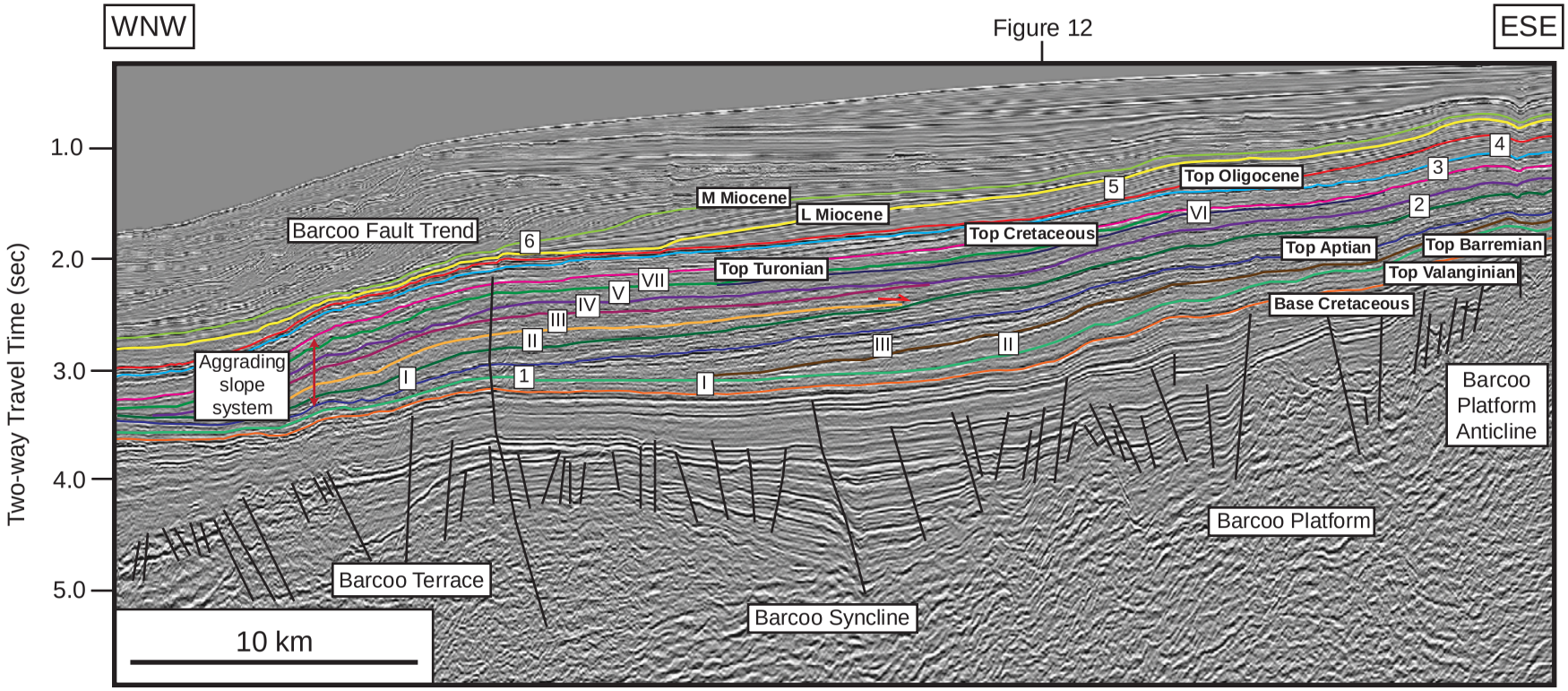

Figure 11b. Regional dip-oriented seismic profile showing all interpreted sequence boundaries from base Cretaceous to middle Miocene. Series of small faults are displayed in the underlying Jurassic strata which caused the irregular surface. The Barcoo Platform Anticline is observed at the eastern part of the profile. The low angle clinoform consists the sediment wedge (yellow shade) which is illustrated in Megasequence 1. Additionally, the aggrading slope system is demonstrated in Megasequence 2. Megasequences 5 and 6 display the distinct prograding clinoform. Location of the profile is shown in Figure 7 and location of where Figure 12 crosses the profile.

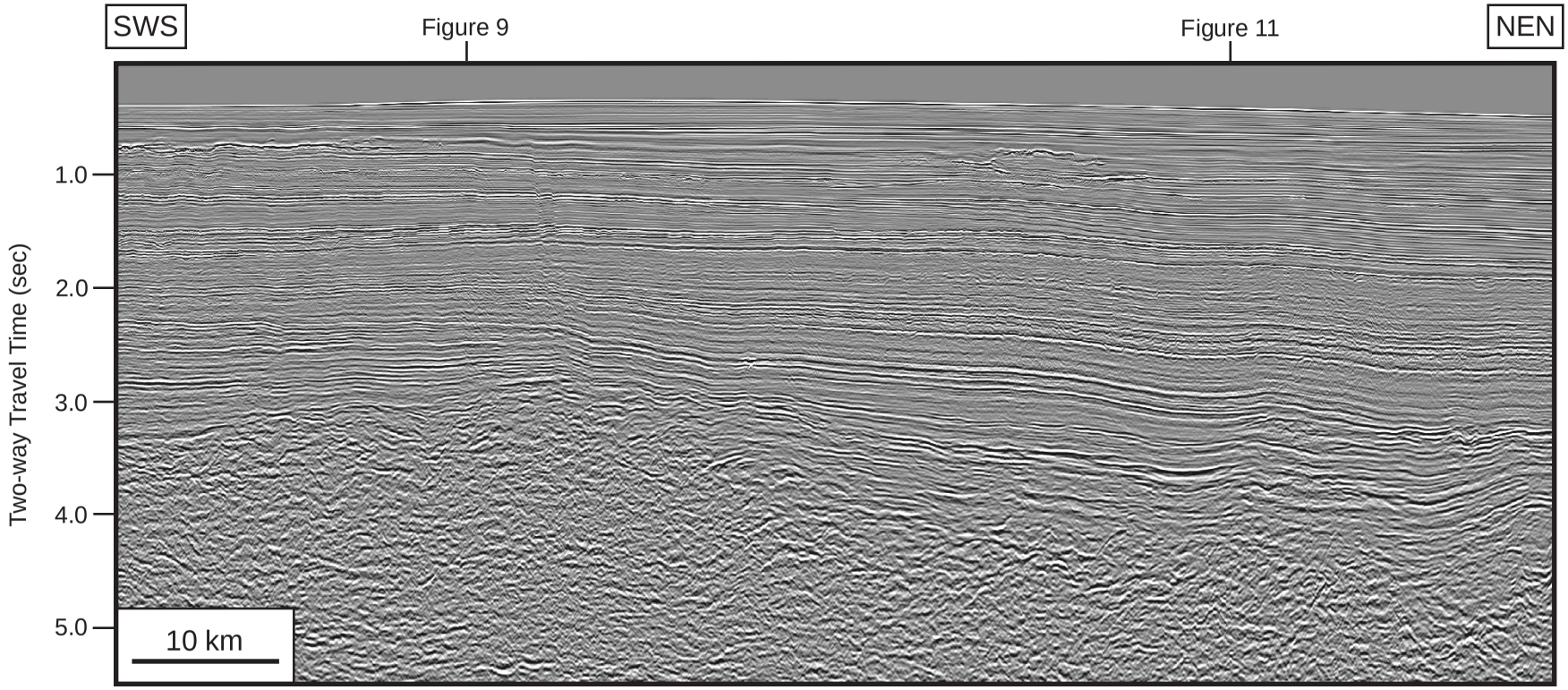

Figure 12a. Uninterpreted regional strike-oriented seismic profile (br-98:br98-071). Location of the profile is shown in Figure 7 and locations of where Figures 9, 11 cross the profile.

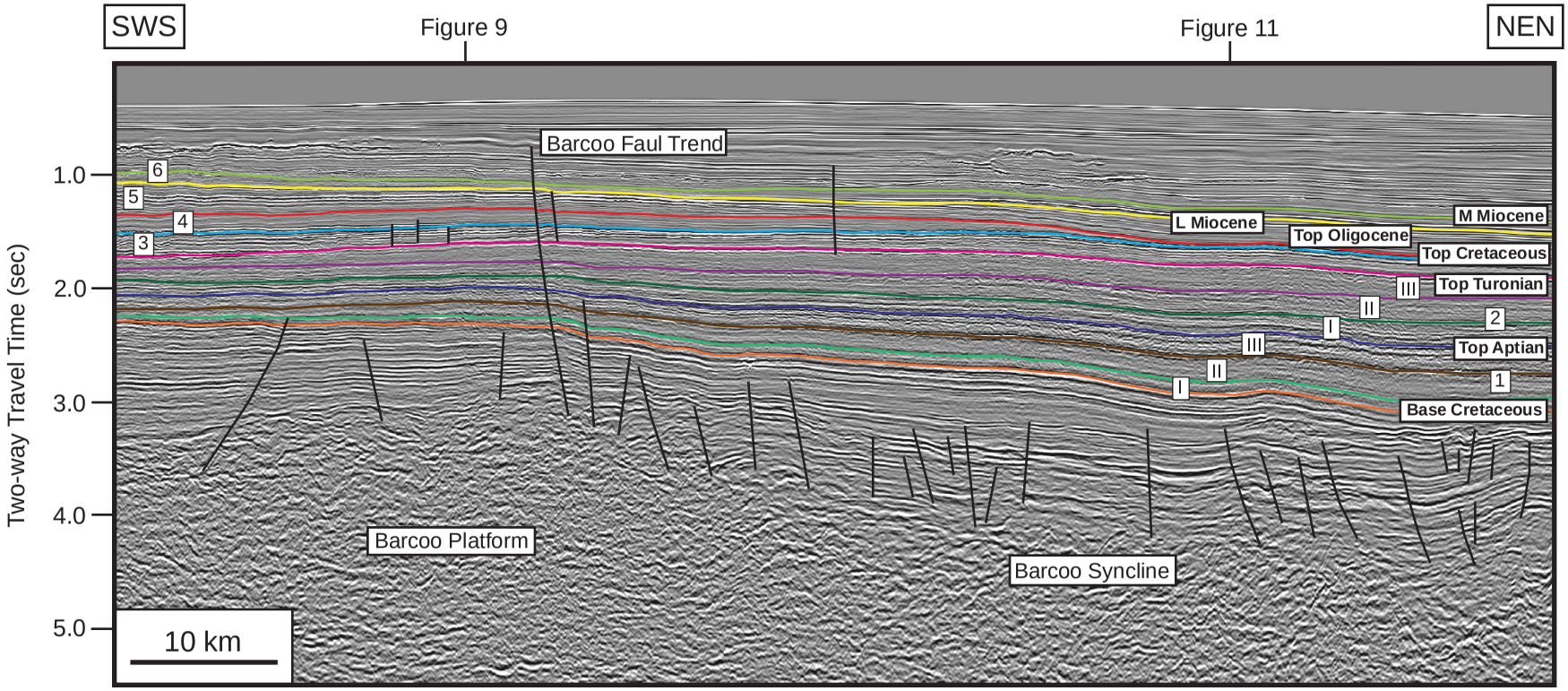

Figure 12b. Regional strike-oriented seismic profile showing all interpreted sequence boundaries from base Cretaceous to middle Miocene. Barcoo fault system cut the underlying Jurassic strata, but does not cut the basal sequence boundary. The pre-existing faulted topography illustrated. Megasequences 1 and 2 demonstrate the clinoform morphology. Location of the profile is shown in Figure 7 and locations of where Figures 9, 11 cross the profile.

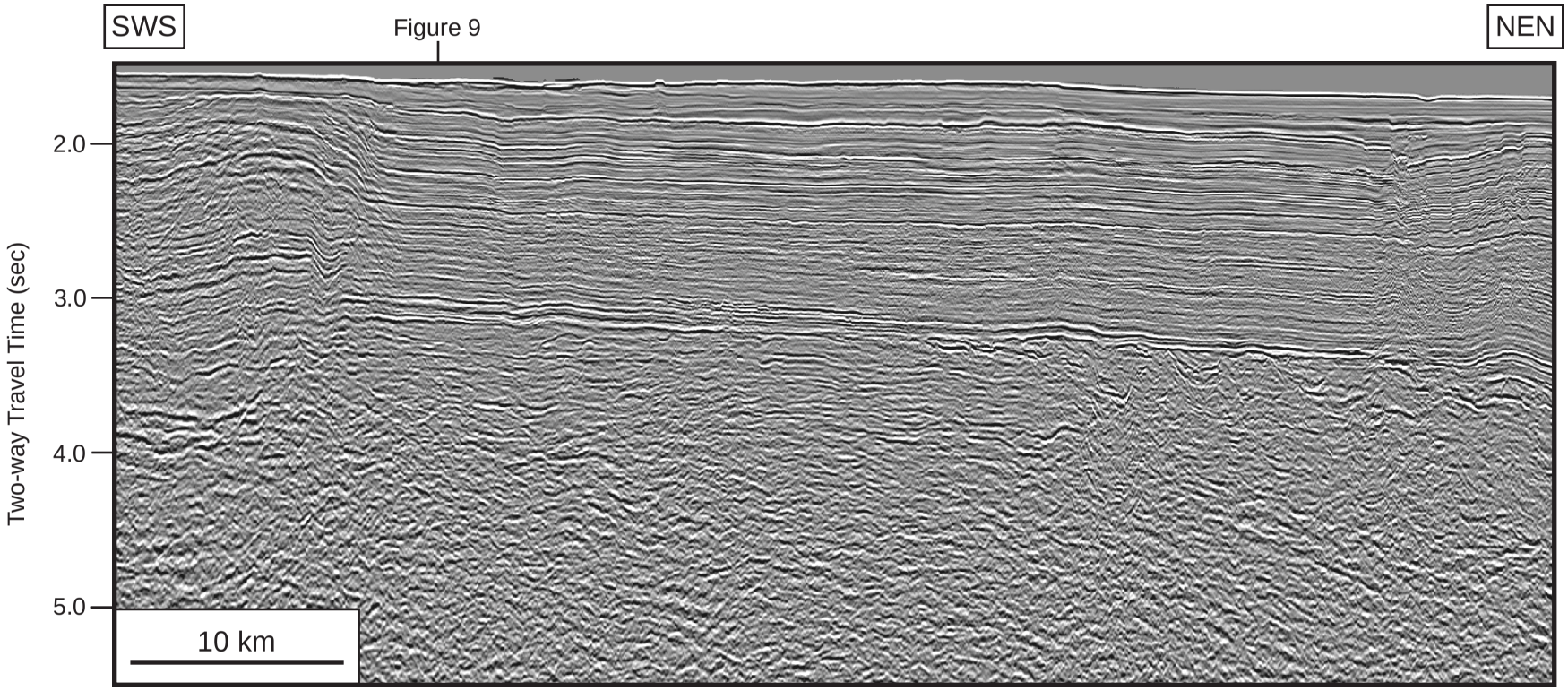

Figure 13a. Uninterpreted regional strike-oriented seismic profile (br-98:br98-065). Location of the profile is shown in Figure 7 and location of where Figure 9 crosses the profile.

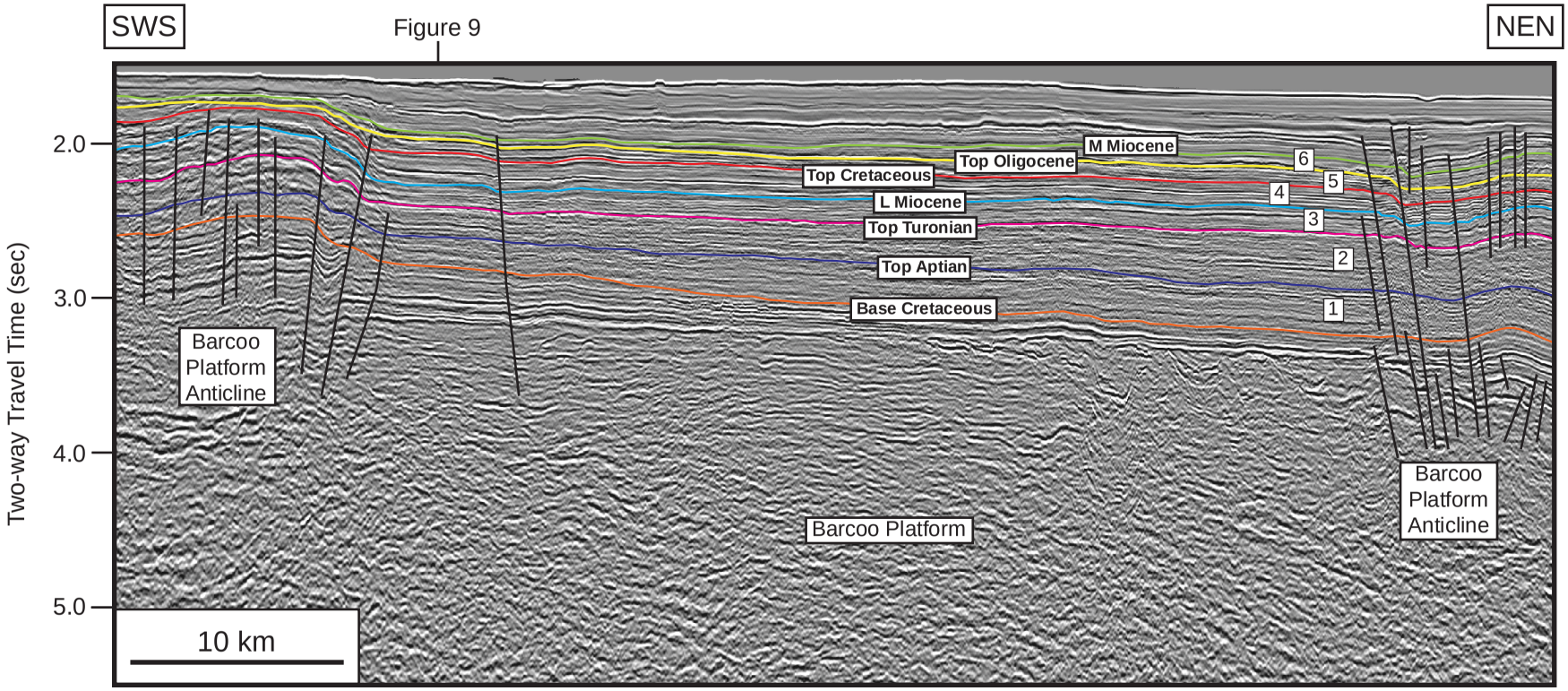

Figure 13b. Regional strike-oriented seismic profile showing all interpreted sequence boundaries from base Cretaceous to middle Miocene. This profile is parallel and cut through the Barcoo Platform Anticline axis at the southern and northern portions. Megasequences 1 and 2 illustrate the low angle prograding clinoform. The seismic reflection of the Barcoo Platform displays the conformable parallel to subparallel seismic reflections. Location of the profile is shown in Figure 7 and location of where Figure 9 crosses the profile.

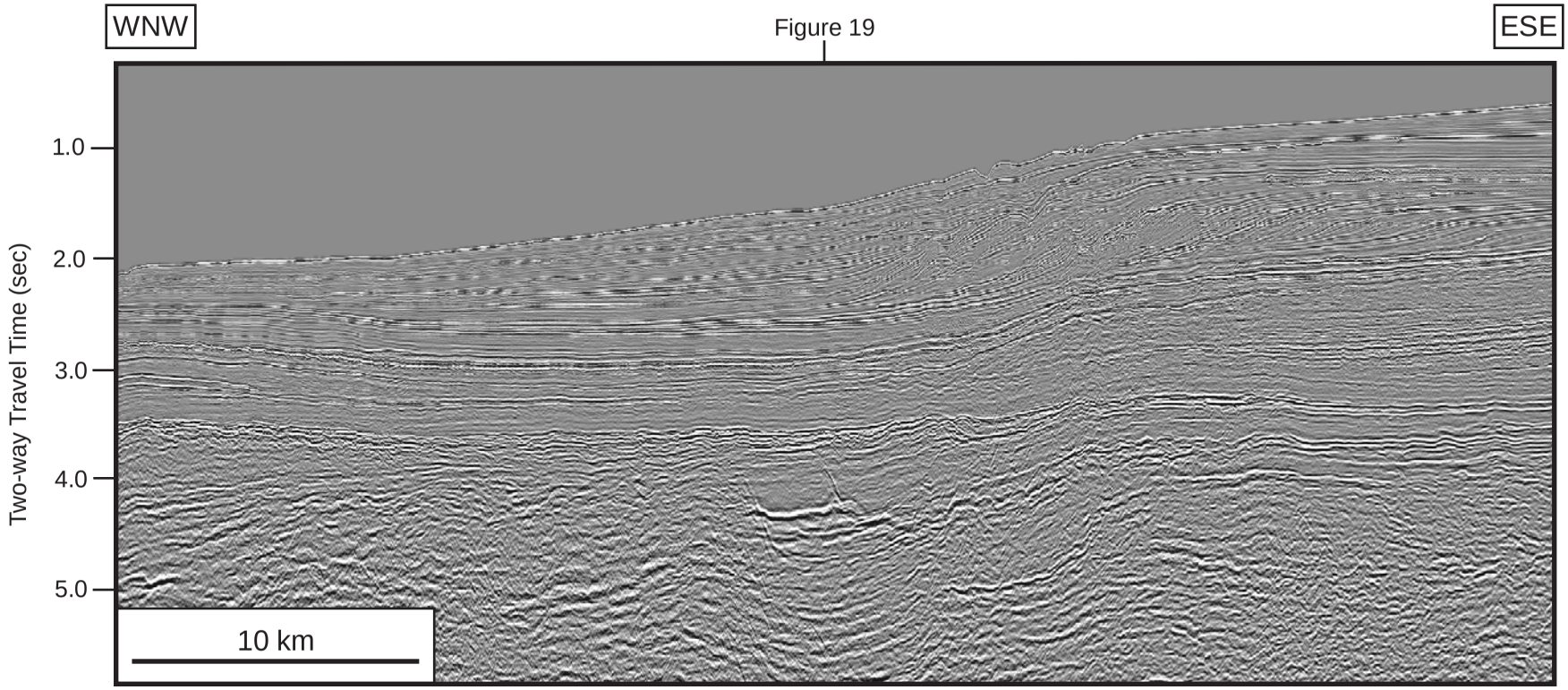

Figure 14a. Uninterpreted regional dip-oriented seismic profile (br-98:br98-025a). Location of the profile is shown in Figure 7 and location of where Figure 19 crosses the profile.

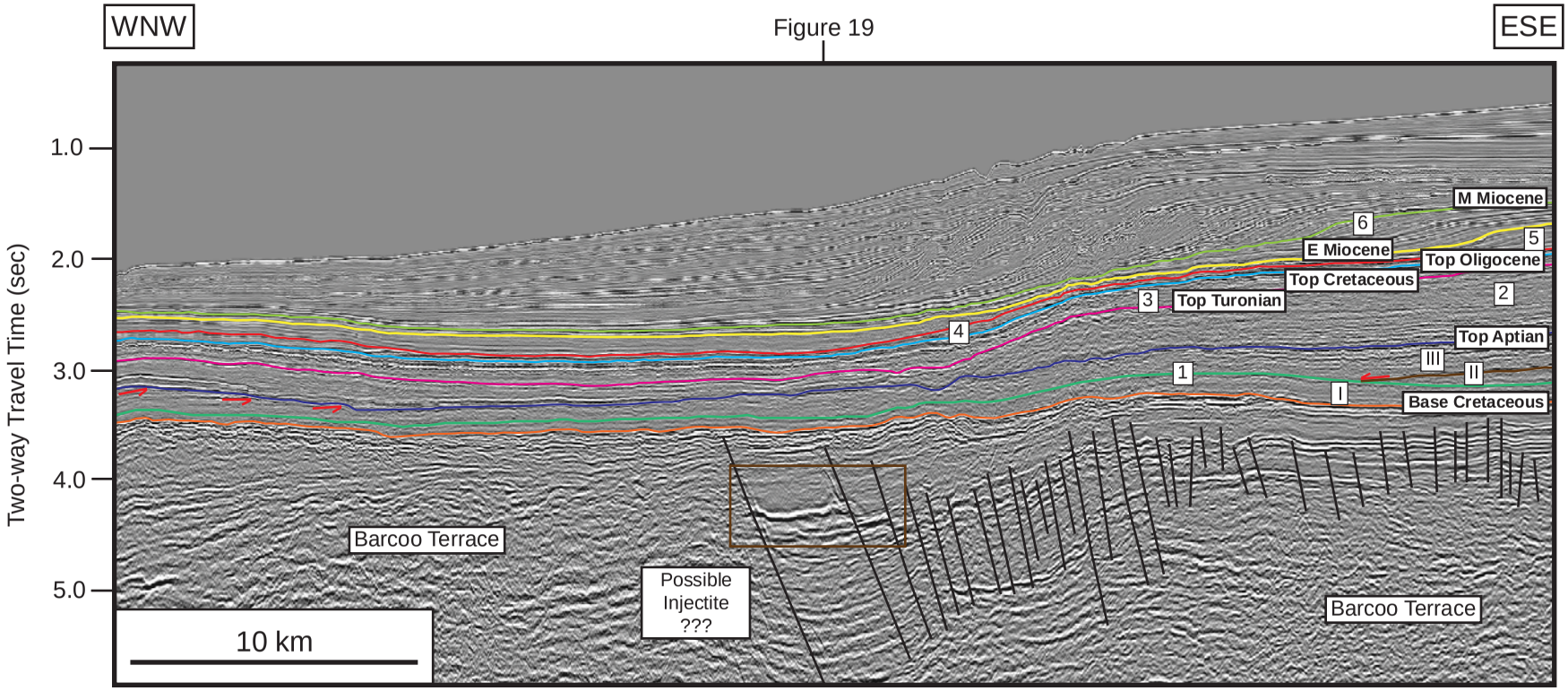

Figure 14b. Regional dip-oriented seismic profile showing all interpreted sequence boundaries from base Cretaceous to middle Miocene. Megasequence 1 consists three depositional sequences (I, II, and III). Megasequences 1, 2, 3 and 4 show the low angle clinoforms which indicate a balance between the rates of subsidence and sediment supply. The type of clinoform and style of progradation is dissimilar to the younger sequences (Megasequences 5 and 6). The Barcoo Fault System and possible injectites are observed in the underlying Jurassic strata. Location of the profile is shown in Figure 7 and location of where Figure 19 crosses the profile.

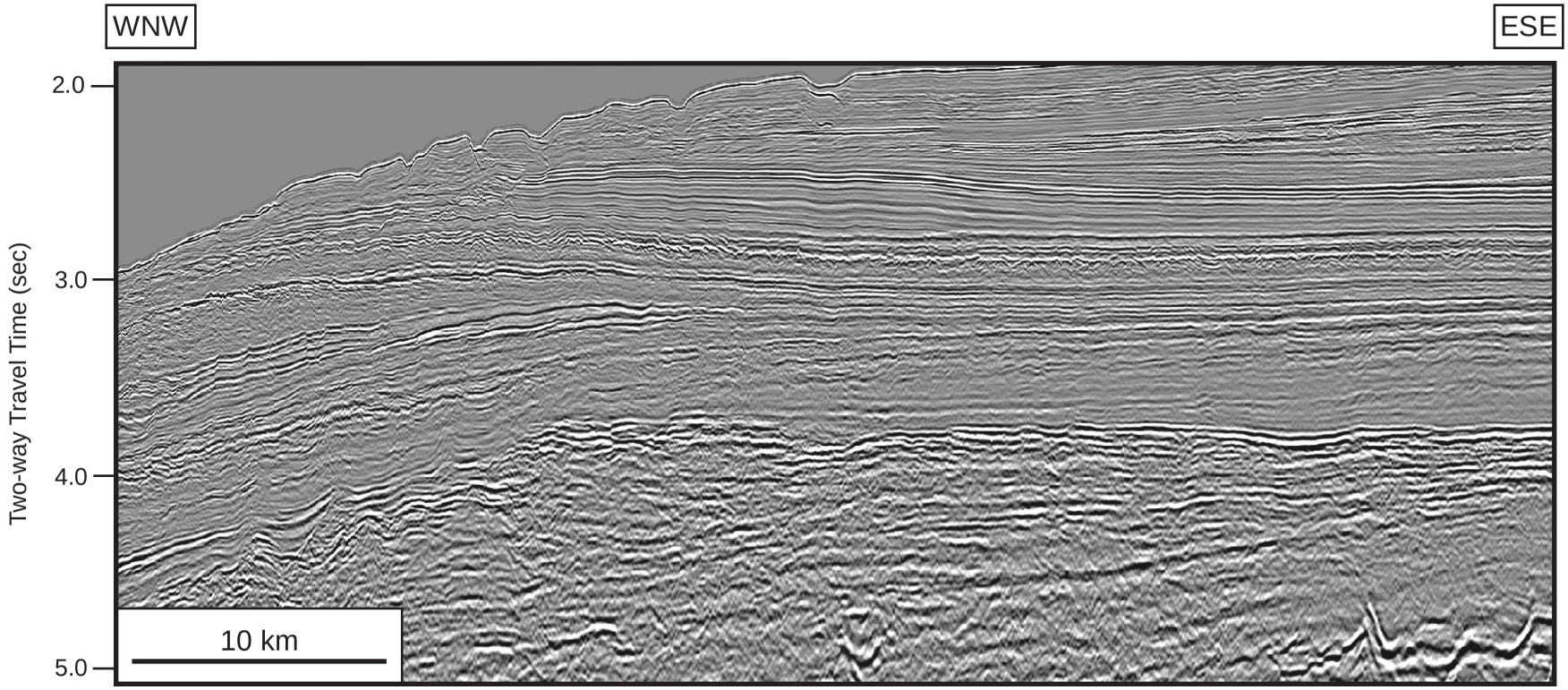

Figure 15a. Uninterpreted regional dip-oriented seismic profile (br-98:br98-029). Location of the profile is shown in Figure 7.

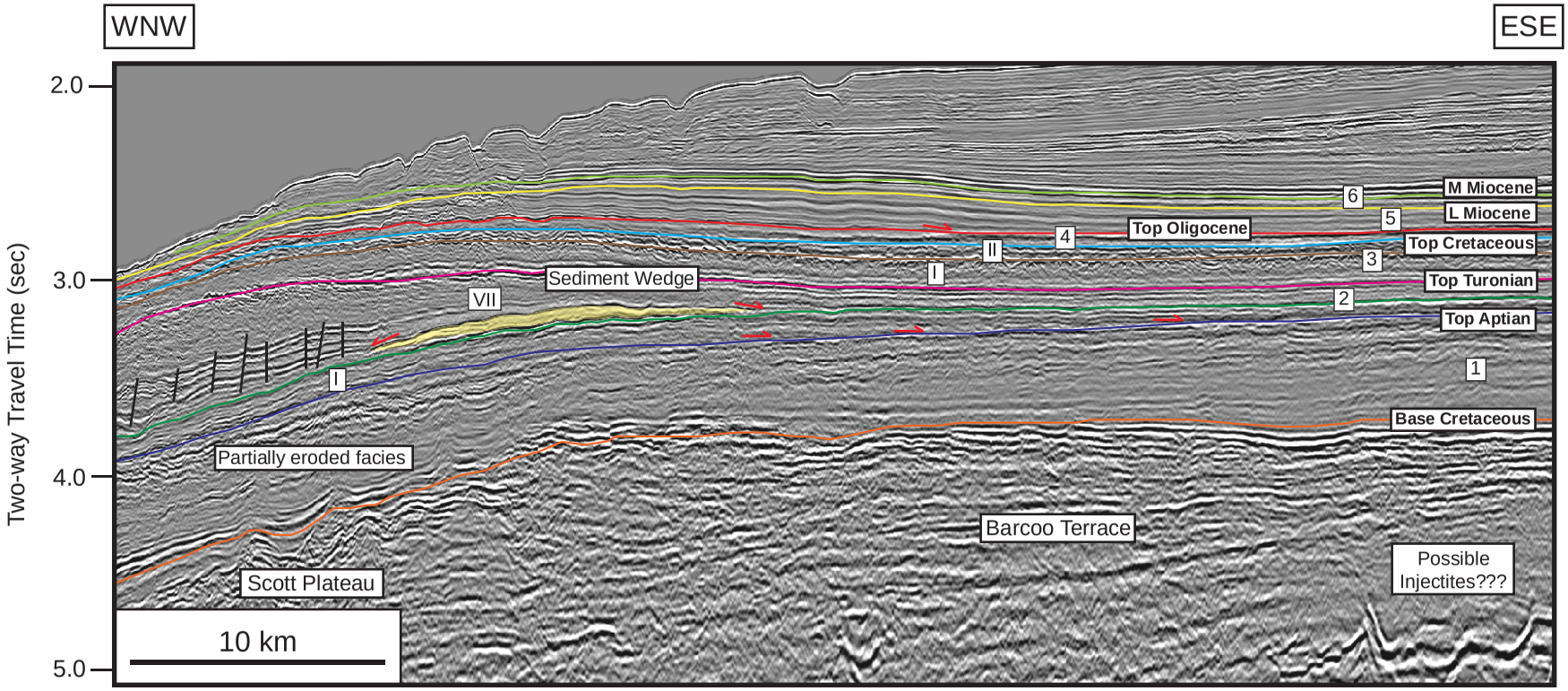

Figure 15b. Regional dip-oriented seismic profile showing all interpreted sequence boundaries from base Cretaceous to middle Miocene. The downlap truncations are identified in order to define the sequence boundaries. The sediment wedge, which is observed in Subsequence VII of Megasequence 2 (yellow shade). It is considered to be the potential petroleum play. Location of the profile is shown in Figures 7.

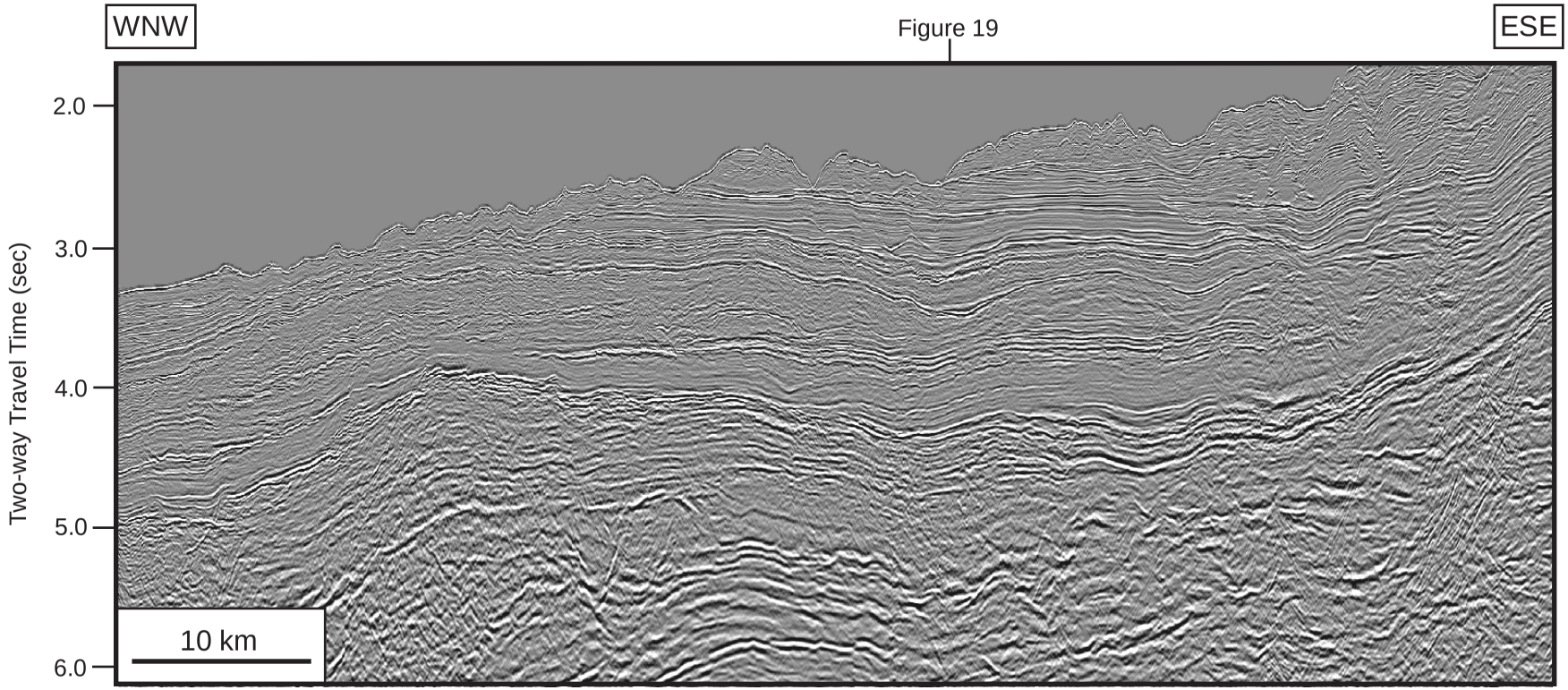

Figure 16a. Uninterpreted regional dip-oriented seismic profile (br-98:br98-035). Location of the profile is shown in Figure 7 and location of where Figure 19 crosses the profile.

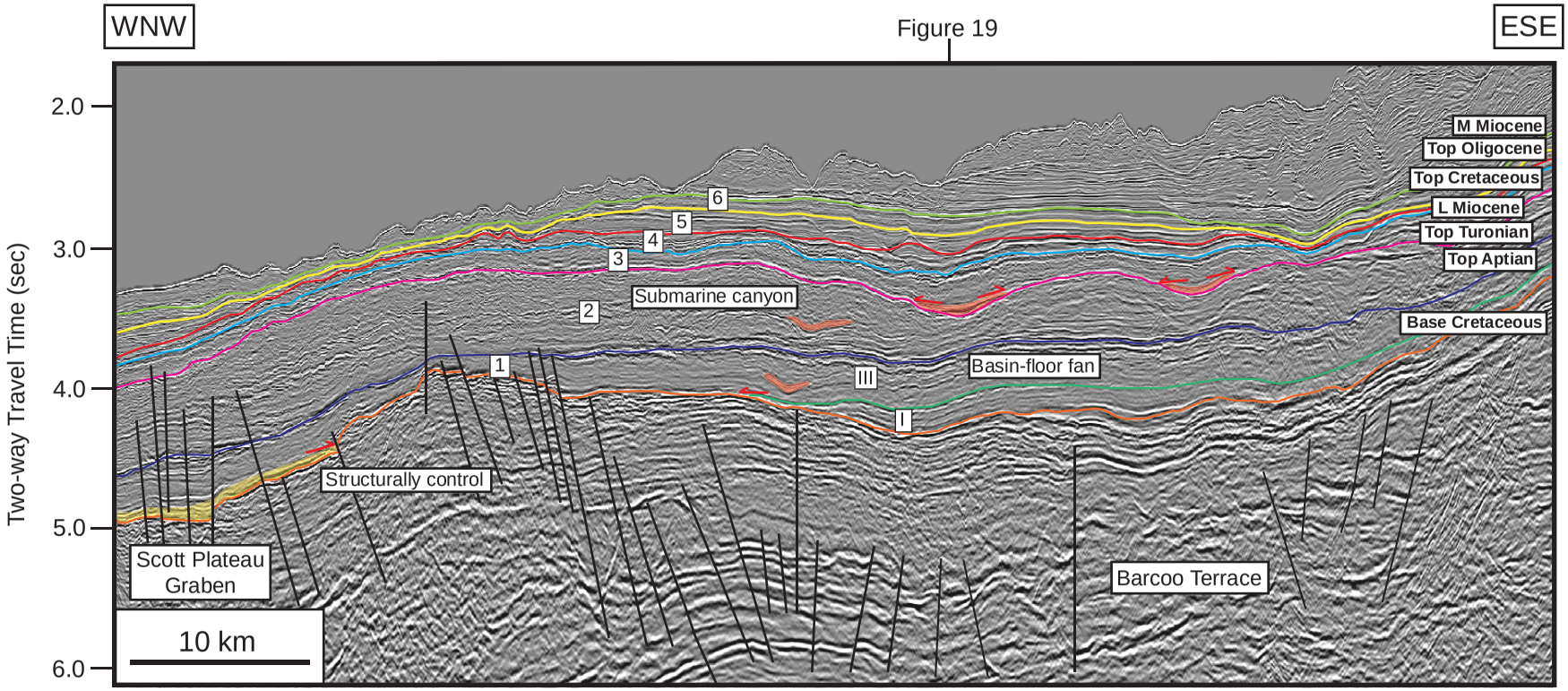

Figure 16b. Regional dip-oriented seismic profile showing all interpreted sequence boundaries from base Cretaceous to middle Miocene. This profile shows the deeper area of the Scott Plateau and the shallower area of the Barcoo Terrace. The basin-floor fan is observed within the low angle clinoform of Megasequence 1 (yellow shade). Distinct submarine canyons are present in gently dipping clinoforms of Megasequences 1, 2 and 3 (red shades). Location of the profile is shown in Figure 7 and location of where Figure 19 crosses the profile.

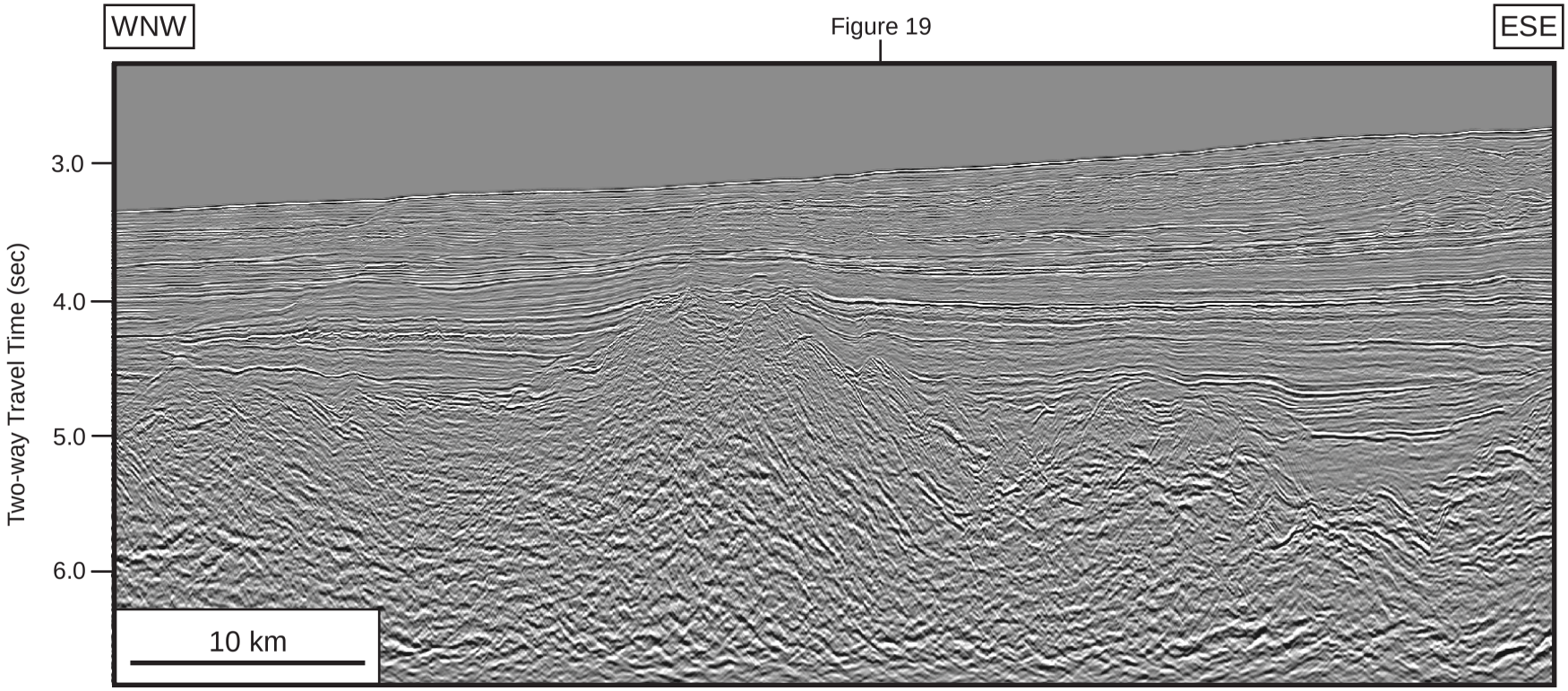

Figure 17a. Uninterpreted regional dip-oriented seismic profile (br-98:br98-048). Location of the profile is shown in Figure 7 and location of where Figure 19 crosses the profile.

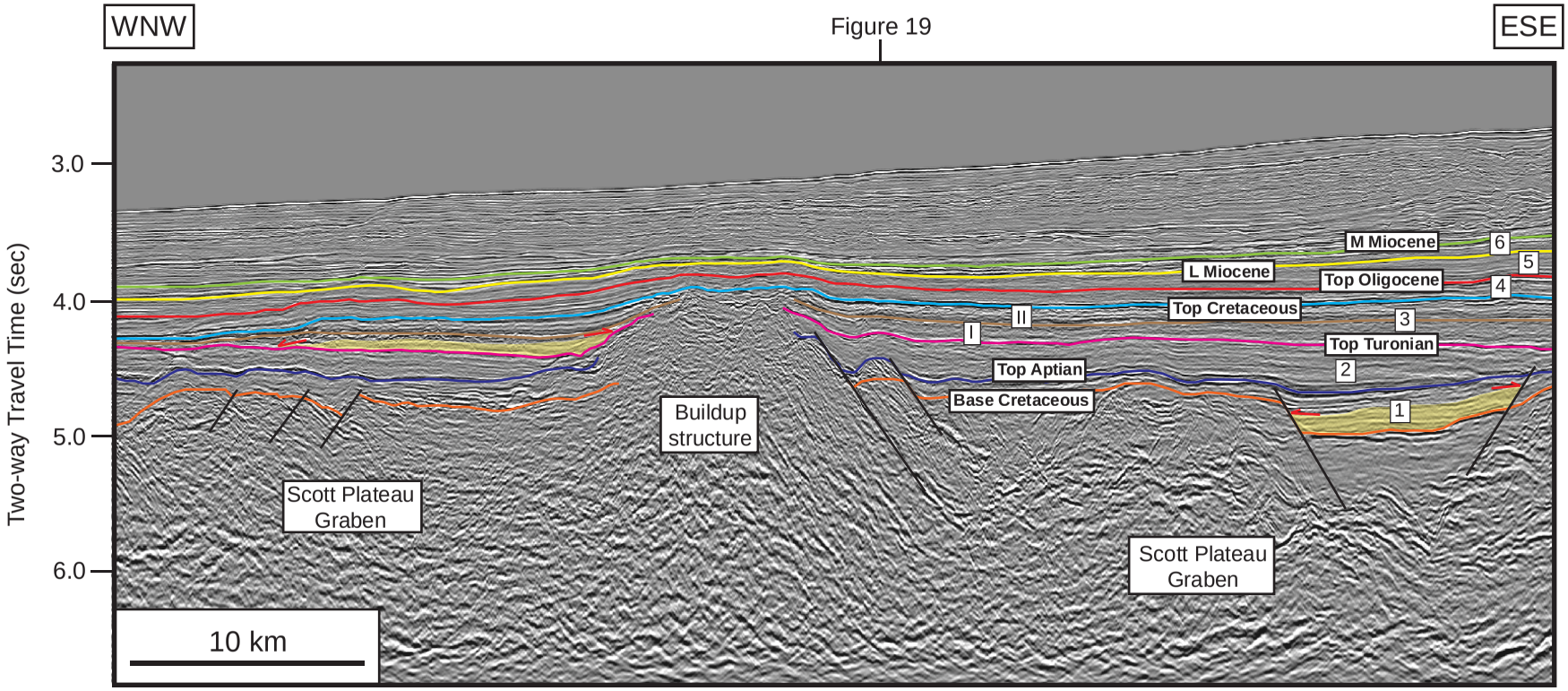

Figure 17b. Regional dip-oriented seismic profile showing all interpreted sequence boundaries from base Cretaceous to middle Miocene. Megasequence 1 shows the potential play which is recognized from the onlap reflection termination onto the bounding faults (orange shade) at the eastern part of the profile. The carbonate buildup which is located in the Scott Plateau Graben is observed. It created the accommodation for sediment to deposit as shown in Megasequence 3 (yellow shade). The block faulting in the underlying Jurassic strata caused the irregular topography. Location of the profile is shown in Figure 7 and location of where Figure 19 crosses the profile.

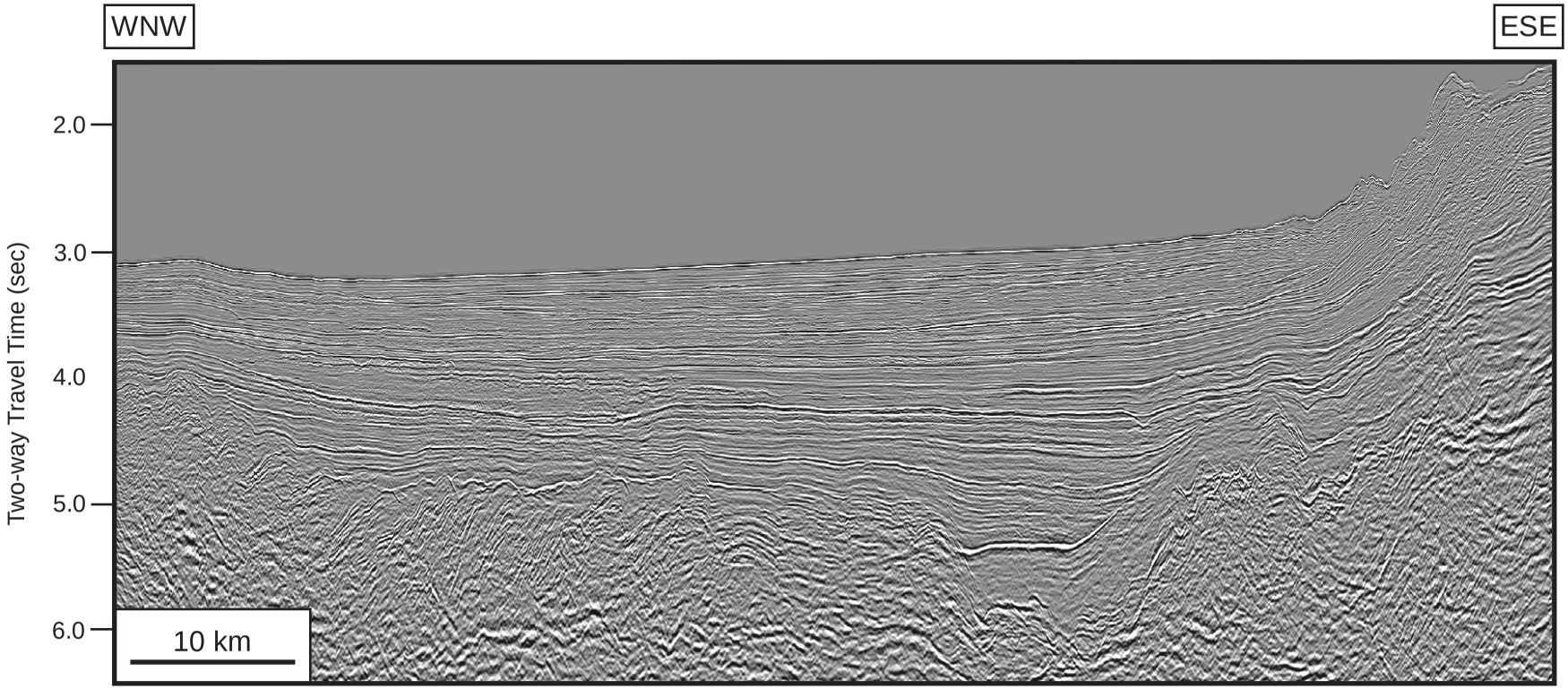

Figure 18a. Uninterpreted regional dip-oriented seismic profile (br-98:br98-057). Location of the profile is shown in Figure 7.

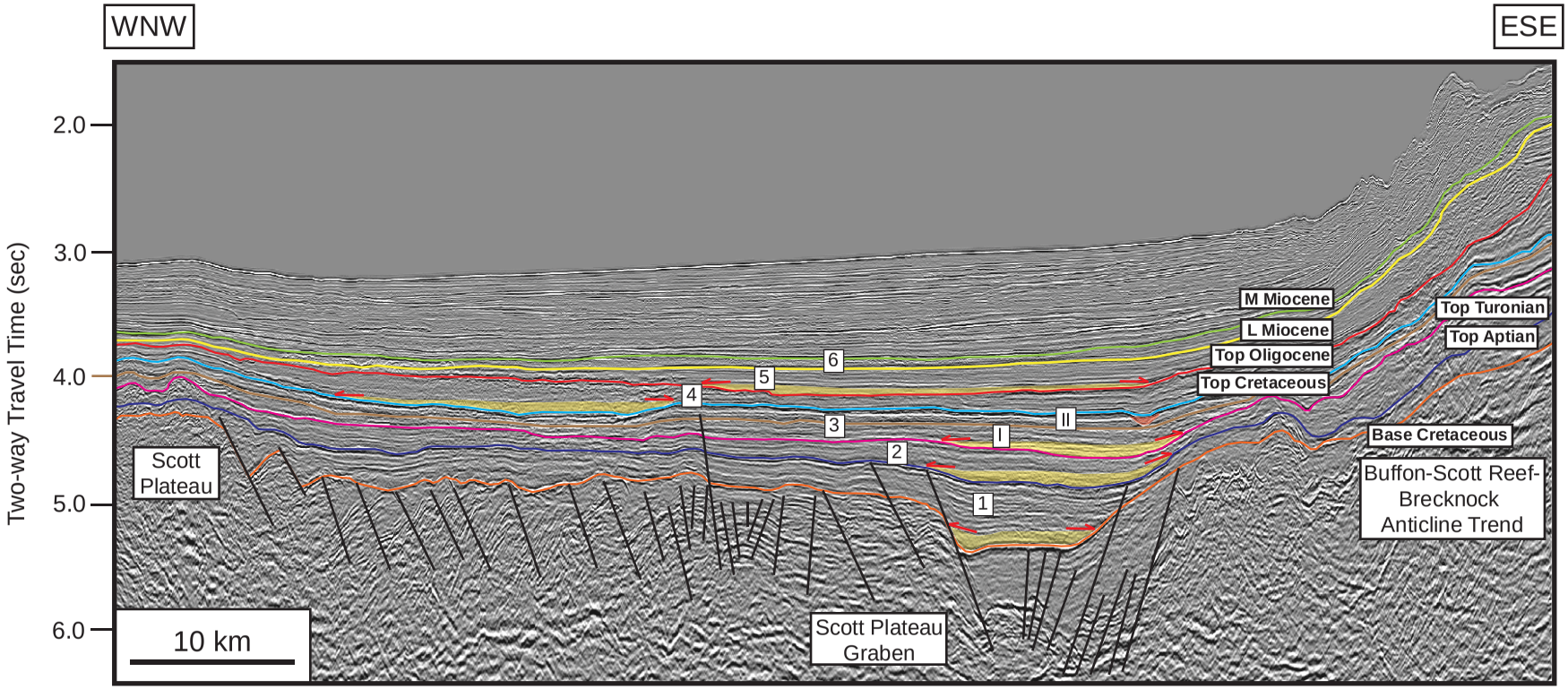

Figure 18b. Regional dip-oriented seismic profile showing all interpreted sequence boundaries from base Cretaceous to middle Miocene. This profile shows the deeper area of the Scott Plateau Graben and shallower area of the Buffon-Scott Reef-Brecknock Anticline Trend in the northern part of the study area. Series of faults in the underlying Jurassic strata caused the irregular topography. Megasequence 1 were structurally confined by faults as shown by the onlap reflection termination (orange shade) at the eastern part of the profile. The sediment wedges are observed in Megasequences 2, 3, 4 and 5 (yellow shades) whereas the submarine canyon is noticed in Megasequence 3 (red shade). Location of the profile is shown in Figure 7.

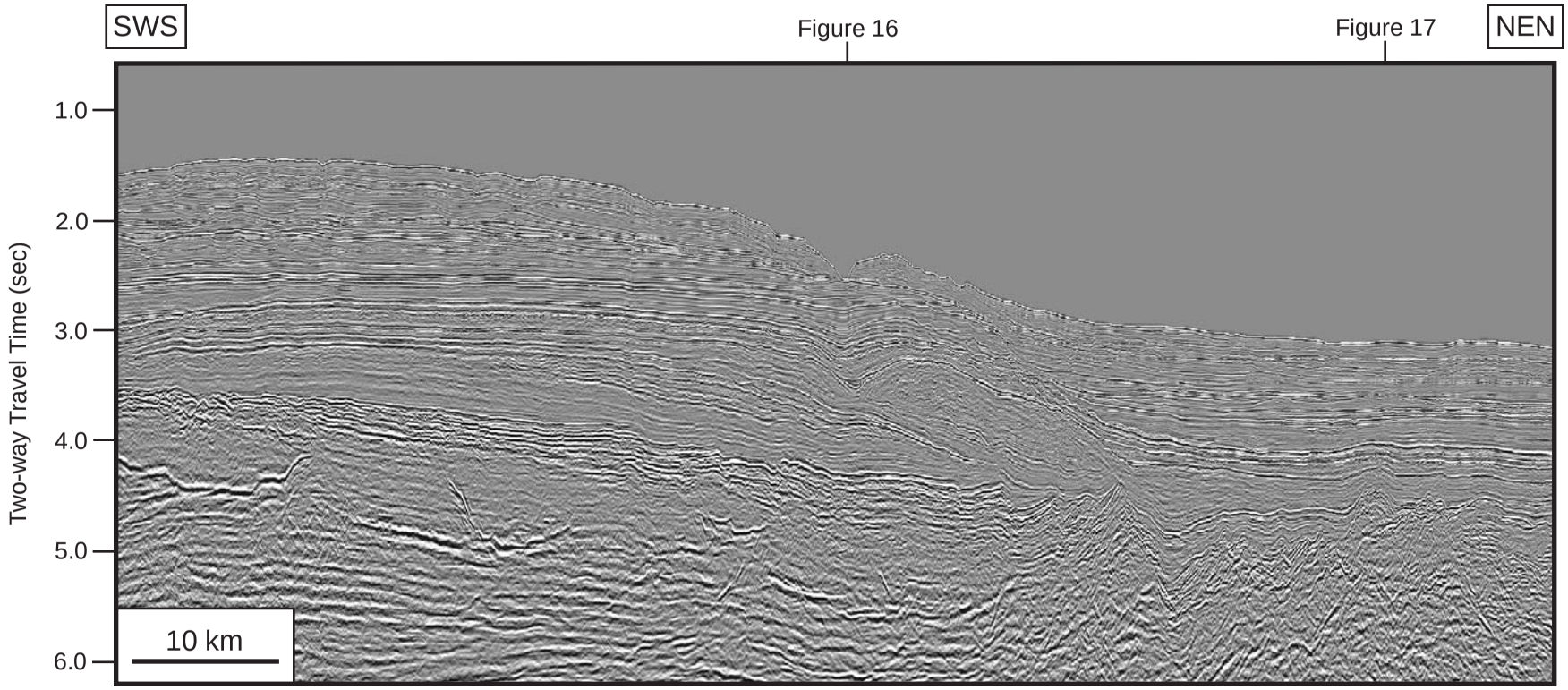

Figure 19a. Uninterpreted regional strike-oriented seismic profile (br-98:br98-082). Location of the profile is shown in Figure 7 and locations of where Figures 16 and 17 cross the profile.

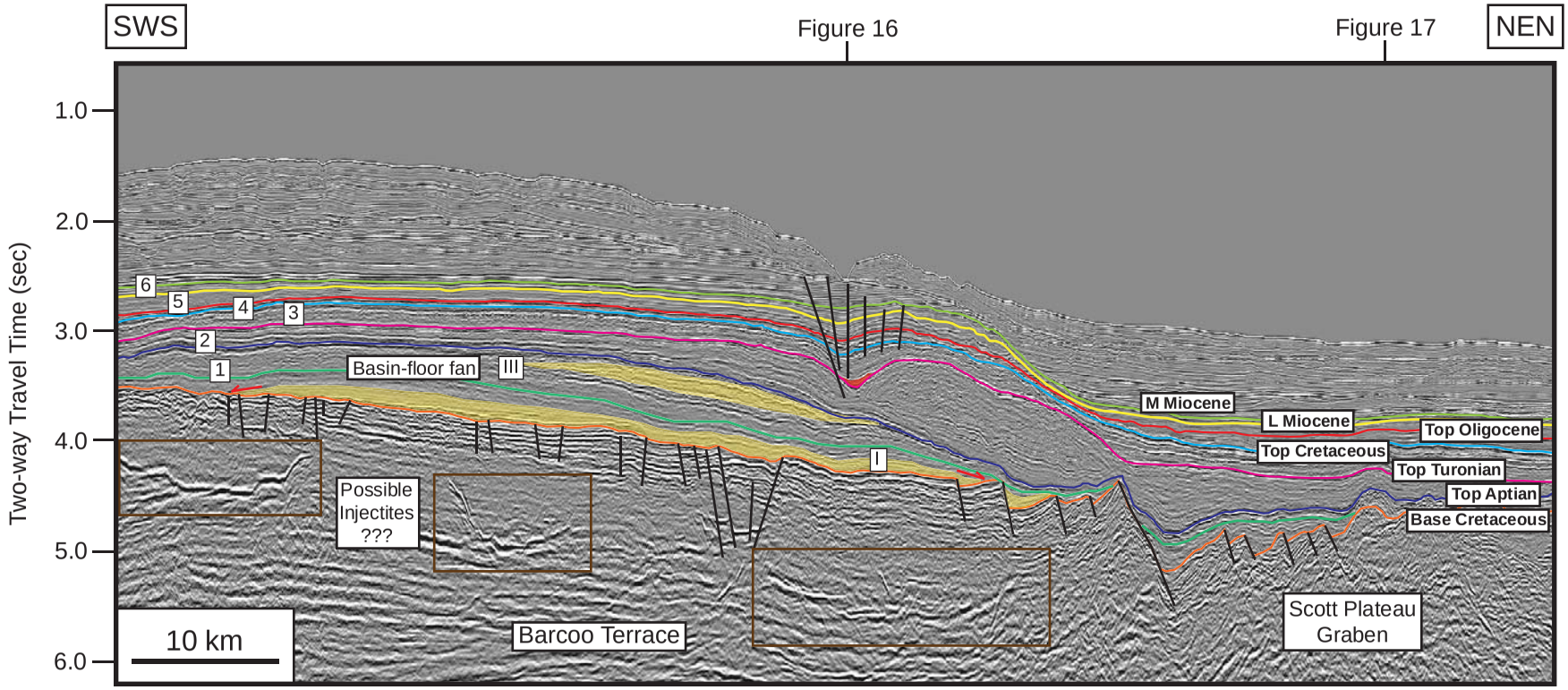

Figure 19b. Regional strike-oriented seismic profile showing all interpreted sequence boundaries from base Cretaceous to middle Miocene. The Barcoo Fault System and possible injectites are observed in the underlying Jurassic strata. The profile displays the shallower area of the Barcoo Terrace and deeper area of the Scott Plateau Graben. Several prograding wedge and basin-floor fan are observed in Megasequence 1 (red shade) whereas an submarine canyon is noticed in Megasequence 3 (red shade). Location of the profile is shown in Figure 7 and locations of where Figures 16 and 17 cross the profile.

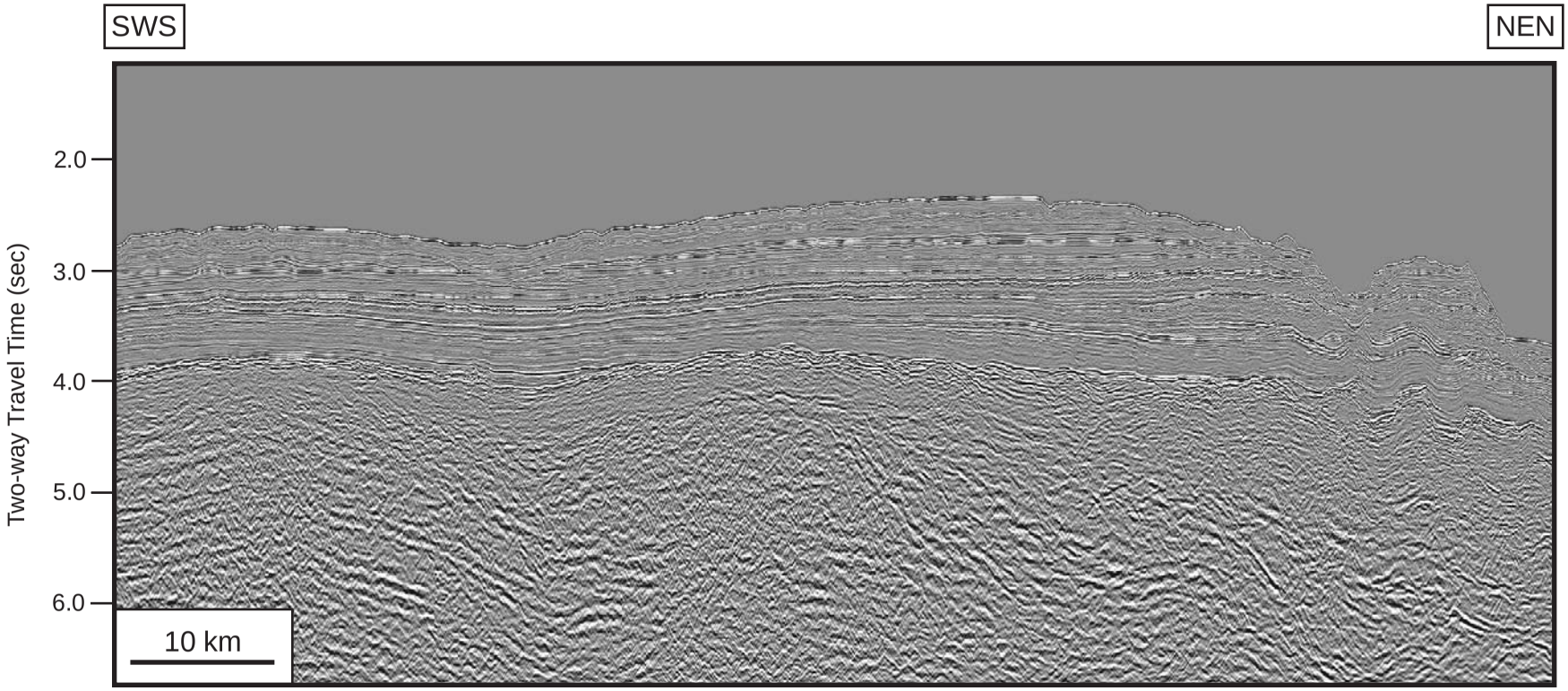

Figure 20a. Uninterpreted regional strike-oriented seismic profile (br-98:br98-089). Location of the profile is shown in Figure 7.

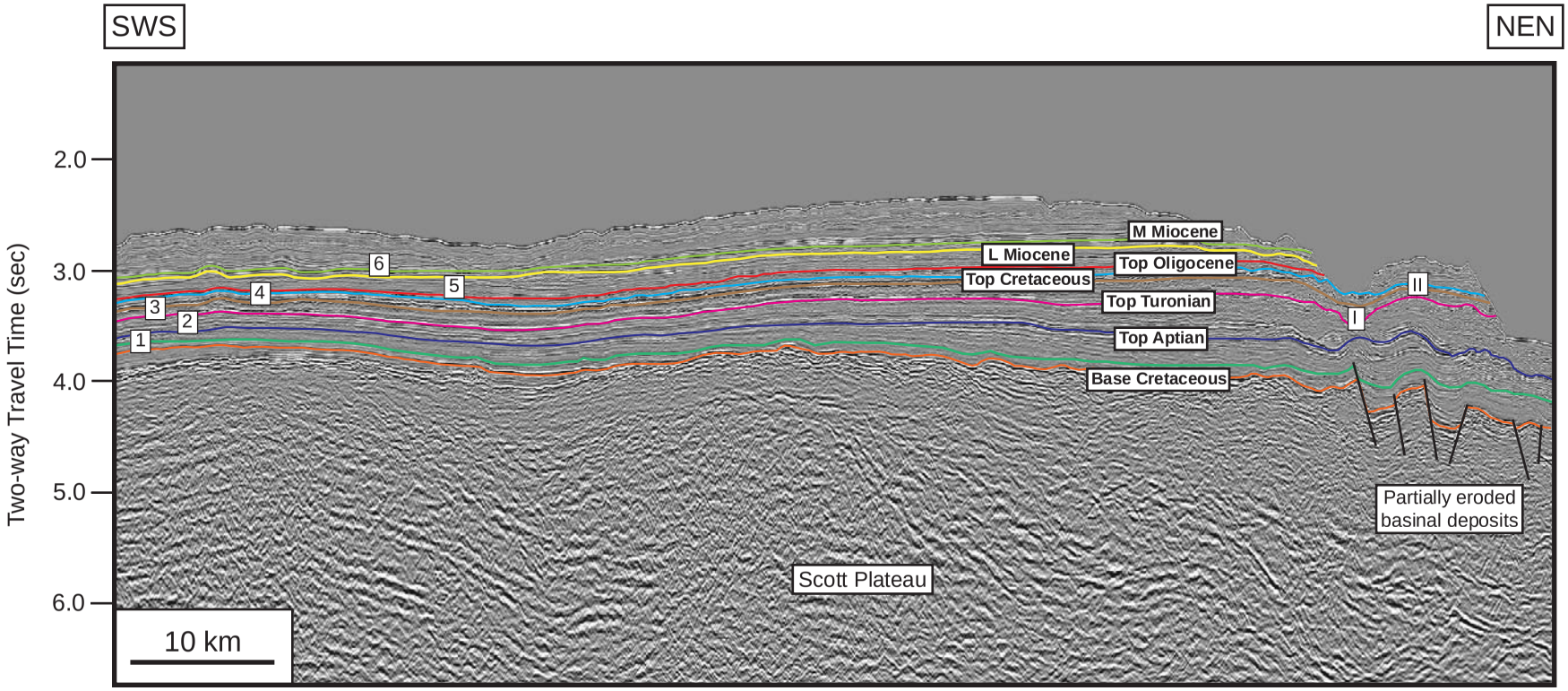

Figure 20b. Regional strike-oriented seismic profile showing all interpreted sequence boundaries from base Cretaceous to middle Miocene. Series of fault blocks are observed in the underlying Jurassic strata. The partailly eroded basinal deposits are recognized in Megasequence 1. All of the sequences display the conformable parallel to subparallel seismic reflections of the Scott Plateau. Location of the profile is shown in Figure 7.

Stratigraphy

The tectonostratigraphic summary of the Browse Basin is illustrates in Figure 21. Major sequences, horizons and tectonic phases are listed from Devonian through Cenozoic. The depocenter of the Browse Basin consists of two series of major tectono-sedimentary sequences separated by a major Callovian (Middle Jurassic) unconformity. The older series were deposited during the two distinct rifting phases (Carboniferous to Permian and Lower to Middle Jurassic).

The Carboniferous section is dominated by fluvio-deltaic and the overlying Lower Permian strata comprises interbedded limestones, mudstone, siltstone and minor sandstone deposited in a marine environment. The Upper Permian section consists of sandstones grading into shales and limestones.

The oldest Triassic rocks penetrated in the Browse Basin are interbedded marine mudstone, siltstones and volcaniclastic strata that were deposited during a regional Lower Triassic marine transgression. Middle to Upper Triassic strata include fluvial and marginal to shallow marine sandstones, shales and minor carbonates. The overlying Triassic rocks include fluvial and marginal to shallow marine sandstones, limestones and shales. The Lower to Middle Jurassic strata comprise sandstones, mudstones and coals that accumulated in deltaic and coastal plain settings with minor marine influence.

The Callovian unconformity coincided with continental breakup and the initiation of sea-floor spreading caused the widespread erosion which occurred onlap onto the Upper Jurassic sandstones and shales. Widespread basalts and pyroclastics associated a new oceanic crust initiating in early Upper Jurassic.

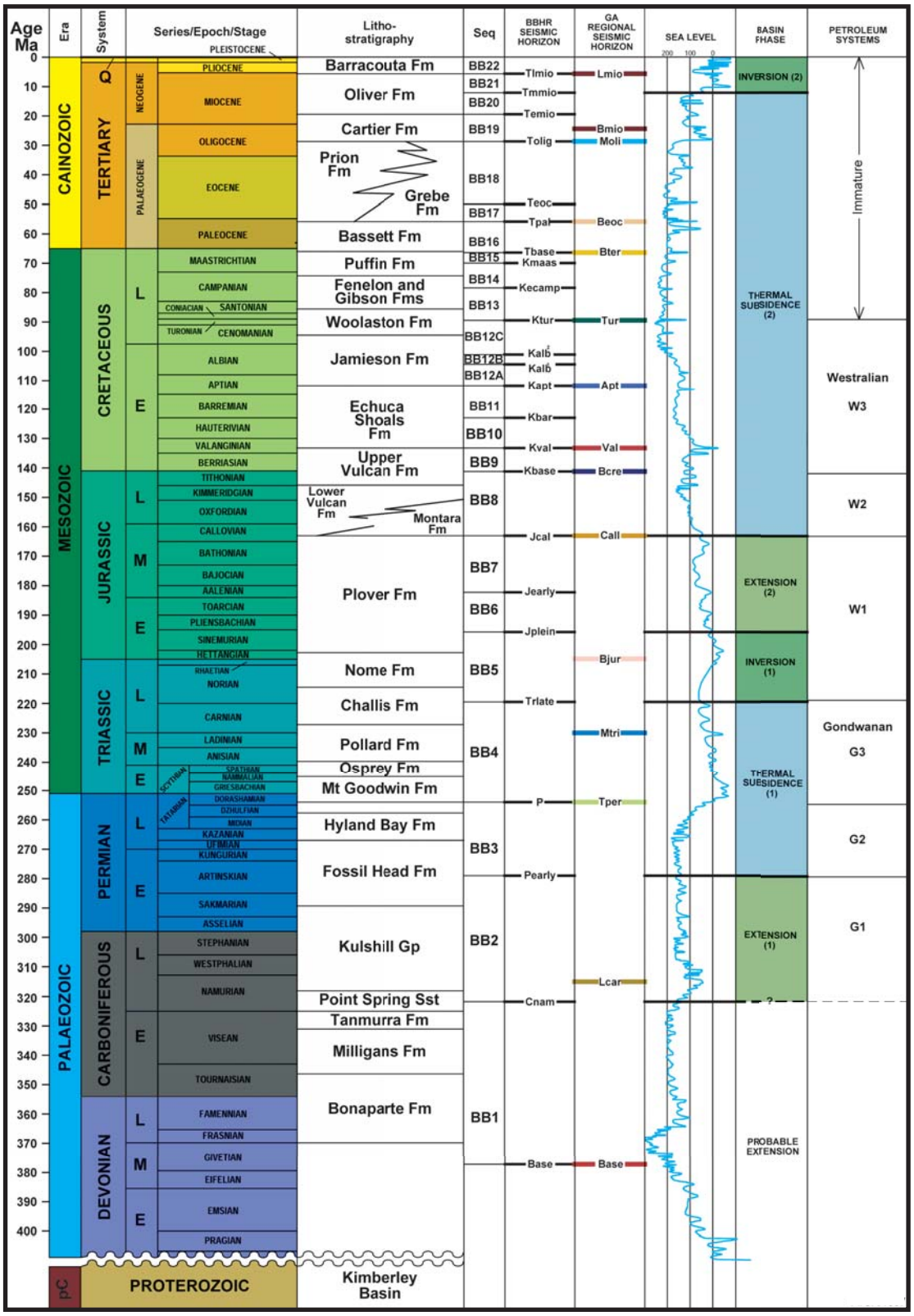

Figure 21. Tectonostratigraphic summary shows sequences, horizons and tectonic phases of the Browse Basin (Department of Resources, Energy and Tourism, Australian Government, 2008)

During the Upper Jurassic to Cenozoic, the accommodation was controlled by the interplay of thermal subsidence, minor reactivation events and eustasy. Upper Jurassic interbedded sandstones and shales onlap onto the pre-Callovian structures. The widespread transgression commenced in the Lower Cretaceous. It peaked in the Turonian and continued until Aptian. The result is the deposition of thick open marine condition. Thick marine claystones deposited during this period recorded at the maximum flooding surfaces of several Lower Cretaceous transgressive cycles.

The Turonian-Cenozoic section represents a major progradational (regressive) cycle in which the shelf edge migrated northwestwards to the outer limits of the Buffon-Scott Reef-Brecknock Anticline Trend.

In term of petroleum systems of the study area, the reservoirs are the Lower to Middle Jurassic marine shelf sandstones and Cretaceous deepwater sandstones. Moreover, the Lower to Middle Jurassic marine and fluvio-deltaic section are also the potential source rocks. The Upper Jurassic shales and the Upper Cretaceous thick marine claystones are regional seal.

Four wells were drilled in the study area (Figures 2, 4, 7): Lombardina-1 (1974), Barcoo-1 (1979), Arquebus-1ST1 (1991) and Sheherazade-1 (1993). Apart from Barcoo-1 well, those three wells penetrated the Late Miocene reactivation structure of Barcoo Platform Anticline, which is located near the eastern margin of the Barcoo Sub-basin and the Leveque Shelf.

Barcoo-1well is the deepest well in the Browse Basin. It was drilled in the central of Barcoo Sub-basin to test the petroleum plays of the Upper Triassic and Lower to Middle Jurassic sandstones within a large northeast-trending Barcoo Anticline along the

Barcoo fault trend. The well penetrated a thick Cenozoic, Cretaceous and Jurassic strata and demonstrated the presence of sandstone with good porosities and permeabilities. The porosities range from 11-21%. The wireline response illustrates thick sand-prone package in the Lower Cretaceous to Tertiary (Figure 22). However, the well was plugged and abandoned as a dry well.

Lombardina-1 well penetrated the Lower Jurassic through Cenozoic strata. From the sidewall cores, it indicates the presence of residual hydrocarbons. However, it shows the poor overall porosity (5-9%) of the sandstone. The wireline log data shows thick sandstone package in the Upper Jurassic and Upper Cretaceous to Tertiary. The claystone interval is observed in Lower Cretaceous (Figure 23). This well was plugged and abandoned.

Arquebus-1ST1 well was drilled further test of Lower to Middle Jurassic sandstones within the Barcoo Platform Anticline. This structure is a large 3-way dip closure against the basin bounding fault. Possible hydrocarbon indicators (flat spots) had been previously recognized in the Lower Jurassic strata on the regional 2D seismic data (Figure 32). The overall porosity of the Upper Jurassic sandstones is relatively poor, ranging from 6-12%, whereas the reservoir quality of the Middle Jurassic sandstones is good with an average porosity of 14%. The wireline log shows the sand interval in Lower Jurassic section. Thick interval of claystone is present in Upper Jurassic to Lower Cretaceous. More sandstone interval is found in the Upper Cretaceous (Figure 24).

Sheherazade-1 well was drilled at the southern portion of the Barcoo Platform Anticline. The prospect has 3-way dip closure against the basin bounding fault. The

primary objective was the Upper Jurassic sandstone that contained potential oil shows in Arquebus-1ST1. The well log data illustrates the coarsening upward sequence ranging from claystone in the Lower Cretaceous to the thick sandstone section from Upper Cretaceous to Tertiary (Figure 25). The failure of this well was to lack of updip lateral seal and/or reactivation by Pliocene faults.

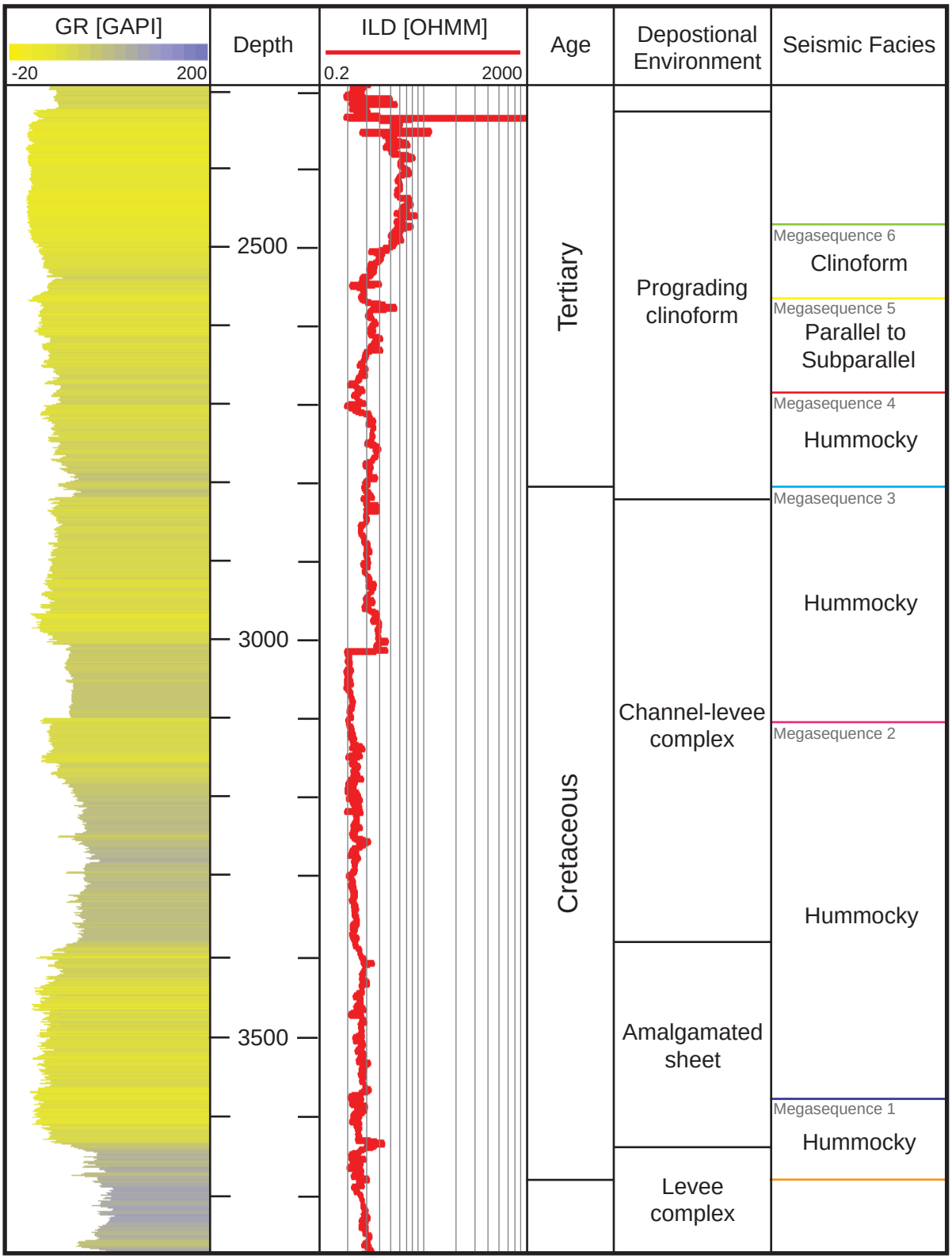

Figure 22. Interpreted wireline response of Barcoo-1 well. See Figures 4 and 7 for the location of well, Figure 26 for time-depth curve and Figure 30 for well-to-seismic tie.

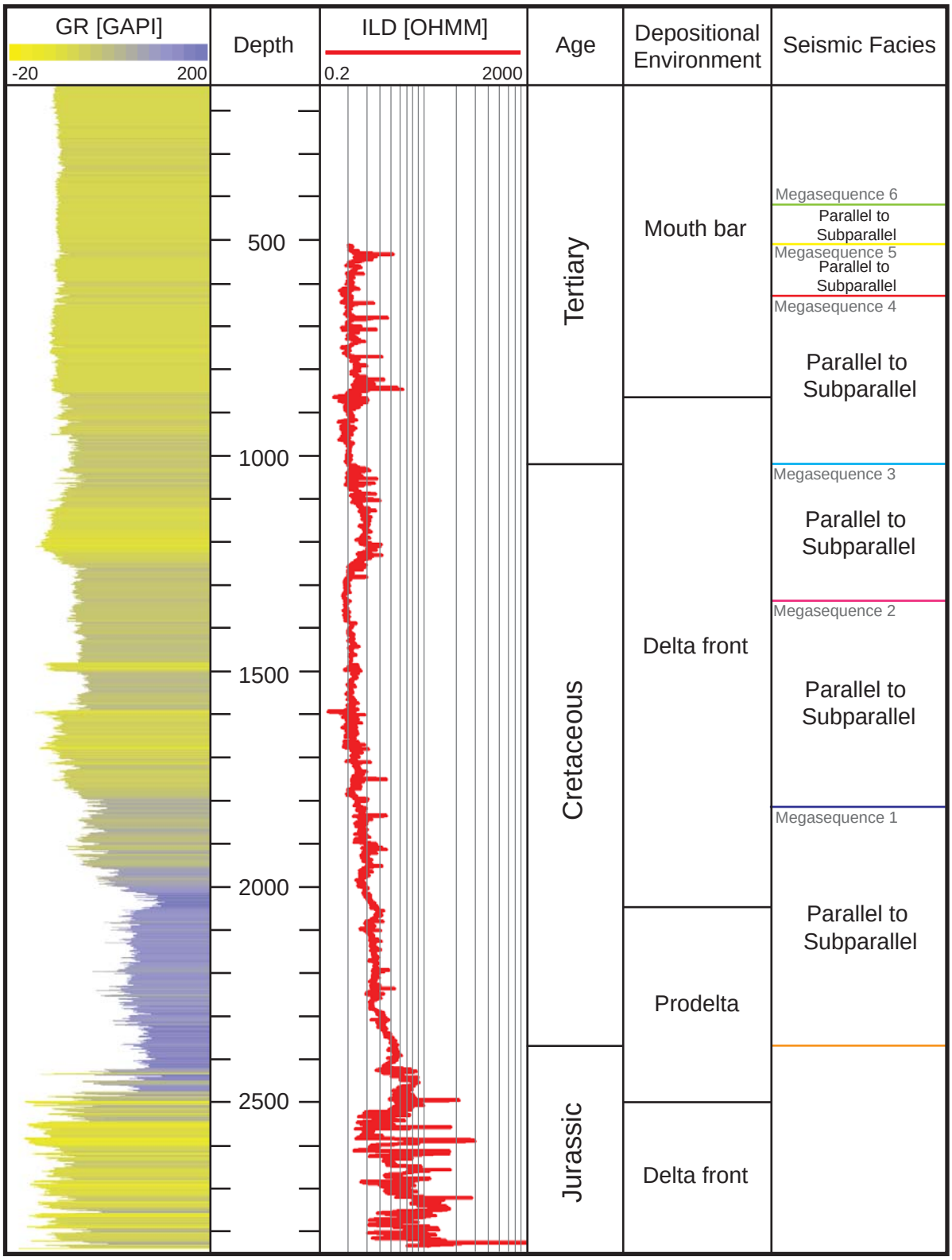

Figure 23. Interpreted wireline response of Lombardina-1 well. See Figures 4 and 7 for the location of well, Figure 27 for time-depth curve and Figure 31 for well-to-seismic tie.

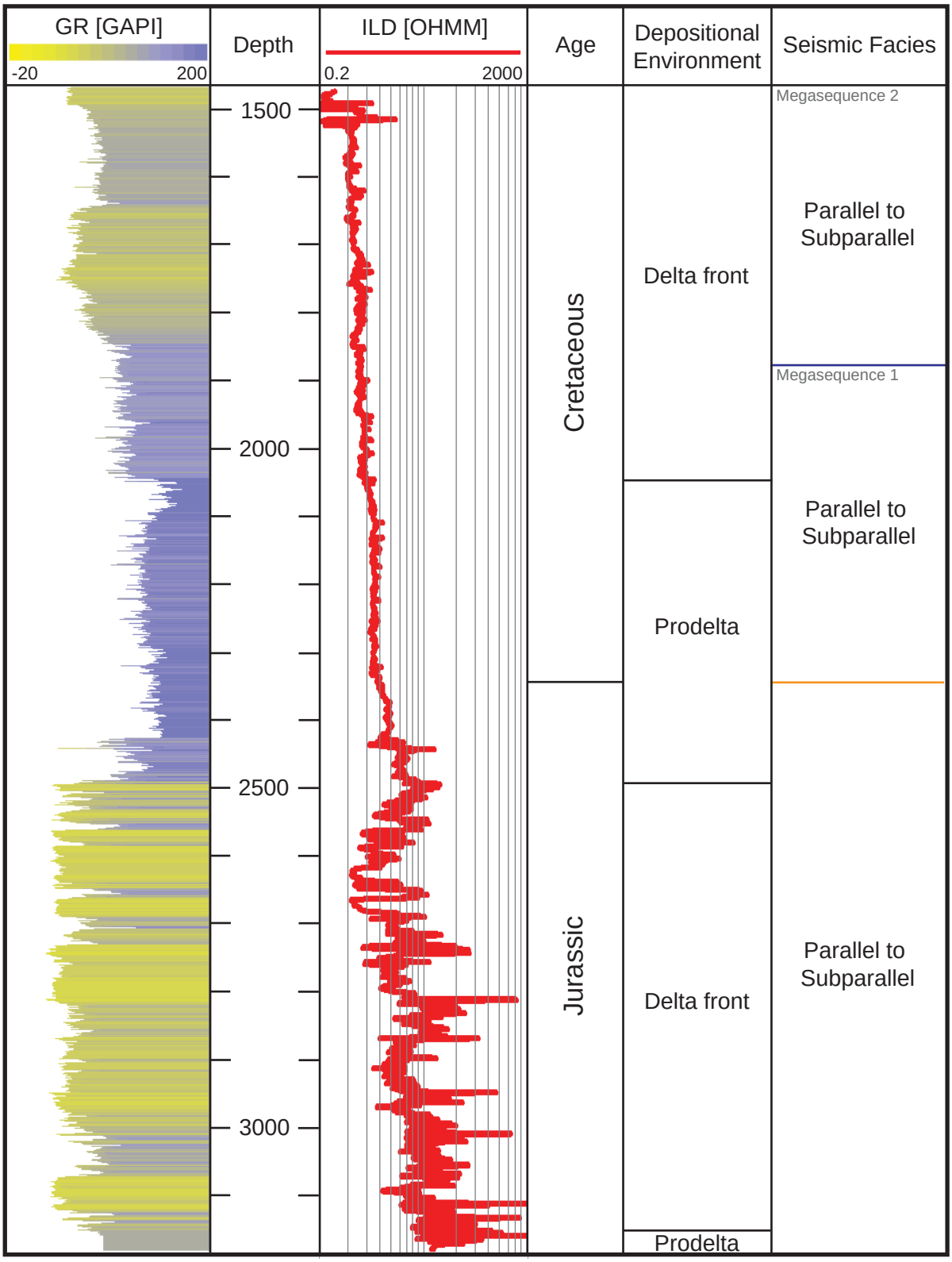

Figure 24. Interpreted wireline response of Arquebus-1ST1 well. See Figures 4 and 7 for the location of well, Figure 28 for time-depth curve and Figure 32 for well-to-seismic tie.

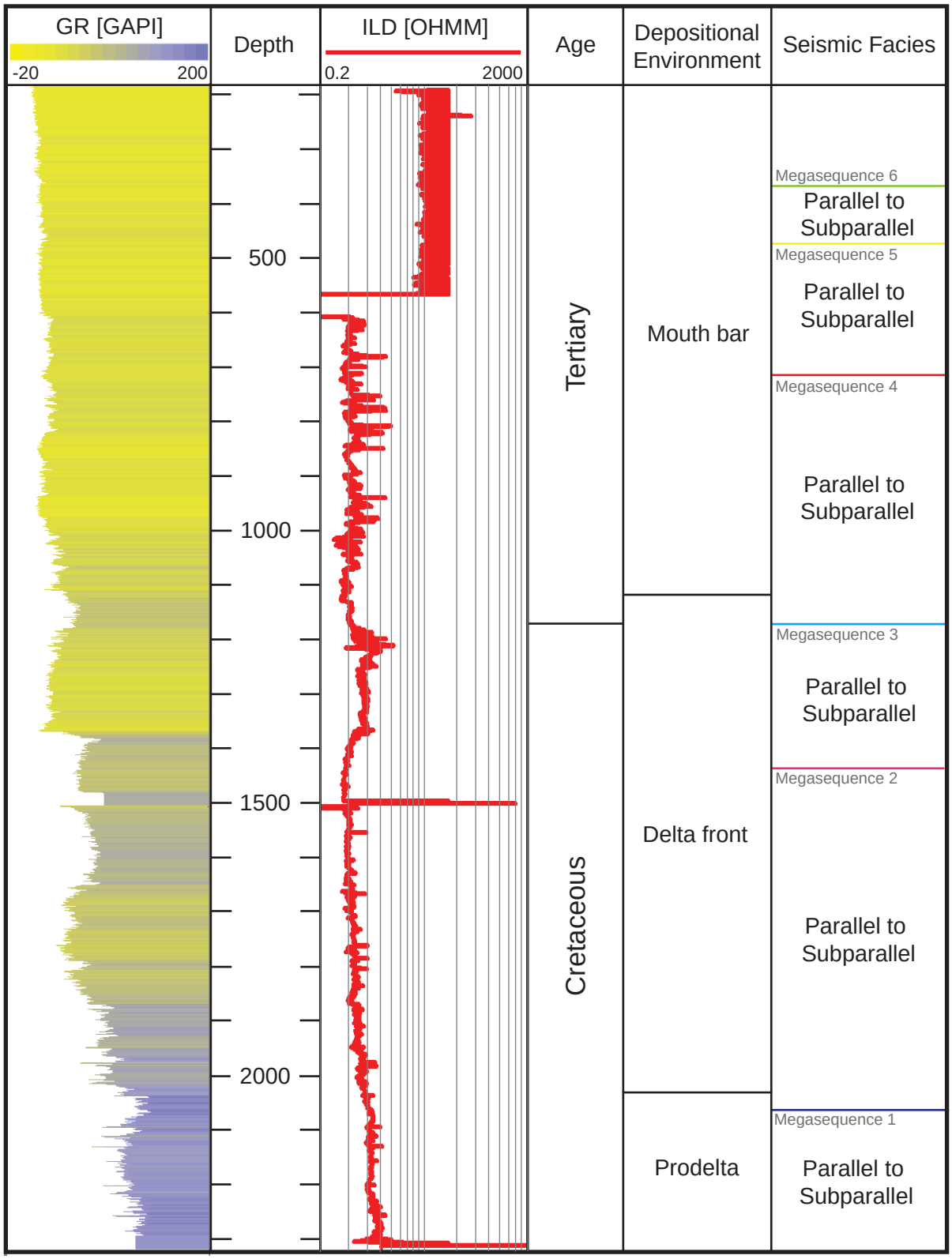

Figure 25. Interpreted wireline response of Sheherazade-1 well. See Figures 4 and 7 for the location of well, Figure 29 for time-depth curve and Figure 33 for well-to-seismic tie.

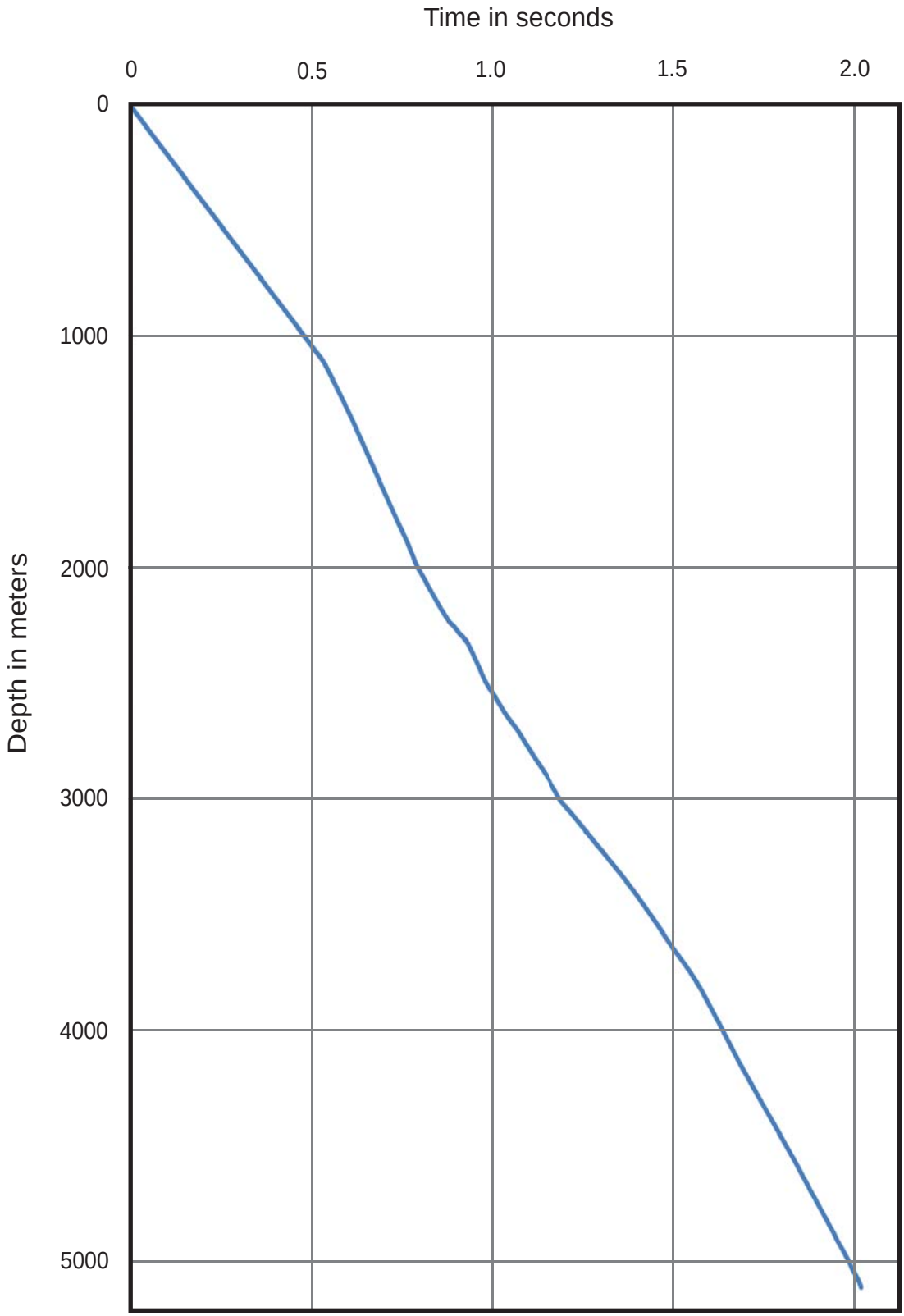

Figure 26. Time-depth curve of Barcoo-1 well. See Figures 4 and 7 for the location of well.

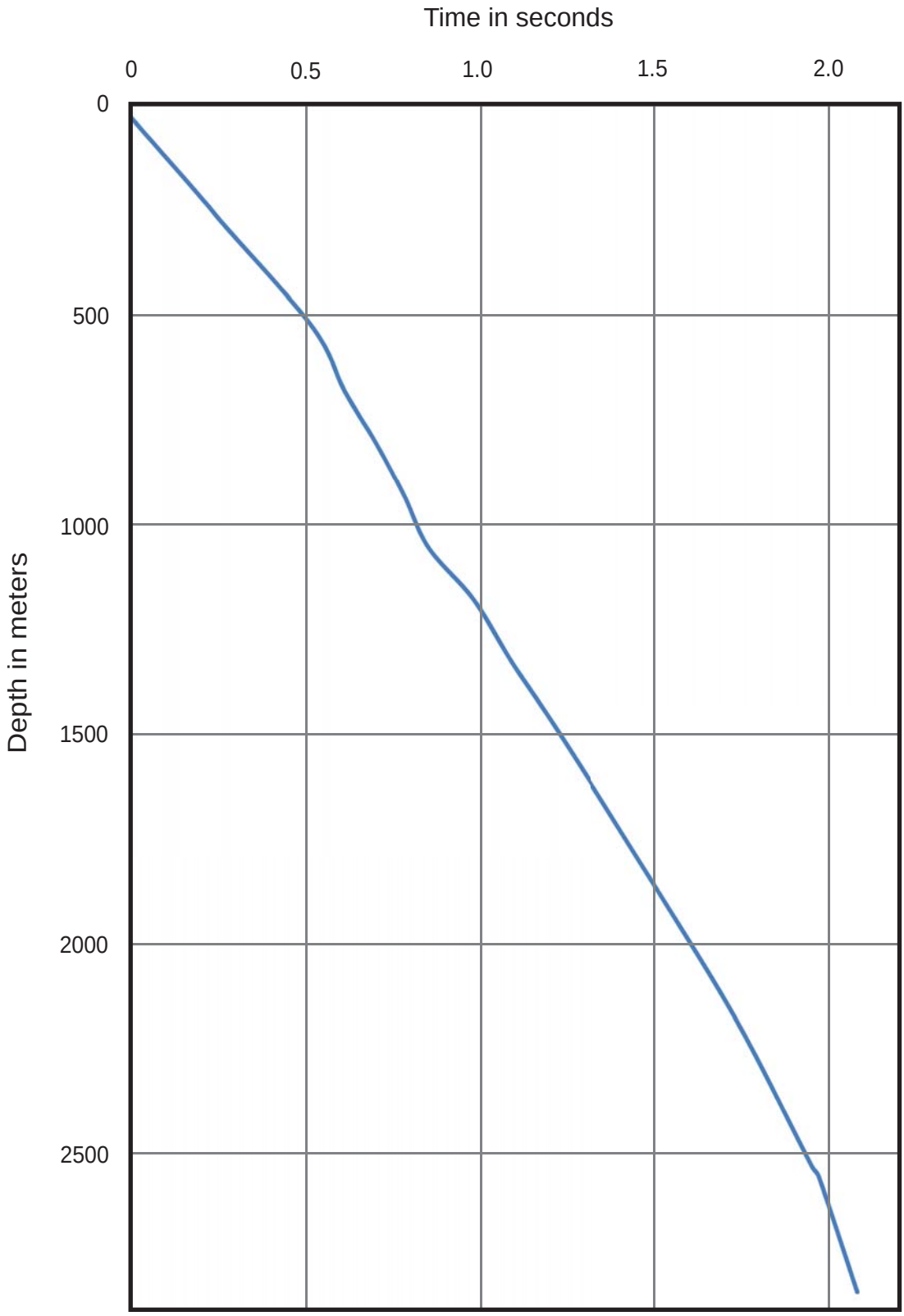

Figure 27. Time-depth curve of Lombardina-1 well. See Figures 4 and 7 for the location of well.

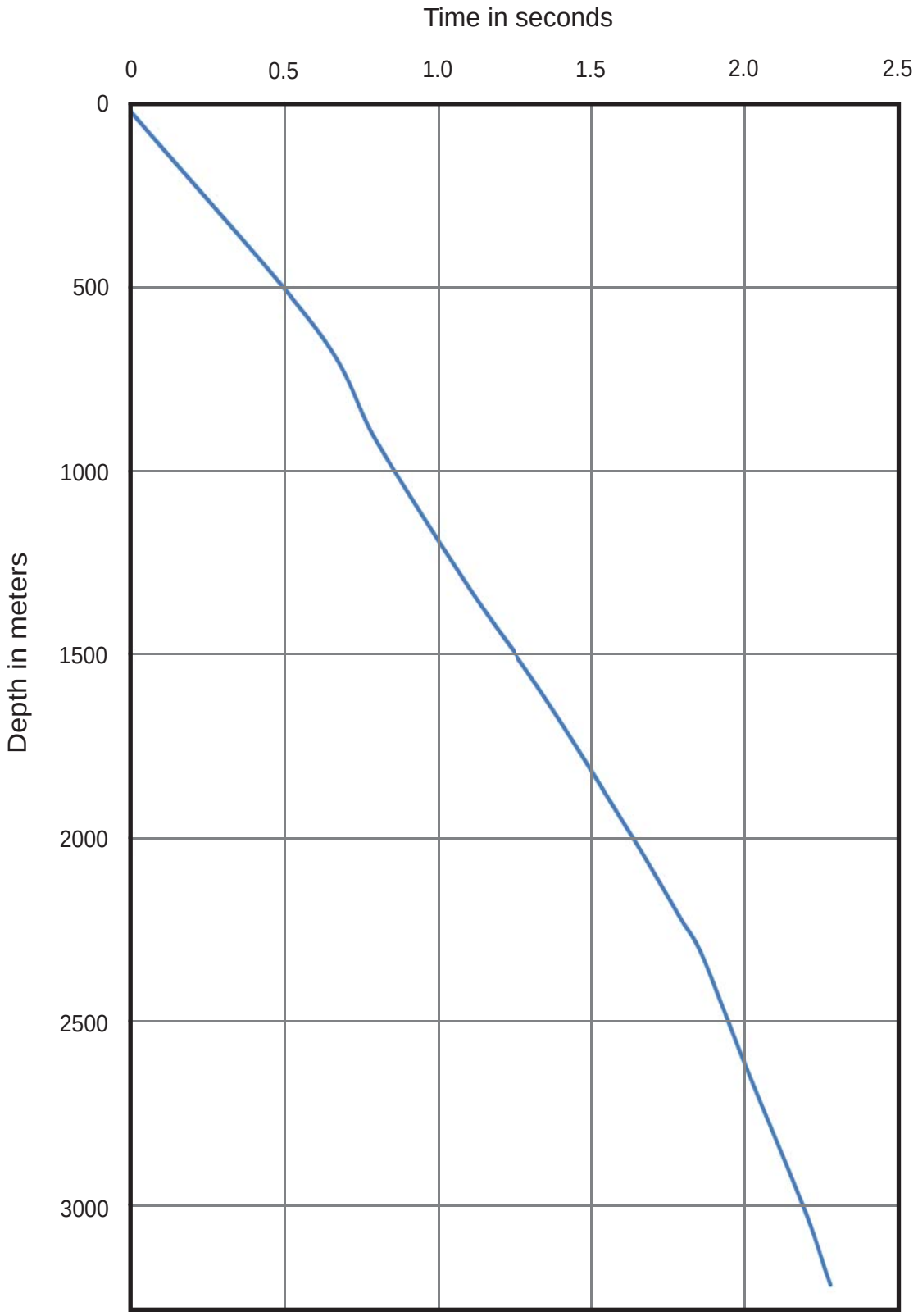

Figure 28. Time-depth curve of Arquebus-1ST1 well. See Figures 4 and 7 for the location of well.

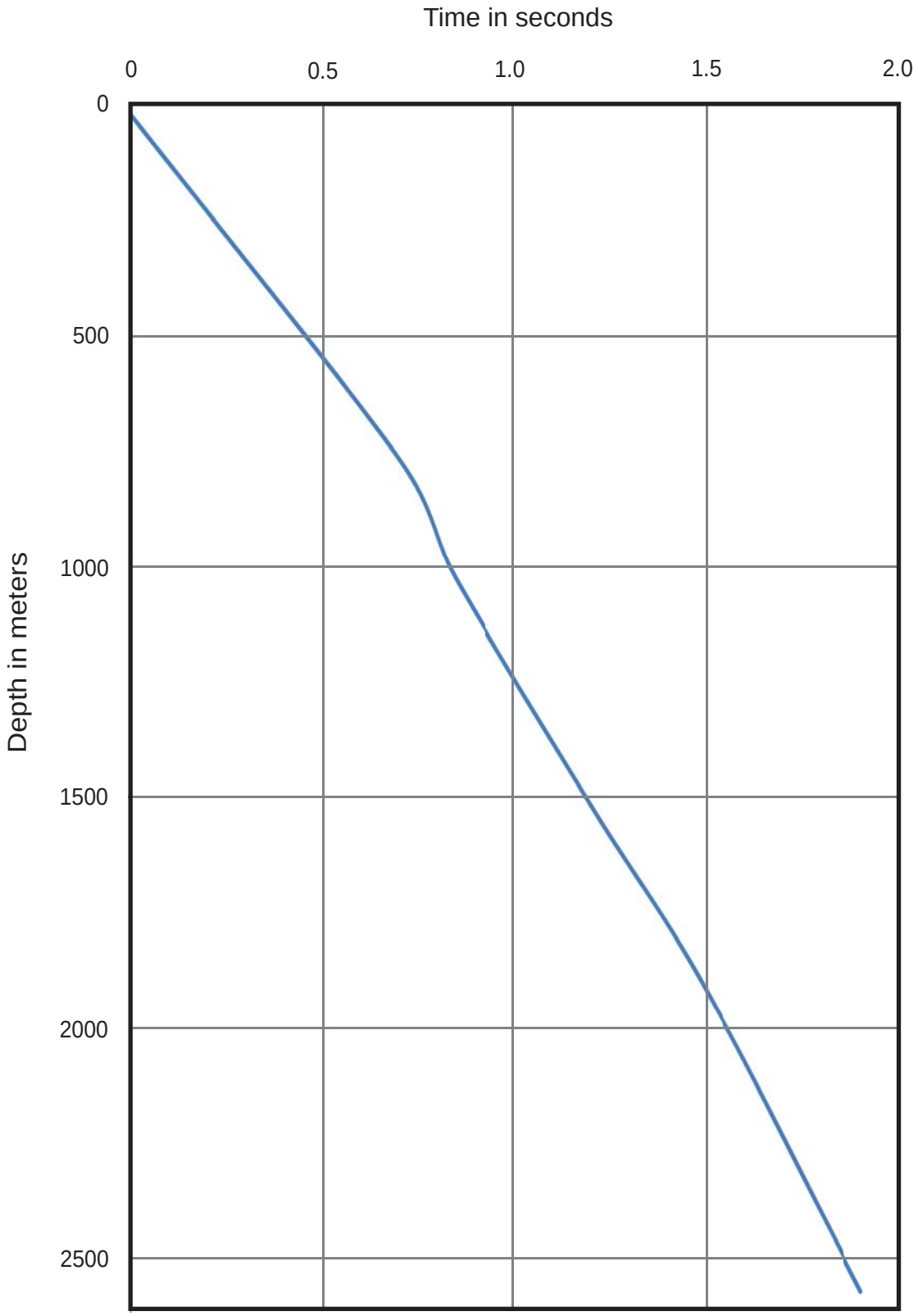

Figure 29. Time-depth curve of Sheherazade-1 well. See Figures 4 and 7 for the location of well.

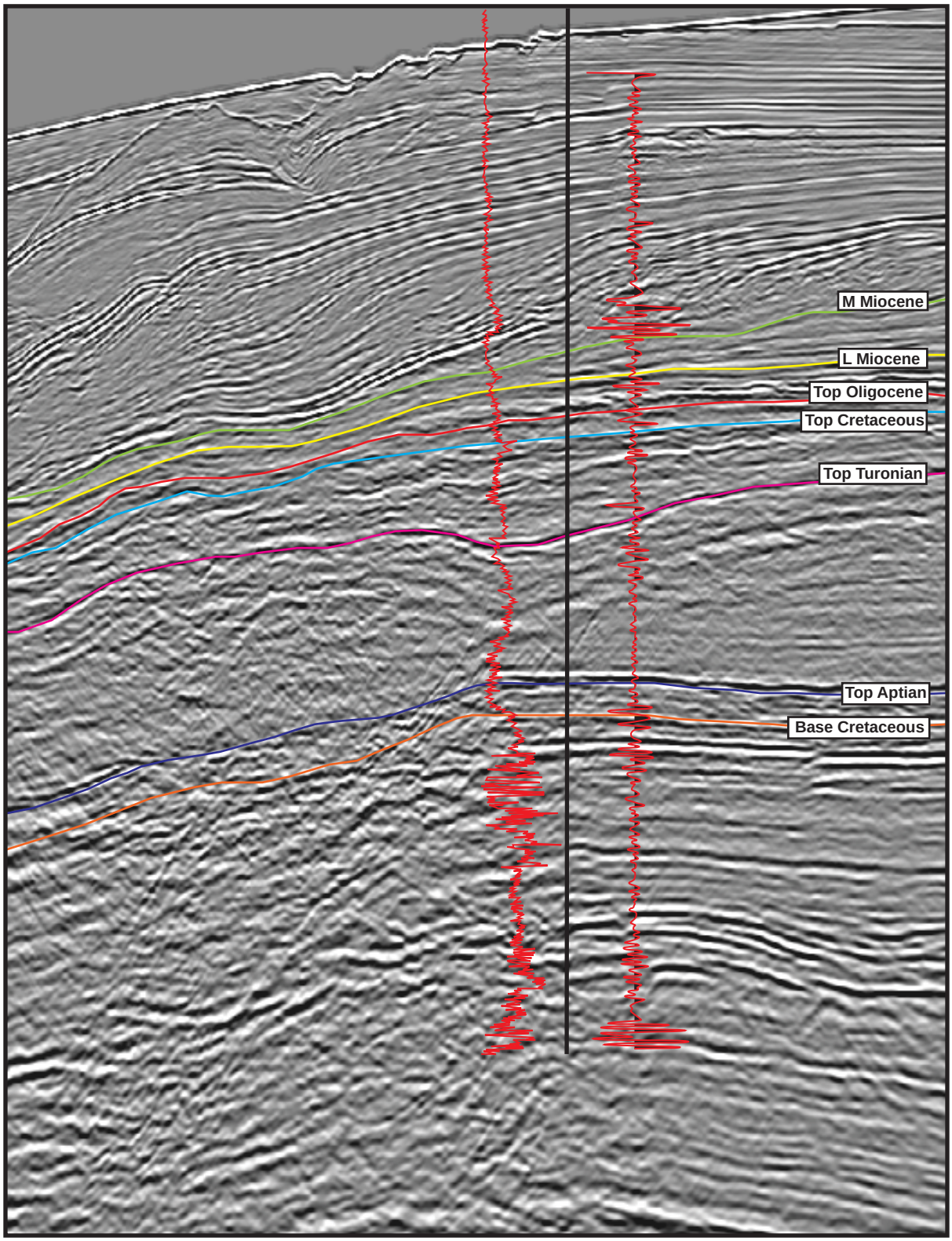

Figure 30. Well-to-seismic tie of Barcoo-1 well. See Figures 4 and 7 for the location of well.

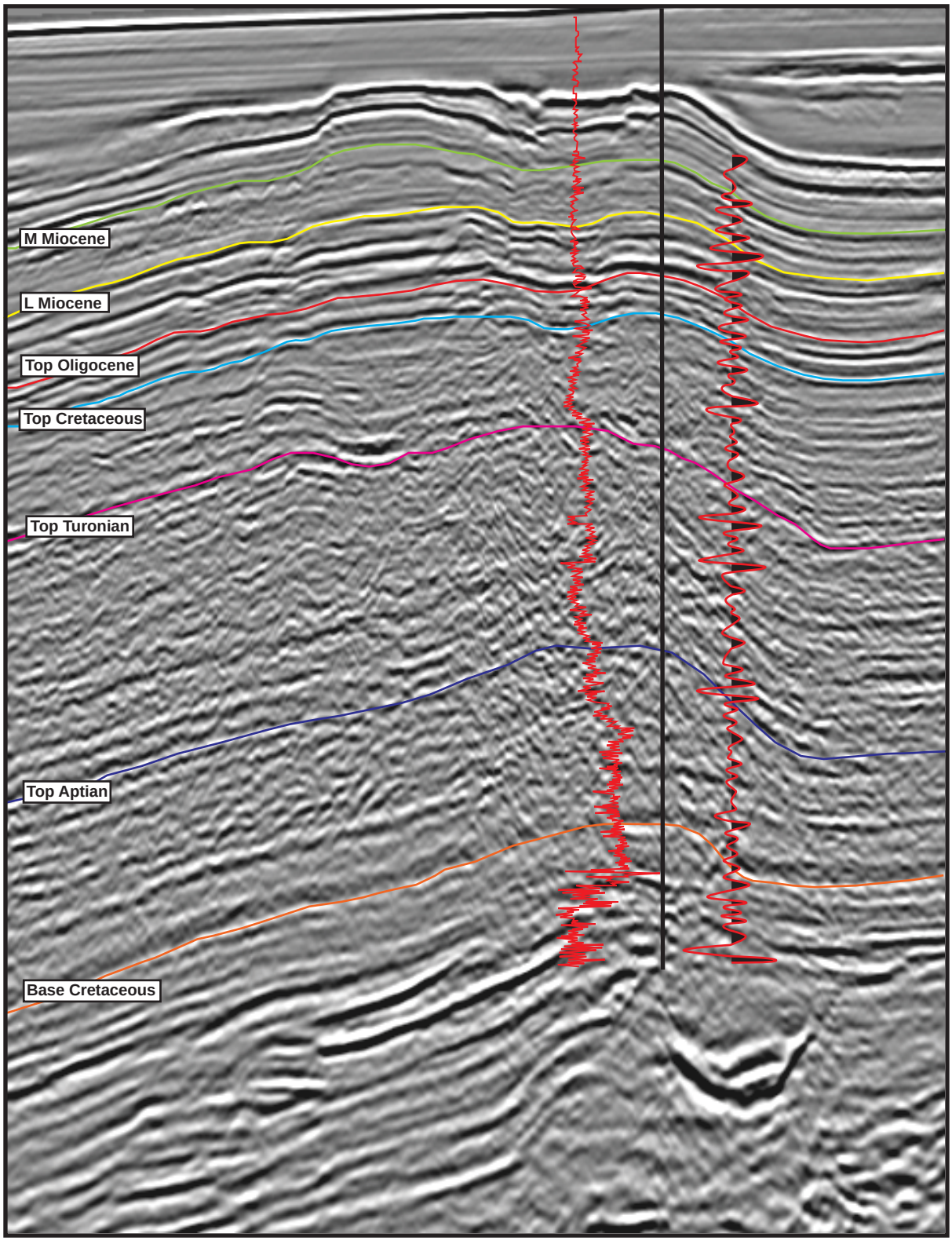

Figure 31. Well-to-seismic tie of Lombardina-1 well. See Figures 4 and 7 for the location of well.

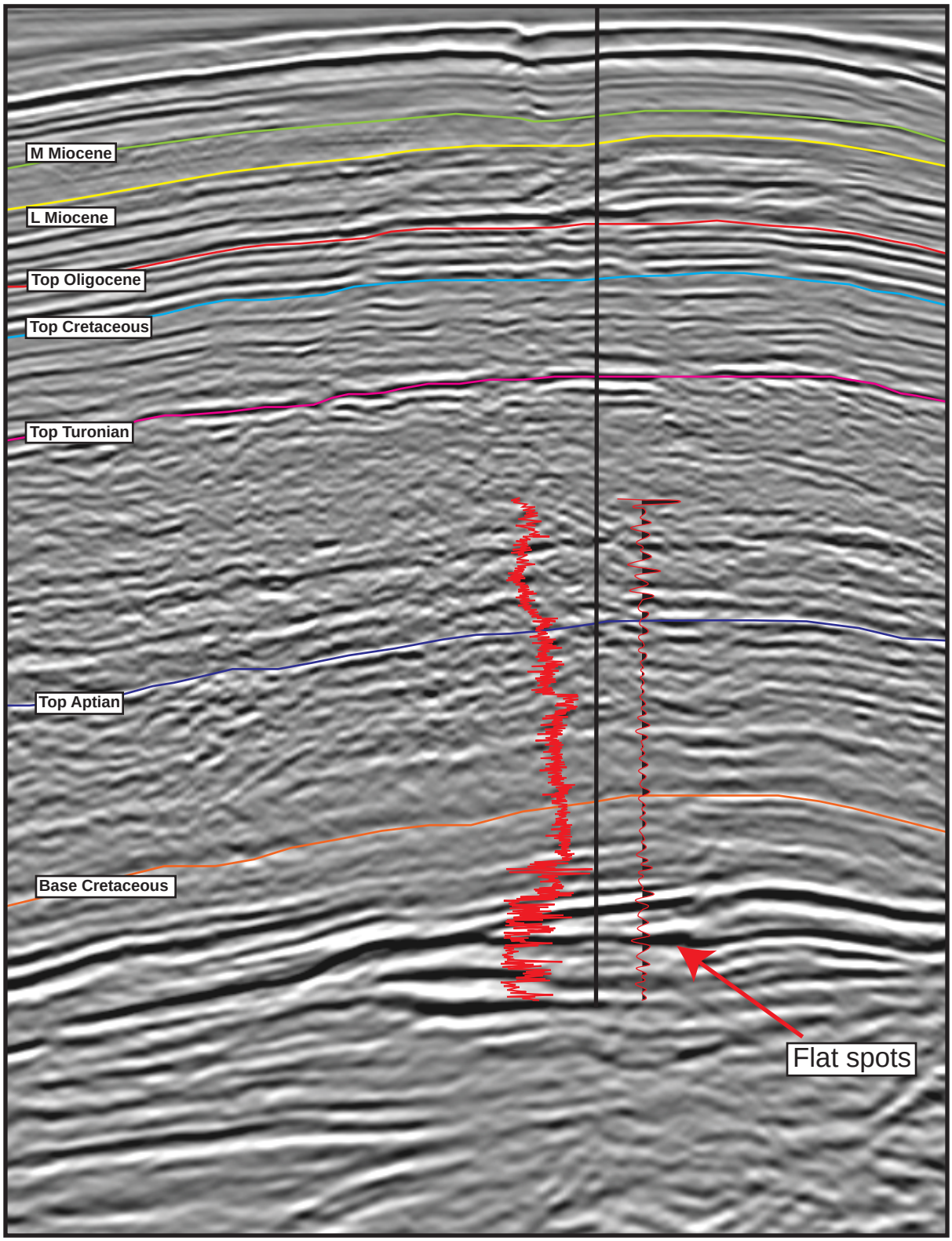

Figure 32. Well-to-seismic tie of Arquebus-1ST1 well. See Figures 4 and 7 for the location of well.

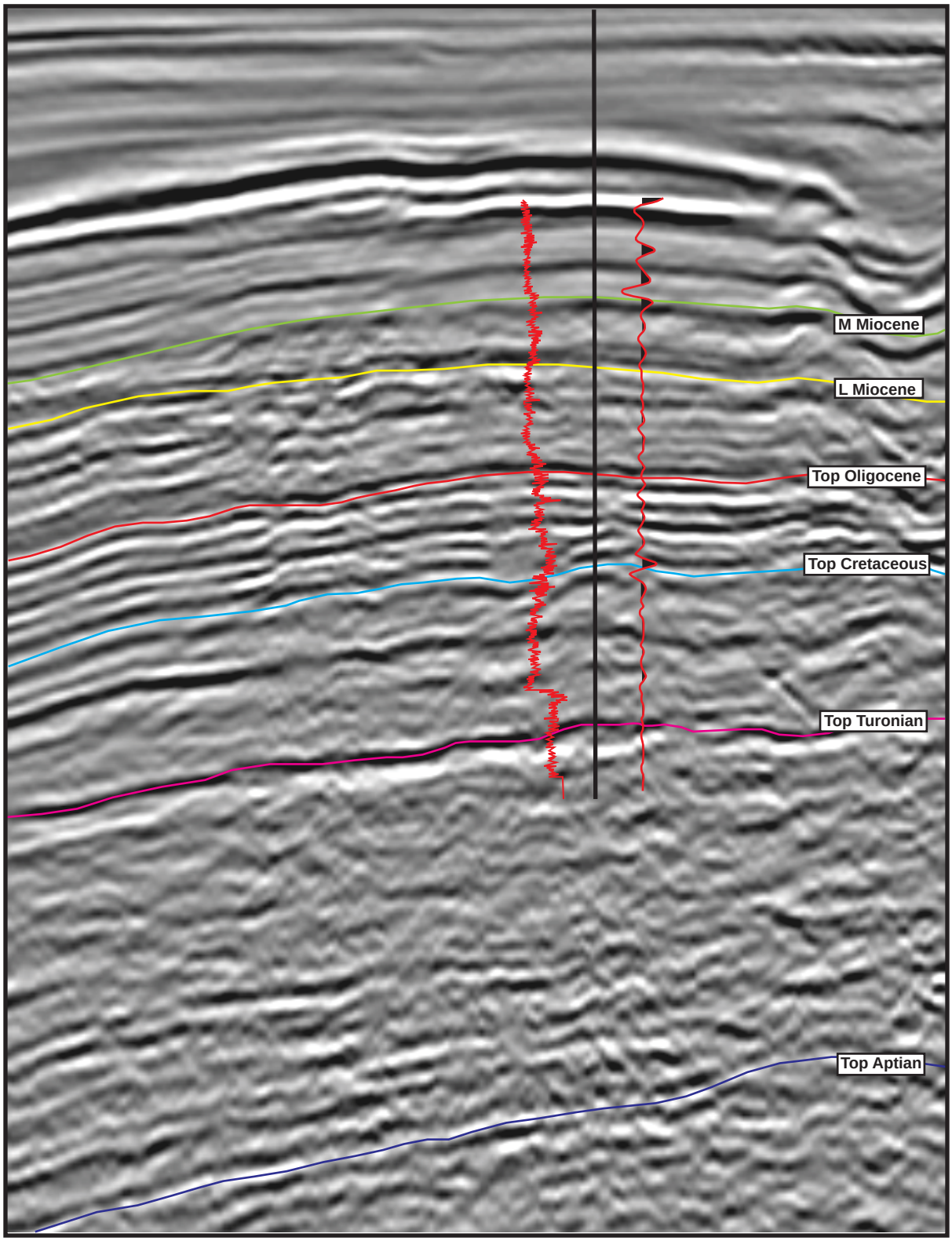

Figure 33. Well-to-seismic tie of Sheherazade-1 well. See Figures 4 and 7 for the location of well.

IV. SEQUENCE STRATIGRAPHY

Methodology and Interpretation Procedure

The sequence stratigraphic analysis used in this study was based on the interpretation procedure outlined by Mitchum and Vail (1977) and Mitchum et al (1993). The integrated 2D multifold seismic and conventional well logs data were used to identify, correlate, and map sequences throughout the study area to establish a time stratigraphic framework.

The first step of this research was to identify and correlate the possible candidates for sequence boundaries or major surfaces. Reflection terminations are used to define these important horizons in seismic lines at the top and base of a seismic sequence (Ramsayer, 1979). Erosional truncation and concordance are the seismic reflection terminations used to delineate the upper surface boundary, whereas onlap, downlap and concordance are used for the lower surface boundary (Table. 2).

With candidates for sequence boundary or major surfaces, the next step was to establish the chronostratigraphic framework of the sequences. The interpreted horizons and their ages were correlated from the previous study of the Department of Resources, Energy and Tourism, Australian Government (2009).

The third step was to analyze and map the seismic facies of each sequence based on the methodology of Ramsayer (1979): A-B/C; where A is the reflection termination or character in the upper surface boundary, B is the reflection termination in the lower surface boundary, and C is the internal reflection configuration or pattern of the seismic reflection. The basic parameters used to describe and map seismic facies units are those dealing with the internal reflection configuration within a sequence as

Table 2. Seismic facies codes used in Table 4-8 and all of the seimic profiles.

Upper Surface Sequence Boundary

Ero: Erosional Truncation

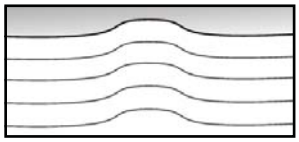

C: Concordant

Lower Surface Sequence Boundary

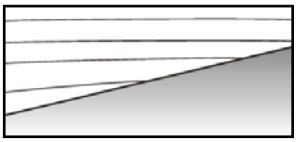

On: Onlap

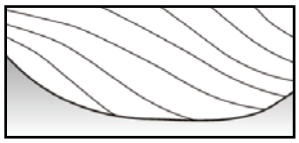

Dwn: Downlap

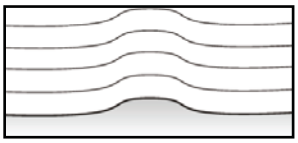

C: Concordant

Internal Reflection Configuration

P: Parallel

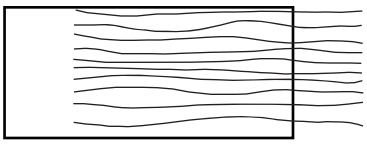

Sbp: Subparallel

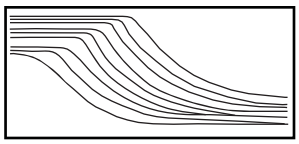

Cli: Clinoform

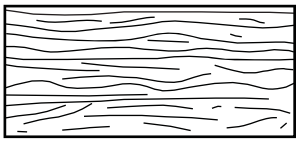

Hum: Hummocky

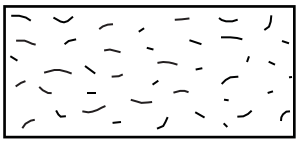

Ch: Chaotic

Amplitude

Low - Moderate - High

Continuity

Poor - Fair - Good

Geologic Facies

Mou	Mound
Ero	Paleo-canyon/Channel
Ant	Anticline

Systems Tracts

LST	Lowstand SystemsTract
TST	Transgressive SystemsTract
HST	Highstand SystemsTract

Seismic Facies Description

$$\frac{A\text{-}B}{C}$$

A	Upper surface
B	Lower surface
C	Reflection Configuration

well as the reflection continuity and amplitude. Then, the structural and isochron maps of each sequence were generated.

Finally, all the maps, well logs data and geological interpretation were integrated to define the different depositional environment of the study area and generate geologic facies maps for each sequence.

Time-Depth Conversion and Synthetic Seismogram

Time-depth curve is the cross-plot between the interval velocity (from sonic logs) and depth. Normally, the velocity value increases with depth. Data from four wells were available in the study area. Sonic logs, density logs and vertical seismic profile (Time-depth curves; Figures 26-29) were used to generate the synthetic seismograms to obtain a direct correlation between the well log and the seismic reflection data. The process to create a synthetic seismogram was done by using SMT 2D/3D seismic interpretation package. The acoustic impedance (AI) was calculated by multiplying the rock's velocity (v) from sonic logs and its density (ρ). The difference of acoustic impedance affects the reflection coefficient (RC) which is the amount of energy to be reflected at the interface between two adjacent layers or body of rocks of different lithology. Then, the reflection coefficient was convolved with the vertical seismic profile to generate the synthetic seismogram (Figures 30-33).

Interval Descriptions

The characteristics of wireline log data (Figures 22-25) where integrated with the seismic facies indicate that the depositional elements in this study area consist of shelf, slope and basinal environments which are shown by the regional seismic profiles (Figures 8-20).

Seven sequence boundaries or maximum flooding surfaces are recognized that define six sequences/ intervals (145.5-112.0, 112.0-89.3, 89.3-65.5, 65.5-23.0, 23.0-19.0 and 19.0-14.2 Ma). Six megasequences (Cretaceous through Middle Miocene) were recognized and studied in the area. Each of the megasequence includes multiple depositional sequences which further subdivided into two to seven third-order depositional sequences. The tops and base of the megasequences consist of major erosional sequence boundaries or second-order maximum flooding surfaces.

Each sequence is described systemically here include the summarized tables, structural maps, isochron maps, seismic facies maps, seismic profiles and geologic facies analyses. Furthermore, the potential petroleum prospects were identified and displayed by strike and dip oriented seismic profiles.

Megasequence 1: base Cretaceous to top Aptian (145.5-112.0 Ma) interval

Megasequence 1 includes the first strata deposited after the major Jurassic rift phase. Many faults cut the underlying Jurassic strata, but do not cut the basal sequence boundary (Figures 8-20). Thus, this megasequence fills an irregular pre-existing faulted topography. At least, three depositional sequences have been recognized within Megasequence 1. The lower and upper sequences (Subsequences I, III) consist parallel to subparallel reflections, whereas the middle sequence (Sequence II) has a distinct wedge shape. Their areal distribution is limited and was difficult to correlate regionally with the widely spaced 2D lines.

The base Cretaceous sequence boundary is the oldest and deepest horizon correlated in this study. It was picked based on the truncation at its base, regional continuity, and high amplitude of the reflection as well as the downlapping reflections in deepwater settings. The time structural contour map (Figure 34) of the base Cretaceous reflection shows the shallower area of the Barcoo Platform to the southeast, the horizon increases in depth to the Barcoo Terrace and the Scott Plateau Graben to the north-northwestern. The two-way travel time ranges from 979 to 4920 msec. The Barcoo Platform Anticline in the southeastern portion of the study area is associated with the major reactivation in the late Miocene time (Figure 36).

The isochron values of this sequence vary from 0 to 1096 msec two-way travel time (TWTT), with the thickest interval on the Barcoo Platform and the northeastern part of the Barcoo Terrace due to the sediment aggrading on slope system (Figure 35).

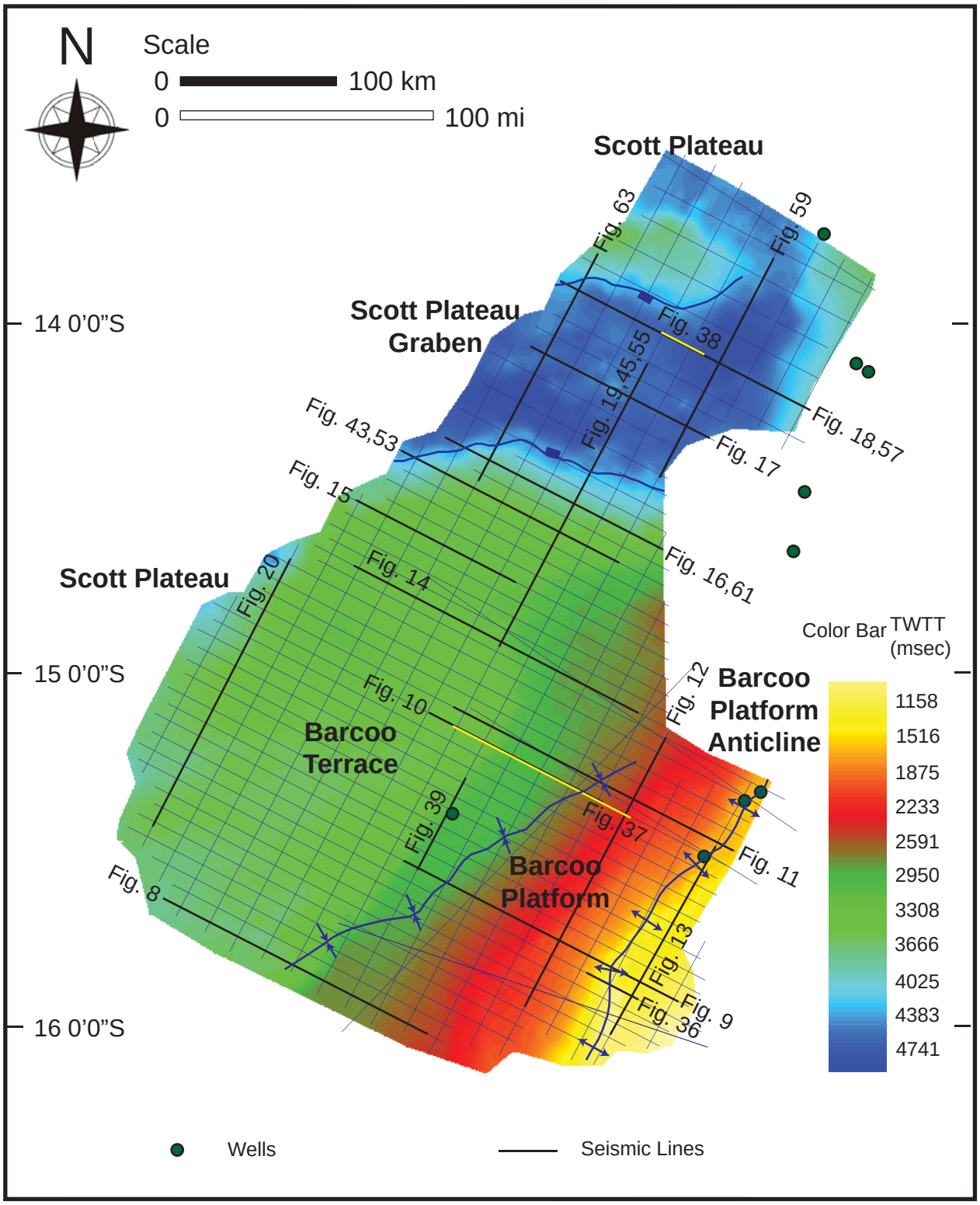

Figure 34. Time structural contour map (in TWTT msecs) of top Aptian (Megasequence 1): 112.0 Ma. Distribution of 2D seismic profiles interpreted to generate the maps are shown by white lines, and wells are shown by green dots. Locations of Figures 8-20, 36-39, 43-46, 53-64 are shown.

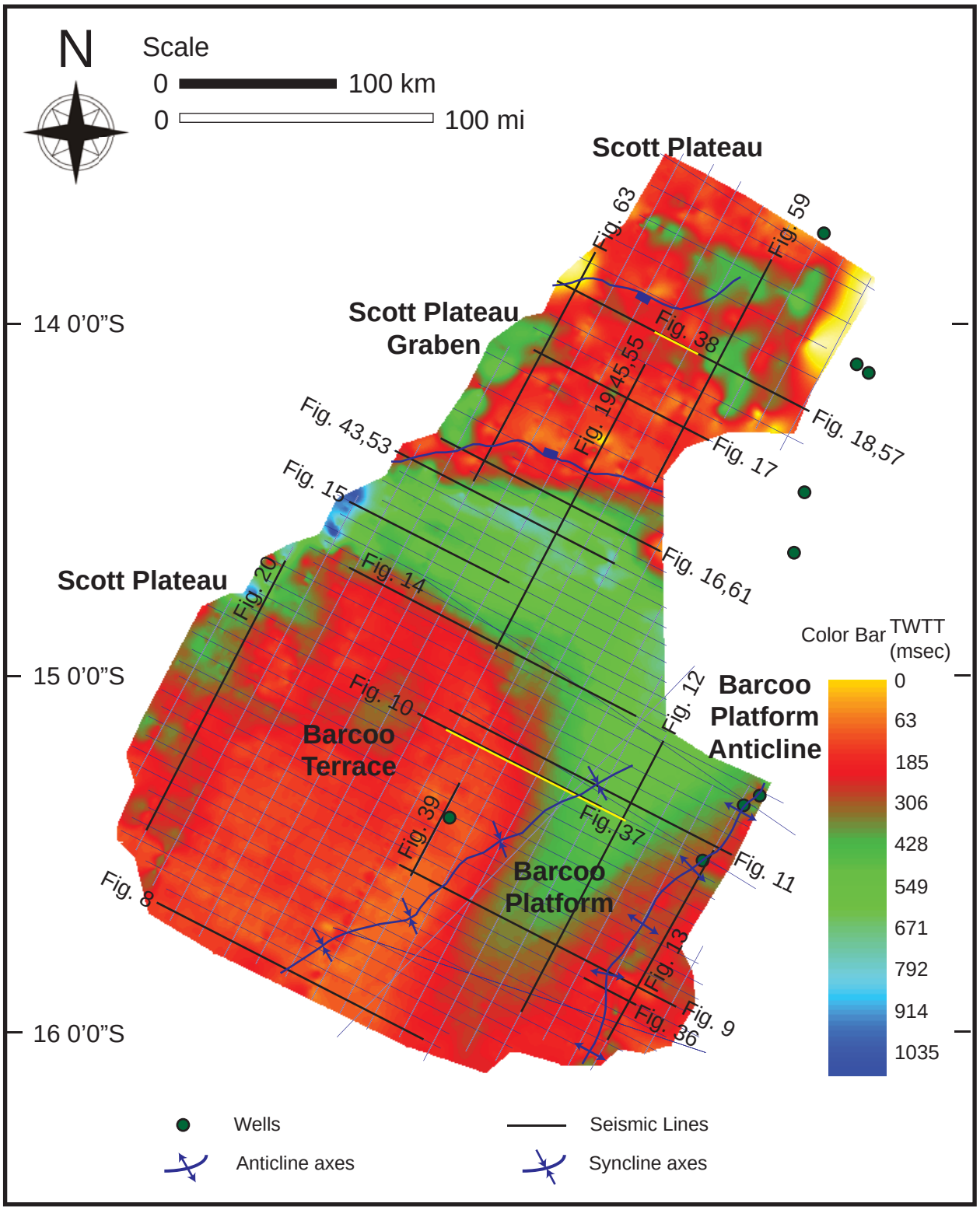

Figure 35. Isochron map (in TWTT msecs) of Megasequence 1 (base Cretaceous to top Valanginian: 145.5-136.4 Ma) interval. Distribution of 2D seismic profiles interpreted to generate the maps are shown by white lines, and wells are shown by green dots. Locations of Figures 8-20, 36-39, 43-46, 53-64 are shown.

Megasequence 1 was penetrated by Barcoo-1, Lombardina-1, Arquebus1-ST1, and Shehearazede-1 wells (Figures 22-25). From the wireline log data, they illustrate the thick interval of fine-grained strata, which are interpreted to be the shale-prone interval of prodelta deposits at the Barcoo Platform Anticline structure and basinal deepwater (levee complex) deposits at the Barcoo-1 well location. The three depositional sequences, Subsequence I-III, were mapped and displayed.

Six seismic facies were identified and mapped for each subsequence (Figures 36-39; Tables 3-5). Seismic facies 1 and 4 are dominant throughout the area. They consist of parallel to subparallel reflections with moderate amplitude and fair to good continuity (Figures 36, 38). Facies 1 is the shelf environment whereas facies 4 is the basinal deposits. Lombardina-1, Arquebus-1ST1, Sheherazaed-1 wells penetrate facies 4 (Figures 30-33). The wireline response shows thick shales or claystones interval (Figures 23-25).

Seismic facies 2 shows the clinoform morphology, which represents the progradation of shelf and primarily a wedge, slope settings (Figures 36, 37). The reflections amplitudes are moderate to high, and continuity is poor to fair. No wells have been penetrated within this facies. Facies 3 consists hummocky reflections with the high amplitude and fair continuity (Figures 37, 39). Barcoo-1 well penetrates in this seismic facies which shows the small grain size interval (Figure 22). Facies 5 and 6 are areally restricted and difficult to analyze due to their chaotic reflections. No wells penetrate these facies. Seismic facies 5 has low amplitude and poor continuity. Facies 6 has a mounded configuration with moderate to high amplitude and poor continuity (Figure 17).

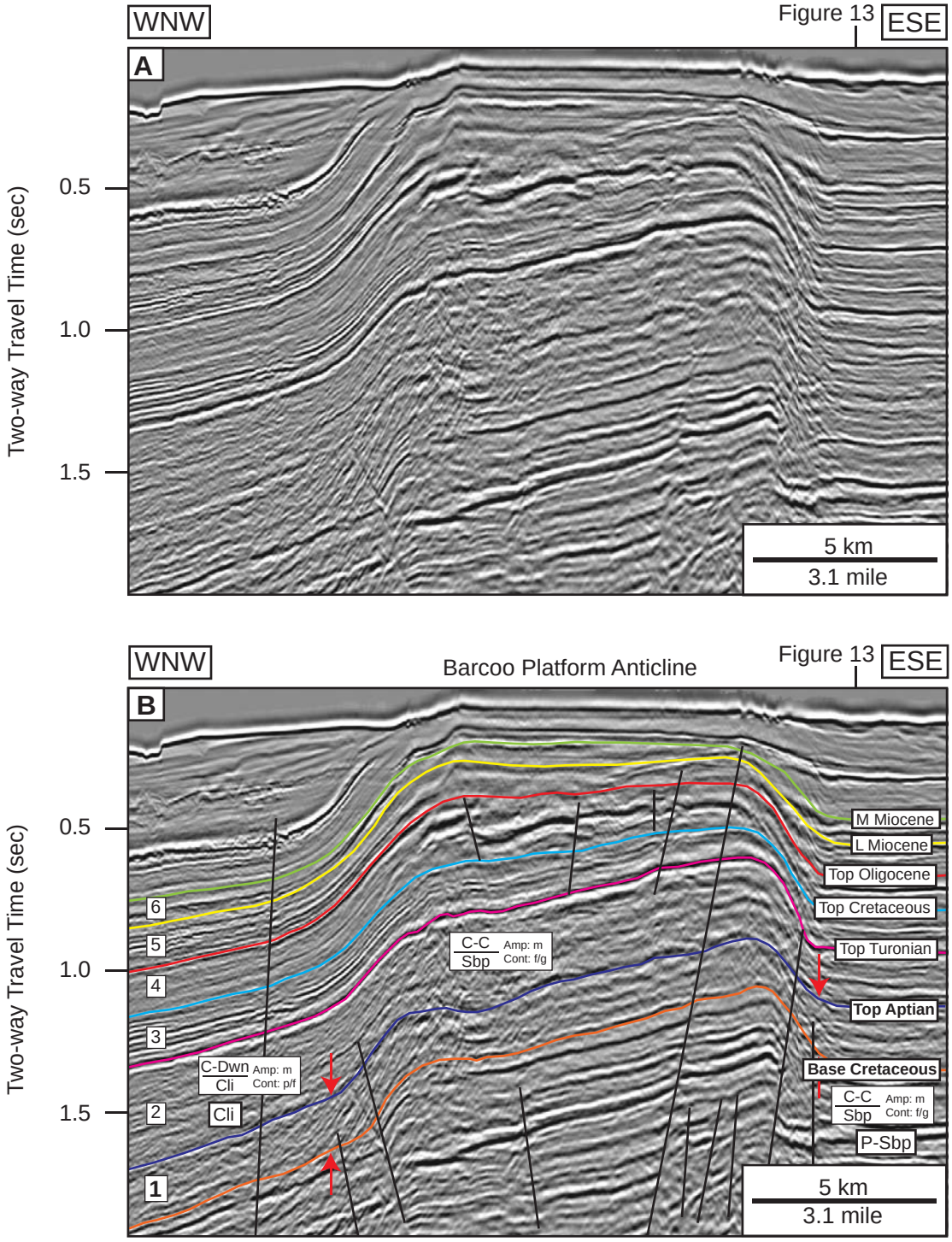

Figure 36. Dip-oriented seismic profile showing seismic facies of Mega-sequence 1: base Cretaceous to top Aptian (145.5-112.0 Ma) interval: (a) uninterpreted, (b) interpreted. See Table 2 for codes and abbreviations and Figures 34-35, 40-42, 47-52 for location of the profile and location of where Figure 13 crosses the profile.

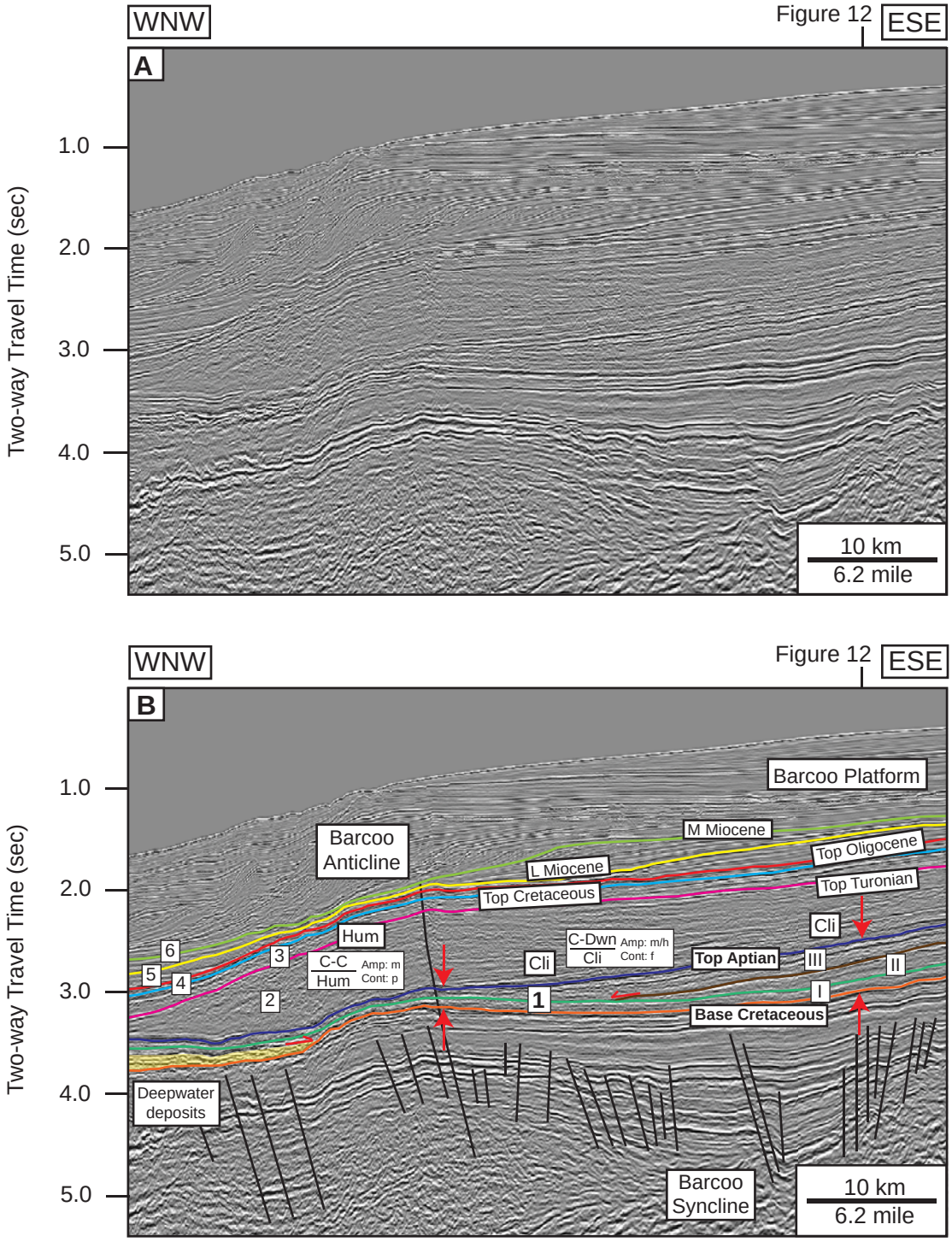

Figure 37. Dip-oriented seismic profile showing seismic facies of Mega-sequence 1 (base Cretaceous to top Aptian:145.5-112.0 Ma) interval: (a) uninterpreted, (b) interpreted. The offset-stacking of deepwater deposits is observed (yellow shade). See Table 2 for codes and abbreviations and Figures 34-35, 40-42, 47-52 for location of the profile and location of where Figure 12 crosses the profile.

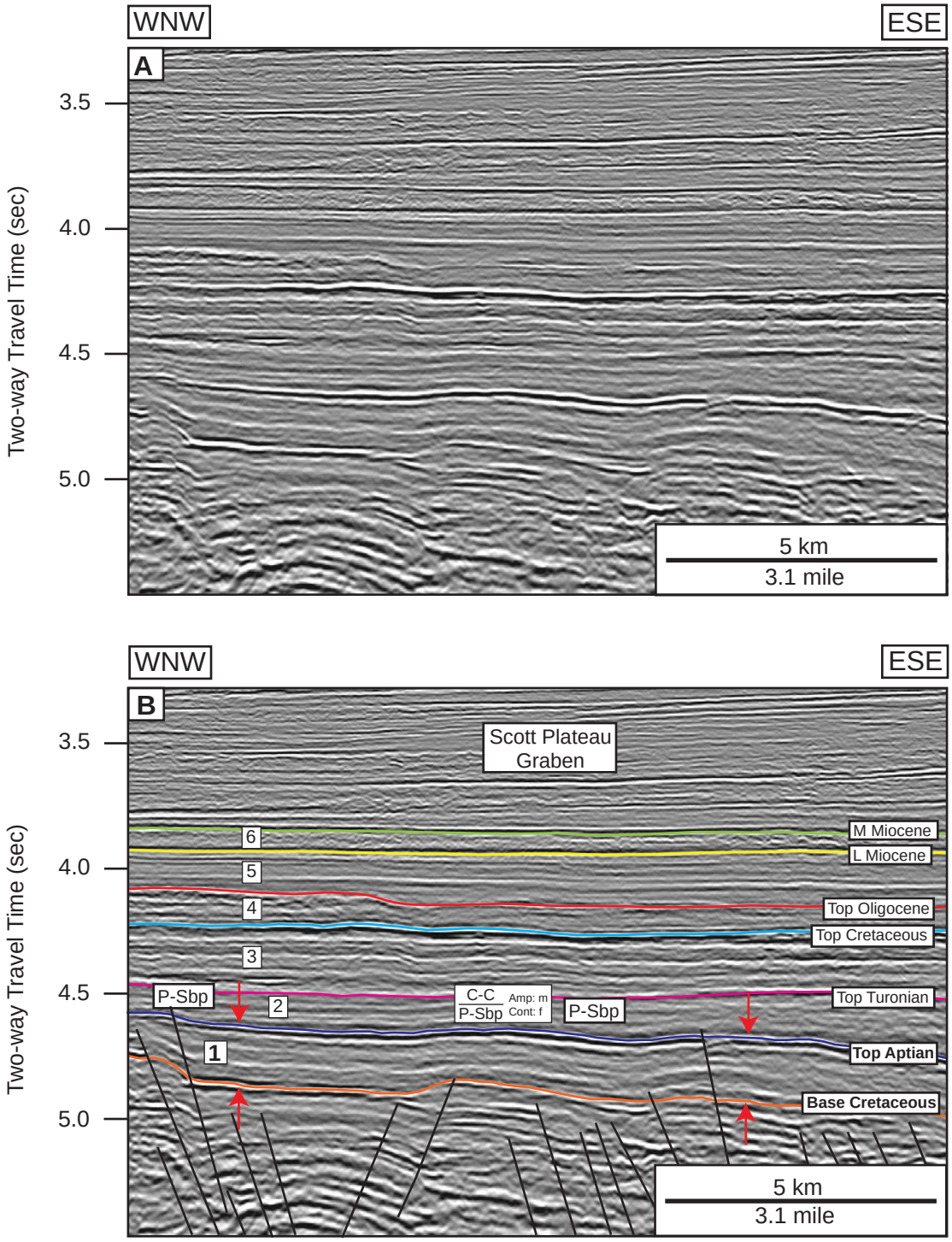

Figure 38. Dip-oriented seismic profile showing seismic facies of Mega-sequence 1 (base Cretaceous to top Aptian: 145.5-112.0 Ma) interval: (a) uninterpreted, (b) interpreted. This profile shows parallel to subparrallel seismic reflections. See Table 2 for codes and abbreviations and Figures 34-35, 40-42, 47-52 for location of the profile.

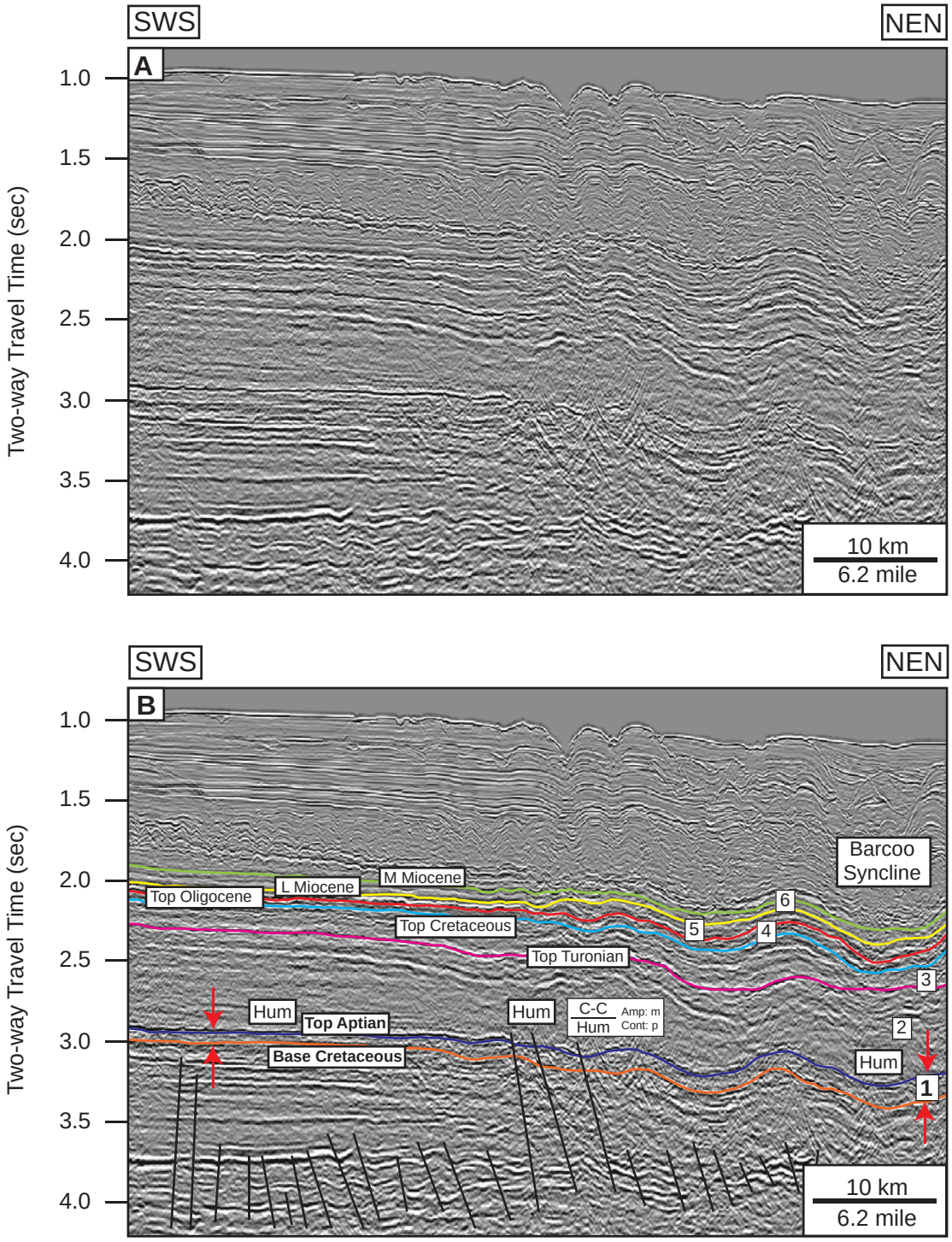

Figure 39. Strike-oriented seismic profile showing seismic facies of Mega-sequence 1 (base Cretaceous to top Aptian: 145.5-112.0 Ma) interval: (a) uninterpreted, (b) interpreted. See Table 2 for codes and abbreviations and Figures 34-35, 40-42, 47-52 for location of the profile.

It is a localized carbonate buildup which has an elongate shape, located in the Scott Plateau Graben in the northern part of the study area.

Subsequence I of Megasequence 1

Subsequence 1 covers more than a half of the study area in the southern part. The isochron map (Figure 40) shows the thicken-most interval in the northeastern part of the Barcoo Terrace which corresponded with the isochron map of the whole sequence of Megasequence 1 (Figure 34). The isochron map shows the value ranges from 0 to 630 msec two-way travel time (TWTT) This might occur due to the accommodation space availability combination with the subsidence (Figures 16, 61-62).

The seismic facies map display 4 facies (Figure 41; Table 3). Seismic facies 1 and 4 illustrate parallel to subparallel internal reflection configuration with moderate amplitude, fair to good continuity which is interpreted to be the shelf environment of the Barcoo Platform and the basinal deposits of the Barcoo Terrace, respectively. The second one is a clinoform facies. This facies has a moderate to high amplitude with poor to fair continuity. In addition, facies 3 demenstrates the hummocky internal reflection configuration. It has moderate amplitude and poor continuity. Those 2 facies (Facies 2 and 3) have been interpreted to be the prograding clinoform of the shelf edge area between the Barcoo Platform and the Barcoo Terrace.

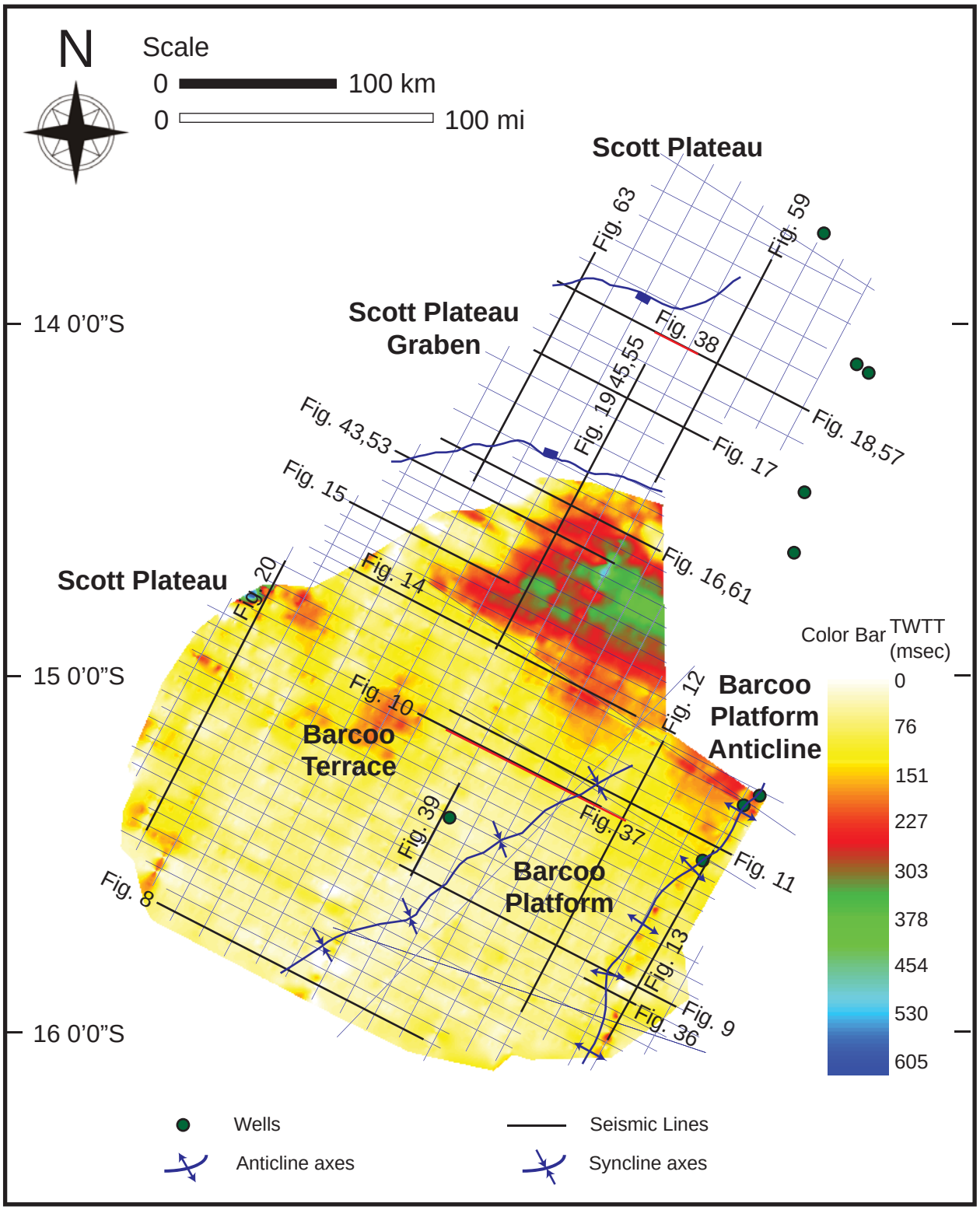

Figure 40. Isochron map (in TWTT msecs) of Subsequence I of Megasequence 1 interval. Distribution of 2D seismic profiles interpreted to generate the maps are shown by white lines, and wells are shown by green dots. Locations of Figures 8-20, 36-39, 43-46, 53-64 are shown.

Table 3. Seismic facies and geologic interpretation of Subsequence I of Megasequence 1

Seismic Facies	Upper Sequence Boundary	Lower Sequence Boundary	Internal Reflection Configuration	Amplitude	Continuity	Geologic Interpretation
1	Concordant	Concordant	Parallel to Subparallel	moderate	fair to good	Shelf deposits
2	Concordant	Downlap	Clinoform	moderate to high	poor to fair	Prograding clinoform
3	Concordant	Concordant	Hummocky	moderate	poor	Inversion – related structure
4	Concordant	Concordant	Parallel to Subparallel	moderate	fair to good	Basinal deposits

The geologic facies map (Figure 42) shows that sediments were transported from the coastal plain environment southeastern part of the study area to shallow marine environment and to the basin-floor in the southeast-northwest direction. The margin of shelf and slope settings prograded across the Barcoo Platform to the Barcoo Terrace. The clinoform wedges consist of low angle clinoform (Figure 8), indicating a balance between the rates of subsidence and sediment supply. The type of clinoform and style of progradation is dissimilar to the younger megasequences (Sequences 5 and 6).

The basin-floor fan has been indicated to be a potential petroleum prospect in this subsequence. This play is identified by the bi-directional onlap truncation to the lower boundary. The dip and strike oriented profiles are shown in Figures 43- 46.

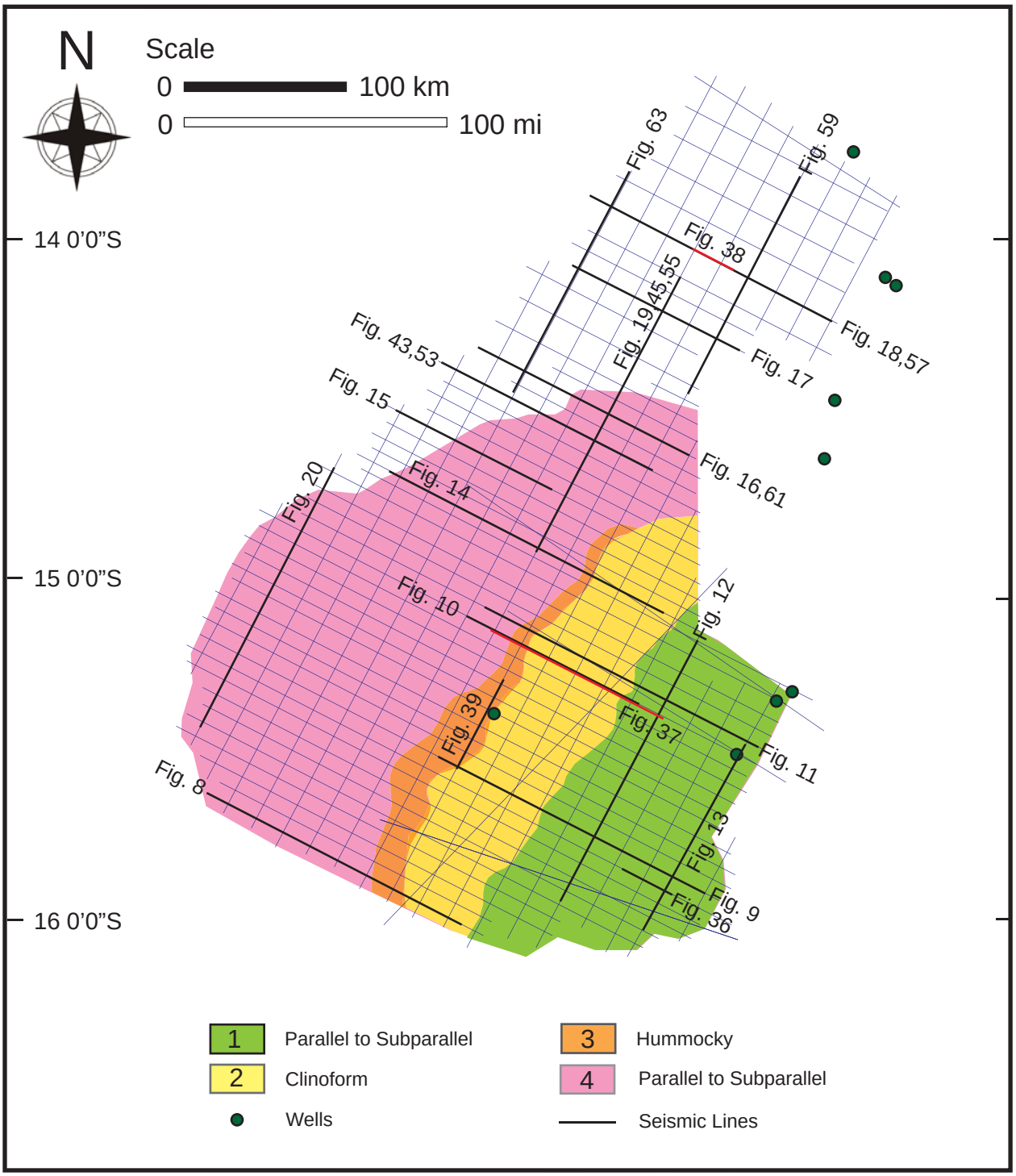

Figure 41. Seismic facies map of Subsequence I of Megasequence 1 interval. Each facies is numbered as described in the text. See Table 2 for seismic facies coding and Table 3 for a summary of seismic facies analysis and geologic interpretation. Locations of Figures 8-20, 36-39, 43-46 and 53-64 (black lines) are shown, and wells are shown by green dots.

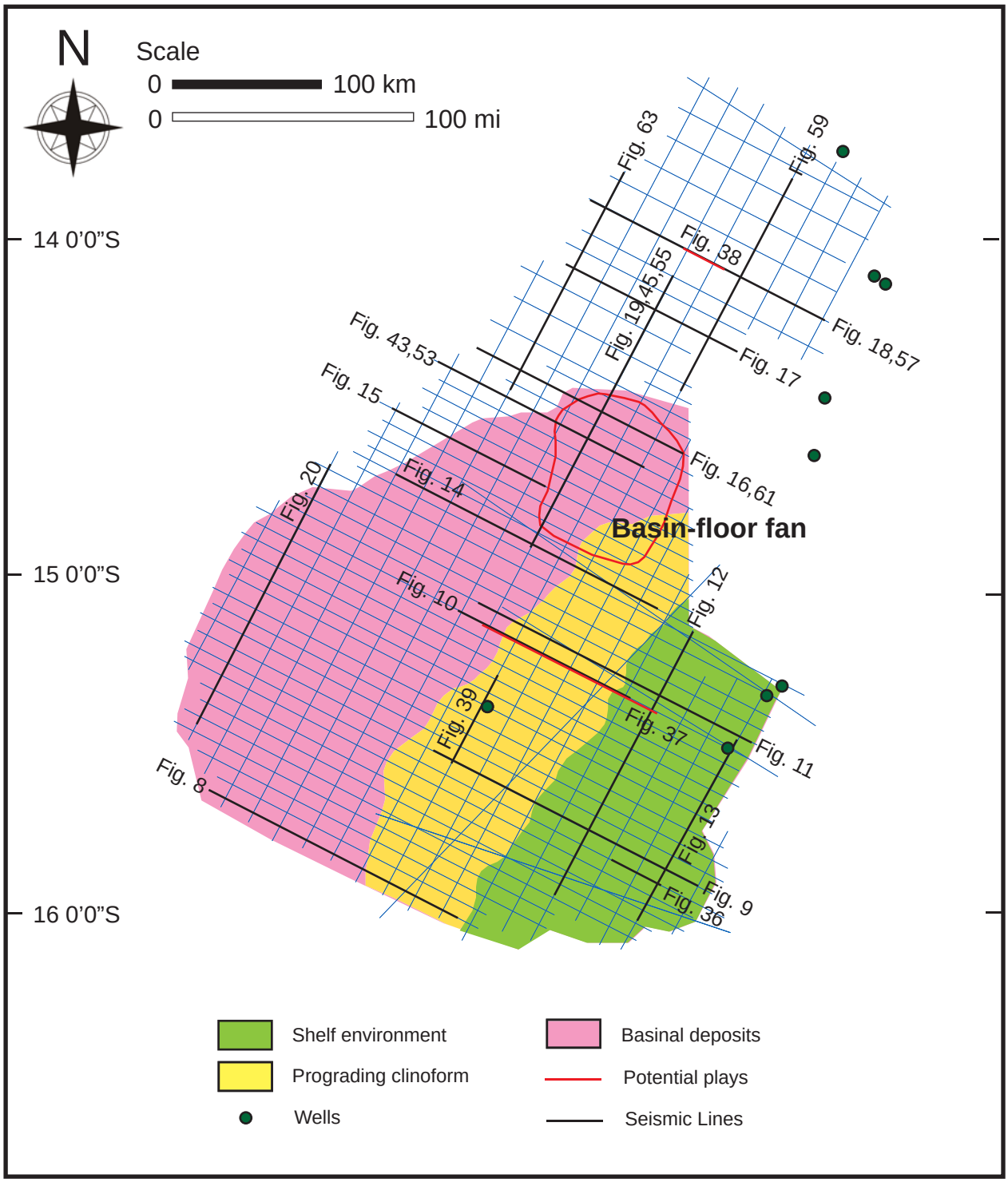

Figure 42. Geologic facies map of Subsequence I of Megasequence 1 (base Cretaceous to top Aptian: 145.5-112.0 Ma) interval. See Table 3 for a summary of seismic facies analysis and geologic interpretation. Locations of Figures 8-20, 36-39, 43-46, 53-64 (black lines) are shown, and wells are shown by green dots.

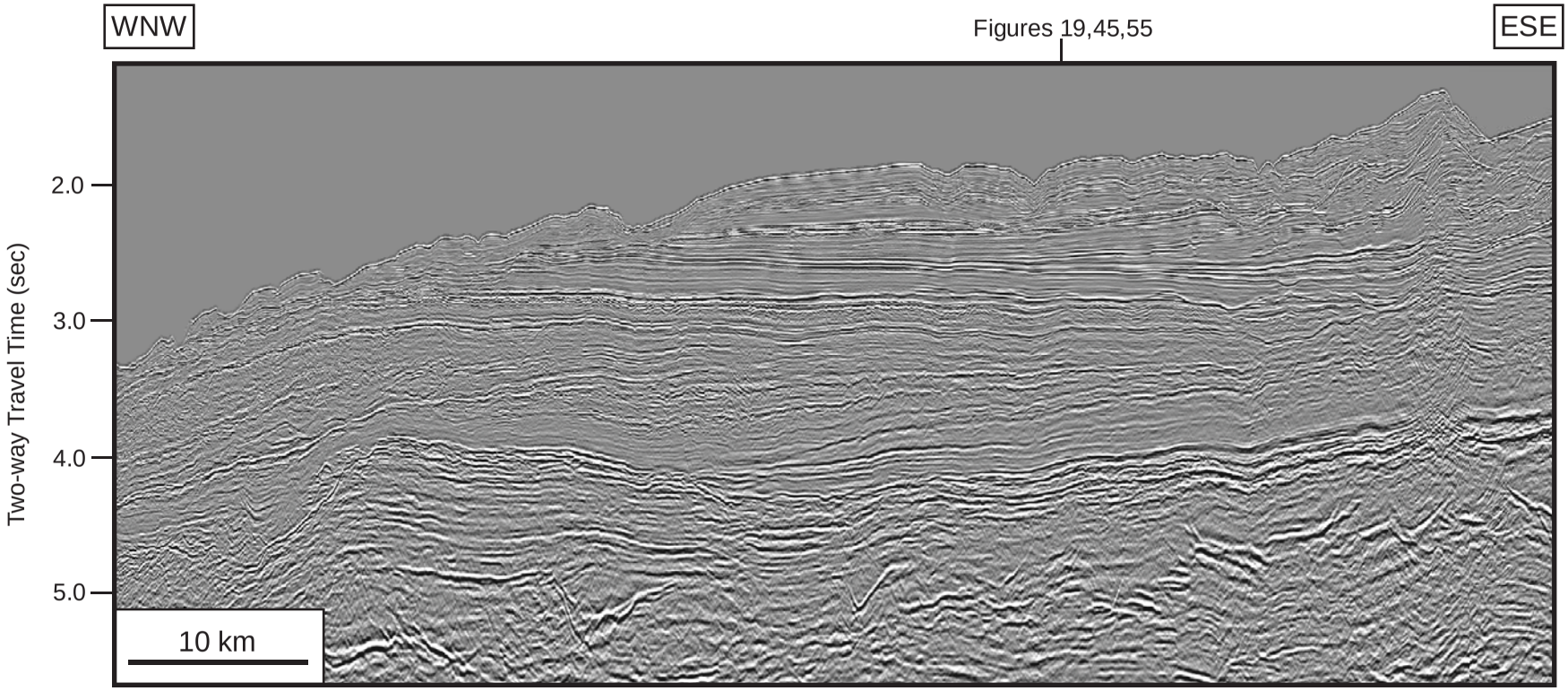

Figure 43a. Uninterpreted regional dip-oriented seismic profile (br-98:br98-033). Location of the profile is shown in Figures 34-35, 40-42, 47-52 and location of where Figures 19, 45, 55 crosses the profile.

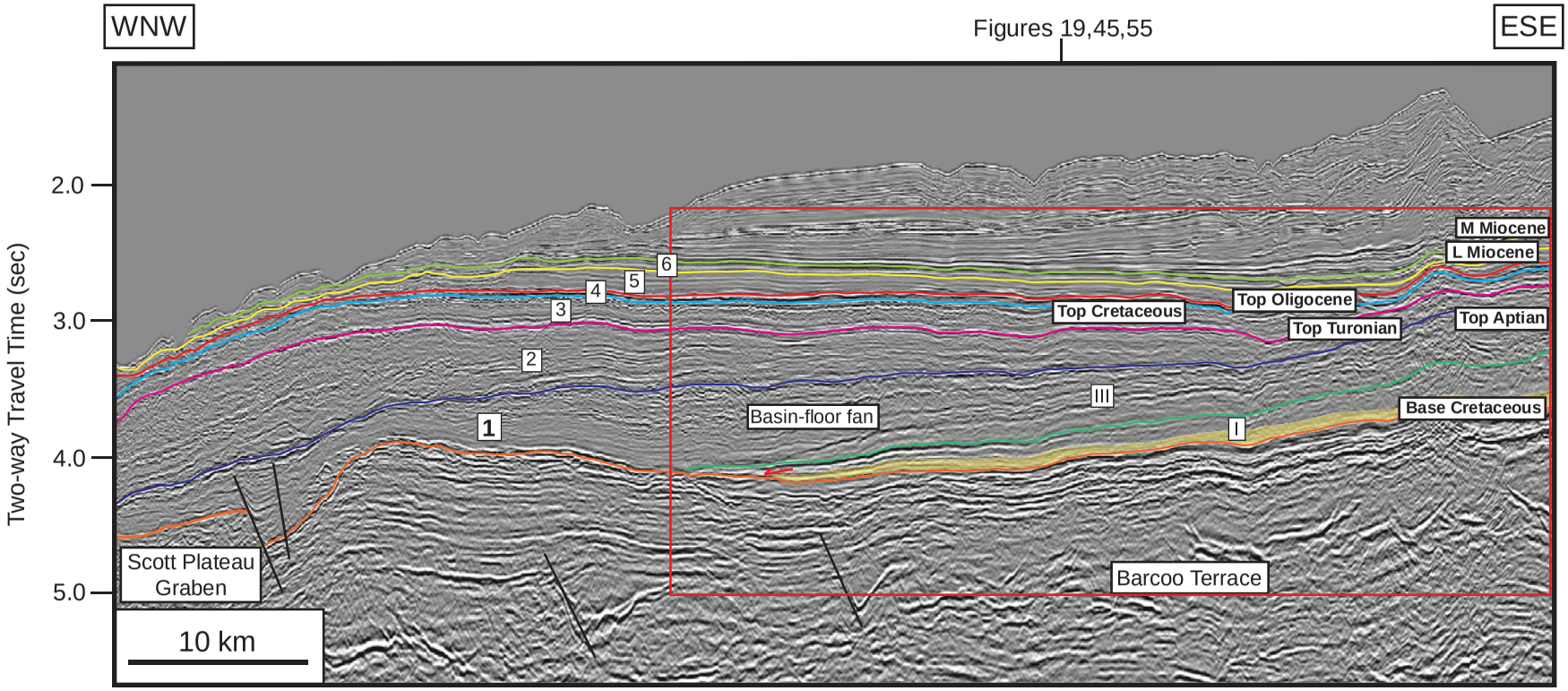

Figure 43b. Regional dip-oriented seismic profile showing all interpreted sequence boundaries from base Cretaceous to middle Miocene. This profile shows the deeper area of the Scott Plateau and the shallower area of the Barcoo Terrace. The basin-floor fan is observed within the low angle clinoform of Subsequence I of Megasequence 1 (yellow shade). Location of the profile is shown in Figures 34-35, 40-42, 47-52 and location of where Figures 19, 45, 55 crosses the profile.

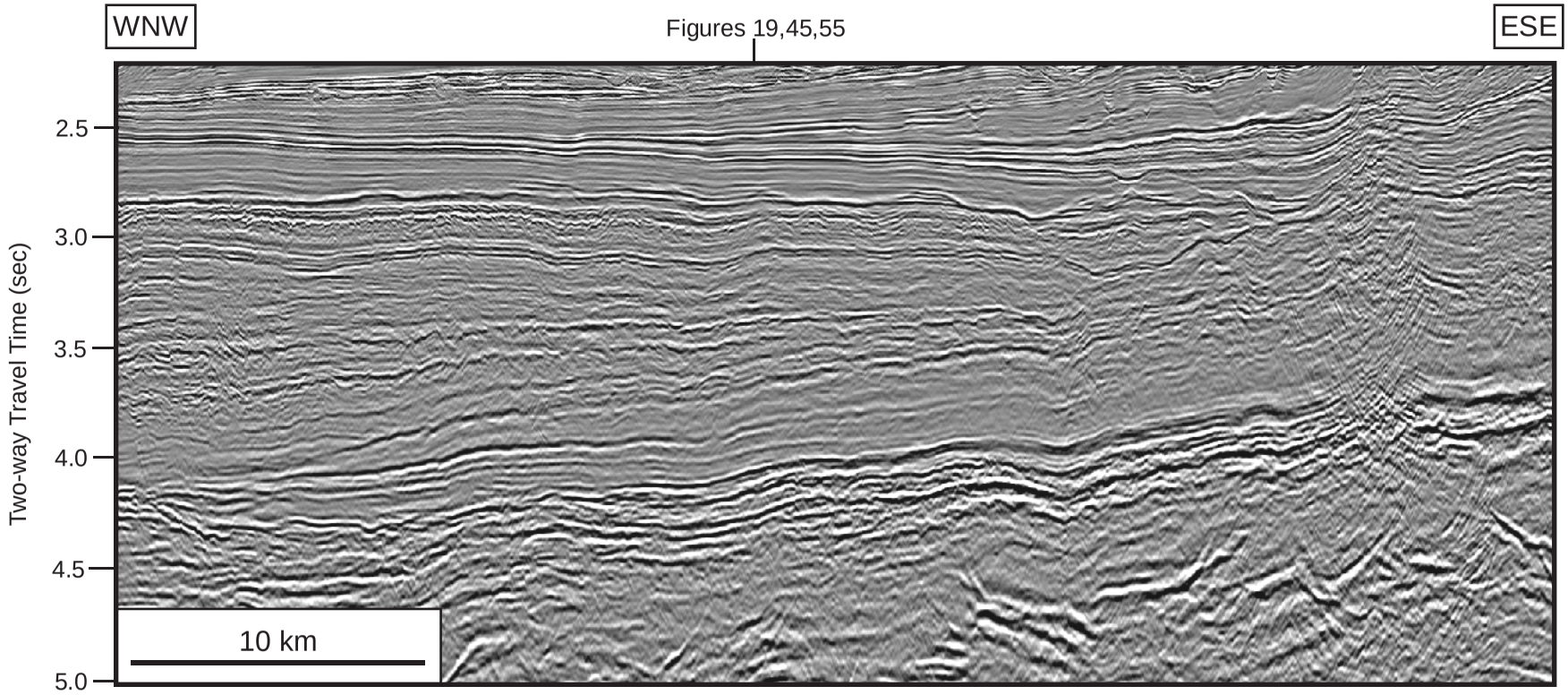

Figure 44a. Uninterpreted regional dip-oriented seismic profile (br-98:br98-033): A closeup view of Figure 43.

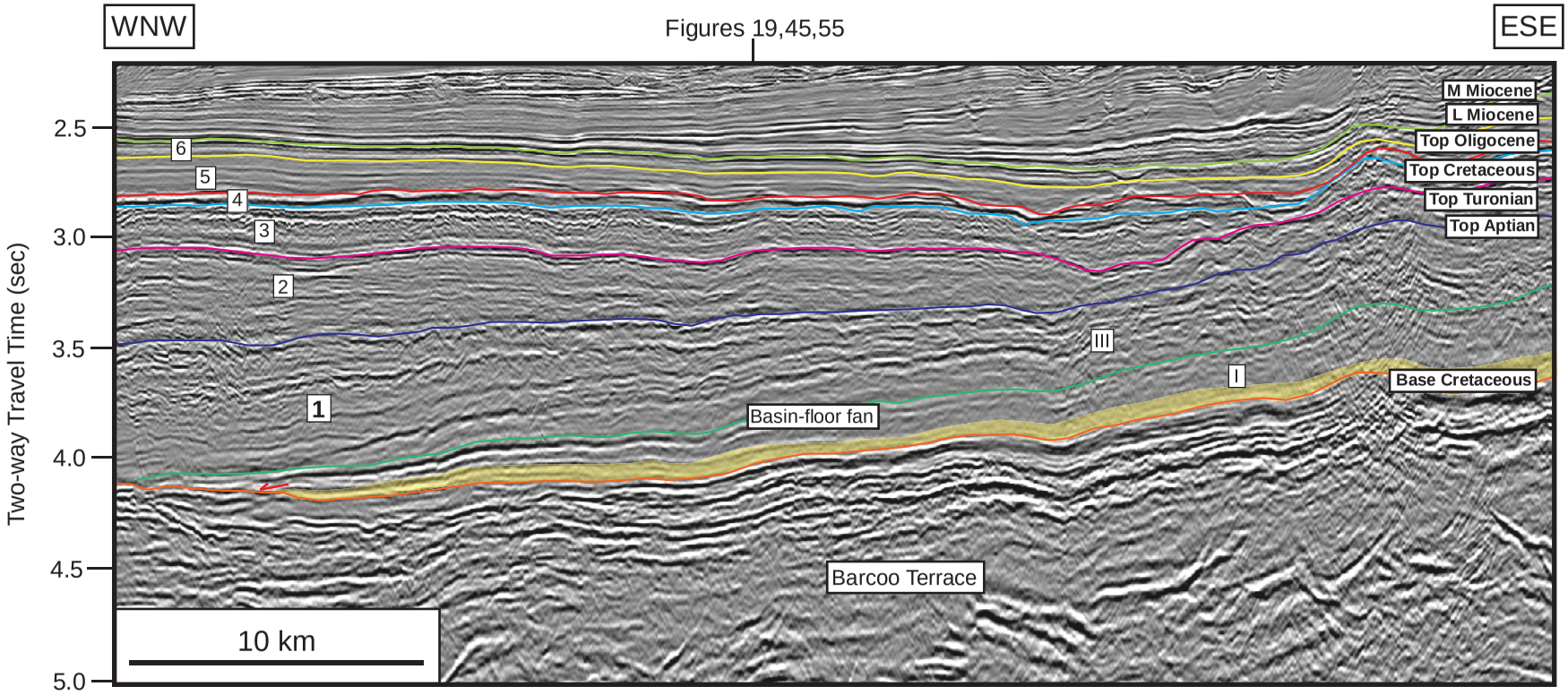

Figure 44b. Regional dip-oriented seismic profile showing all interpreted sequence boundaries from base Cretaceous to middle Miocene: A closeup view of Figure 43. The basin-floor fan is observed within the low angle clinoform of Subsequence I of Megasequence 1 (yellow shade).

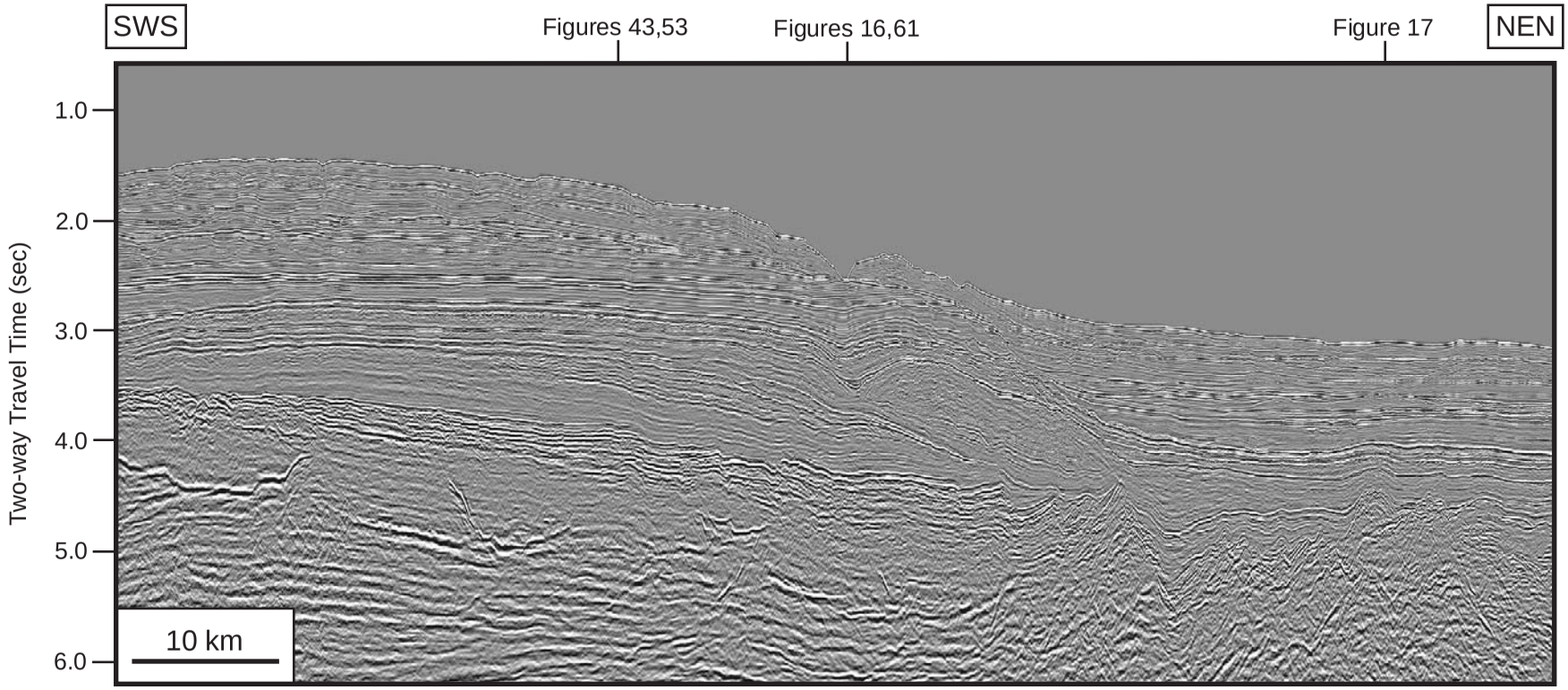

Figure 45a. Uninterpreted regional strike-oriented seismic profile (br-98:br98-082). Location of the profile is shown in Figures 34-35, 40-42, 47-52 and locations of where Figures 16, 17, 43, 53, 61 cross the profile.

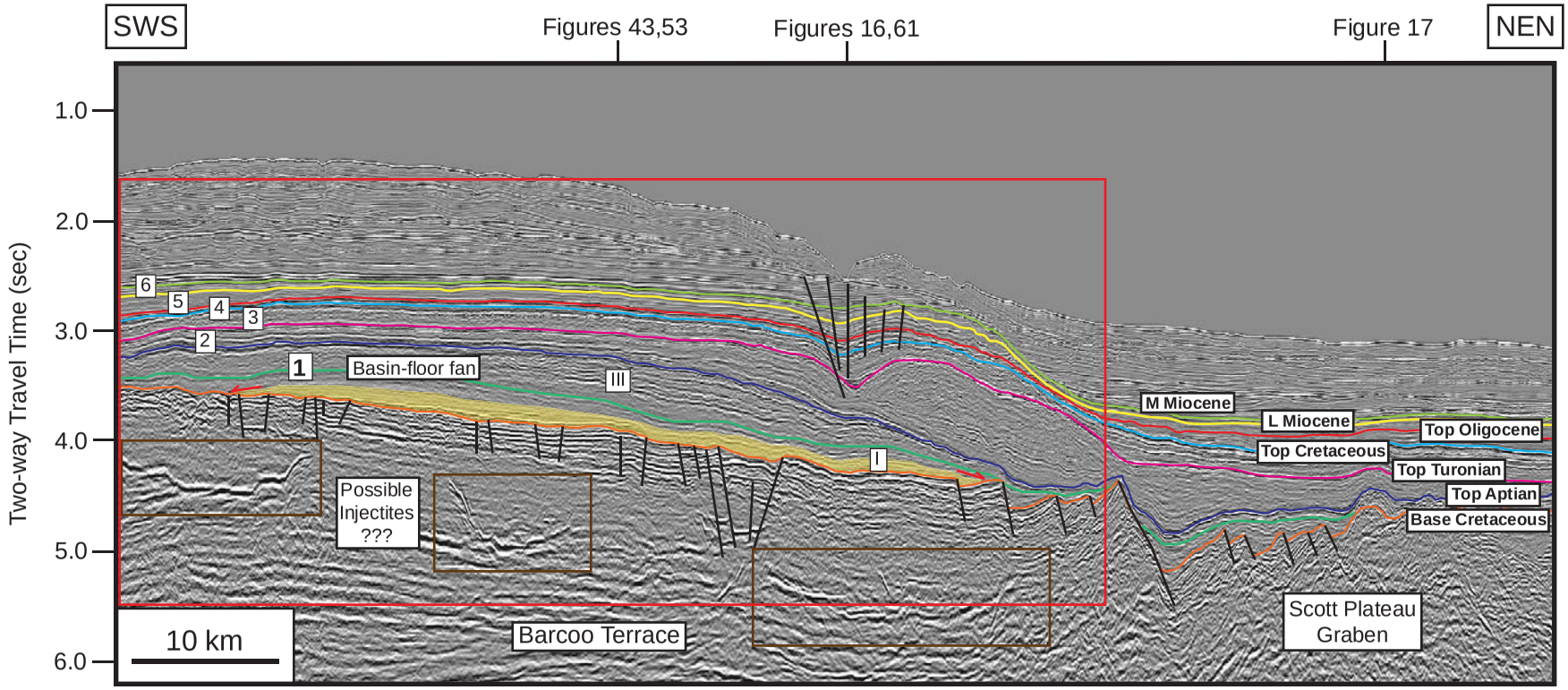

Figure 45b. Regional strike-oriented seismic profile showing all interpreted sequence boundaries from base Cretaceous to middle Miocene. The Barcoo Fault System and possible injectites are observed in the underlying Jurassic strata. The profile displays the shallower area of the Barcoo Terrace and deeper area of the Scott Plateau Graben. The basin-floor fan is observed in Subsequence I of Megasequence 1 (yellow shade). Location of the profile is shown in Figures 34-35, 40-42, 47-52 and locations of where Figures 16, 17, 43, 53, 61 cross the profile.

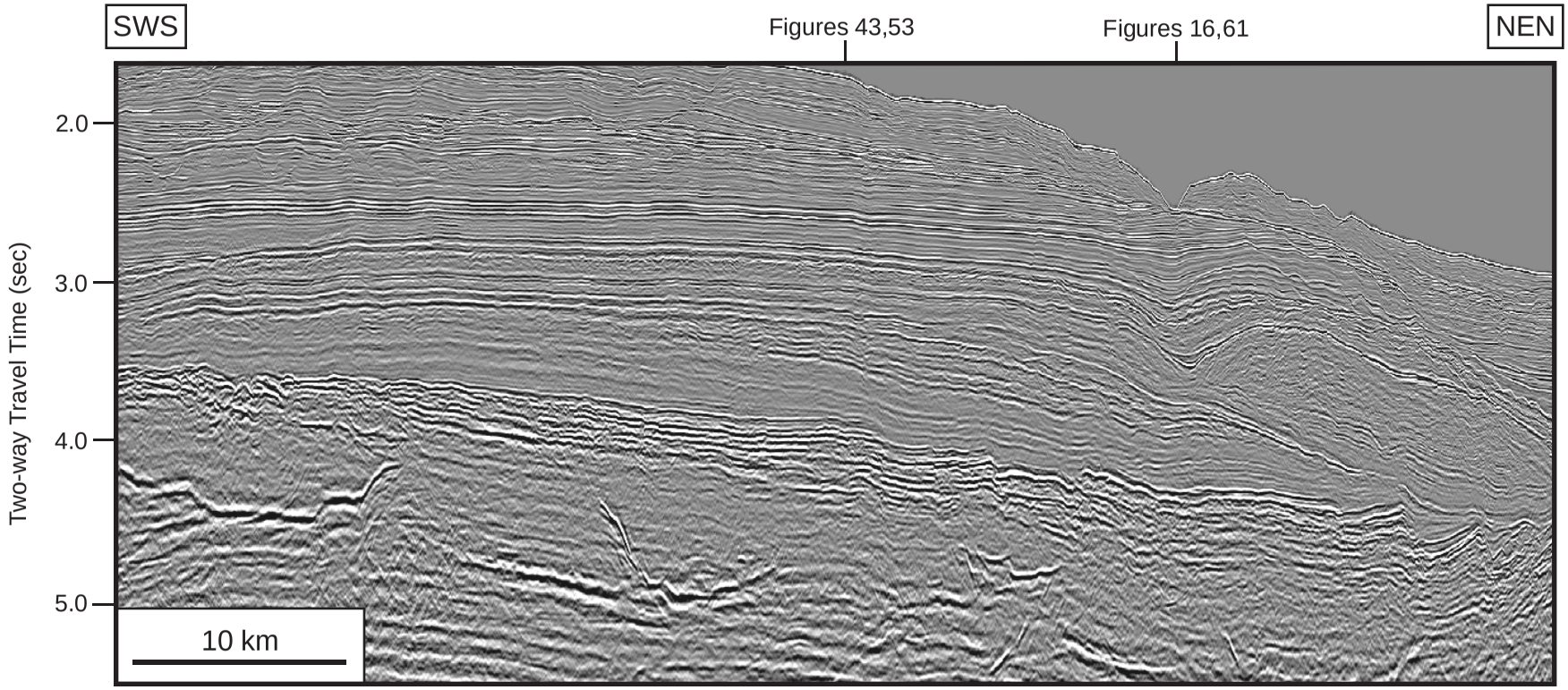

Figure 46a. Uninterpreted regional strike-oriented seismic profile (br-98:br98-082): A closeup view of Figure 45.

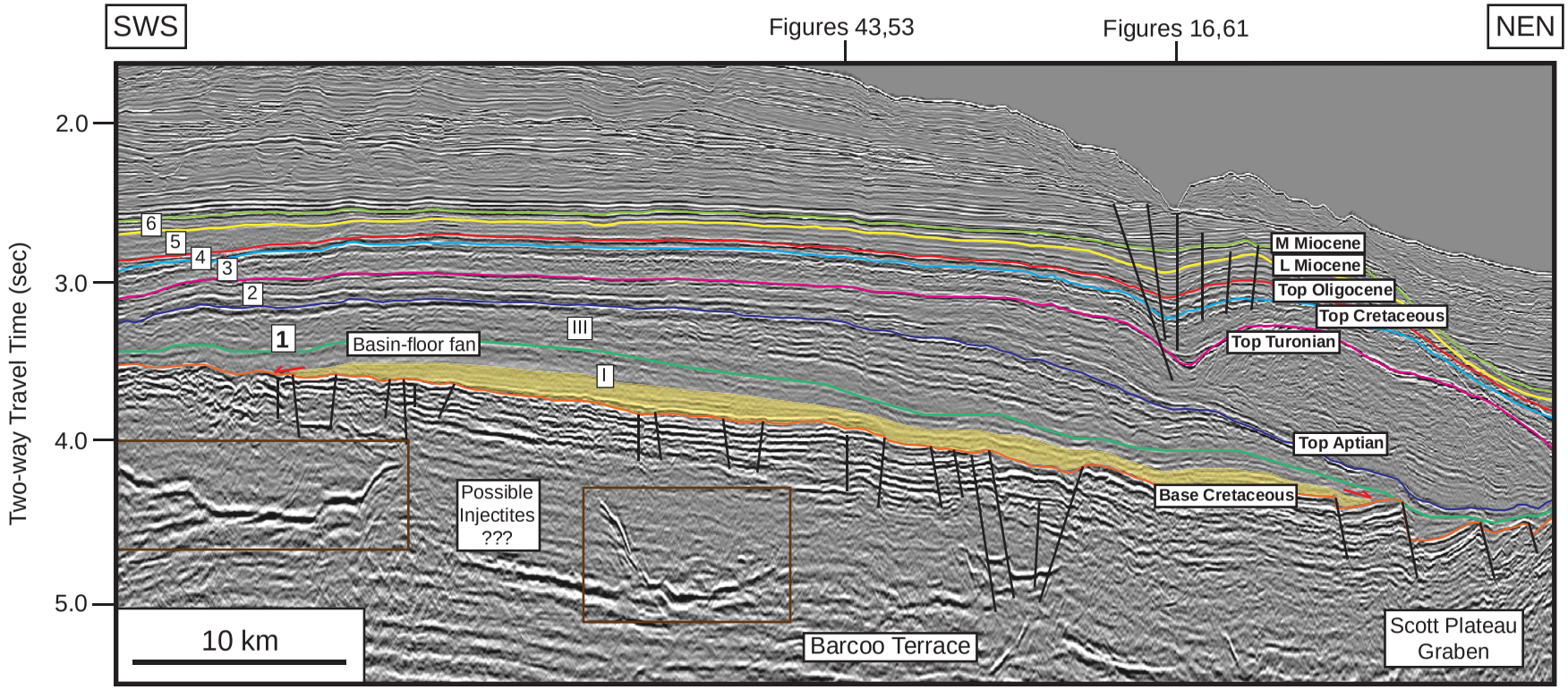

Figure 46b. Regional strike-oriented seismic profile showing all interpreted sequence boundaries from base Cretaceous to middle Miocene: A closeup view of Figure 45. The basin-floor fan is observed in Subsequence I of Mega sequence 1 (yellow shade).

Subsequence II of Megasequence 1

This subsequence is present only in the area of the Barcoo Platform at the southeastern part of the study area. This subsequence displays the sediment wedge shape of deepwater deposit (Figures 9, 12, 13). The thickest area is located at the Barcoo Platform. The isochron map of this subsequence illustrates the thickness values varying from 0 to 240 msec two-way travel time (TWTT) (Figure 47).

Seismic Facies 2 and 3 are recognized within this subsequence (Figures 48; Table 4). The facies 2 is the prograding clinoform which illustrates the moderate to high amplitude and poor to fair continuity whereas the facies 3 shows the hummocky reflection configuration which is interpreted to be the shelf environment.

Table 4. Seismic facies and geologic interpretation of Subsequence II of Megasequence 1

Seismic Facies	Upper Sequence Boundary	Lower Sequence Boundary	Internal Reflection Configuration	Amplitude	Continuity	Geologic Interpretation
2	Concordant	Downlap	Clinoform	moderate to high	poor to fair	Prograding clinoform
3	Concordant	Concordant	Hummocky	moderate	poor	Inversion – related structure

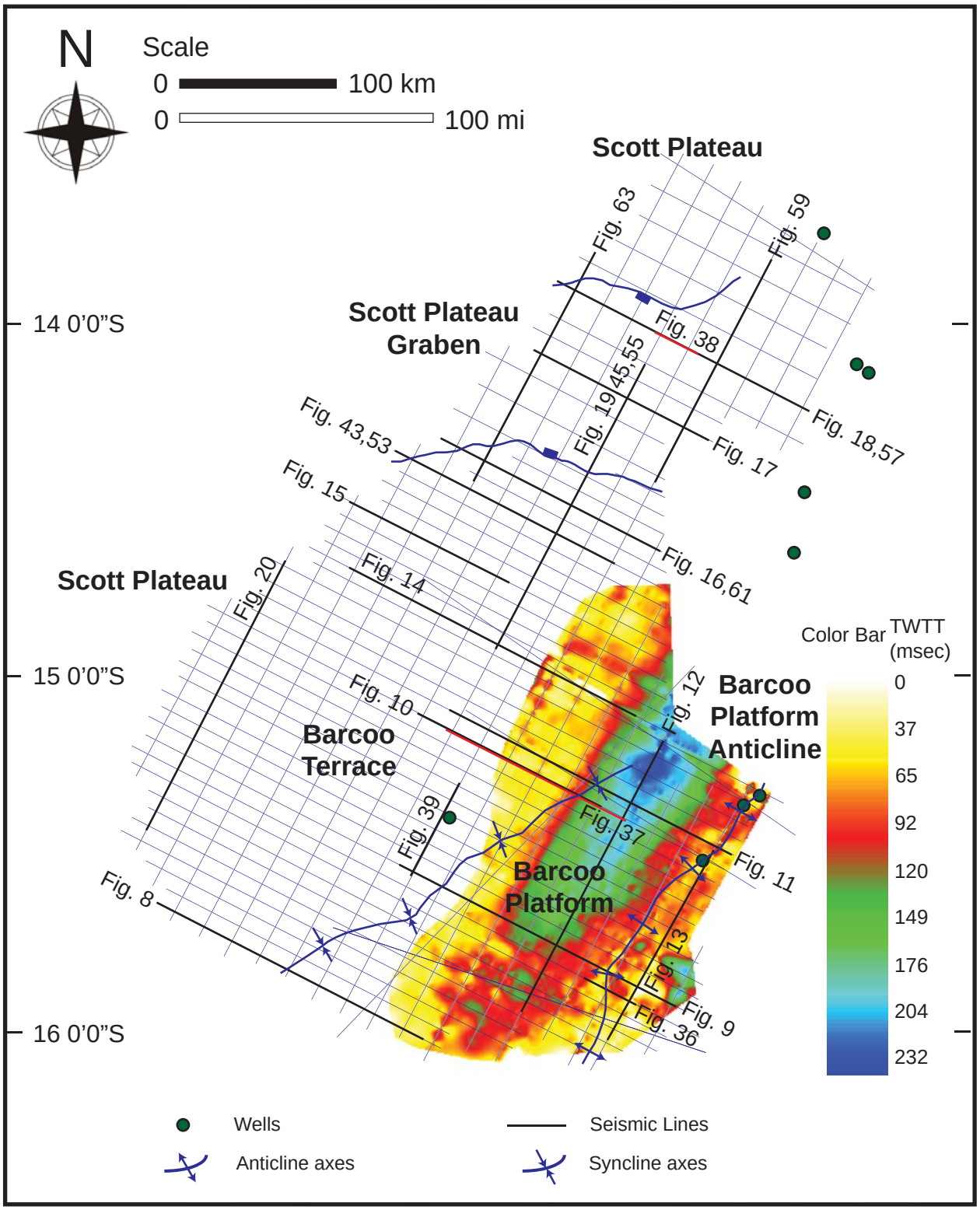

Figure 47. Isochron map (in TWTT msecs) of Subsequence II of Megasequence 1 interval. Distribution of 2D seismic profiles interpreted to generate the maps are shown by white lines, and wells are shown by green dots. Locations of Figures 8-20, 36-39, 43-46, 53-64 are shown.

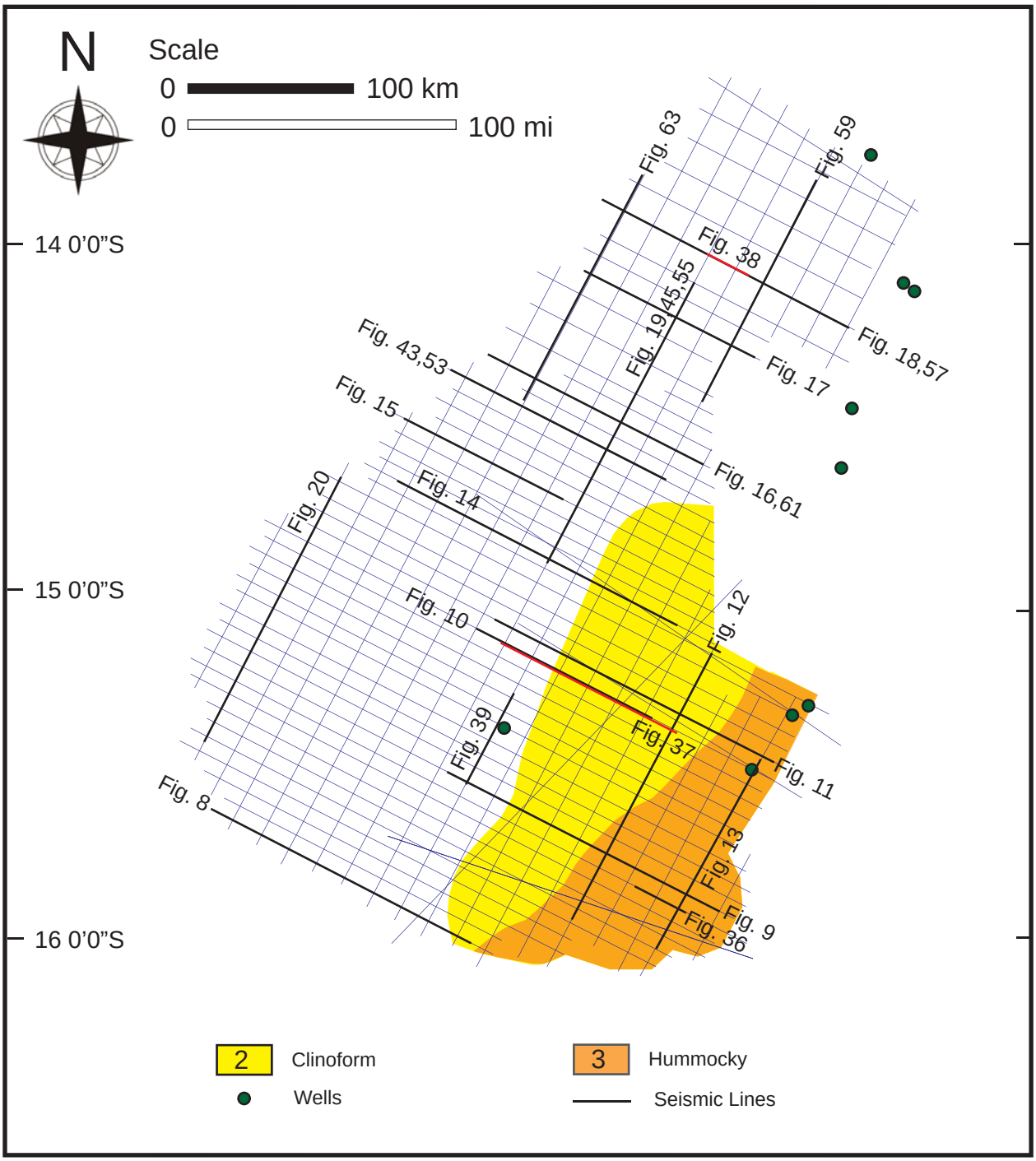

Figure 48. Seismic facies map of Subsequence II of Megasequence 1 interval. Each facies is numbered as described in the text. See Table 2 for seismic facies coding and Table 3 for a summary of seismic facies analysis and geologic interpretation. Locations of Figures 8-20, 36-39, 43-46 and 53-64 (black lines) are shown, and wells are shown by green dots.

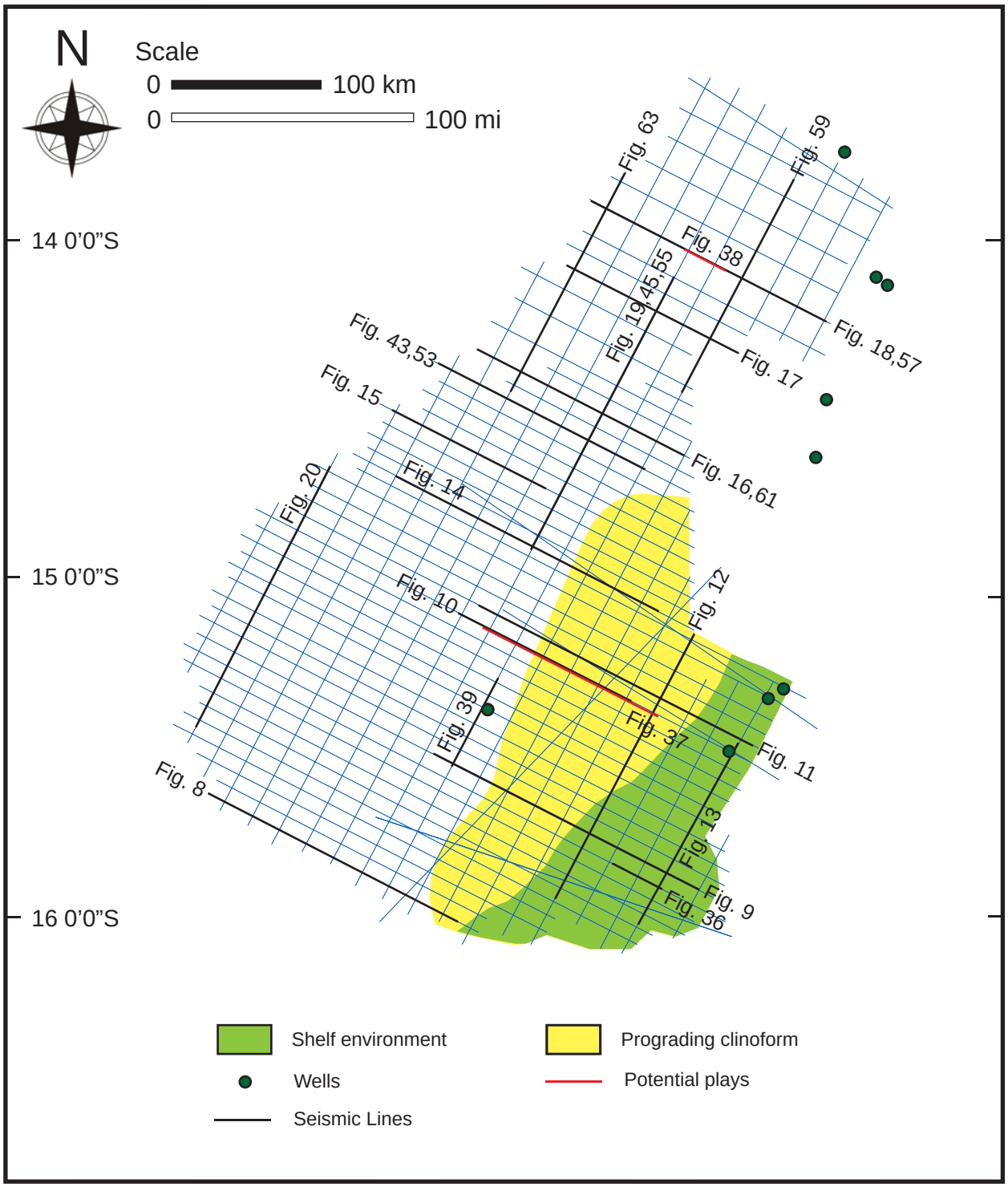

Figure 49. Geologic facies map of Subsequence II of Megasequence 1 (base Cretaceous to top Aptian: 145.5-112.0 Ma) interval. See Table 3 for a summary of seismic facies analysis and geologic interpretation. Locations of Figures 8-20, 36-39, 43-46, 53-64 (black lines) are shown, and wells are shown by green dots.

Subsequence III of Megasequence 1

Subsequence III is the main interval of Megasequence 1. The isochron map shows the value ranges from 0 to 1094 msec two-way travel time (TWTT) (Figure 50). The thickest sediment deposited on the Barcoo Terrace, at the edge of the Scott Plateau Graben.

Six seismic facies are identified in this subsequence (Figure 43; Table 5). Facies 1 and 4 covers the large part of the study area. Both of them illustrated the seismic reflections concordant to the upper and lower sequence boundaries. They are interpreted to be the shelf and basin-floor environments, respectively.

Seismic facies 2 demonstrates the concordant to the upper sequence boundary whereas the downlap termination on to the lower sequence boundary. Its amplitude is moderate to high with poor to fair continuity. The internal reflection configuration of Facies 3 is the hummocky. The amplitude is moderate whereas the continuity is poor to good. The seismic facies 2 and 3 are interpreted to be the prograding clinoform at the shelf edge between the Barcoo Platform and the Barcoo Terrace.

Table 5. Seismic facies and geologic interpretation of Subsequence III of Megasequence 1

Seismic Facies	Upper Sequence Boundary	Lower Sequence Boundary	Internal Reflection Configuration	Amplitude	Continuity	Geologic Interpretation
1	Concordant	Concordant	Parallel to Subparallel	moderate	fair to good	Shelf deposits
2	Concordant	Downlap	Clinoform	moderate to high	poor to fair	Prograding clinoform
3	Concordant	Concordant	Hummocky	moderate	poor	Inversion – related structure
4	Concordant	Concordant	Parallel to Subparallel	moderate	fair to good	Basinal deposits
5	-	-	Chaotic	low	poor	Basinal deposits
6	-	-	Chaotic	moderate to high	poor	Carbonate buildup

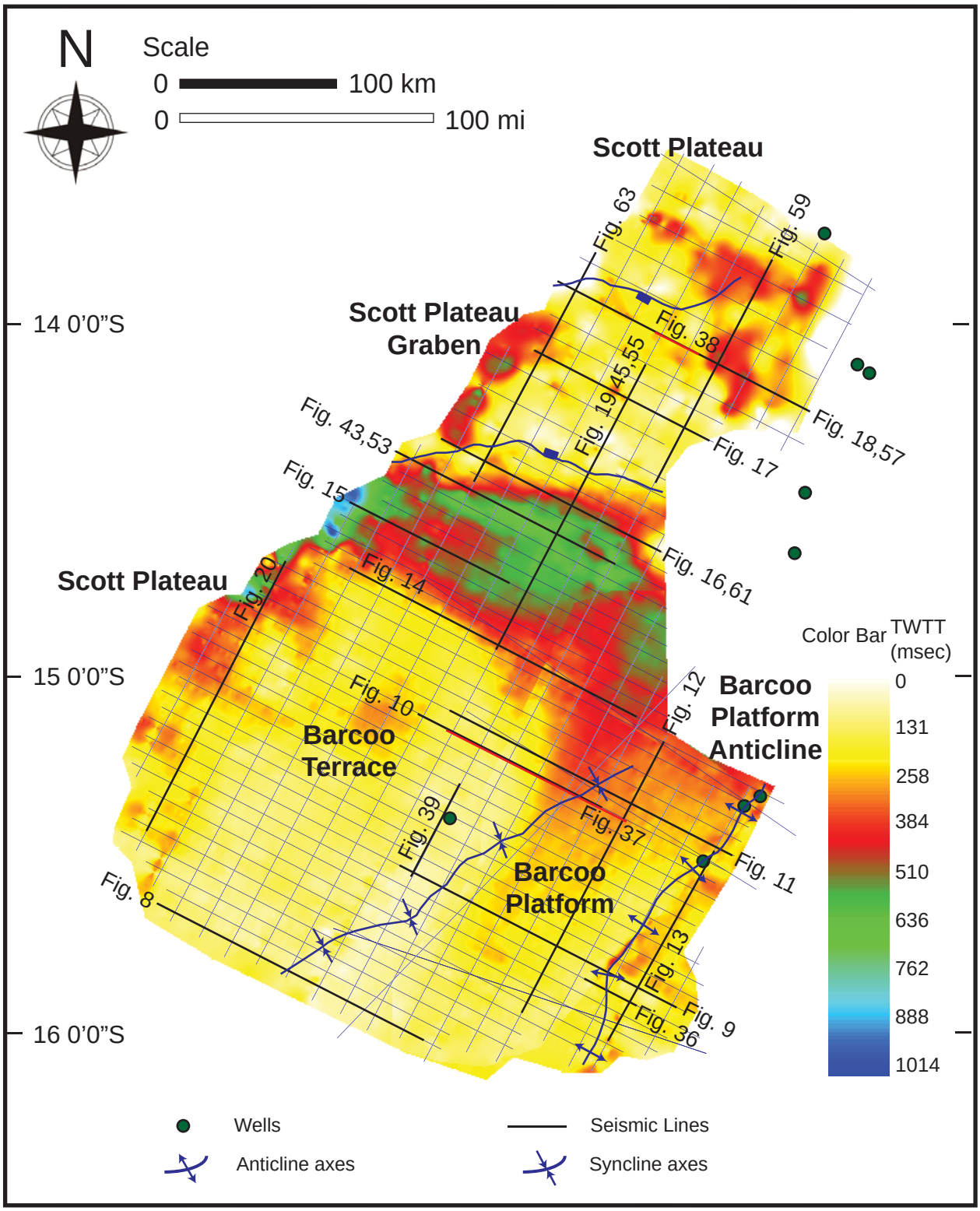

Figure 50. Isochron map (in TWTT msecs) of Subsequence III of Megasequence 1 interval. Distribution of 2D seismic profiles interpreted to generate the maps are shown by white lines, and wells are shown by green dots. Locations of Figures 8-20, 36-39, 43-46, 53-64 are shown.

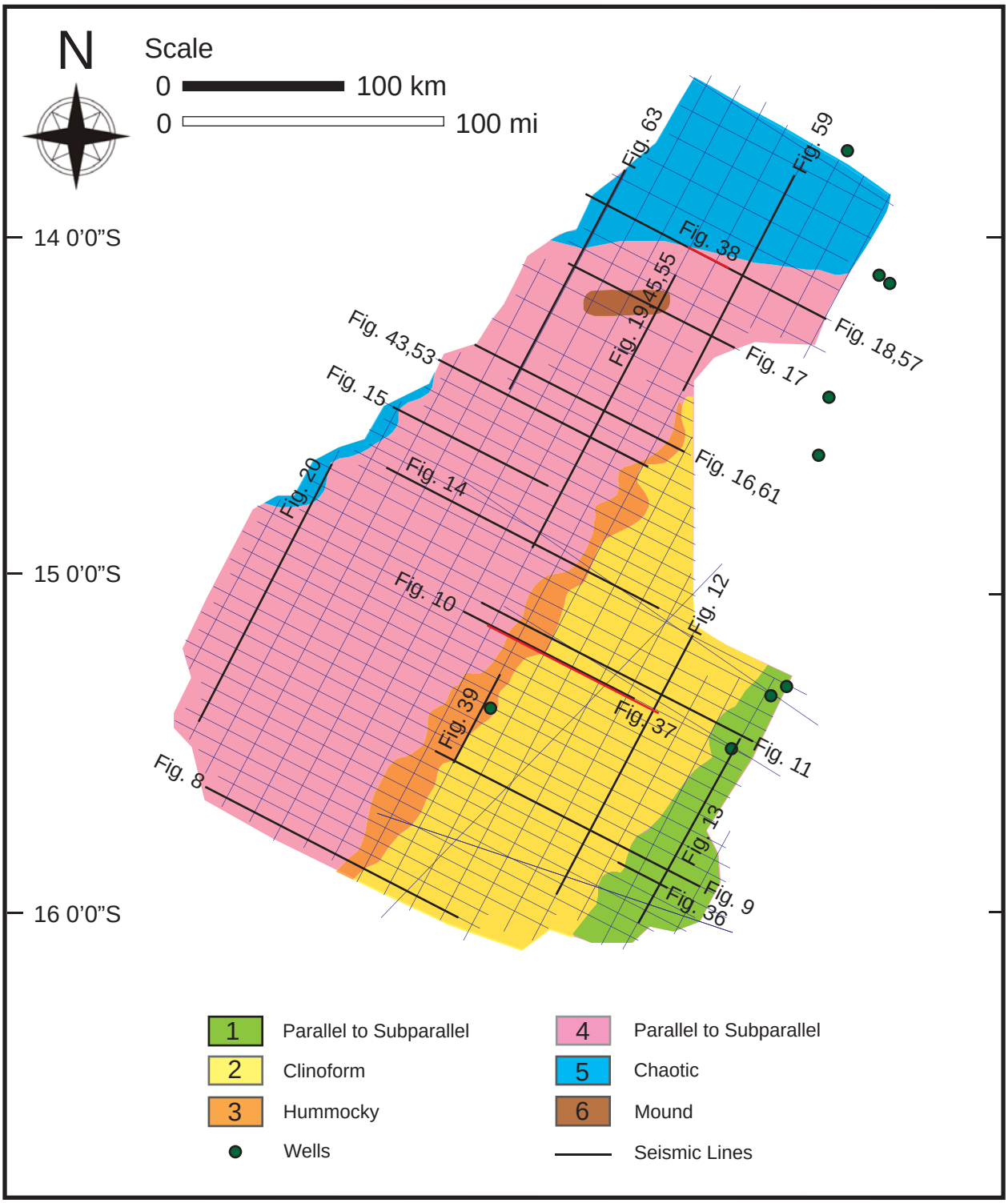

Figure 51. Seismic facies map of Subsequence III of Megasequence 1 interval. Each facies is numbered as described in the text. See Table 2 for seismic facies coding and Table 3 for a summary of seismic facies analysis and geologic interpretation. Locations of Figures 8-20, 8-20, 36-39, 43-46 and 53-64 (black lines) are shown, and wells are shown by green dots.

Facies 5 shows the chaotic internal reflection configuration with low amplitude and poor continuity. However, this facies is interpreted to be the part of the basin environment same as facies 4. The last seismic facies, 6, is the build-up structure which could be either carbonate or volcanic. However, from the previous study and data availibity, it is interpreted to be the carbonate build-up structure. One more feature which could be found in this subsequence is the partially eroded of the basinal environment (Figures 15, 20).

At least 3 potential prospects are identified. One is the basin-floor fan and other two are the potential deepwater sediments which are controlled by structural features. These prospects are indicated by the bi-directional downlap termination to the lower sequence boundary. The dip and strike oriented seismic profile are shown in Figures 53-64.

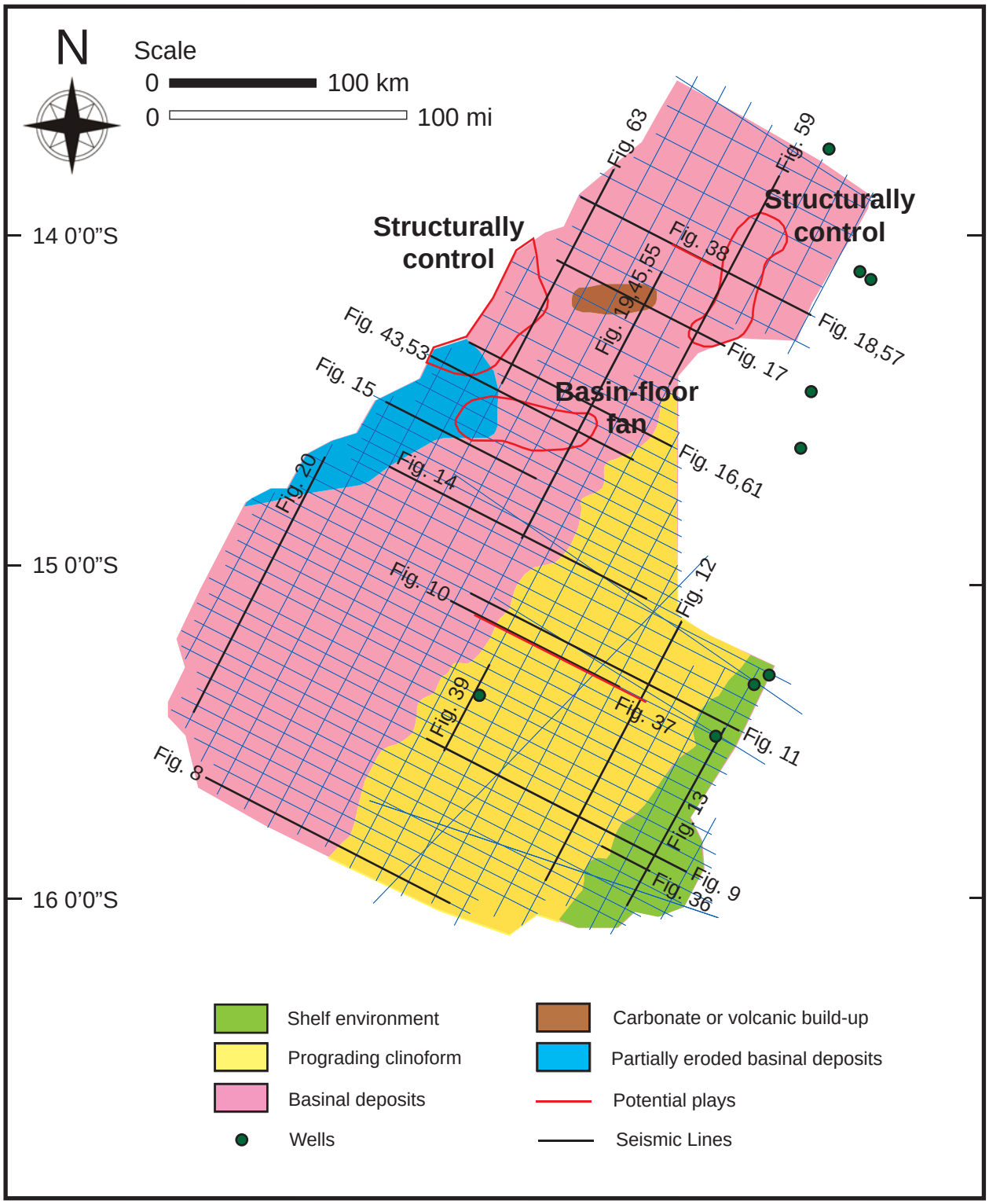

Figure 52. Geologic facies map of Subsequence III of Megasequence 1 (base Cretaceous to top Aptian: 145.5-112.0 Ma) interval. See Table 3 for a summary of seismic facies analysis and geologic interpretation. Locations of Figures 8-20, 36-39, 43-46, 53-64 (black lines) are shown, and wells are shown by green dots.

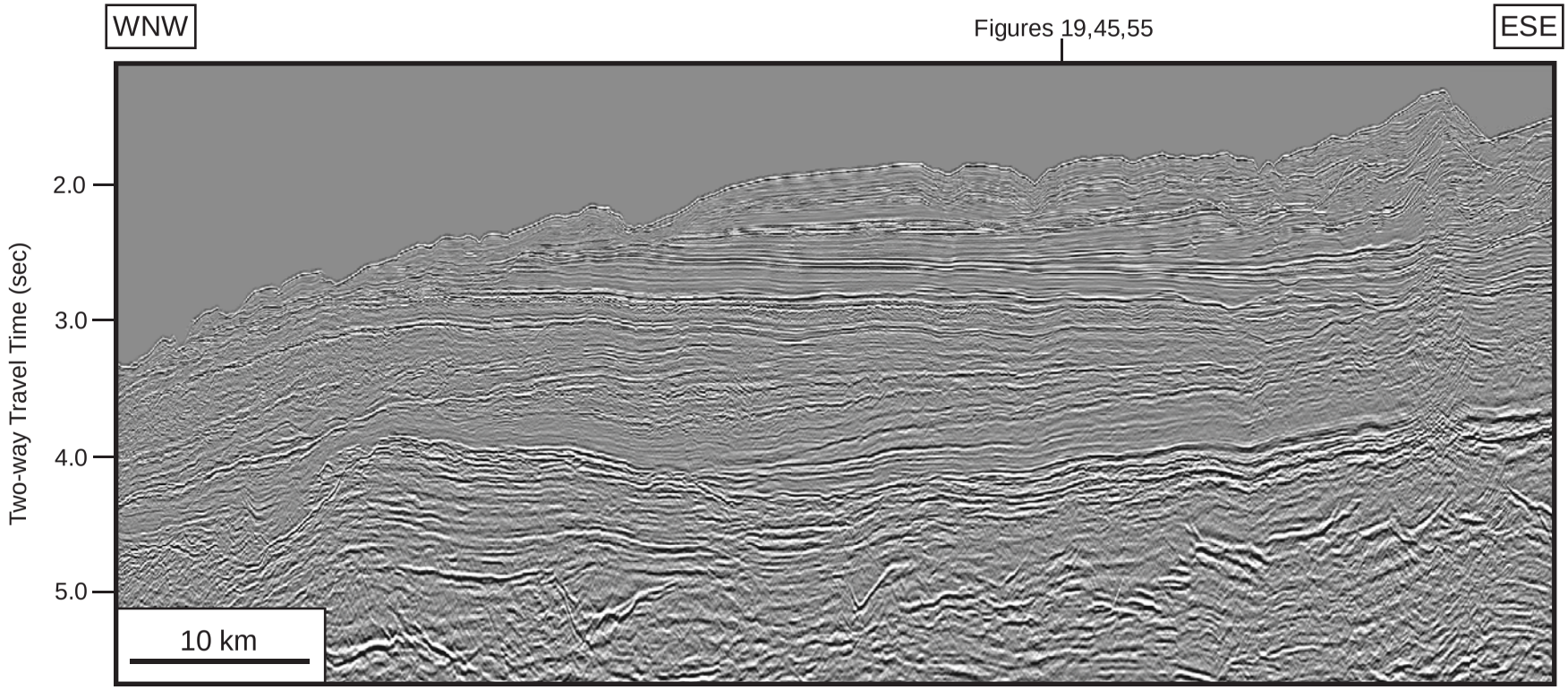

Figure 53a. Uninterpreted regional dip-oriented seismic profile (br-98:br98-033). Location of the profile is shown in Location of the profile is shown in Figures 34-35, 40-42, 47-52 and location of where Figures 19, 45, 55 crosses the profile.

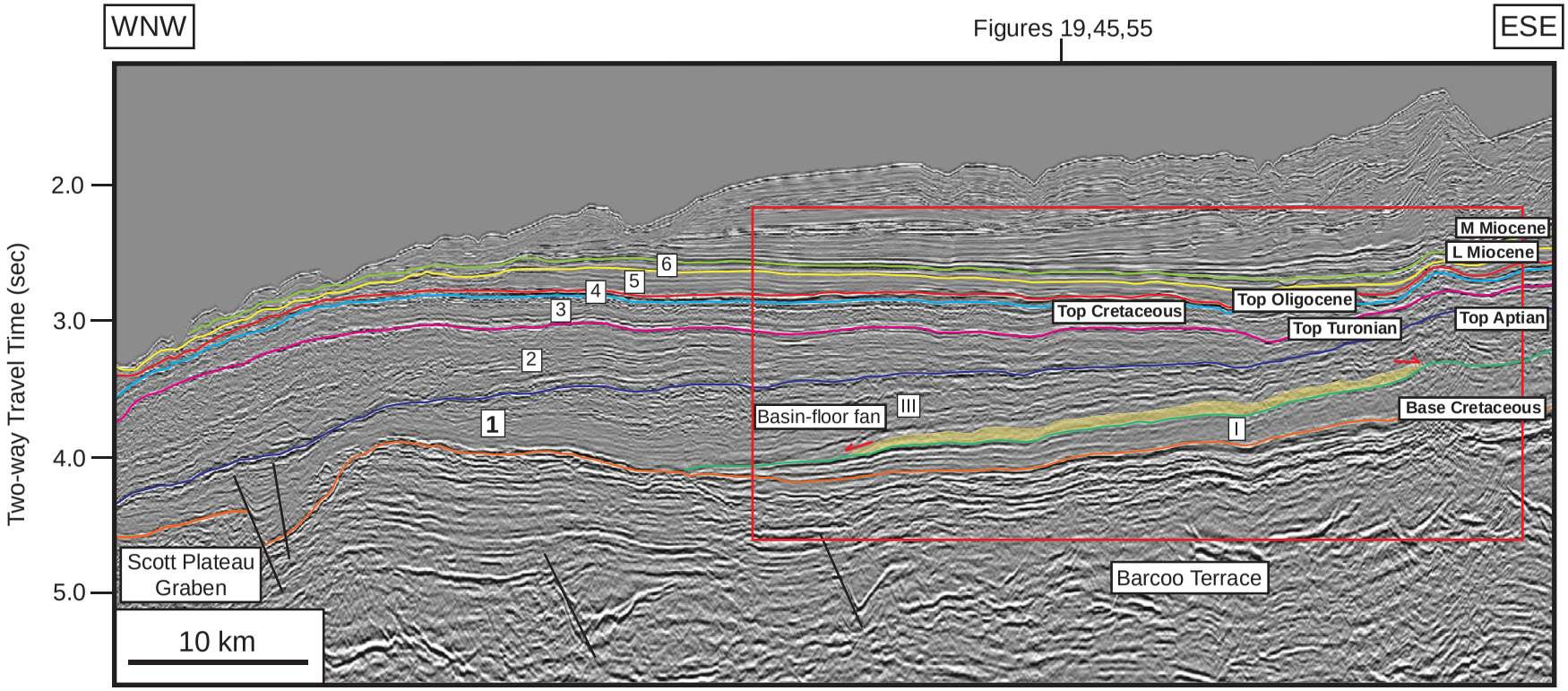

Figure 53b. Regional dip-oriented seismic profile showing all interpreted sequence boundaries from base Cretaceous to middle Miocene. This profile shows the deeper area of the Scott Plateau and the shallower area of the Barcoo Terrace. The basin-floor fan is observed within the low angle clinoform of Subsequence III of Megasequence 1 (yellow shade). Location of the profile is shown in Location of the profile is shown in Figures 34-35, 40-42, 47-52 and location of where Figures 19, 45, 55 crosses the profile.

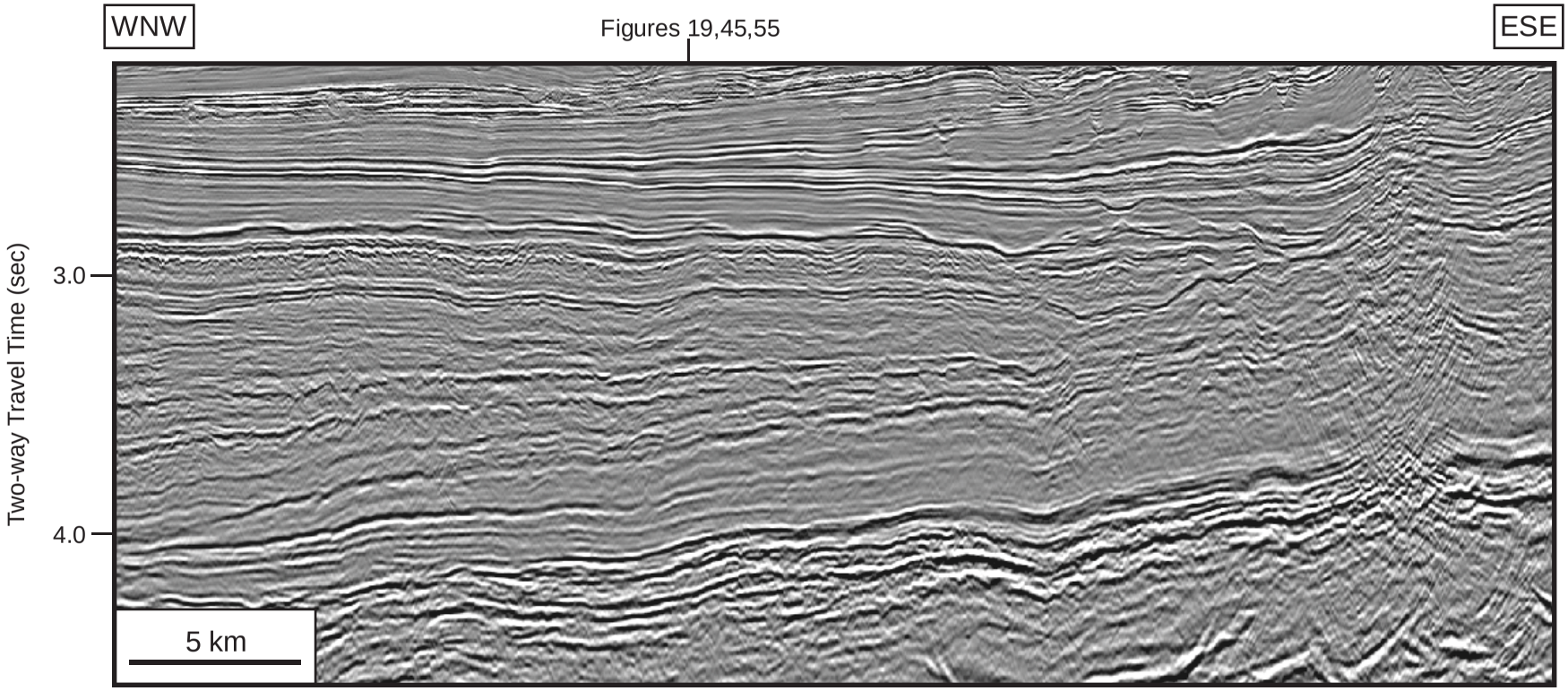

Figure 54a. Uninterpreted regional dip-oriented seismic profile (br-98:br98-033): A closeup view of Figure 53.

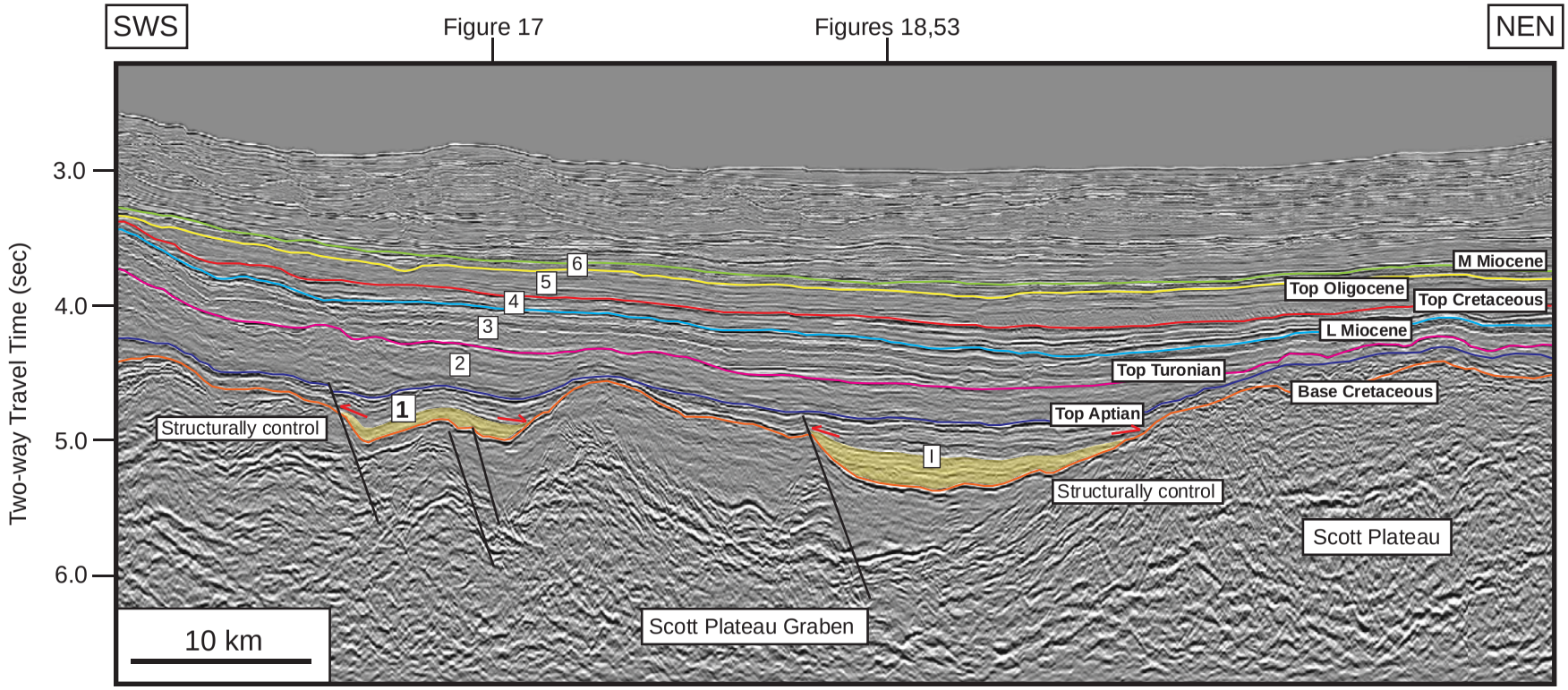

Figure 54b. Regional strike-oriented seismic profile showing all interpreted sequence boundaries from base Cretaceous to middle Miocene. This profile shows the area of the Scott Plateau and the shallower area of the Barcoo Terrace. The basin-floor fan is observed within Subsequence I of Megasequence 1 (yellow shade). Location of the profile is shown in Figures 34-35, 40-42, 45-50 and locations of where Figures 17, 18, 53 cross the profile.

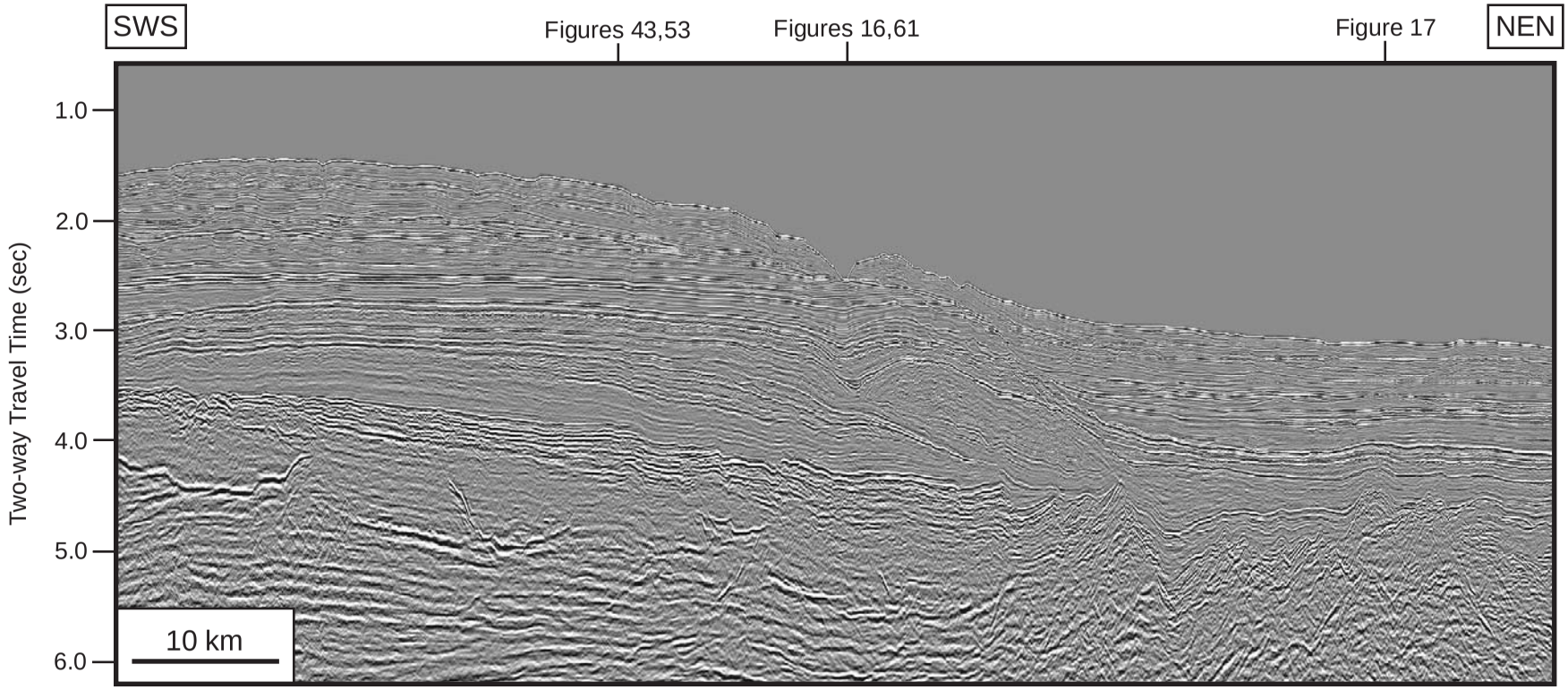

Figure 55a. Uninterpreted regional strike-oriented seismic profile (br-98:br98-082). Location of the profile is shown in Figures 34-35, 40-42, 47-52 and locations of where Figures 16, 17, 43, 53, 61 cross the profile.

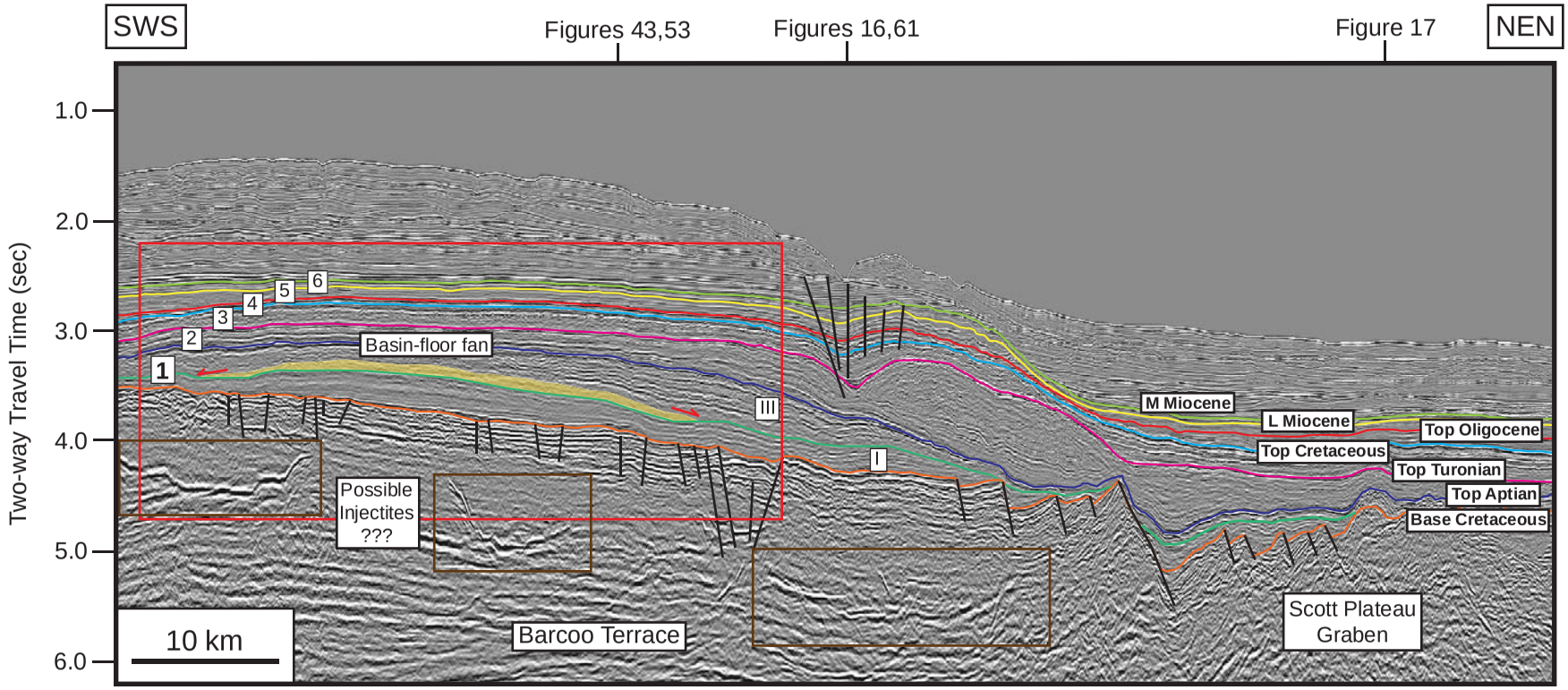

Figure 55b. Regional strike-oriented seismic profile showing all interpreted sequence boundaries from base Cretaceous to middle Miocene. The Barcoo Fault System and possible injectites are observed in the underlying Jurassic strata. The profile displays the areas of the Barcoo Terrace and the Scott Plateau Graben. The basin-floor fan is observed in Subsequence III of Megasequence 1 (yellow shade). Location of the profile is shown in Figures 34-35, 40-42, 47-52 and locations of where Figures 16, 17, 43, 53, 61 cross the profile.

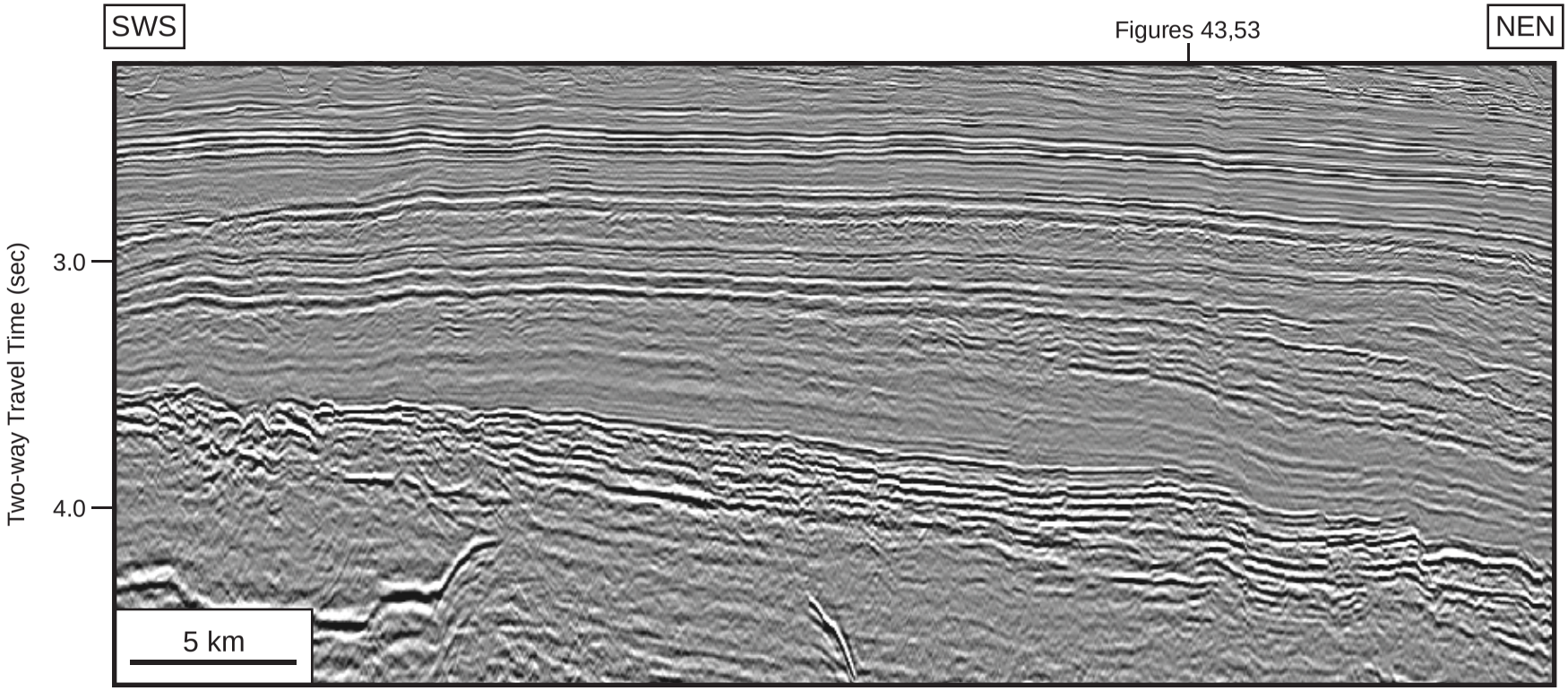

Figure 56a. Uninterpreted regional strike-oriented seismic profile (br-98:br98-082): A closeup view of Figure 55.

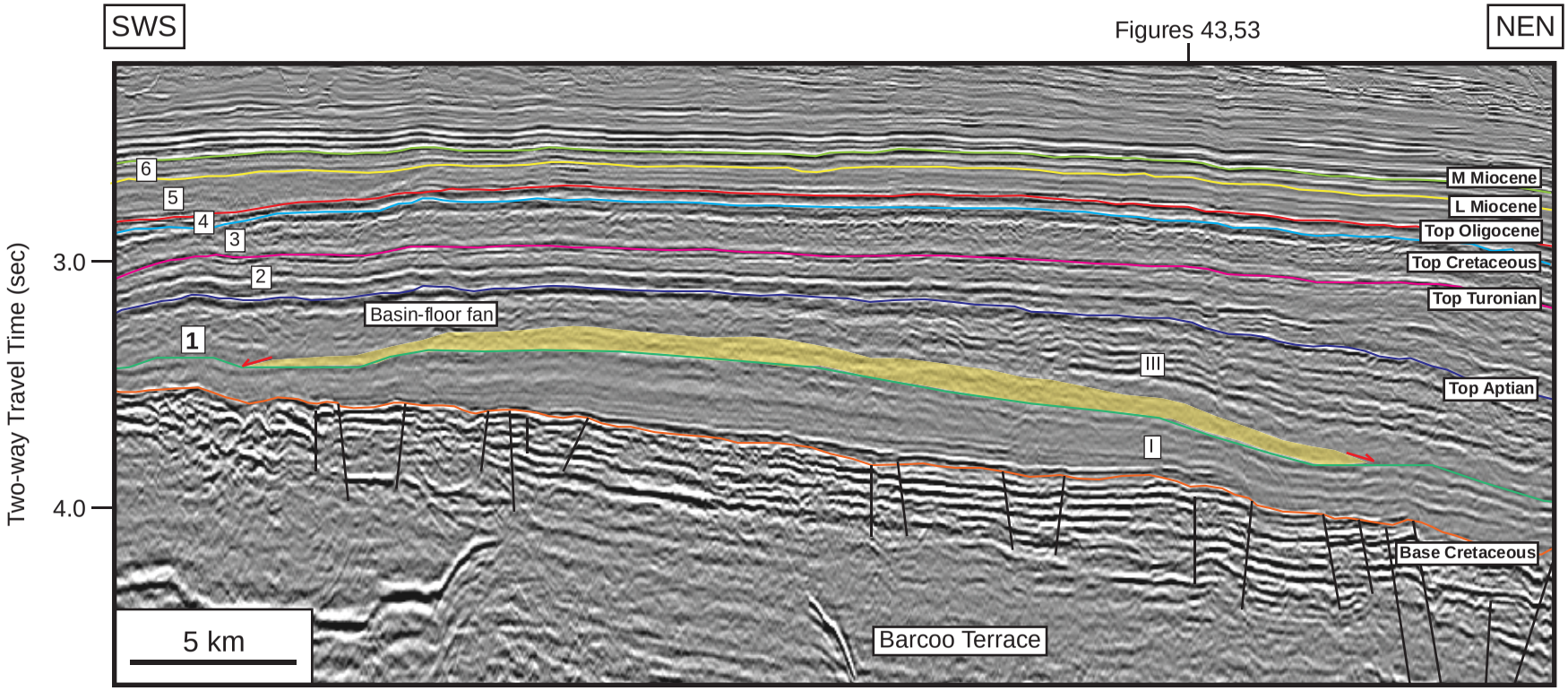

Figure 56b. Regional strike-oriented seismic profile showing all interpreted sequence boundaries from base Cretaceous to middle Miocene: A closeup view of Figure 55. The basin-floor fan is observed in Subsequence III of Megasequence 1 (yellow shade).

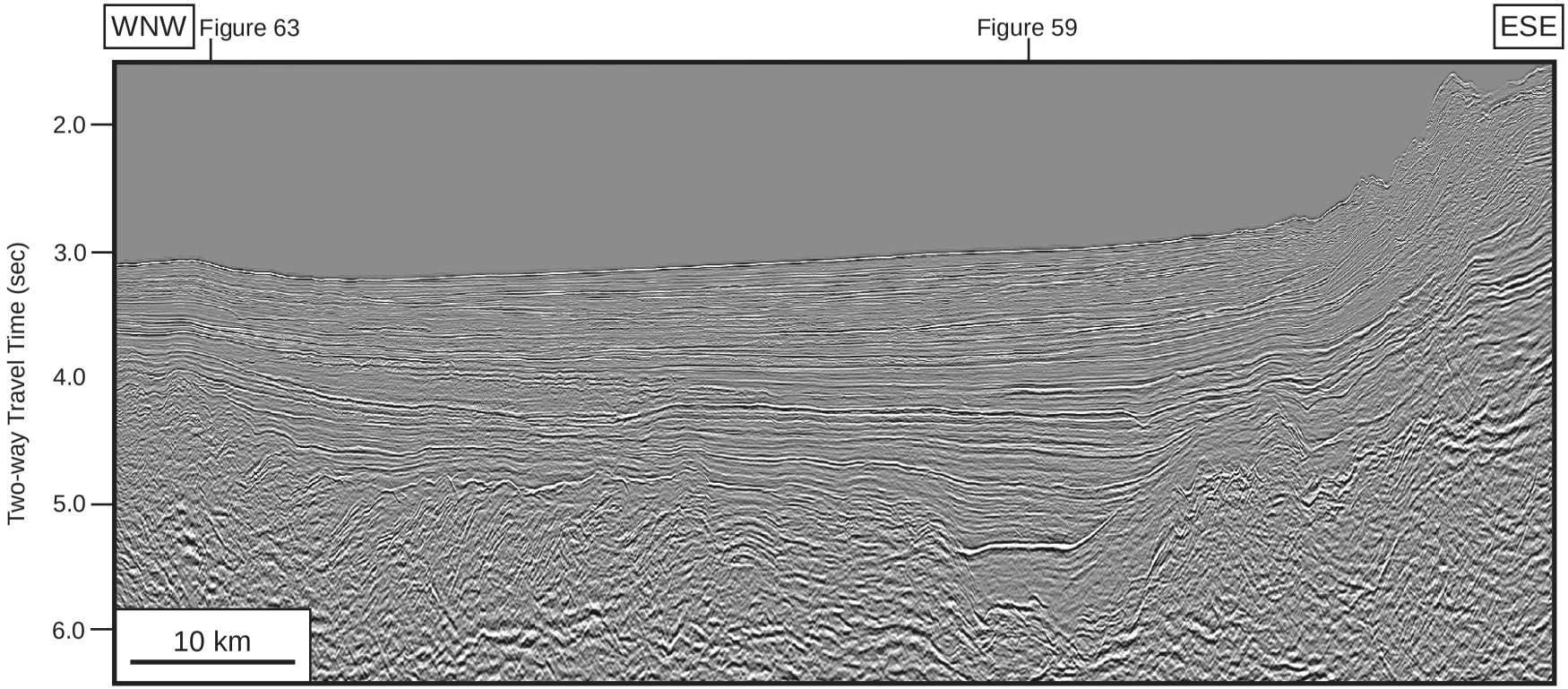

Figure 57a. Uninterpreted regional dip-oriented seismic profile (br-98:br98-057). Location of the profile is shown in Figures 34-35, 40-42, 47-52 and locations of where Figures 59, 63 cross the profile.

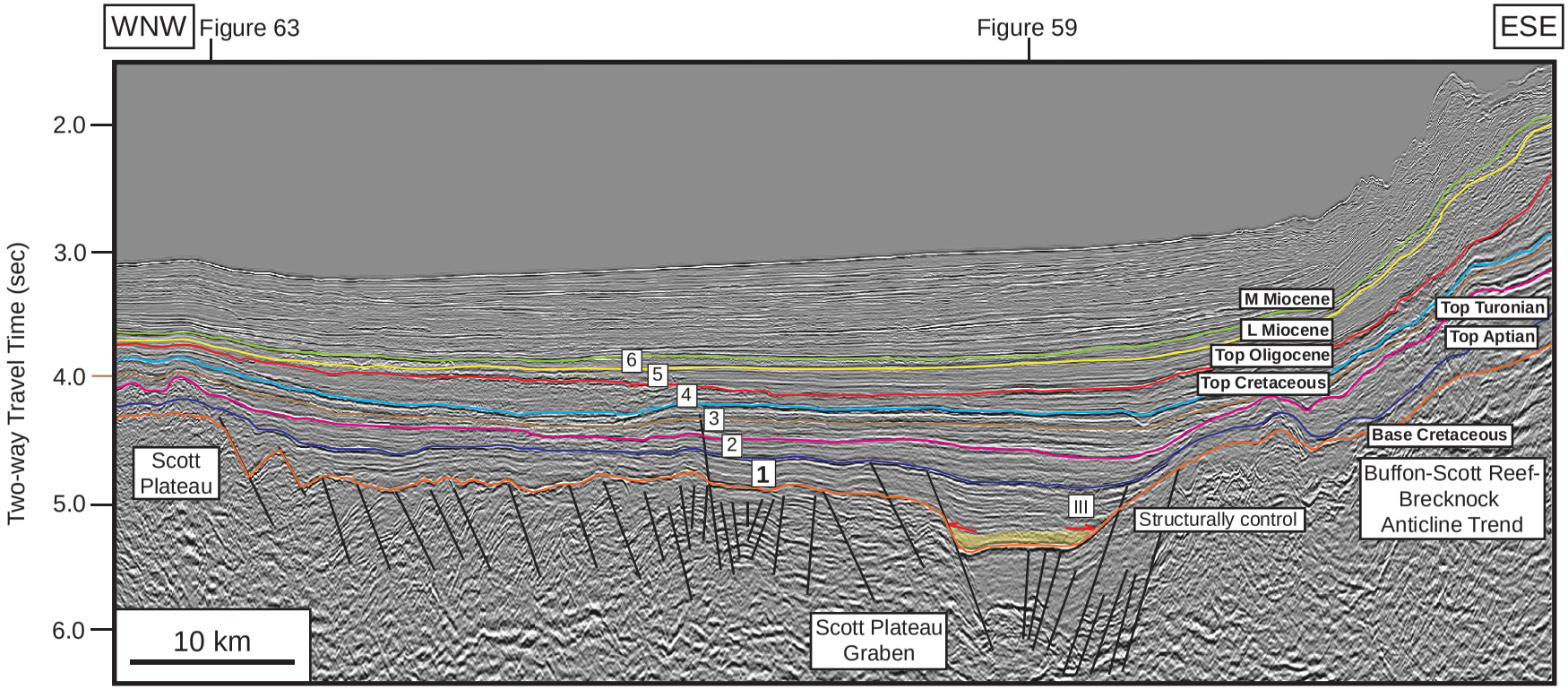

Figure 57b. Regional dip-oriented seismic profile showing all interpreted sequence boundaries from base Cretaceous to middle Miocene. This profile shows the deeper area of the Scott Plateau Graben and the shallower area of the Buffon-Scott Reef-Brecknock Anticline Trend in the northern part of the study area. Series of faults in the underlying Jurassic strata caused the irregular topography. Some part within Subsequence III of Megasequence 1 were structurally confined by faults as shown by the onlap reflection termination (orange shade) at the eastern part of the profile. Location of the profile is shown in Figures 34-35, 40-42, 47-52 and locations of where Figures 59, 63 cross the profile.

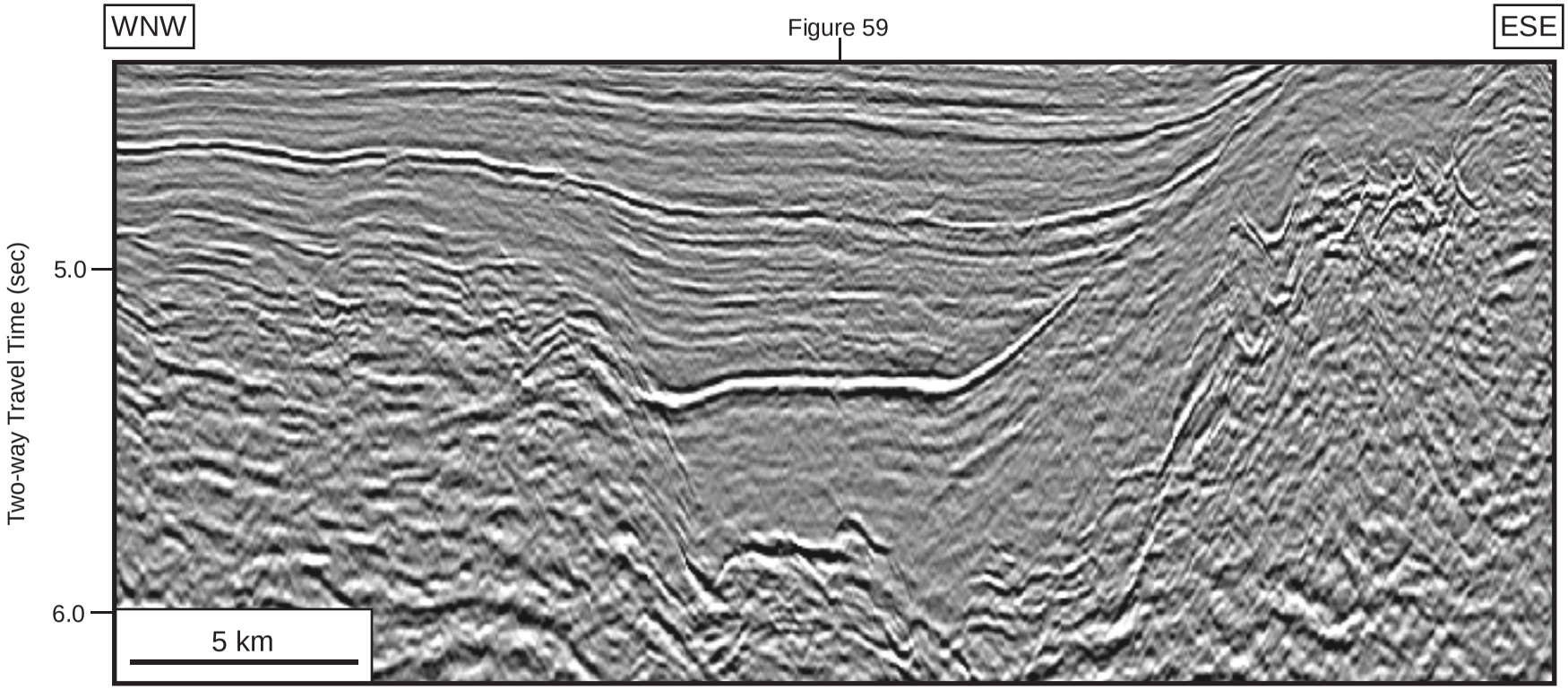

Figure 58a. Uninterpreted regional dip-oriented seismic profile (br-98:br98-057): A closeup view of Figure 57.

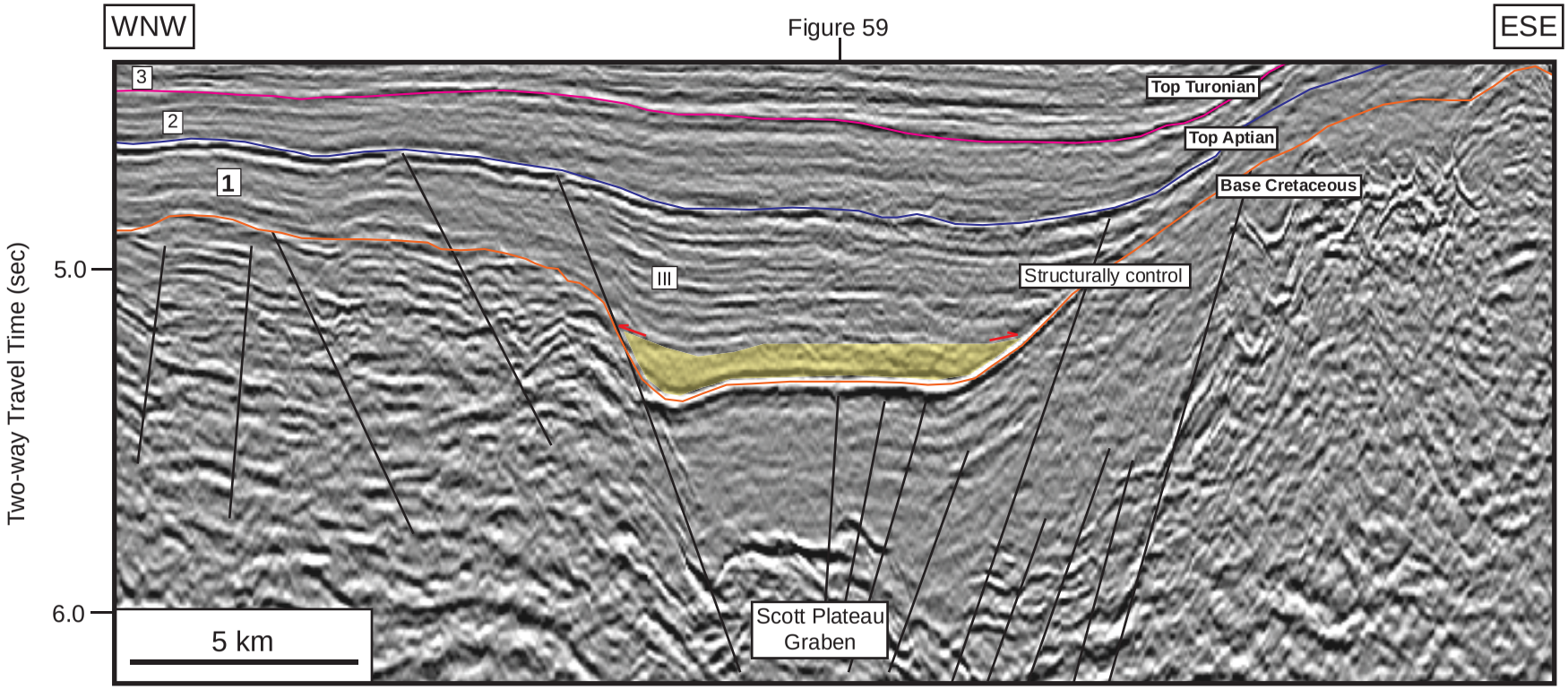

Figure 58b. Regional dip-oriented seismic profile showing all interpreted sequence boundaries from base Cretaceous to middle Miocene: A closeup view of Figure 57. Some part within Subsequence III of Megasequence 1 were structurally confined by faults as shown by the onlap reflection termination (orange shade) at the eastern part of the profile.

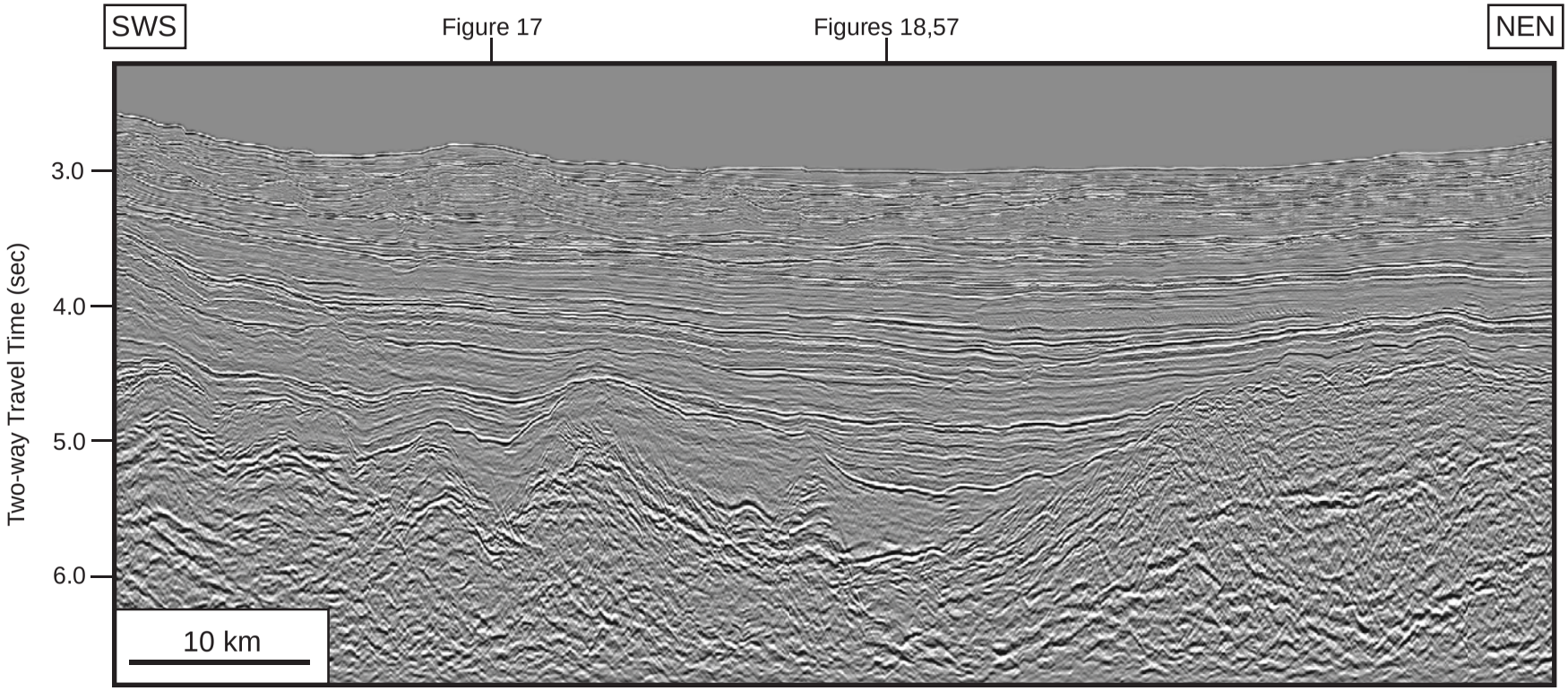

Figure 59a. Uninterpreted regional strike-oriented seismic profile (br-98:br98-080). Location of the profile is shown in Figures 34-35, 40-42, 47-52 and locations of where Figures 17, 18, 57 cross the profile.

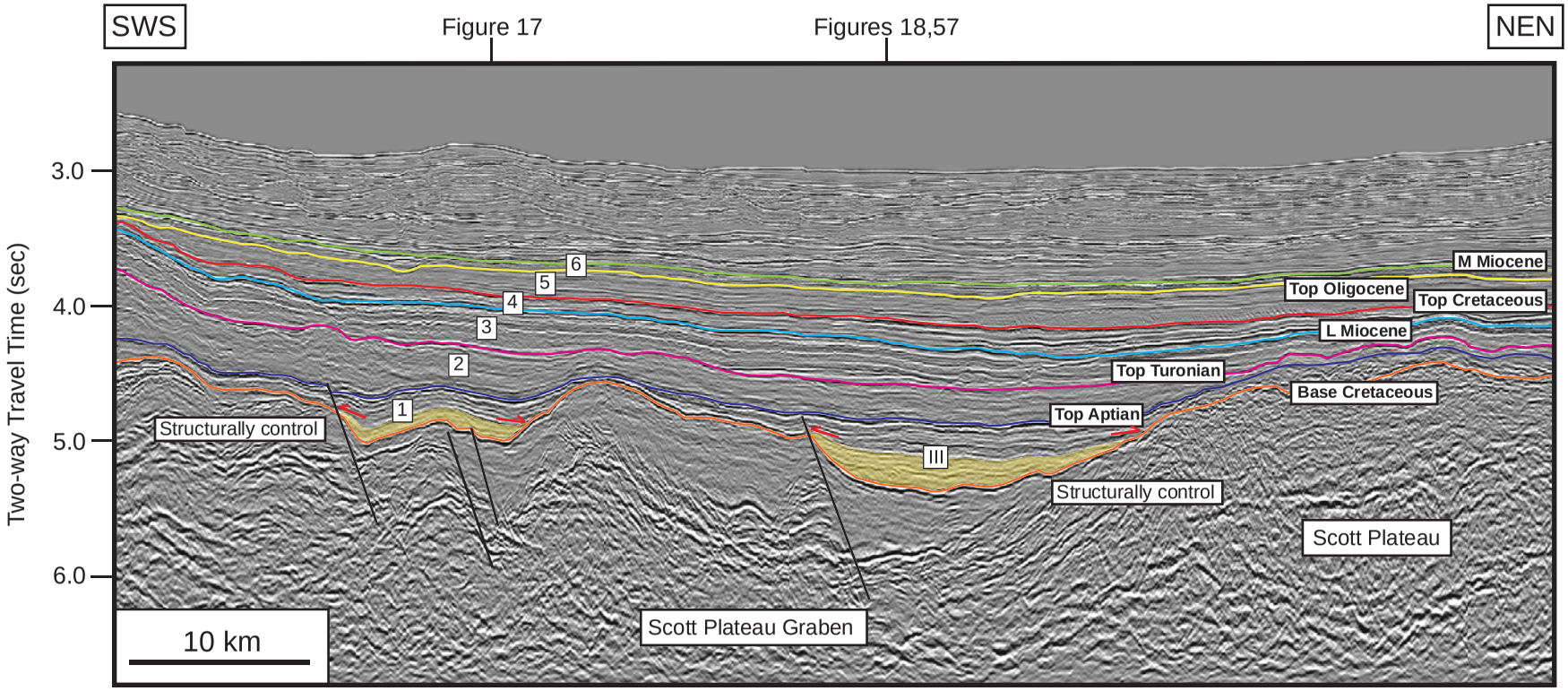

Figure 59b. Regional strike-oriented seismic profile showing all interpreted sequence boundaries from base Cretaceous to middle Miocene. This profile shows the area of the Scott Plateau and the shallower area of the Barcoo Terrace. The basin-floor fan is observed within Subsequence III of Megasequence 1 (yellow shade). Location of the profile is shown in Figures 34-35, 40-42, 47-52 and locations of where Figures 17, 18, 57 cross the profile.

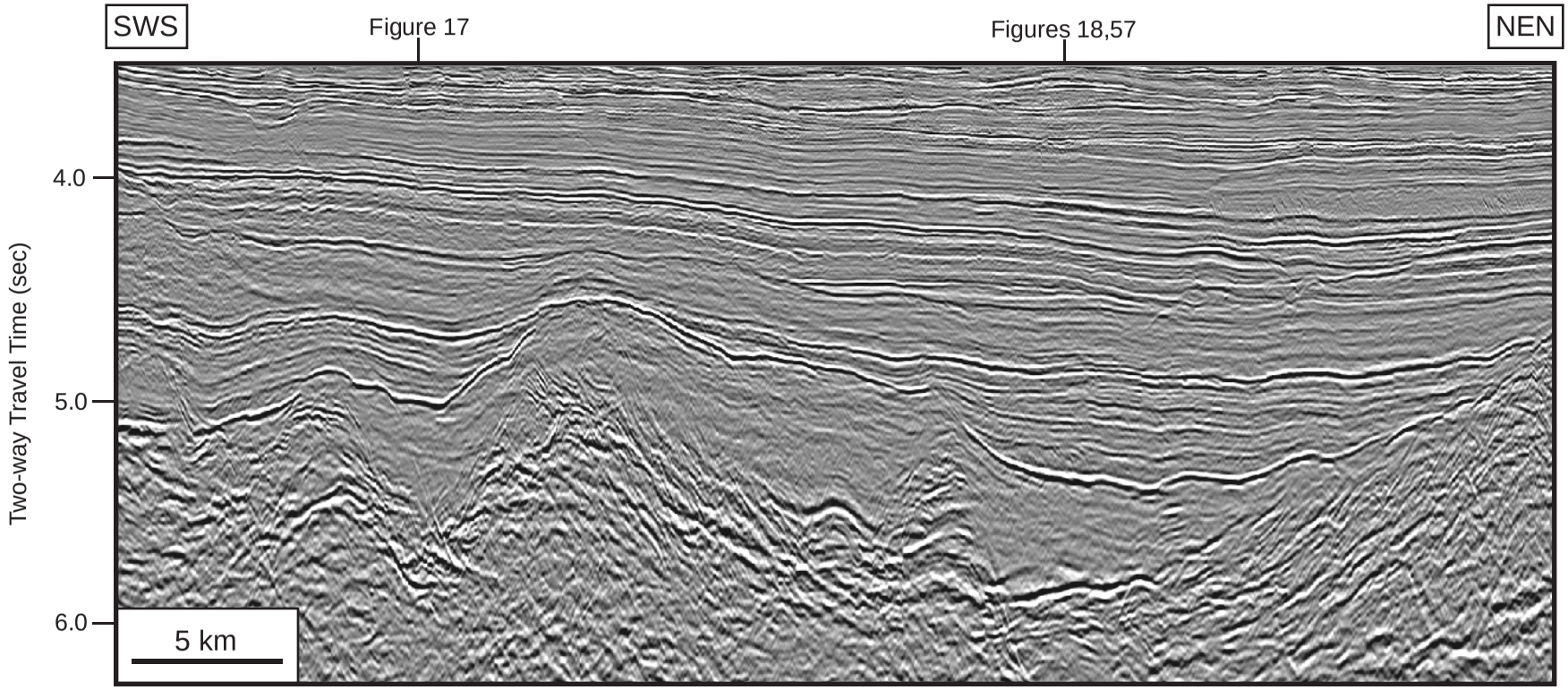

Figure 60a. Uninterpreted regional strike-oriented seismic profile (br-98:br98-080): A closeup view of Figure 59.

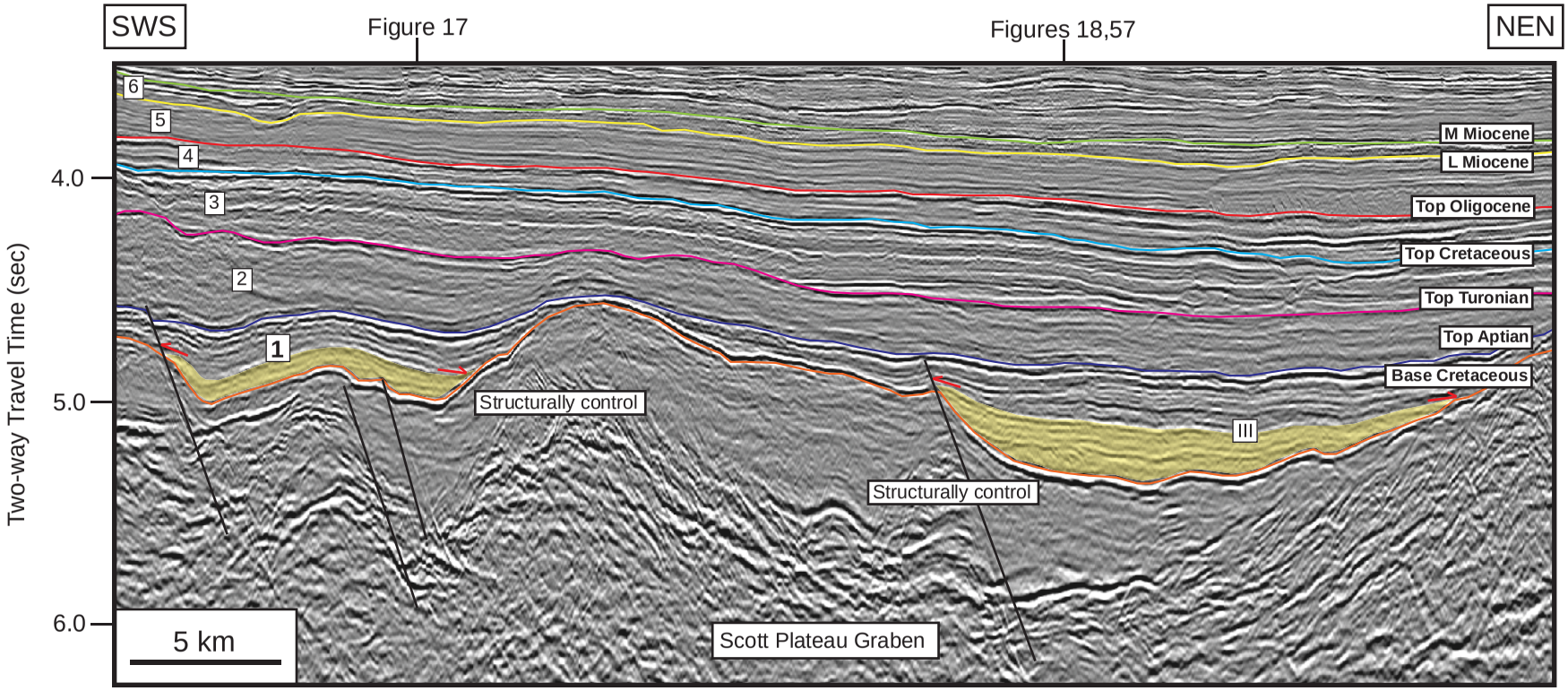

Figure 60b. Regional strike-oriented seismic profile showing all interpreted sequence boundaries from base Cretaceous to middle Miocene: A closeup view of Figure 59. The basin-floor fan is observed within Subsequence III of Megasequence 1 (yellow shade).

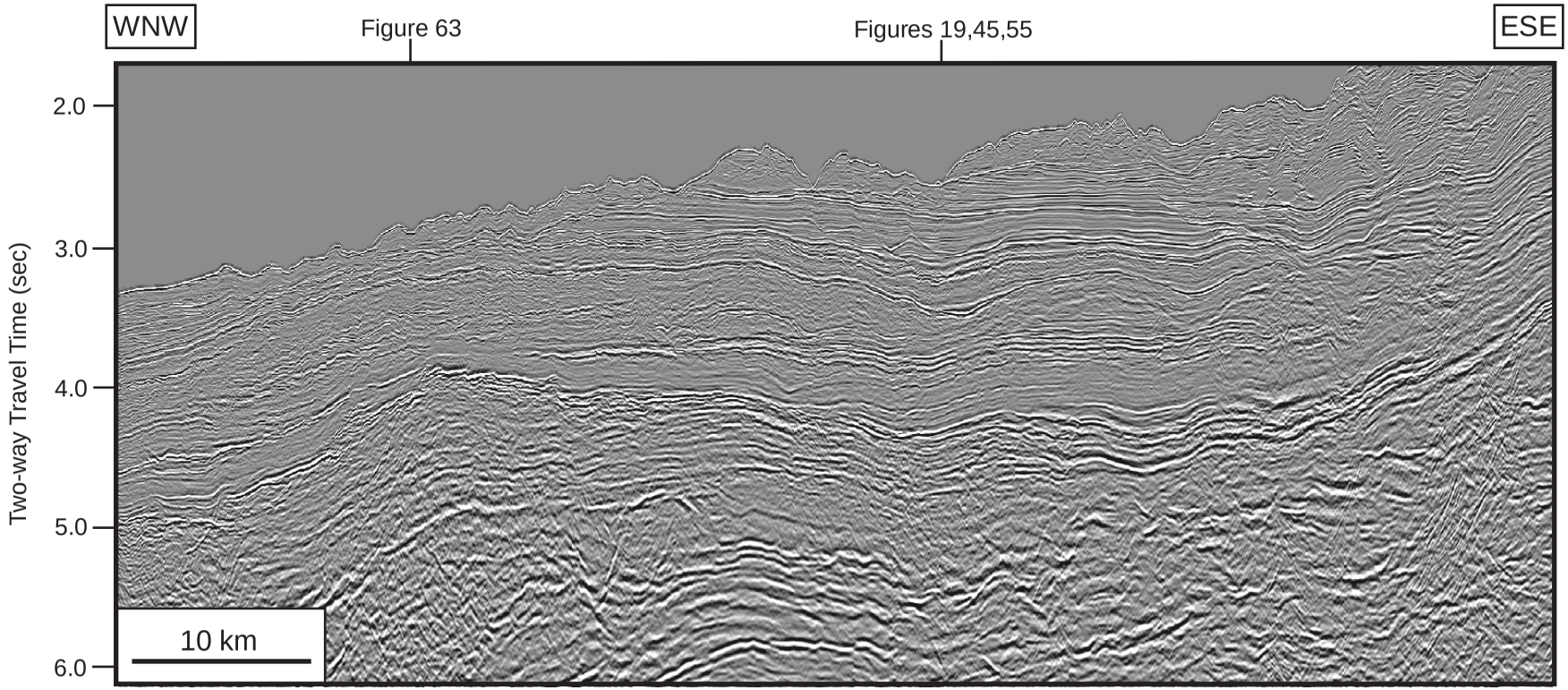

Figure 61a. Uninterpreted regional dip-oriented seismic profile (br-98:br98-035). Location of the profile is shown in Figures 34-35, 40-42, 47-52 and locations of where Figures 19, 44, 55, 63 cross the profile.

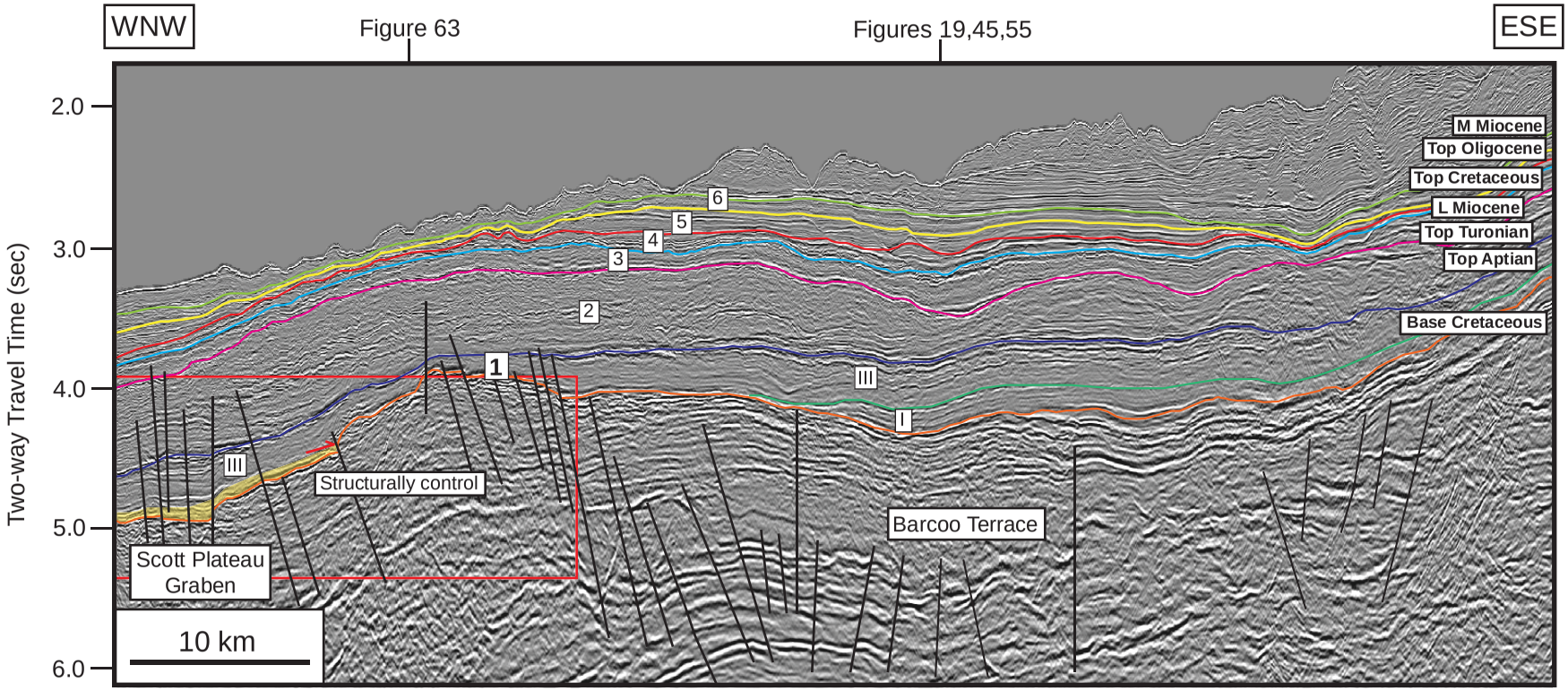

Figure 61b. Regional dip-oriented seismic profile showing all interpreted sequence boundaries from base Cretaceous to middle Miocene. This profile shows the deeper area of the Scott Plateau and the shallower area of the Barcoo Terrace. The basin-floor fan is observed within the low angle clinoform of Subsequence III of Megasequence 1 (yellow shade). Location of the profile is shown in Figures 34-35, 40-42, 47-52 and locations of where Figures 19, 44, 55, 63 cross the profile.

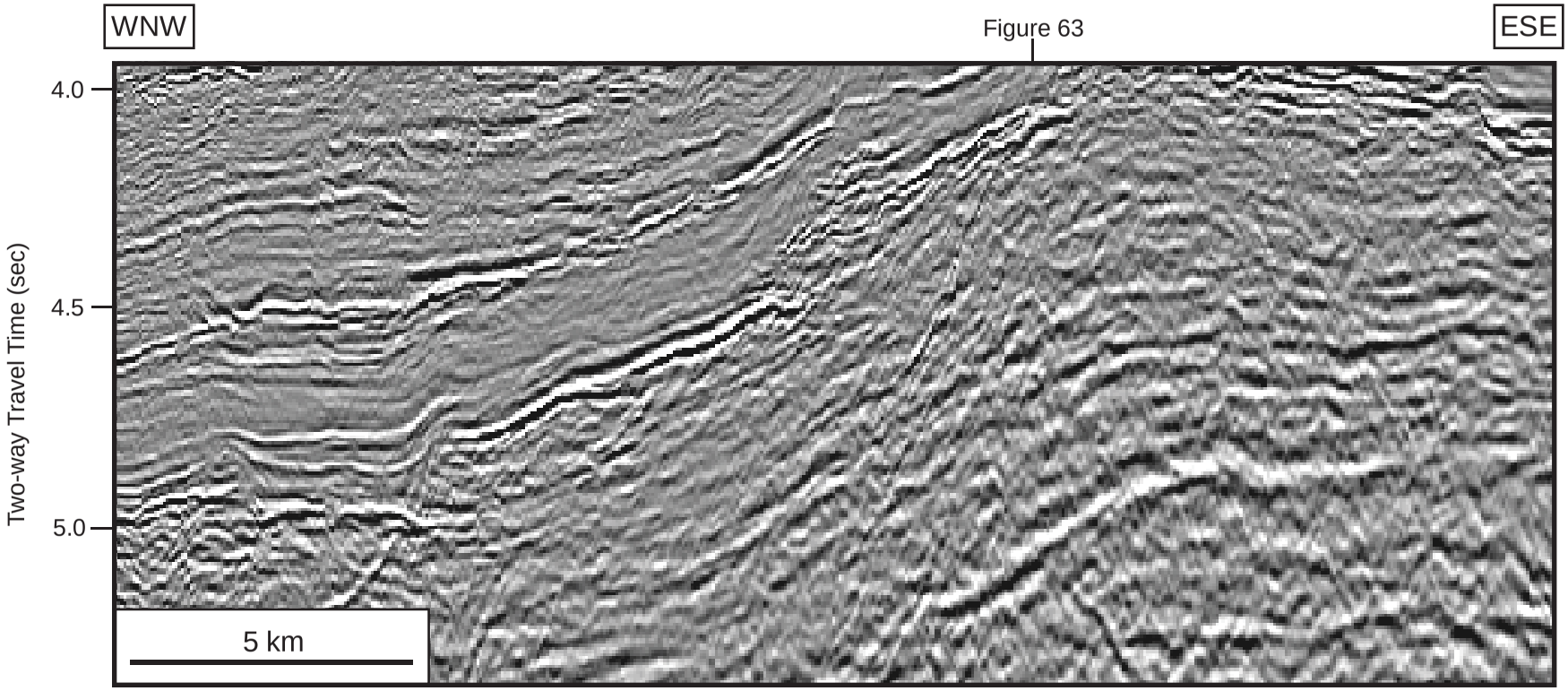

Figure 62a. Uninterpreted regional dip-oriented seismic profile (br-98:br98-035): A closeup view of Figure 61.

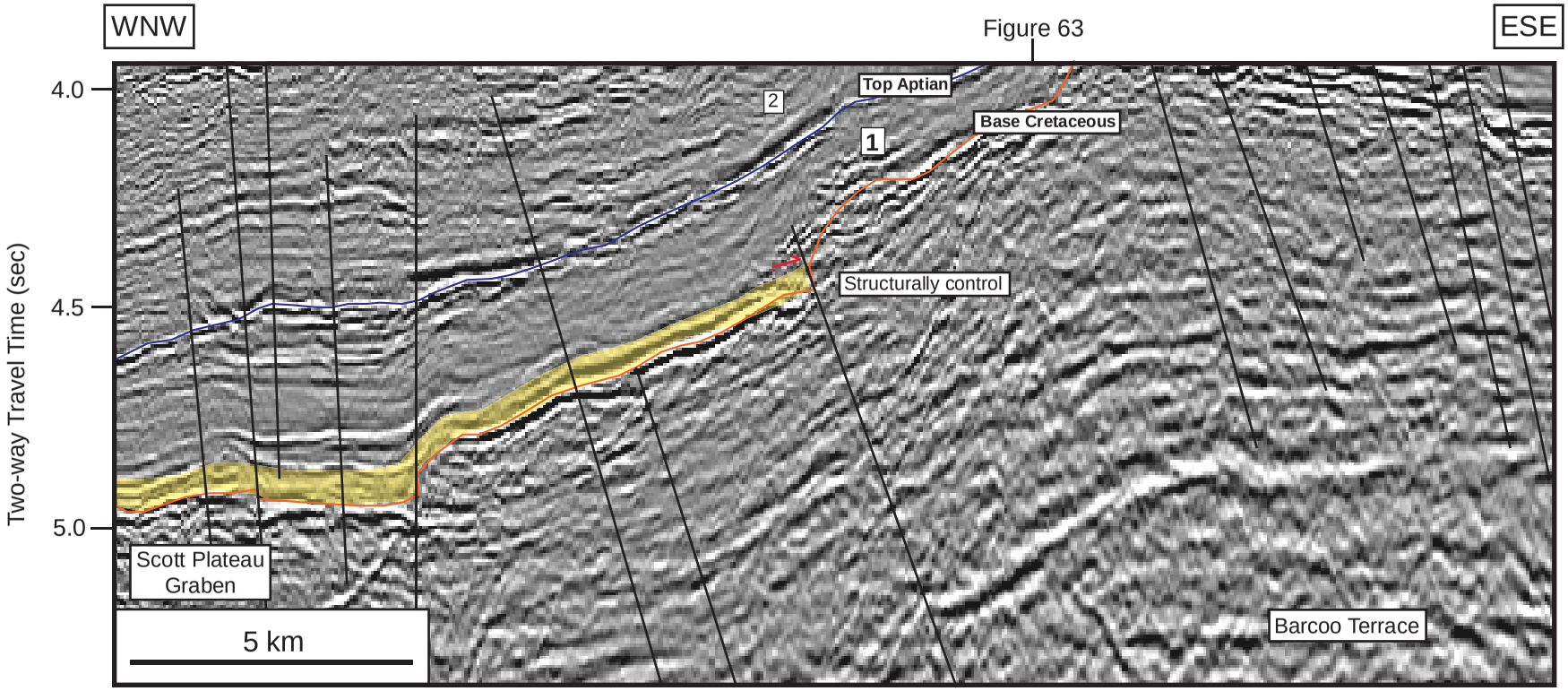

Figure 62b. Regional dip-oriented seismic profile showing all interpreted sequence boundaries from base Cretaceous to middle Miocene: A closeup view of Figure 61. The basin-floor fan is observed within the low angle clinoform of Subsequence III of Megasequence 1 (yellow shade).

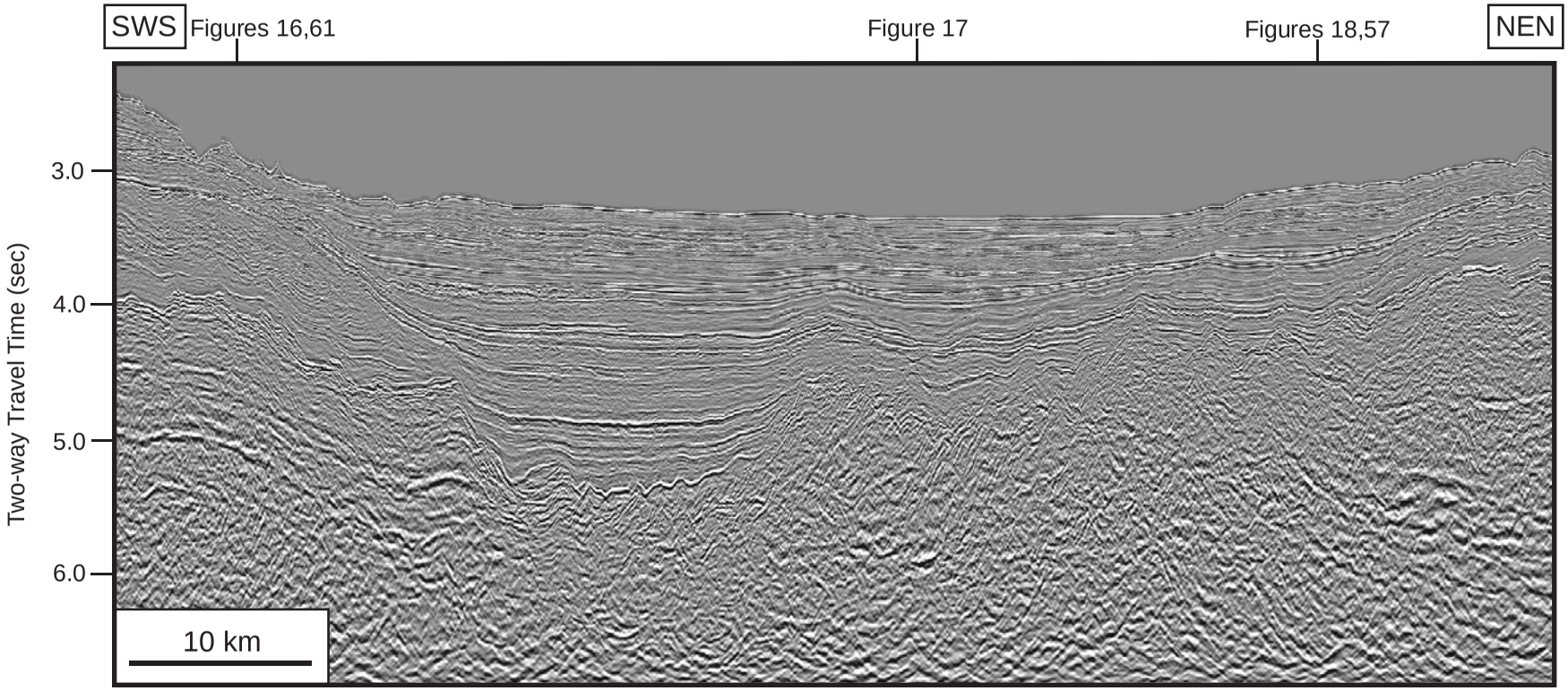

Figure 63a. Uninterpreted regional strike-oriented seismic profile (br-98:br98-085). Location of the profile is shown in Figures 34-35, 40-42, 47-52 and locations of where Figures 16, 17, 18, 57, 61 cross the profile.

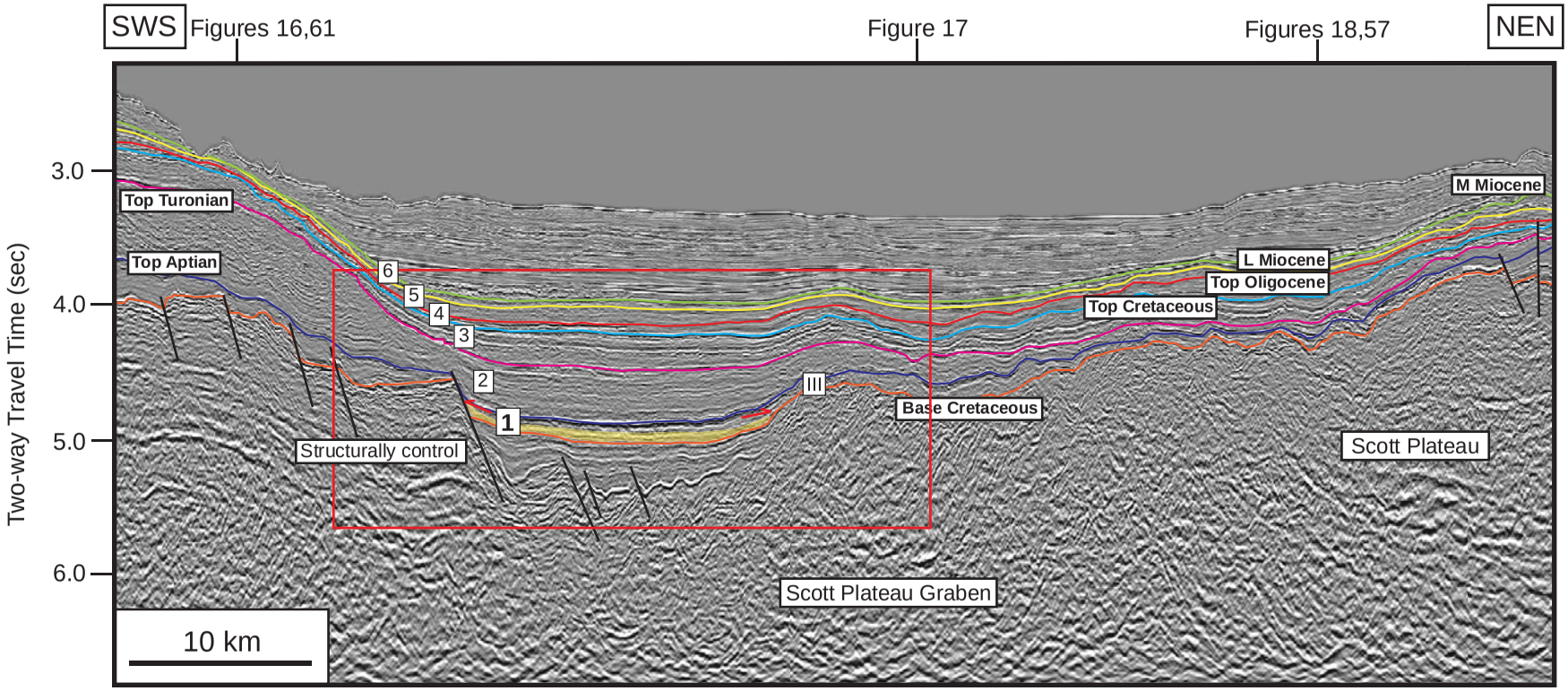

Figure 63b. Regional strike-oriented seismic profile showing all interpreted sequence boundaries from base Cretaceous to middle Miocene. This profile shows the paleogeography of the Scott Plateau Graben and the shallower area of the Scott Plateau. The basin-floor fan is observed within the low angle clinoform of Subsequence III of Megasequence 1 (yellow shade). Location of the profile is shown in Figures 34-35, 40-42, 47-52 and locations of where Figures 16, 17, 18, 57, 61 cross the profile.

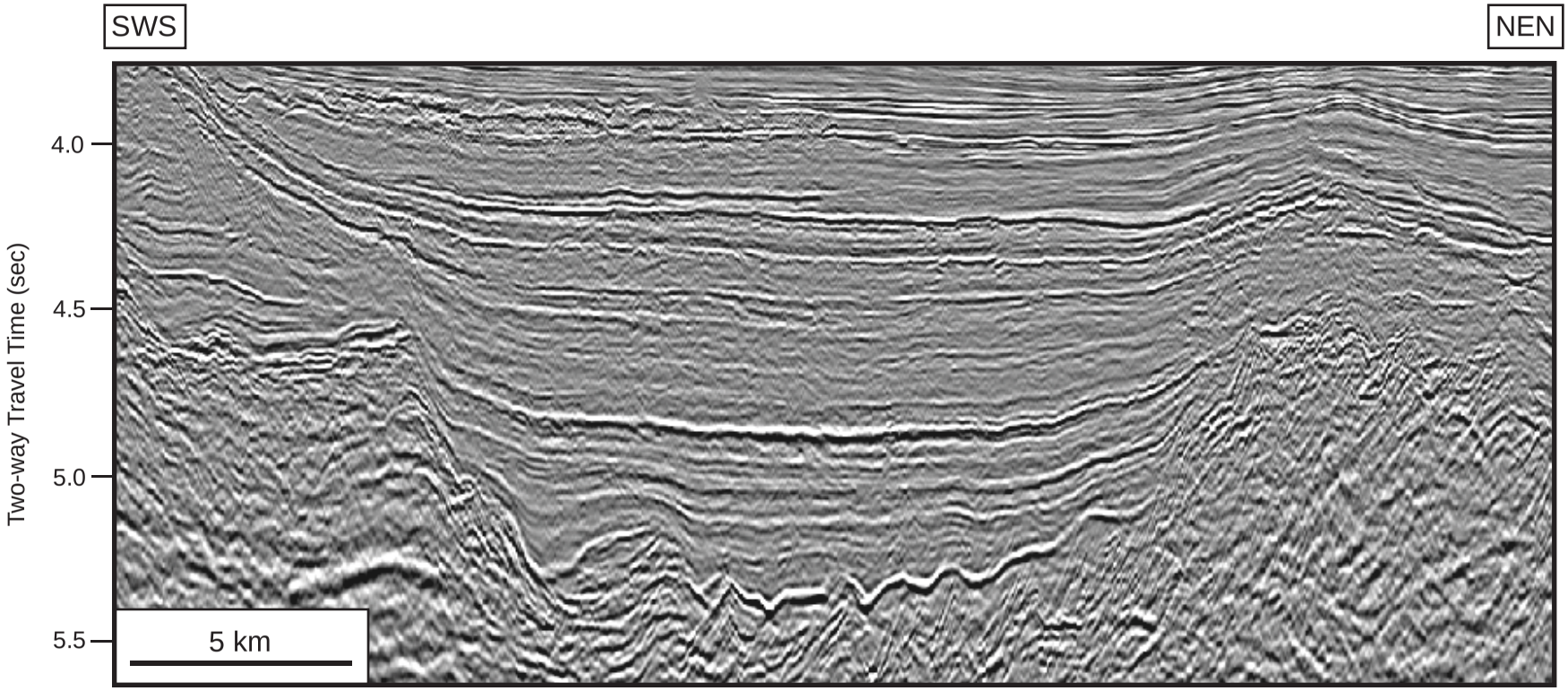

Figure 64a. Uninterpreted regional strike-oriented seismic profile (br-98:br98-085): A closeup view of Figure 63.

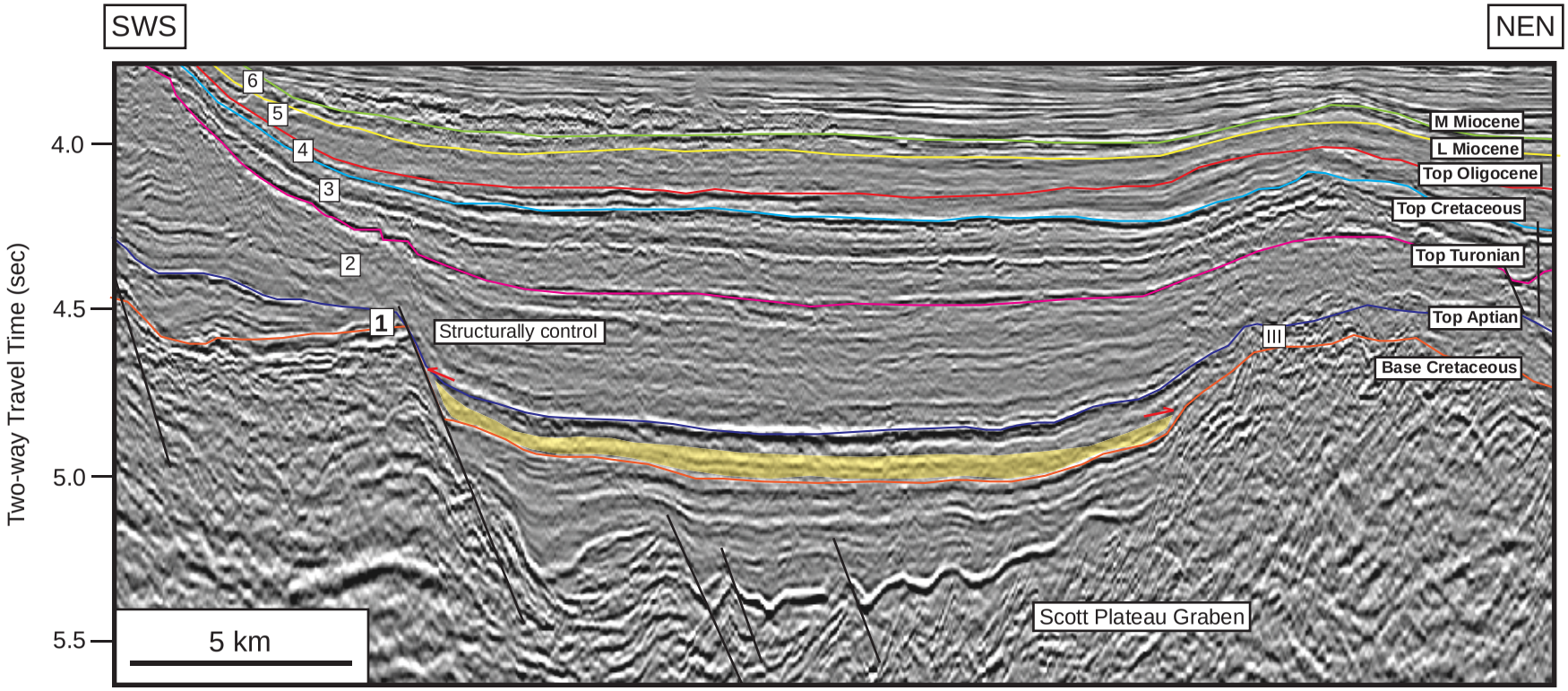

Figure 64b. Regional strike-oriented seismic profile showing all interpreted sequence boundaries from base Cretaceous to middle Miocene: A closeup view of Figure 63. The basin-floor fan is observed within the low angle clinoform of Subsequence III of Megasequence 1 (yellow shade).

Megasequence 2: top Aptian to top Turonian (112.0- 89.3 Ma) interval

Megasequence 2 includes at least seven depositional sequences (I-VII; Figure 10). Top Aptian horizon was picked as a major flooding surface based on the regional downlap, and its lateral continuity as well as high amplitude (Figures 8, 11). The top Turonian unconformity is an irregular surface due to erosion (Figures 8, 14, 16, 18, 19, 20). This megasequence demonstrates the sediment aggradation of slope system (Figures 8, 9, 10, 11, 14).

The time structural contour map of the top Turonian has the similar characteristic to the top Aptian horizon. The two-way travel time values range from 837 to 4645 msec. Barcoo Platform is the shallowest area whereas Scott Plateau Graben is the deepest (Figure 65). The Barcoo Platform Anticline and Barcoo syncline axes trend southwest-northeast in the southern part of the sub-basin. (Figure 7)

Isochron map shows values vary from 177 to 1433 msec two-way travel time (TWTT). The greatest thickness of Megasequence 2 is in the Barcoo Syncline in the southeastern part, and along the southern flank of Scott Plateau Graben in the northern part of the study area (Figure 66).

Six distinct seismic facies are identified. Facies 1 and 4 are parallel to subparallel internal reflections with moderate to high amplitude and fair to good continuity (Figures 67, 68, 70). Seismic facies 2 consists of the low-angle prograding clinoforms within external wedge shape (Figure 8). The amplitude reflections is moderate and the continuity is fair (Figures 10, 14, 15, 18, 67). Facies 3 has hummocky reflections with moderate to high amplitude and fair continuity. Barcoo-1 well penetrates in this facies.

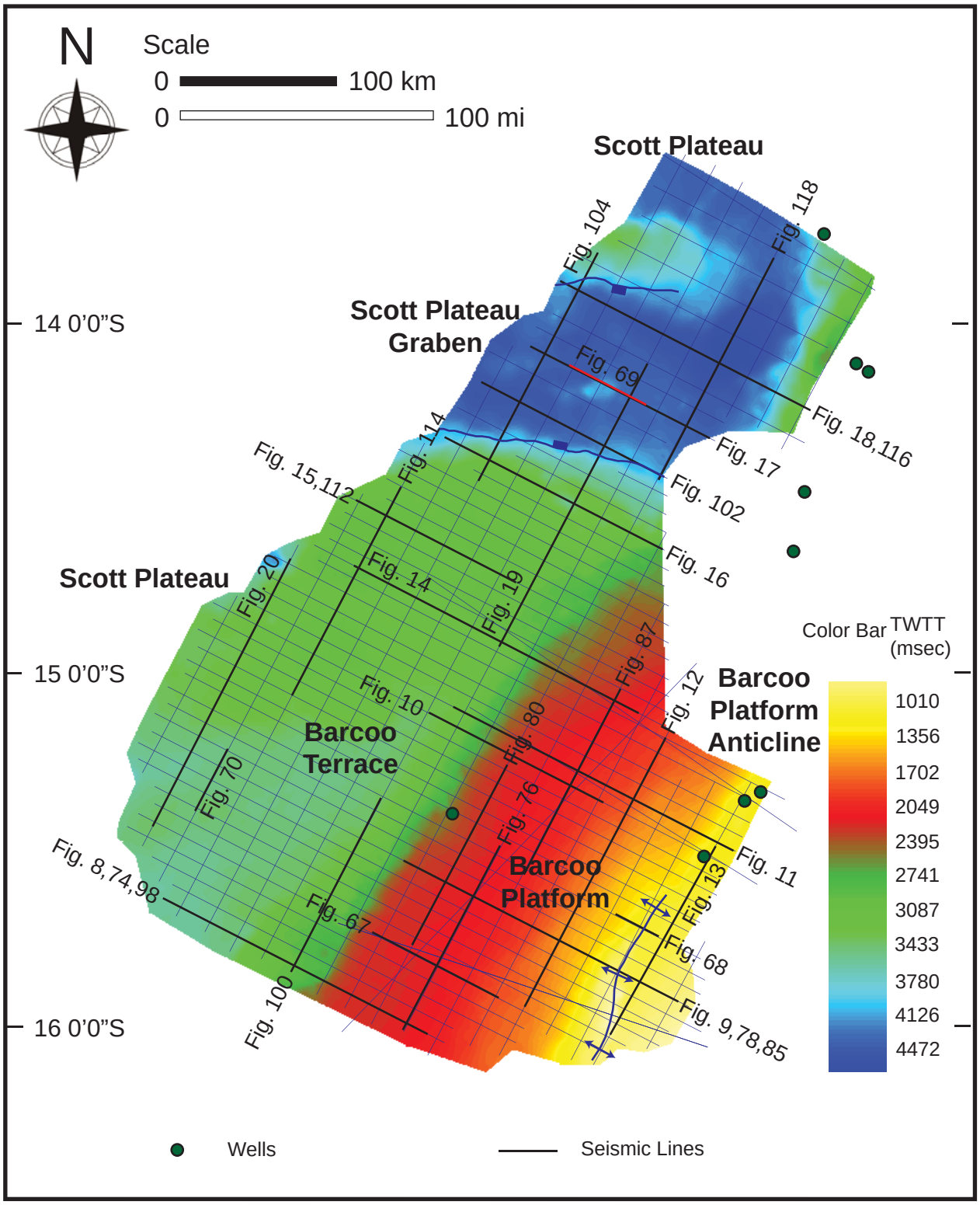

Figure 65. Time structural contour map (in TWTT msecs) of top Turonian: 89.3 Ma (Megasequence 2). Distribution of 2D seismic profiles interpreted to generate the maps are shown by white lines, and wells are shown by green dots. Locations of Figures 8-20, 67-70, 74-81, 85-88, 98-105, 112-119 are shown.

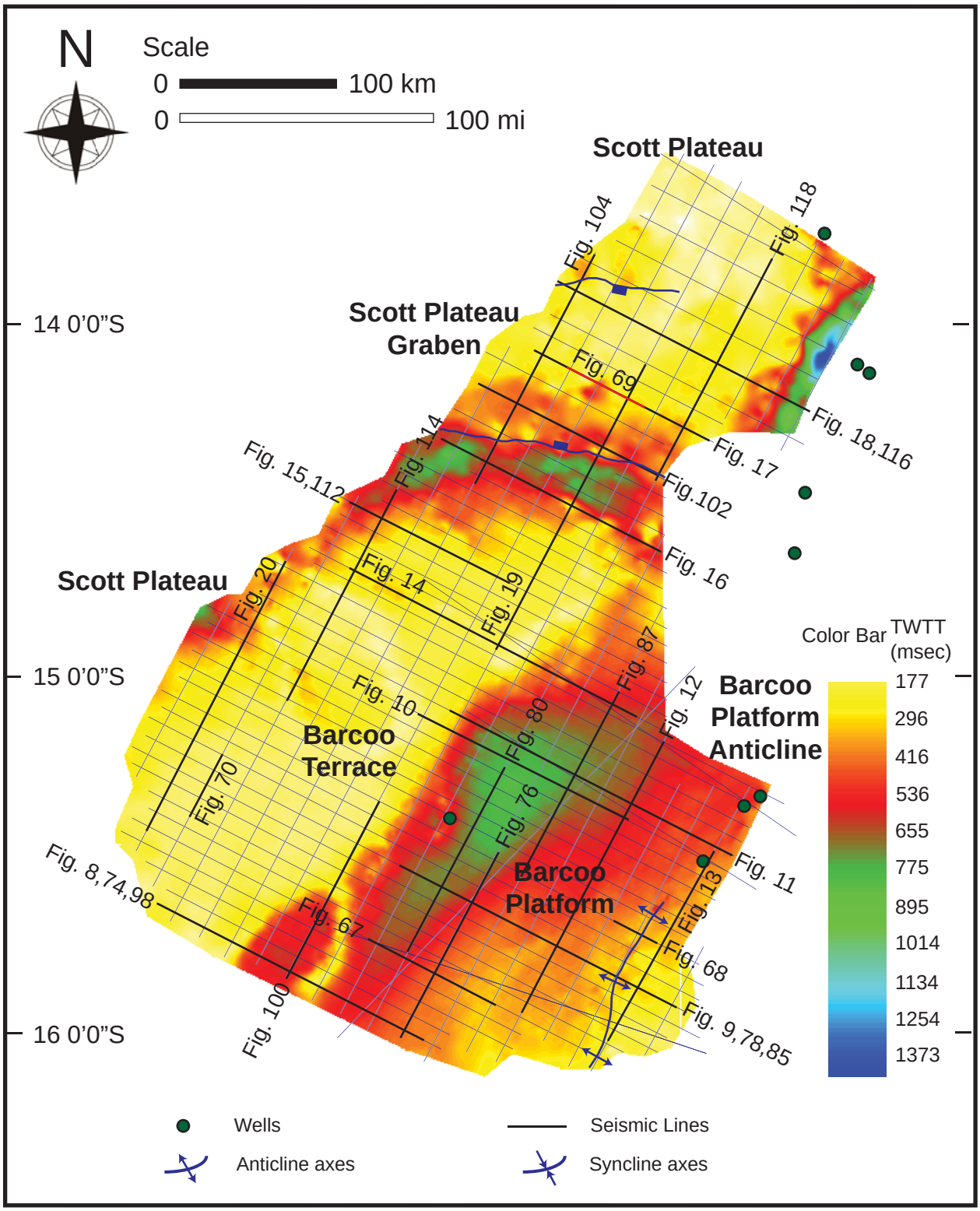

Figure 66. Isochron map (in TWTT msecs) of Megasequence 2 (top Aptian to top Turonian: 112.0-89.3 Ma) interval. Distribution of 2D seismic profiles interpreted to generate the maps are shown by blue lines, and wells are shown by green dots. Locations of Figures 8-20, 67-70, 74-81, 85-88, 98-105, 112-119 are shown.

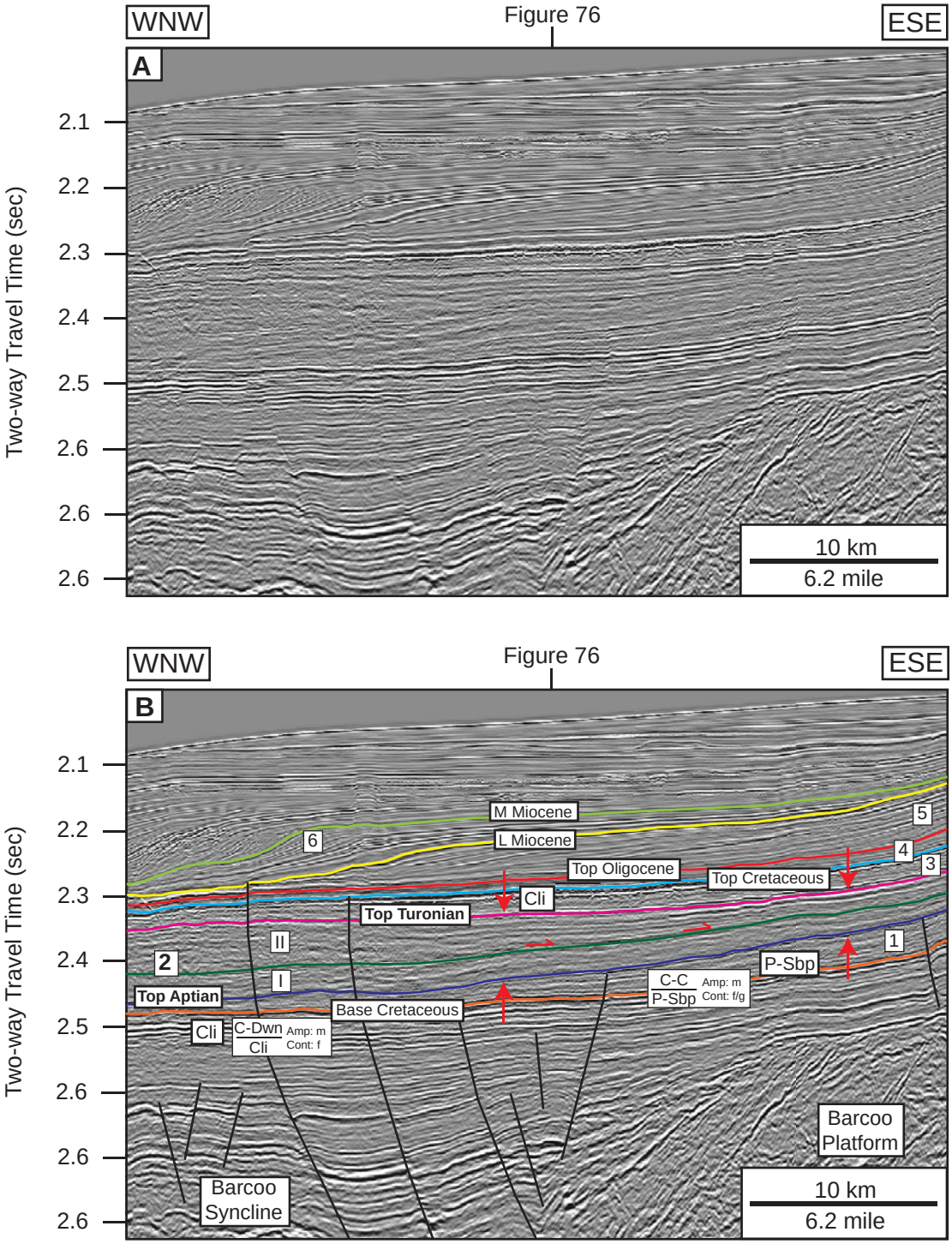

Figure 67. Dip-oriented seismic profile showing seismic facies of Megasequence 2 (top Aptian to top Turonian: 112.0-89.3 Ma) interval: (a) uninterpreted, (b) interpreted. This megasequence consists of at least two depositional sequences. See Table 2 for codes and abbreviations and Figures 65-66, 71-73, 82-84, 89-97, 106-111 for location of the profile and location of where Figure 76 crosses the profile.

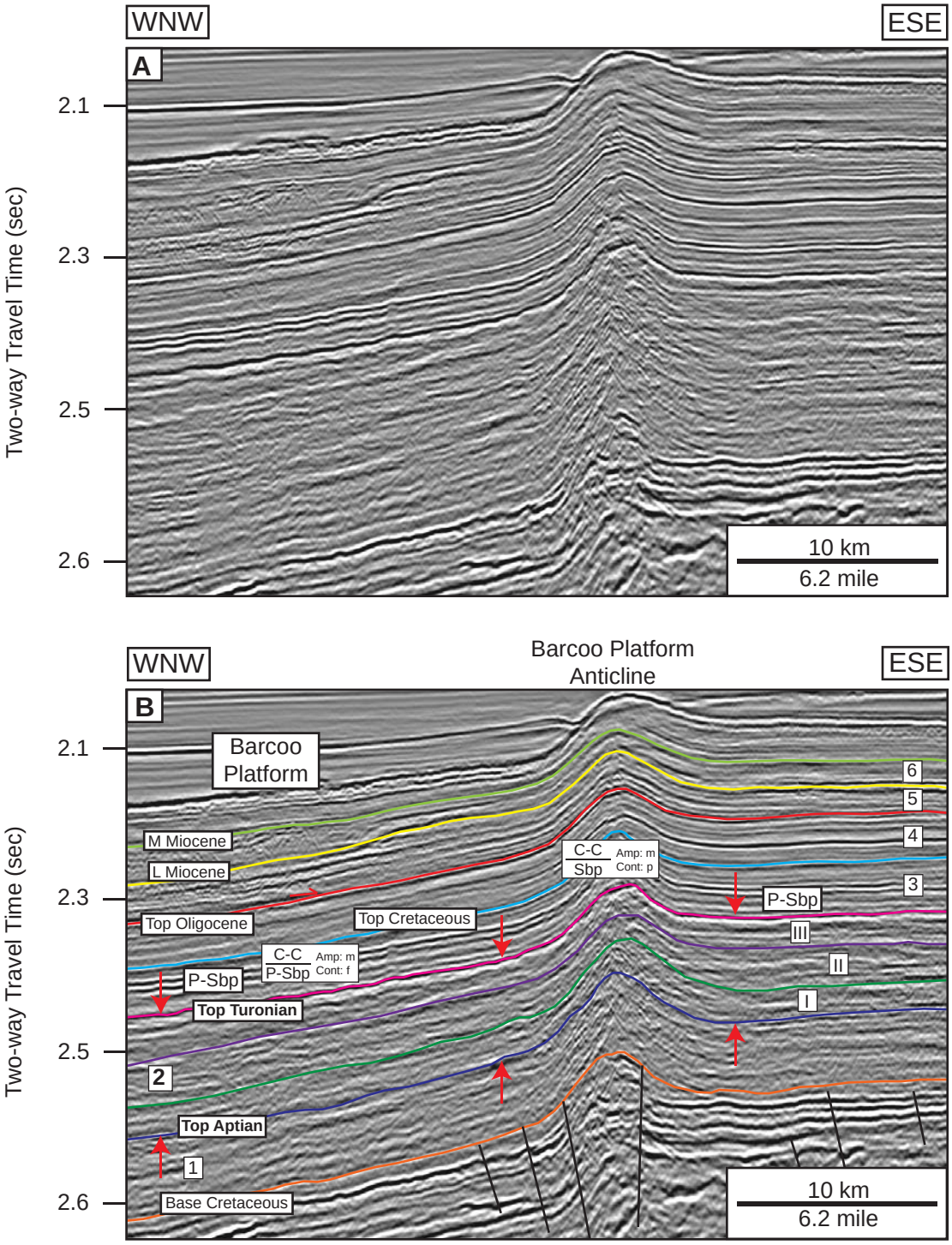

Figure 68. Dip-oriented seismic profile showing seismic facies of Megasequence 2 (top Aptian to top Turonian: 112.0-89.3 Ma) interval: (a) uninterpreted, (b) interpreted. At least three depositional sequences are observed in this megasequence. See Table 2 for codes and abbreviations and Figures 65-66, 71-73, 82-84, 89-97, 106-111 for location of the profile.

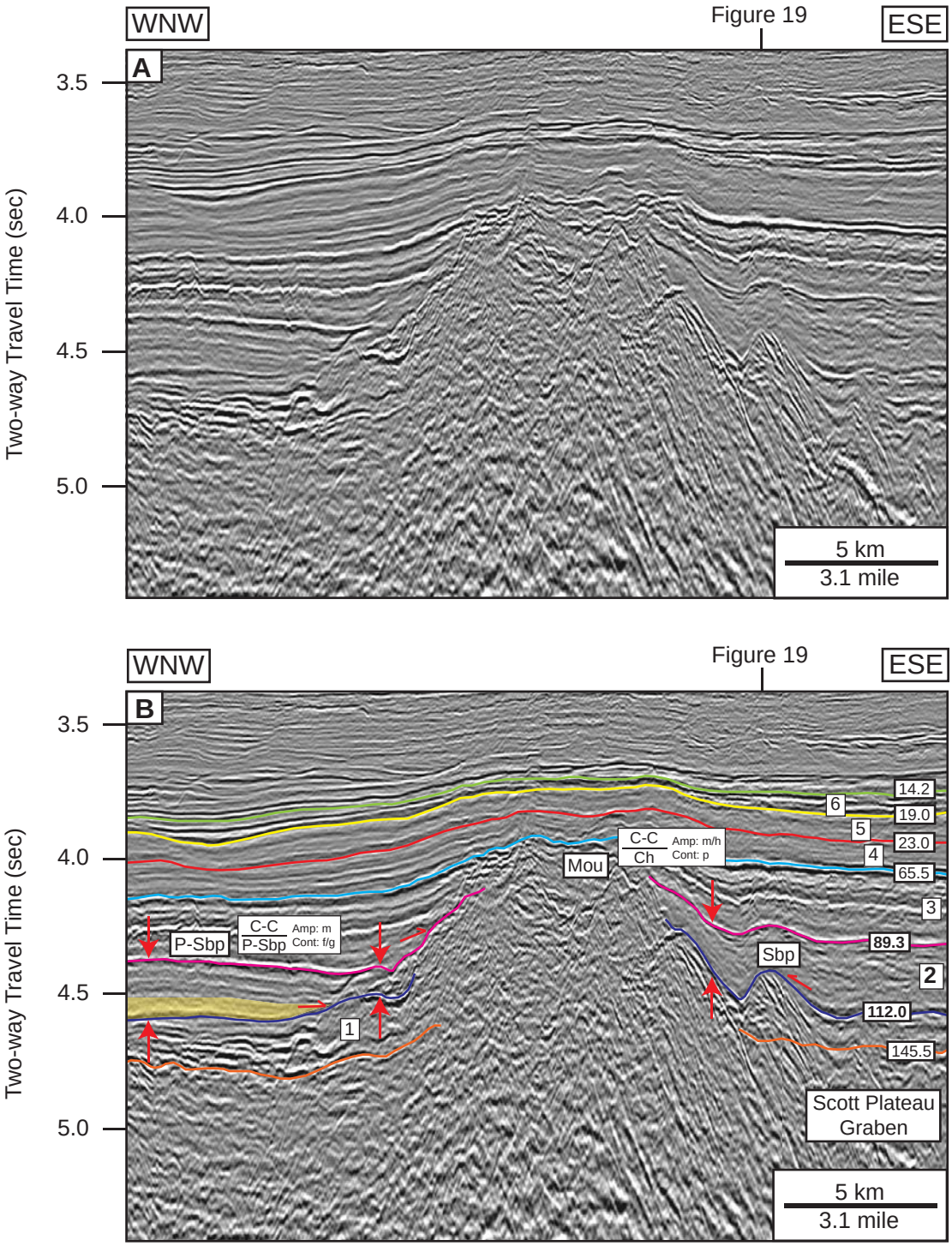

Figure 69. Dip-oriented seismic profile showing seismic facies of Megasequence 2 (top Aptian to top Turonian: 112.0-89.3 Ma) interval: (a) uninterpreted, (b) interpreted. This profile shows a mounded feature of carbonate buildup which is located in the northern portion of the study area. See Table 2 for codes and abbreviations and Figures 65-66, 71-73, 82-84, 89-97, 106-111 for location of the profile and location of where Figure 19

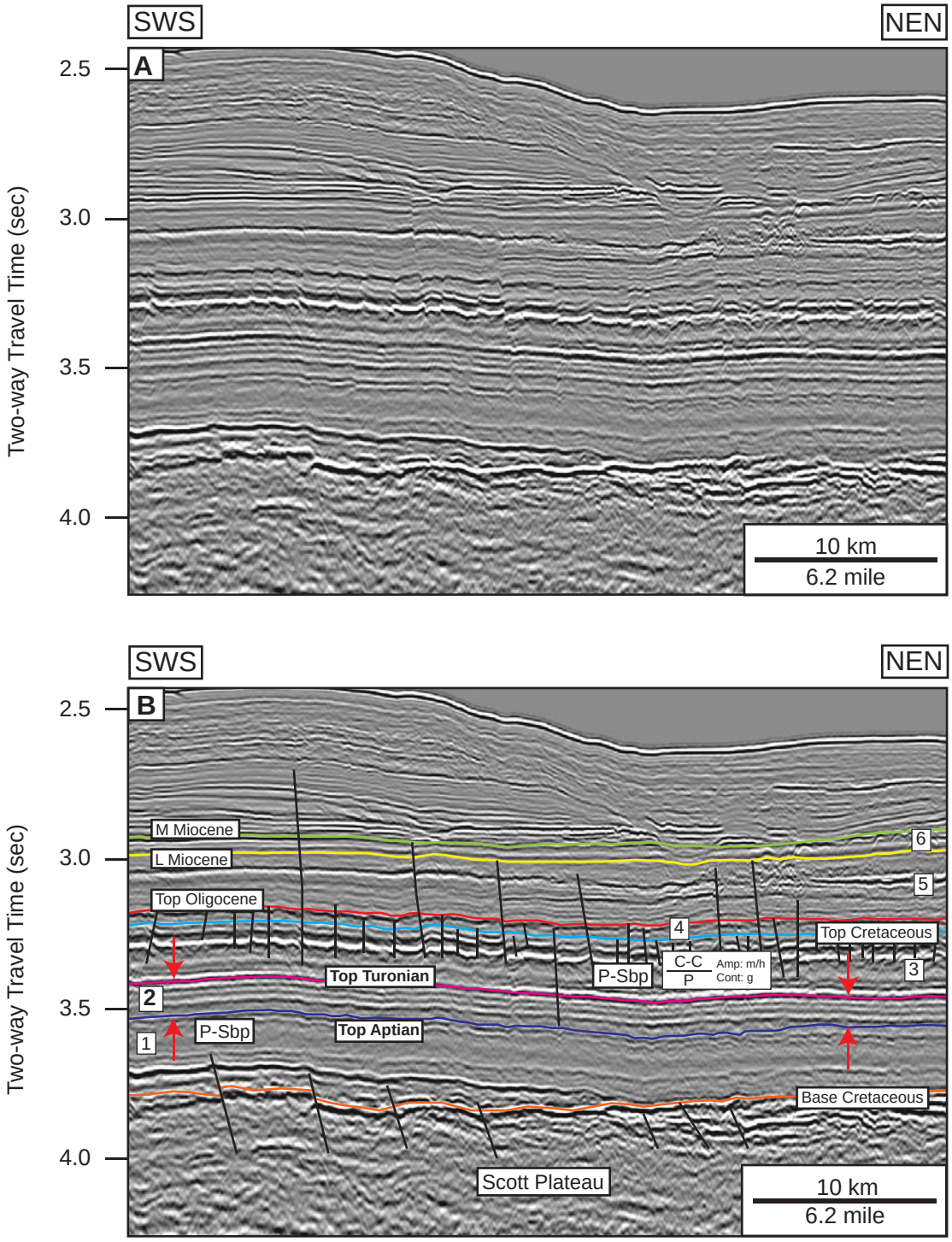

Figure 70. Strike-oriented seismic profile showing seismic facies of Megasequence 2 (top Aptian to top Turonian: 112.0-89.3 Ma) interval: (a) uninterpreted, (b) interpreted. This profile illustrates the conformable parallel seismic reflections of the Scott Plateau. See Table 2 for codes and abbreviations and Figures 65-66, 71-73, 82-84, 89-97, 106-111 for location of the profile.

The well log data shows sand-prone at the lower part of the megasequence and the smaller grain size in the upper interval (Figure 22). Facies 5 and 6 were defined to be the chaotic internal reflection configuration. They have low amplitude and poor continuity. Seismic facies 6, which is a mound (Figure 69), has moderate to high amplitude and poor continuity. No wells penetrate in these two seismic facies.

Lombardina-1, Arquebus-1ST1, Sheherazaed-1 wells penetrate seismic facies 4 (Figures 4, 7). Wireline log data show the interval of sandstone interbedded with shales (Figures 23-25).

Subsequence I of Megasequence 2

The isochron map of this subsequence illustrates the thickness values varying from 0 to 240 msec two-way travel time (TWTT) (Figure 71). The thickest stratum is deposited in the Barcoo Platform.

Two seismic facies in this subsequence are facies 1 and 3 (Figure 72; Table 6). Seismic facies 1 is the parallel to subparallel internal reflection configurations with concordant to the upper and lower sequence boundaries. The amplitude is moderate to high whereas the continuity is fair to good. It has been interpreted to be the shelf environment (Figures 9, 11, 10). On the other hand, the internal reflection configuration of facies 3 is a hummocky with moderate amplitude and fair continuity. This facies is interpreted to be part of the inversion phase which related to the structure.

Table 6. Seismic facies and geologic interpretation of Subsequence I of Megasequence 2

Seismic Facies	Upper Sequence Boundary	Lower Sequence Boundary	Internal Reflection Configuration	Amplitude	Continuity	Geologic Interpretation
1	Concordant	Concordant	Parallel to Subparallel	moderate to high	fair to good	Shelf deposits
3	Concordant	Concordant	Hummocky	moderate	fair	Inversion – related structure

The analysis of geological facies shows the shelf deposit and the prograding clinoform (Figure 73). Two basin-floor fans are indicated in the southern part of the study area. Each of them is shown by the dip and strike oriented seismic profile in Figures 74-77 and 78-81, respectively. The bi-directional downlap termination is the main indicators for these kinds of prospects.

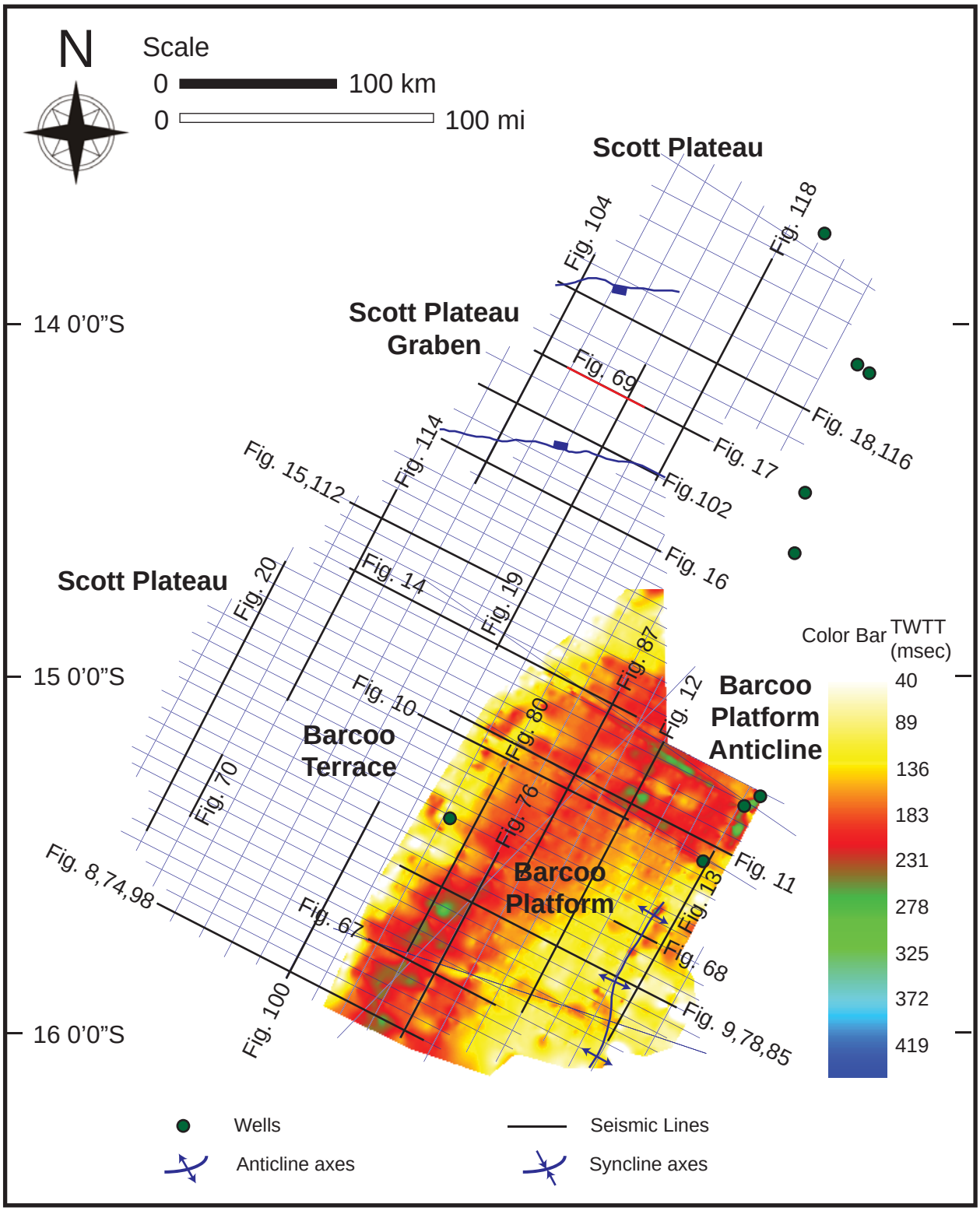

Figure 71. Isochron map (in TWTT msecs) of Subsequence I of Megasequence 2 interval. Distribution of 2D seismic profiles interpreted to generate the maps are shown by blue lines, and wells are shown by green dots. Locations of Figures 8-20, 67-70, 74-81, 85-88, 98-105, 112-119 are shown.

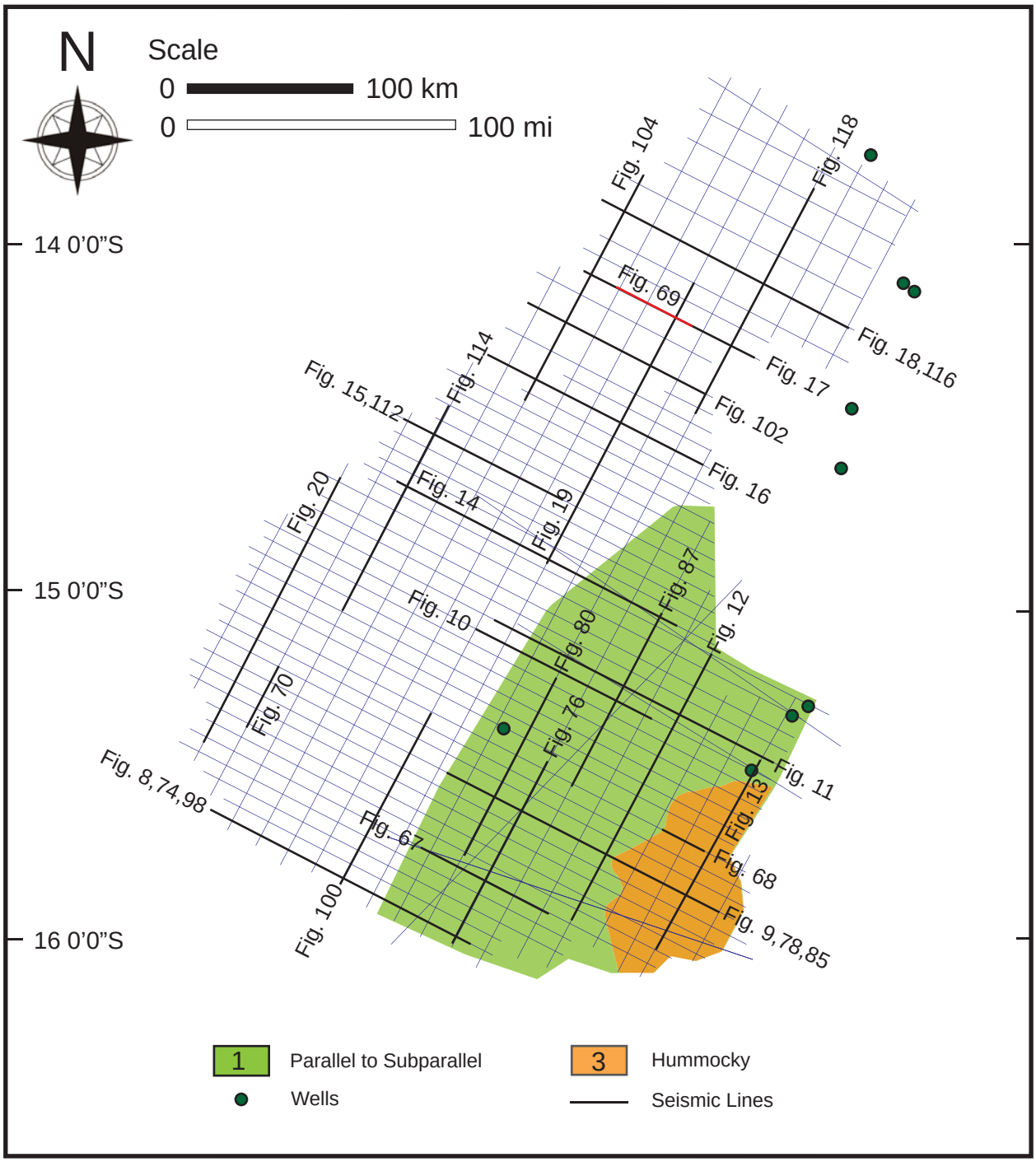

Figure 72. Seismic facies map of Subsequence I of Megasequence 2 interval. Each facies is numbered as described in the text. See Table 2 for seismic facies coding and Table 4 for a summary of seismic facies analysis and geologic interpretation. Locations of Figures 8-20, 67-70, 74-81, 85-88, 98-105, 112-119 (black lines) are shown, and wells are shown by green dots.

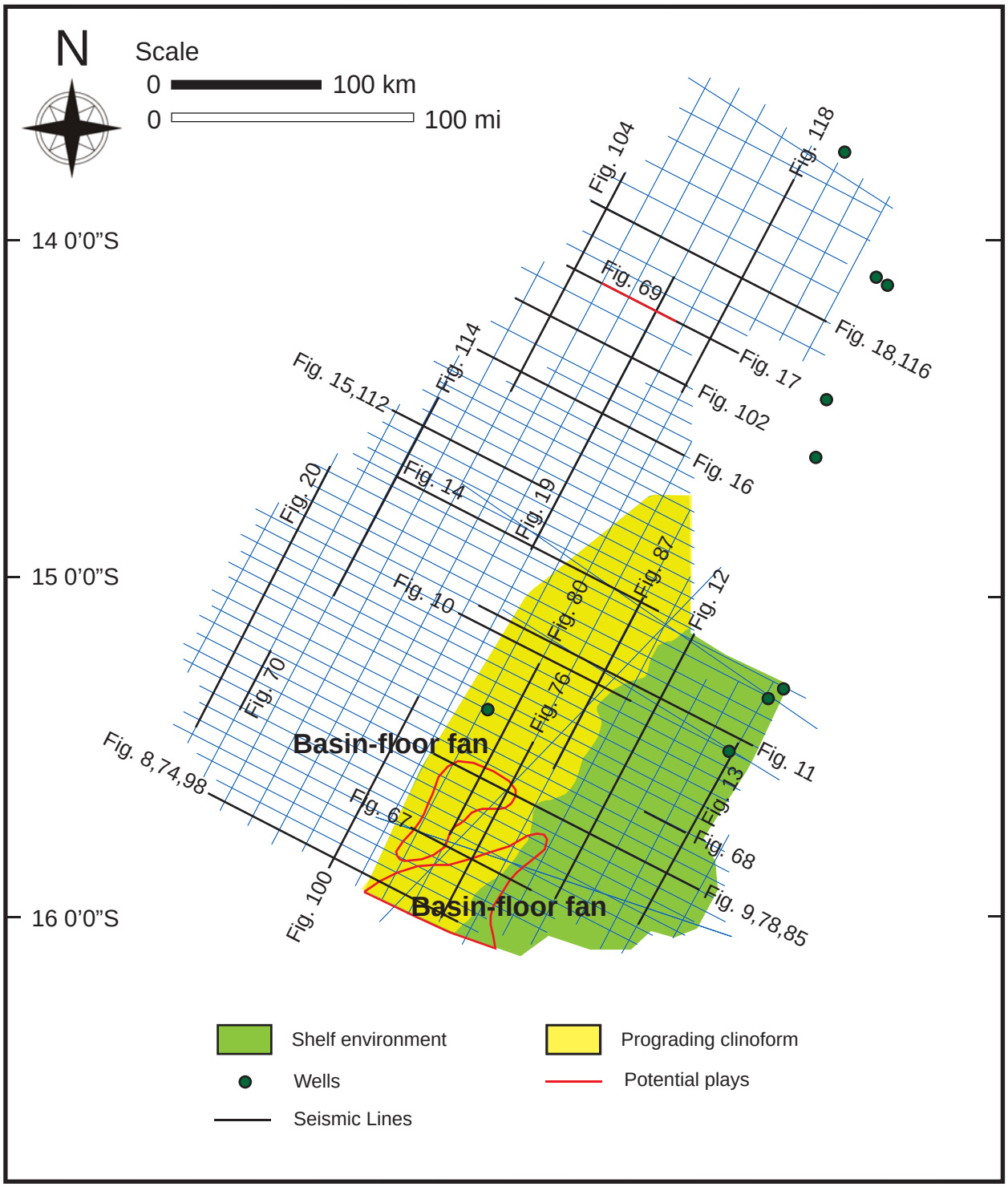

Figure 73 . Geologic facies map of Subsequence I of Megasequence 2 (top Aptian to top Turonian: 112.0-89.3 Ma) interval. See Table 4 for a summary of seismic facies analysis and geologic interpretation. Locations of Figures 8-20, 67-70, 74-81, 85-88, 98-105, 112-119 (black lines) are shown, and wells are shown by green dots.

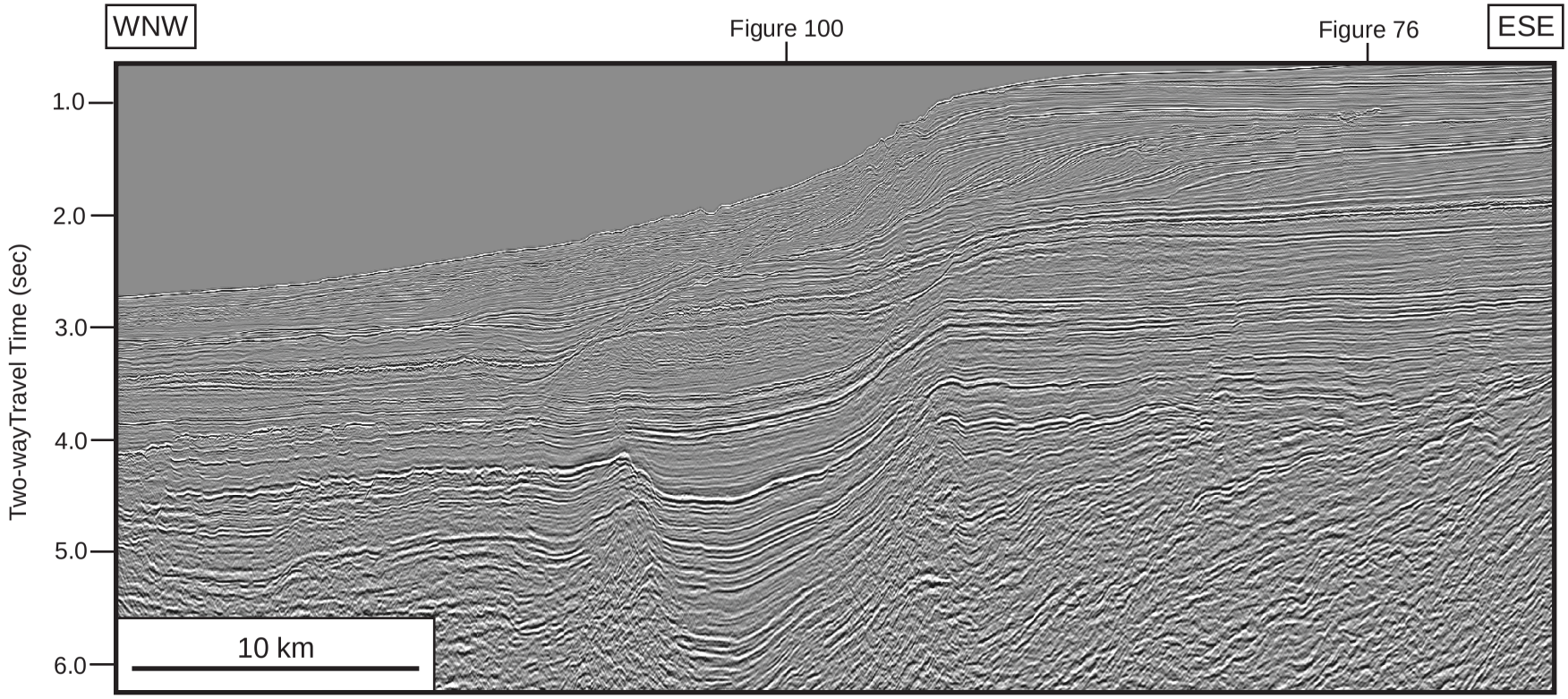

Figure 74a. Uninterpreted regional dip-oriented seismic profile (br-98:br98-001). Location of the profile is shown in Figures 65-66, 71-73, 82-84, 89-97, 106-111 and locations of where Figures 76, 100 cross the profile.

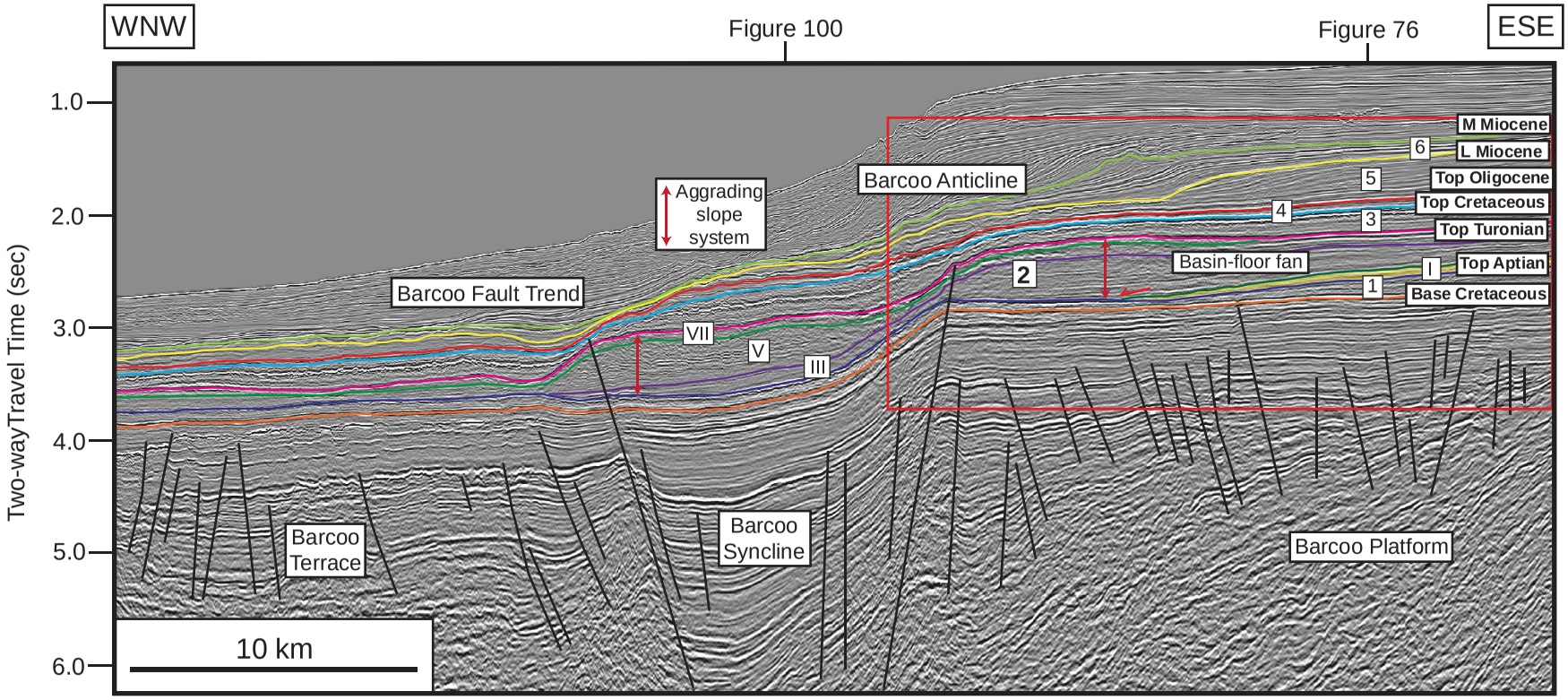

Figure 74b. Regional dip-oriented seismic profile showing all interpreted sequence boundaries from base Cretaceous to middle Miocene. This profile shows the deeper are of the Barcoo Terrace, The major graben structure of the Barcoo Syncline and the shallower area of the Barcoo Platform. The external wedges of low angle clinoform indicate a balance between the rates of subsudence and sediment supply. This Megasequence 2 shows the aggrading slope system (red arrow). The basin floor-fan is observed within Subsequence I of Megasequences 2 (yellow shade). Location of the profile is shown in Figures 65-66, 71-73, 82-84, 89-97, 106-111 and locations of where Figures 76, 100 cross the profile.

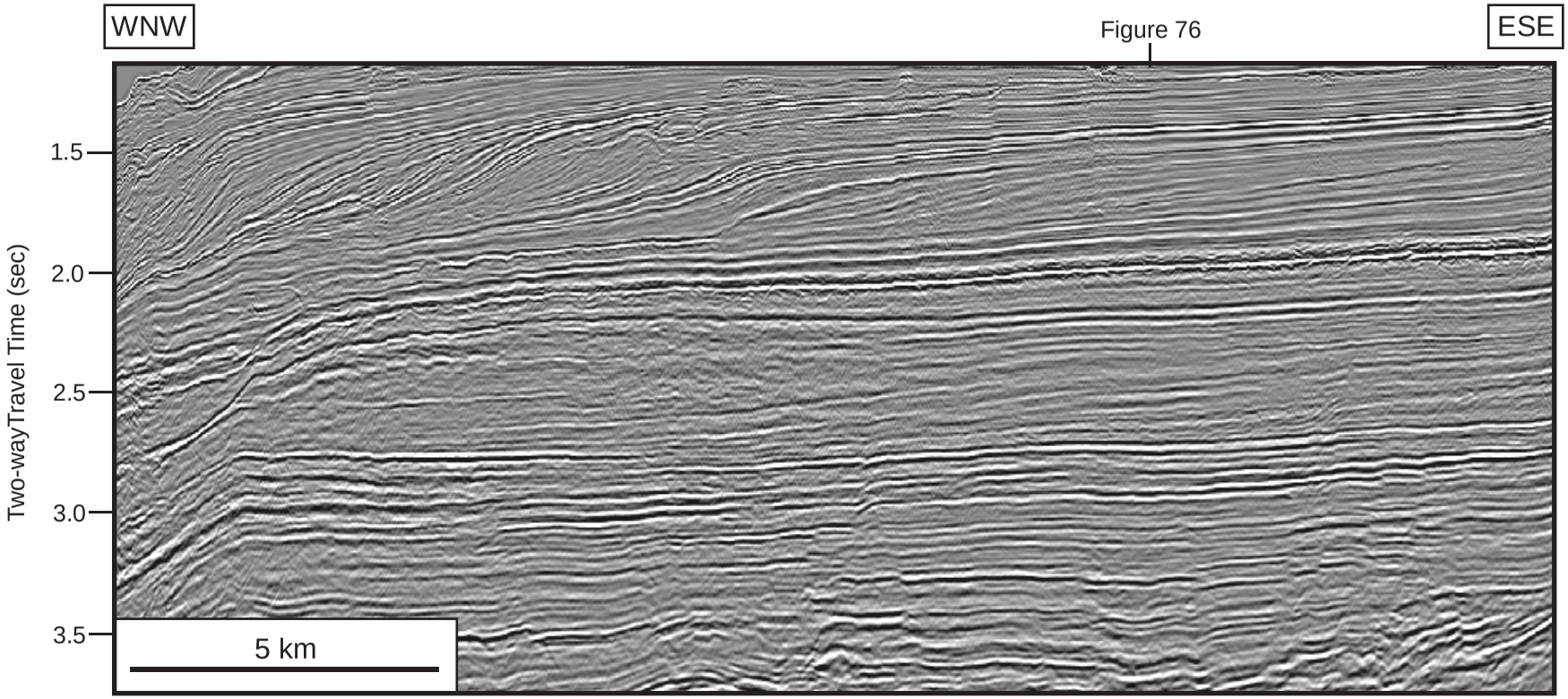

Figure 75a. Uninterpreted regional dip-oriented seismic profile (br-98:br98-001): A closeup view of Figure 73.

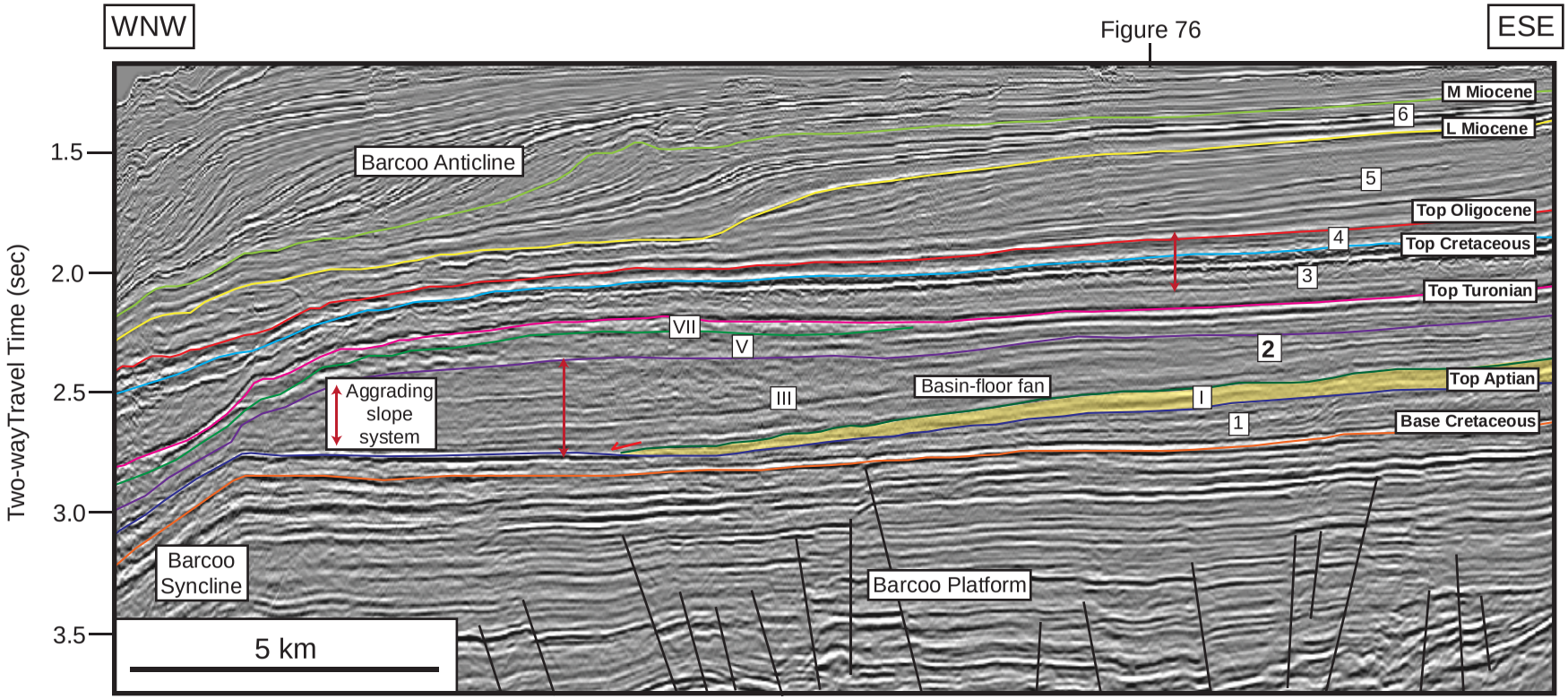

Figure 75b. Regional dip-oriented seismic profile showing all interpreted sequence boundaries from base Cretaceous to middle Miocene: A closeup view of Figure 73. The external wedges of low angle clinoform indicate a balance between the rates of subsudence and sediment supply. This Megasequence 2 shows the aggrading slope system (red arrow). The basin floor-fan is observed within Subsequence I of Megasequences 2 (yellow shade).

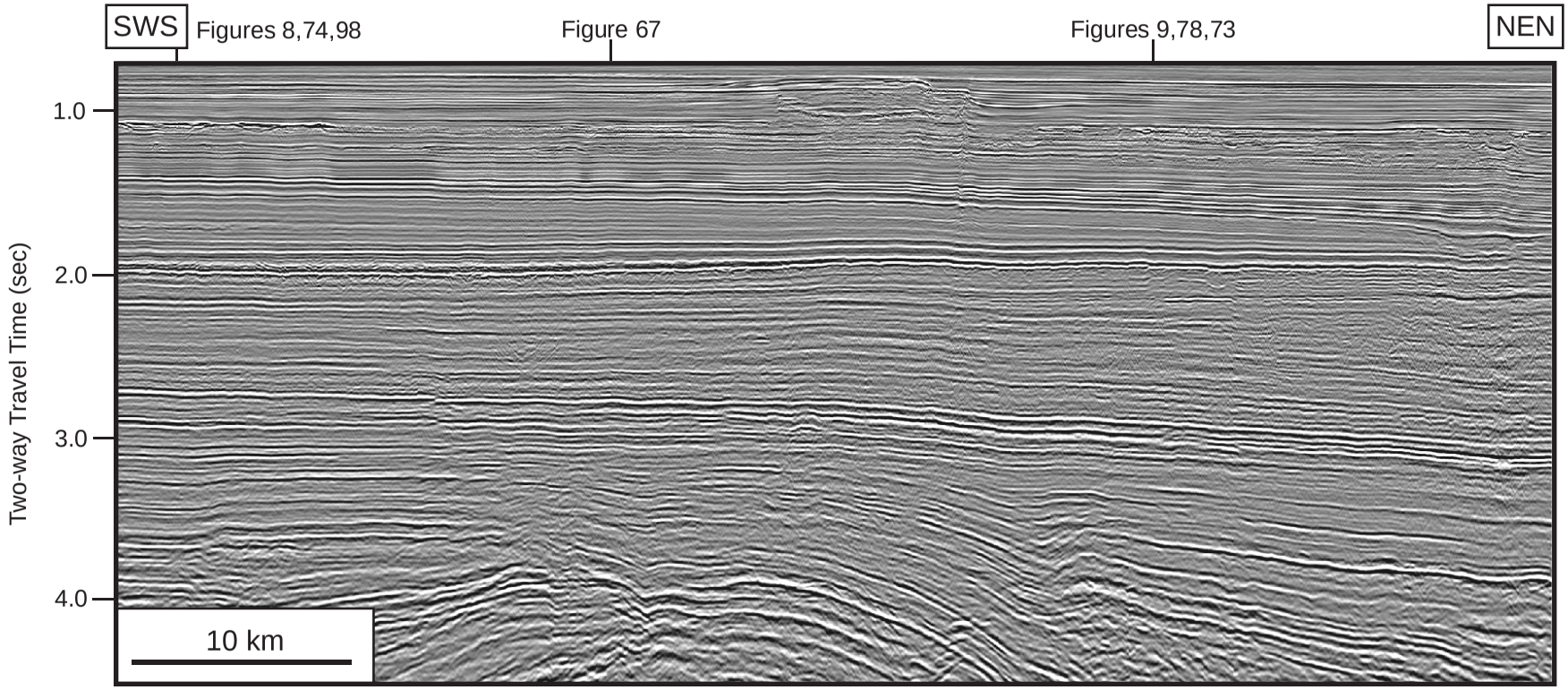

Figure 76a. Uninterpreted regional strike-oriented seismic profile (br-98:br98-078a). Location of the profile is shown in Figures 65-66, 71-73, 82-84, 89-97, 106-111 and locations of where Figures 8, 9, 67, 74, 78, 85, 98 cross the profile.

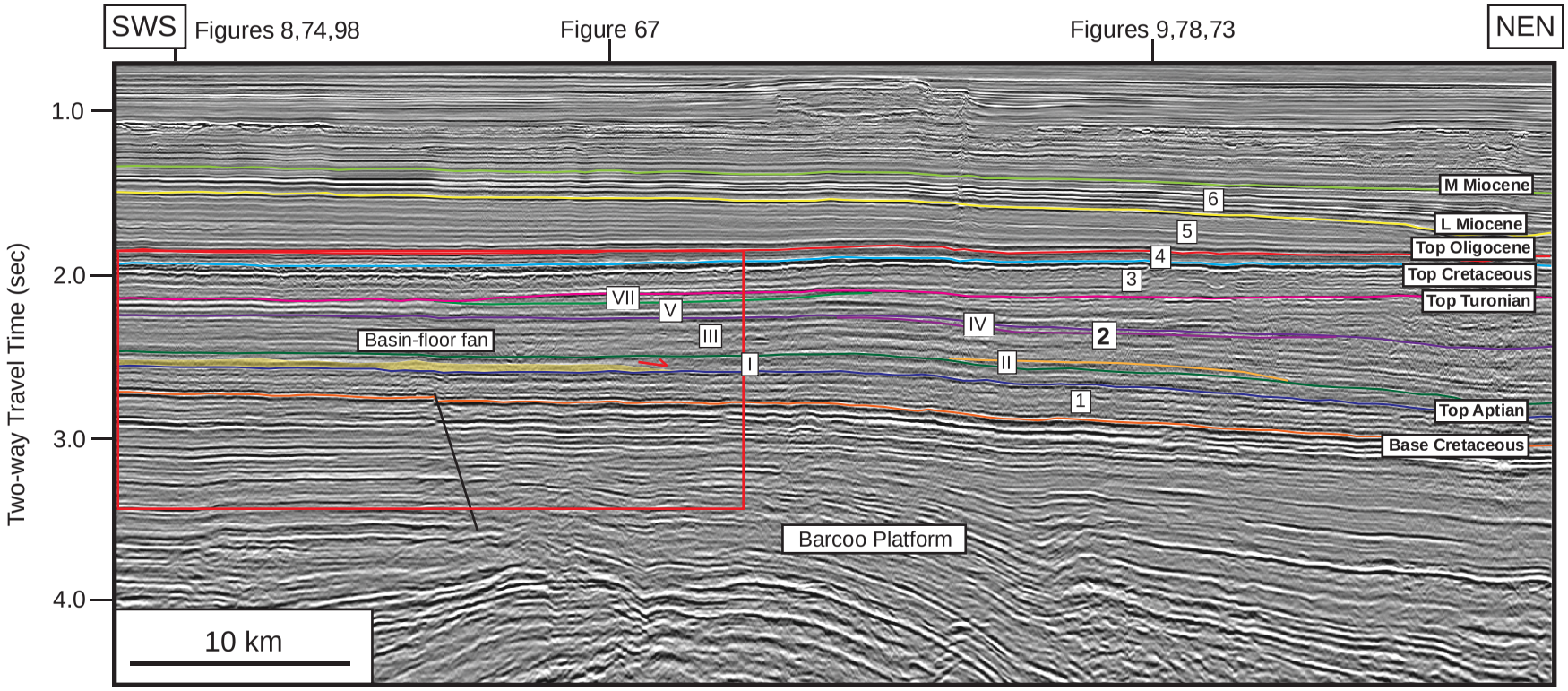

Figure 76b. Regional strike-oriented seismic profile showing all interpreted sequence boundaries from base Cretaceous to middle Miocene. This profile shows the area of the Barcoo Platform. The basin-floor fan is observed in Subsequence I of Megasequence 1 (yellow shade). Location of the profile is shown in Figures 65-66, 71-73, 82-84, 89-97, 106-111 and locations of where Figures 76, 100 cross the profile.

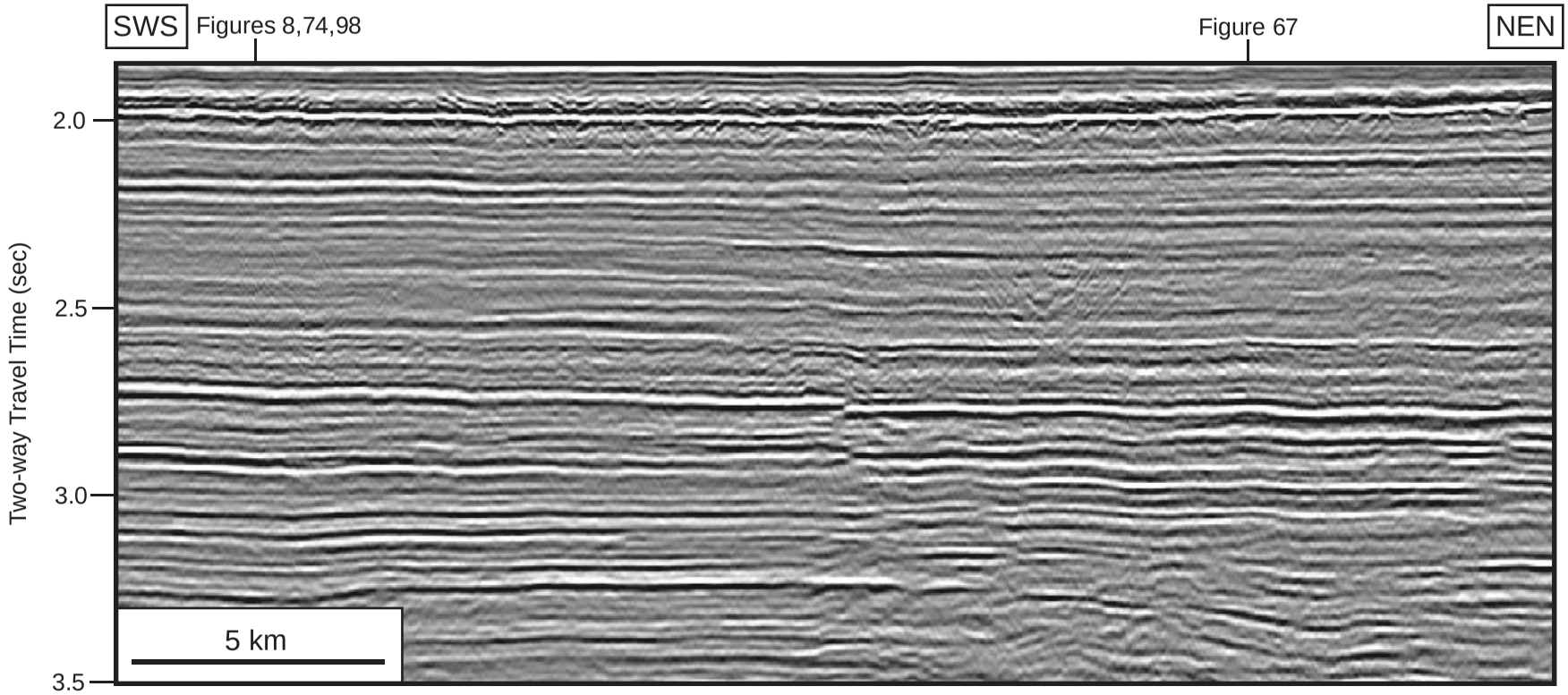

Figure 77a. Uninterpreted regional strike-oriented seismic profile (br-98:br98-078a): A closeup view of Figure 76.

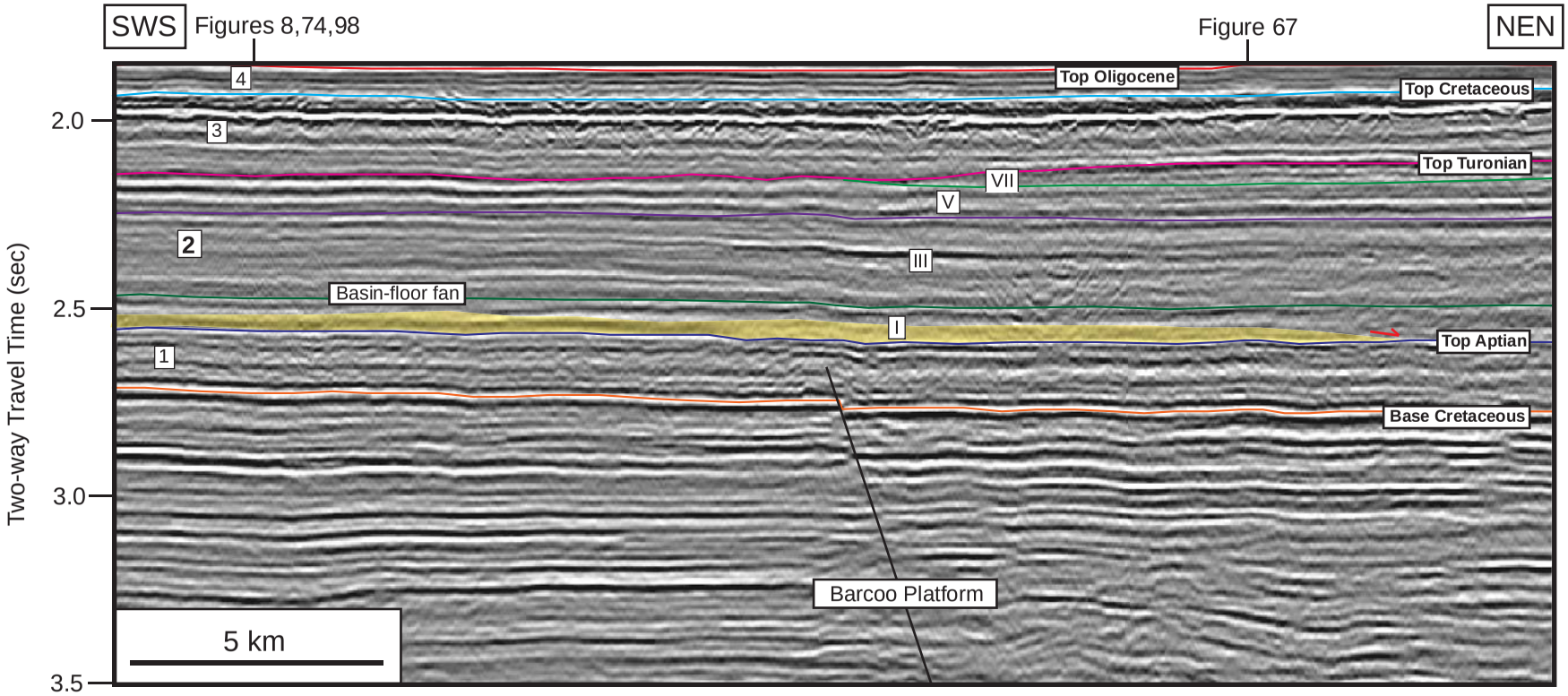

Figure 77b. Regional strike-oriented seismic profile showing all interpreted sequence boundaries from base Cretaceous to middle Miocene: A closeup view of Figure 76. The basin-floor fan is observed in Subsequence I of Megasequence 1 (yellow shade).

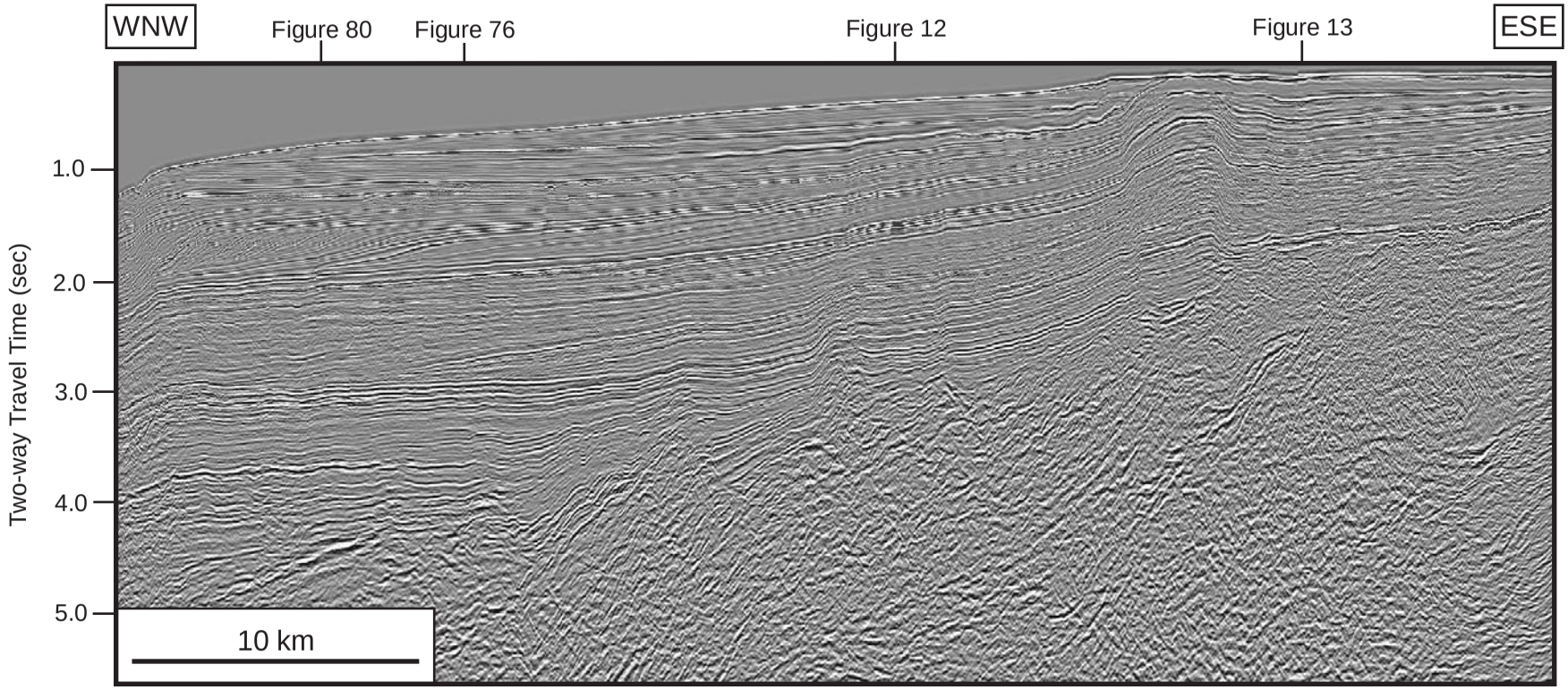

Figure 78a. Uninterpreted regional dip-oriented seismic profile (br-98:br98-010). Location of the profile is shown in Figures 65-66, 71-73, 82-84, 89-97, 106-111 and locations of where Figures 12, 13, 76, 80 cross the profile.

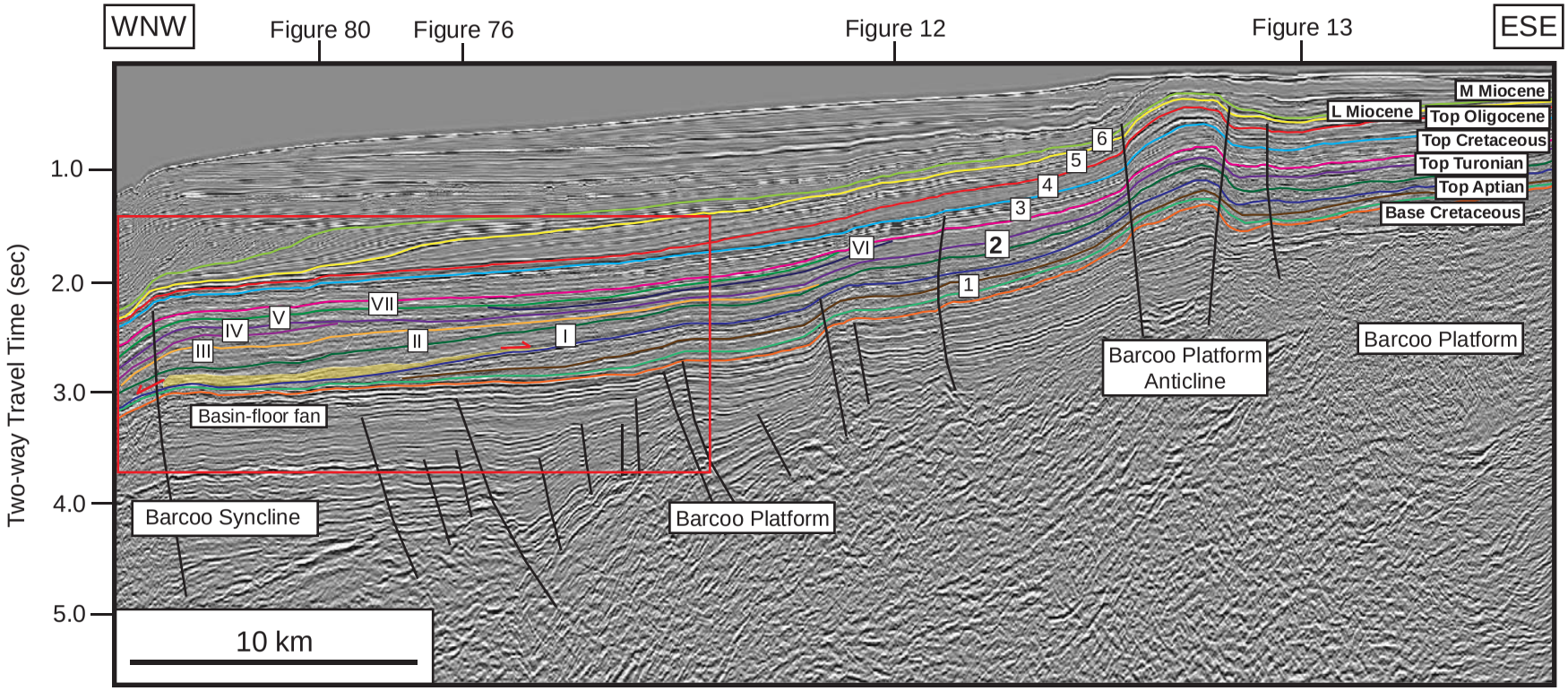

Figure 78b. Regional dip-oriented seismic profile showing all interpreted sequence boundaries from base Cretaceous to middle Miocene. The Barcoo Anticline and small faults of Barcoo fault system in the underlying Jurassic strata are observed. The Barcoo Platform anticline, which formed at the eastern margin of the Barcoo Sub-basin next to the Leveque Shelf, is associated with the fault reactivation during the late Miocene. The prograding sediment wedge is recognized within Subsequence I of Megasequence 2. Location of the profile is shown in Figures 65-66, 71-73, 82-84, 89-97, 106-111 and locations of where Figures 12, 13, 76, 80 cross the profile.

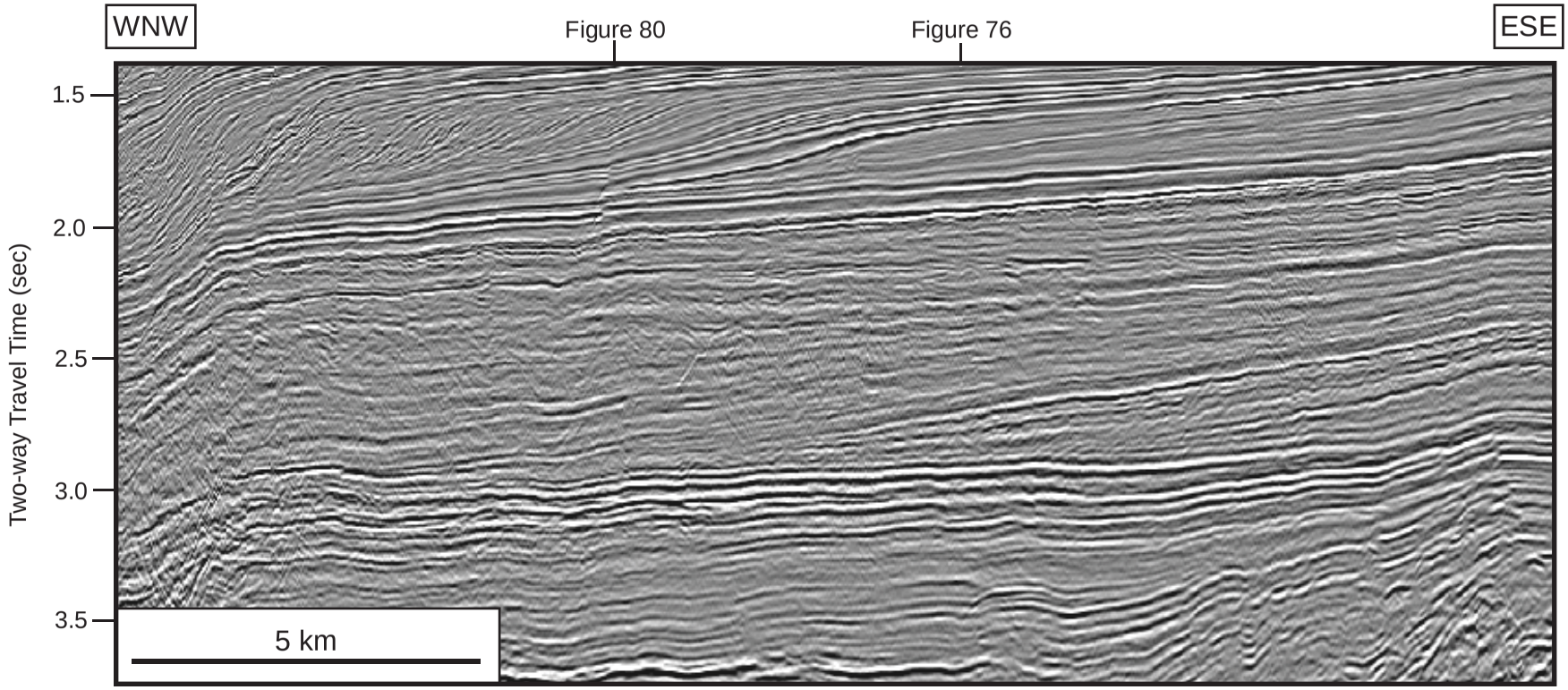

Figure 79a. Uninterpreted regional dip-oriented seismic profile (br-98:br98-010): A closeup view of Figure 78.

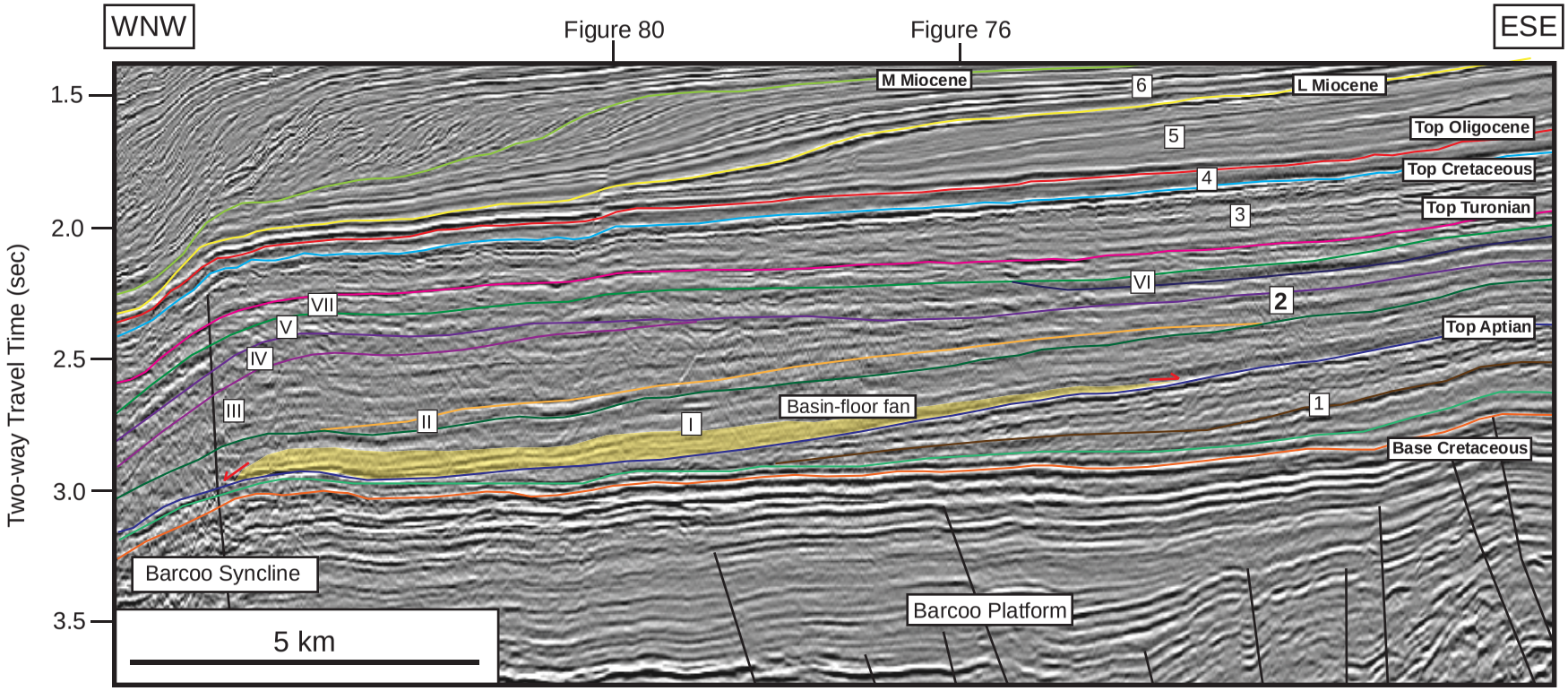

Figure 79b. Regional dip-oriented seismic profile showing all interpreted sequence boundaries from base Cretaceous to middle Miocene: A closeup view of Figure 78. The basin-floor fan is recognized within Subsequence I of Megasequence 2.

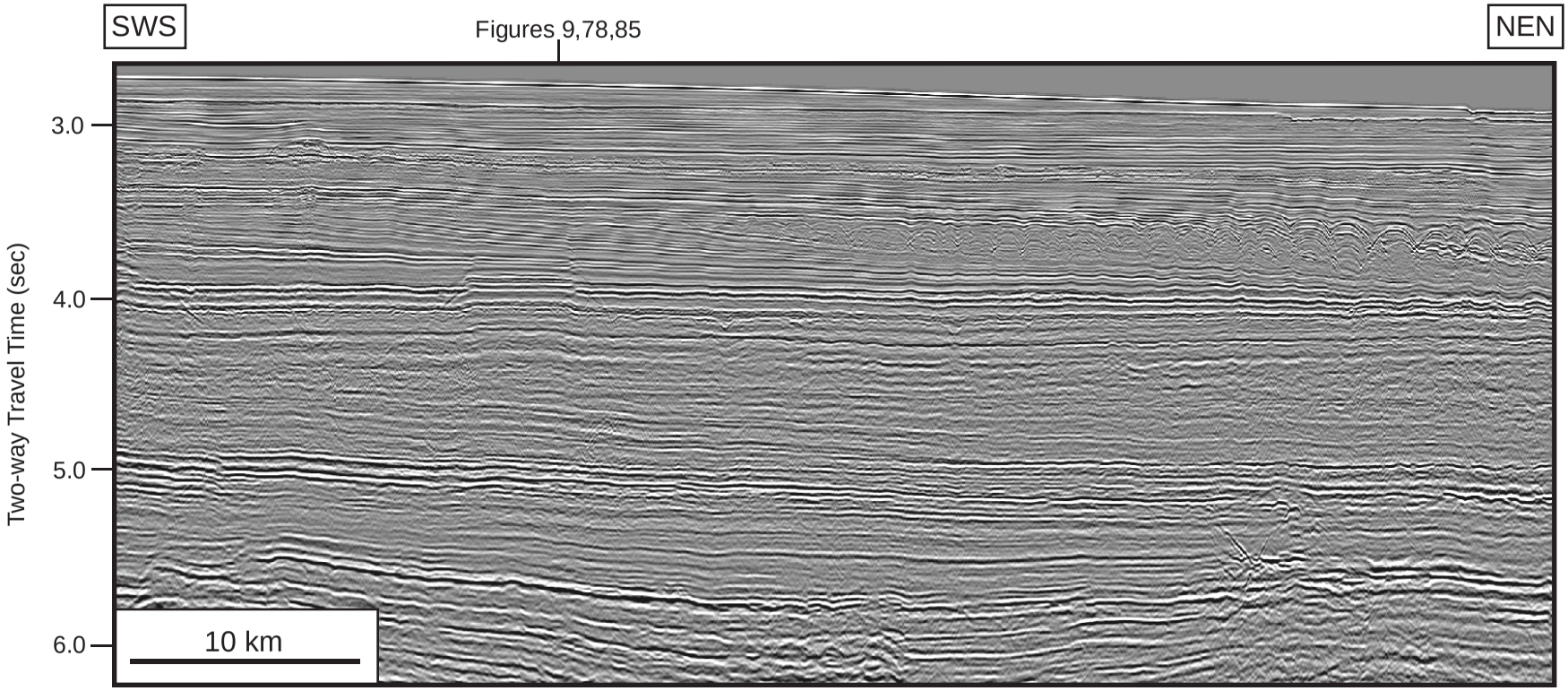

Figure 80a. Uninterpreted regional dip-oriented seismic profile (br-98:br98-080). Location of the profile is shown in Figures 65-66, 71-73, 82-84, 89-97, 106-111 and location of where Figures 9, 78, 85 cross the profile.

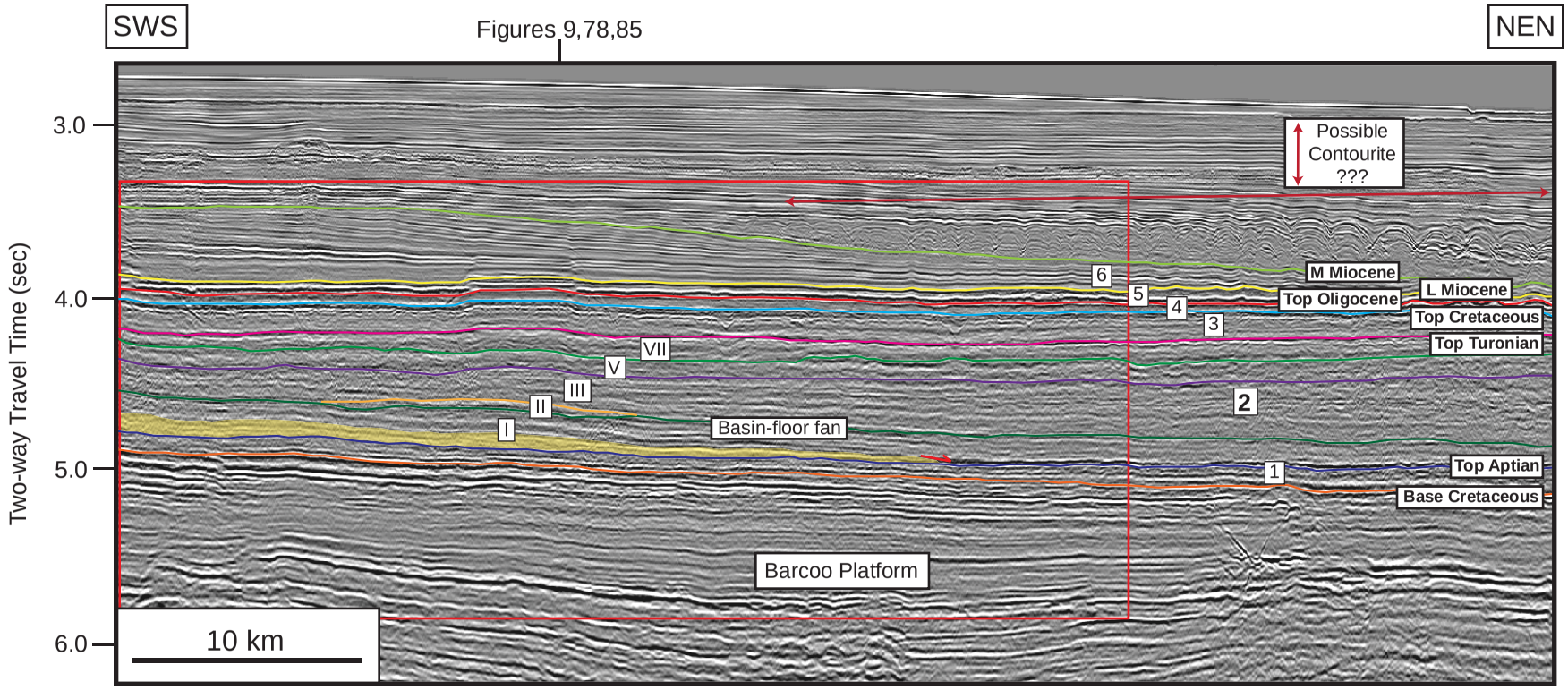

Figure 80b. Regional strike-oriented seismic profile showing all interpreted sequence boundaries from base Cretaceous to middle Miocene. This profile shows the area of the Barcoo Platform. The basin-floor fan is observed within the low angle clinoform of Subsequence I of Megasequence 1 (yellow shade). Location of the profile is shown in Figures 65-66, 71-73, 82-84, 89-97, 106-111 and location of where Figures 9, 78, 85 cross the profile.

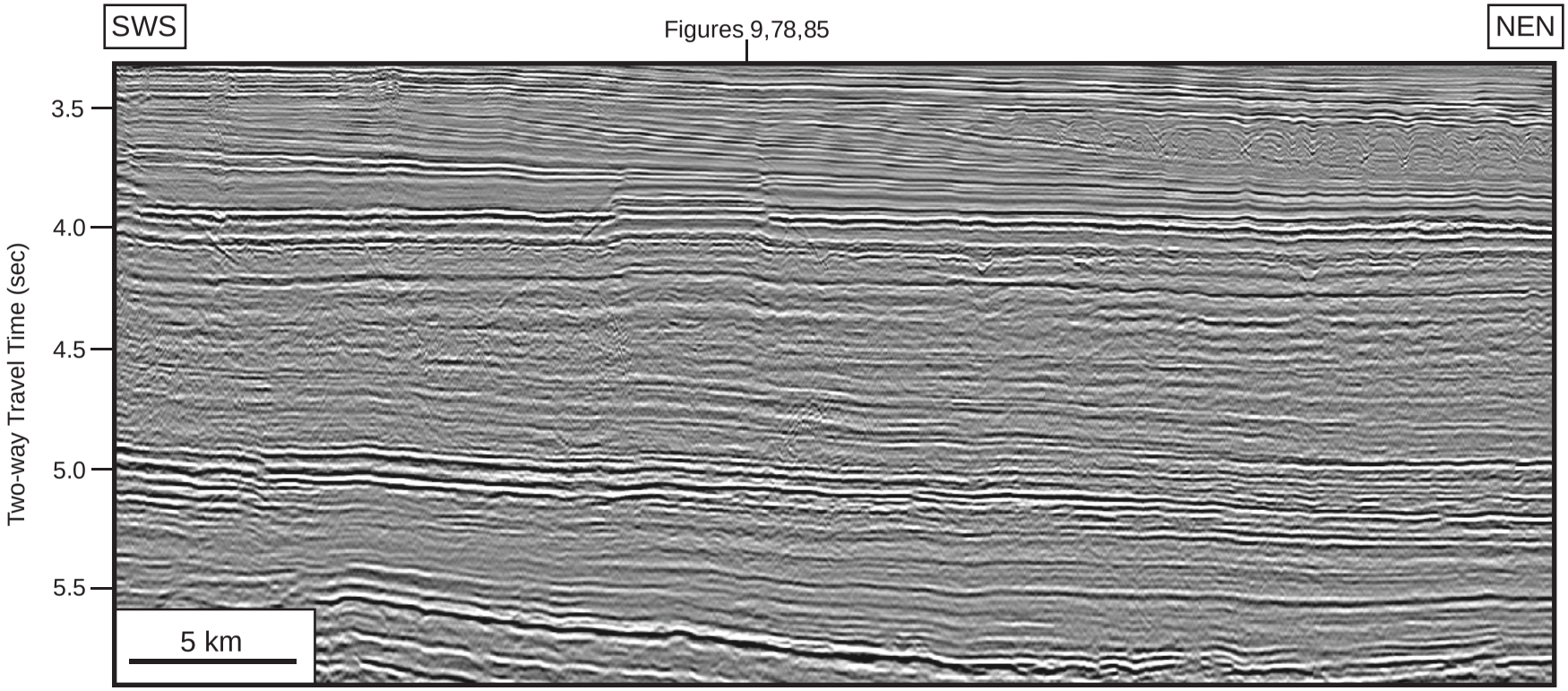

Figure 81a. Uninterpreted regional dip-oriented seismic profile (br-98:br98-080): A closeup view of Figure 80.

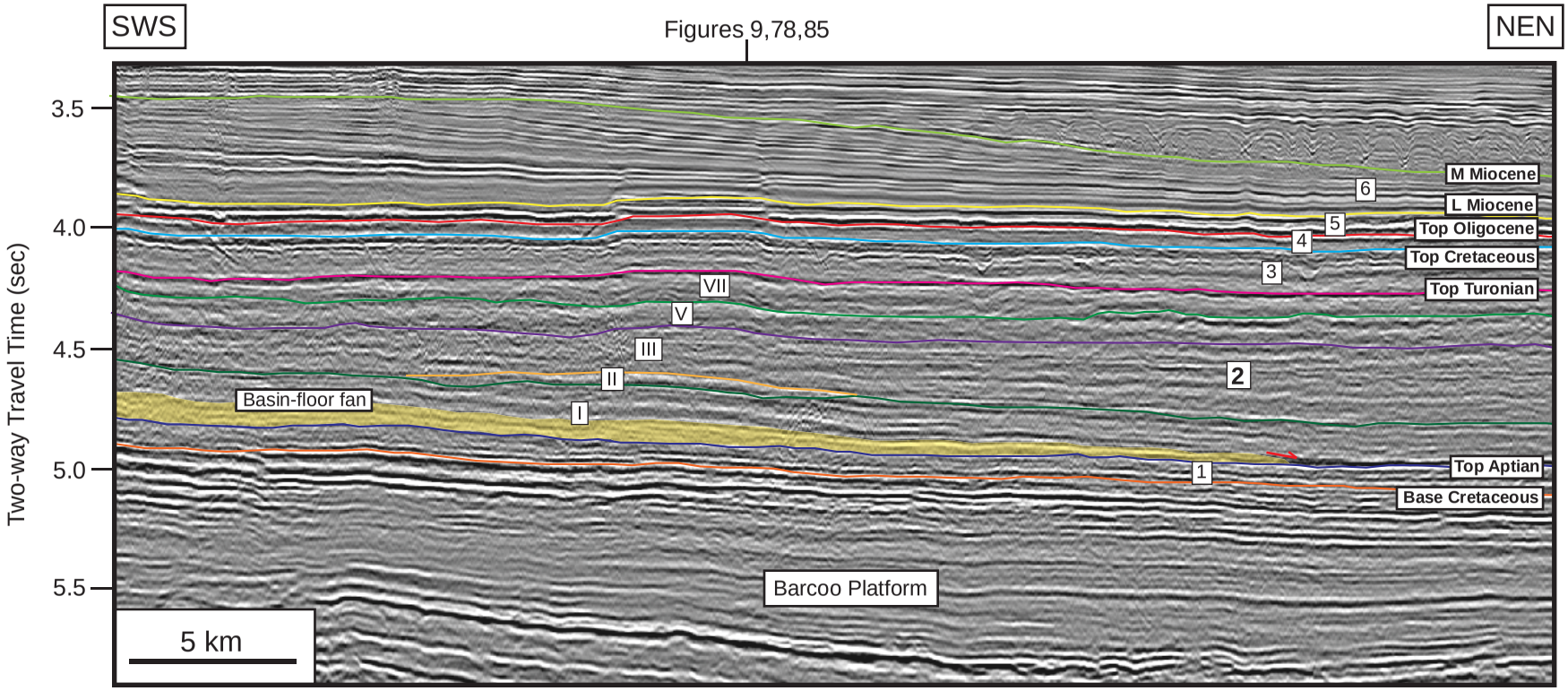

Figure 81b. Regional strike-oriented seismic profile showing all interpreted sequence boundaries from base Cretaceous to middle Miocene: A closeup view of Figure 80. The basin-floor fan is observed within the low angle clinoform of Subsequence I of Megasequence 1 (yellow shade).

Subsequence II of Megasequence 2

The isochron map of this subsequence illustrates the thickness values varying from 0 to 241 msec two-way travel time (TWTT) (Figure 82). These sediments deposited covering the area of the Barcoo Anticline.

Only one of seismic facies 5 is specified (Figure 83; Table 7). This facies is present as the concordant to both upper and lower sequence boundaries. The internal reflection configuration is chaotic with low amplitude and poor continuity. From the geological analysis, it is interpreted to be a prograding wedge deposited on a graben flank (Figure 84). This subsequence is one of the potential prospects in this area. The dip and strike oriented seismic profiles are shown in Figures 85-88.

Table 7. Seismic facies and geologic interpretation of Subsequence II of Megasequence 2

Seismic Facies	Upper Sequence Boundary	Lower Sequence Boundary	Internal Reflection Configuration	Amplitude	Continuity	Geologic Interpretation
5	Concordant	Concordant	Chaotic	low	poor	Basinal deposits on graben flank

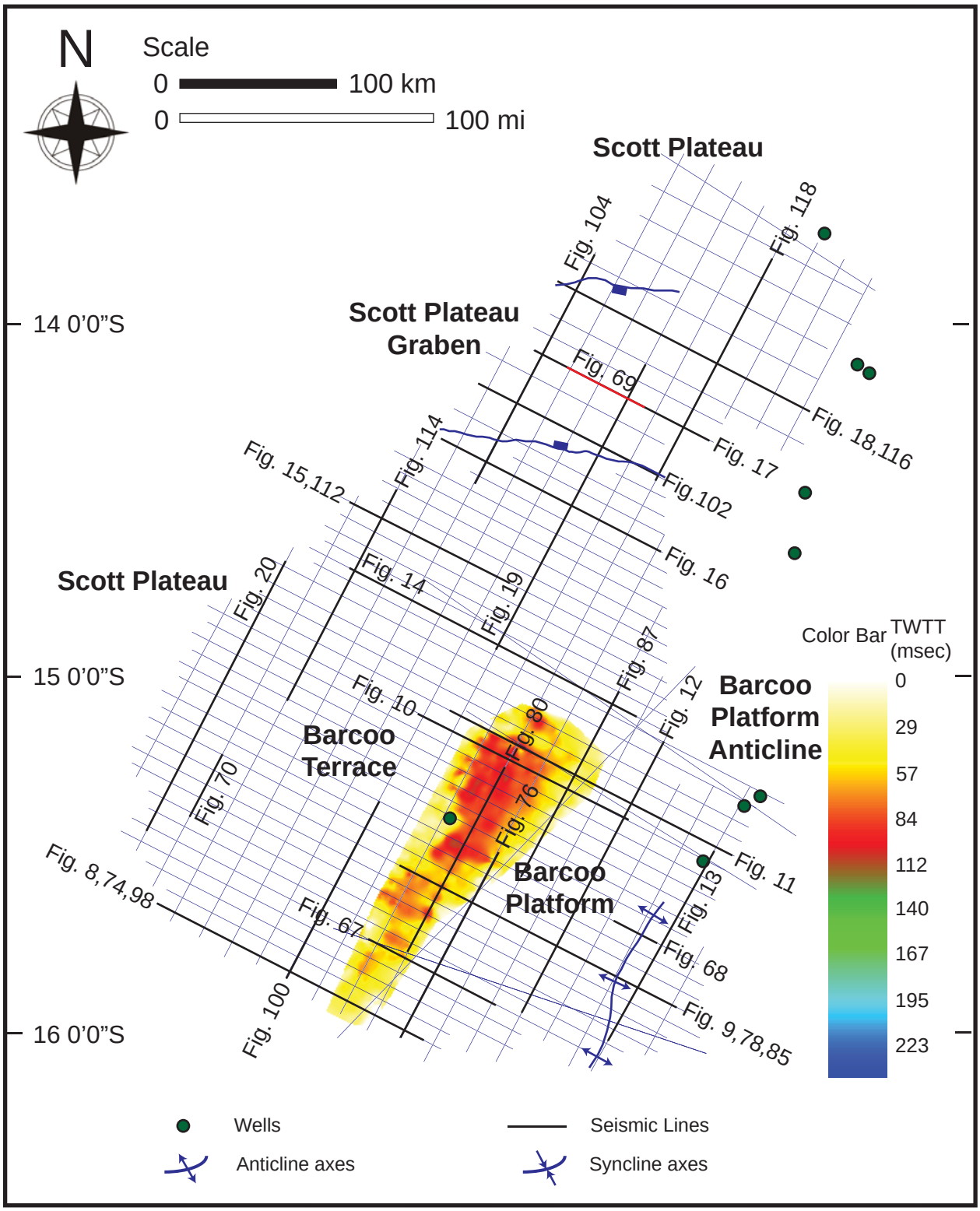

Figure 82. Isochron map (in TWTT msecs) ofSubsequence II of Megasequence 2 interval. Distribution of 2D seismic profiles interpreted to generate the maps are shown by blue lines, and wells are shown by green dots. Locations of Figures 8-20, 67-70, 74-81, 85-88, 98-105, 112-119 are shown.

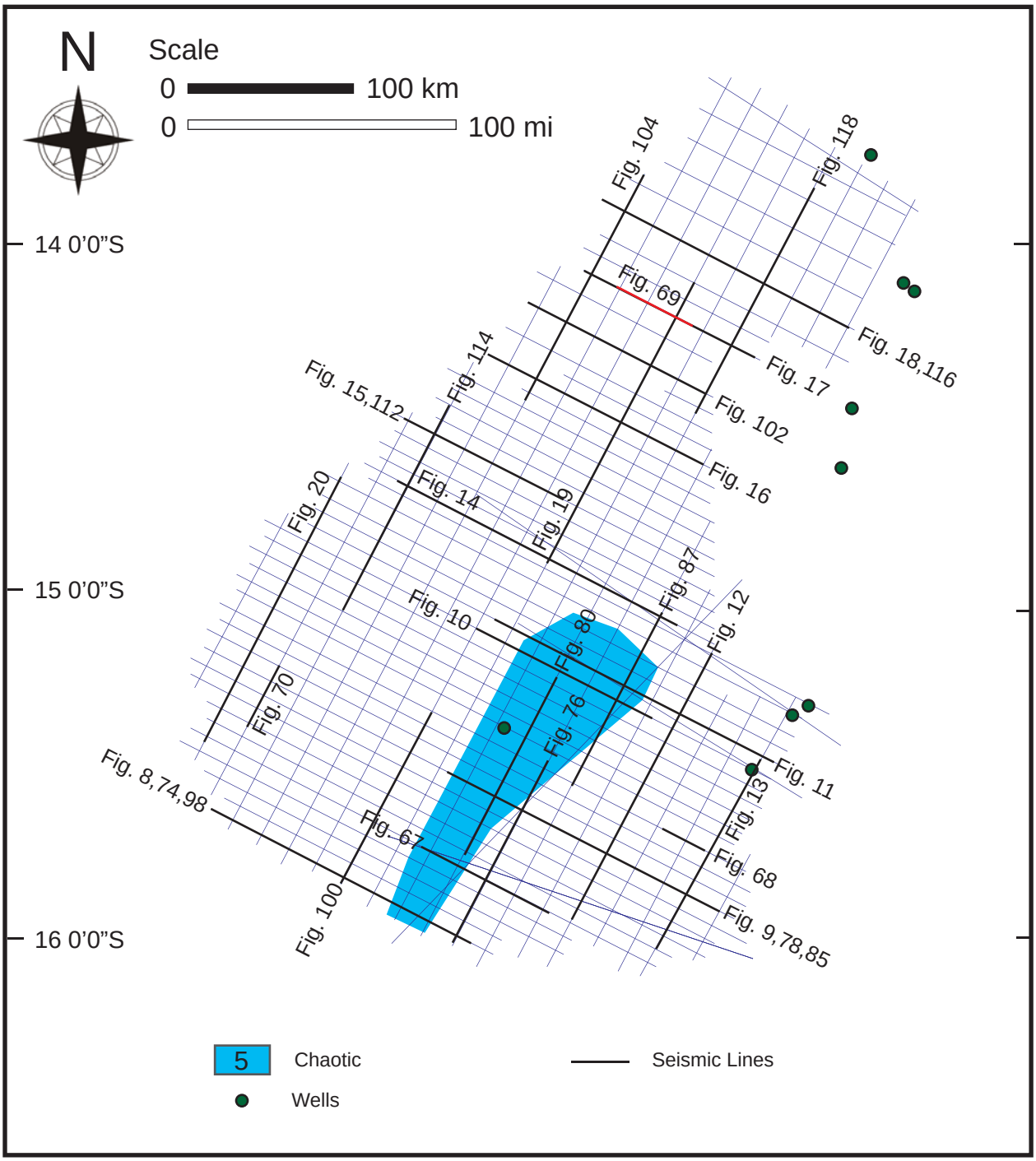

Figure 83. Seismic facies map of Subsequence II of Megasequence 2 interval. Each facies is numbered as described in the text. See Table 2 for seismic facies coding and Table 4 for a summary of seismic facies analysis and geologic interpretation. Locations of Figures 8-20, 67-70, 74-81, 85-88, 98-105, 112-119 (black lines) are shown, and wells are shown by green dots.

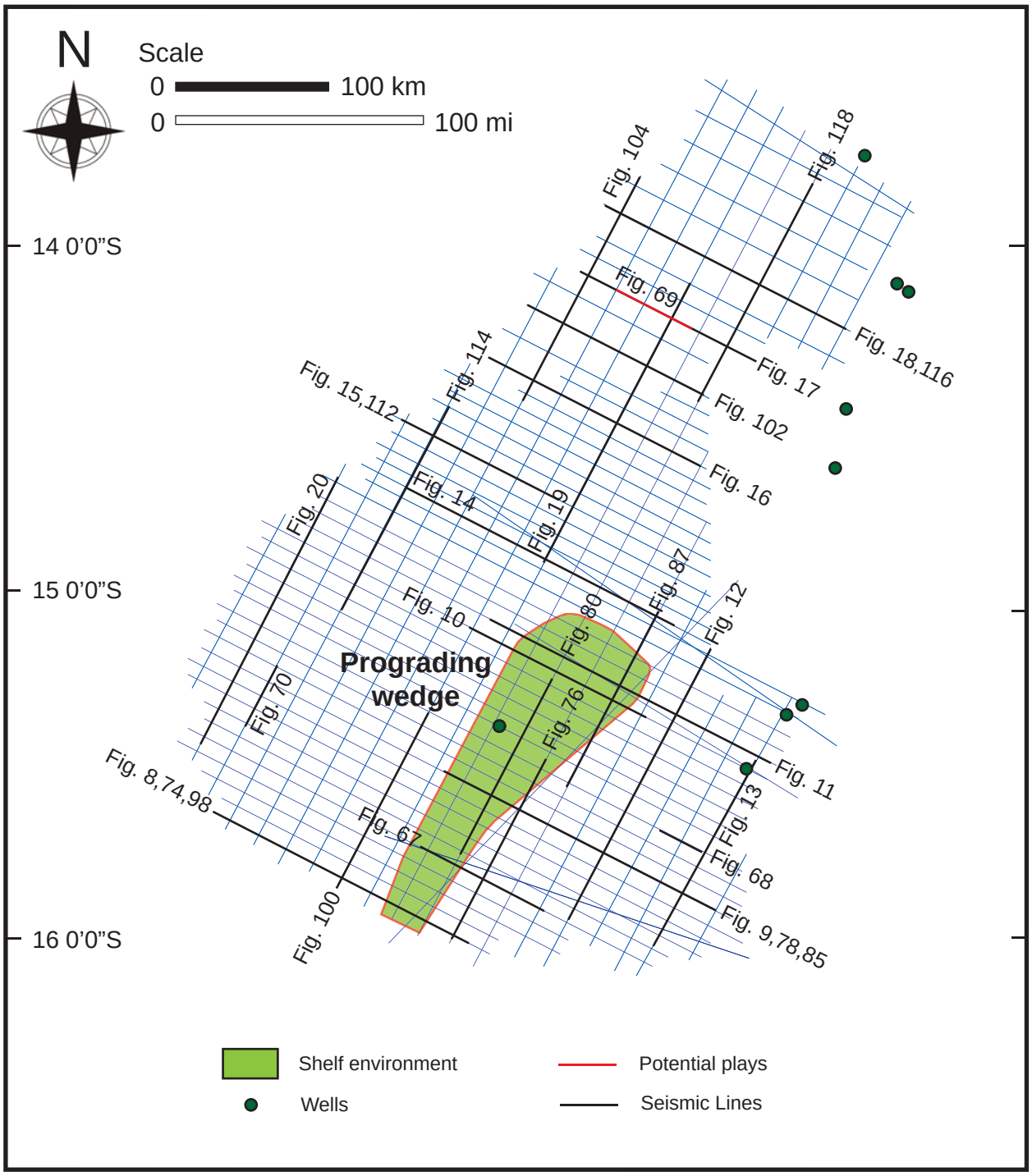

Figure 84. Geologic facies map of Subsequence II of Megasequence 2 (top Aptian to top Turonian: 112.0-89.3 Ma) interval. See Table 4 for a summary of seismic facies analysis and geologic interpretation. Locations of Figures 8-20, 67-70, 74-81, 85-88, 98-105, 112-119 (black lines) are shown, and wells are shown by green dots.

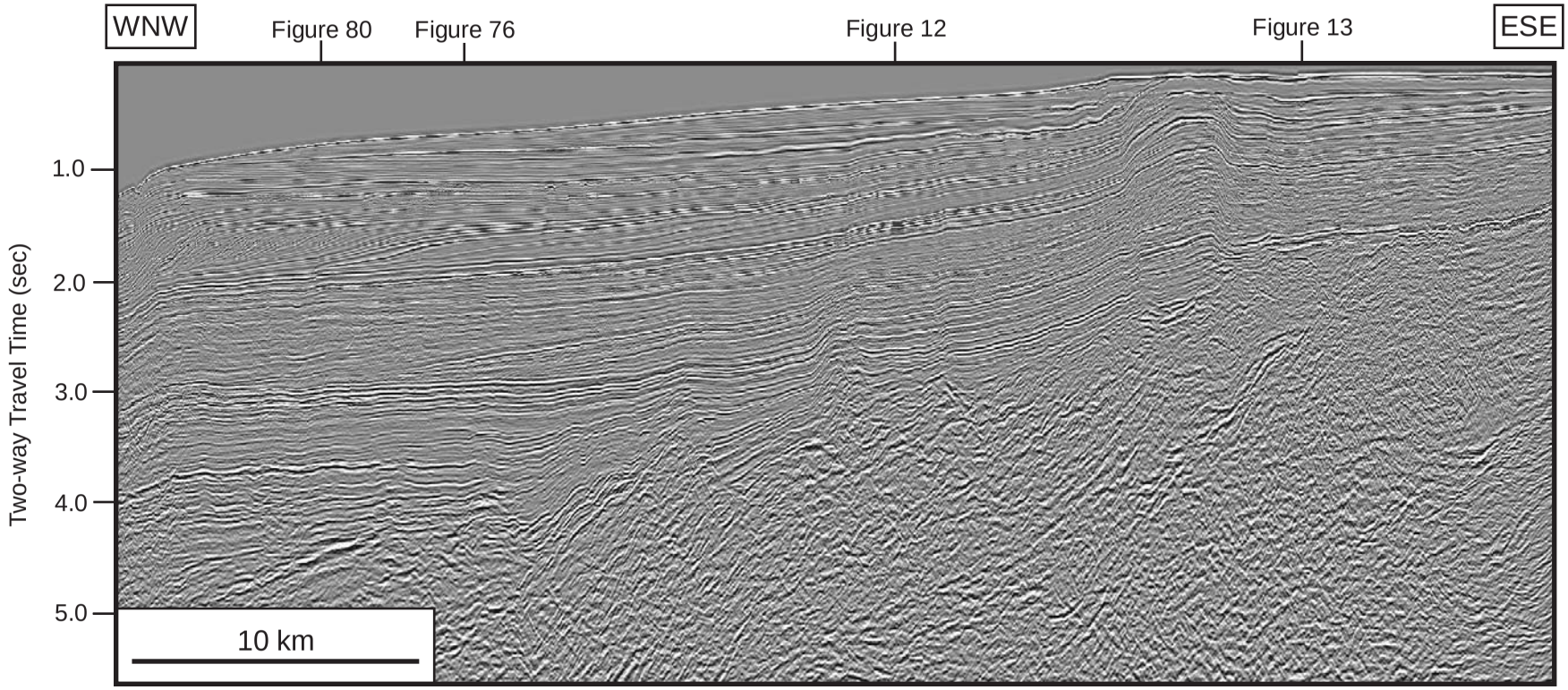

Figure 85a. Uninterpreted regional dip-oriented seismic profile (br-98:br98-010). Location of the profile is shown in Figures 65-66, 71-73, 82-84, 89-97, 106-111 and locations of where Figures 12, 13, 76, 80 cross the profile.

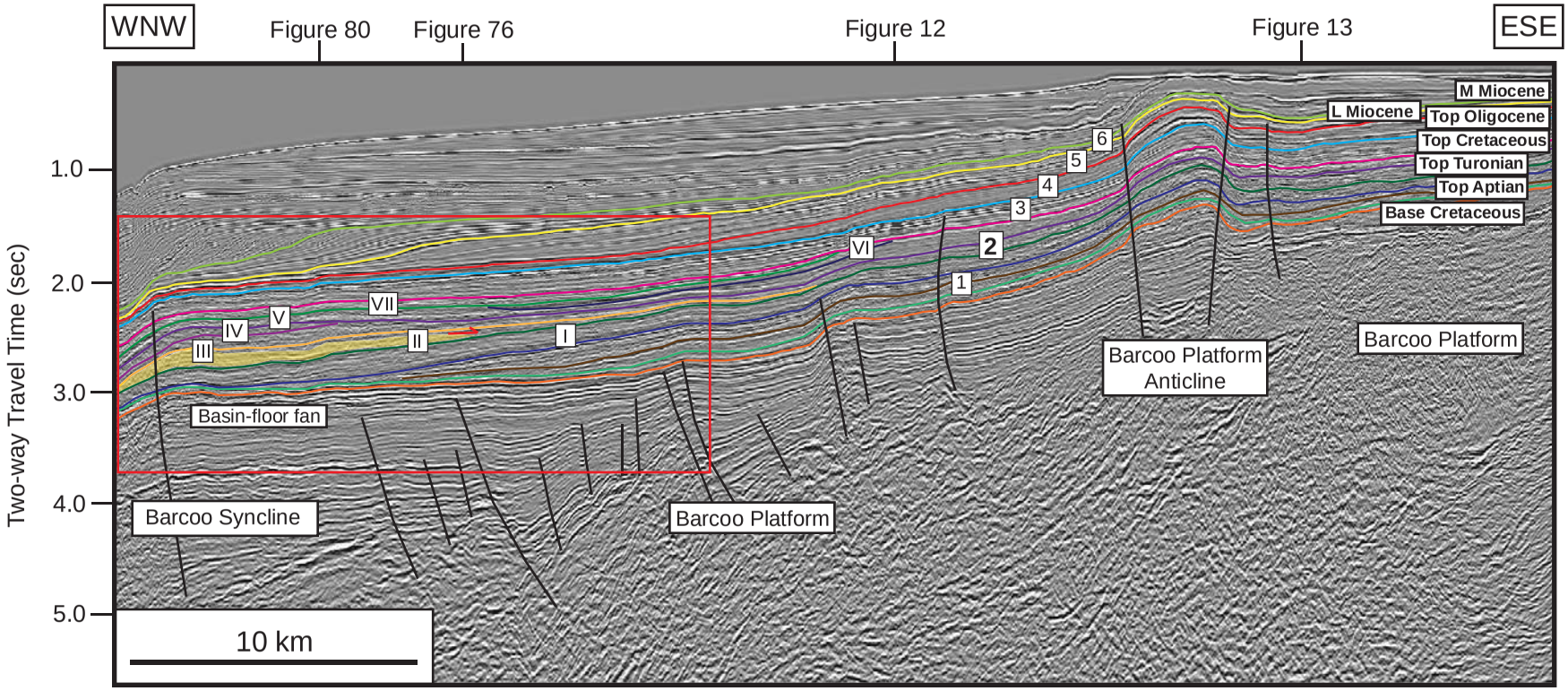

Figure 85b. Regional dip-oriented seismic profile showing all interpreted sequence boundaries from base Cretaceous to middle Miocene. The Barcoo Anticline and small faults of Barcoo fault system in the underlying Jurassic strata are observed. The Barcoo Platform anticline, which formed at the eastern margin of the Barcoo Sub-basin next to the Leveque Shelf, is associated with the fault reactivation during the late Miocene. The prograding sediment wedge is recognized within Subsequence I of Megasequence 2. Location of the profile is shown in Figures 65-66, 71-73, 82-84, 75-83, 106-111 and locations of where Figures 12, 13, 76, 80 cross the profile.

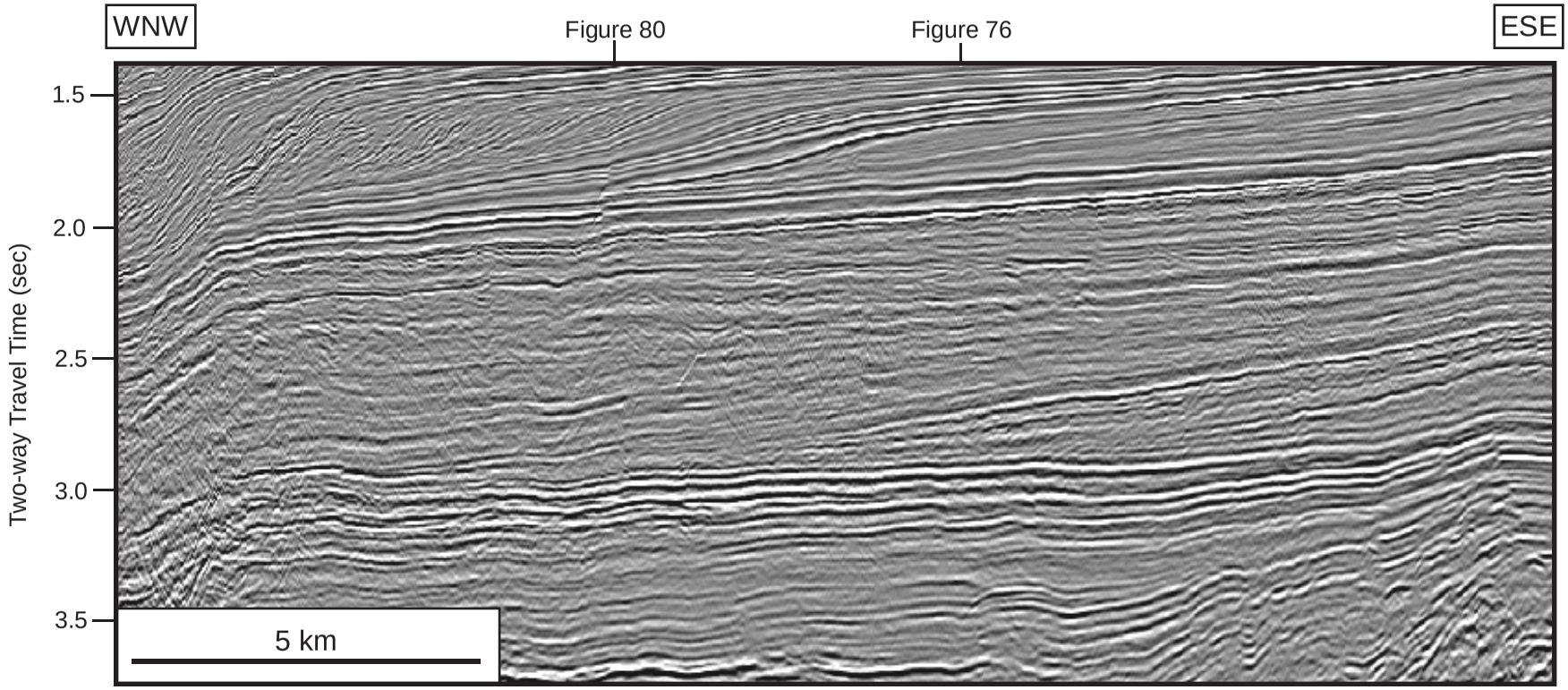

Figure 86a. Uninterpreted regional dip-oriented seismic profile (br-98:br98-010): A closeup view of Figure 85.

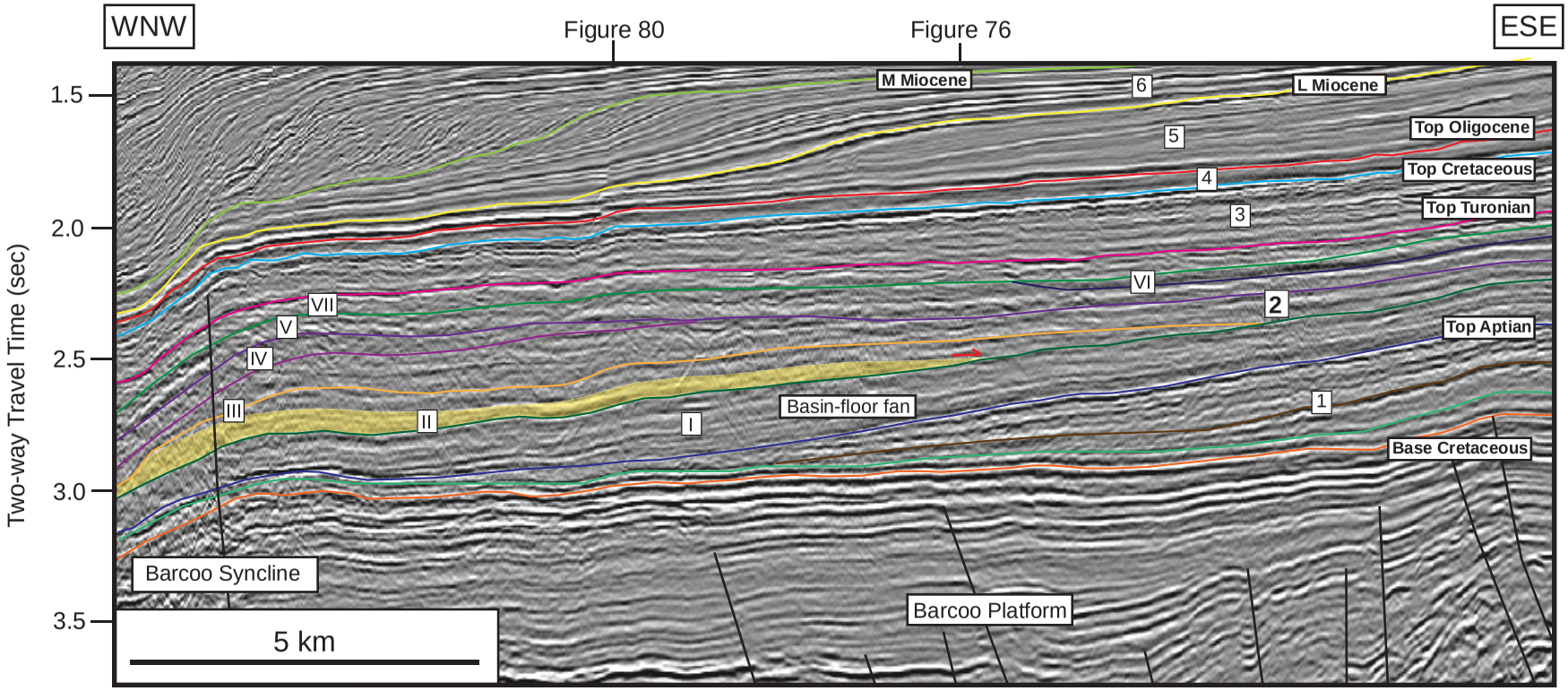

Figure 86b. Regional dip-oriented seismic profile showing all interpreted sequence boundaries from base Cretaceous to middle Miocene: A closeup view of Figure 85. The basin-floor fan is recognized within Subsequence I of Megasequence 2.

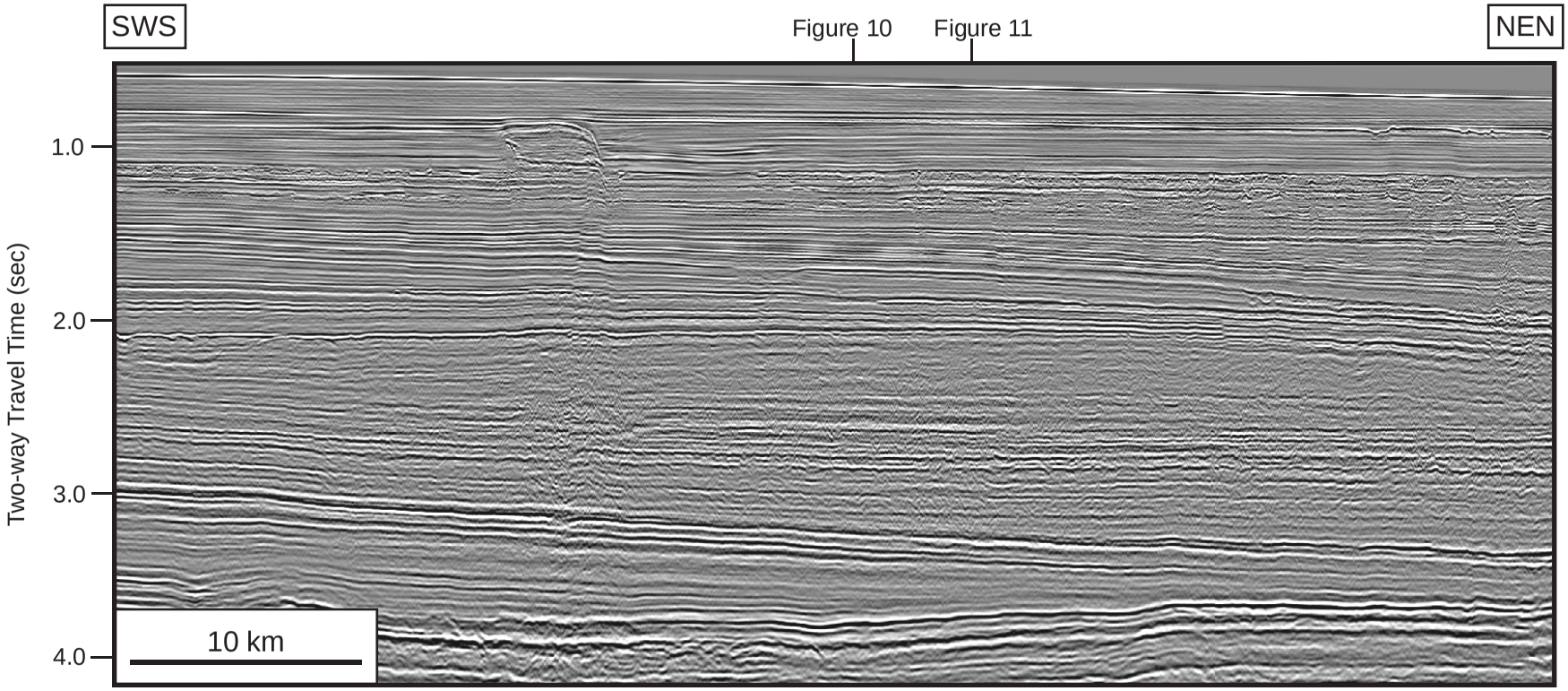

Figure 87a. Uninterpreted regional strike-oriented seismic profile (br-98:br98-075b). Location of the profile is shown in Figures 65-66, 71-73, 82-84, 89-97, 106-111 and locations of where Figures 10, 11 cross the profile.

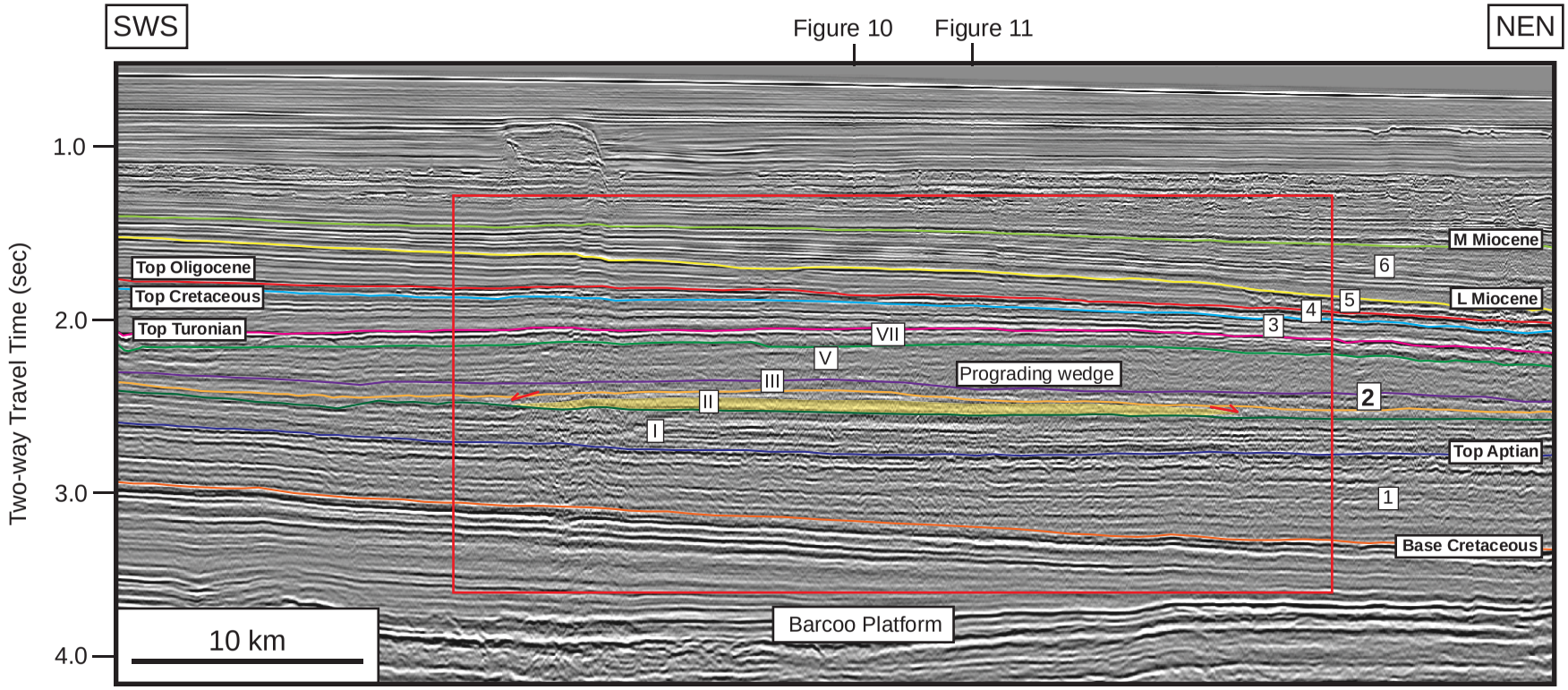

Figure 87b. Regional strike-oriented seismic profile showing all interpreted sequence boundaries from base Cretaceous to middle Miocene. This profile shows the area of the Barcoo Platform. The basin-floor fan is observed within the Subsequence II of Megasequence 2 (yellow shade). Location of the profile is shown in Figures 65-66, 71-73, 82-84, 89-97, 106-111 and locations of where Figures 10, 11 cross the profile.

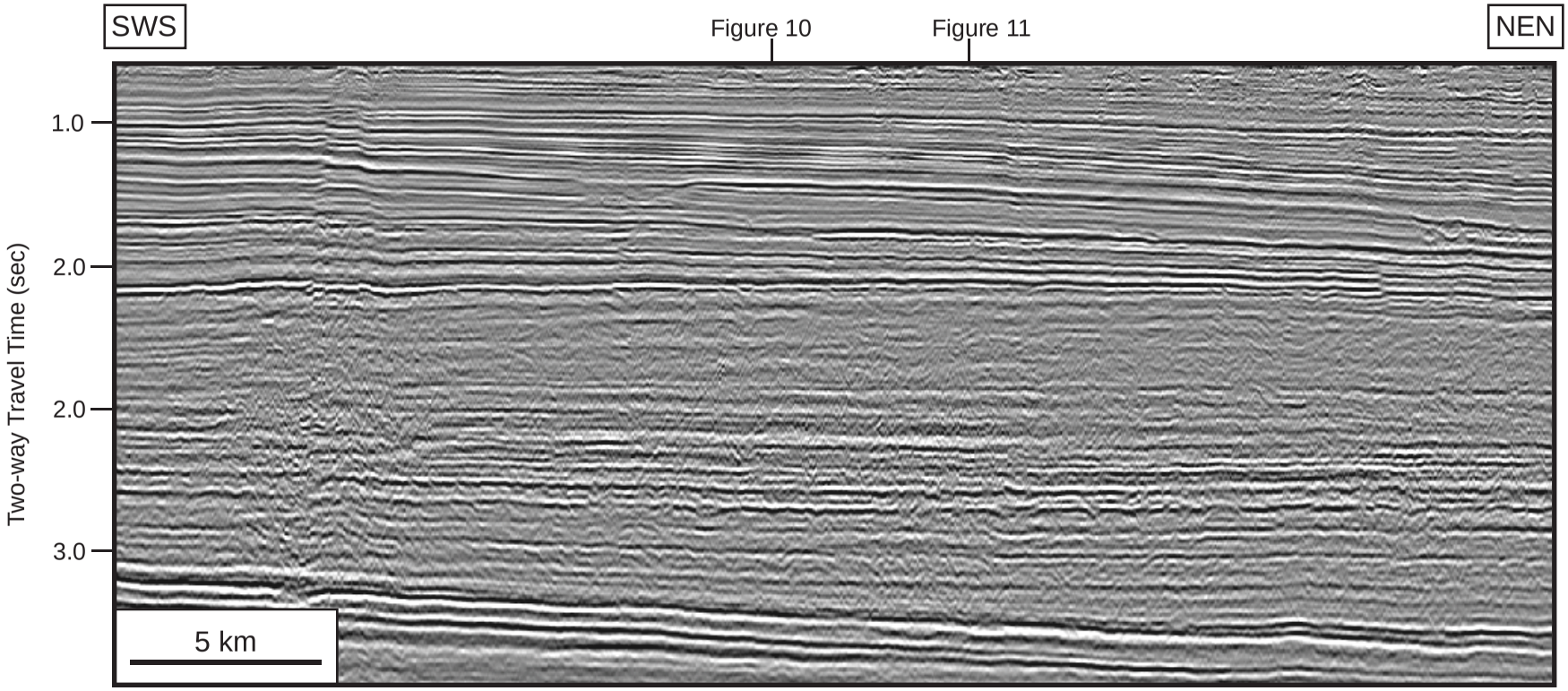

Figure 88a. Uninterpreted regional strike-oriented seismic profile (br-98:br98-075b): A closeup view of Figure 87.

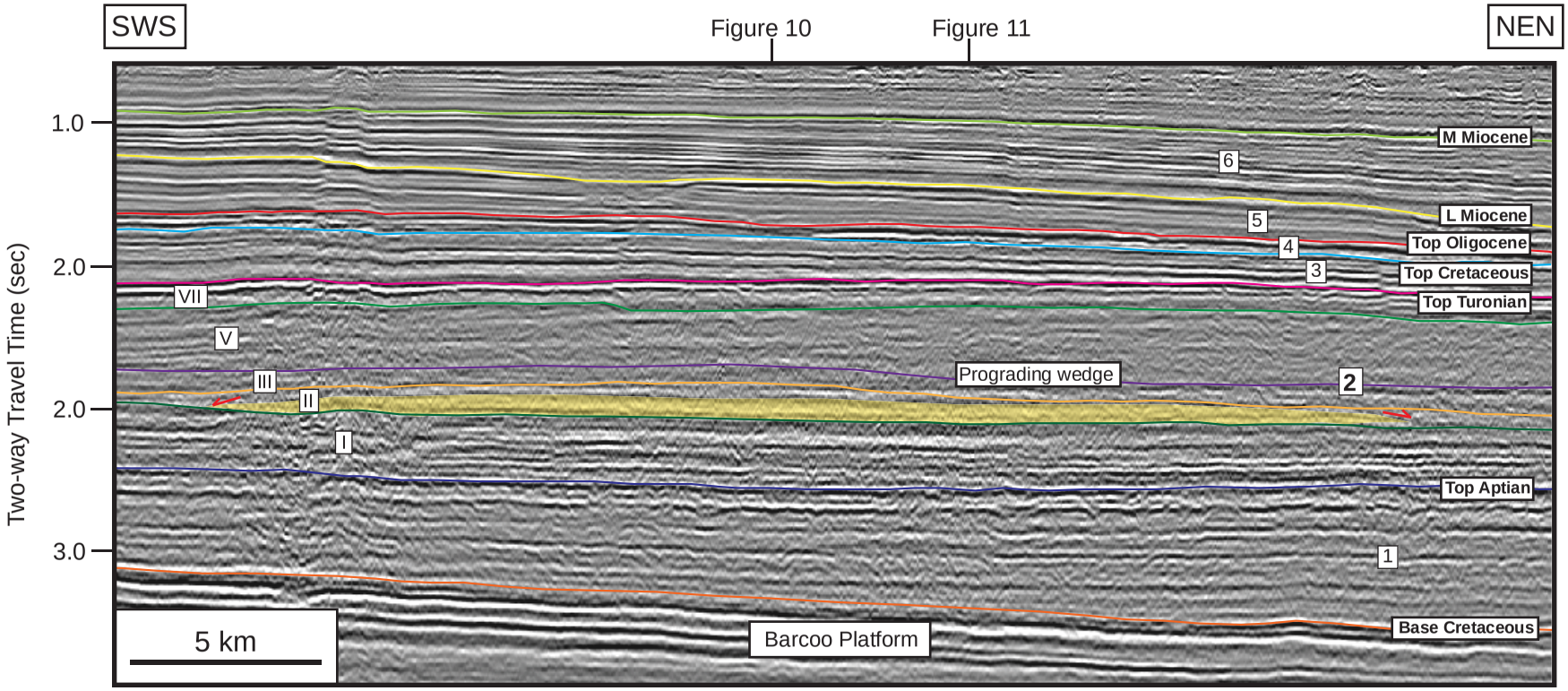

Figure 88b. Regional strike-oriented seismic profile showing all interpreted sequence boundaries from base Cretaceous to middle Miocene: A closeup view of Figure 87. The basin-floor fan is observed within the Subsequence II of Megasequence 2 (yellow shade).

Subsequence III of Megasequence 2

Figure 89 shows the isochron map of Subsequence III, the thickness value ranges from 0 to 295 msec two-way travel time (TWTT). The greatest thickness of this interval is in the Barcoo Syncline.

Three seismic facies are pointed out (Figure 90; Table 8). All of them show the concordant reflection to the upper and lower sequence boundaries. Facies 1 is the parallel to subparallel internal reflection configuration with moderate to high amplitude and fair to good continuity. Seismic facies 2 is the clinoform which has moderate amplitude and fair continuity. The geological facies map illustrates the shelf environment and prograding clinoform (Figure 91). No potential petroleum prospect is identified in this subsequence.

Table 8. Seismic facies and geologic interpretation of Subsequence III of Megasequence 2

Seismic Facies	Upper Sequence Boundary	Lower Sequence Boundary	Internal Reflection Configuration	Amplitude	Continuity	Geologic Interpretation
1	Concordant	Concordant	Parallel to Subparallel	moderate to high	fair to good	Shelf deposits
2	Concordant	Concordant	Clinoform	moderate	fair	Prograding clinoform
3	Concordant	Concordant	Hummocky	moderate	fair	Inversion – related structure

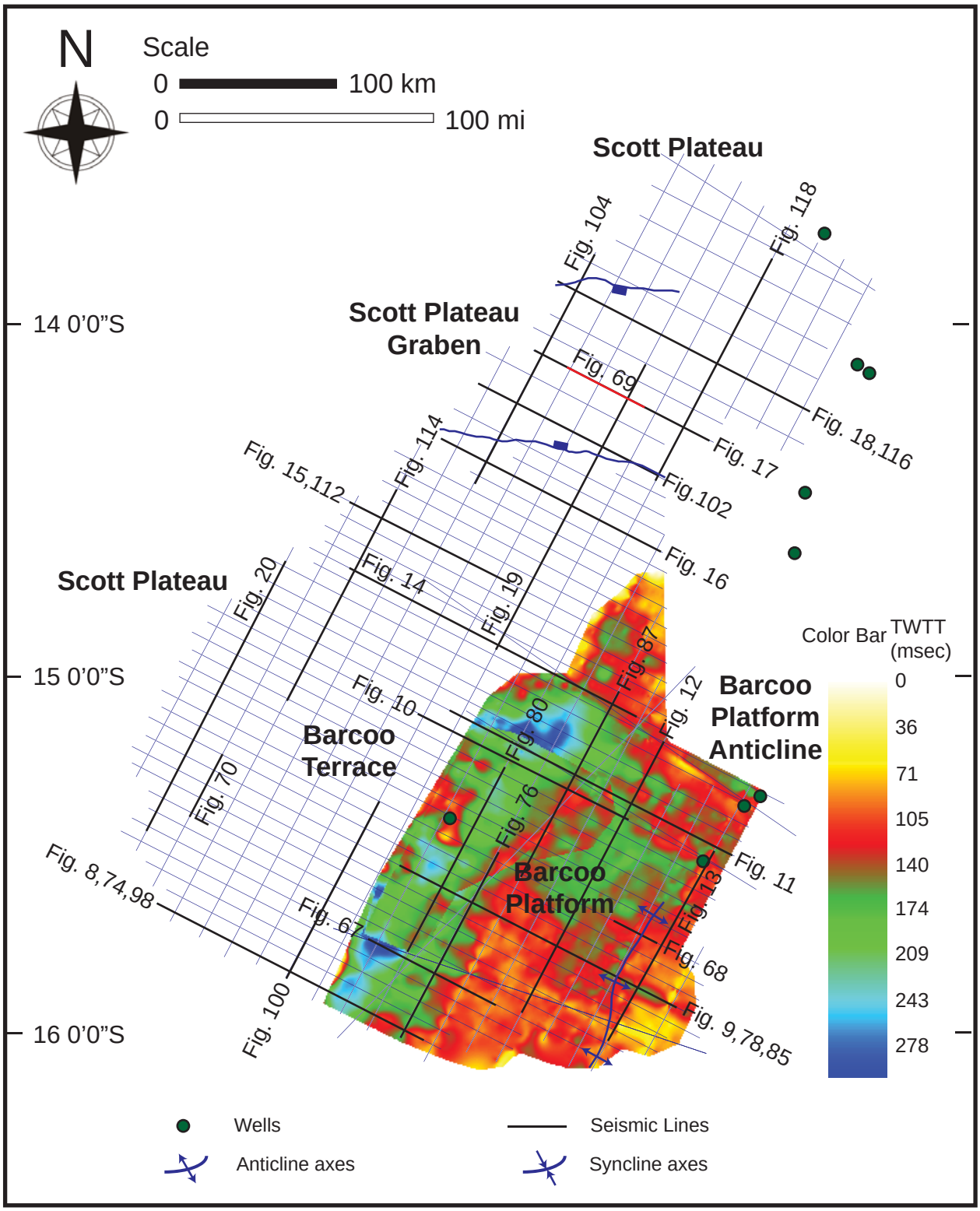

Figure 89. Isochron map (in TWTT msecs) of Subsequence III of Megasequence 2 interval. Distribution of 2D seismic profiles interpreted to generate the maps are shown by blue lines, and wells are shown by green dots. Locations of Figures 8-20, 67-70, 74-81, 85-88, 98-105, 112-119 are shown.

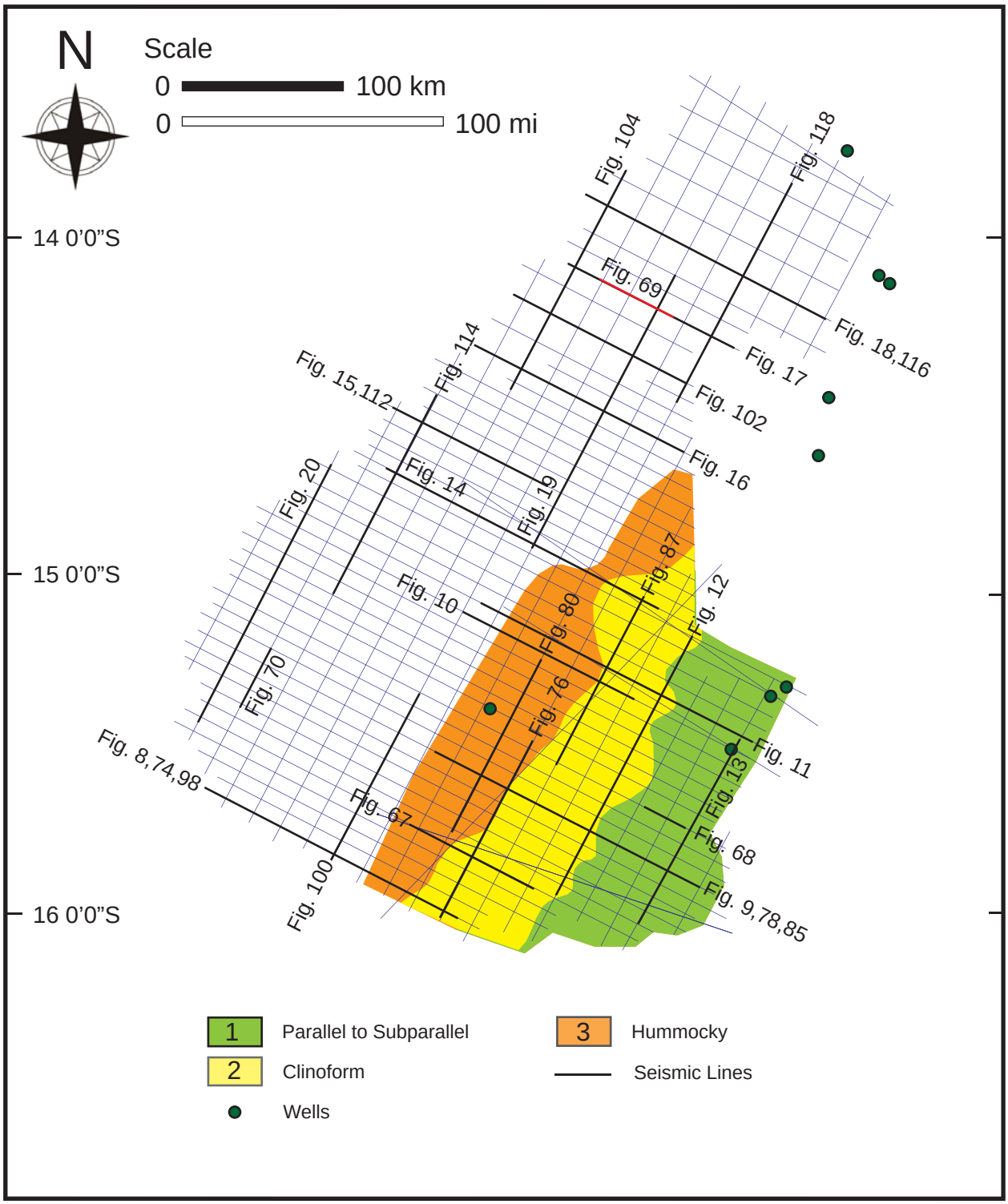

Figure 90. Seismic facies map of Subsequence III of Megasequence 2 interval. Each facies is numbered as described in the text. See Table 2 for seismic facies coding and Table 4 for a summary of seismic facies analysis and geologic interpretation. Locations of Figures 8-20, 67-70, 74-81, 85-88, 98-105, 112-119 (black lines) are shown, and wells are shown by green dots.

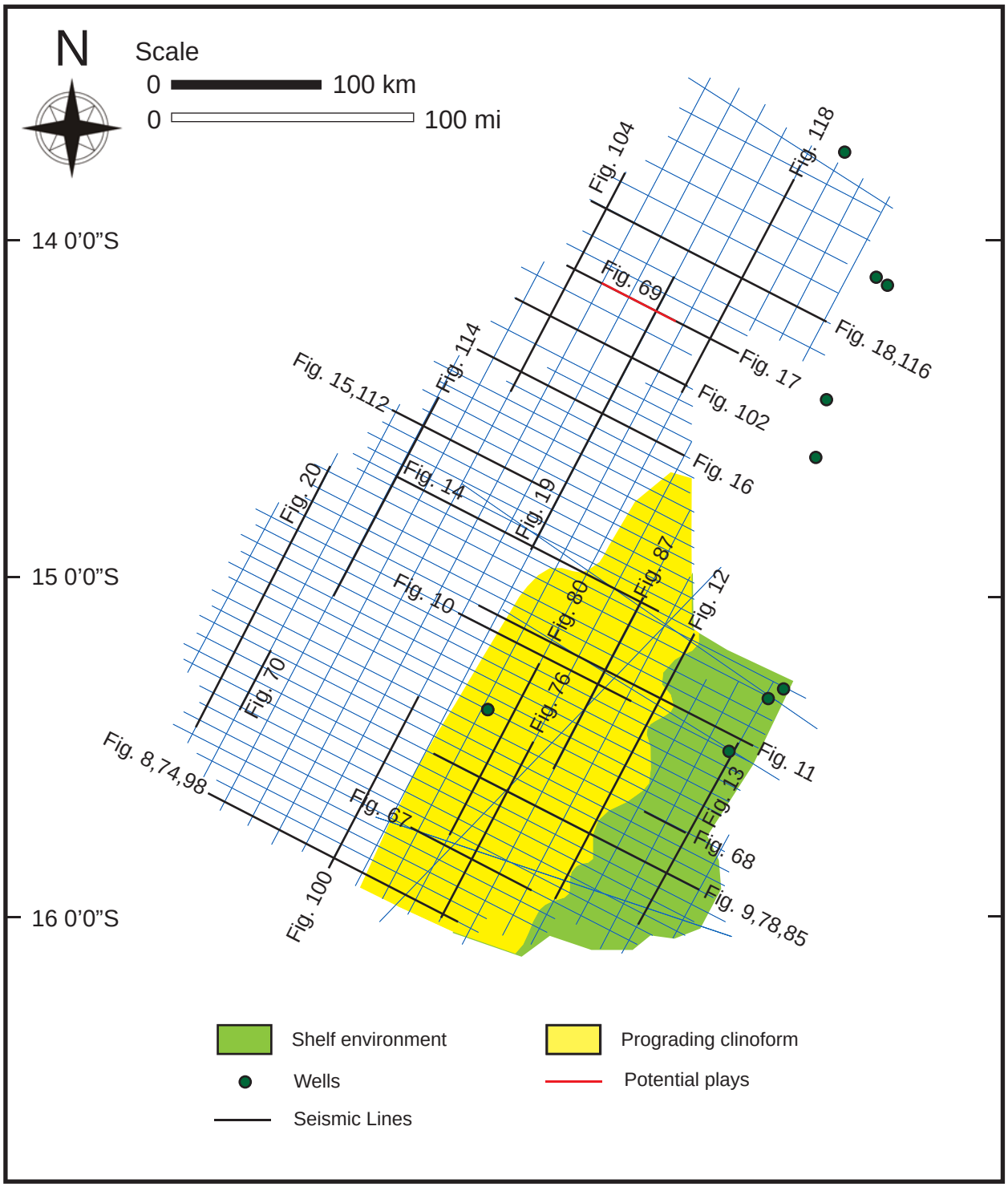

Figure 91 . Geologic facies map of Subsequence III of Megasequence 2 (top Aptian to top Turonian: 112.0-89.3 Ma) interval. See Table 4 for a summary of seismic facies analysis and geologic interpretation. Locations of Figures 8-20, 67-70, 74-81, 85-88, 98-105, 112-119 (black lines) are shown, and wells are shown by green dots.

Subsequence IV of Megasequence 2

The isochron map of this subsequence illustrates the thickness values varying from 0 to 119 msec two-way travel time (TWTT) (Figure 92). It deposited on the shelf-edge between the area of the Barcoo Platform and the Barcoo Terrace.

Seismic facies map is shown in Figure 93 and Table 9. Only two facies are subdivided. Facies 3 and 4 have the concordant seismic reflection to both upper and lower sequence boundaries. The hummocky facies shows moderate amplitude and fair continuity. The other facies displays parallel to subparallel internal reflection configuration with moderate to high amplitude and fair to good continuity. Those of these facies are interpreted to be related to the inversion phase and the basinal deposit, respectively (Figure 94).

Table 9. Seismic facies and geologic interpretation of Subsequence IV of Megasequence 2

Seismic Facies	Upper Sequence Boundary	Lower Sequence Boundary	Internal Reflection Configuration	Amplitude	Continuity	Geologic Interpretation
3	Concordant	Concordant	Hummocky	moderate	fair	Inversion – related structure
4	Concordant	Concordant	Parallel to Subparallel	moderate to high	fair to good	Basinal deposits

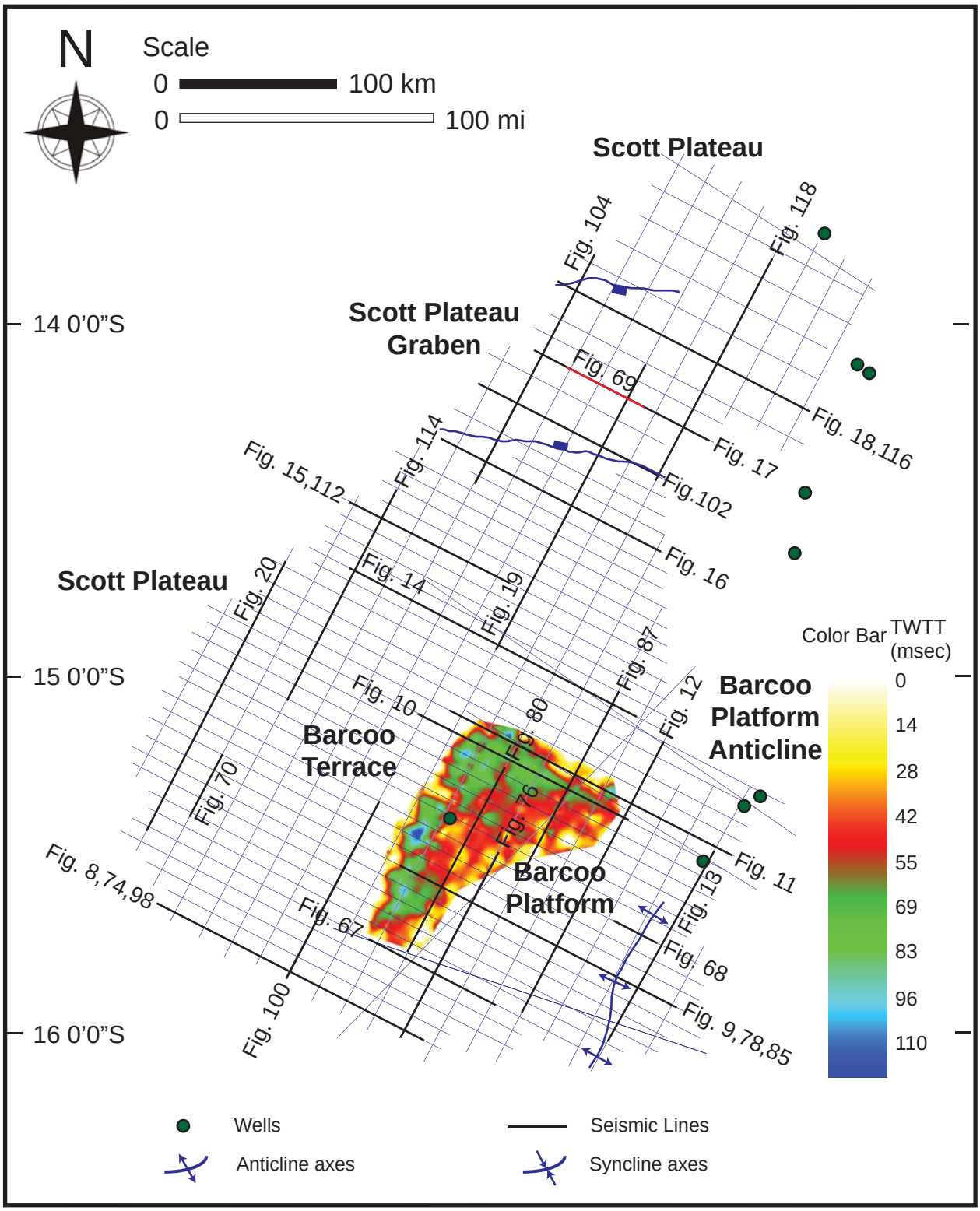

Figure 92. Isochron map (in TWTT msecs) of Subsequence IV of Megasequence 2 interval. Distribution of 2D seismic profiles interpreted to generate the maps are shown by blue lines, and wells are shown by green dots. Locations of Figures 8-20, 67-70, 74-81, 85-88, 98-105, 112-119 are shown.

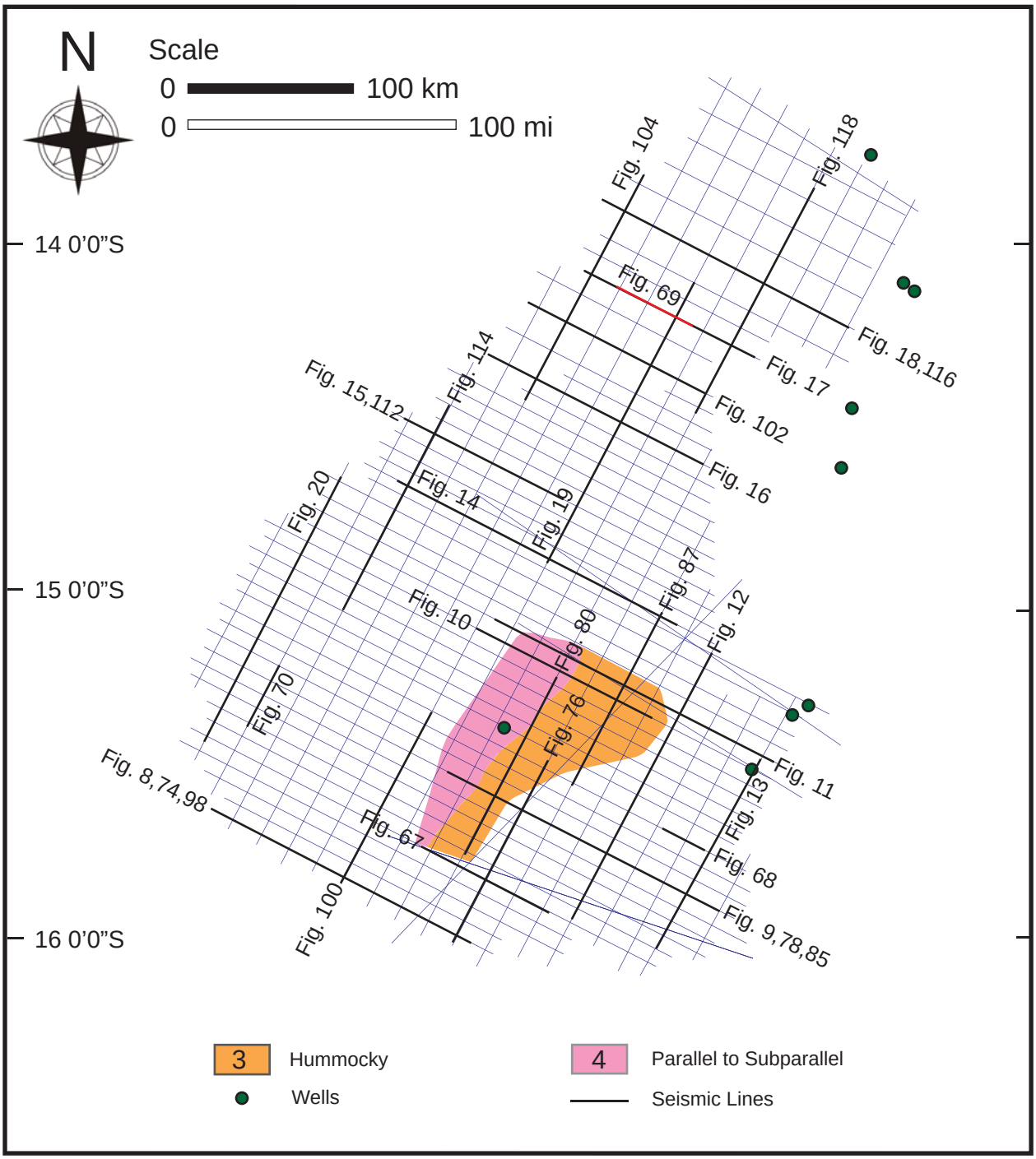

Figure 93. Seismic facies map of Subsequence IV of Megasequence 2 interval. Each facies is numbered as described in the text. See Table 2 for seismic facies coding and Table 4 for a summary of seismic facies analysis and geologic interpretation. Locations of Figures 8-20, 67-70, 74-81, 85-88, 98-105, 112-119 (black lines) are shown, and wells are shown by green dots.

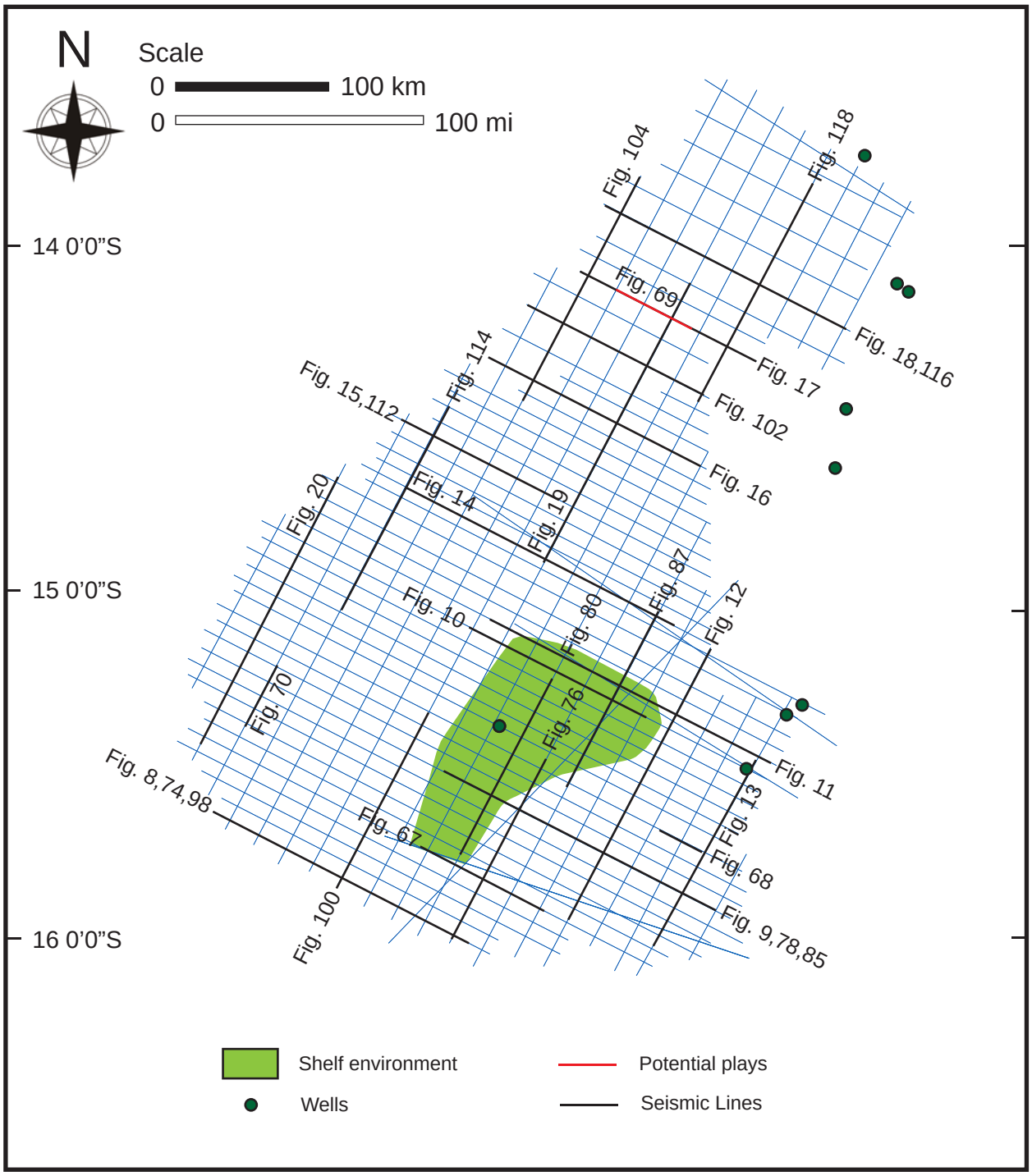

Figure 94 . Geologic facies map of Subsequence IV of Megasequence 2 (top Aptian to top Turonian: 112.0-89.3 Ma) interval. See Table 4 for a summary of seismic facies analysis and geologic interpretation. Locations of Figures 8-20, 67-70, 74-81, 85-88, 98-105, 112-119 (black lines) are shown, and wells are shown by green dots.

Subsequence V of Megasequence 2

The isochron map shows the value ranges from 0 to 388 msec two-way travel time (TWTT) (Figure 95). This subsequence covers almost all of the study area. The greatest thickness areas are in the Barcoo Syncline and part of the Barcoo Terrace.

Five seismic facies have been specified (Figure 96; Table 10). Facies 1, 3, 4 and 5 show the concordant seismic reflection at both upper and lower sequence boundaries. Seismic facies 1 and 4 displays the parallel to subparallel internal reflection configuration with moderated to high amplitude and fair to good continuity. Facies 1 is interpreted to be the shelf. On the other hand, facies 4 is interpreted to be the basin-floor environment same as facies 5 which has the chaotic internal reflection configuration with low amplitude and poor continuity. This sediment deposited on the graben flank. The hummocky configuration shows moderate amplitude and fair continuity. This facies is related to the inversion phase of the structural evolution in this area. Faceis 6 is characterized to be a chaotic facies. The amplitude is varied from moderate to high whereas the continuity is poor. The external configuration illustrates the mound feature which is assumed to be the carbonate build-up.

Table 10. Seismic facies and geologic interpretation of Subsequence V of Megasequence 2

Seismic Facies	Upper Sequence Boundary	Lower Sequence Boundary	Internal Reflection Configuration	Amplitude	Continuity	Geologic Interpretation
1	Concordant	Concordant	Parallel to Subparallel	moderate to high	fair to good	Shelf deposits
3	Concordant	Concordant	Hummocky	moderate	fair	Inversion – related structure
4	Concordant	Concordant	Parallel to Subparallel	moderate to high	fair to good	Basinal deposits
5	Concordant	Concordant	Chaotic	low	poor	Basinal deposits on graben flank
6	-	-	Chaotic	moderate to high	poor	Carbonate buildup

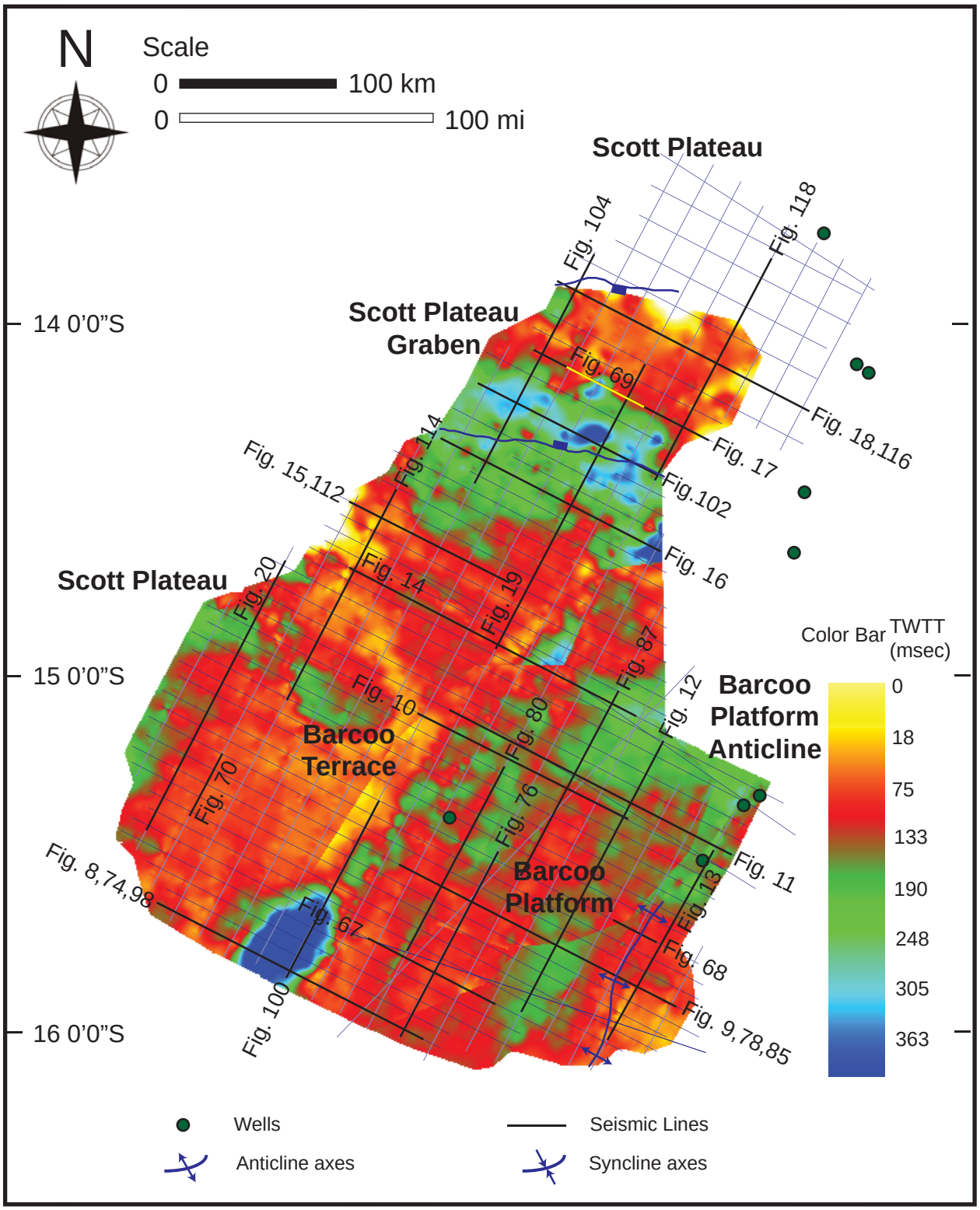

Figure 95. Isochron map (in TWTT msecs) of Subsequence V of Megasequence 2 interval. Distribution of 2D seismic profiles interpreted to generate the maps are shown by blue lines, and wells are shown by green dots. Locations of Figures 8-20, 67-70, 74-81, 85-88, 98-105, 112-119 are shown.

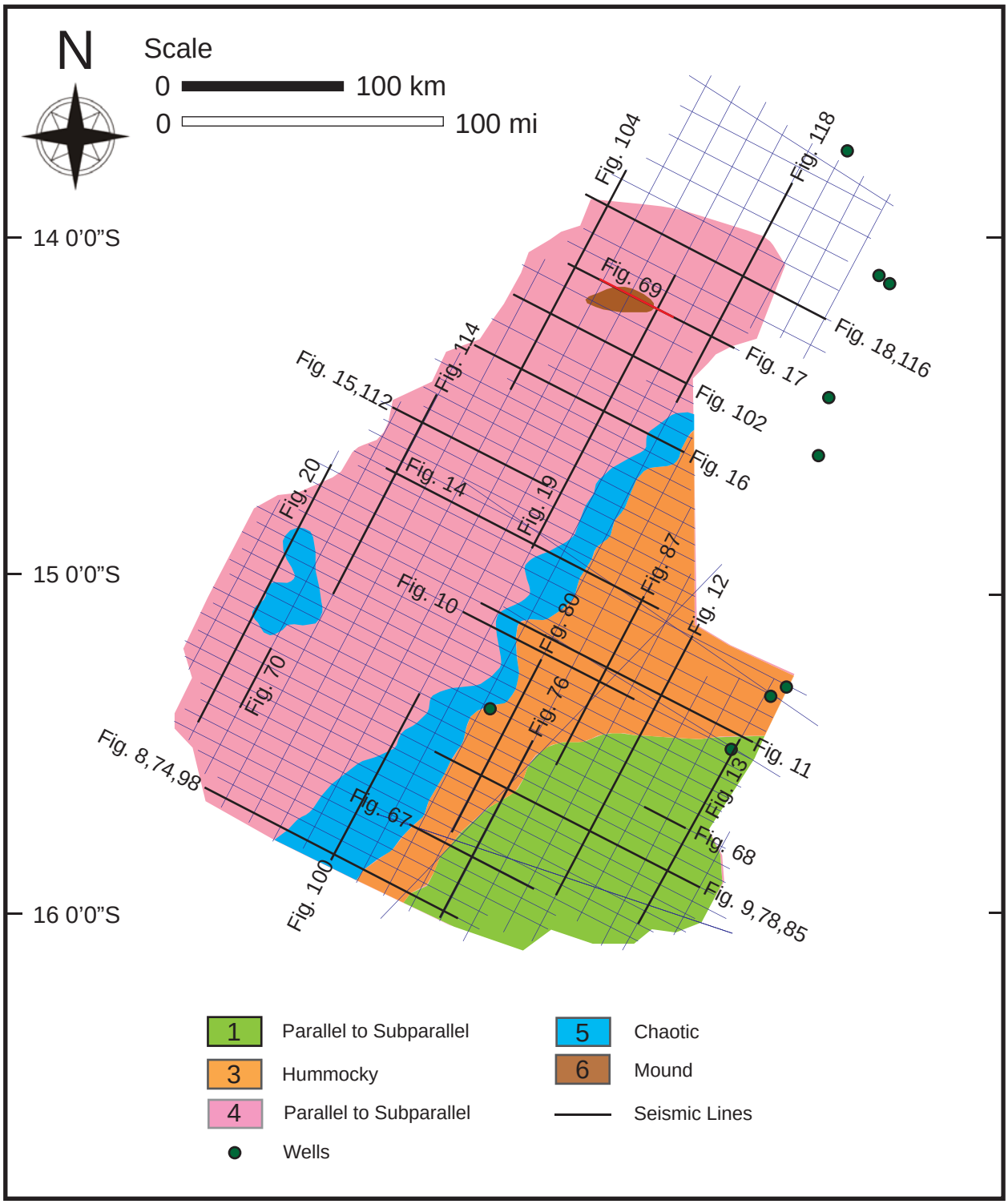

Figure 96. Seismic facies map of Subsequence V of Megasequence 2 interval. Each facies is numbered as described in the text. See Table 2 for seismic facies coding and Table 4 for a summary of seismic facies analysis and geologic interpretation. Locations of Figures 8-20, 67-70, 74-81, 85-88, 98-105, 112-119 (black lines) are shown, and wells are shown by green dots.

The geologic facies map of megasequence 2 shows that sediments were transported from the shelf environment into the basin in the southeast-northwest direction (Figure 97). The prograding wedge within the low angle clinoform (Figure 8) and the sediment aggrading on slope setting (Figures 10, 11) are the main characteristics of this megasequence. The low angle clinoform indicates the relatively low rate of sediment supply compared to the subsidence rate. In comparison with Megasequence 1, the shelf edge in Megasequence 2 prograded basinward associated with the regressive cycle. Some erosional features of submarine canyons were recognized (Figure 16). In addition, the carbonate or volcanic buildup is observed in the northern portion of the study area (Figures 17, 69).

There are potential petroleum prospect are found in this subsequence. One is the basin-floor fan which deposited in the Barcoo Syncline. It has been identified by its bi-directional downlap terminations (Figures 100-101). The other prospect is the structurally control sediments which deposited in the Scott Plateau Graben. The dip and strike oriented seismic profiles are shown in Figures 98-105.

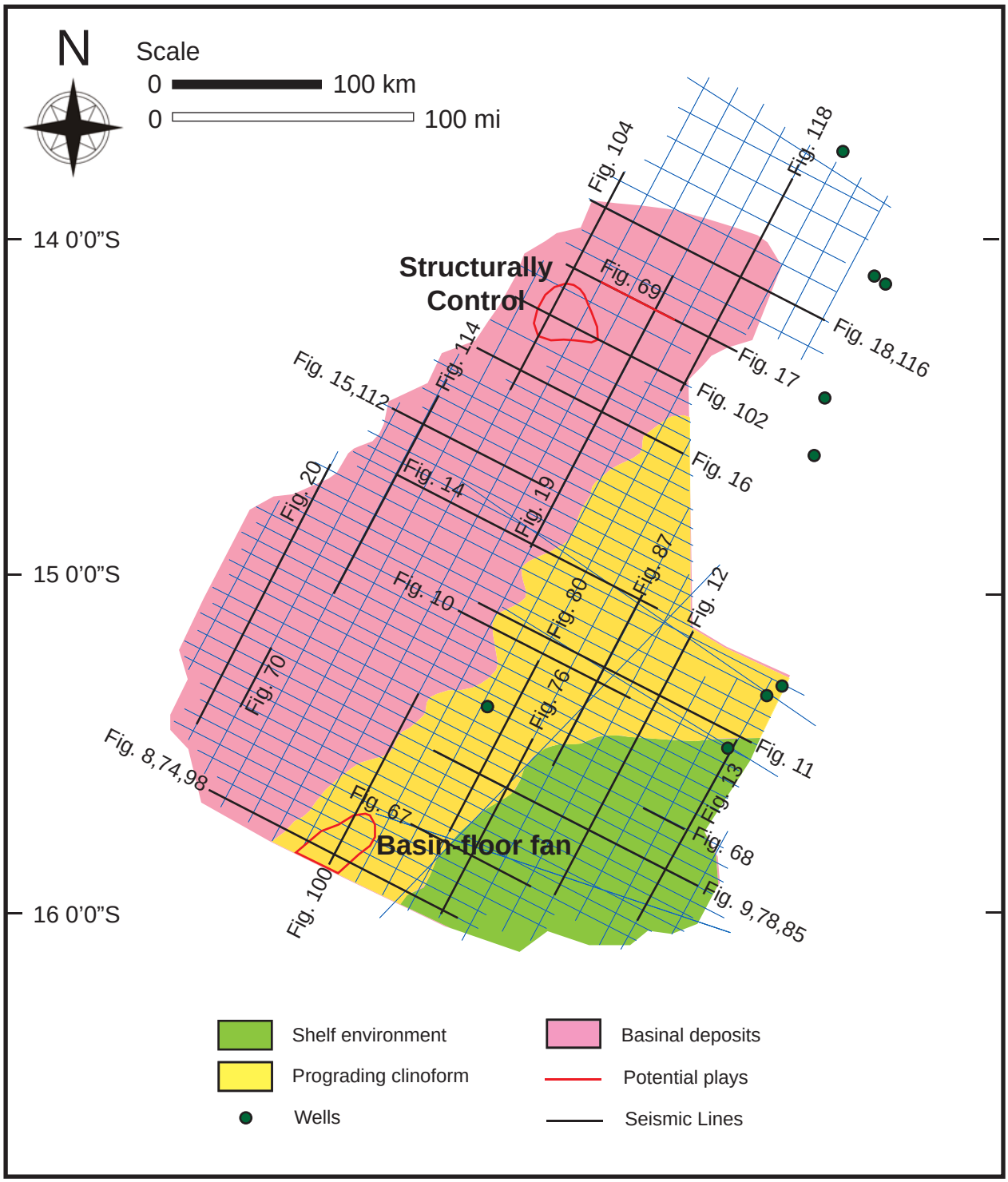

Figure 97. Geologic facies map of Subsequence V of Megasequence 2 (top Aptian to top Turonian: 112.0-89.3 Ma) interval. See Table 4 for a summary of seismic facies analysis and geologic interpretation. Locations of Figures 8-20, 67-70, 74-81, 85-88, 98-105, 112-119 (black lines) are shown, and wells are shown by green dots.

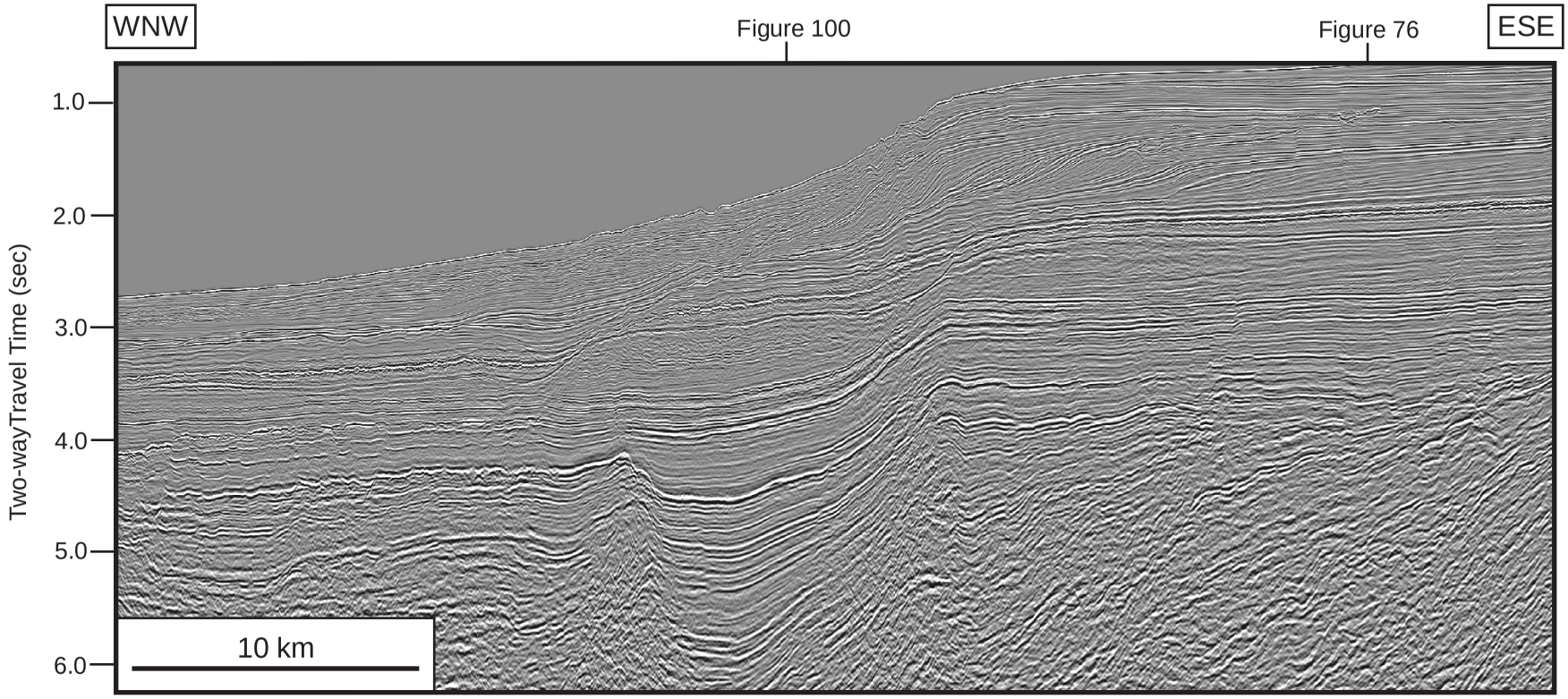

Figure 98a. Uninterpreted regional dip-oriented seismic profile (br-98:br98-001). Location of the profile is shown in Figures 65-66, 71-73, 82-84, 89-97, 106-111 and locations of where Figures 76, 100 cross the profile.

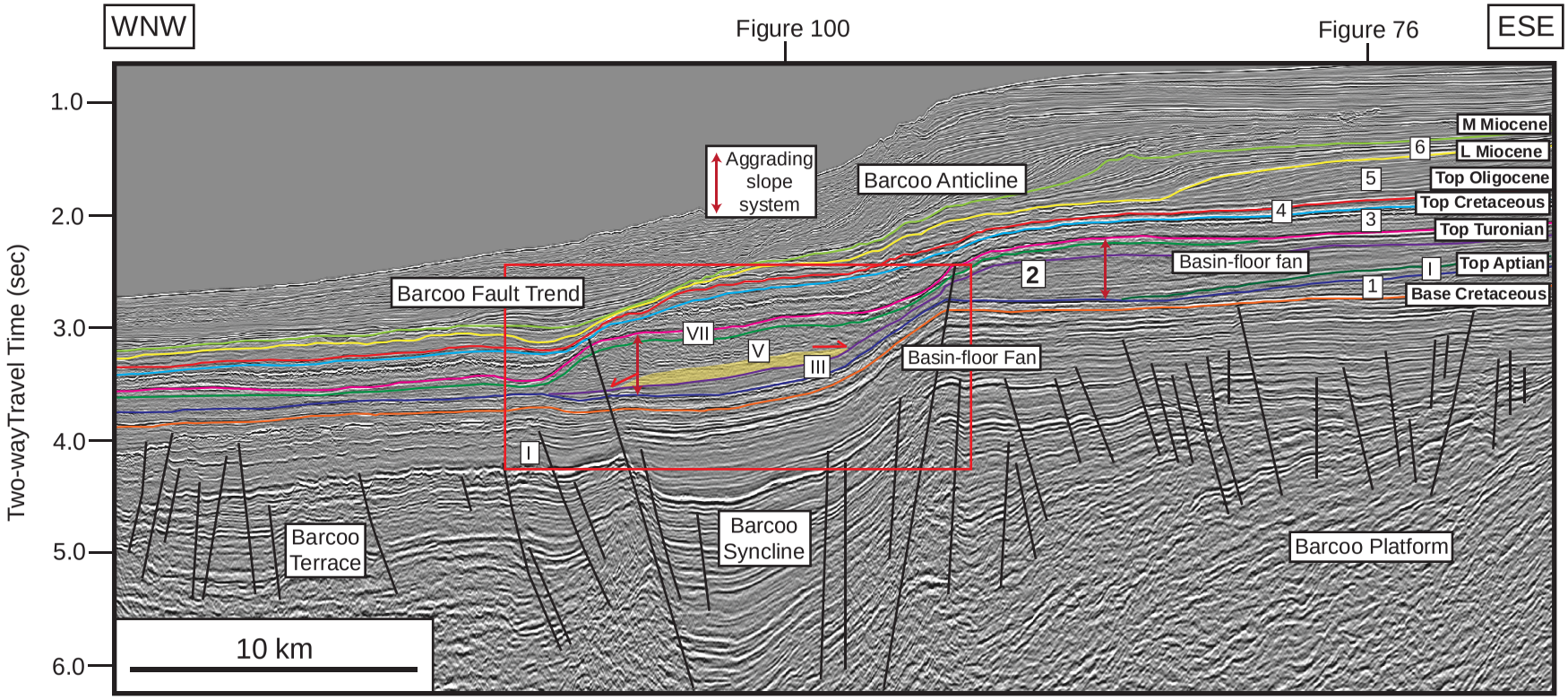

Figure 98b. Regional dip-oriented seismic profile showing all interpreted sequence boundaries from base Cretaceous to middle Miocene. The major graben structure of the Barcoo Syncline was overlain by the Upper Jurassic and younger strata. The prograding wedge is observed within Subsequence V of Megasequence 2 (yellow shade) which shows the aggrading slope system (red arrow). Location of the profile is shown in Figures 65-66, 71-73, 82-84, 89-97, 106-111 and locations of where Figures 76, 100 cross the profile.

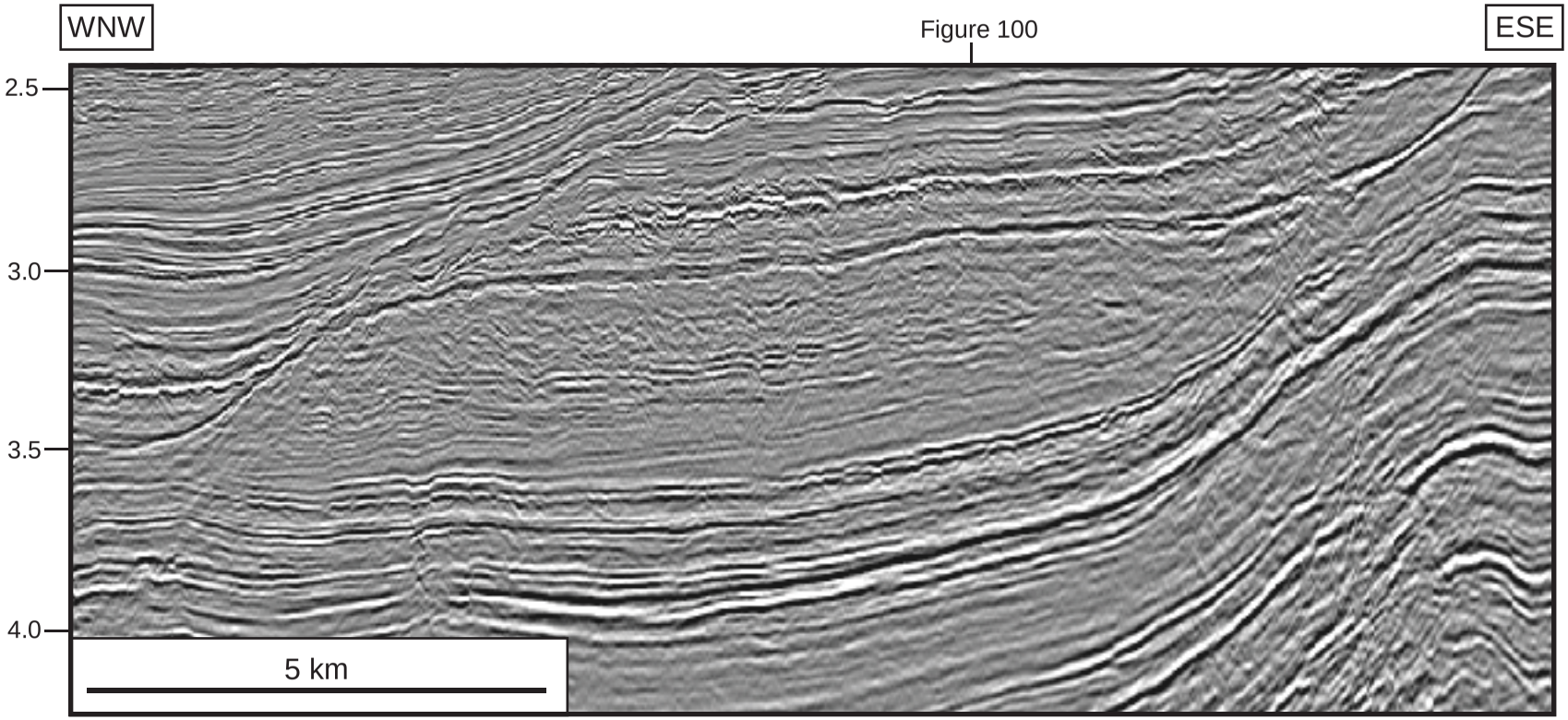

Figure 99a. Uninterpreted regional dip-oriented seismic profile (br-98:br98-001): A closeup view of Figure 98.

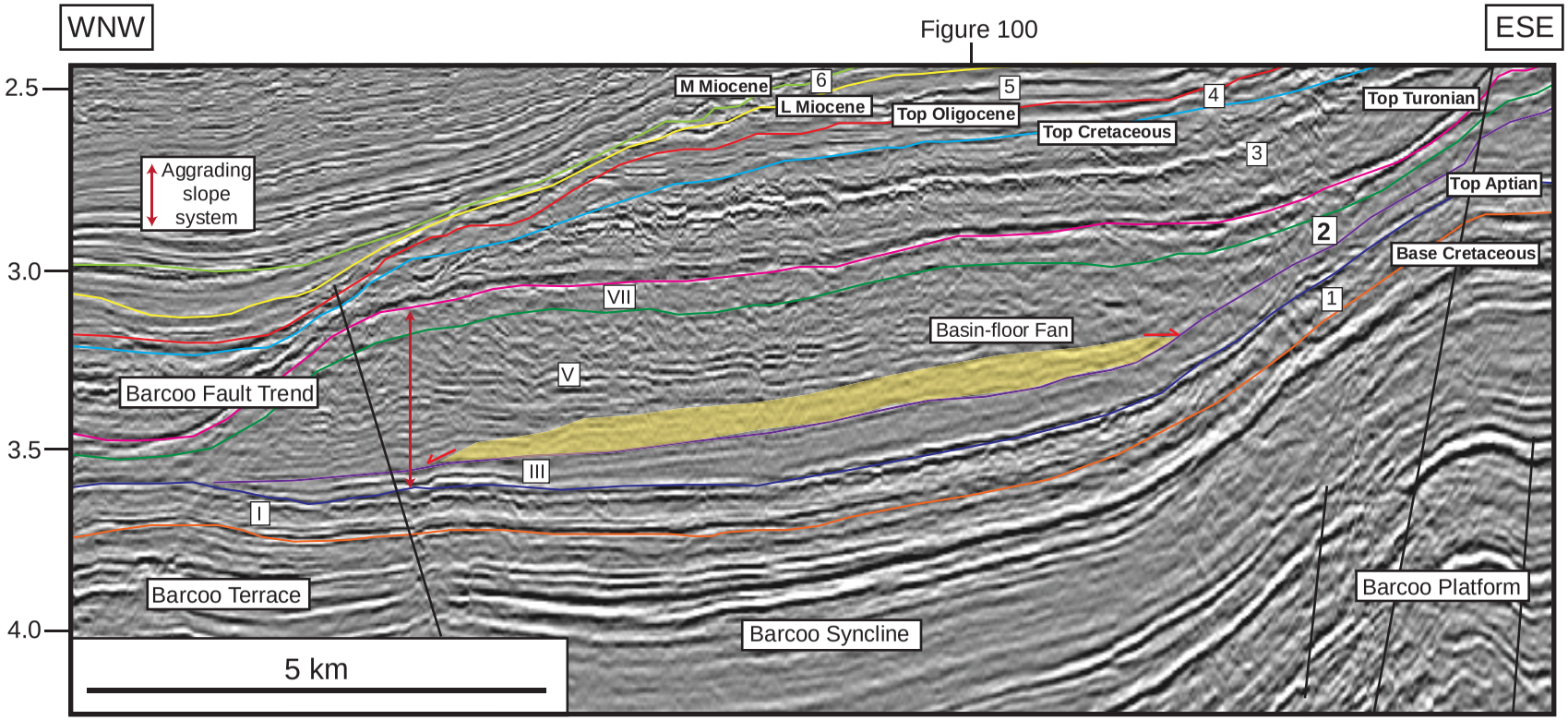

Figure 99b. Regional dip-oriented seismic profile showing all interpreted sequence boundaries from base Cretaceous to middle Miocene: A closeup view of Figure 98. The prograding wedge is observed within Subsequence V of Megasequence 2 (yellow shade) which shows the aggrading slope system (red arrow).

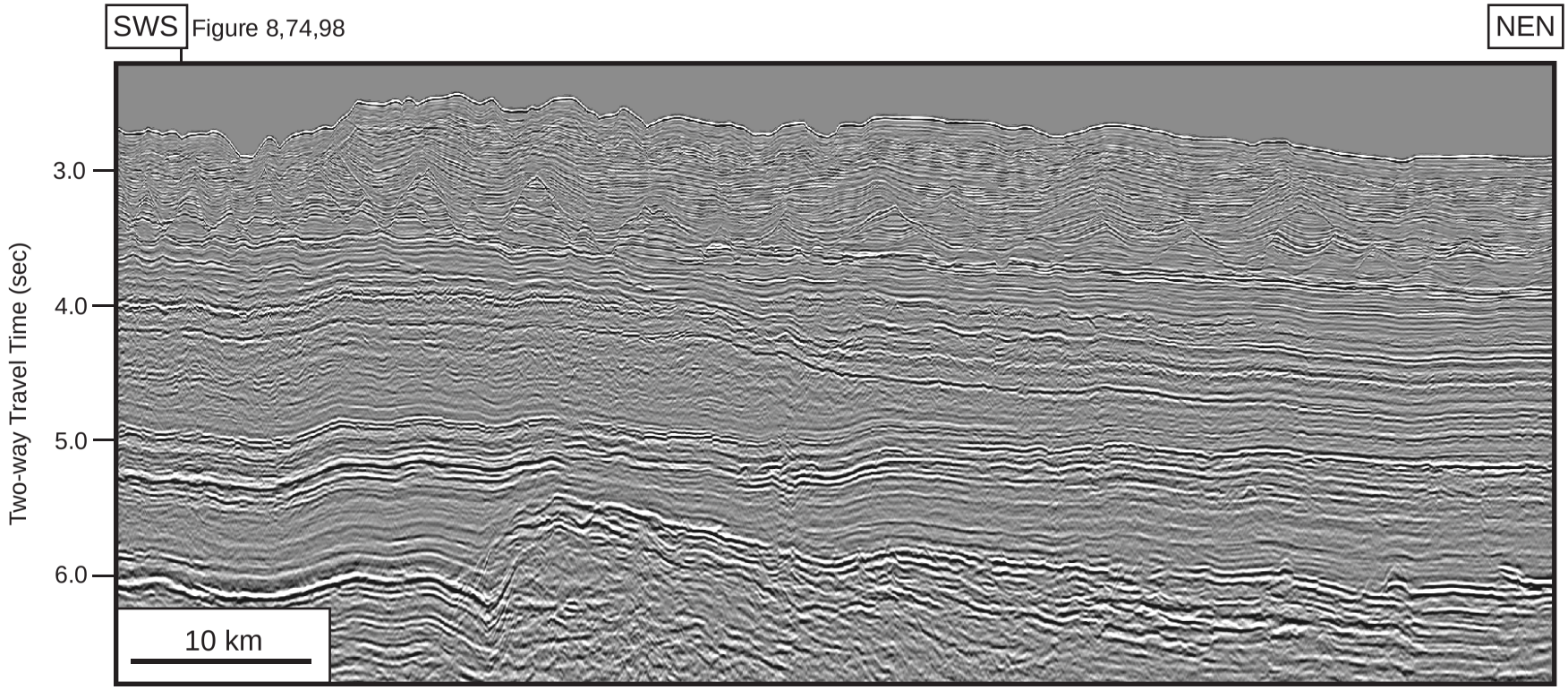

Figure 100a. Uninterpreted regional strike-oriented seismic profile (br-98:br98-083). Location of the profile is shown in Figures 65-66, 71-73, 82-84, 89-97, 106-111 and locations of where Figures 8, 74, 98 cross the profile.

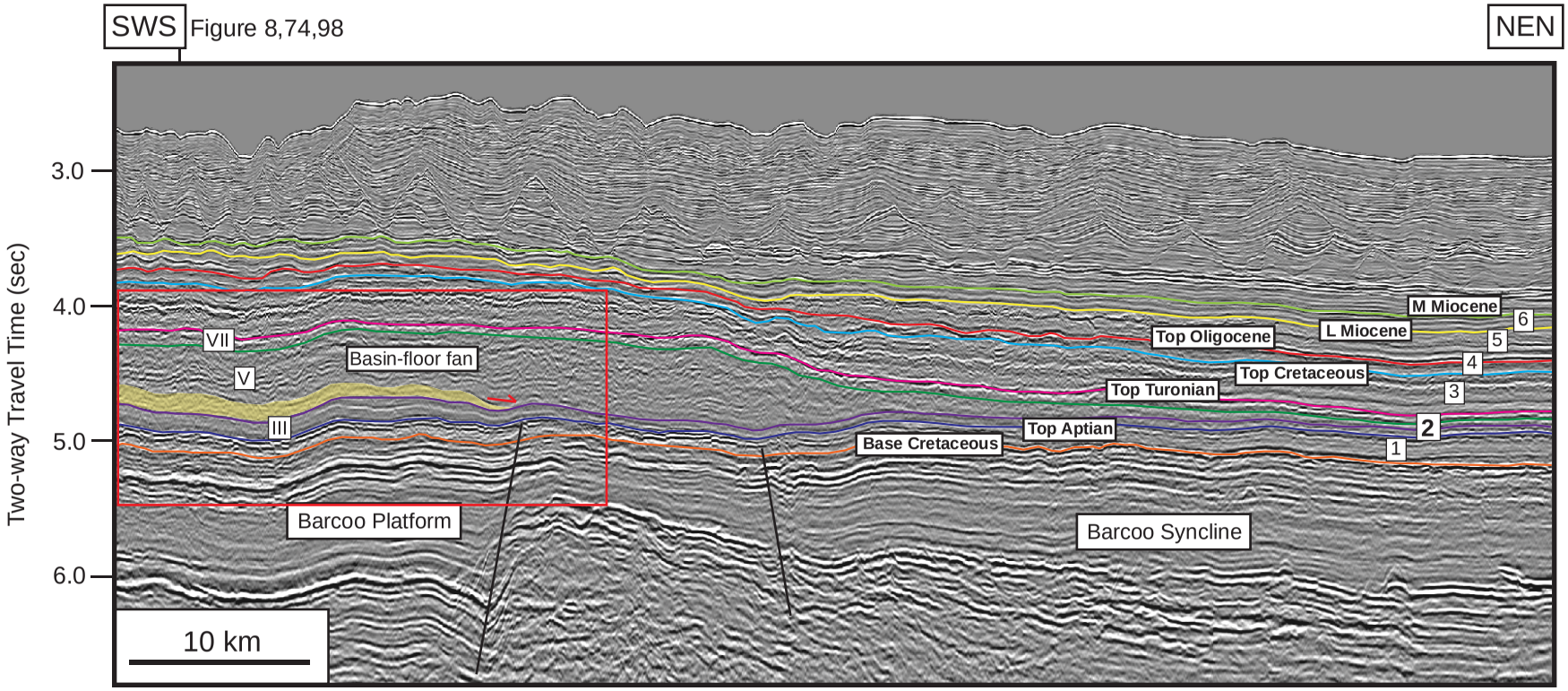

Figure 100b. Regional strike-oriented seismic profile showing all interpreted sequence boundaries from base Cretaceous to middle Miocene. This profile shows the areas of the Barcoo Plaform and the Barcoo Syncline. The basin-floor fan is observed within Subsequence V of Megasequence 1 (yellow shade). Location of the profile is shown in Figures 65-66, 71-73, 82-84, 89-97, 106-111 and locations of where Figures 8, 74, 98 cross the profile.

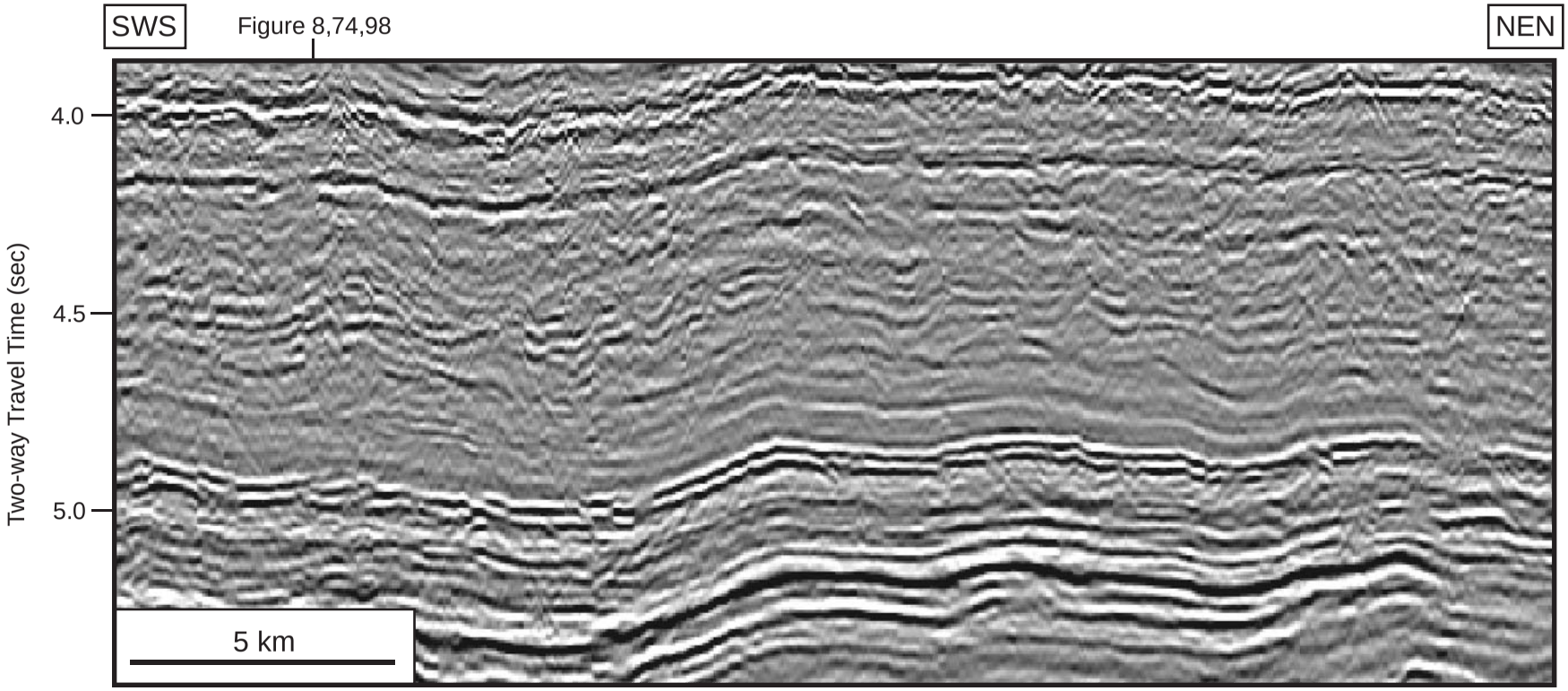

Figure 101a. Uninterpreted regional strike-oriented seismic profile (br-98:br98-083): A closeup view of Figure 100.

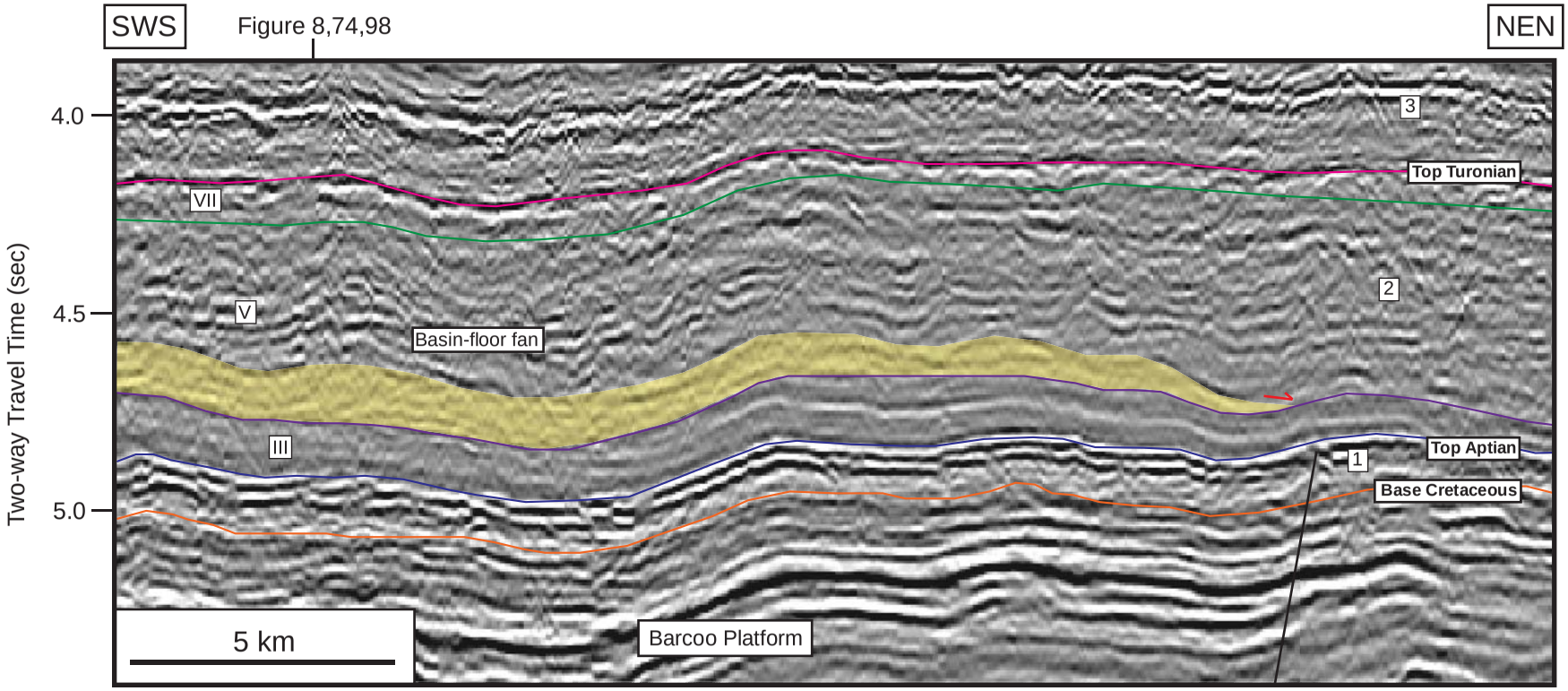

Figure 101b. Regional strike-oriented seismic profile showing all interpreted sequence boundaries from base Cretaceous to middle Miocene: A closeup view of Figure 100. The basin-floor fan is observed within Subsequence V of Megasequence 1 (yellow shade).

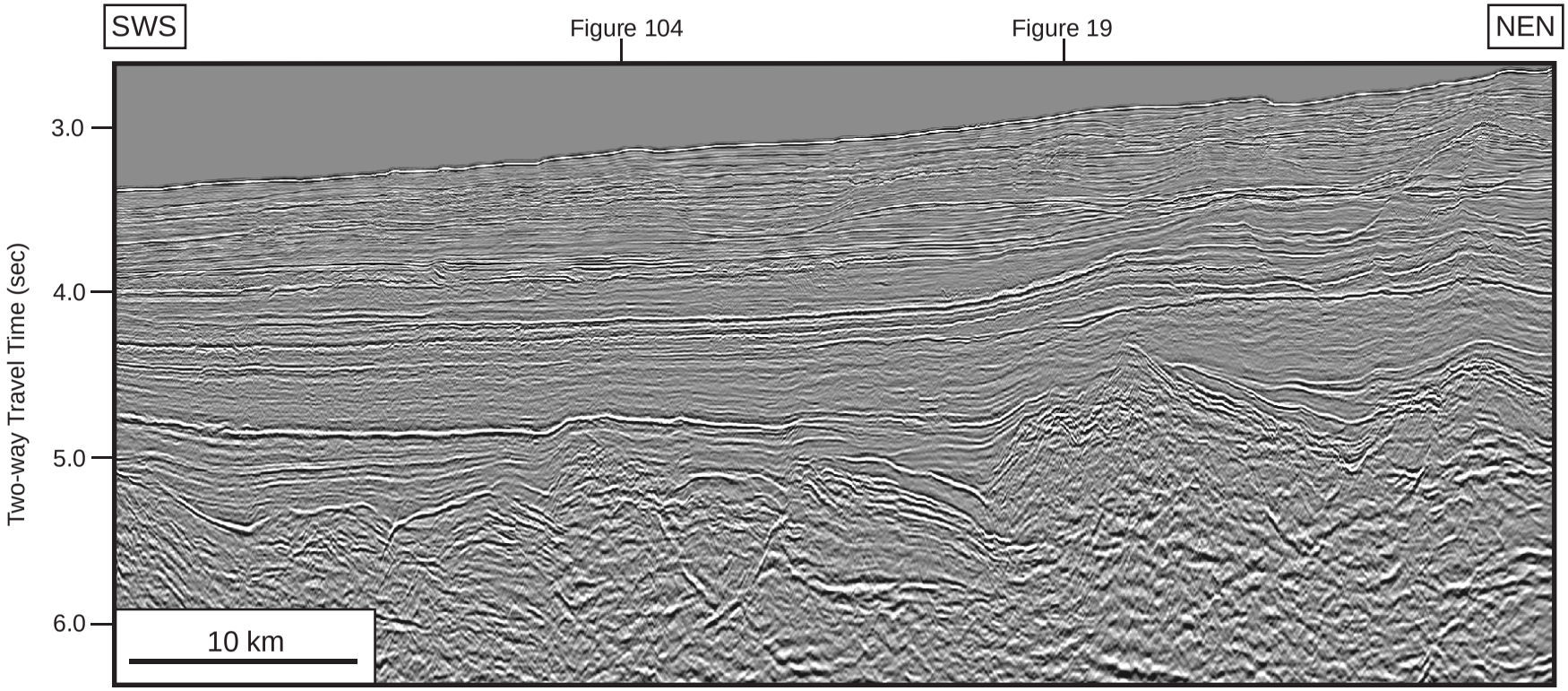

Figure 102a. Uninterpreted regional dip-oriented seismic profile (br-98:br98-039). Location of the profile is shown in Figures 65-66, 71-73, 82-84, 89-97, 106-111 and locations of where Figures 19, 104 cross the profile.

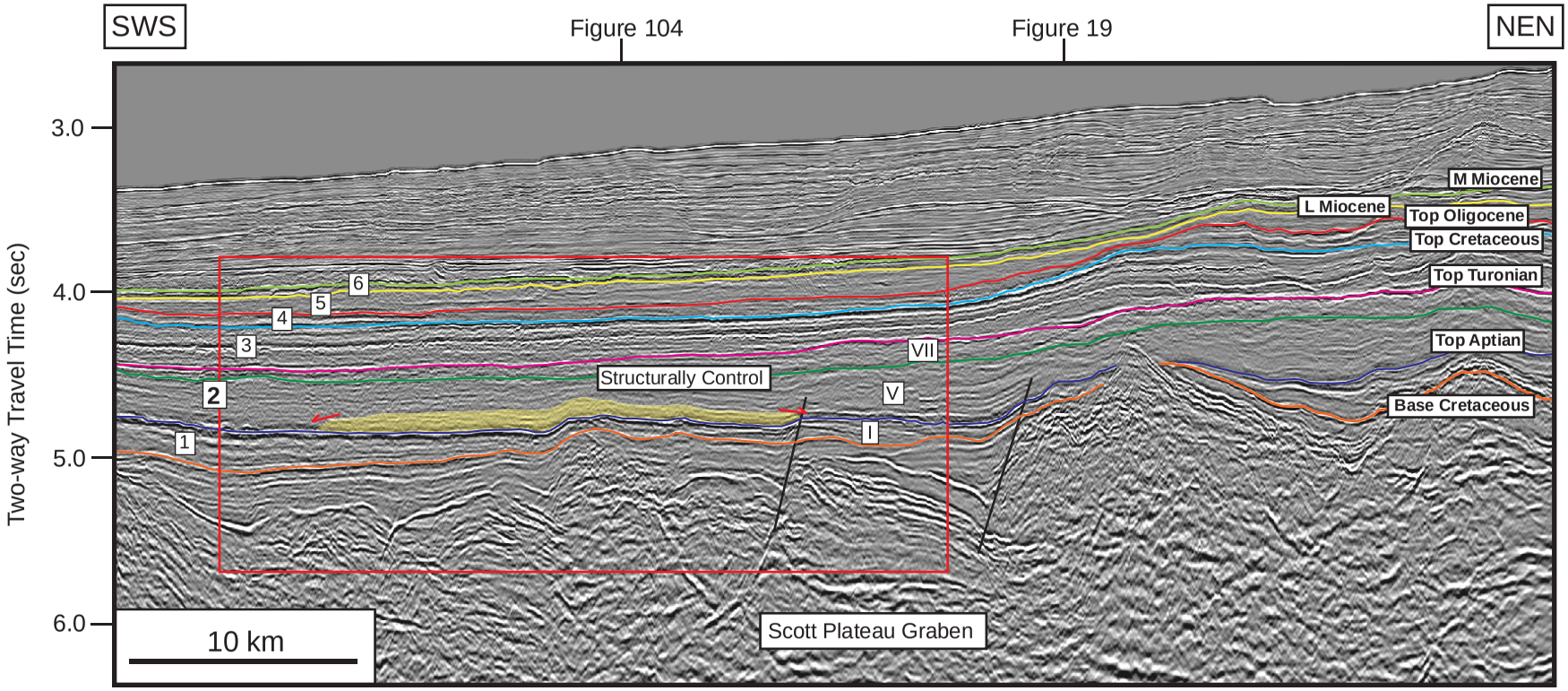

Figure 102b. Regional dip-oriented seismic profile showing all interpreted sequence boundaries from base Cretaceous to middle Miocene. This profile shows the area of the Scott Plateau. The deepwater deposit is observed within Subsequence V of Megasequence 2 which caused by the structurally control (yellow shade). Location of the profile is shown in Figures 65-66, 71-73, 82-84, 89-97, 106-111 and locations of where Figures 19, 104 cross the profile.

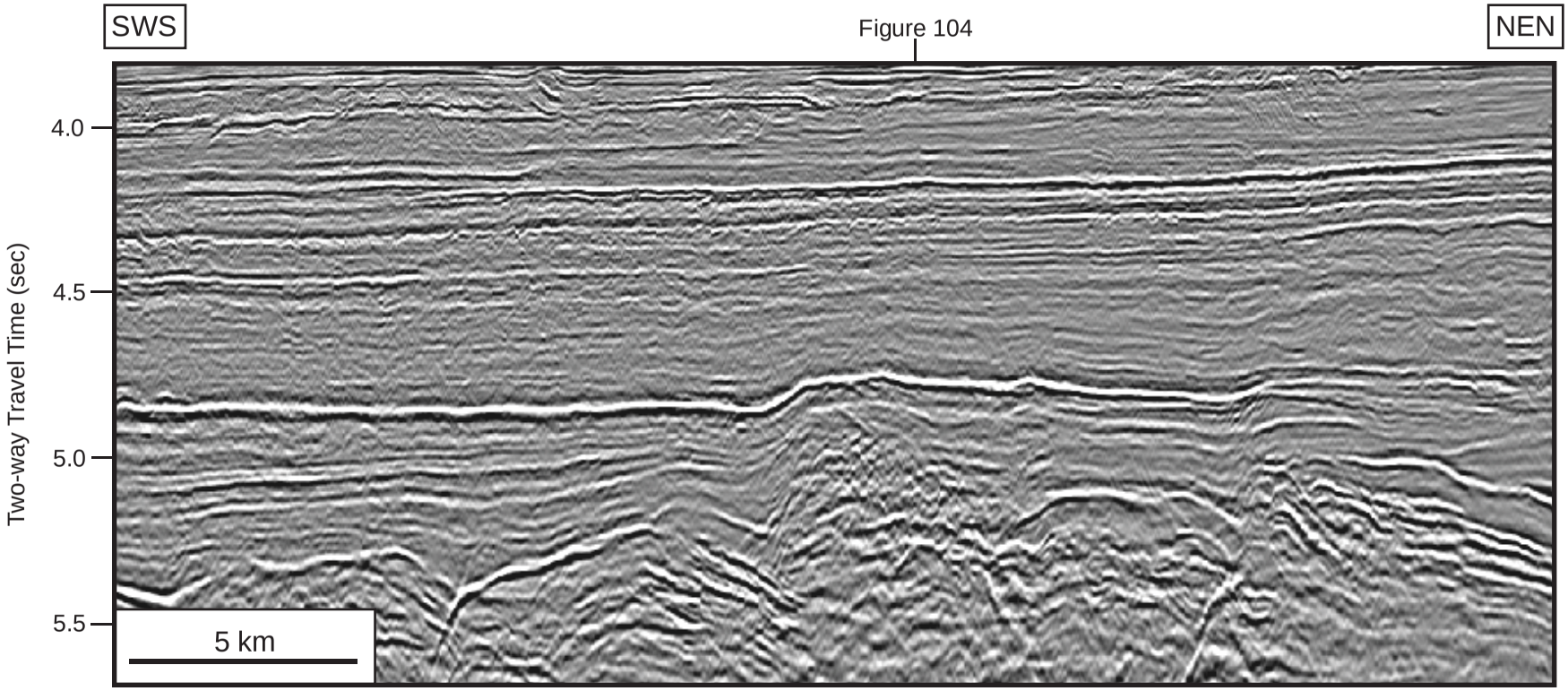

Figure 103a. Uninterpreted regional dip-oriented seismic profile (br-98:br98-039): A closeup view of Figure 102.

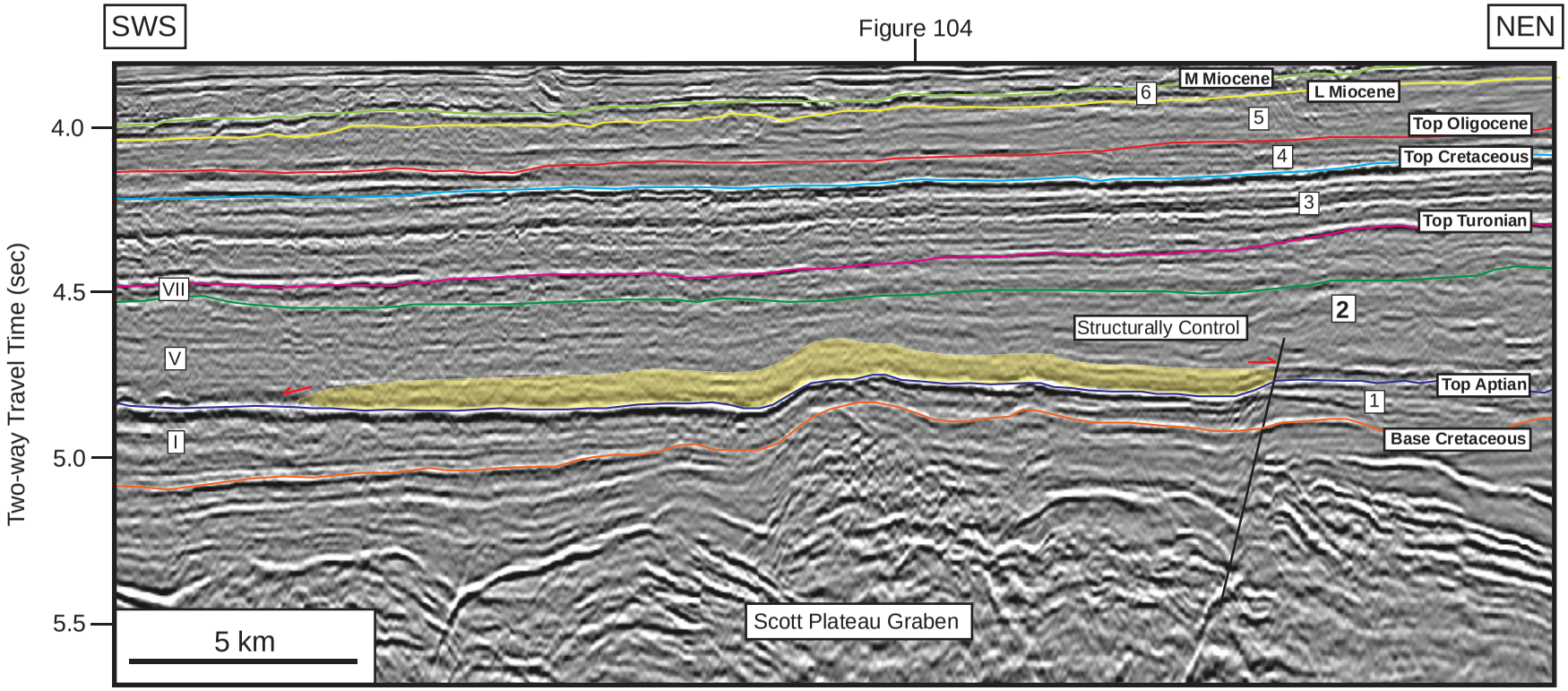

Figure 103b. Regional dip-oriented seismic profile showing all interpreted sequence boundaries from base Cretaceous to middle Miocene: A closeup view of Figure 102. The deepwater deposit is observed within Subsequence V of Megasequence 2 which caused by the structurally control (yellow shade).

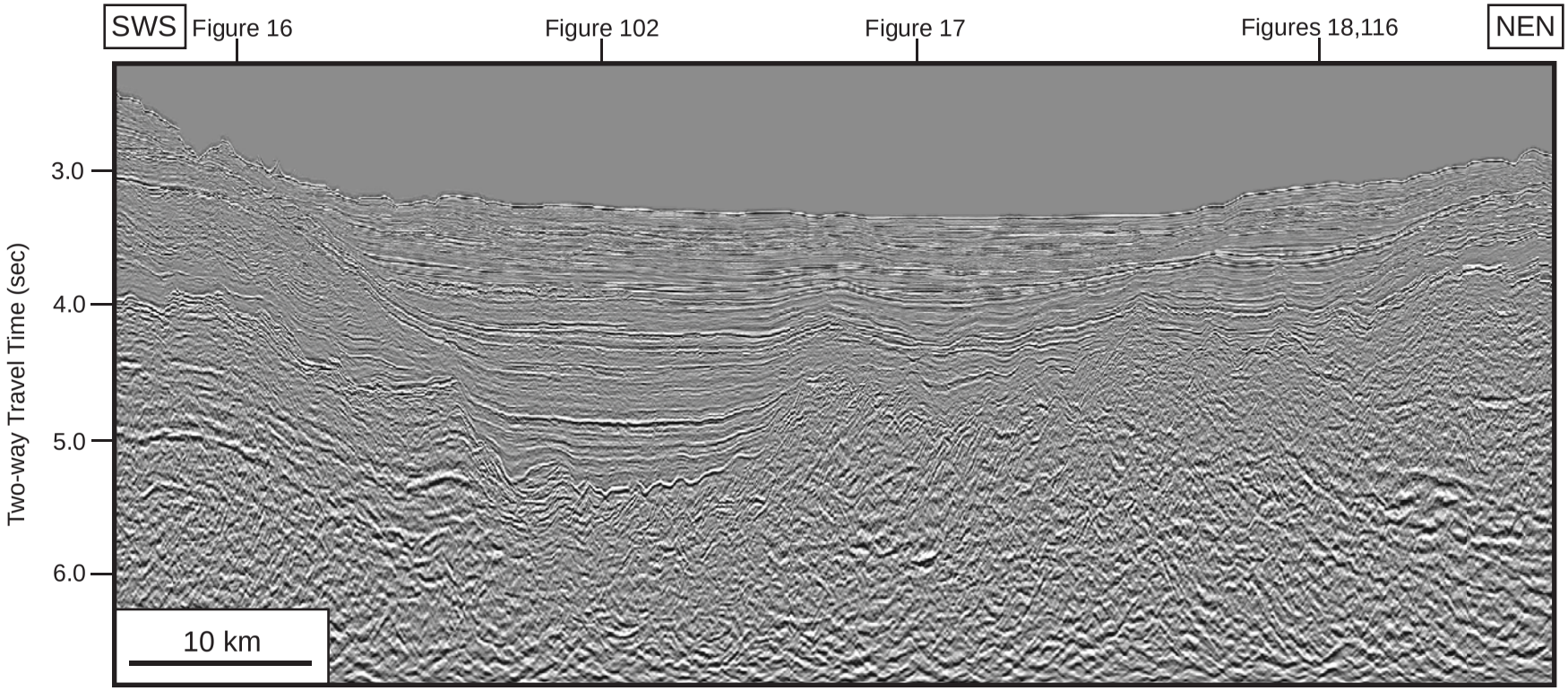

Figure 104a. Uninterpreted regional strike-oriented seismic profile (br-98:br98-085). Location of the profile is shown in Figures 65-66, 71-73, 82-84, 89-97, 106-111 and locations of where Figures 16, 17, 18, 102, 116 cross the profile.

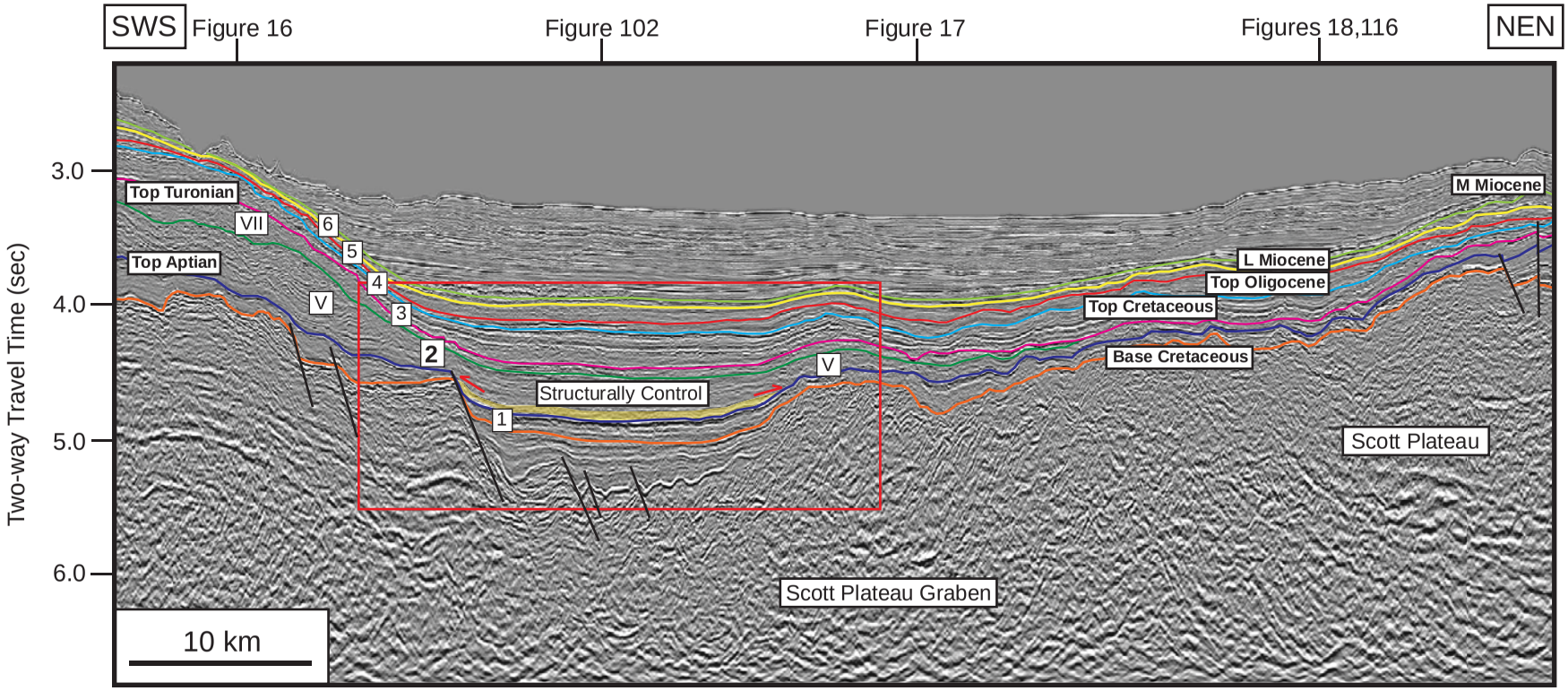

Figure 104b. Regional strike-oriented seismic profile showing all interpreted sequence boundaries from base Cretaceous to middle Miocene. This profile shows the paleogeography of the Scott Plateau Graben and the shallower area of the Scott Plateau. The deepwater deposit is observed within Subsequence V of Megasequence 2 (yellow shade) which caused be the structurally control. Location of the profile is shown in Figures 65-66, 71-73, 82-84, 89-97, 106-111 and locations of where Figures 16, 17, 18, 102, 116 cross the profile.

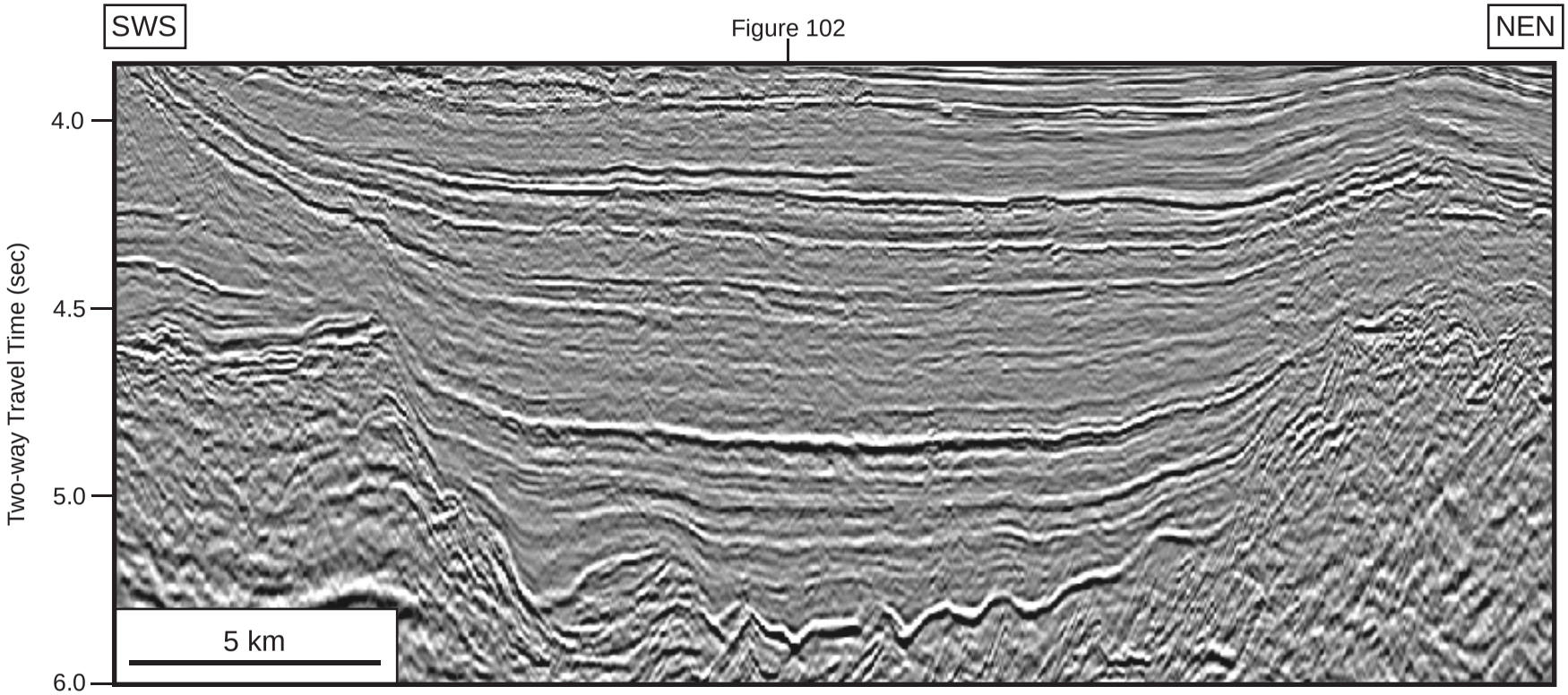

Figure 105a. Uninterpreted regional strike-oriented seismic profile (br-98:br98-085): A closeup view of Figure 104.

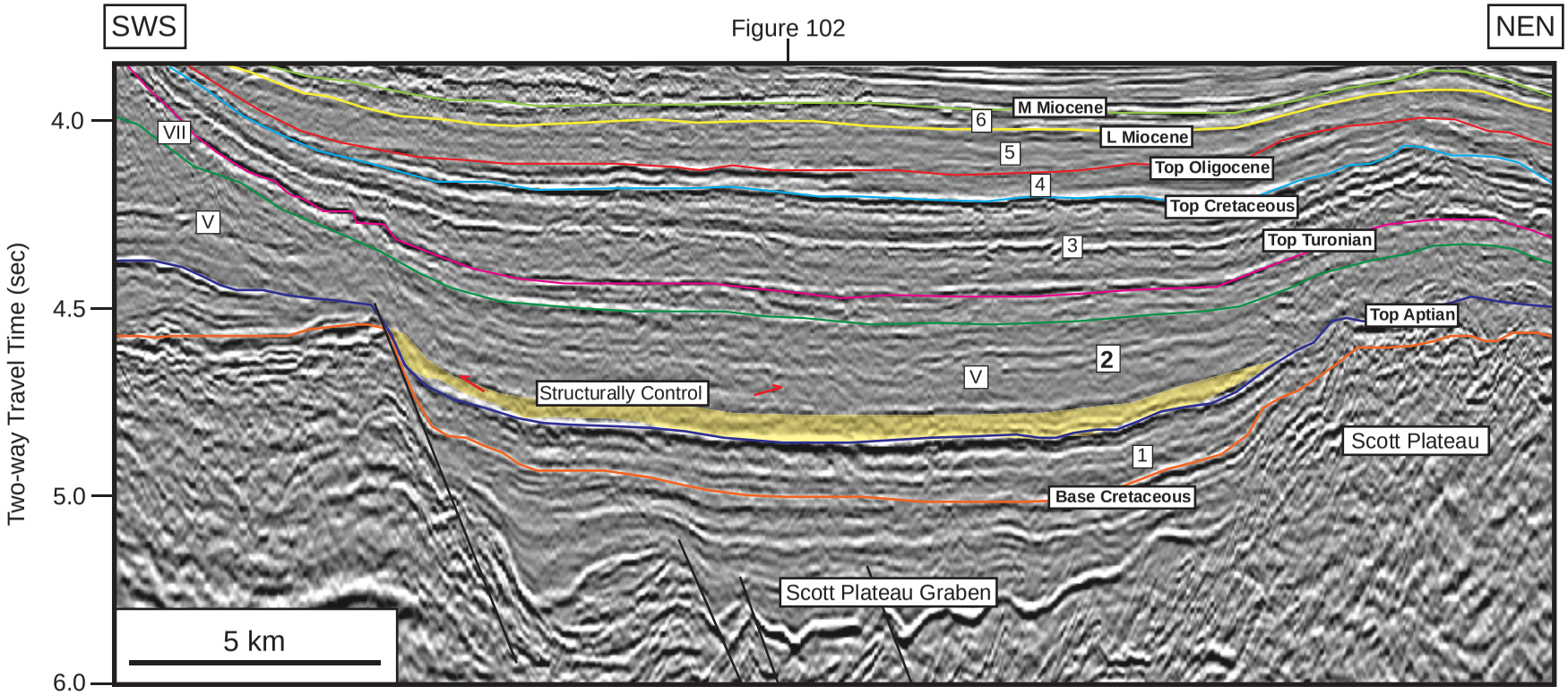

Figure 105b. Regional strike-oriented seismic profile showing all interpreted sequence boundaries from base Cretaceous to middle Miocene: A closeup view of Figure 104. The deepwater deposit is observed within Subsequence V of Megasequence 2 (yellow shade) which caused be the structurally control.

Subsequence VI of Megasequence 2

The isochron map of this subsequence illustrates the thickness values varying from 0 to 660 msec two-way travel time (TWTT) (Figure 106). This interval is the deepwater sediment which deposited on the Barcoo Platform. Only one seismic facies has been identified. The hummocky facies shows the seismic reflections are concordant to both upper and lower sequence boundaries. Its amplitude is moderate whereas the continuity is fair (Figure 107; Table 11).

Table 11. Seismic facies and geologic interpretation of Subsequence VI of Megasequence 2

Seismic Facies	Upper Sequence Boundary	Lower Sequence Boundary	Internal Reflection Configuration	Amplitude	Continuity	Geologic Interpretation
3	Concordant	Concordant	Hummocky	moderate	fair	Inversion – related structure

The geological facies analysis indicates 1 facies of the shelf environment which is shown in Figure 108. No potential prospect is identified.

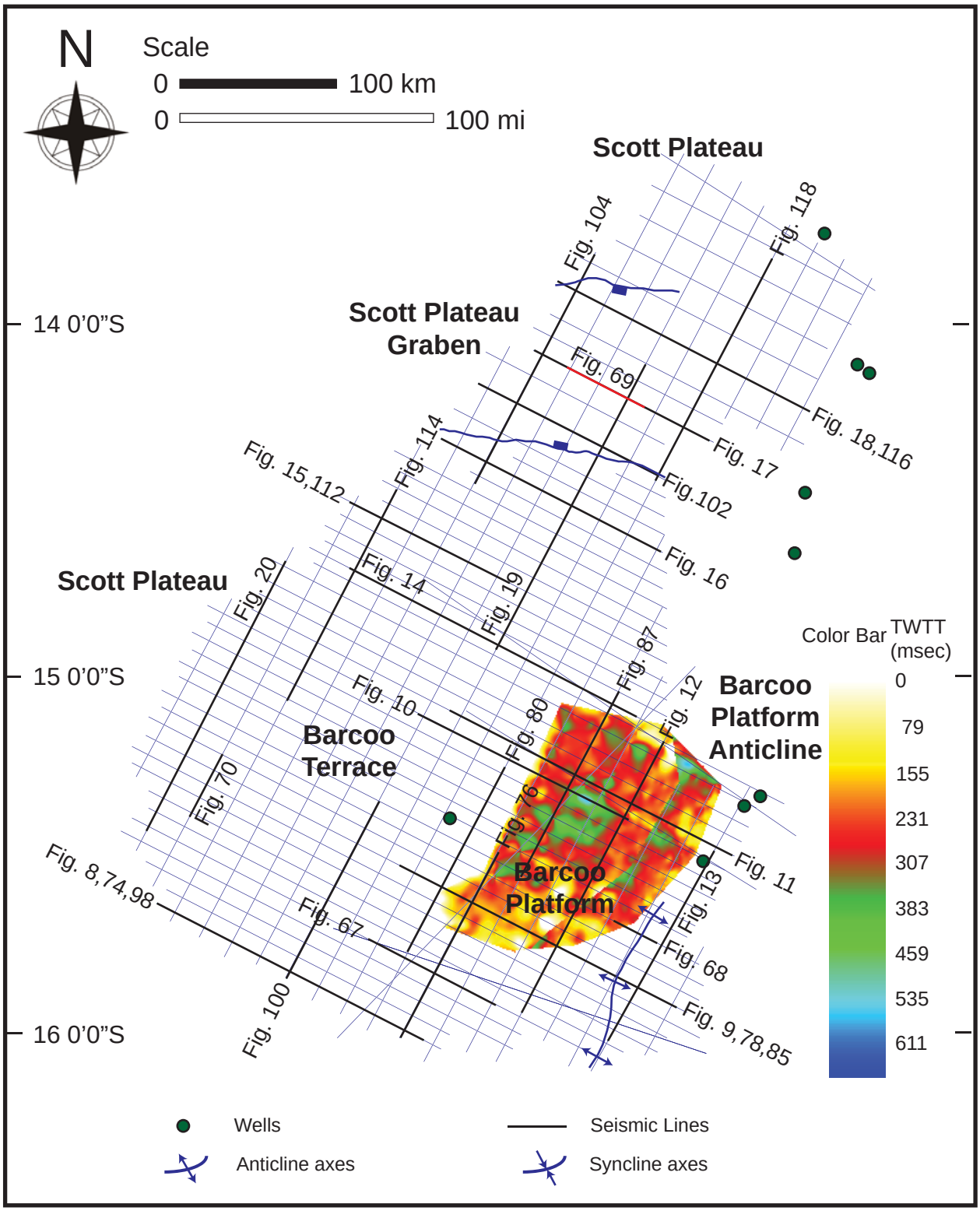

Figure 106. Isochron map (in TWTT msecs) of Subsequence VI of Megasequence 2 interval. Distribution of 2D seismic profiles interpreted to generate the maps are shown by blue lines, and wells are shown by green dots. Locations of Figures 8-20, 67-70, 74-81, 85-88, 98-105, 112-119 are shown.

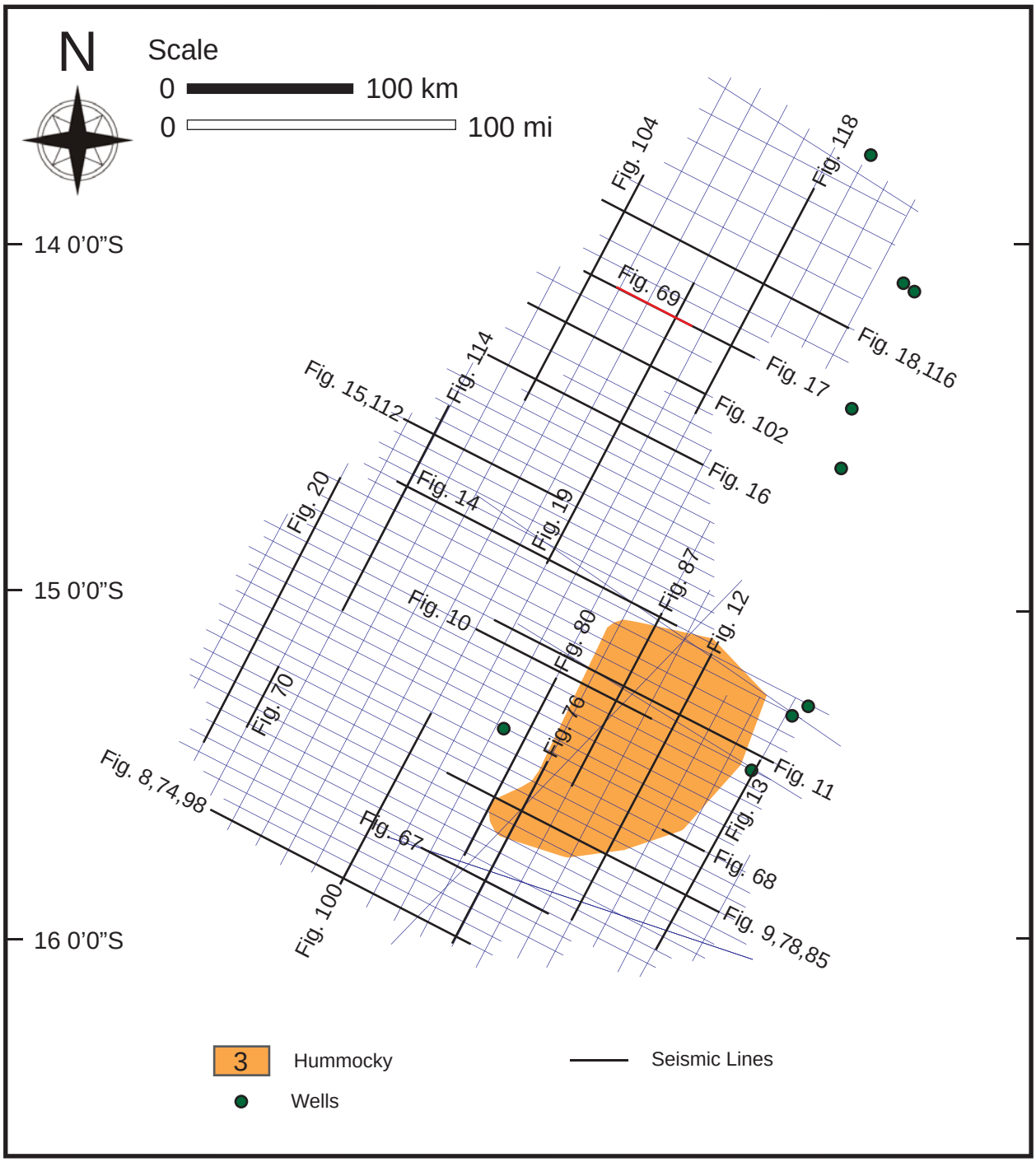

Figure 107. Seismic facies map of Subsequence VI of Megasequence 2 interval. Each facies is numbered as described in the text. See Table 2 for seismic facies coding and Table 4 for a summary of seismic facies analysis and geologic interpretation. Locations of Figures 8-20, 67-70, 74-81, 85-88, 98-105, 112-119 (black lines) are shown, and wells are shown by green dots.

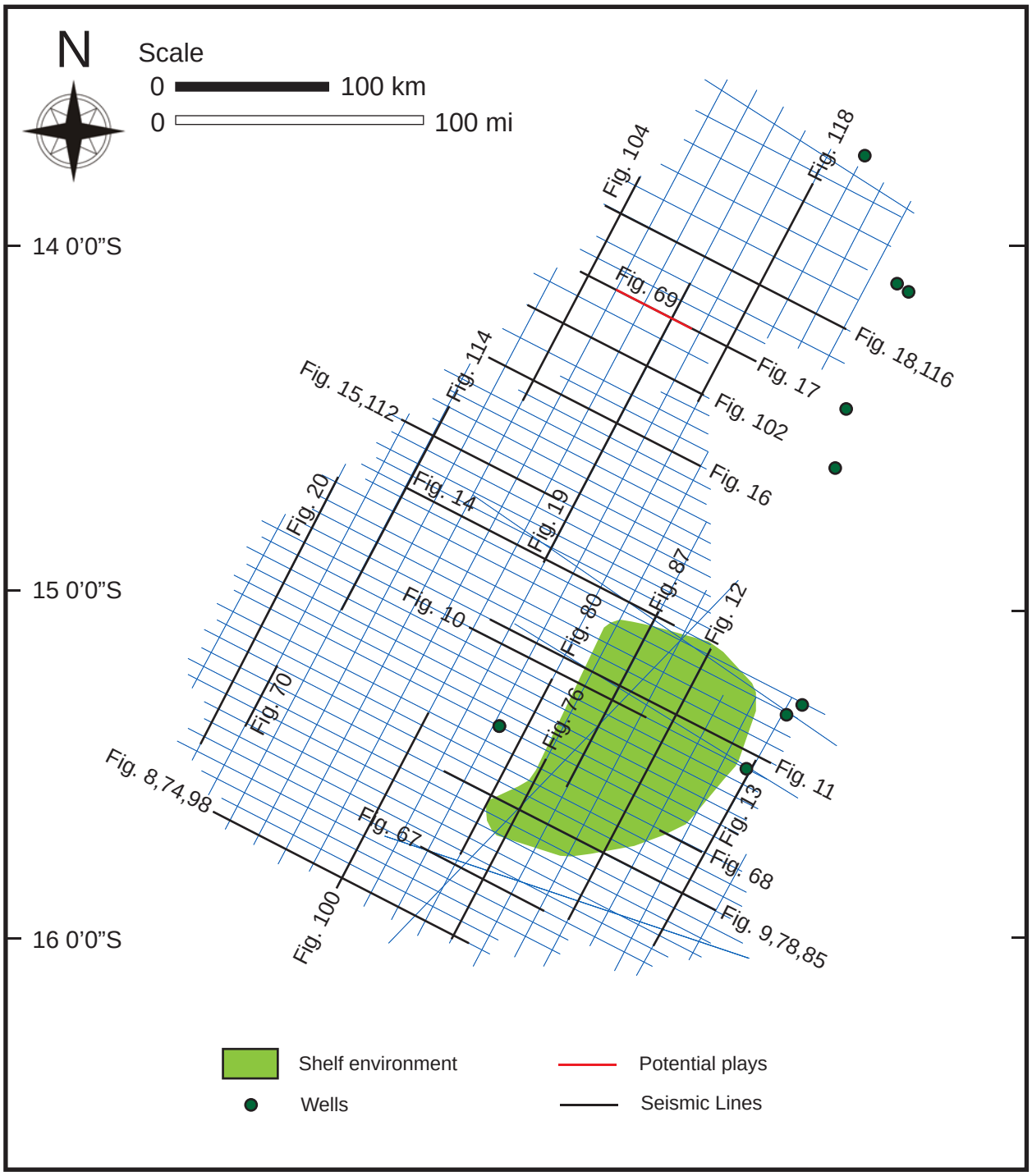

Figure 108. Geologic facies map of Subsequence VI of Megasequence 2 (top Aptian to top Turonian: 112.0-89.3 Ma) interval. See Table 4 for a summary of seismic facies analysis and geologic interpretation. Locations of Figures 8-20, 67-70, 74-81, 85-88, 98-105, 112-119 (black lines) are shown, and wells are shown by green dots.

Subsequence VII of Megasequence 2

The isochron map shows the value ranges from 0 to 660 msec two-way travel time (TWTT) (Figure 109). The sediments deposited greatly on the Scott Plateau, at the southern and eastern flanks of the Scott Plateau Graben.

There are six seismic facies are specified in this subsequence (Figure 110; Table 12). Facies 1 and 4 show the concordant seismic reflection onto both upper and lower sequence boundaries. They have the parallel to subparallel internal reflection configuration with moderate to high amplitude and fair to good continuity. Facies 1 is interpreted to be the shelf deposits whereas facies 4 assumes to be the basin-floor environment. Seismic facies 3 displays the hummocky configuration with moderate amplitude and fair continuity. The other two facies are facies 5 and 6. Both of them, illustrates the chaotic internal reflection configuration. The amplitude ranges from low to moderate to high whereas the continuity is poor. Facies 5 interpreted to be the basinal deposits on graben flank. On the other hand, due to its mounded external feature, facies 6 is assumed to the build-up structure of carbonate rock.

Table 12. Seismic facies and geologic interpretation of Subsequence VII of Megasequence 2

Seismic Facies	Upper Sequence Boundary	Lower Sequence Boundary	Internal Reflection Configuration	Amplitude	Continuity	Geologic Interpretation
1	Concordant	Concordant	Parallel to Subparallel	moderate to high	fair to good	Shelf deposits
3	Concordant	Concordant	Hummocky	moderate	fair	Inversion – related structure
4	Concordant	Concordant	Parallel to Subparallel	moderate to high	fair to good	Basinal deposits
5	Concordant	Concordant	Chaotic	low	poor	Basinal deposits on graben flank
6	-	-	Chaotic	moderate to high	poor	Carbonate buildup

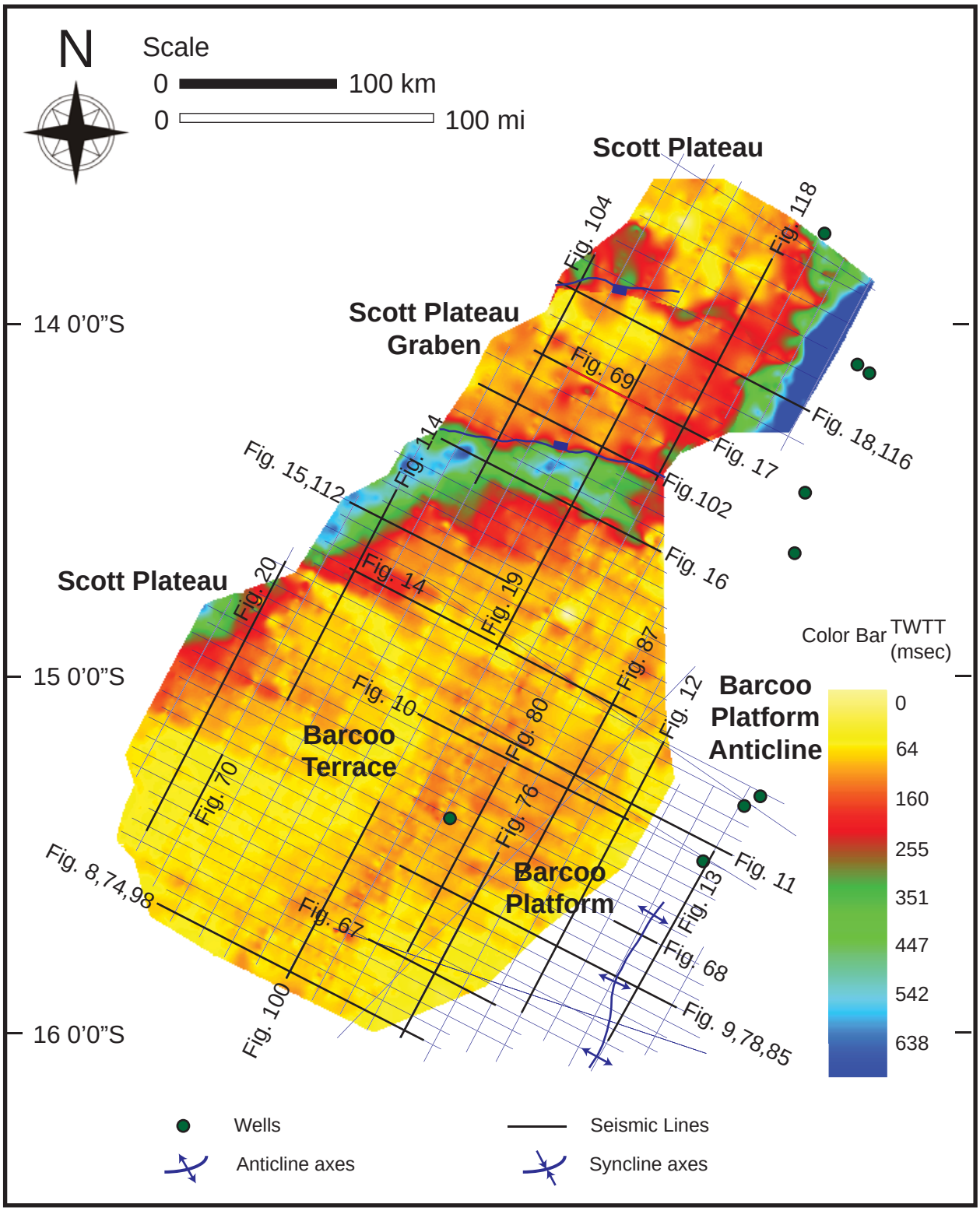

Figure 109. Isochron map (in TWTT msecs) of Subsequence VII of Megasequence 2 interval. Distribution of 2D seismic profiles interpreted to generate the maps are shown by blue lines, and wells are shown by green dots. Locations of Figures 8-20, 67-70, 74-81, 85-88, 98-105, 112-119 are shown.

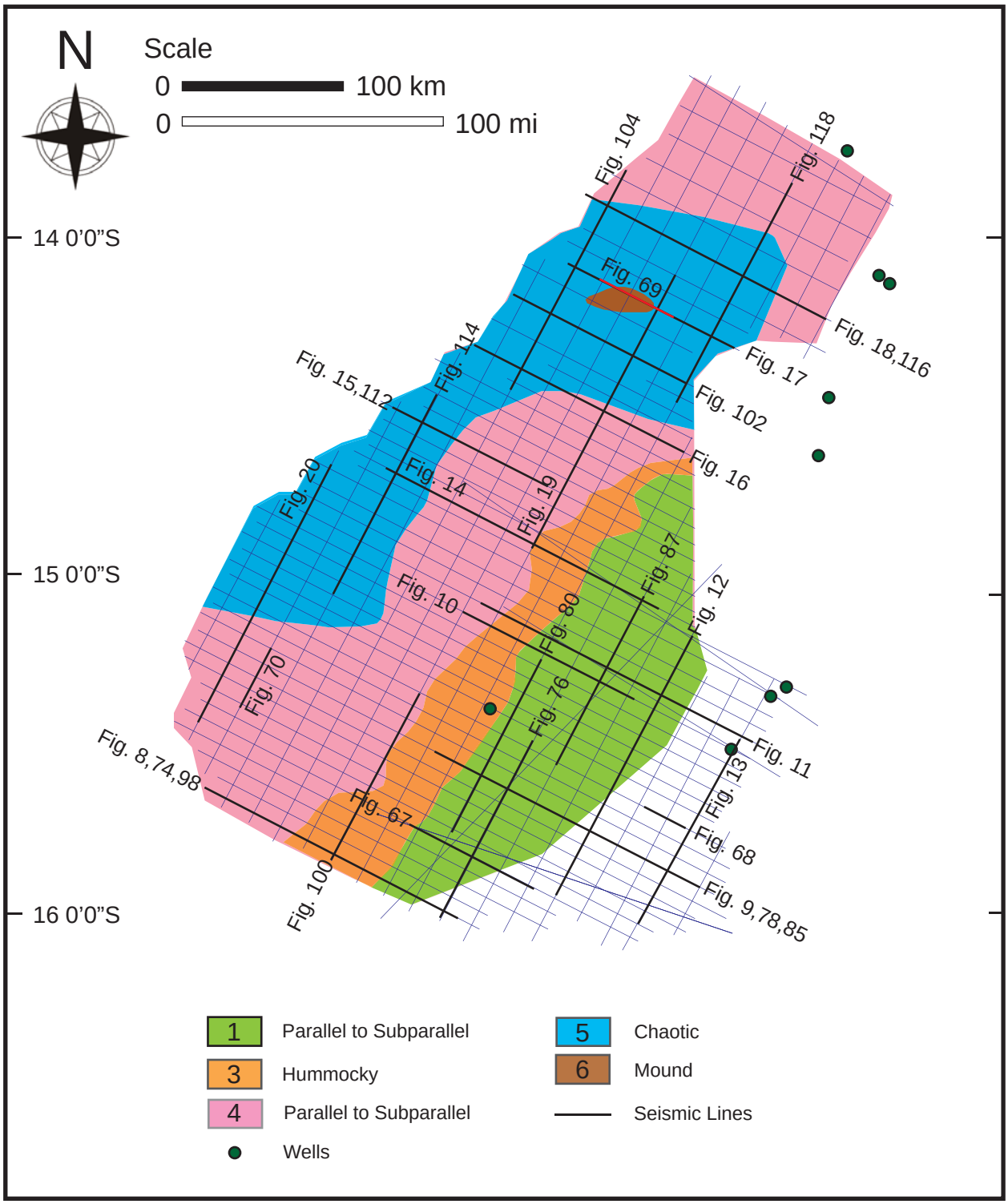

Figure 110. Seismic facies map of Subsequence VII of Megasequence 2 interval. Each facies is numbered as described in the text. See Table 2 for seismic facies coding and Table 4 for a summary of seismic facies analysis and geologic interpretation. Locations of Figures 8-20, 67-70, 74-81, 85-88, 98-105, 112-119 (black lines) are shown, and wells are shown by green dots.

Two potential petroleum prospects are identified. Figures 112-115 display the dip and strike oriented seismic profiles of the sediment wedge which deposited on the Barcoo Terrace. The other one is the basin-floor fan which deposited in the Scott Plateau Graben. The dip and strike oriented seismic profile are shown in Figures 112-119. Both of these prospects are pointed out because of its bi-directional downlap truncations.

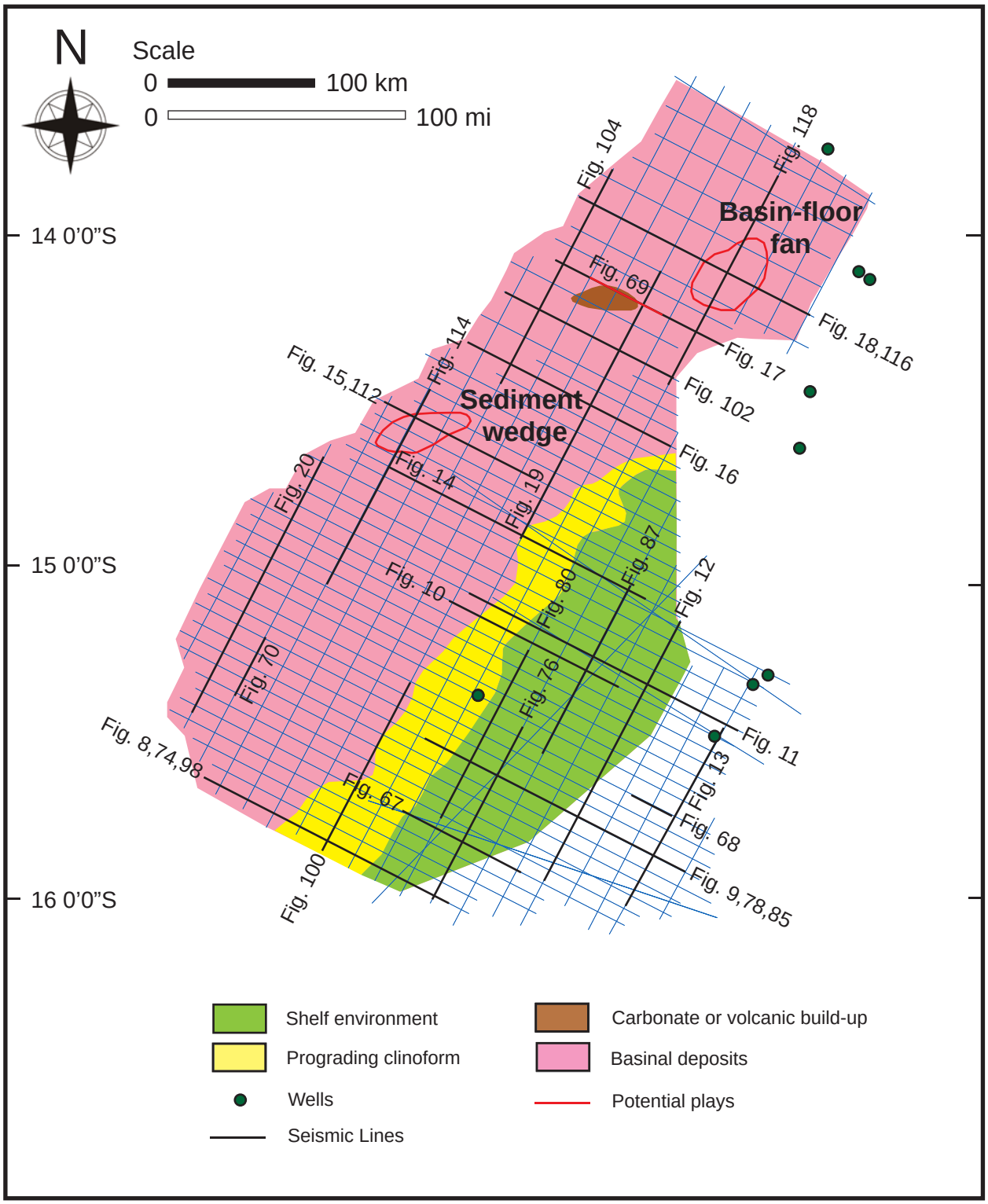

Figure 111. Geologic facies map of Subsequence VII of Megasequence 2 (top Aptian to top Turonian: 112.0-89.3 Ma) interval. See Table 4 for a summary of seismic facies analysis and geologic interpretation. Locations of Figures 8-20, 67-70, 74-81, 85-88, 98-105, 112-119 (black lines) are shown, and wells are shown by green dots.

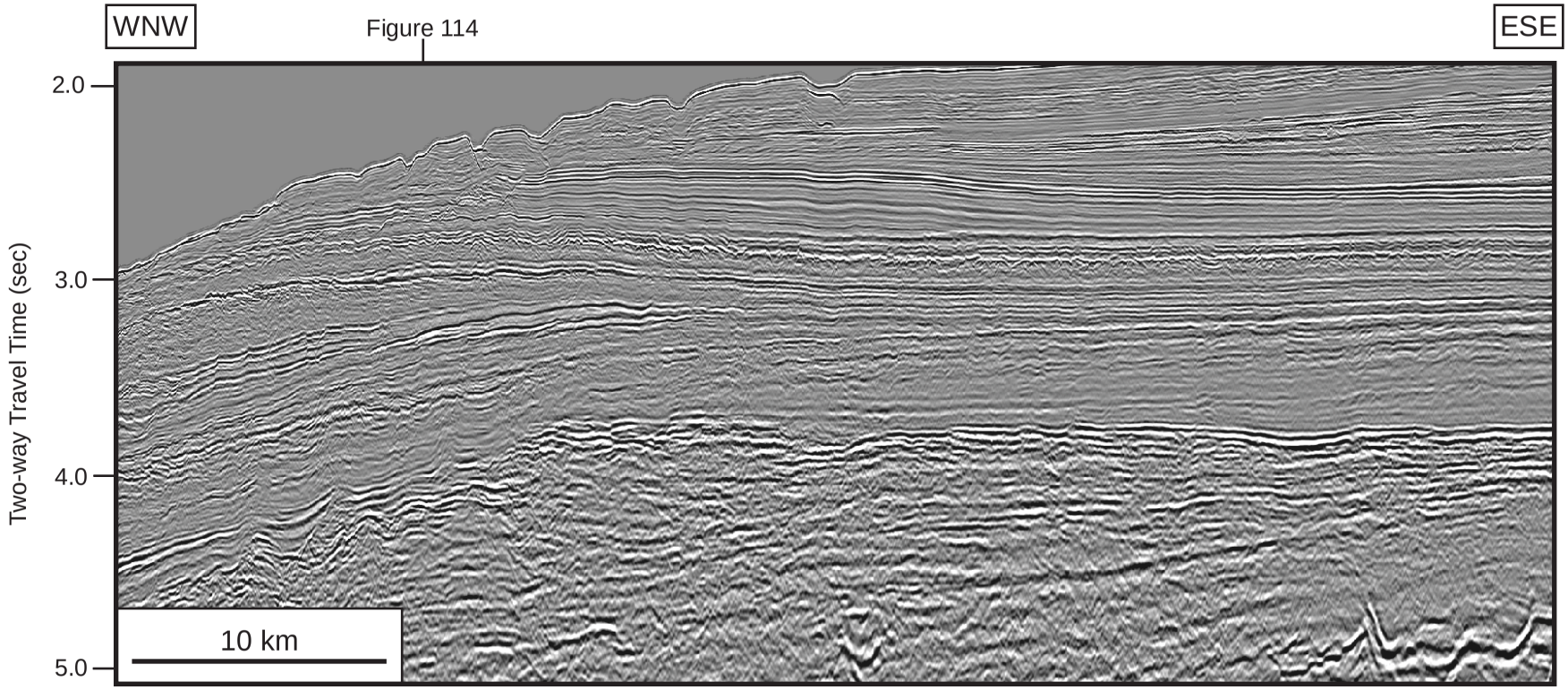

Figure 112a. Uninterpreted regional dip-oriented seismic profile (br-98:br98-029). Location of the profile is shown in Figures 65-66, 71-73, 82-84, 89-97, 106-111 and location of where Figure 114 crosses the profile.

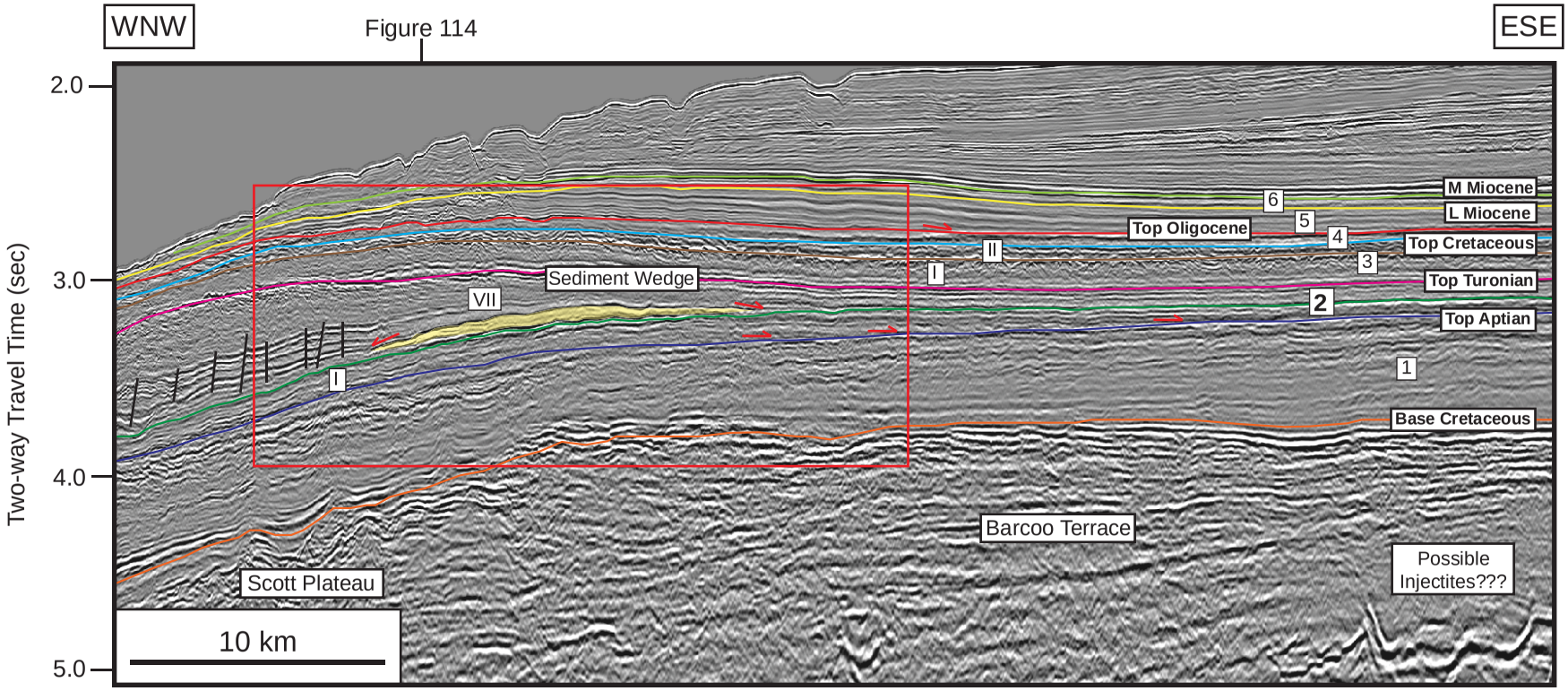

Figure 112b. Regional dip-oriented seismic profile showing all interpreted sequence boundaries from base Cretaceous to middle Miocene. The sediment wedge, which is observed within Subsequence VII of Megasequence 2 (yellow shade), is considered to be the potential petroleum play. Location of the profile is shown in Figures 65-66, 71-73, 82-84, 89-97, 106-111 and location of where Figure 114 crosses the profile.

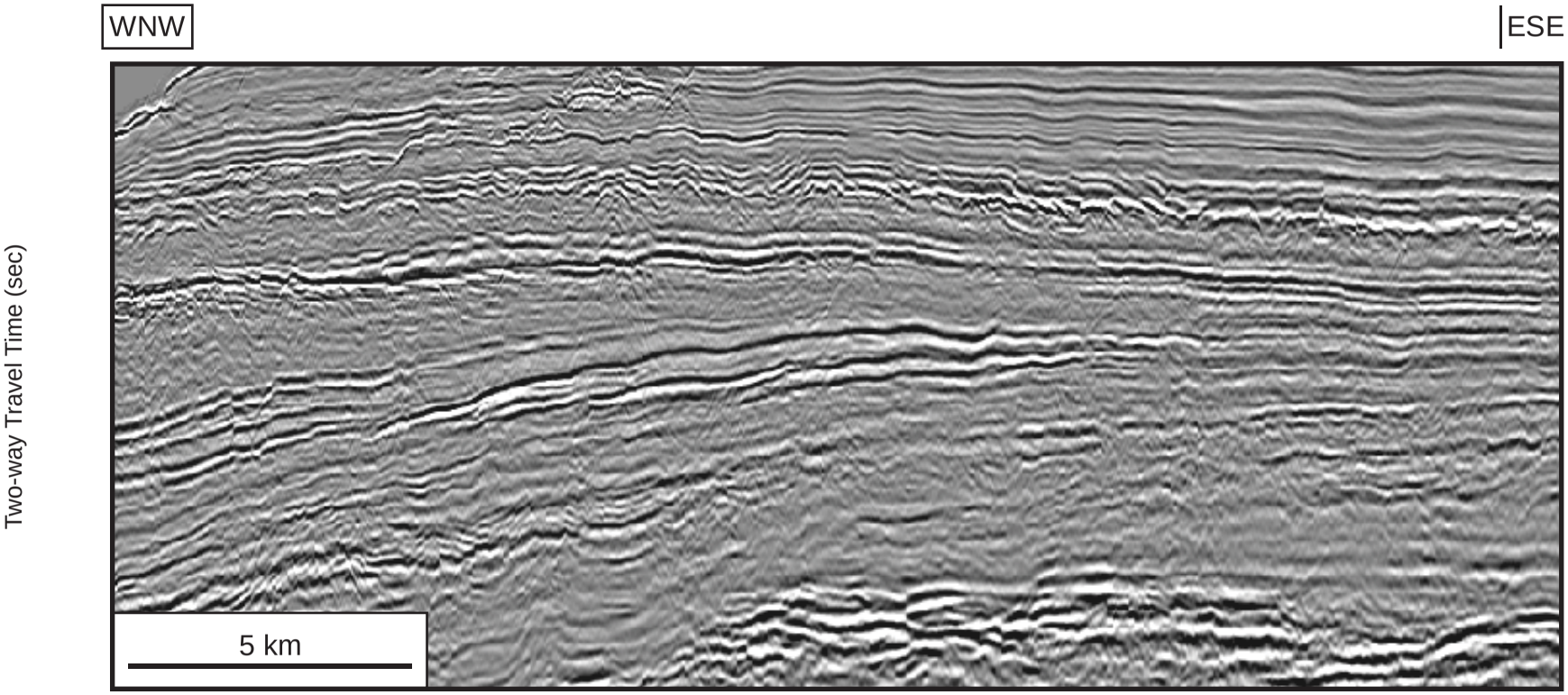

Figure 113a. Uninterpreted regional dip-oriented seismic profile (br-98:br98-029): A closeup view of Figure 112.

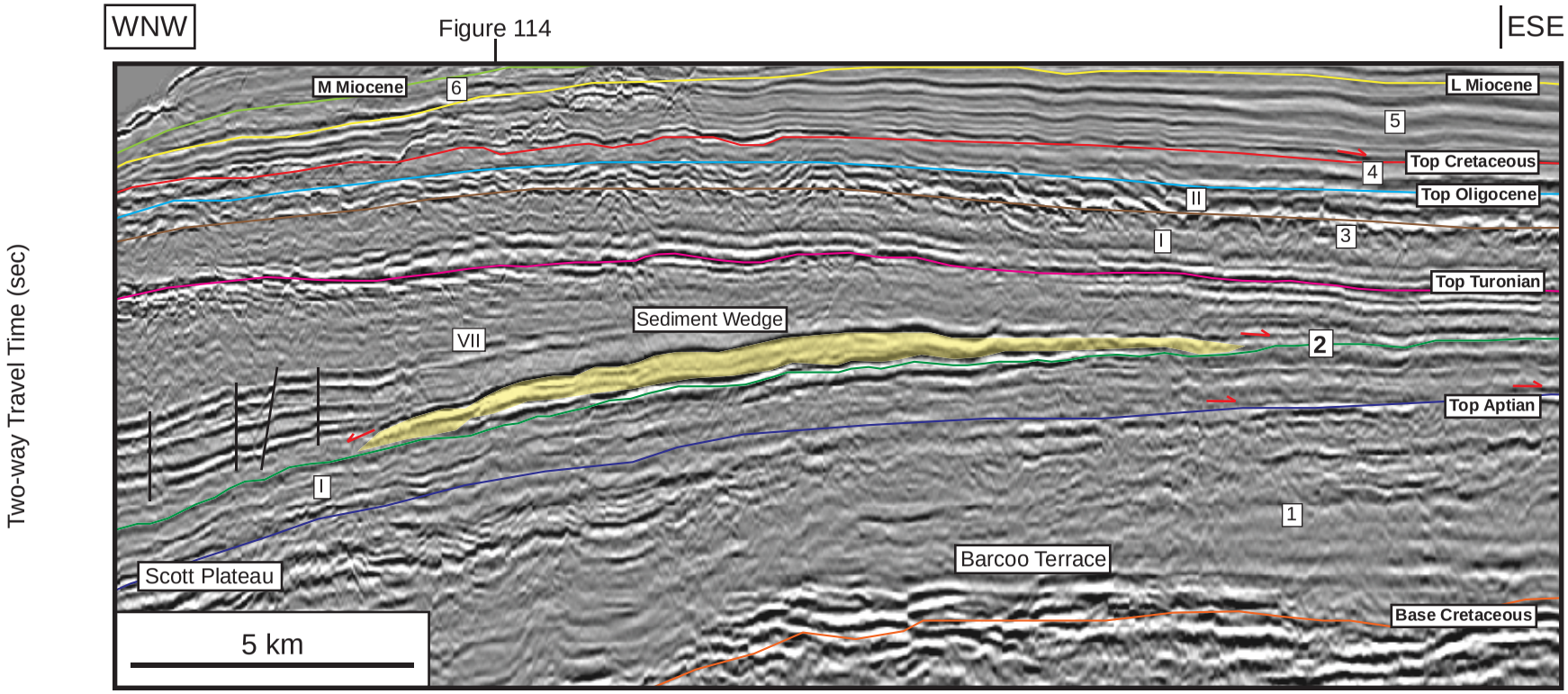

Figure 113b. Regional dip-oriented seismic profile showing all interpreted sequence boundaries from base Cretaceous to middle Miocene: A closeup view of Figure 112. The sediment wedge, which is observed within Subsequence VII of Megasequence 2 (yellow shade), is considered to be the potential petroleum play.

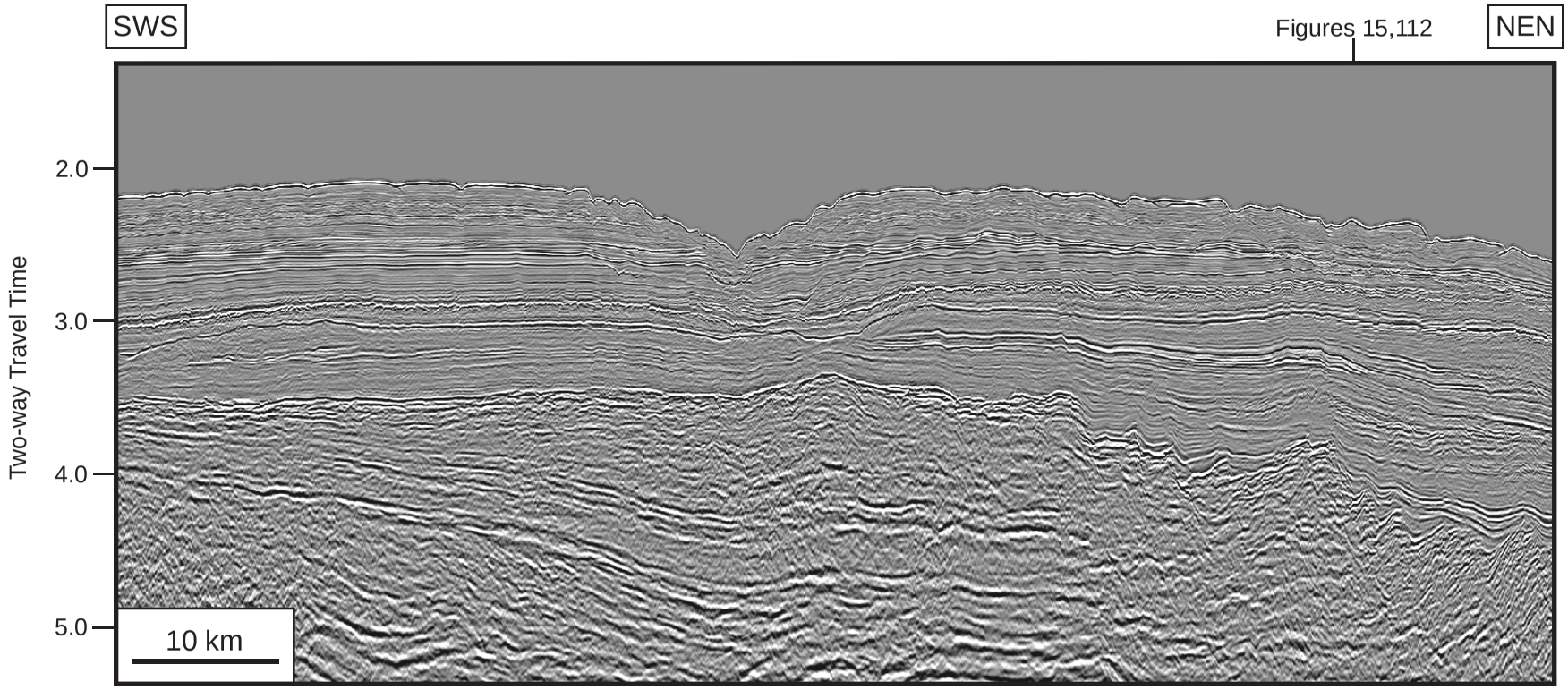

Figure 114a. Uninterpreted regional strike-oriented seismic profile (br-98:br98-087). Location of the profile is shown in Figures 65-66, 71-73, 782-84, 89-97, 106-111 and location of where Figures 15, 112 crosses the profile.

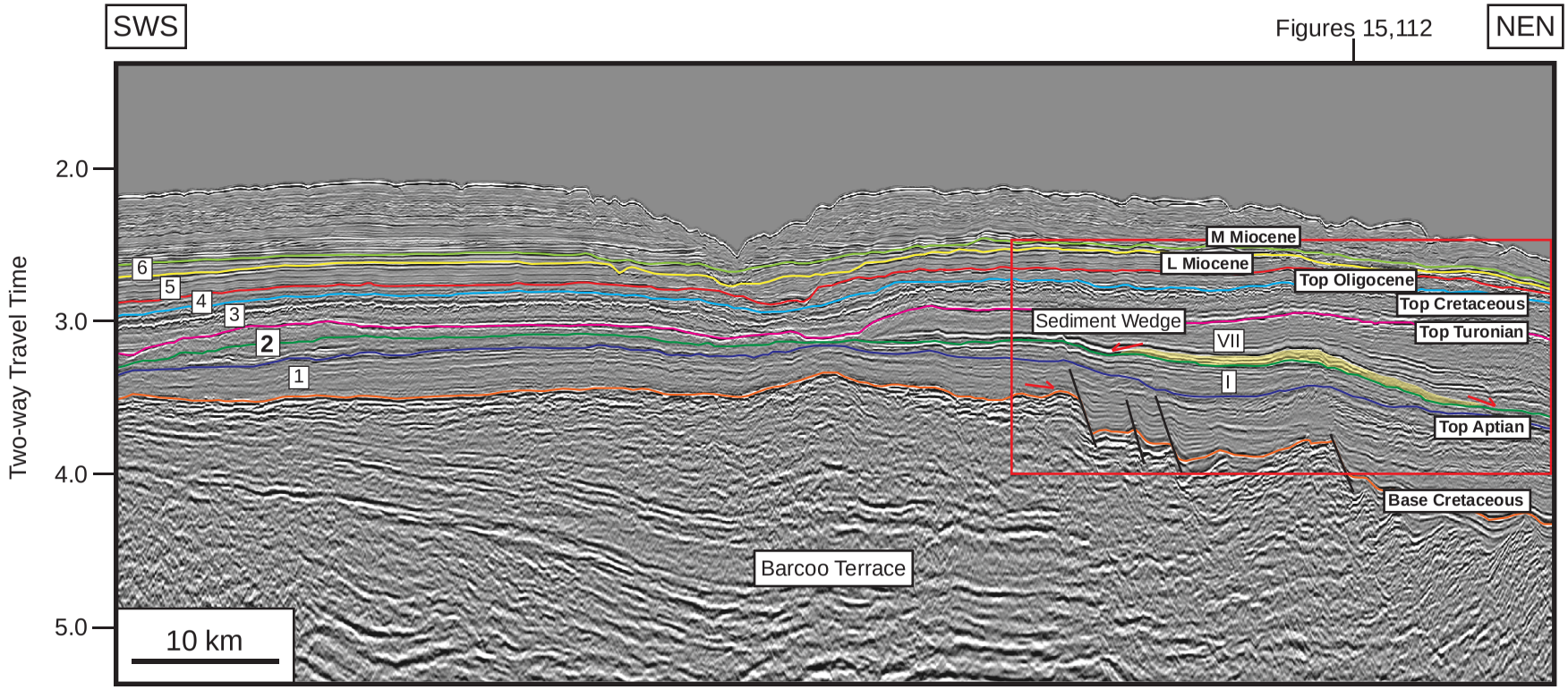

Figure 114b. Regional strike-oriented seismic profile showing all interpreted sequence boundaries from base Cretaceous to middle Miocene. This profile shows the area of the Barcoo Terrace. The basin-floor fan is observed within Subsequence VII of Megasequence 1 (yellow shade). Location of the profile is shown in Figures 65-66, 71-73, 782-84, 89-97, 106-111 and location of where Figures 15, 112 crosses the profile.

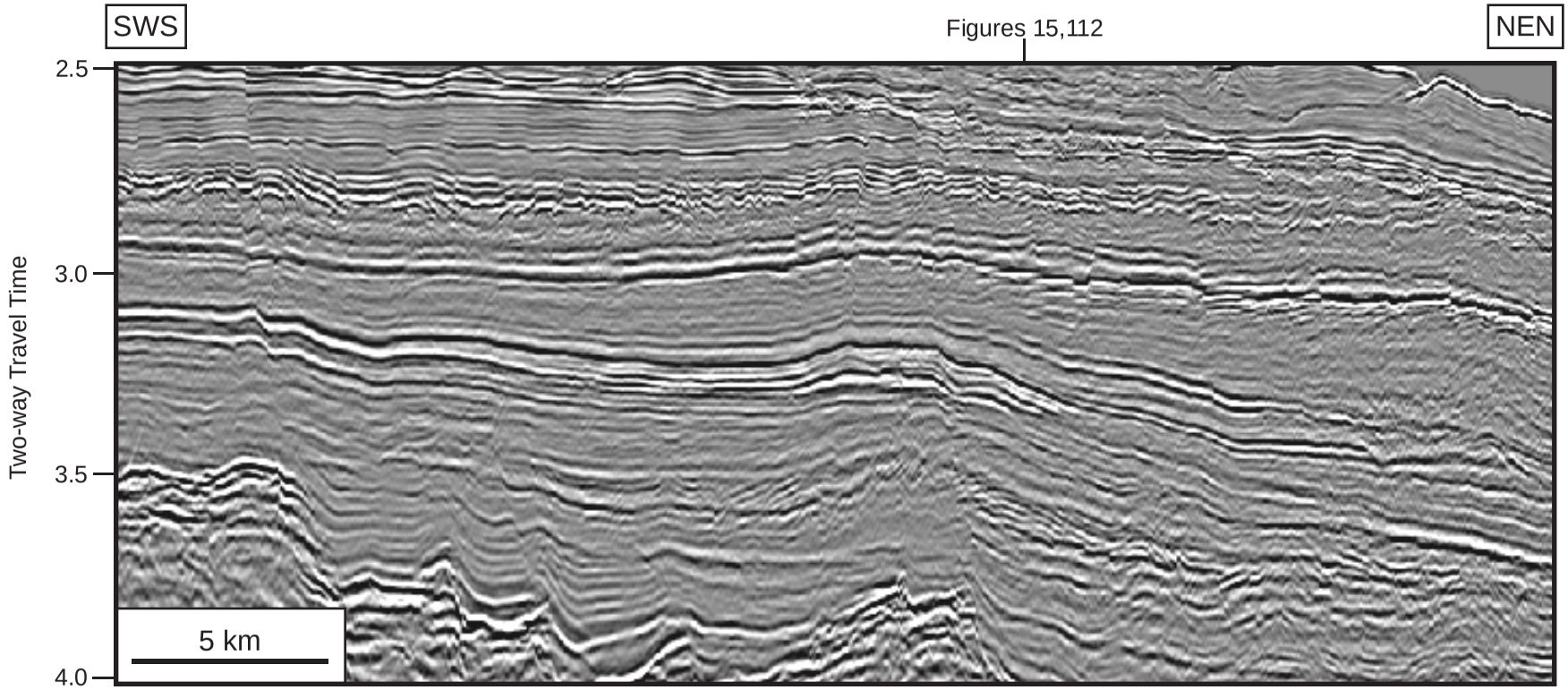

Figure 115a. Uninterpreted regional strike-oriented seismic profile (br-98:br98-087): A closeup view of Figure 114.

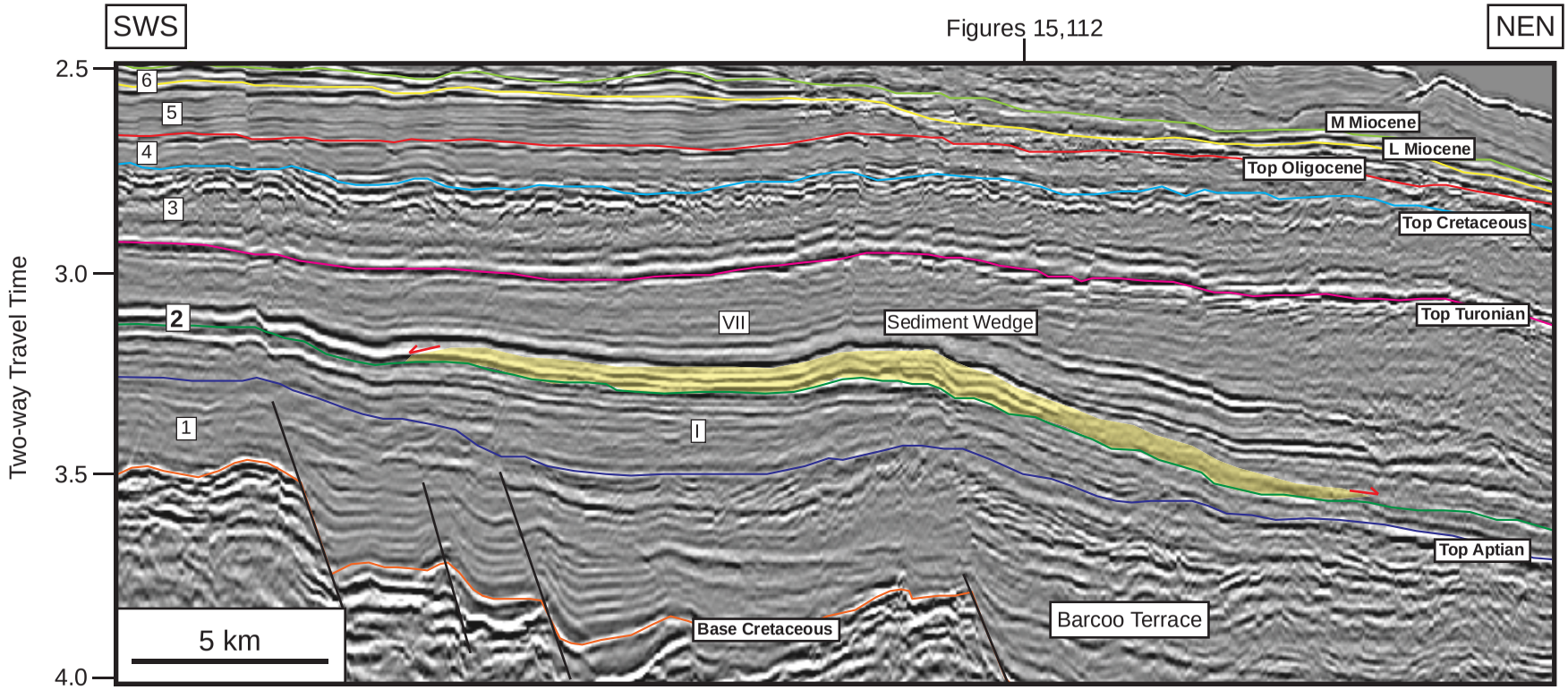

Figure 115b. Regional strike-oriented seismic profile showing all interpreted sequence boundaries from base Cretaceous to middle Miocene: A closeup view of Figure 114. The basin-floor fan is observed within Subsequence VII of Megasequence 1 (yellow shade).

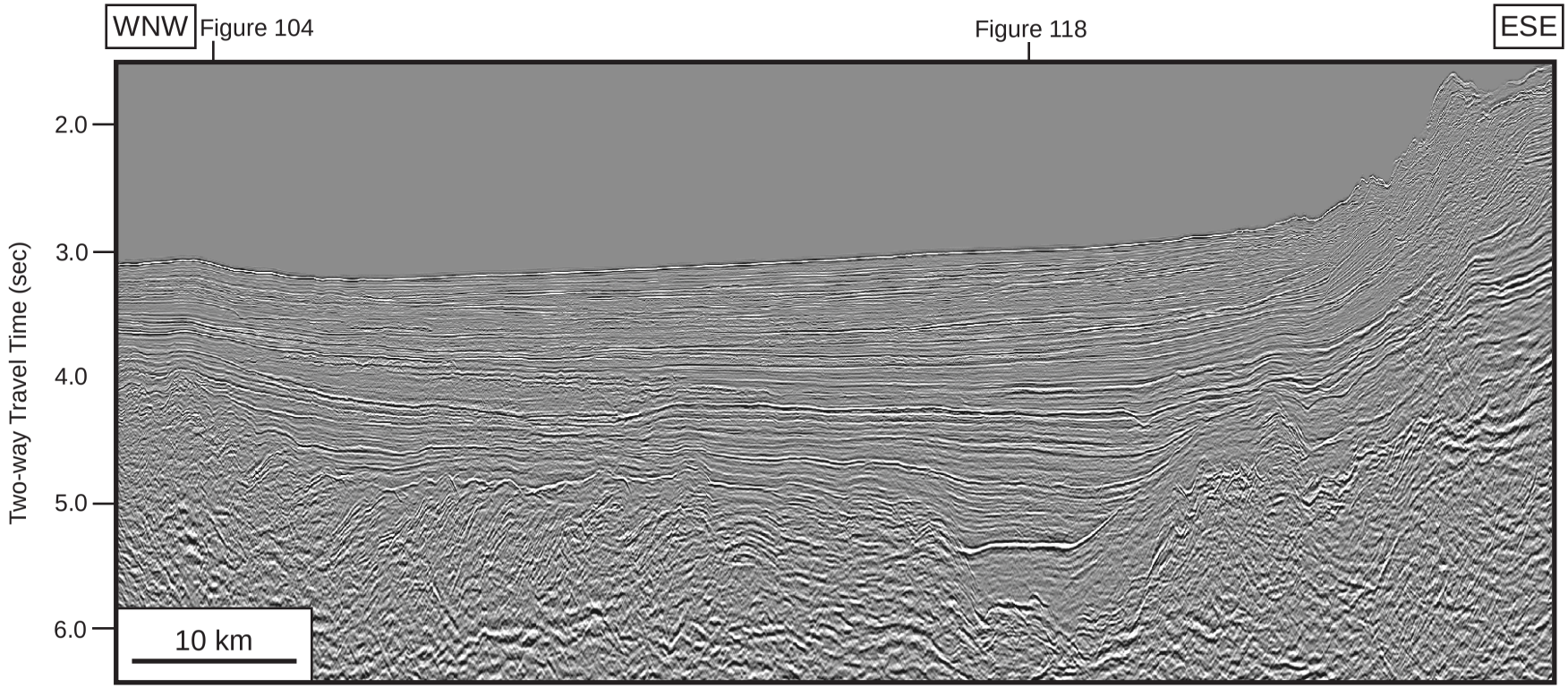

Figure 116a. Uninterpreted regional dip-oriented seismic profile (br-98:br98-057). Location of the profile is shown in Figures 65-66, 71-73, 82-84, 89-97, 106-111 and locations of where Figures 104, 118 cross the profile.

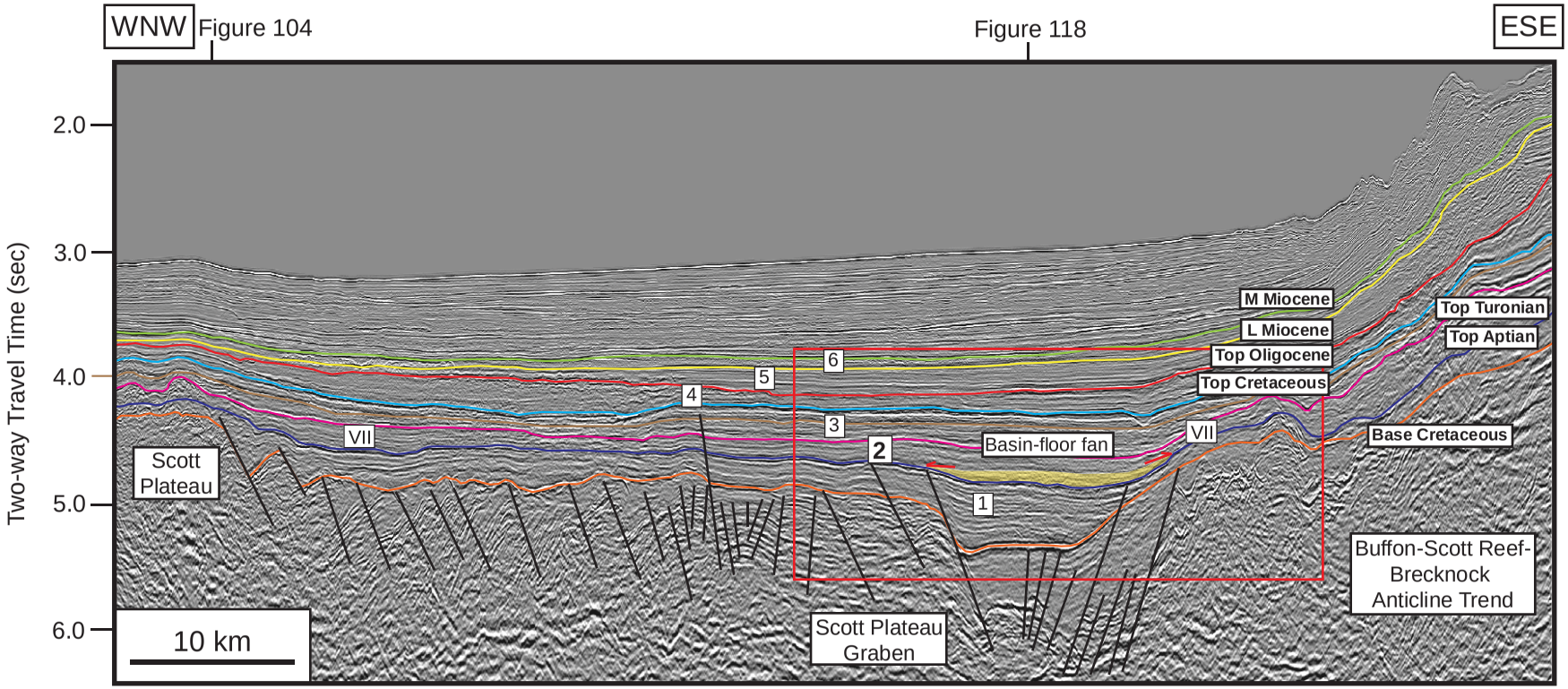

Figure 116b. Regional dip-oriented seismic profile showing all interpreted sequence boundaries from base Cretaceous to middle Miocene. This profile shows the deeper area of the Scott Plateau Graben and shallower area of the Buffon-Scott Reef-Brecknock Anticline Trend in the northern part of the study area. Series of faults in the underlying Jurassic strata caused the irregular topography. The basin-floor fan is observed within Subsequence VII of Megasequence 2 (yellow shade). Location of the profile is shown in Figures 65-66, 71-73, 82-84, 89-97, 106-111 and locations of where Figures 104, 118 cross the profile.

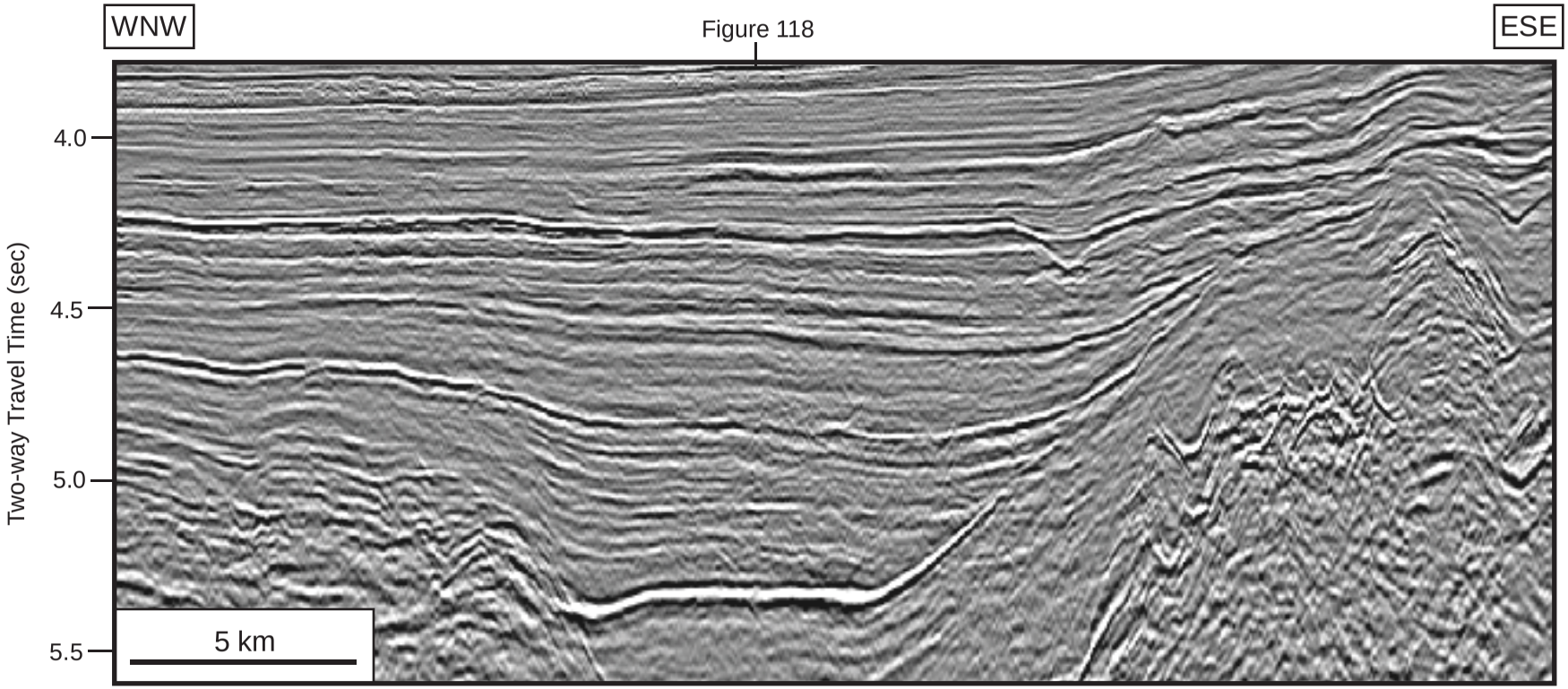

Figure 117a. Uninterpreted regional dip-oriented seismic profile (br-98:br98-057)A closeup view of Figure 116.

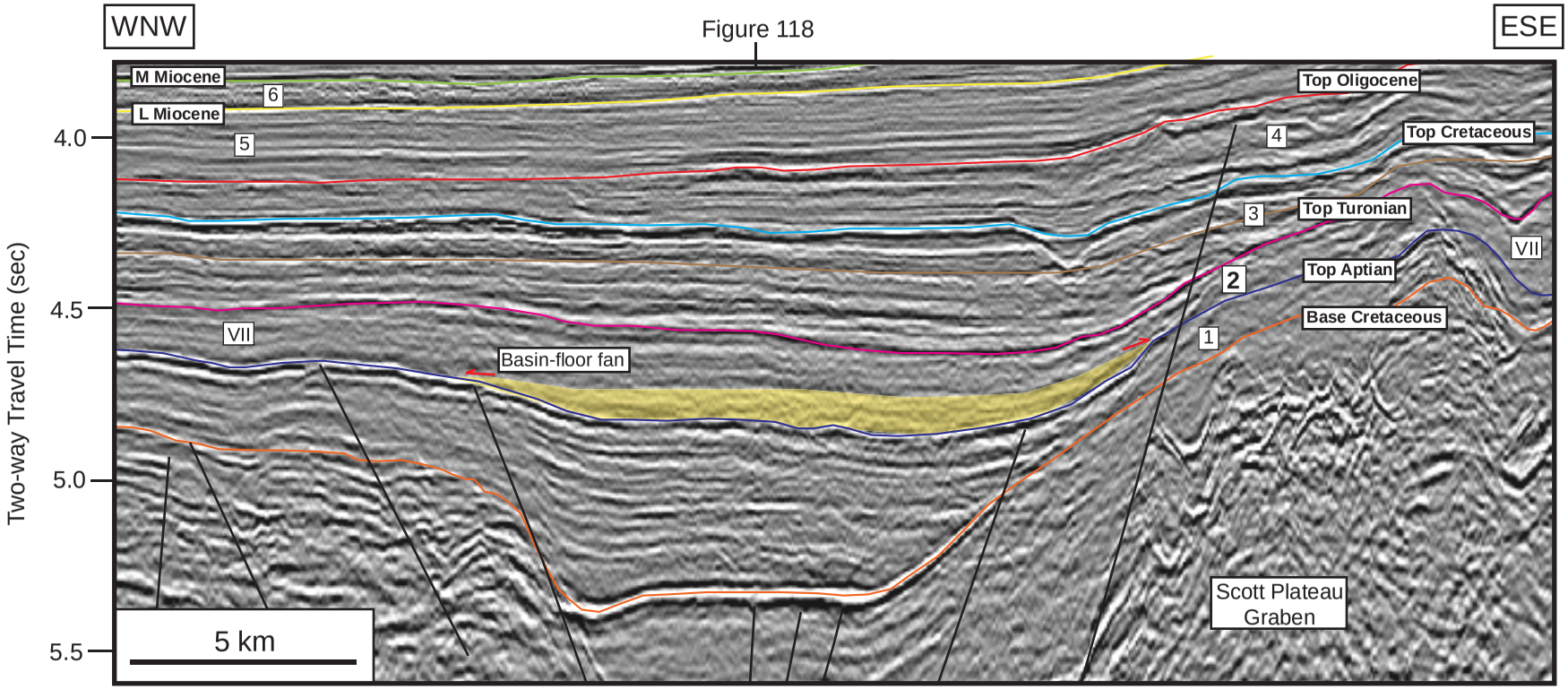

Figure 117b. Regional dip-oriented seismic profile showing all interpreted sequence boundaries from base Cretaceous to middle Miocene: A closeup view of Figure 116. The basin-floor fan is observed within Subsequence VII of Megasequence 2 (yellow shade).

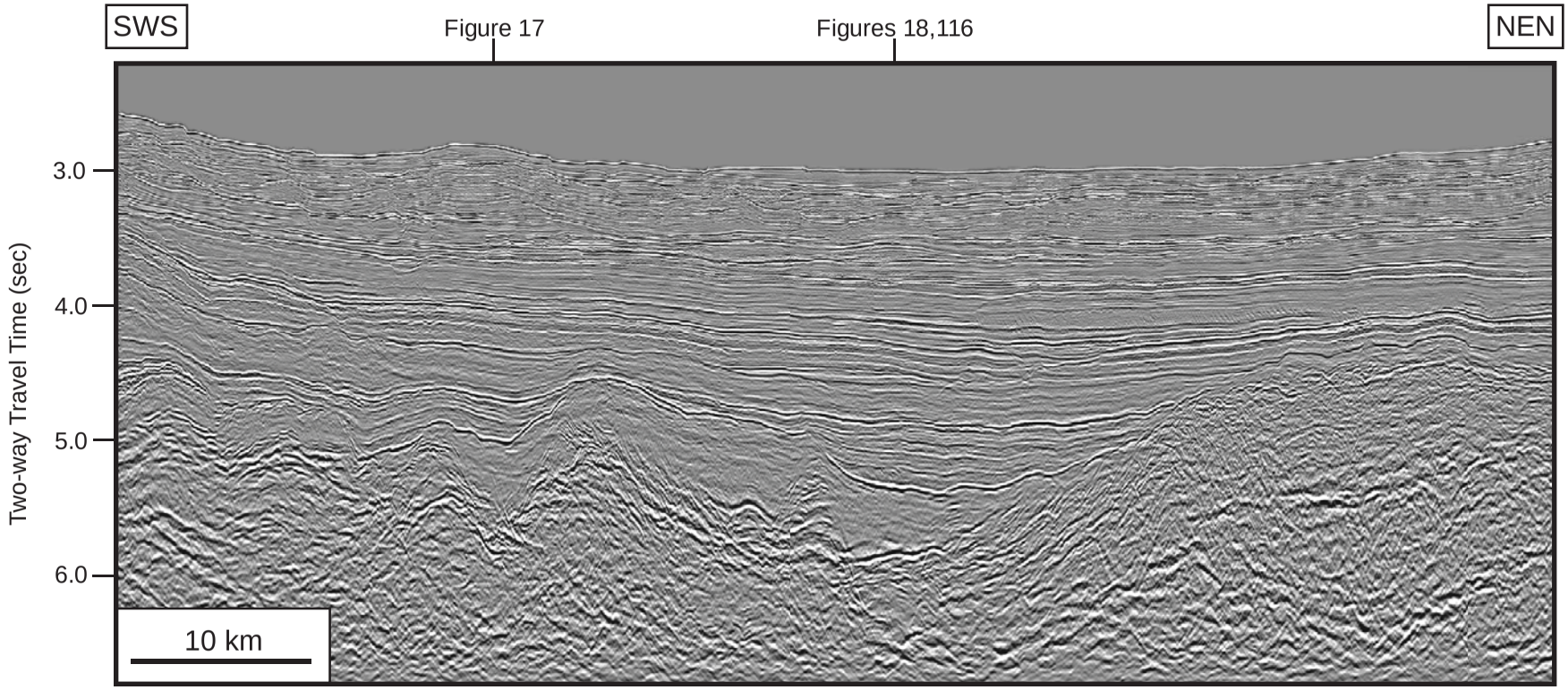

Figure 118a. Uninterpreted regional strike-oriented seismic profile (br-98:br98-080). Location of the profile is shown in Figures 65-66, 71-73, 82-84, 89-97, 106-111 and locations of where Figures 17, 18, 116 cross the profile.

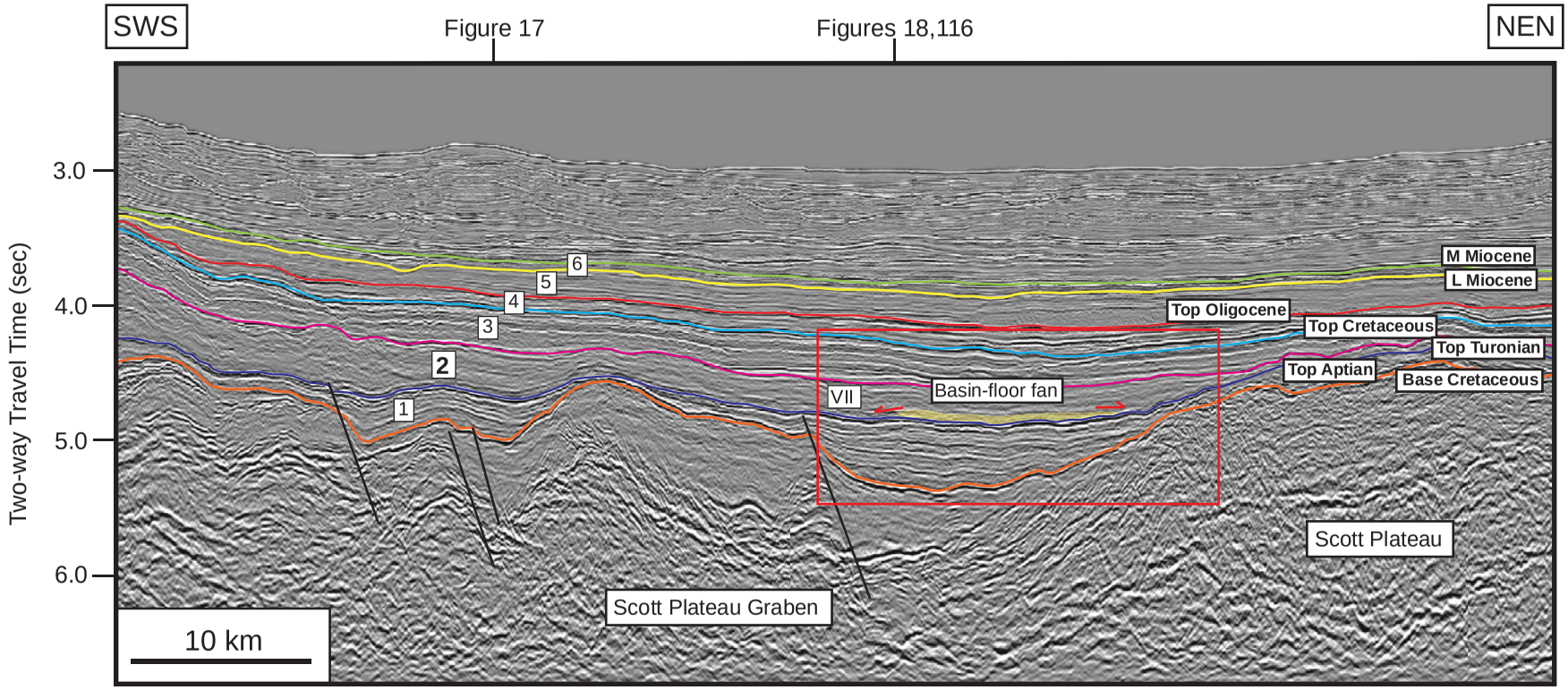

Figure 118b. Regional strike-oriented seismic profile showing all interpreted sequence boundaries from base Cretaceous to middle Miocene. This profile shows the area of the Scott Plateau and the shallower area of the Scott Plateau. The basin-floor fan is observed within Subsequence VII of Megasequence 2 (yellow shade). Location of the profile is shown in Figures 65-66, 71-73, 82-84, 89-97, 106-111 and locations of where Figures 17, 18, 116 cross the profile.

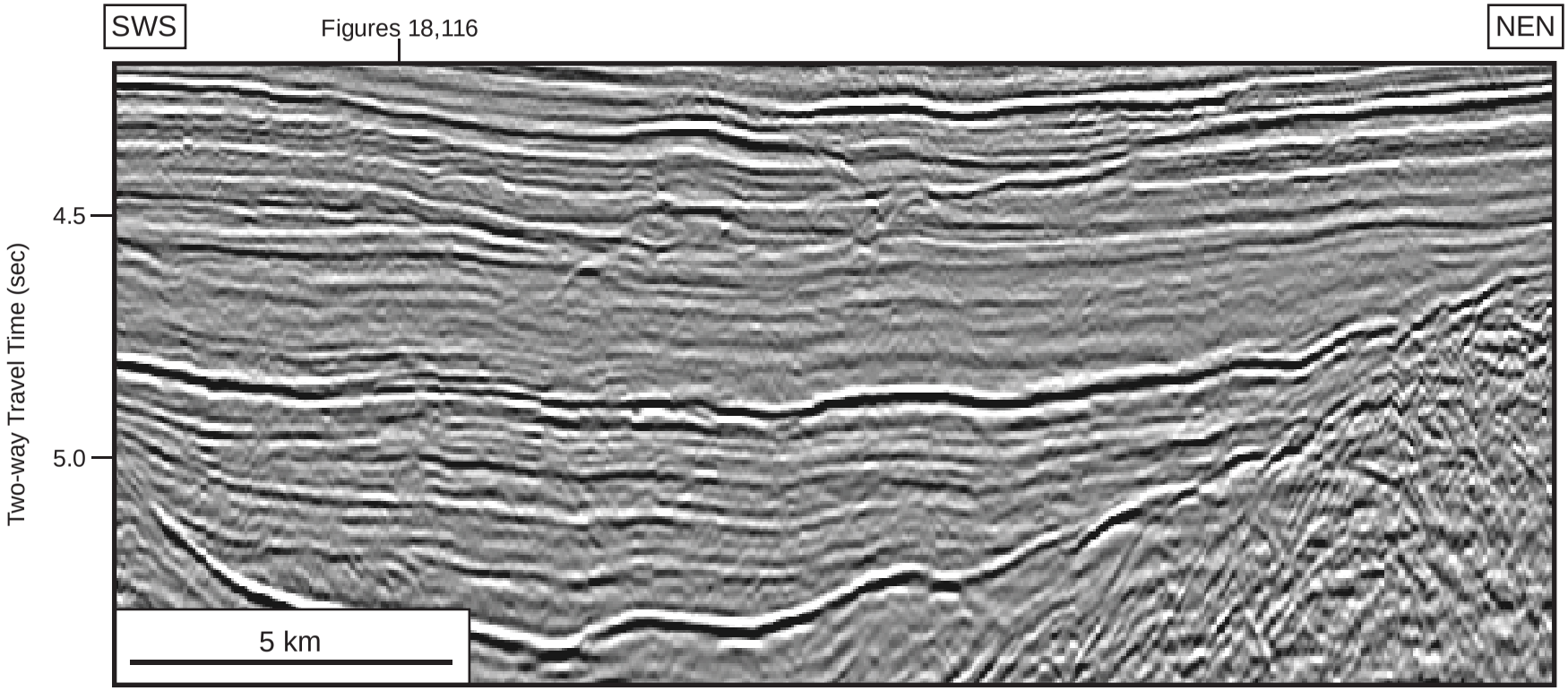

Figure 119a. Uninterpreted regional strike-oriented seismic profile (br-98:br98-080): A closeup view of Figure 118.

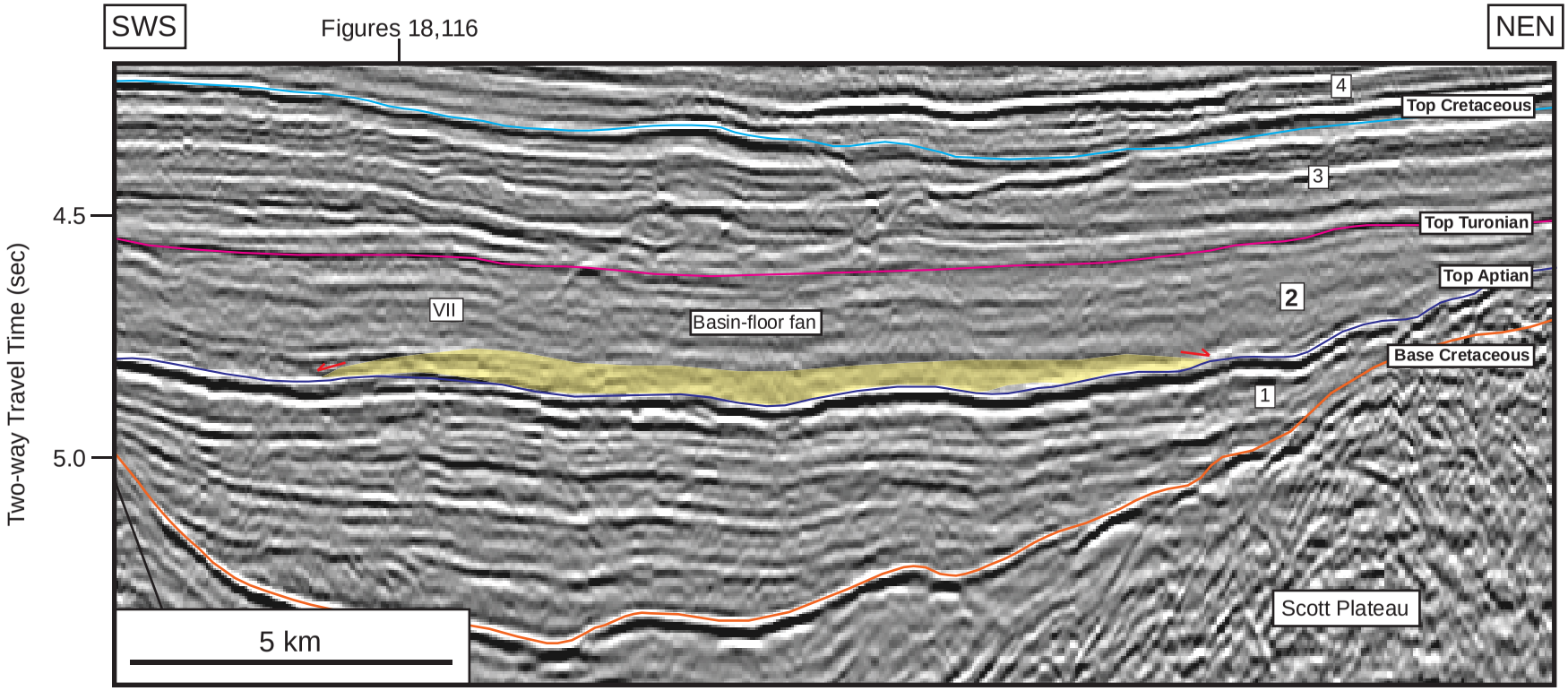

Figure 119b. Regional strike-oriented seismic profile showing all interpreted sequence boundaries from base Cretaceous to middle Miocene: A closeup view of Figure 118. The basin-floor fan is observed within Subsequence VII of Megasequence 2 (yellow shade).

Megasequence 3: top Turonian to top Cretaceous (89.3-65.5 Ma) interval

Megasequence 3 shows a major progradational cycle and aggrading slope system towards northwest. At least two depositional sequences are present (I-II; Figures 16, 18). The top Turonian sequence boundary is easily recognized throughout the study area due to the prominent erosional truncation and its high amplitude (Figure 10). The top Cretaceous sequence boundary horizon illustrates the irregular surface which caused by the erosion. Sediments bypassed and deposited in the lower relief area (Figures 8, 18, 19).

The time structural contour map shows the values vary between 700 to 4432 msec (Figure 120). The deepest area is in the Scott Plateau Graben, whereas the shallowest area is in the Barcoo Platform area. At the eastern margin of the sub-basin, the Barcoo Platform anticline is observed next to the Leveque Shelf (Figures 9, 11, 13). The Barcoo syncline shows its axis in the southwest-northeast.

The isochron map shows the value ranges from 0 to 356 msec two-way travel time (TWTT) (Figure 121). The greatest thickness of this megasequence is in the Scott Plateau Graben. Six seismic facies were recognized in the study. Seismic facies 1 and 4 are the most prominent facies within this sequence. They consist of parallel to subparallel reflections with moderate to high amplitude and fair to good continuity (Figures 122-125). Lombardina-1 and Sheherazade-1 wells were penetrated in facies 1. Well results show fining upward sequence of sand-prone interval (Figures 23, 25). Barcoo-1 well was penetrated in this megasequence. The well log data shows the fining

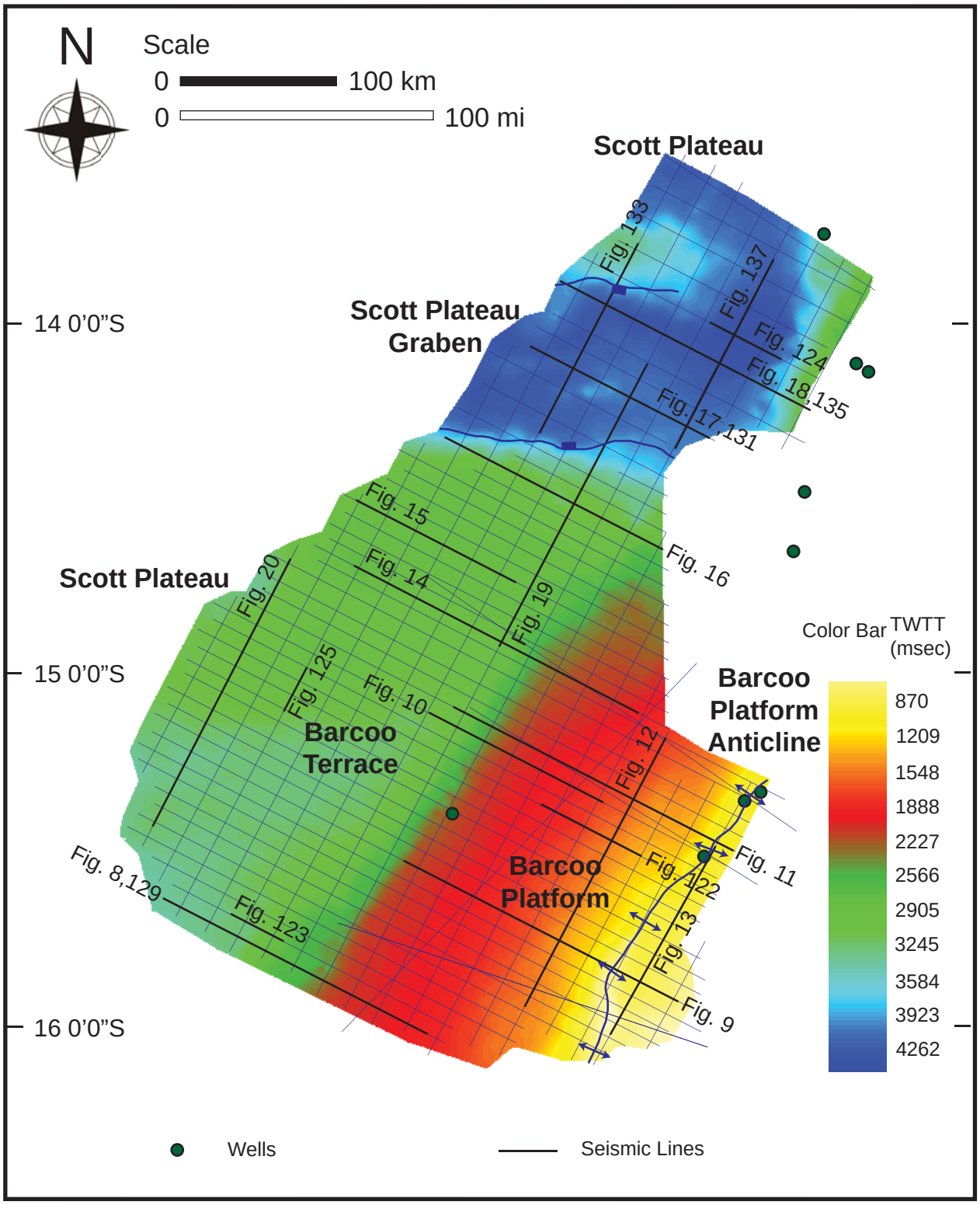

Figure 120. Time structural contour map (in TWTT msecs) of top Cretaceous: 65.5 Ma (Megasequence 3). Distribution of 2D seismic profiles interpreted to generate the maps are shown by white lines, and wells are shown by green dots. Locations of Figures 8-20, 122-125, 129-138 are shown.

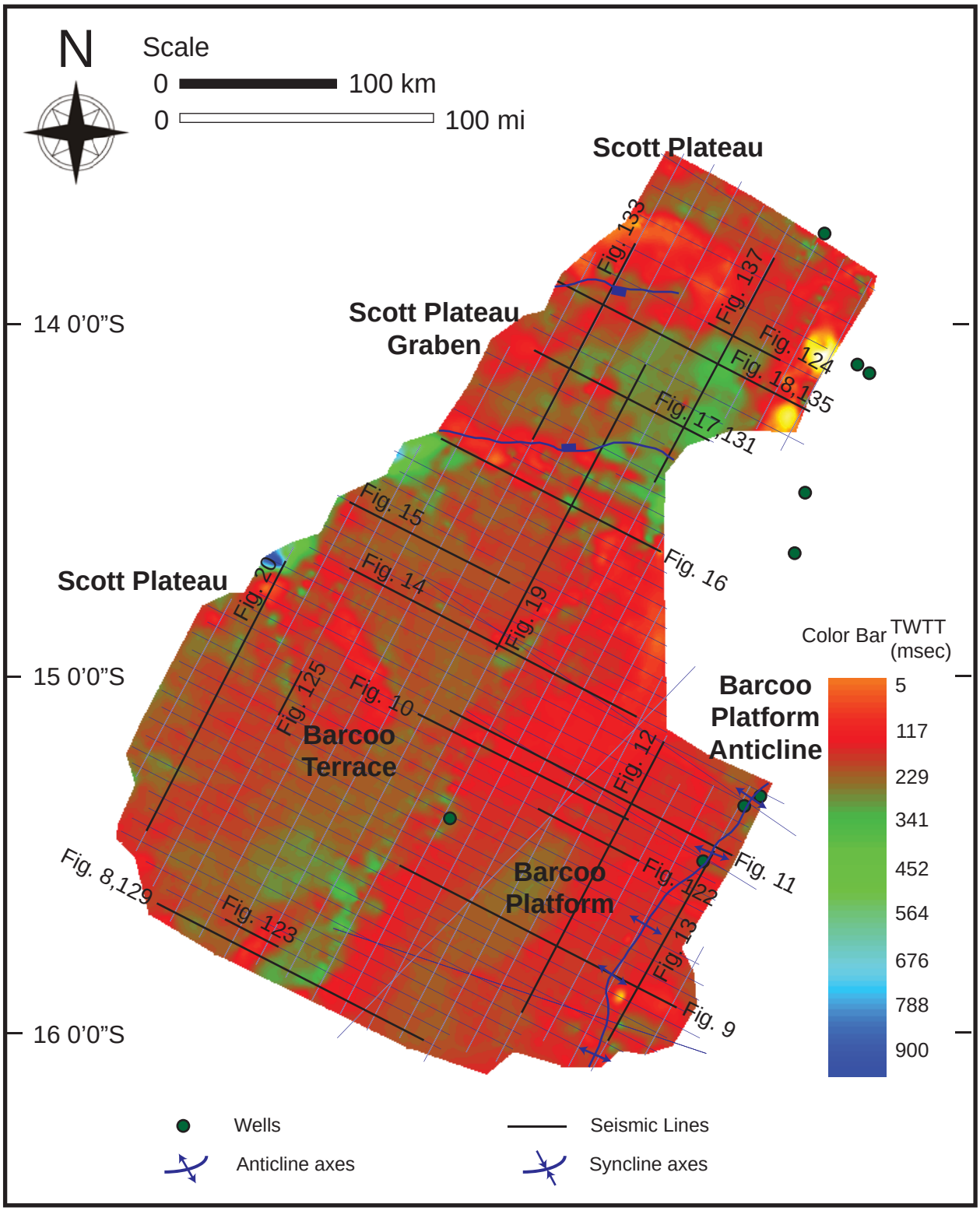

Figure 121. Isochron map (in TWTT msecs) of Megasequence 3 (top Turonian to top Cretaceous: 89.3-65.5 Ma) interval. Distribution of 2D seismic profiles interpreted to generate the maps are shown by white lines, and wells are shown by green dots. Locations of Figures 8-20, 122-125, 129-138 are shown.

onlapping deepwater sand deposit play of megasequence 5 is observed in the northern portion of the study area.

A basin-floor which deposited in the Scott Plateau Graven is considered to be one of the potential prospects. It has been recognized due to its bi-directional downlap truncation to the Top Oligocene horizon. The dip and strike oriented seismic profiles are shown in Figures 162-165.

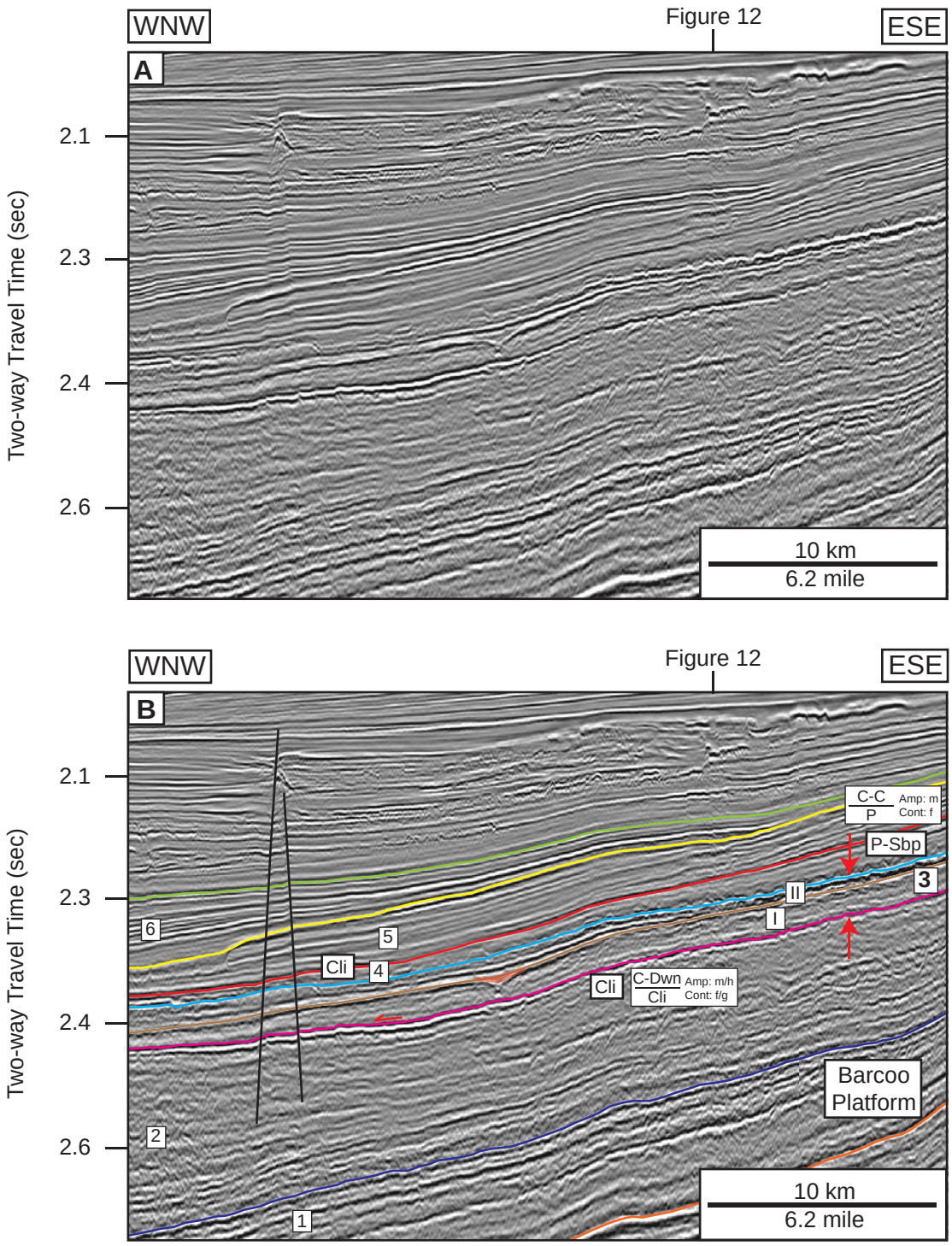

Figure 122. Dip-oriented seismic profile showing seismic facies of Mega-sequence 3 (top Turonian to top Cretaceous: 89.3-65.5 Ma) interval: (a) uninterpreted, (b) interpreted. The submarine canyon is observed (red shade). See Table 2 for codes and abbreviations and Figures 120-121, 126-128, 139-141 for location of the profile and location of where Figure 12 crosses the profile.

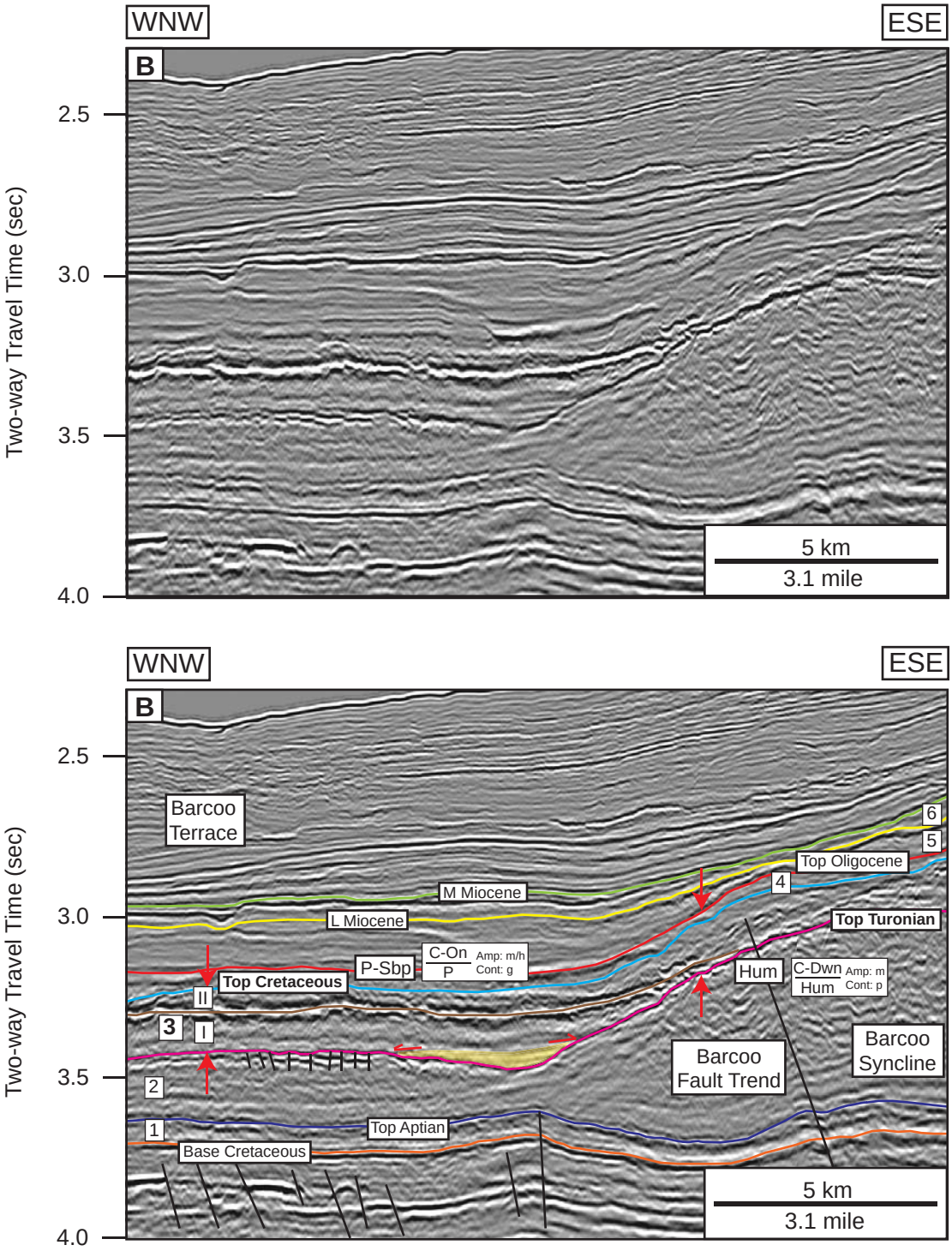

Figure 123. Dip-oriented seismic profile showing seismic facies of Mega-sequence 3 (top Turonian to top Cretaceous: 89.3-65.5 Ma) interval: (a) uninterpreted, (b) interpreted. This megasequence consists at least two depositional sequences. The seidment wedge is observed (yellow shade). See Table 2 for codes and abbreviations and Figures 120-121, 126-128, 139-141 for location of the profile.

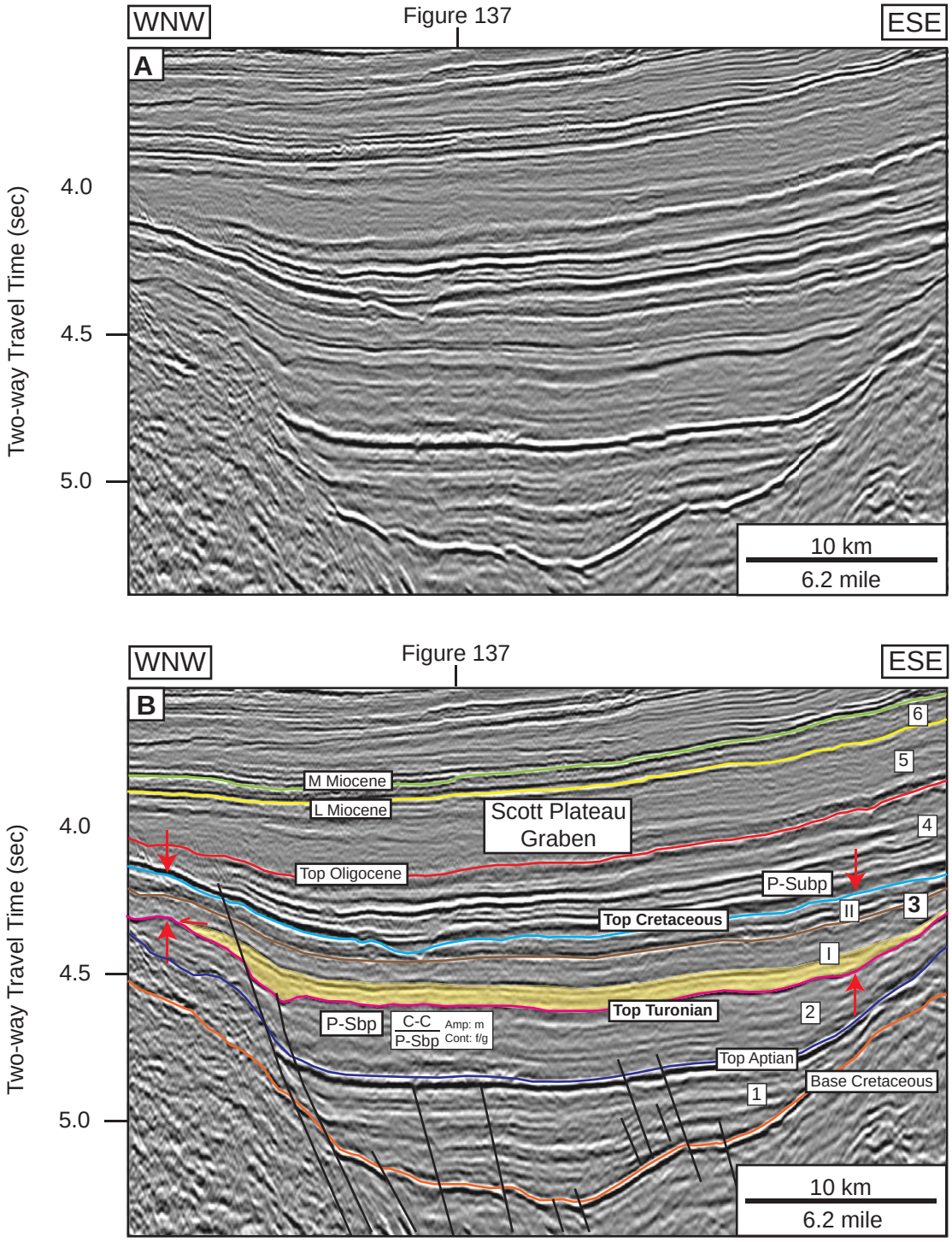

Figure 124. Dip-oriented seismic profile showing seismic facies of Megasequence 3 (top Turonian to top Cretaceous: 89.3-65.5 Ma) interval: (a) uninterpreted, (b) interpreted. The potential play concept is observed in the Scott Plateau Graben (yellow shade). See Table 2 for codes and abbreviations and Figures 120-121, 126-128, 139-141 for location of the profile and location of where Figure 137 crosses the profile.

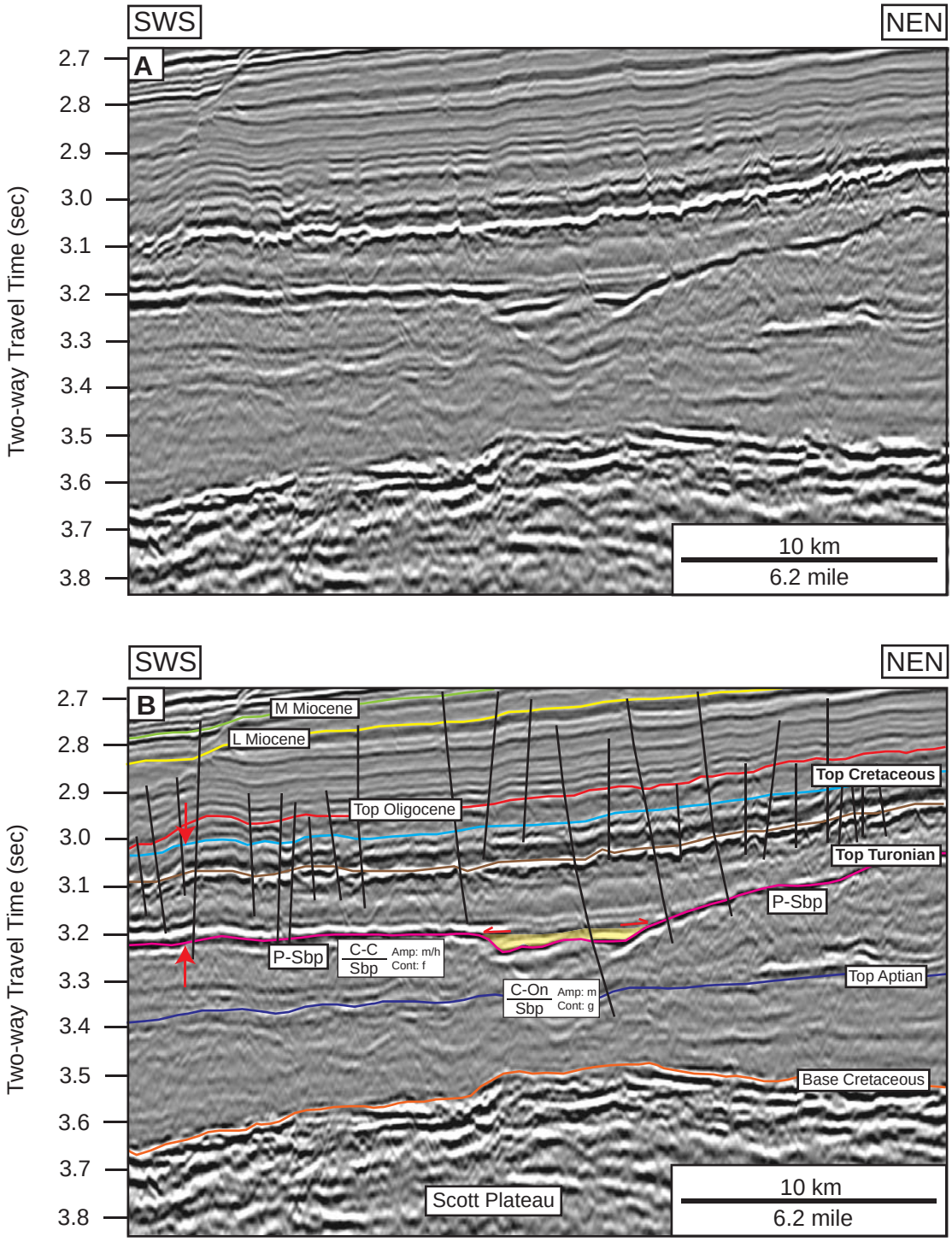

Figure 125. Strike-oriented seismic profile showing seismic facies of Mega-sequence 3 (top Turonian to top Cretaceous: 89.3-65.5 Ma) interval: (a) uninterpreted, (b) interpreted. The submarine canyon is oberved (red shade). See Table 2 for codes and abbreviations and Figures 120-121, 126-128, 139-141 for location of the profile.

upward sequence of sand-prone interval (Figure 22). No wells penetrate in either seismic facies 5 and 6.

Subsequence I of Megasequence 3

The isochron map of this subsequence illustrates the thickness values varying from 0 to 1074 msec two-way travel time (TWTT) (Figure 126). The thickness of this interval is generally constant covering all of the study area.

Six seismic facies are identified (Figure 127; Table 13). Facies 1 and 4 illustrates the parallel to subparallel internal reflection configuration with moderate to high amplitude and fair to good continuity. The reflection is concordant to the upper sequence boundary whereas terminates onlap on to the lower sequence boundary. Seismic facies 2 shows moderate to high amplitude and fair to good continuity which is the prograding clinoform sediments. The reflection is concordant to the upper boundary and downlap to the lower sequence boundary.

Table 13. Seismic facies and geologic interpretation of Subsequence I of Megasequence 3

Seismic Facies	Upper Sequence Boundary	Lower Sequence Boundary	Internal Reflection Configuration	Amplitude	Continuity	Geologic Interpretation
1	Concordant	Concordant /Onlap	Parallel to Subparallel	moderate to high	fair to good	Shelf deposits
2	Concordant	Downlap	Clinoform	moderate to high	fair to good	Prograding clinoform
3	Concordant	Concordant /Downlap	Hummocky	moderate	poor	Inversion – related structure
4	Concordant	Concordant /Onlap	Parallel to Subparallel	moderate to high	fair to good	Basinal deposits
5	Concordant	Concordant	Chaotic	low	poor	Poor quality data
6	-	-	Chaotic	moderate	poor	Carbonate buildup

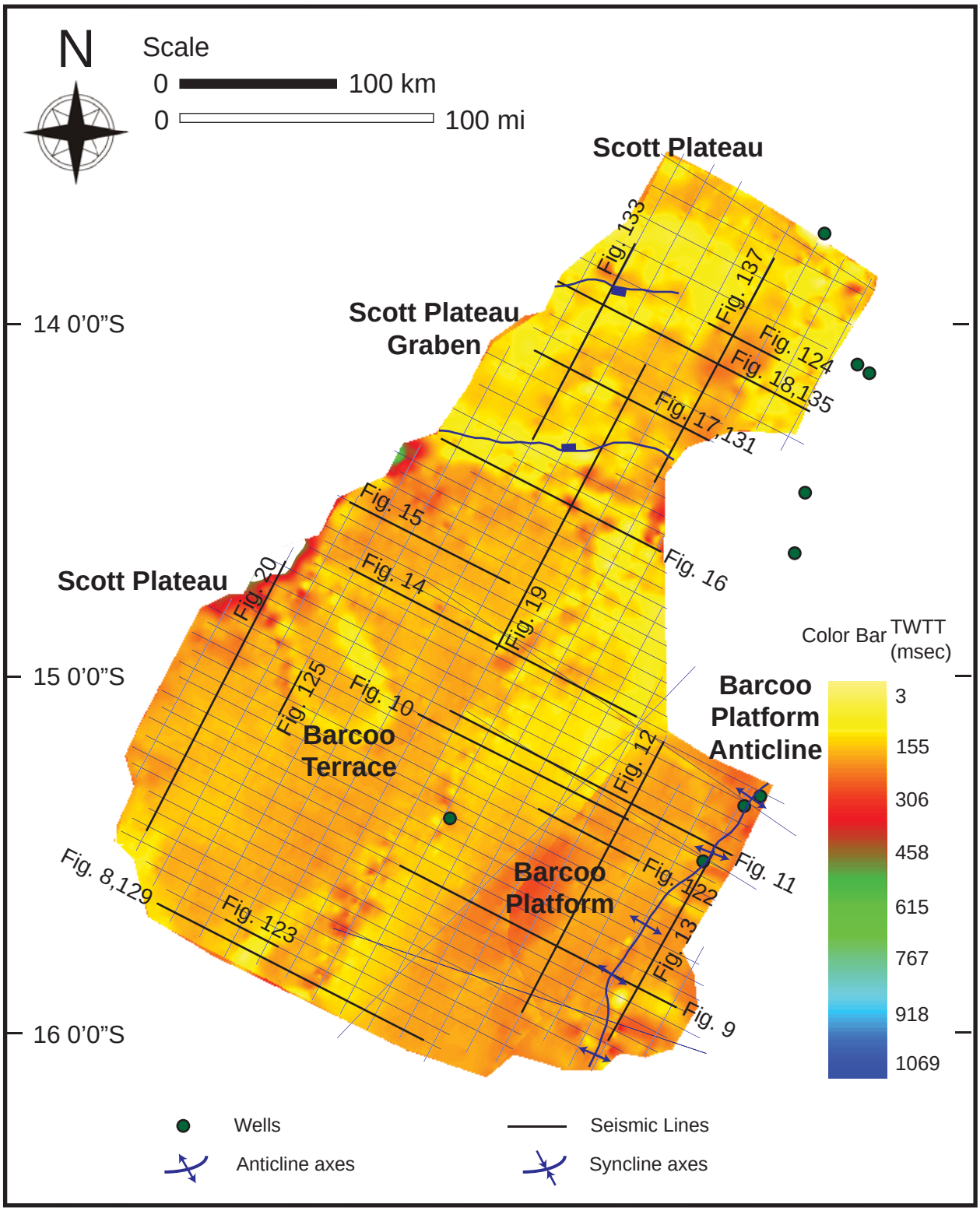

Figure 126. Isochron map (in TWTT msecs) of Subsequence I of Megasequence 3 interval. Distribution of 2D seismic profiles interpreted to generate the maps are shown by white lines, and wells are shown by green dots. Locations of Figures 8-20, 122-125, 129-138 are shown.

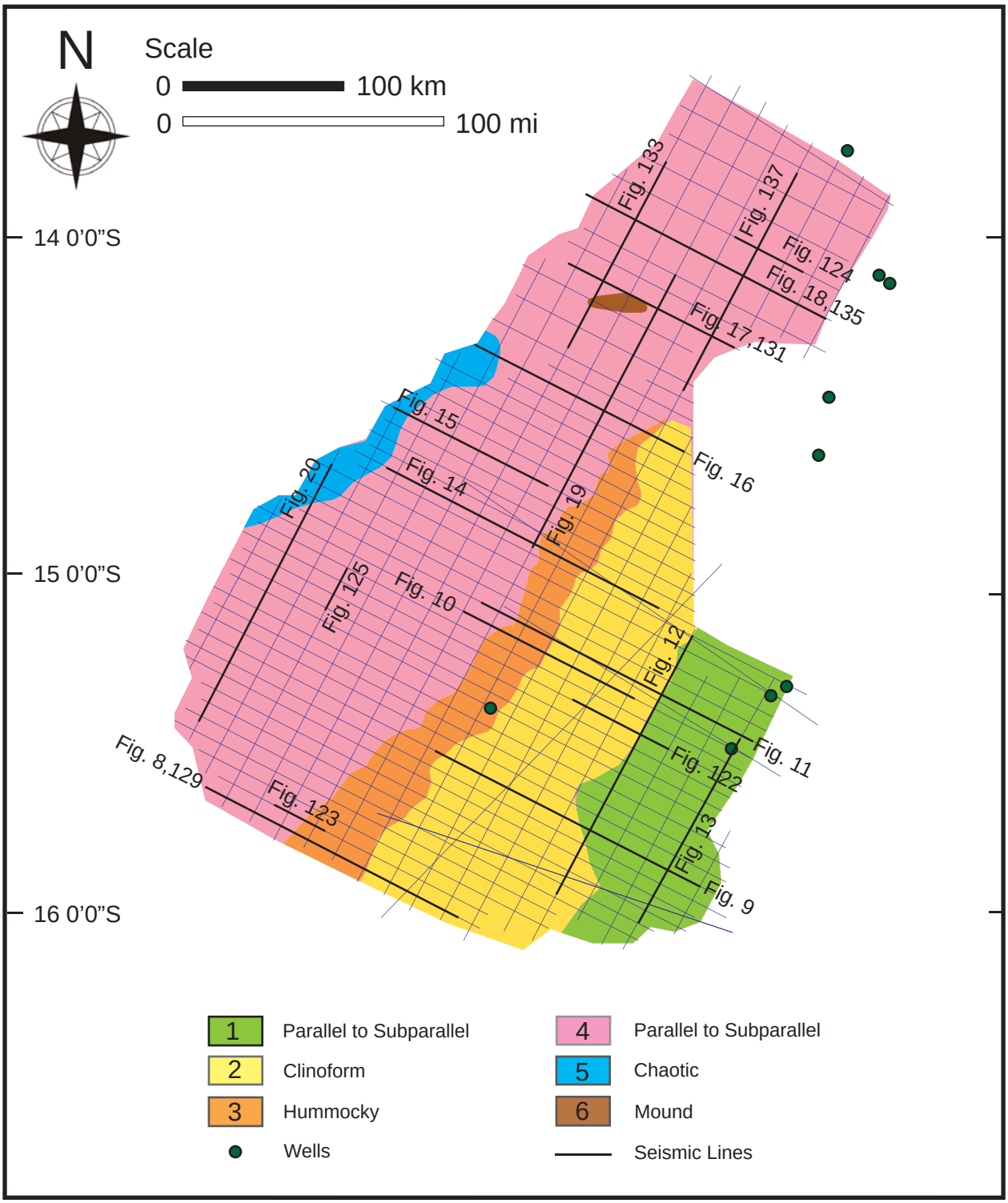

Figure 127. Seismic facies map of Subsequence I of Megasequence 3 interval. Each facies is numbered as described in the text. See Table 2 for seismic facies coding and Table 5 for a summary of seismic facies analysis and geologic interpretation. Locations of Figures 8-20, 122-125, 129-138 (black lines) are shown, and wells are shown by green dots.

Another facies is hummocky facies. It illustrates moderate amplitude with poor continuity. This facies is interpreted to be the inversion related structure. Facies 5 and 6 shows the chaotic internal reflection configuration which could be by the real structure or the poor data quality. Facies 5 has a low amplitude and poor continuity whereas Facies 6 has moderate amplitude with poor continuity. This facies has a mounded morphology. It is located in the northern portion of the study area (Figure 17).

The geologic facies map is shown in Figure 128. The parallel to subparallel of shelf and basinal deposits cover most of the study area. The sediments were transported from the shelf environment to the basin center in the southeast to northwest direction. The fluid escape structure is recognized in this megasequence (Figure 15). The basin-floor fan, which deposited onlap onto the top Turonian horizon in the Scott Plateau Graben, is recognized (Figure 123). At the northern part of the study area, the carbonate buildup structure caused the accommodation for the sediments to be deposited (Figure 17). The structurally confined sediment is recognized due to the significant onlap onto the lower surface boundary (top Turonian horizon; Figure 124). Several erosional features of the submarine canyons are observed due to their bidirectional onlap reflection terminations on to the top Turonian unconformity (Figures 16, 122, 125).

Four potential prospects are recognized. To the south, there are two basin-floor fans deposited on the Barcoo Platform (Figures 129-130). They have been identified due to their bi-directional downlap terminations. A sediment wedge is found deposited adjacent to the carbonate build-up structure in the Scott Plateau Graben. The last one is

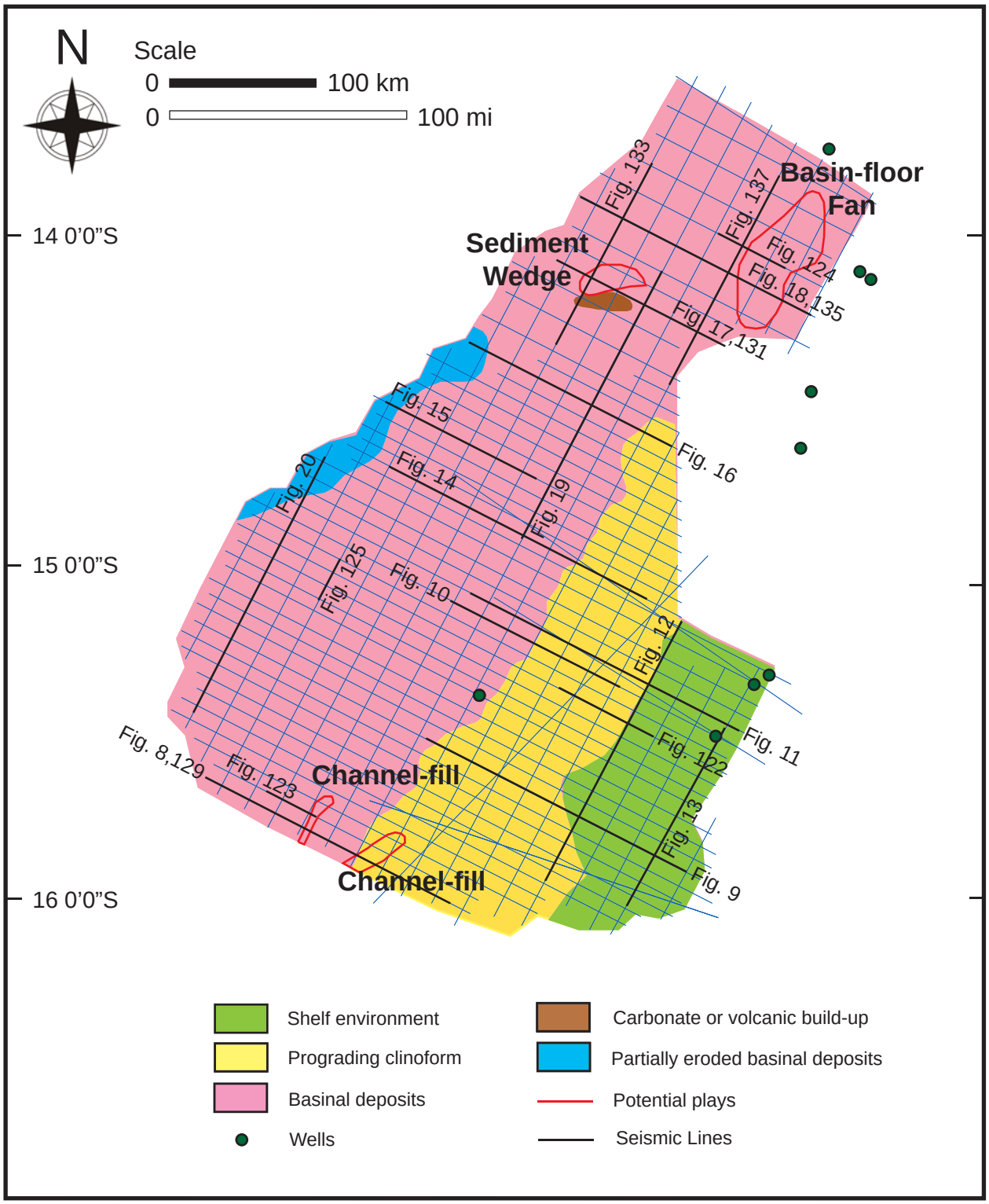

Figure 128. Geologic facies map of of Subsequence I of Megasequence 3 (top Turonian to top Cretaceous: 89.3-65.5 Ma) interval. See Table 5 for a summary of seismic facies analysis and geologic interpretation. Locations of Figures 8-20, 122-125, 129-138 (black lines) are shown, and wells are shown by green dots.

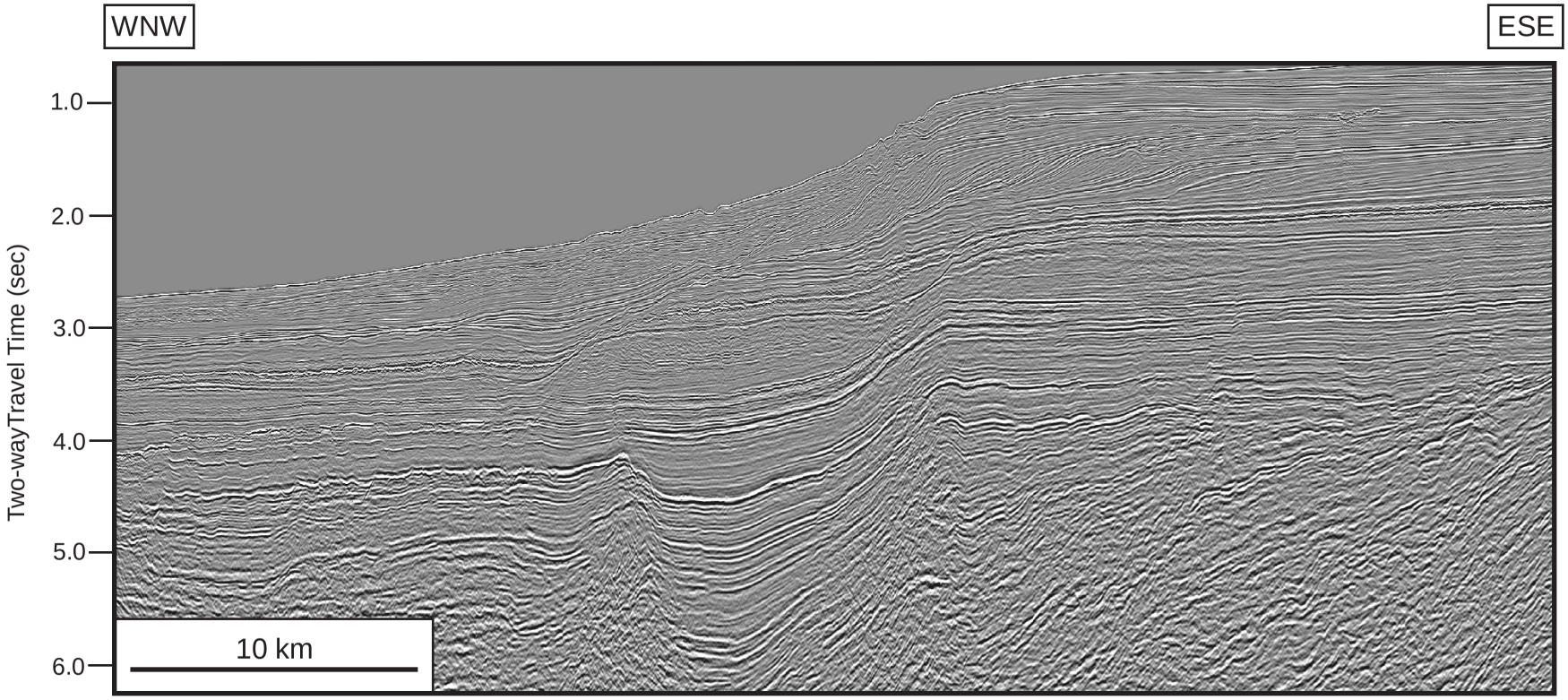

Figure 129a. Uninterpreted regional dip-oriented seismic profile (br-98:br98-001). Location of the profile is shown in Figures 120-120, 126-128, 139-141.

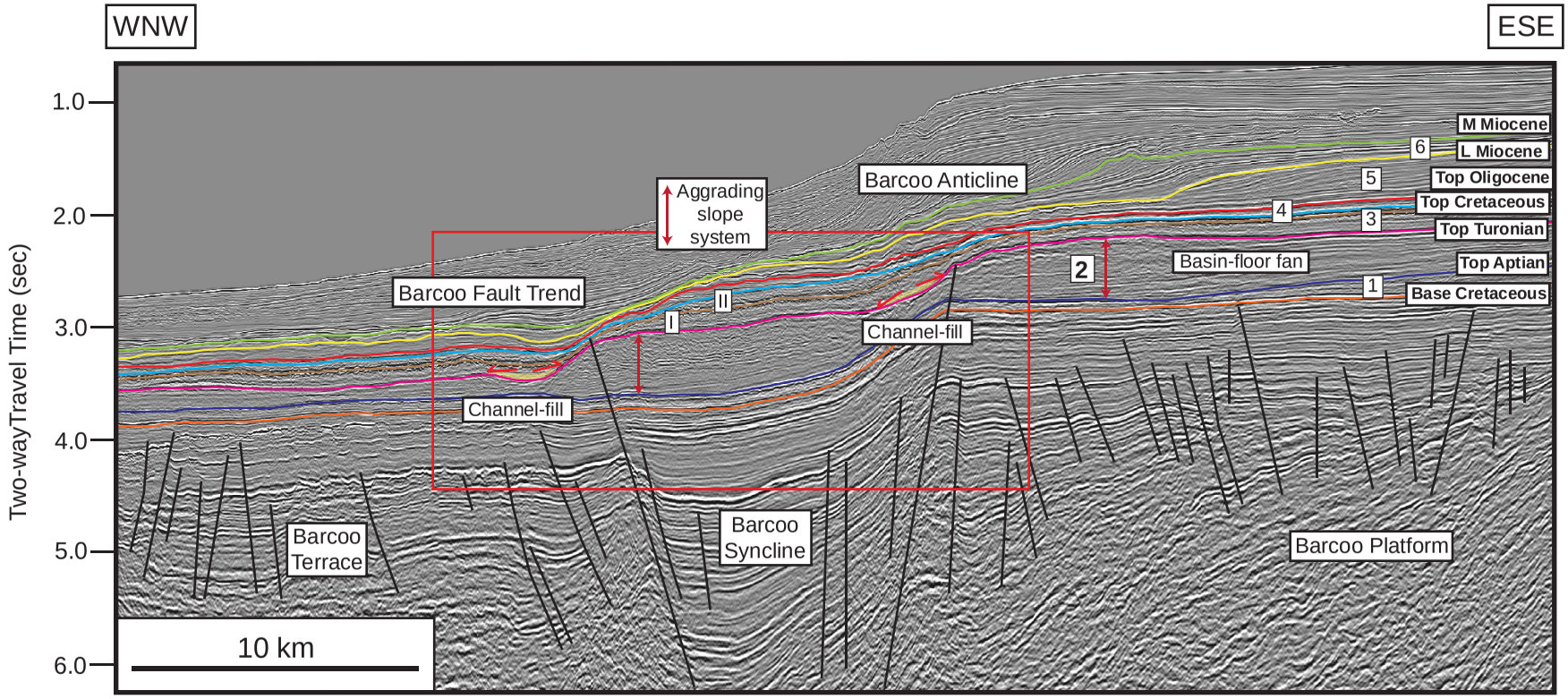

Figure 129b. Regional dip-oriented seismic profile showing all interpreted sequence boundaries from base Cretaceous to middle Miocene. The major graben structure of the Barcoo Syncline was overlain by the Upper Jurassic and younger strata. The channel-fill features are observed within Subsequence I of Megasequences 3 (yellow shades). Location of the profile is shown in Figures 120-120, 126-128, 139-141.

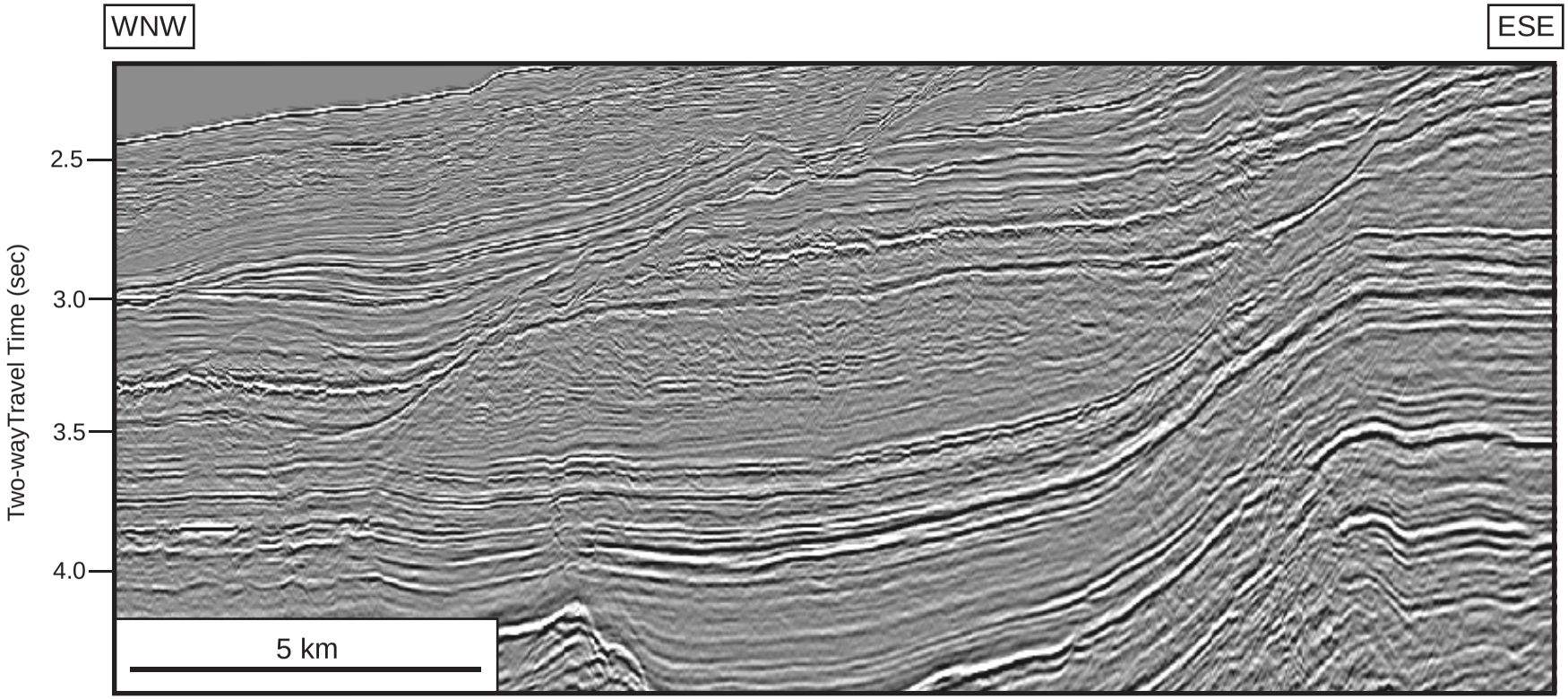

Figure 130a. Uninterpreted regional dip-oriented seismic profile (br-98:br98-001): A closeup view of Figure 129.

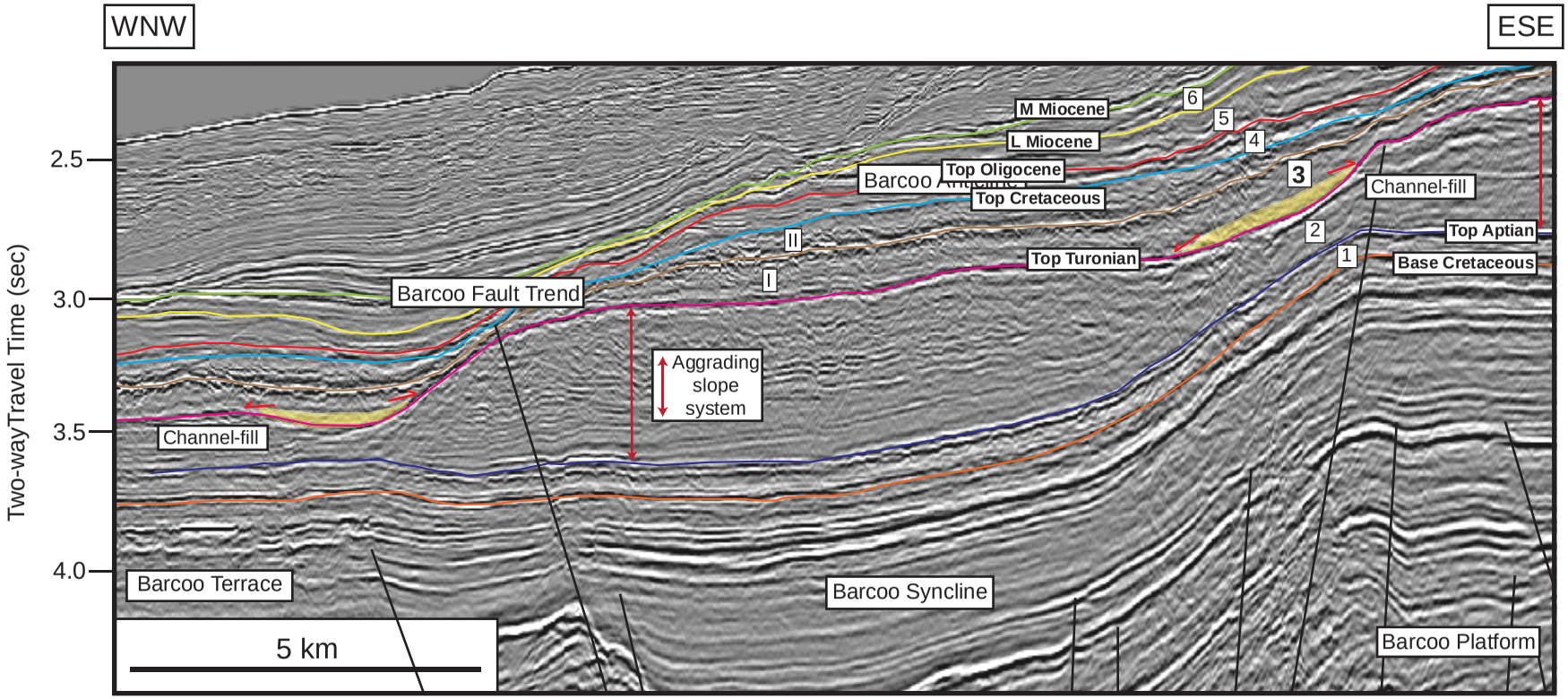

Figure 130b. Regional dip-oriented seismic profile showing all interpreted sequence boundaries from base Cretaceous to middle Miocene: A closeup view of Figure 129. The channel-fill features are observed within Subsequence I of Megasequences 3 (yellow shades).

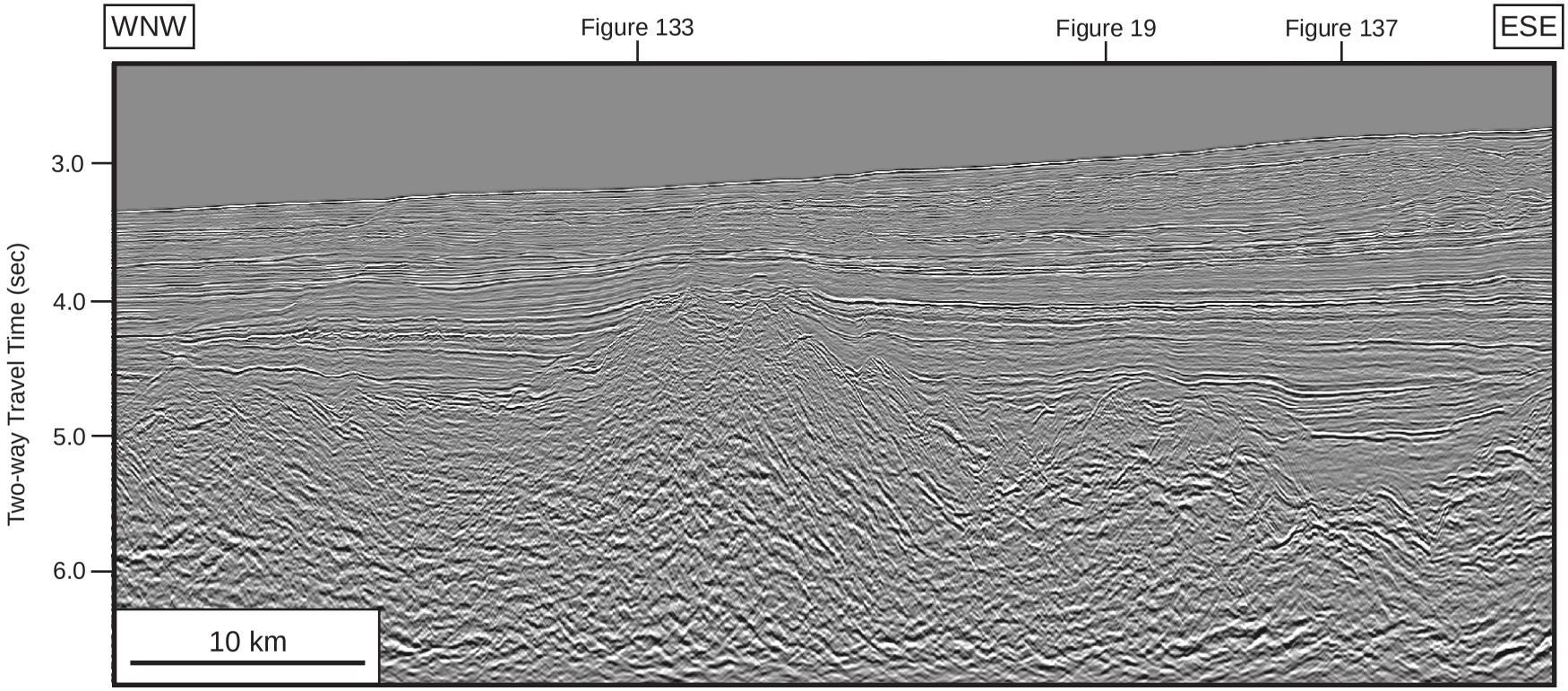

Figure 131a. Uninterpreted regional dip-oriented seismic profile (br-98:br98-048). Location of the profile is shown in Figures 120-121, 126-128, 139-141 and locations of where Figures 19, 133, 137 cross the profile.

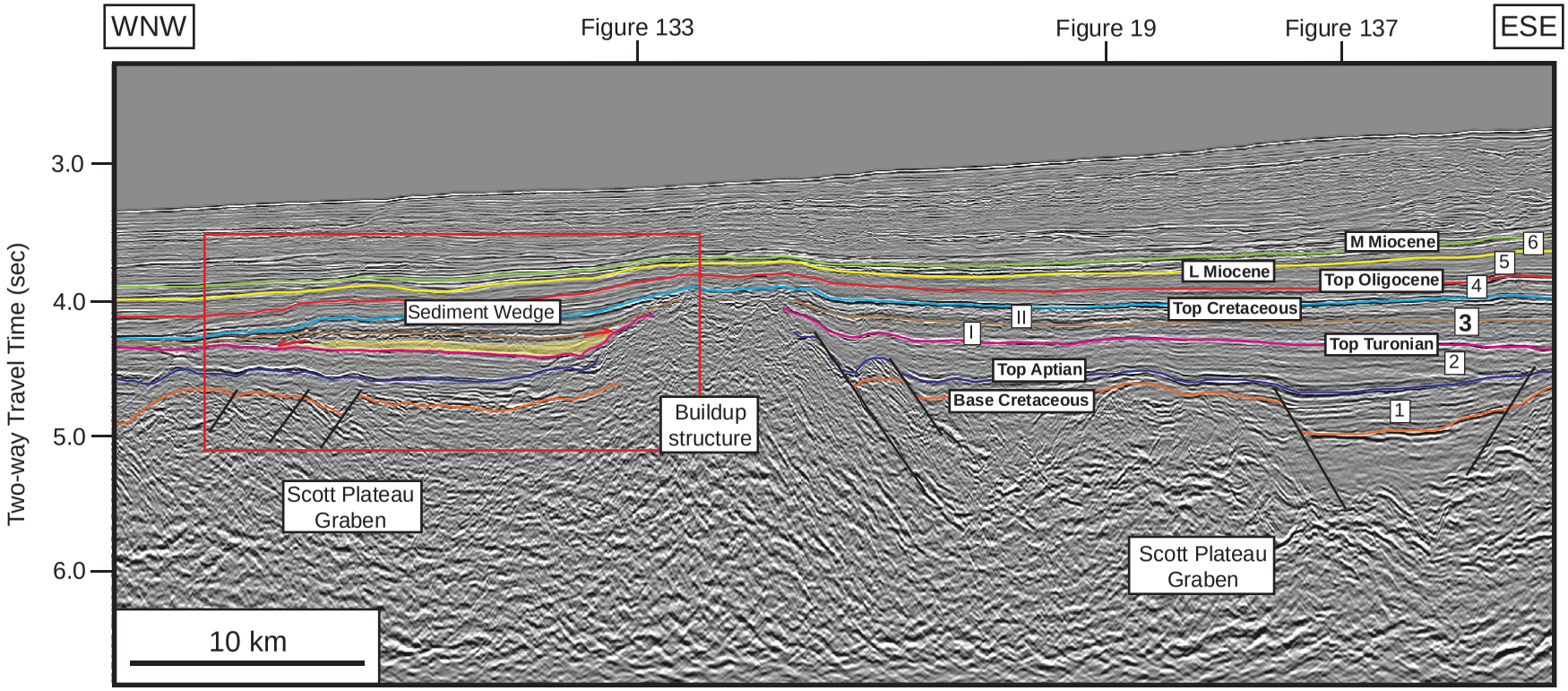

Figure 131b. Regional dip-oriented seismic profile showing all interpreted sequence boundaries from base Cretaceous to middle Miocene. The carbonate buildup which is located in the Scott Plateau Graben is observed. It created the accommodation for sediment to deposit as shown with in Subsequence I of Megasequence 3 (yellow shade). The block faulting in the underlying Jurassic strata caused the irregular topography. Location of the profile is shown in Figures 120-121, 126-128, 139-141 and locations of where Figures 19, 133, 137 cross the profile.

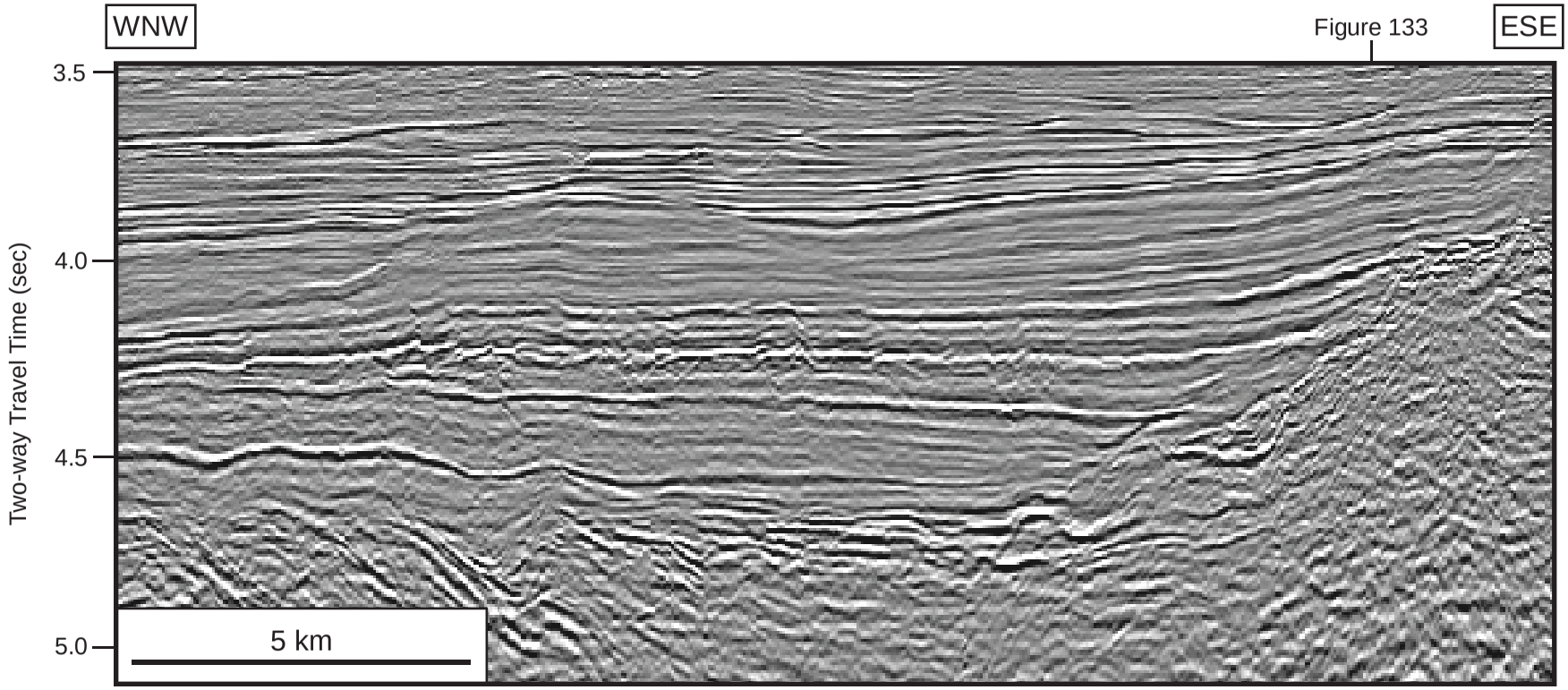

Figure 132a. Uninterpreted regional dip-oriented seismic profile (br-98:br98-048): A closeup view of Figure 131.

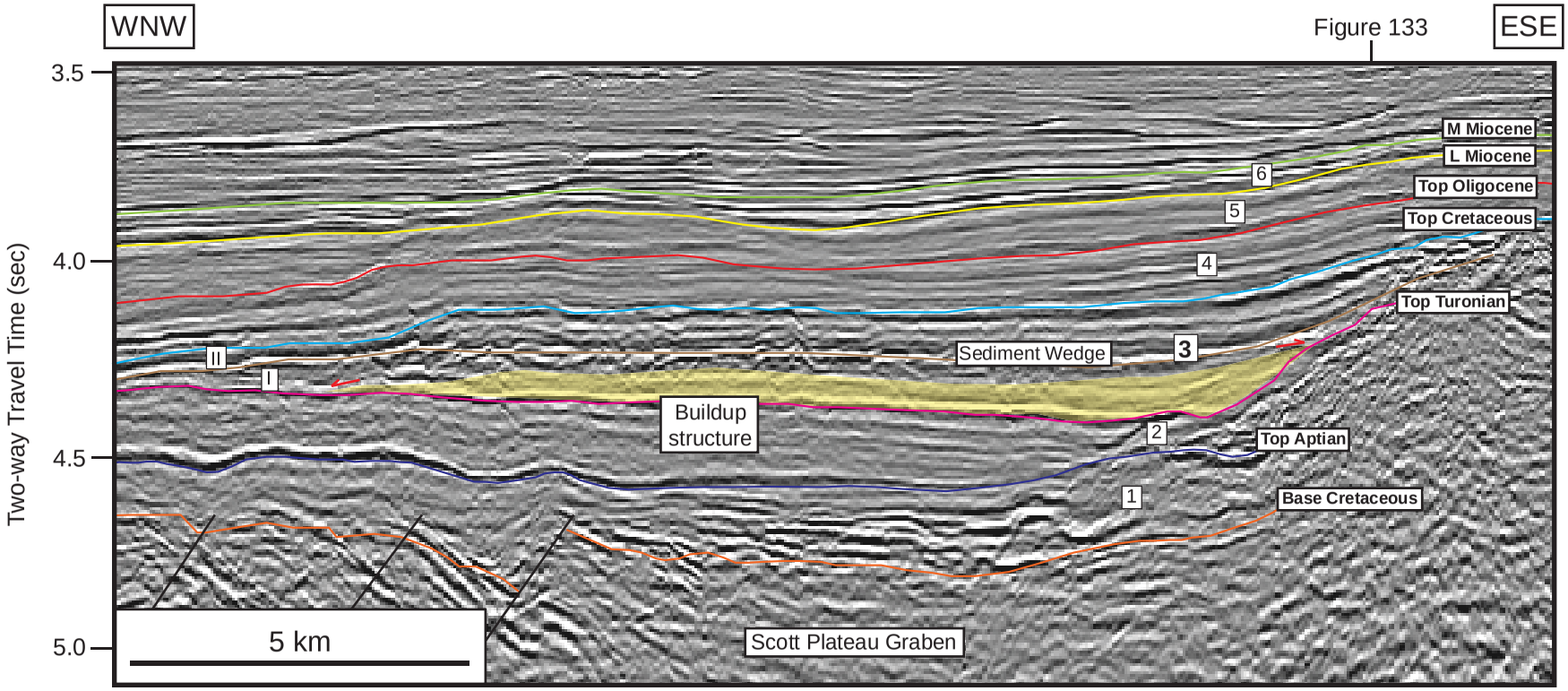

Figure 132b. Regional dip-oriented seismic profile showing all interpreted sequence boundaries from base Cretaceous to middle Miocene: A closeup view of Figure 131. The carbonate buildup which is located in the Scott Plateau Graben is observed. It created the accommodation for sediment to deposit as shown with in Subsequence I of Megasequence 3 (yellow shade).

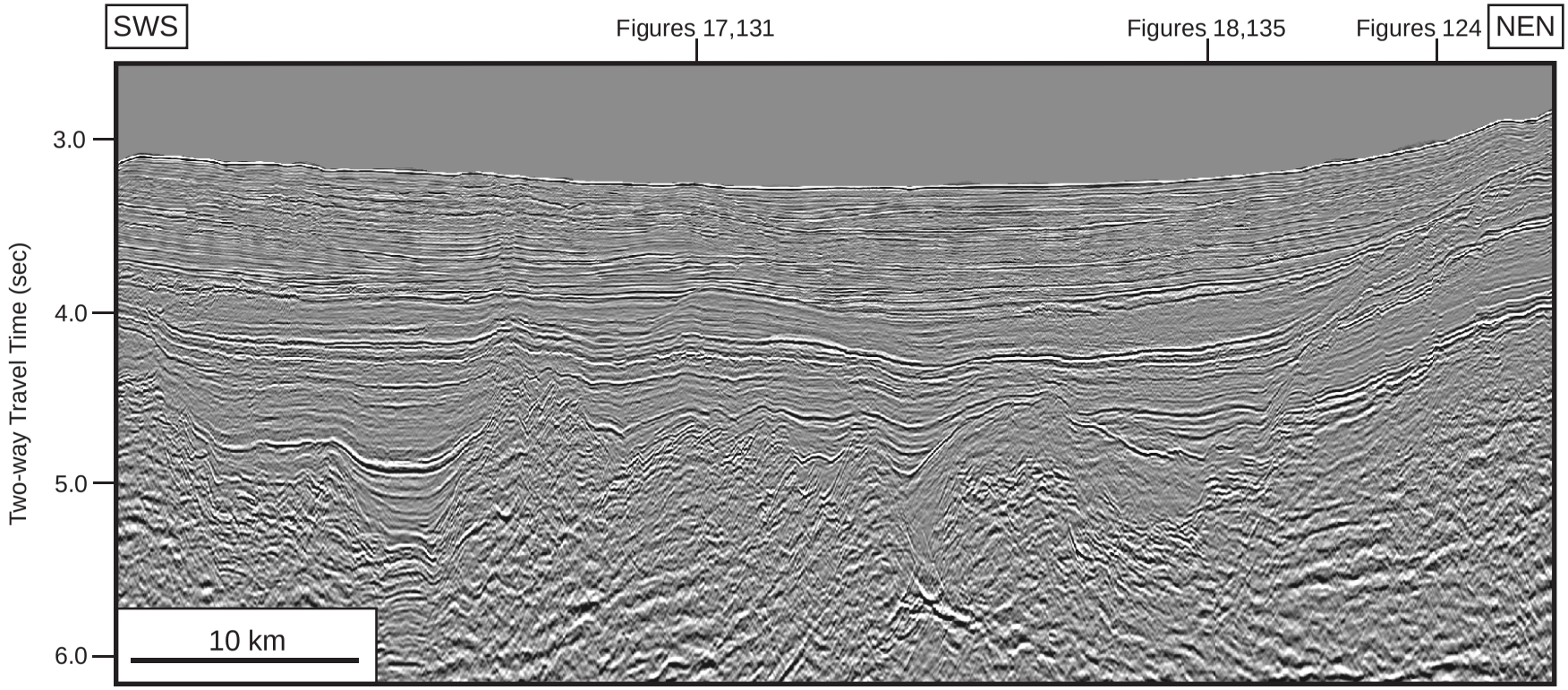

Figure 133a. Uninterpreted regional strike-oriented seismic profile (br-98:br98-084). Location of the profile is shown in Figures 120-121, 126-128, 139-141 and locations of where Figures 17, 18, 124, 131, 135 cross the profile.

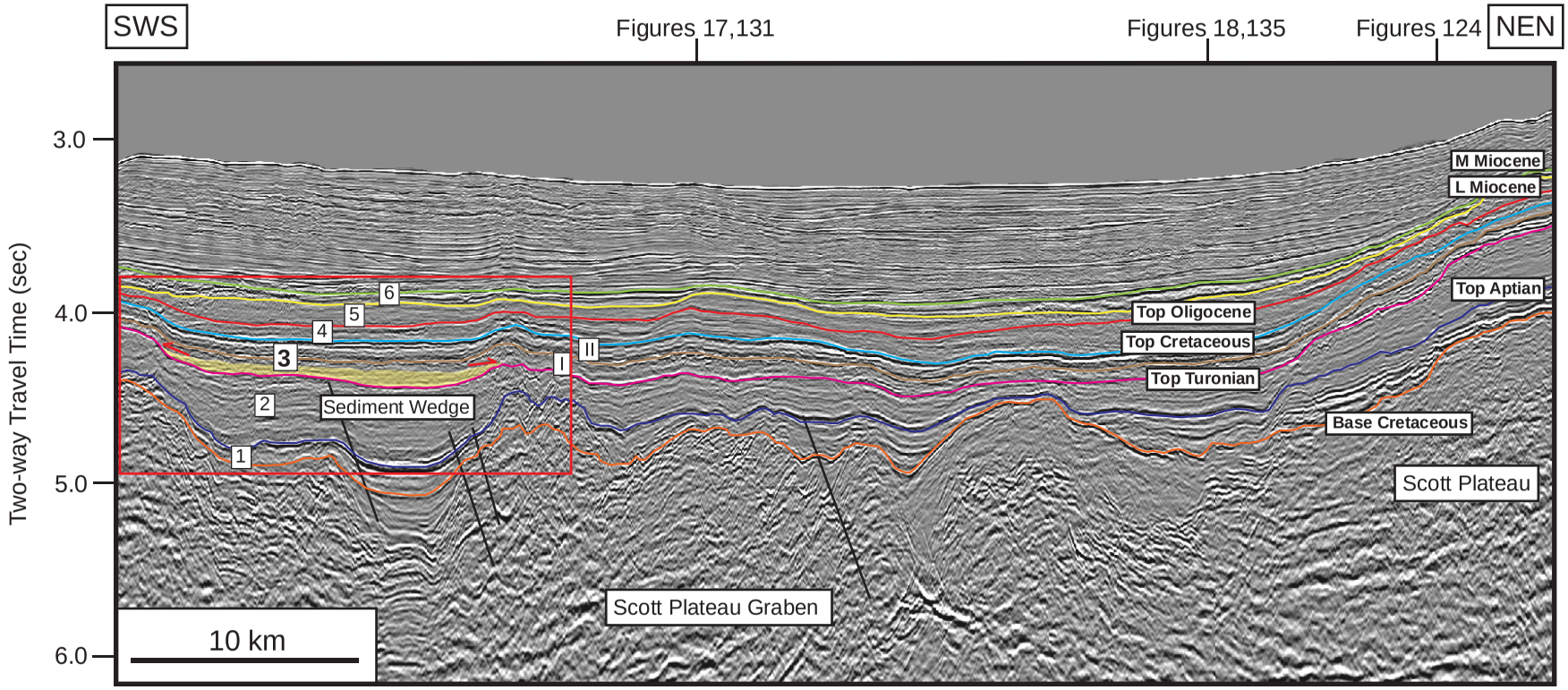

Figure 133b. Regional strike-oriented seismic profile showing all interpreted sequence boundaries from base Cretaceous to middle Miocene. This profile shows the deeper area of the Scott Plateau Graben and the shallower area of the Scott Plateau. The deepwater deposit is observed within Subsequence I of Megasequence 3 (yellow shade). Location of the profile is shown in Figures 120-121, 126-128, 139-141 and locations of where Figures 17, 18, 124, 131, 135 cross the profile.

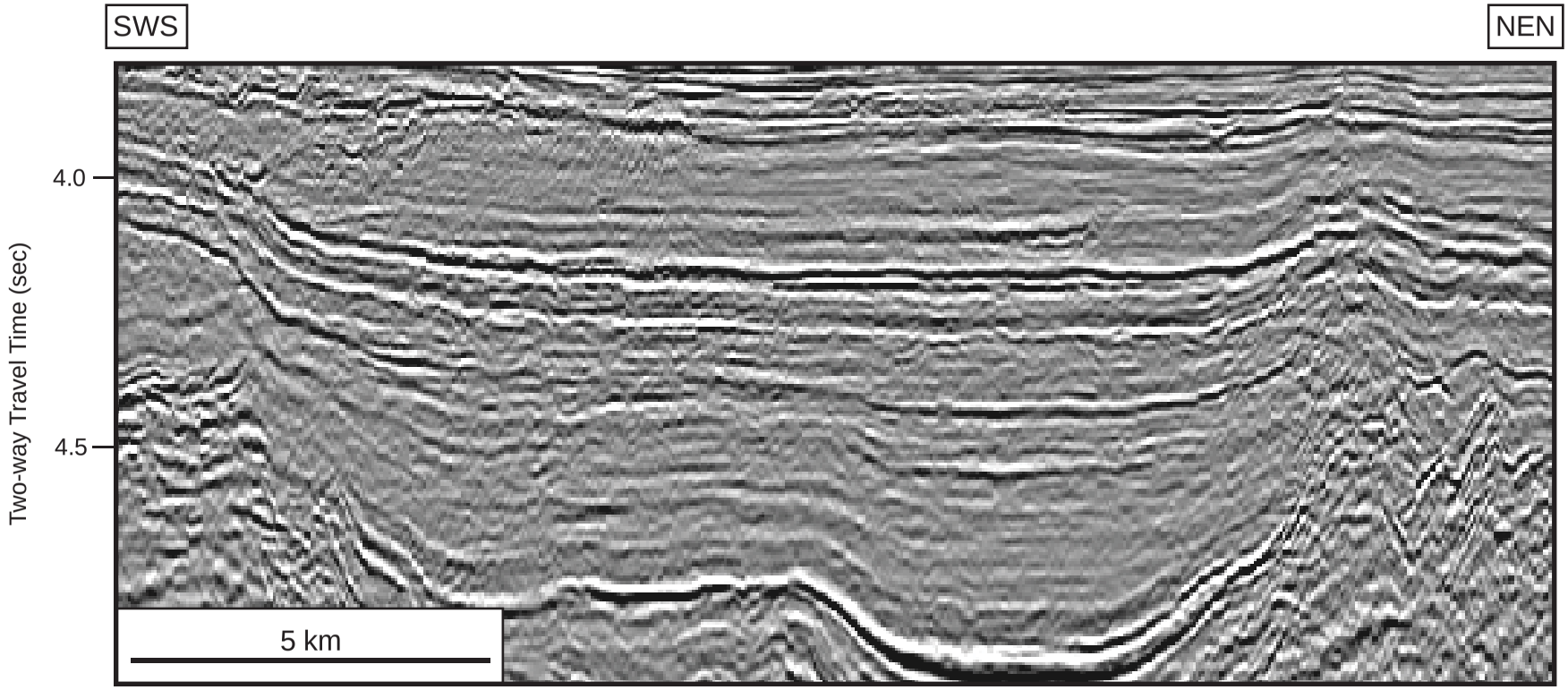

Figure 134a. Uninterpreted regional strike-oriented seismic profile (br-98:br98-084): A closeup view of Figure 133.

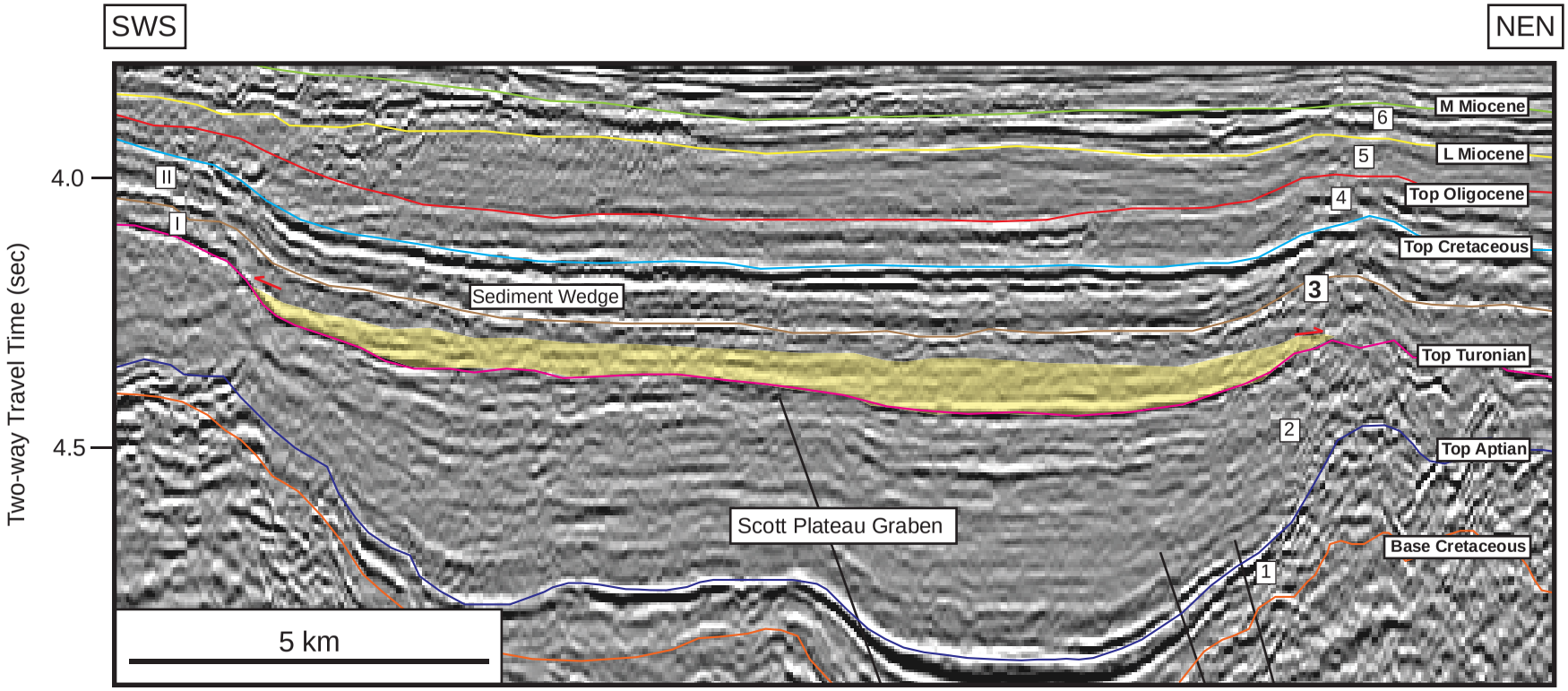

Figure 134b. Regional strike-oriented seismic profile showing all interpreted sequence boundaries from base Cretaceous to middle Miocene: A closeup view of Figure 133. The deepwater deposit is observed within Subsequence I of Megasequence 3 (yellow shade).

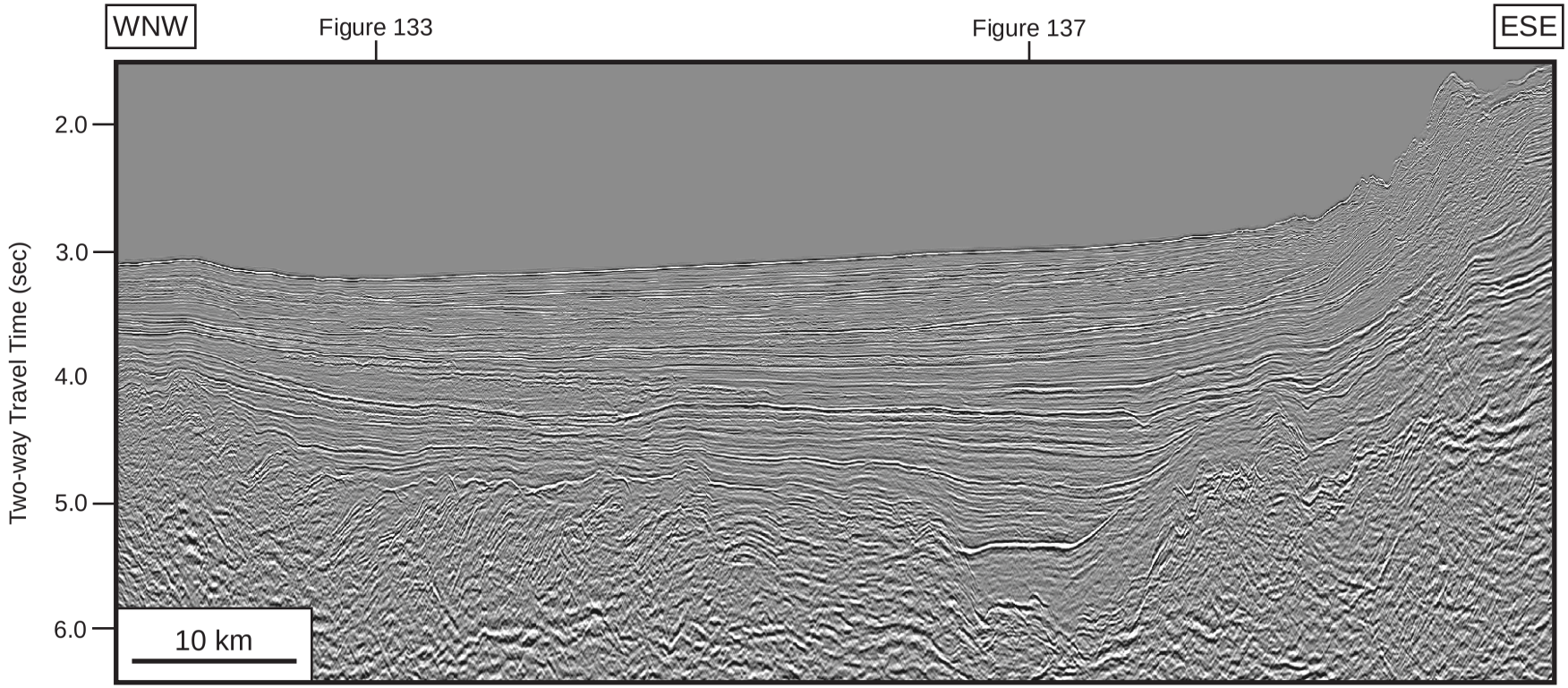

Figure 135a. Uninterpreted regional dip-oriented seismic profile (br-98:br98-057). Location of the profile is shown in Figures 120-121, 126-128, 139-141 and locations of where Figures 133 and 137 cross the profile.

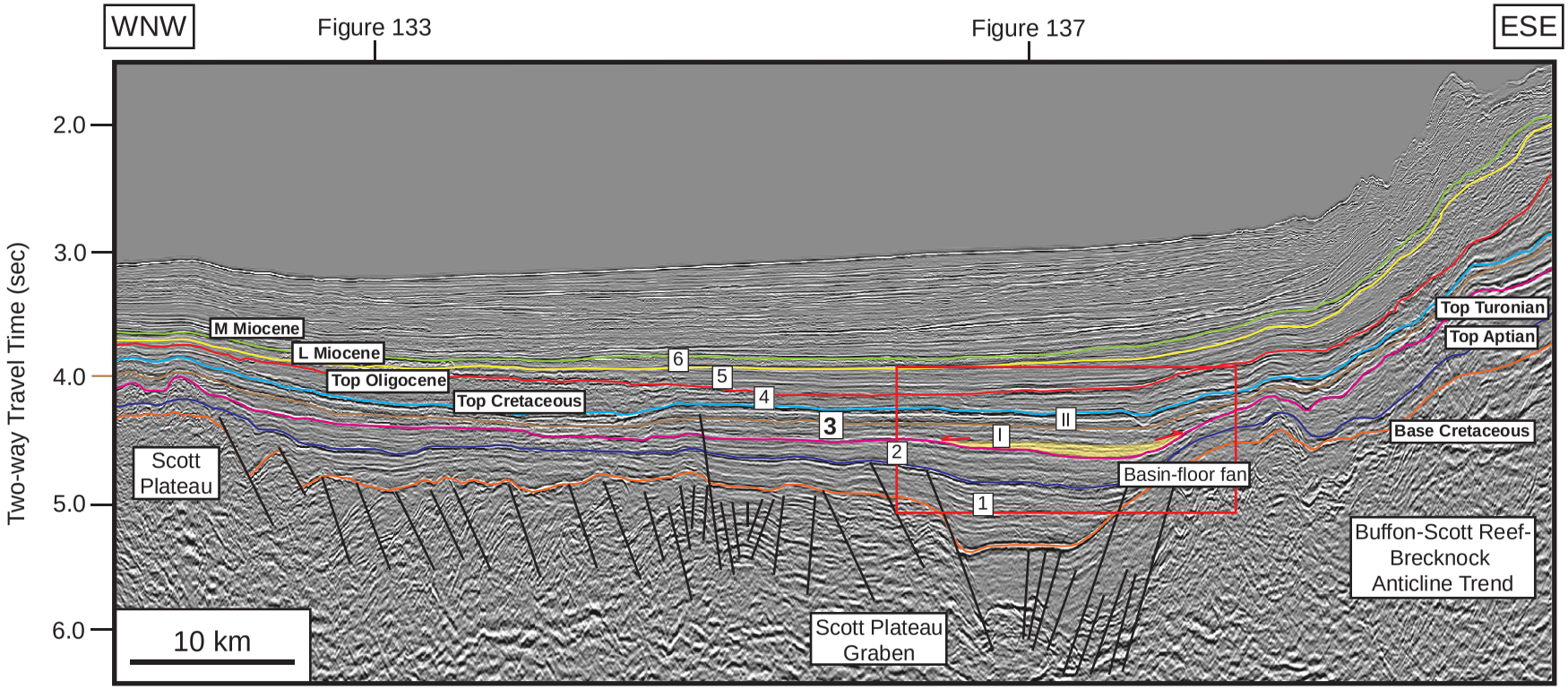

Figure 135b. Regional dip-oriented seismic profile showing all interpreted sequence boundaries from base Cretaceous to middle Miocene. This profile shows the deeper area of the Scott Plateau Graben and shallower/high area of the Buffon-Scott Reef-Brecknock Anticline Trend in the northern part of the study area. Series of faults in the underlying Jurassic strata caused the irregular topography. The basin-floor fan is observed within Subsequence I of Megasequences 3 (yellow shade). Location of the profile is shown in Figures 120-121, 126-128, 139-141 and locations of where Figures 133 and 137 cross the profile.

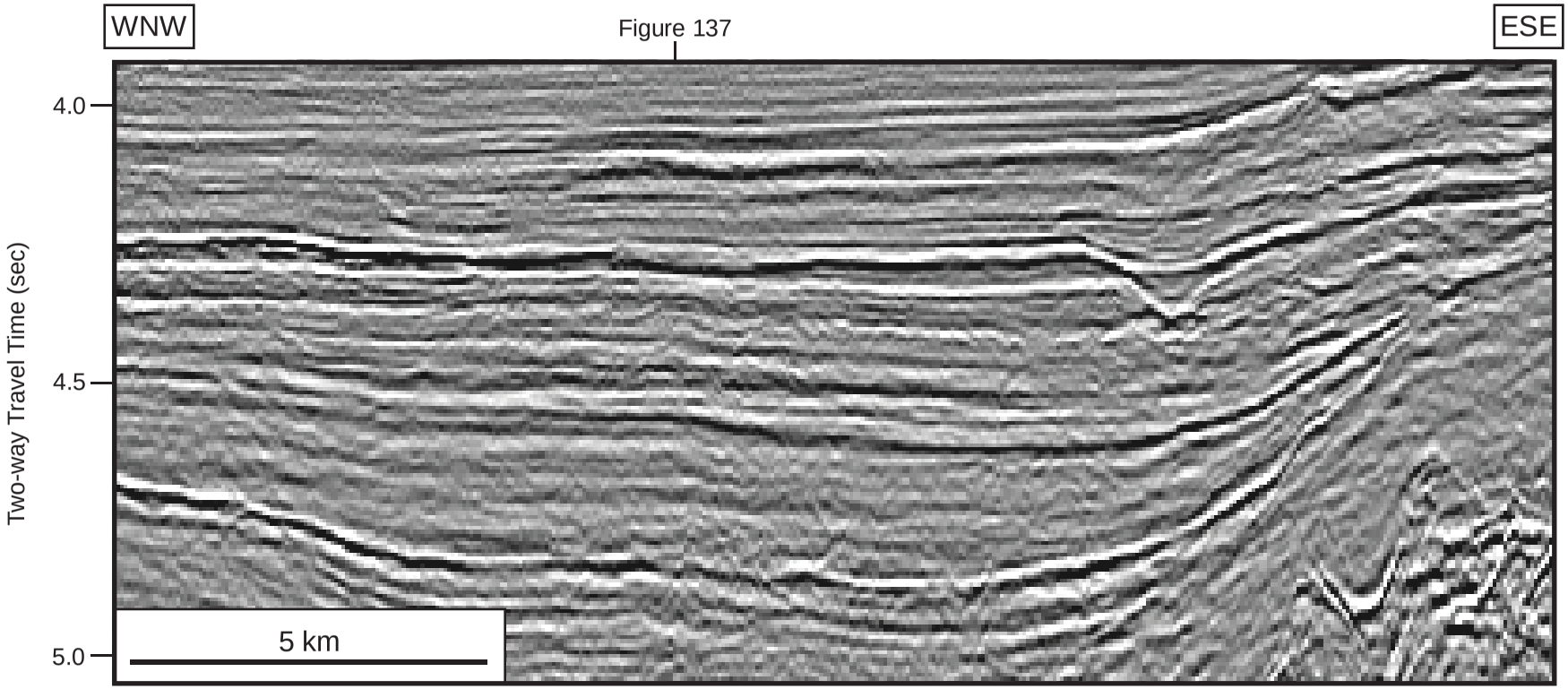

Figure 136a. Uninterpreted regional dip-oriented seismic profile (br-98:br98-057): A closeup view of Figure 135.

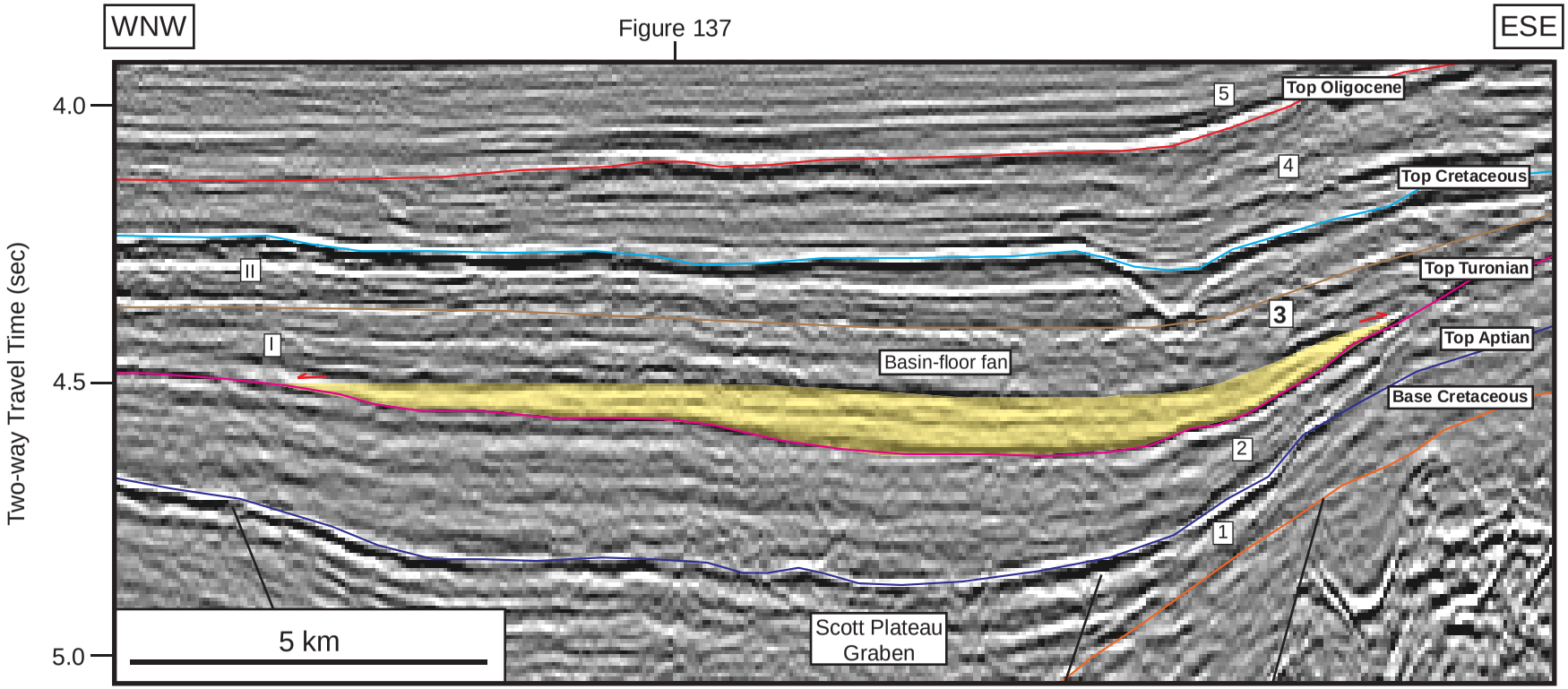

Figure 136b. Regional dip-oriented seismic profile showing all interpreted sequence boundaries from base Cretaceous to middle Miocene: A closeup view of Figure 135. The basin-floor fan is observed within Subsequence I of Megasequences 3 (yellow shade).

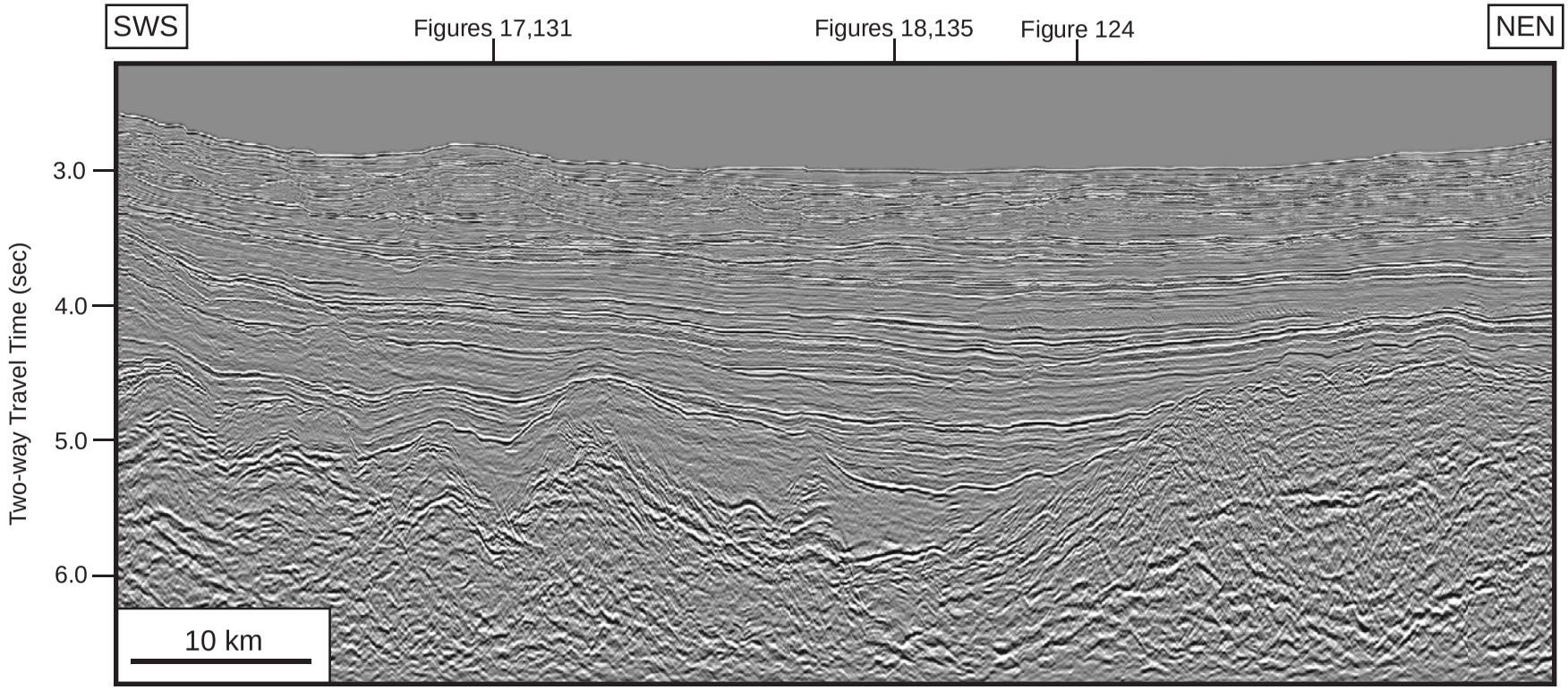

Figure 137a. Uninterpreted regional strike-oriented seismic profile (br-98:br98-080). Location of the profile is shown in Figures 120-121, 126-128, 139-141 and locations of where Figures 17, 18, 124, 131, 135 cross the profile.

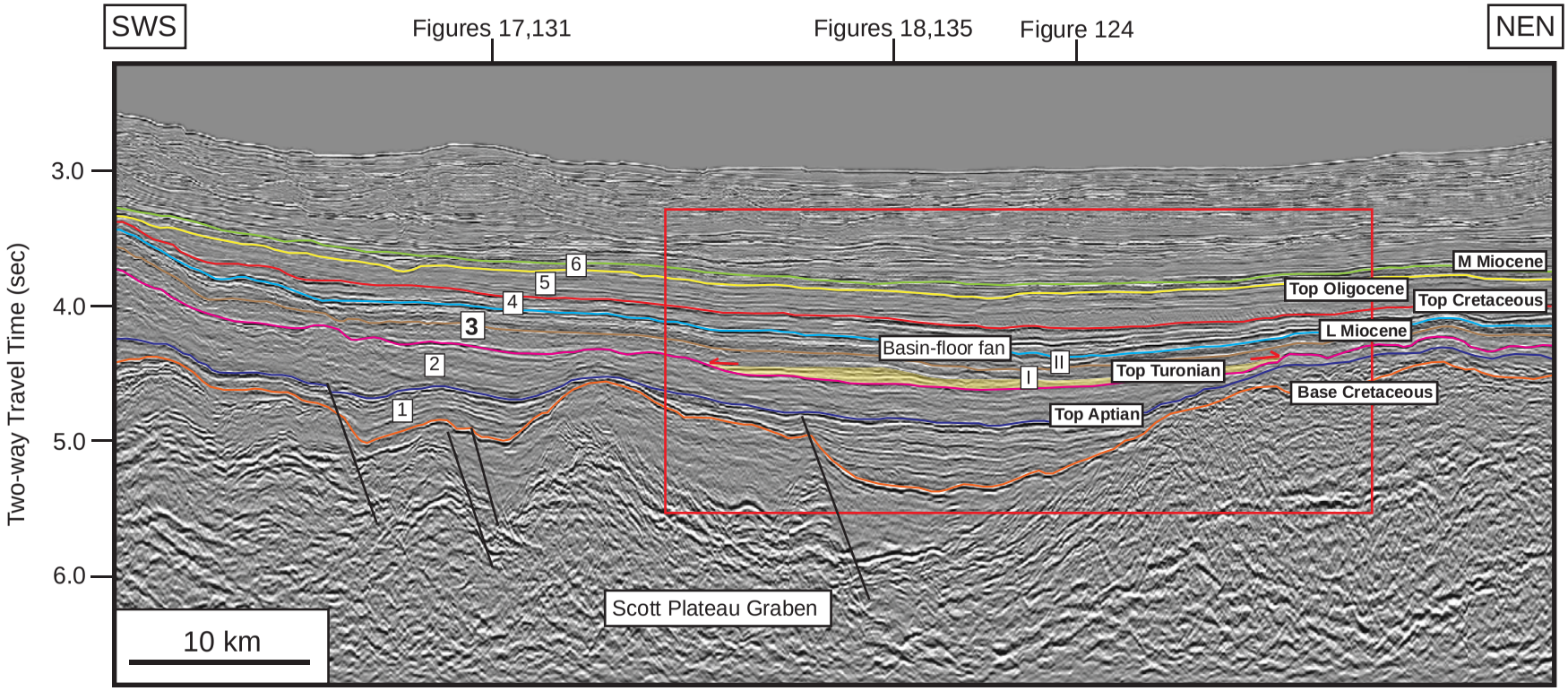

Figure 137b. Regional strike-oriented seismic profile showing all interpreted sequence boundaries from base Cretaceous to middle Miocene. This profile shows the area of the Scott Plateau and the shallower area of the Barcoo Terrace. The basin-floor fan is observed within Subsequence I of Megasequence 3 (yellow shade). Location of the profile is shown in Figures 120-121, 126-128, 139-141 and locations of where Figures 17, 18, 124, 131, 135 cross the profile.

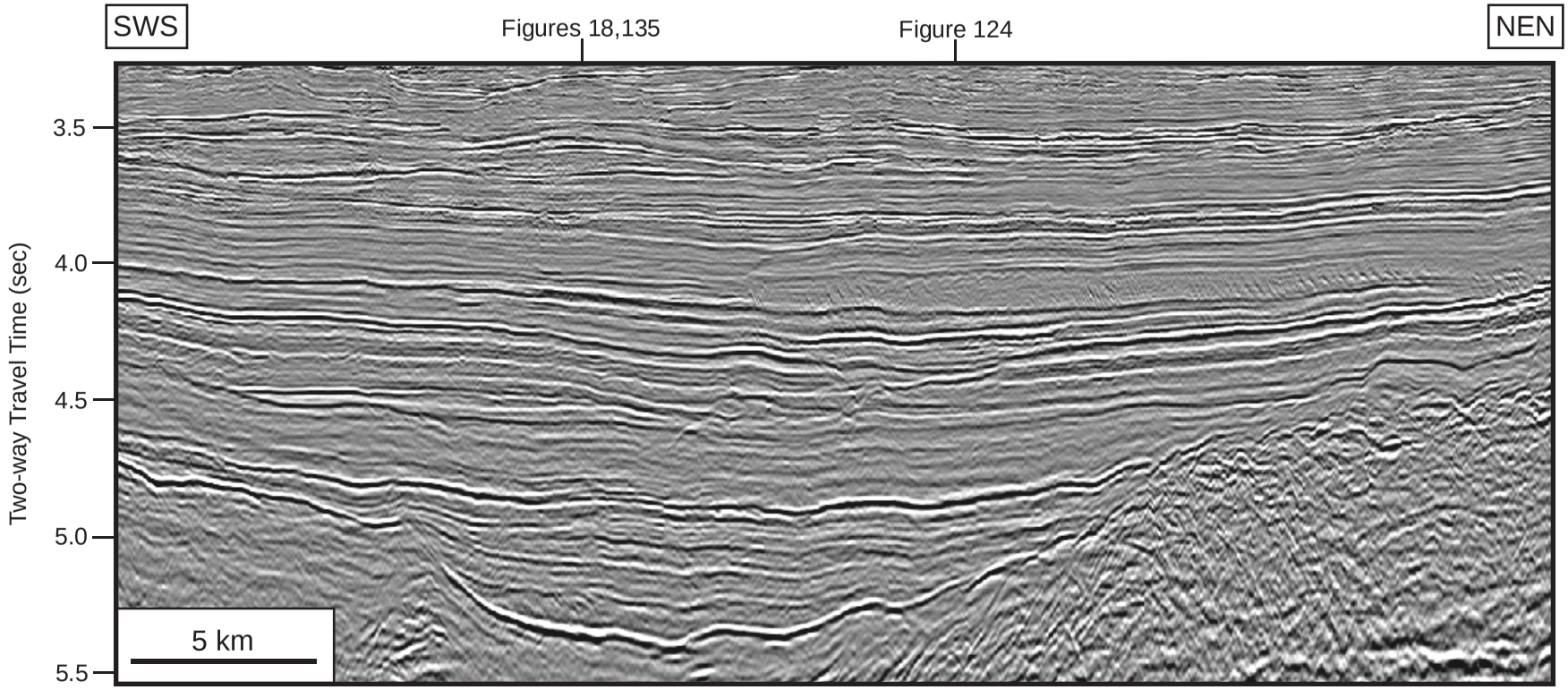

Figure 138a. Uninterpreted regional strike-oriented seismic profile (br-98:br98-080): A closeup view of Figure 137.

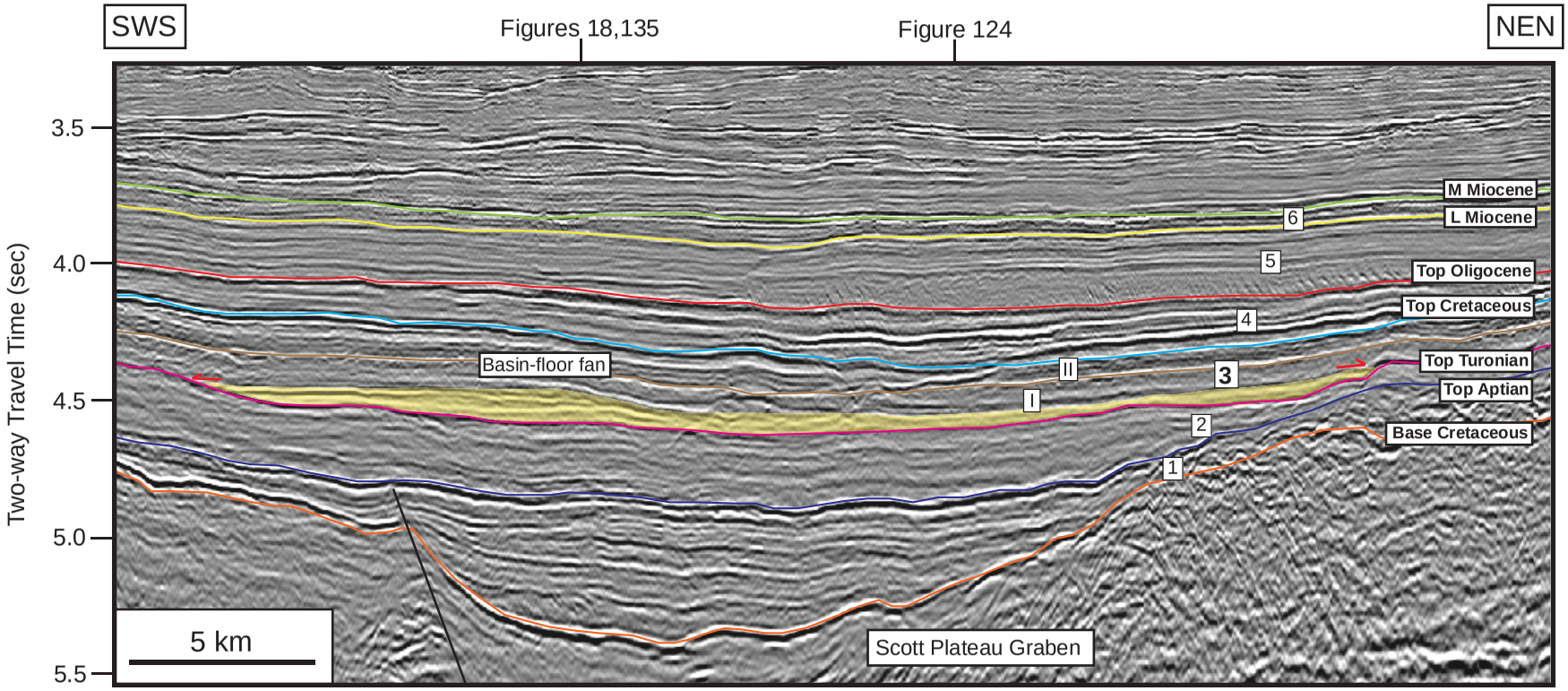

Figure 138b. Regional strike-oriented seismic profile showing all interpreted sequence boundaries from base Cretaceous to middle Miocene: A closeup view of Figure 137. The basin-floor fan is observed within Subsequence I of Megasequence 3 (yellow shade).

another basin-floor fan deposited in the area of Scott Plateau. The dip and strike oriented seismic profiles are shown in Figures 129-138.

Subsequence II of Megasequence 3

The isochron map shows the constant thickness along the Barcoo Terrace. The values range from 0 to 314 msec two-way travel time (TWTT) (Figure 139). This interval does not cover all over the study area. It is limited mainly in the area of the Barcoo Terrace. The greatest thickness deposition is in the Scott Plateau Graben to the north of the study area.

Only one seismic facies of facies 5 is recognized (Figure 140). The analysis was significantly difficult due to highly faulted reflections with variable amplitude and poor continuity (Figure 125). This seismic facies sits on the Scott Plateau at the edge of seismic coverage area to the west. No wells penetrate in either seismic facies 5 and 6.

Table 14. Seismic facies and geologic interpretation of Subsequence II of Megasequence 3

Seismic Facies	Upper Sequence Boundary	Lower Sequence Boundary	Internal Reflection Configuration	Amplitude	Continuity	Geologic Interpretation
3	Concordant	Concordant /Downlap	Hummocky	moderate	poor	Inversion – related structure

The geological facies map is shown in Figure 141. This interval is interpreted to be the shelf and basin-floor depositional environments. No interesting petroleum play is recognized.

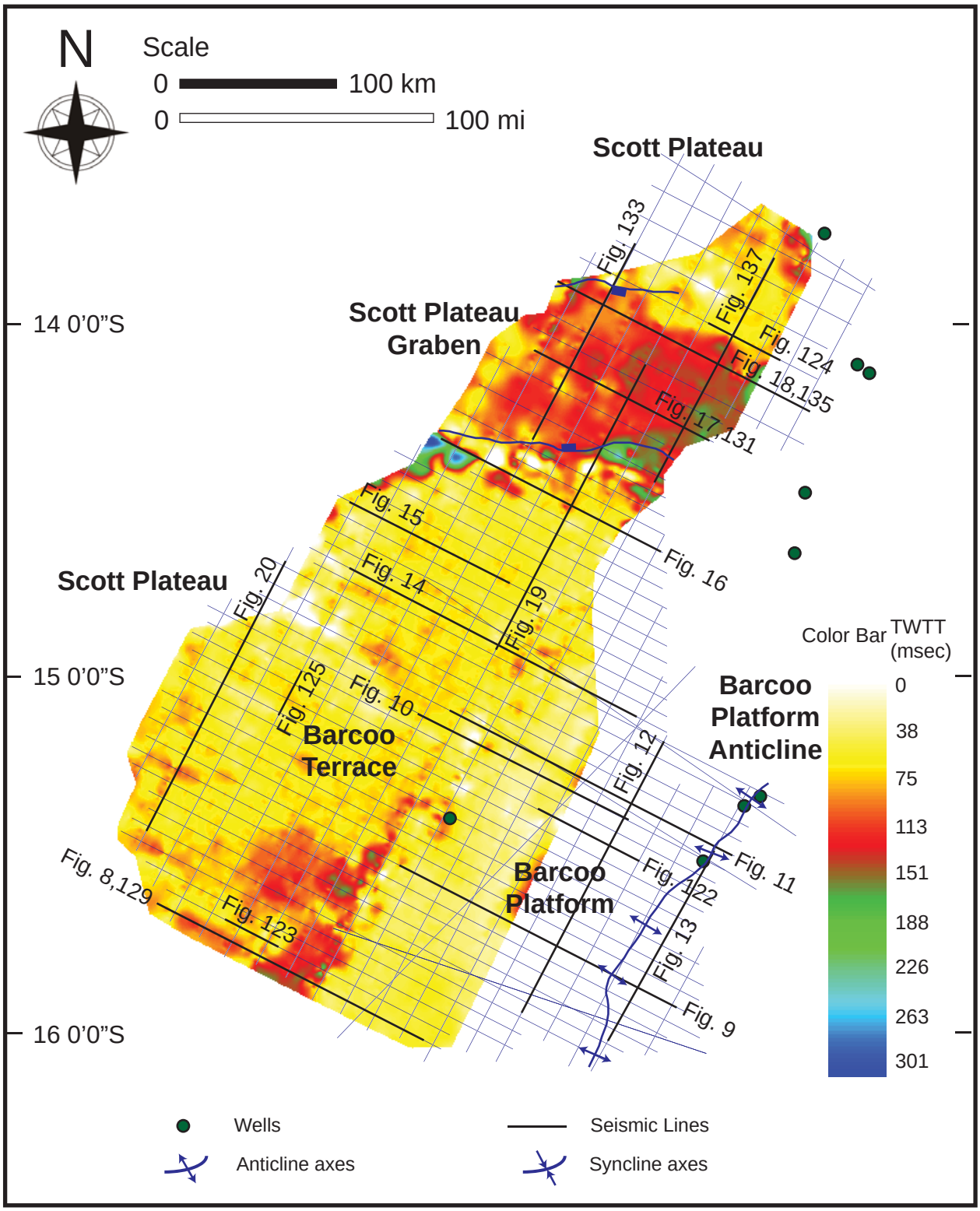

Figure 139. Isochron map (in TWTT msecs) of Subsequence II of Megasequence 3 interval. Distribution of 2D seismic profiles interpreted to generate the maps are shown by white lines, and wells are shown by green dots. Locations of Figures 8-20, 122-125, 129-138 are shown.

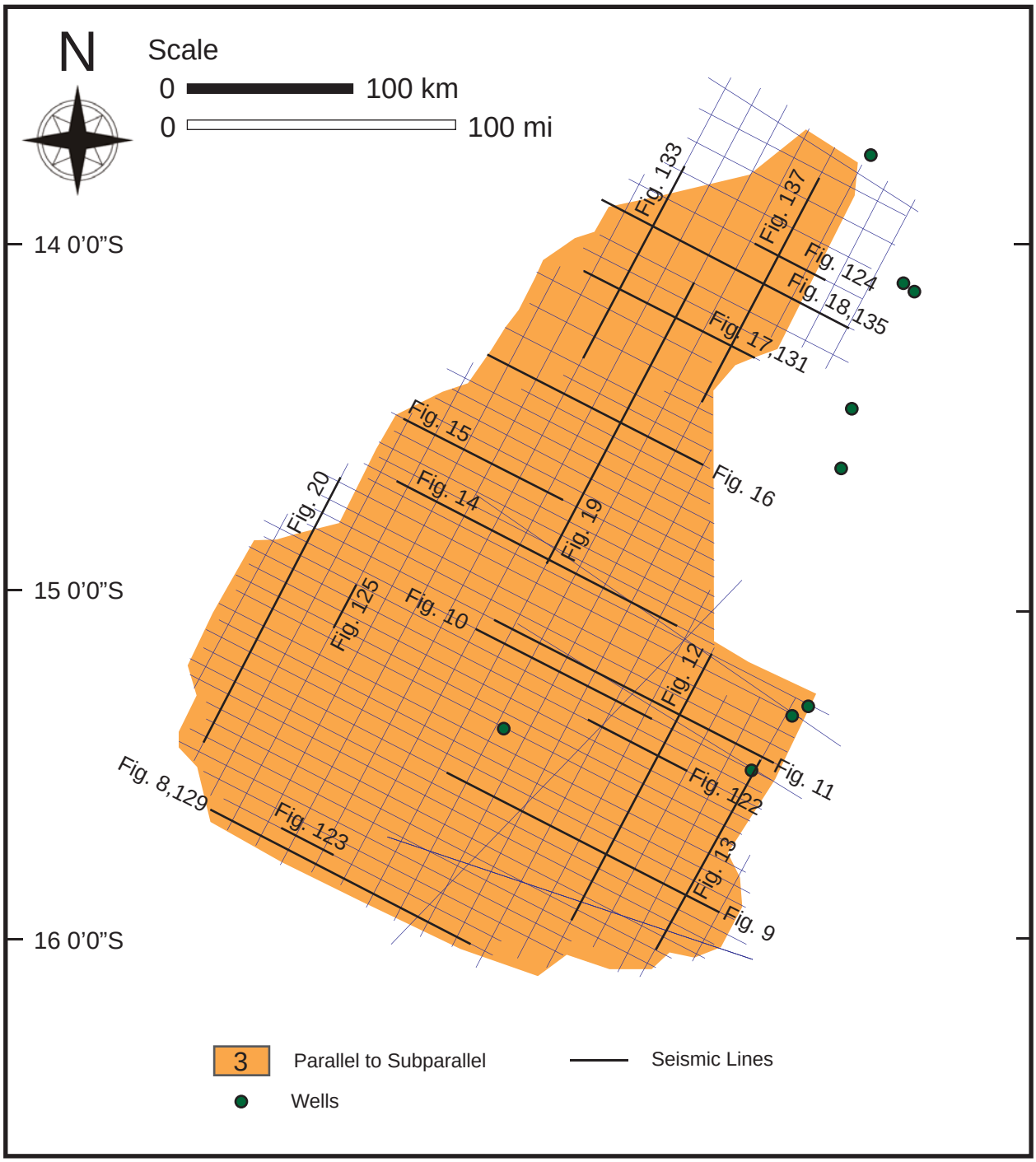

Figure 140. Seismic facies map of Subsequence II of Megasequence 3 interval. Each facies is numbered as described in the text. See Table 2 for seismic facies coding and Table 5 for a summary of seismic facies analysis and geologic interpretation. Locations of Figures 8-20, 122-125, 129-138 (black lines) are shown, and wells are shown by green dots.

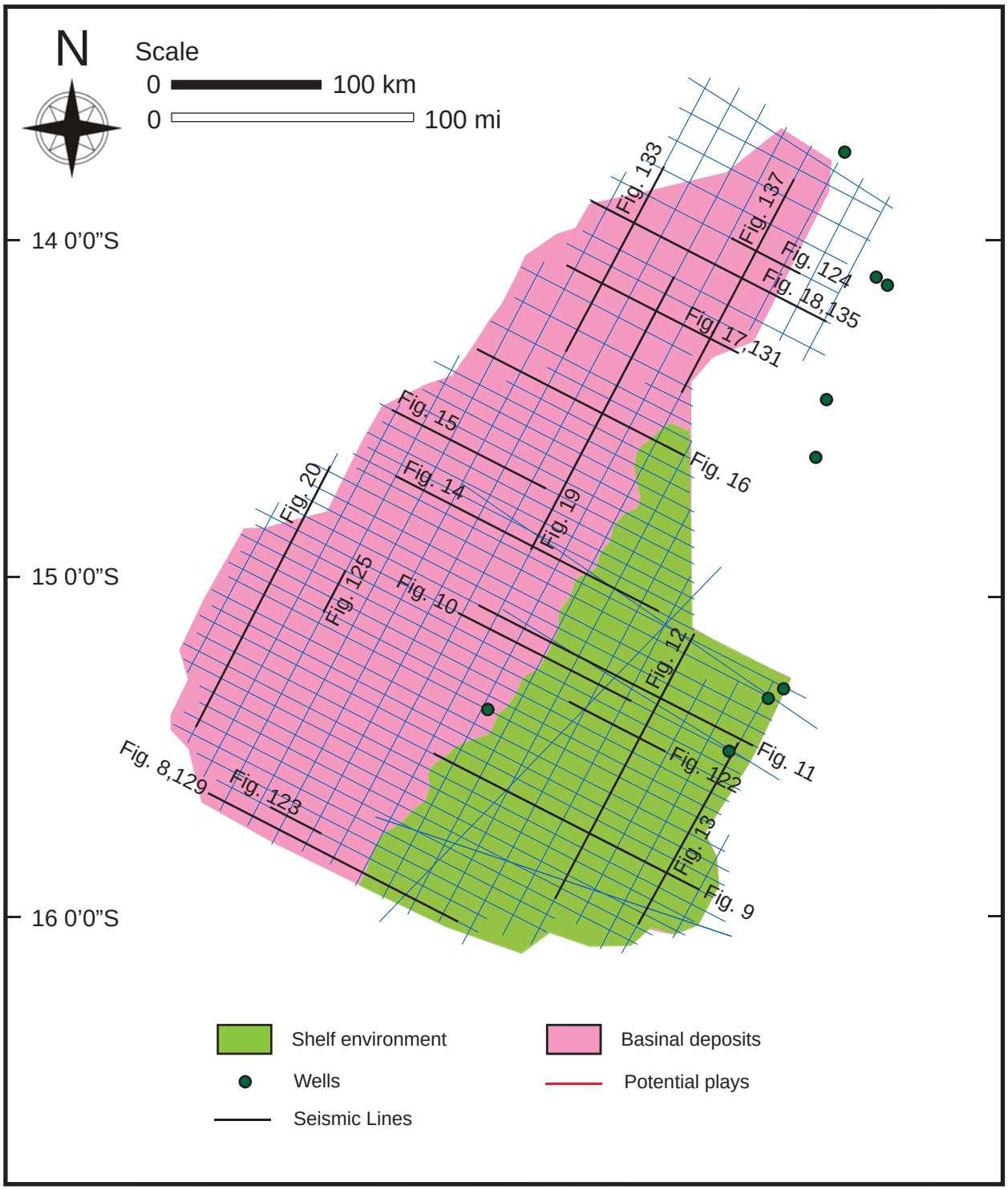

Figure 141. Geologic facies map of of Subsequence II of Megasequence 3 (top Turonian to top Cretaceous: 89.3-65.5 Ma) interval. See Table 5 for a summary of seismic facies analysis and geologic interpretation. Locations of Figures 8-20, 122-125, 129-138 (black lines) are shown, and wells are shown by green dots.

Megasequence 4: top Cretaceous to top Oligocene (65.5-23.0 Ma) interval

Megasequence 4 is markedly different from than the three underlying megasequences, specifically it is considerably thinner in terms of the amount of geologic time versus thickness. This relative thin is due to a major regional transgressive in the basin at the end of Cretaceous. The major backstep in the margin area followed by significant reduction in the rates of sedimentation. As a consequence, this megasequence comprises several depositional sequences that are below resolution of the seismic data. The top Oligocene horizon is the major flooding surface (condensed section) that can be identified a major downlap surface at the base of megasequence 5 (Figures 8-11).

The time structural contour map values range from 579 to 4102 msec (Figure 142). The Scott Plateau graben is the deepest relief of the megasequence where is shallower is at the southern flank of the Scott Plateau Graben. The Barcoo Platform anticline can be seen in the eastern margin of the sub-basin (Figures 9, 11, 13).

The isochron map of this megasequence illustrates the thickness values varying from 0 to 764 msec two-way travel time (TWTT) (Figure 143). The lowest thickness of this sequence is at the southern flank of Scott Plateau Graben.

Five distinct seismic facies were recognized in the megasequence (Figure 148; Table 15). Most of this sequence displays predominantly parallel to subparallel seismic reflection with moderate to high amplitude and fair to good continuity of seismic facies 1 and 4 (Figures 144-126). Lombardina-1 and Sheherazade-1 wells penetrate in seismic facies 1. The well log data shows the thick sand-prone interval.

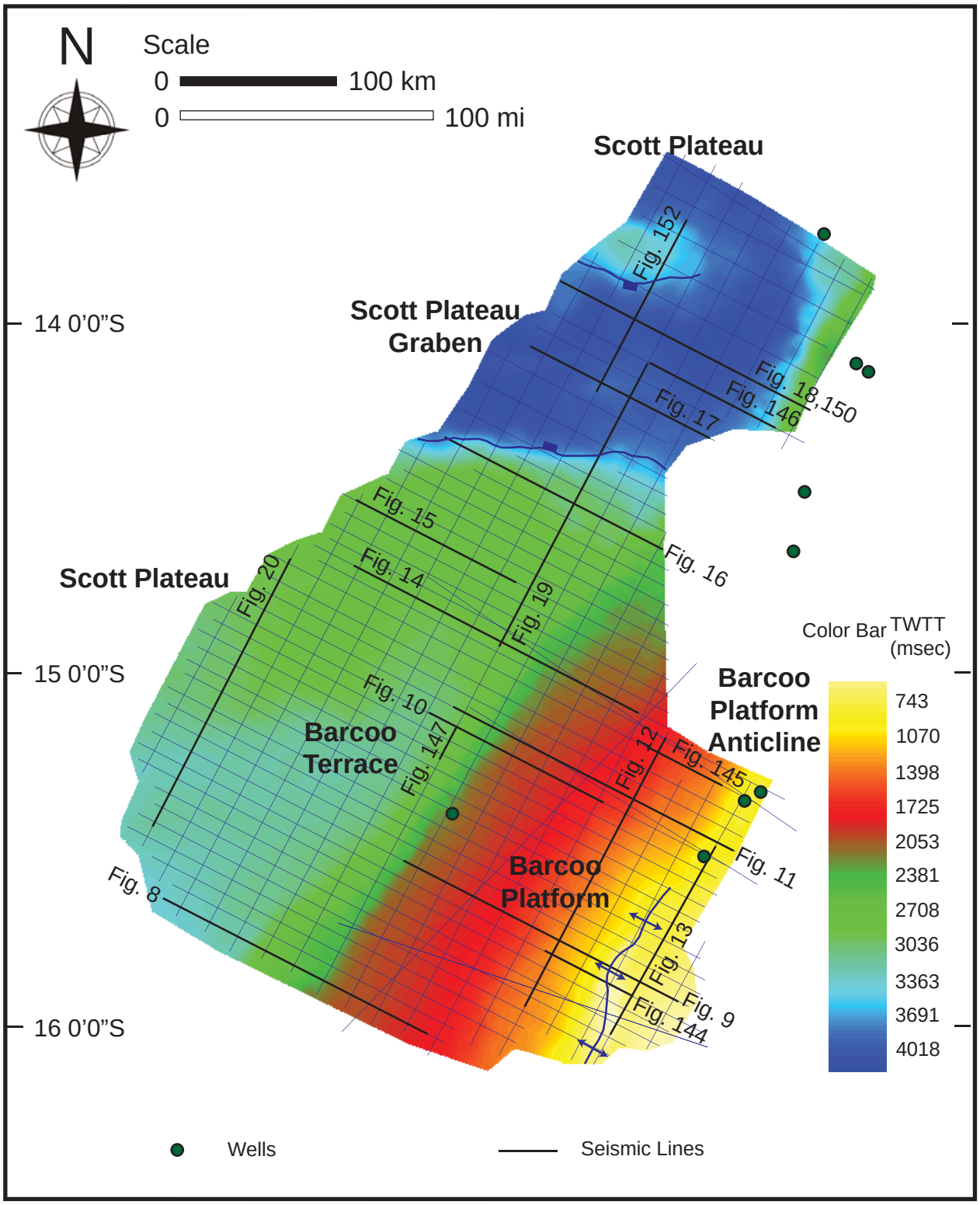

Figure 142. Time structural contour map (in TWTT msecs) of Oligocene: 23.0 Ma (Megasequence 4). Distribution of 2D seismic profiles interpreted to generate the maps are shown by white lines, and wells are shown by green dots. Locations of Figures 8-20, 144-147, 150-153 are shown.

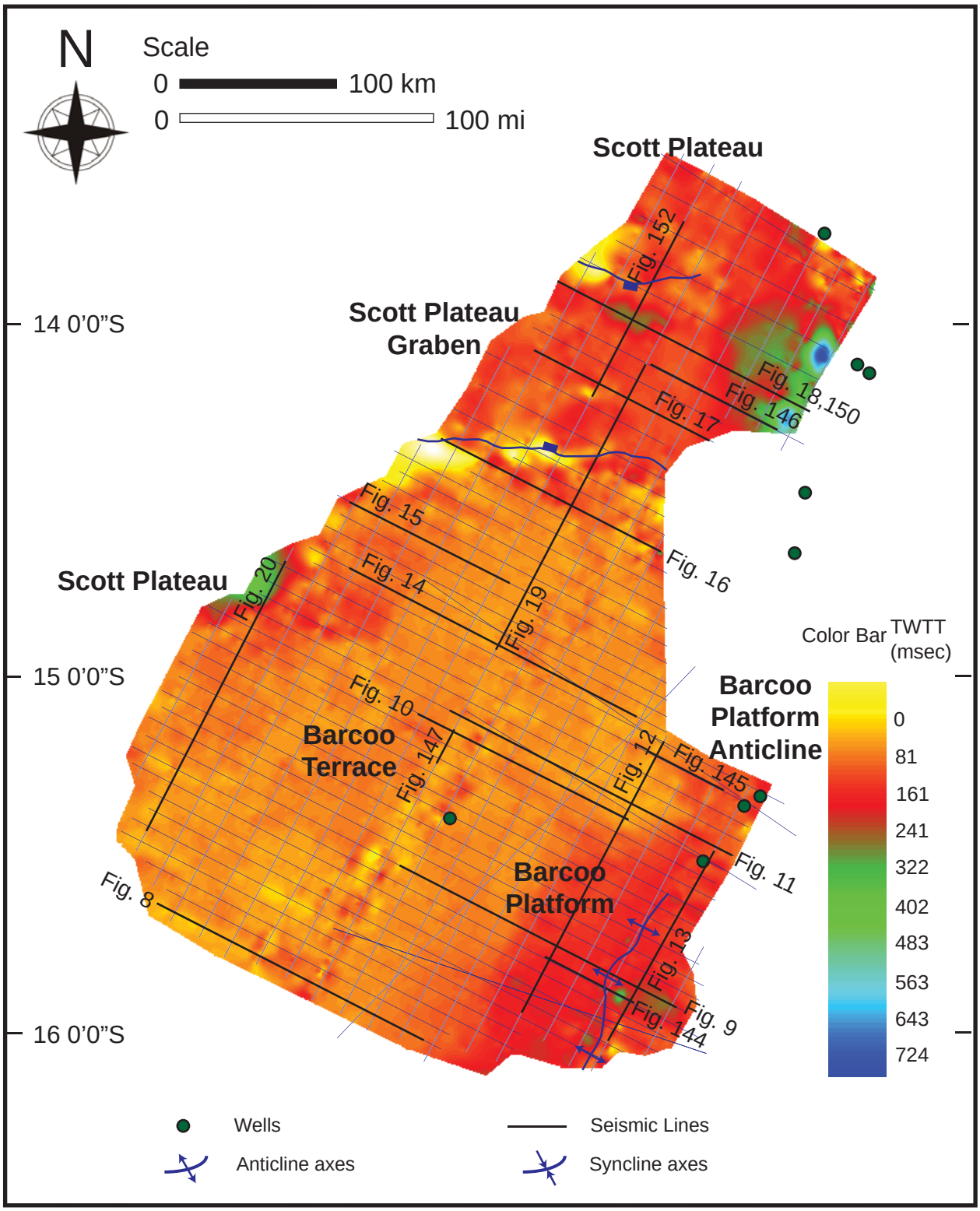

Figure 143. Isochron map (in TWTT msecs) of Megasequence 4 (top Cretaceous to top Oligocene: 65.5-23.0 Ma) interval. Distribution of 2D seismic profiles interpreted to generate the maps are shown by white lines, and wells are shown by green dots. Locations of Figures 8-20, 144-147, 150-153 are shown.

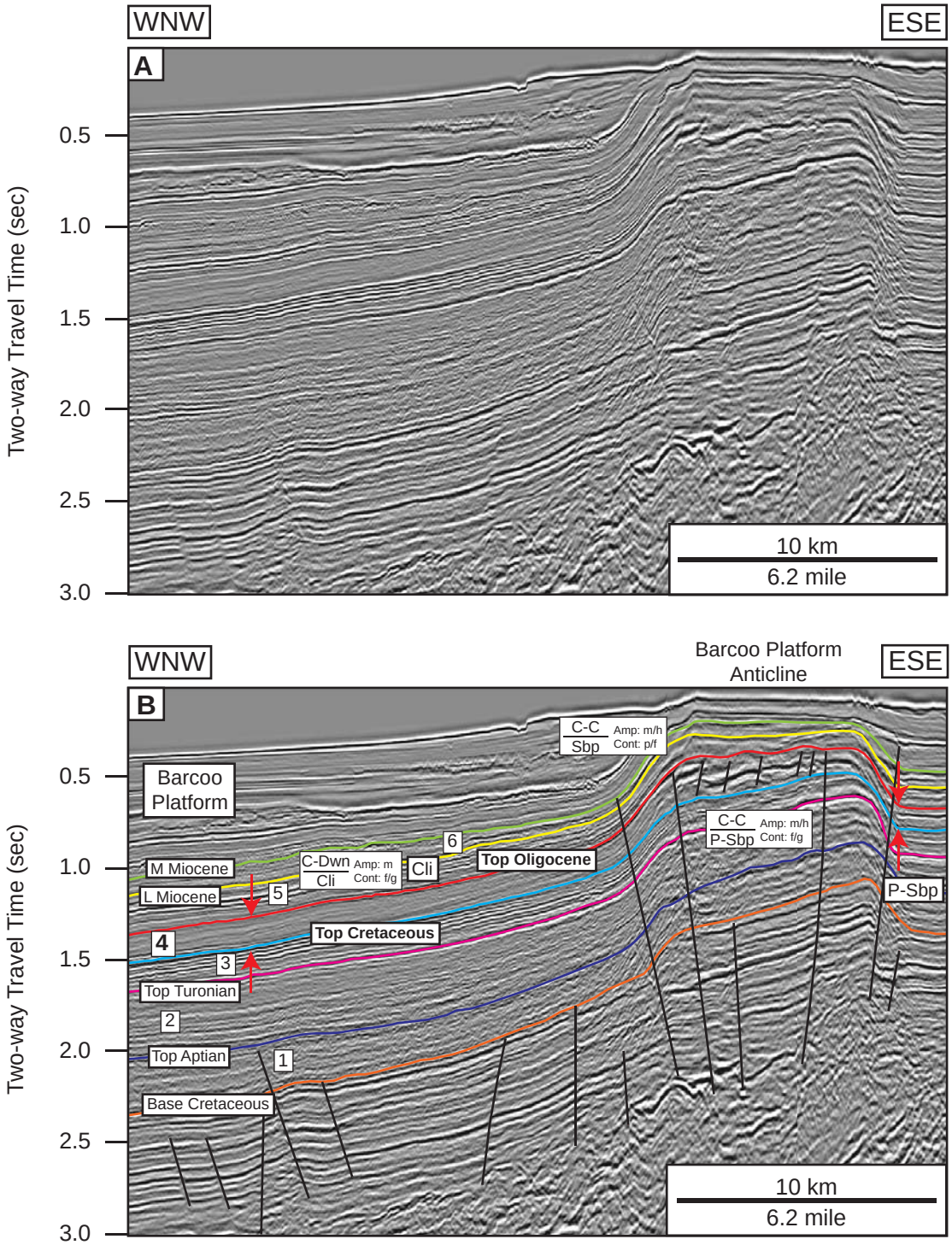

Figure 144. Dip-oriented seismic profile showing seismic facies of Mega-sequence 4 (top Cretaceous to top Oligocene: 65.5-23.0 Ma) interval: (a) uninterpreted, (b) interpreted. See Table 2 for codes and abbreviations and Figures 142-143, 148-149 for location of the profile

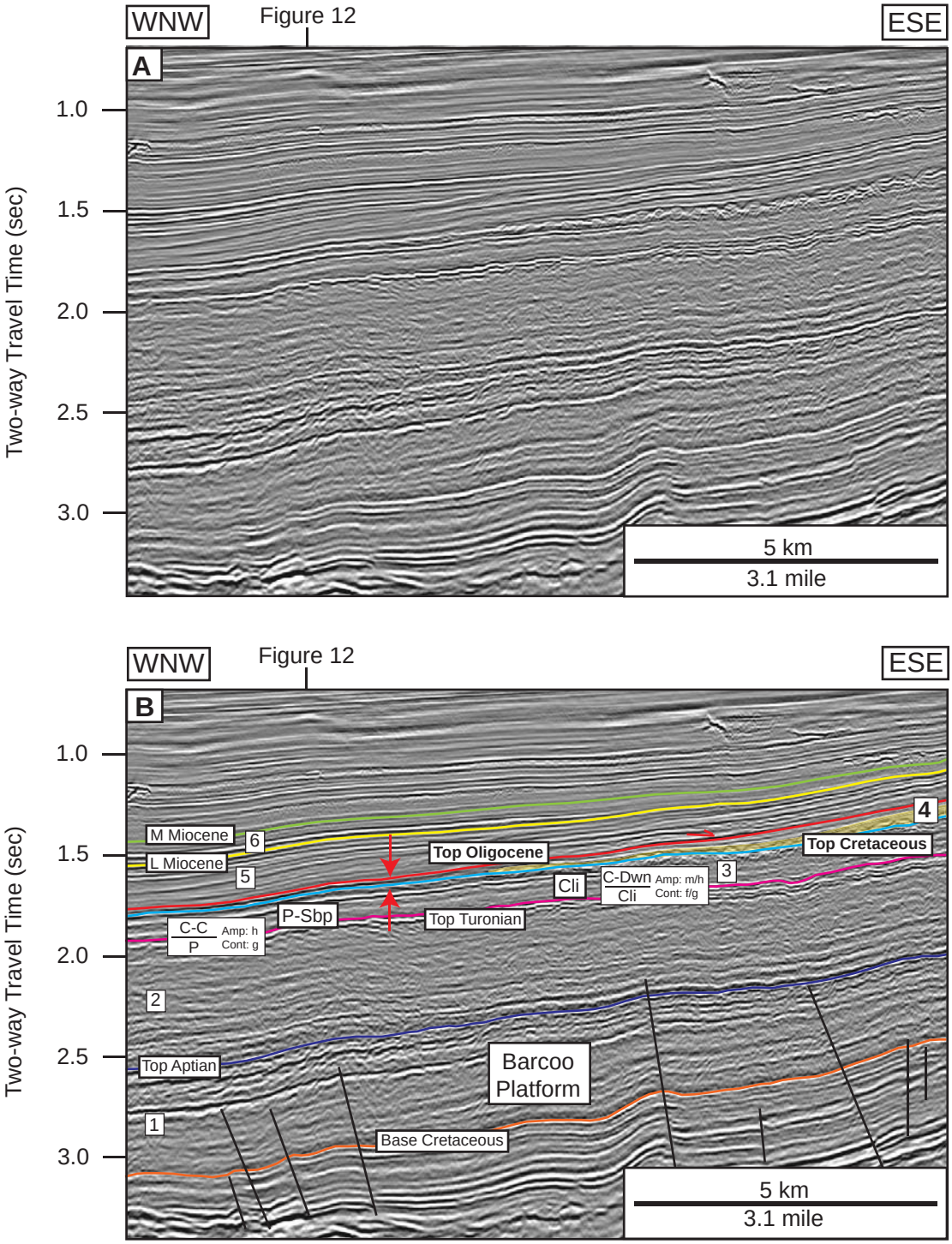

Figure 145. Dip-oriented seismic profile showing seismic facies of Mega-sequence 4 (top Cretaceous to top Oligocene: 65.5-23.0 Ma) interval: (a) uninterpreted, (b) interpreted. The mass transport deposit is observed (yellow shade). See Table 2 for codes and abbreviations and Figures 142-143, 148-149 for location of the profile and location of where Figure 12 crosses the profile.

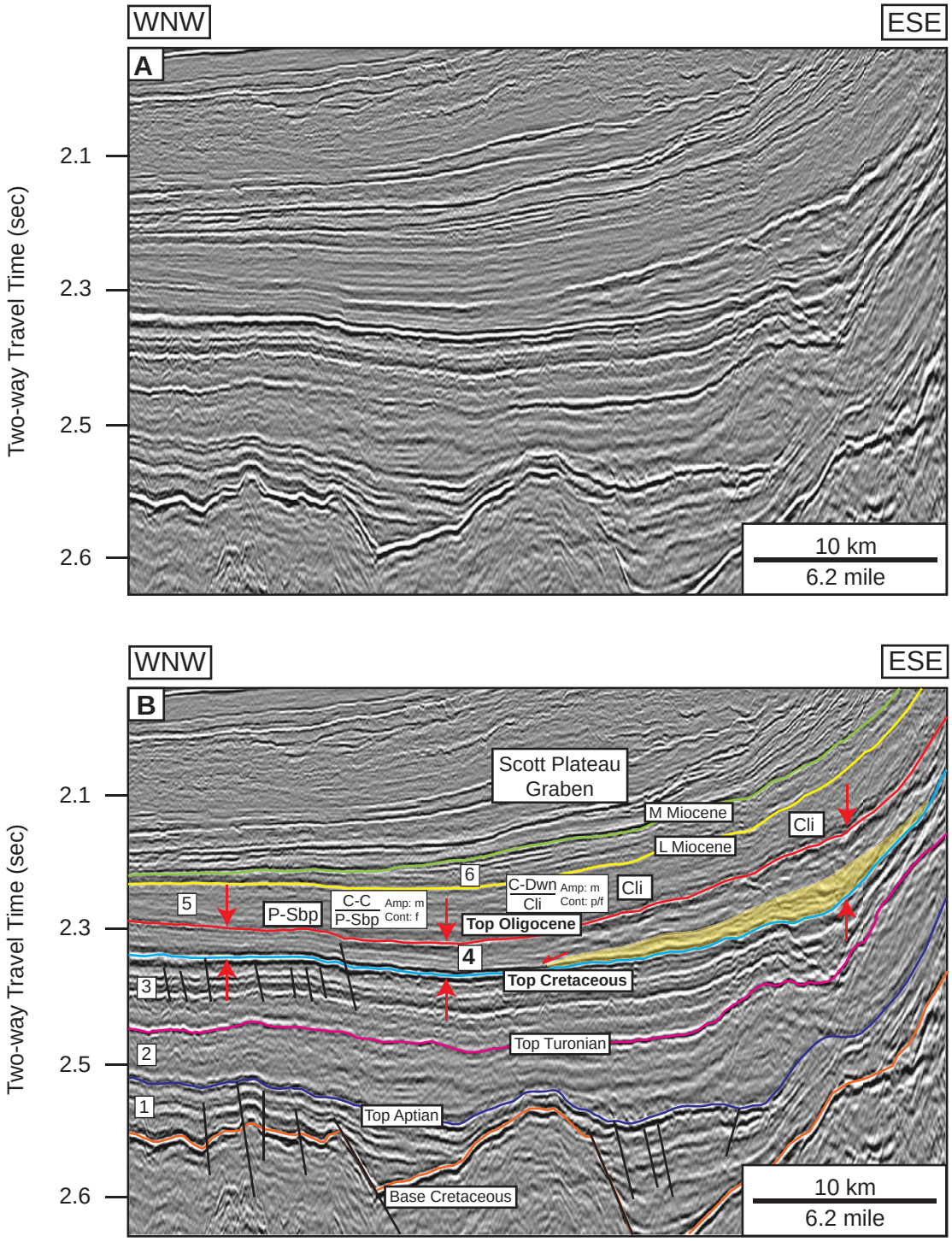

Figure 146. Dip-oriented seismic profile showing seismic facies of Mega-sequence 4 (top Cretaceous to top Oligocene: 65.5-23.0 Ma) interval: (a) uninterpreted, (b) interpreted. The deepwater deposits is recognized (yellow shade). See Table 2 for codes and abbreviations and Figures 142-143, 148-149 for location of the profile.

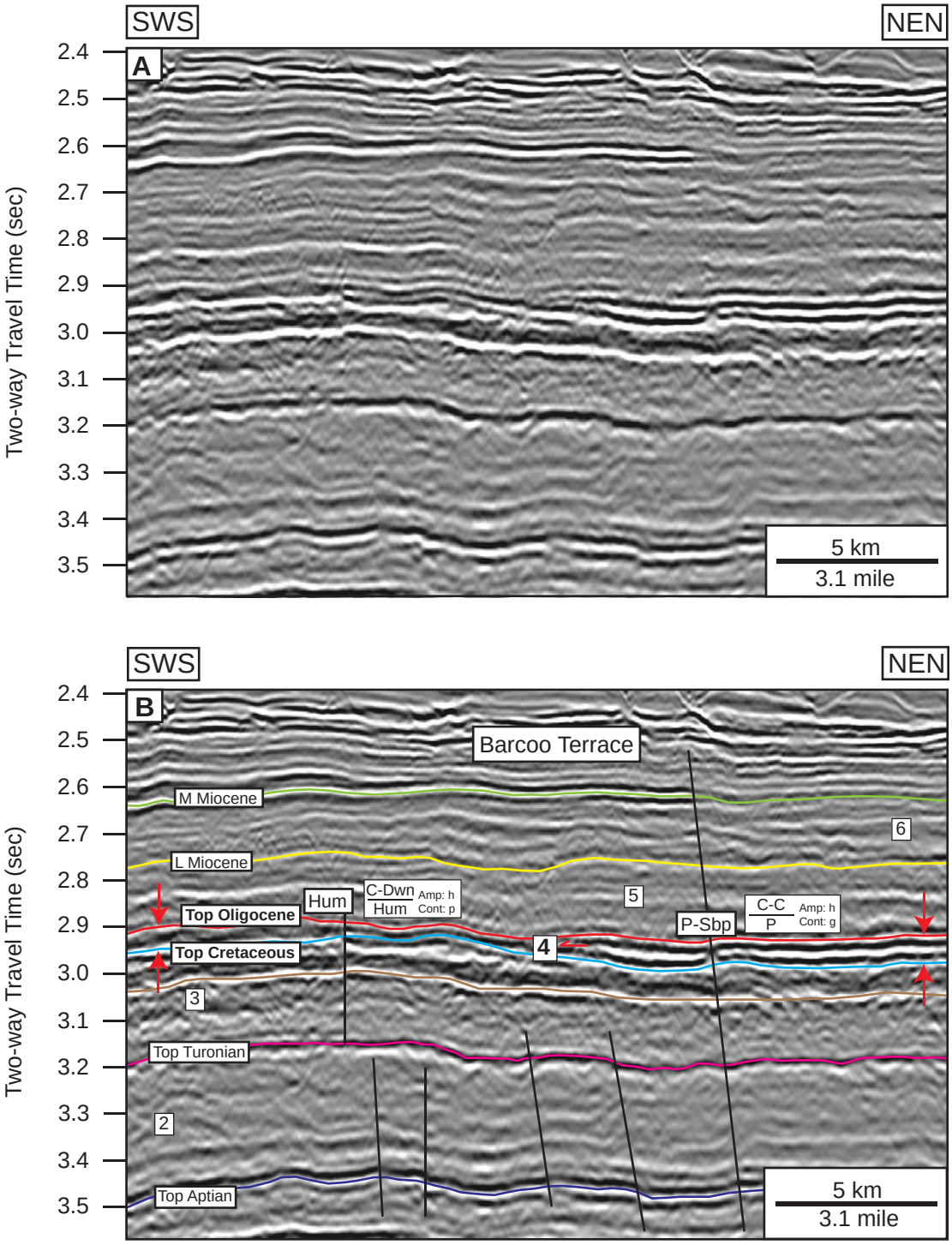

Figure 147. Strike-oriented seismic profile showing seismic facies of Mega-sequence 4 (top Cretaceous to top Oligocene: 65.5-23.0 Ma) interval: (a) uninterpreted, (b) interpreted. See Table 2 for codes and abbreviations and Figures 142-143, 148-149 for location of the profile.

Facies 2 consists of clinoform reflections, with moderate to high amplitude and poor to good continuity (Figures 144-147). No well penetrated in facies 2.

Table 15. Seismic facies and geologic interpretation of Megasequence 4: 65.5-23.0 Ma.

Seismic Facies	Upper Sequence Boundary	Lower Sequence Boundary	Internal Reflection Configuration	Amplitude	Continuity	Geologic Interpretation
1	Concordant	Concordant	Parallel to Subparallel	moderate to high	fair to good	Shelf deposits
2	Concordant	Downlap	Clinoform	moderate to high	poor to good	Prograding clinoform
3	Concordant	Concordant /Downlap	Hummocky	high	poor	Inversion – related structure
4	Concordant	Concordant	Parallel to Subparallel	moderate to high	fair to good	Basinal deposits
5	-	-	Chaotic	low	poor	Poor quality data

Seismic facies 3 displays hummocky internal configuration with high seismic amplitude and poor seismic continuity. This facies is related to the tectonic activity of the Barcoo fault trend. Barcoo-1 well penetrates this facies. The wireline data shows the coarsening upward of sandstone interval. Seismic facies 5 illustrates chaotic internal reflection configuration with low amplitude and poor continuity. No well penetrates in this seismic facies.

The geologic facies map for megasequence 4 is in Figure 149. The sediments were transported from the shelf into the basin in the southeast to northwest direction. This main characteristic of this sequence is the very low angle clinoform morphology (Figure 9) due to the relatively low rates of sediment supply compared to the rates of subsidence. Most of this sequence shows the channels and overbanks deposits of slope environment as well as the deepwater deposits on the basin floor (Figure 18). The basin-floor fan is recognized in the northern part of the study area. This is one of the

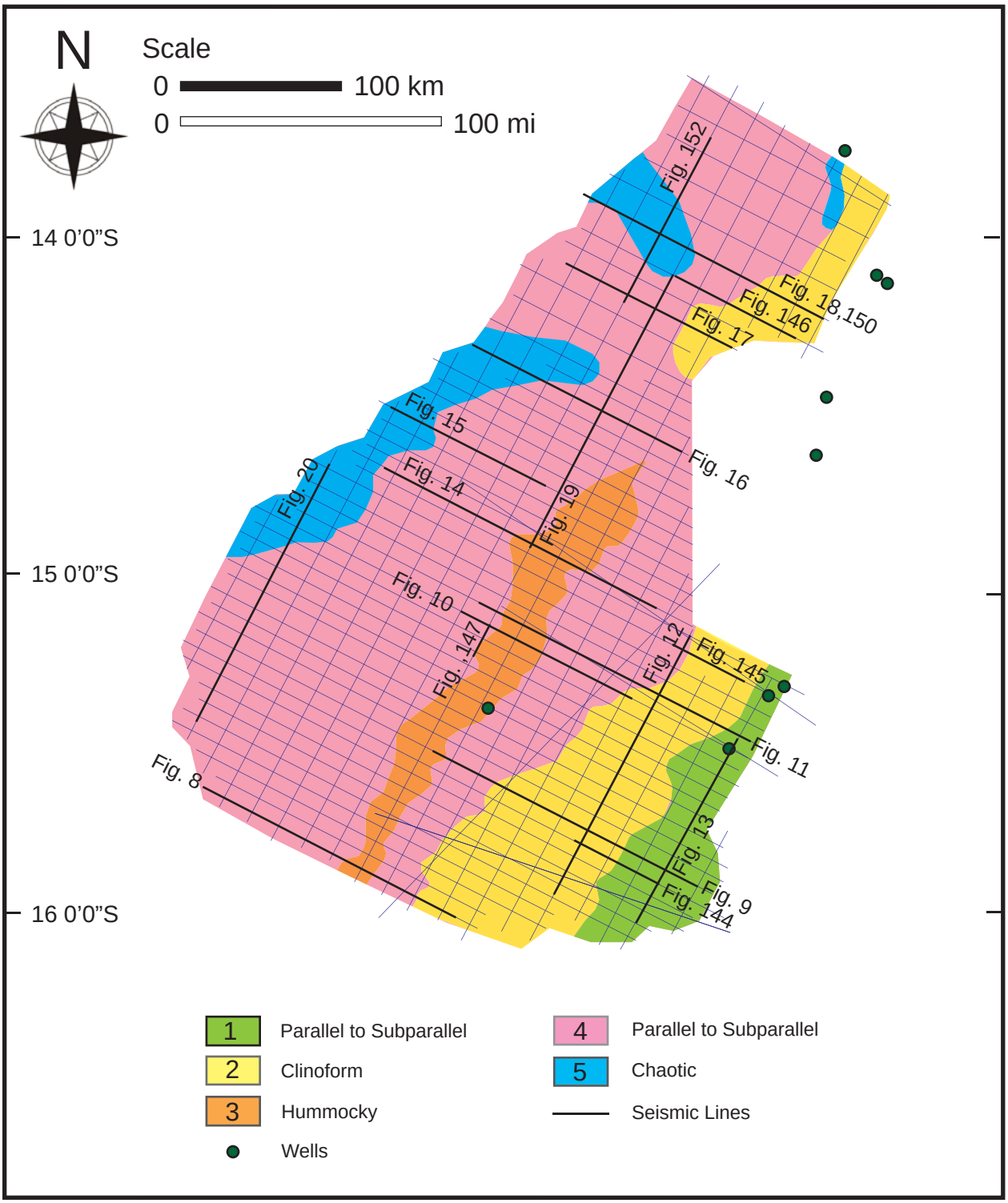

Figure 148. Seismic facies map of Megasequence 4 (top Cretaceous to top Oligocene: 65.5-23.0 Ma) interval. Each facies is numbered as described in the text. See Table 2 for seismic facies coding and Table 6 for a summary of seismic facies analysis and geologic interpretation. Locations of Figures 8-20, 144-147, 150-153 (black lines) are shown, and wells are shown by green dots.

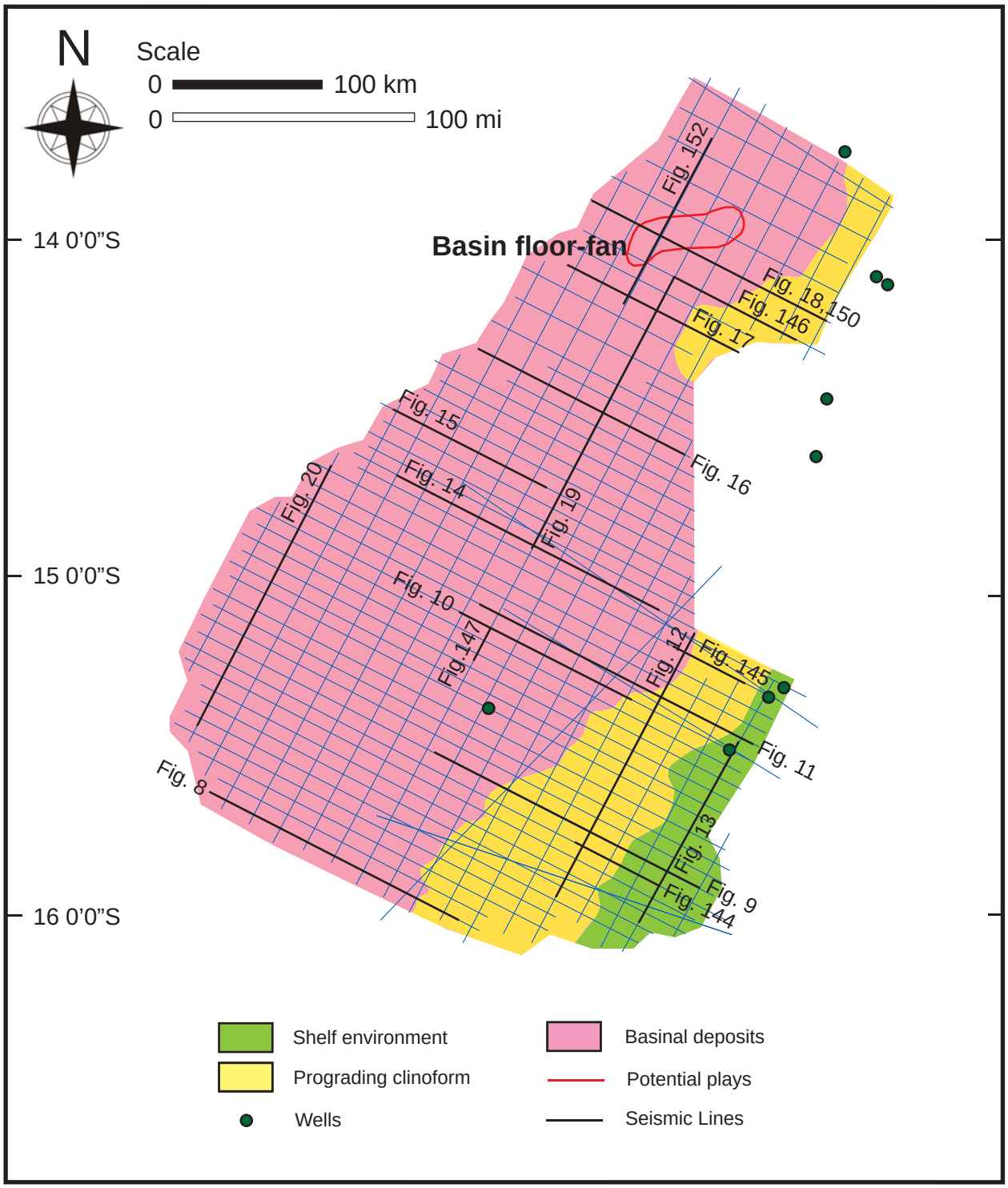

Figure 149. Geologic facies map of Megasequence 4 (top Cretaceous to top Oligocene: 65.5-23.0 Ma) interval. See Table 6 for a summary of seismic facies analysis and geologic interpretation. Locations of Figures 8-20, 144-147, 150-153 (black lines) are shown, and wells are shown by green dots.

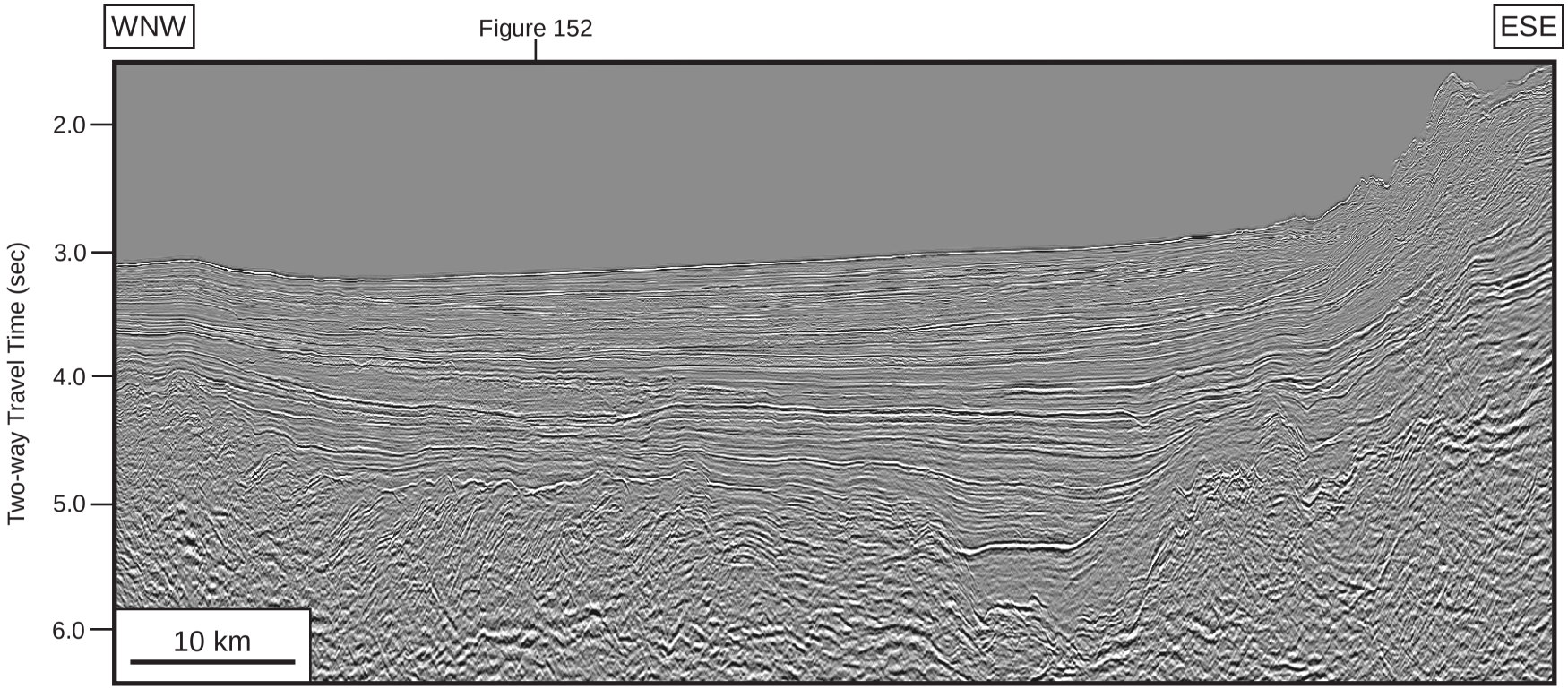

Figure 150a. Uninterpreted regional dip-oriented seismic profile (br-98:br98-057). Location of the profile is shown in Figures 142-143, 148-149 and location of where Figure 152 crosses the profile.

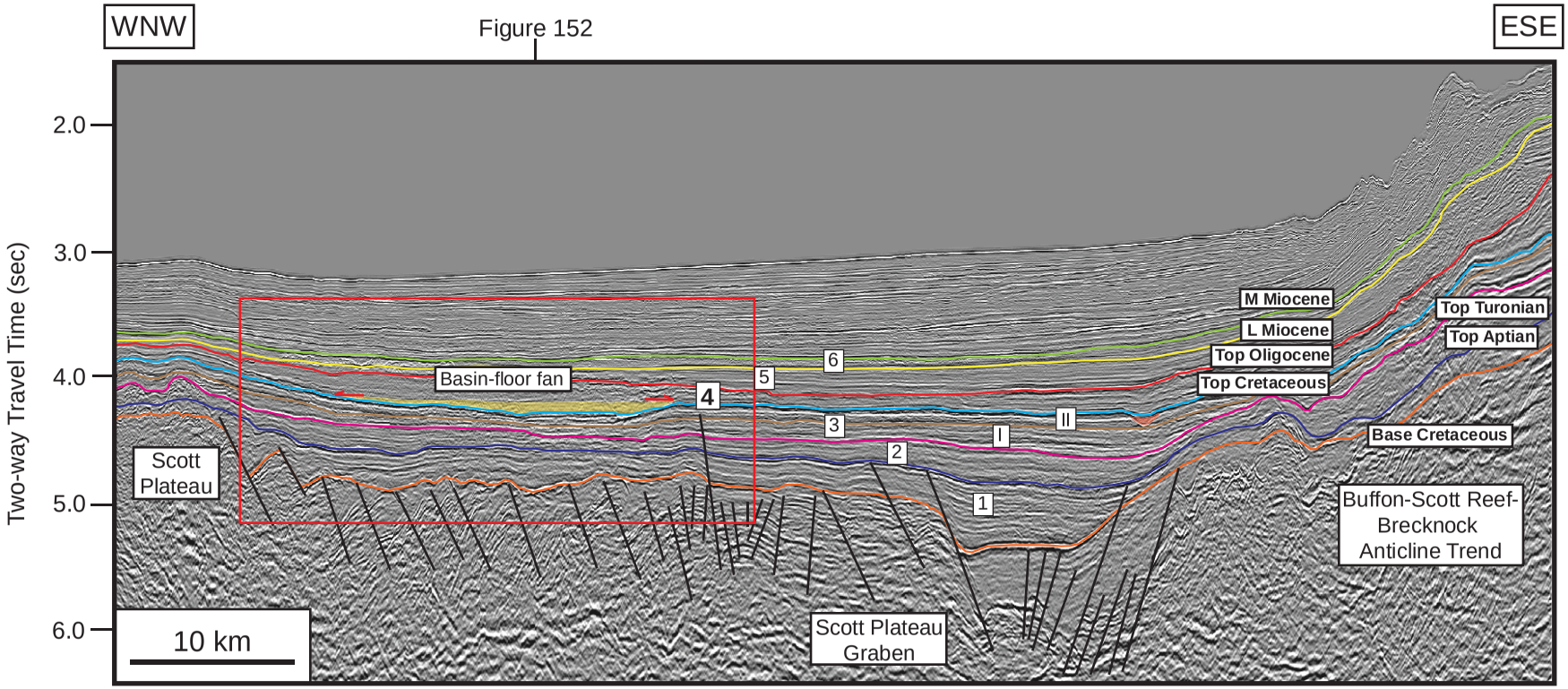

Figure 150b. Regional dip-oriented seismic profile showing all interpreted sequence boundaries from base Cretaceous to middle Miocene. This profile shows the deeper area of the Scott Plateau Graben and shallower area of the Buffon-Scott Reef-Brecknock Anticline Trend in the northern part of the study area. Series of faults in the underlying Jurassic strata caused the irregular topography. The basin floor-fan and the erosional feature (submarine canyon?) are observed within Megasequence 4 (yellow and red shades, respectively). Location of the profile is shown in Figures 142-143, 148-149 and location of where Figure 152 crosses the profile.

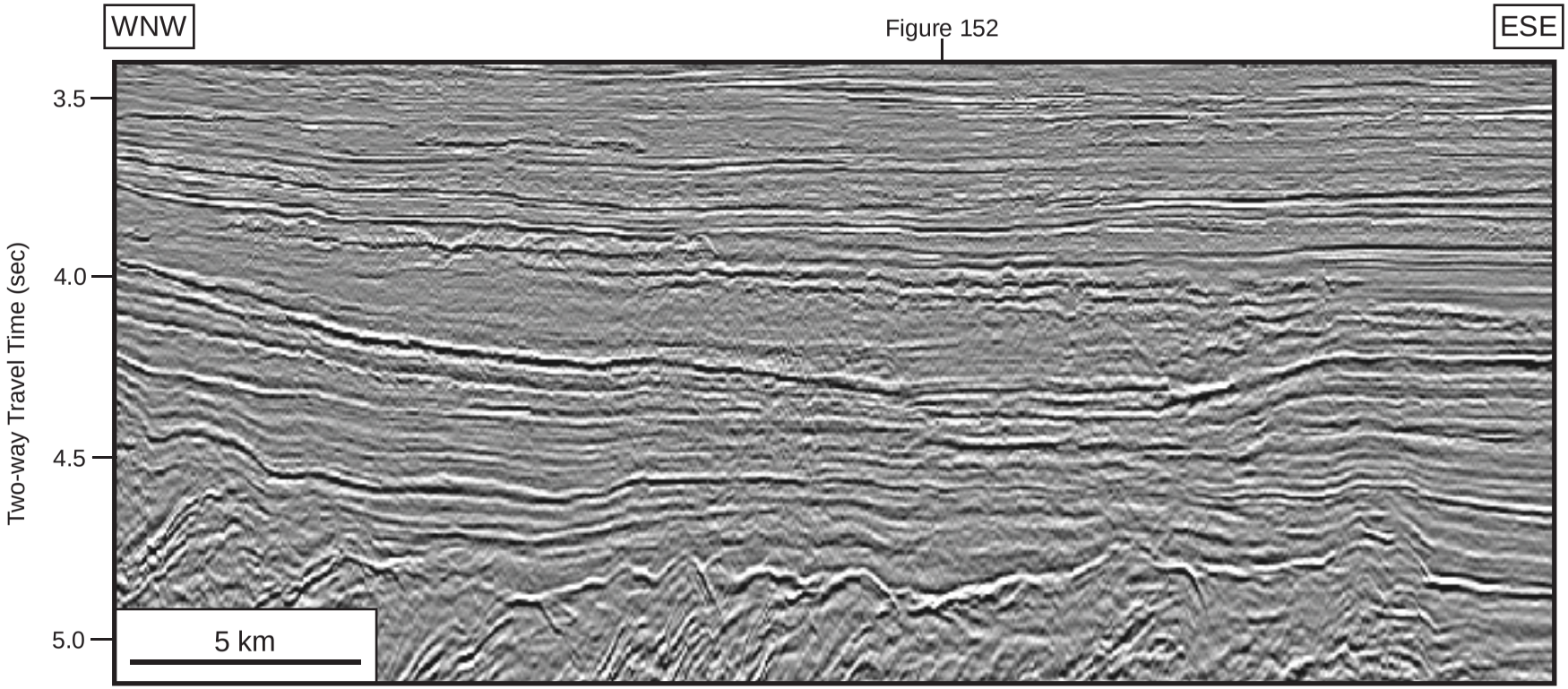

Figure 151a. Regional dip-oriented seismic profile showing all interpreted sequence boundaries from base Cretaceous to middle Miocene: A closeup view of Figure 150.

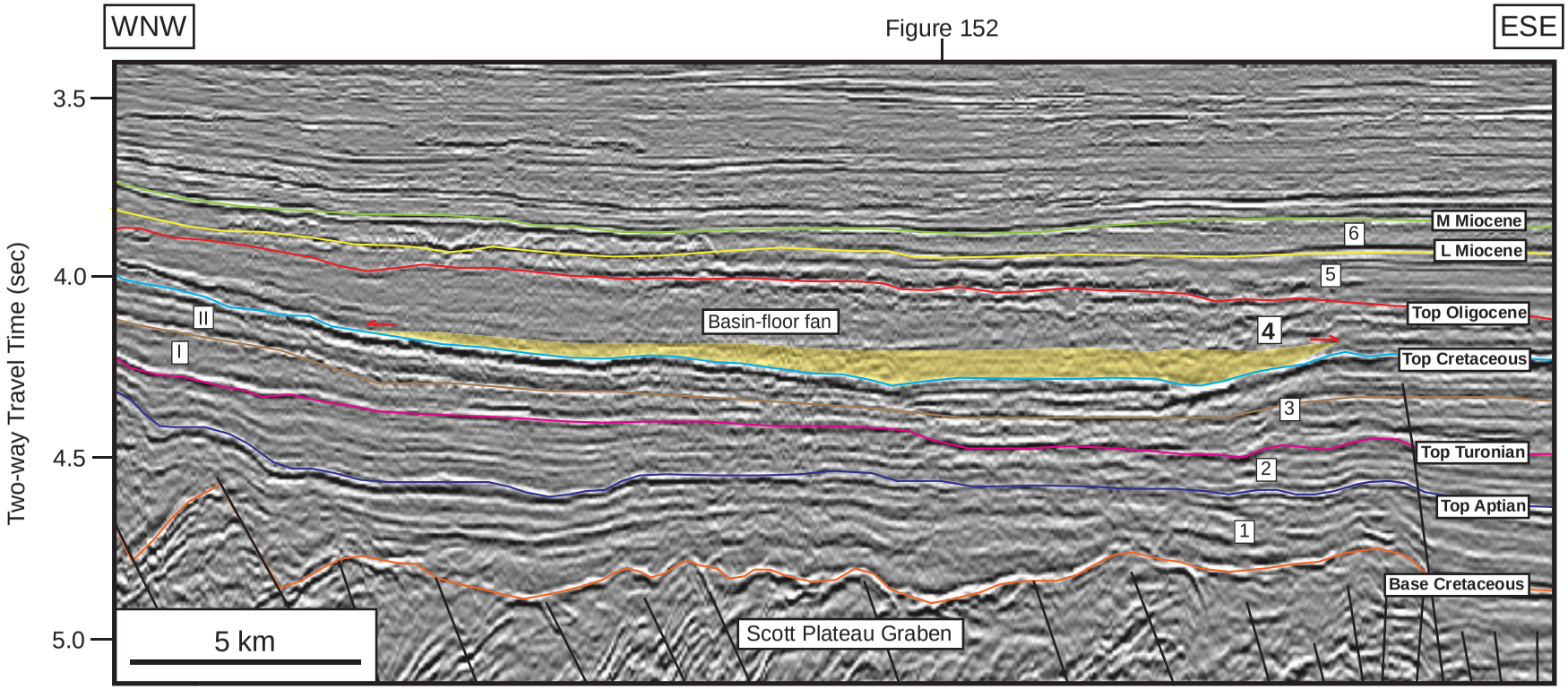

Figure 151b. Regional dip-oriented seismic profile showing all interpreted sequence boundaries from base Cretaceous to middle Miocene: A closeup view of Figure 150. The basin floor-fan is observed within Megasequence 4 (yellow shade).

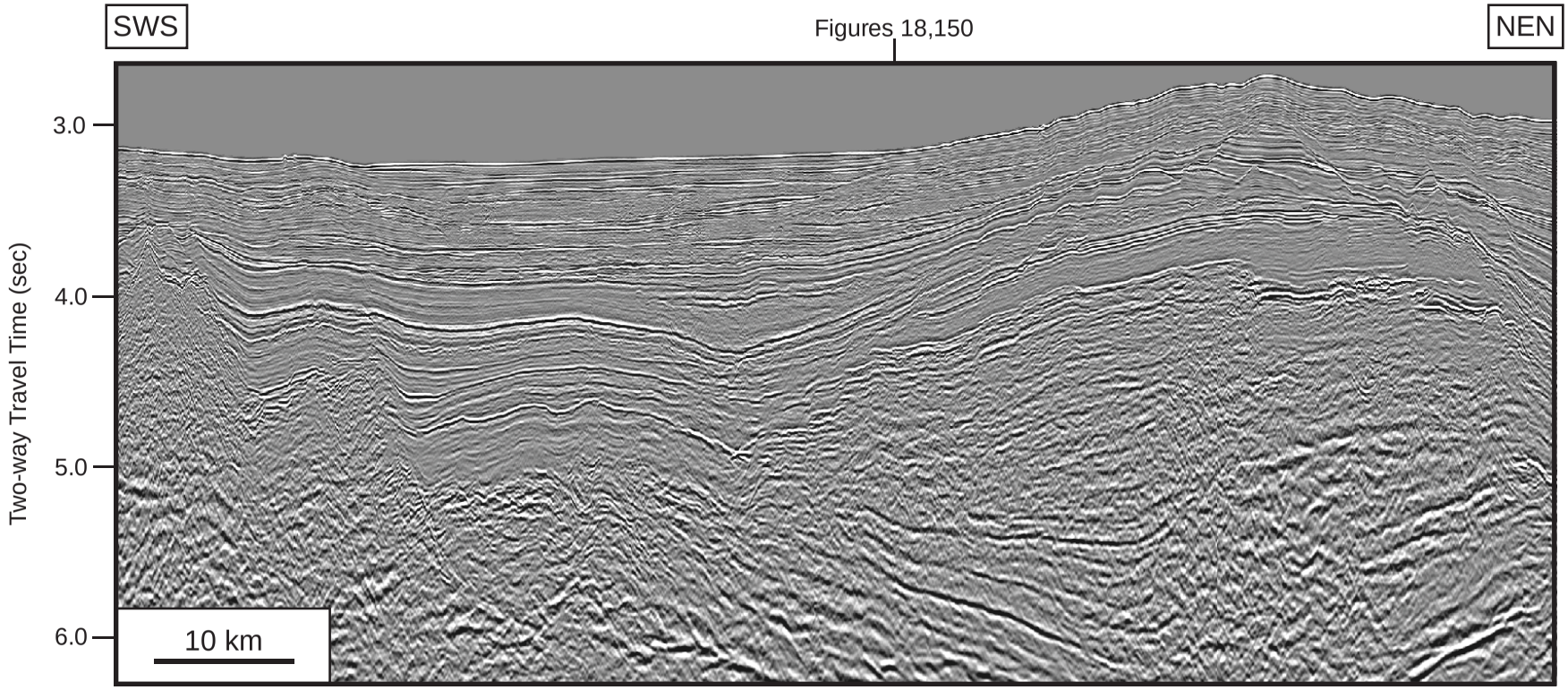

Figure 152a. Uninterpreted regional strike-oriented seismic profile (br-98:br98-083). Location of the profile is shown in Figures 142-143, 148-149 and location of where Figures 18, 150 crosses the profile.

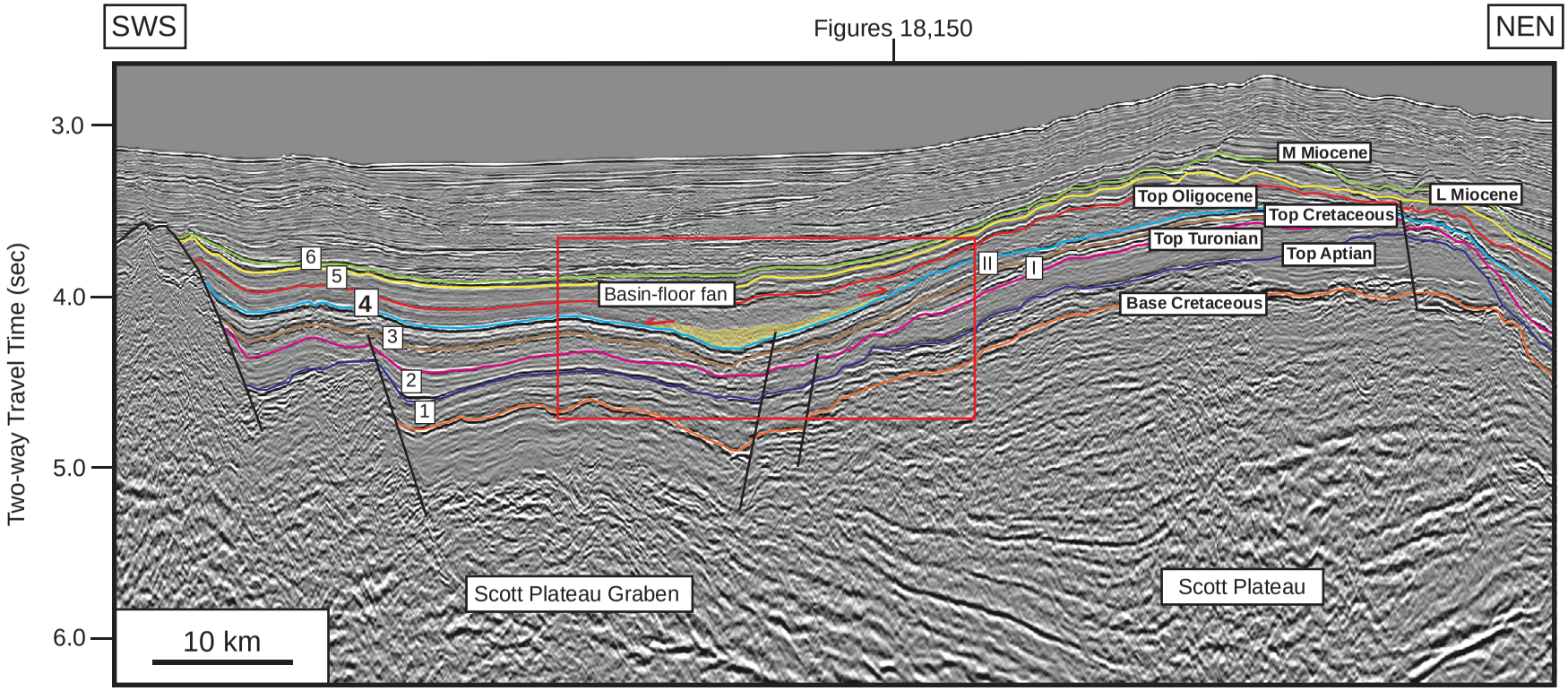

Figure 152b. Regional strike-oriented seismic profile showing all interpreted sequence boundaries from base Cretaceous to middle Miocene. This profile shows the deeper area of the Scott Plateau and the shallower area of the Scott Plateau. The basin-floor fan is observed within the Megasequence 4 (yellow shade). Location of the profile is shown in Figures 142-143, 148-149 and location of where Figures 18, 150 crosses the profile.

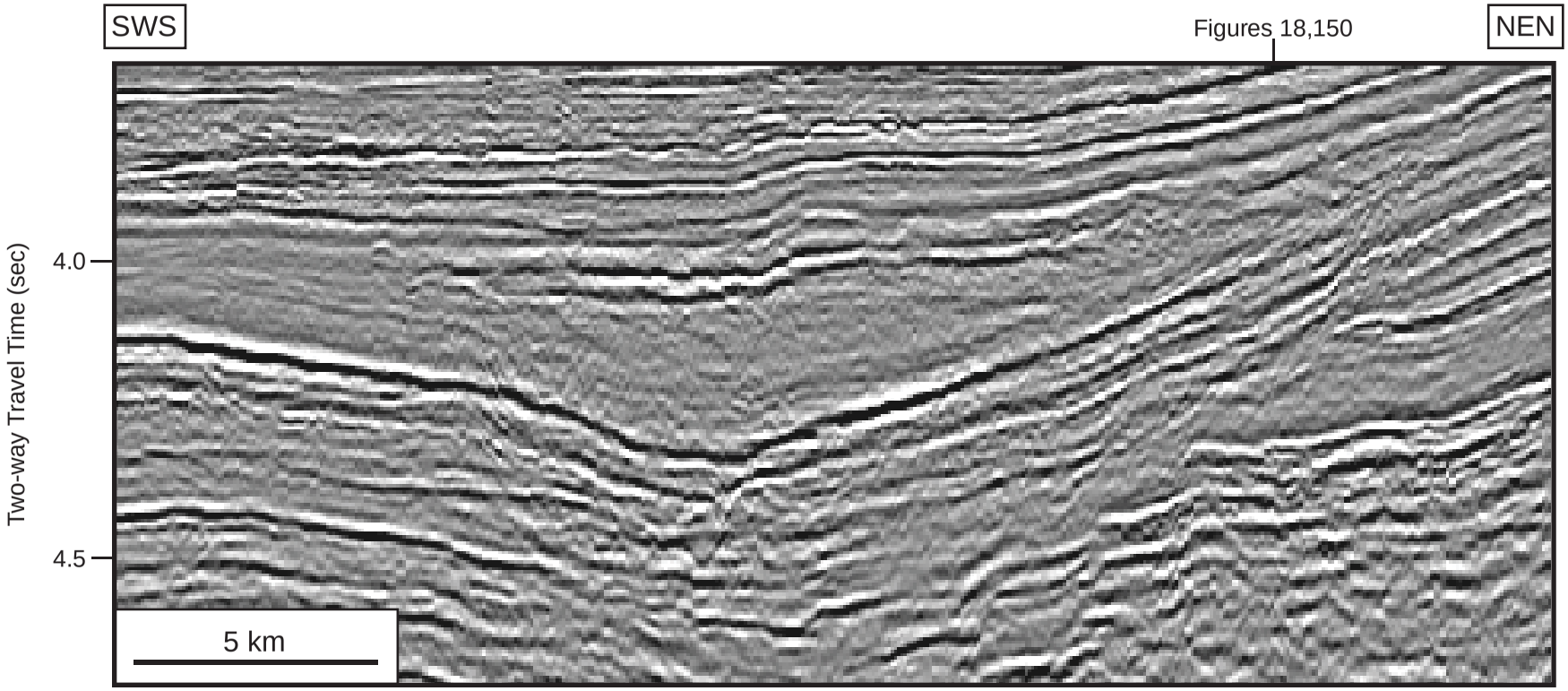

Figure 153a. Uninterpreted regional strike-oriented seismic profile (br-98:br98-083): A closeup view of Figure 152.

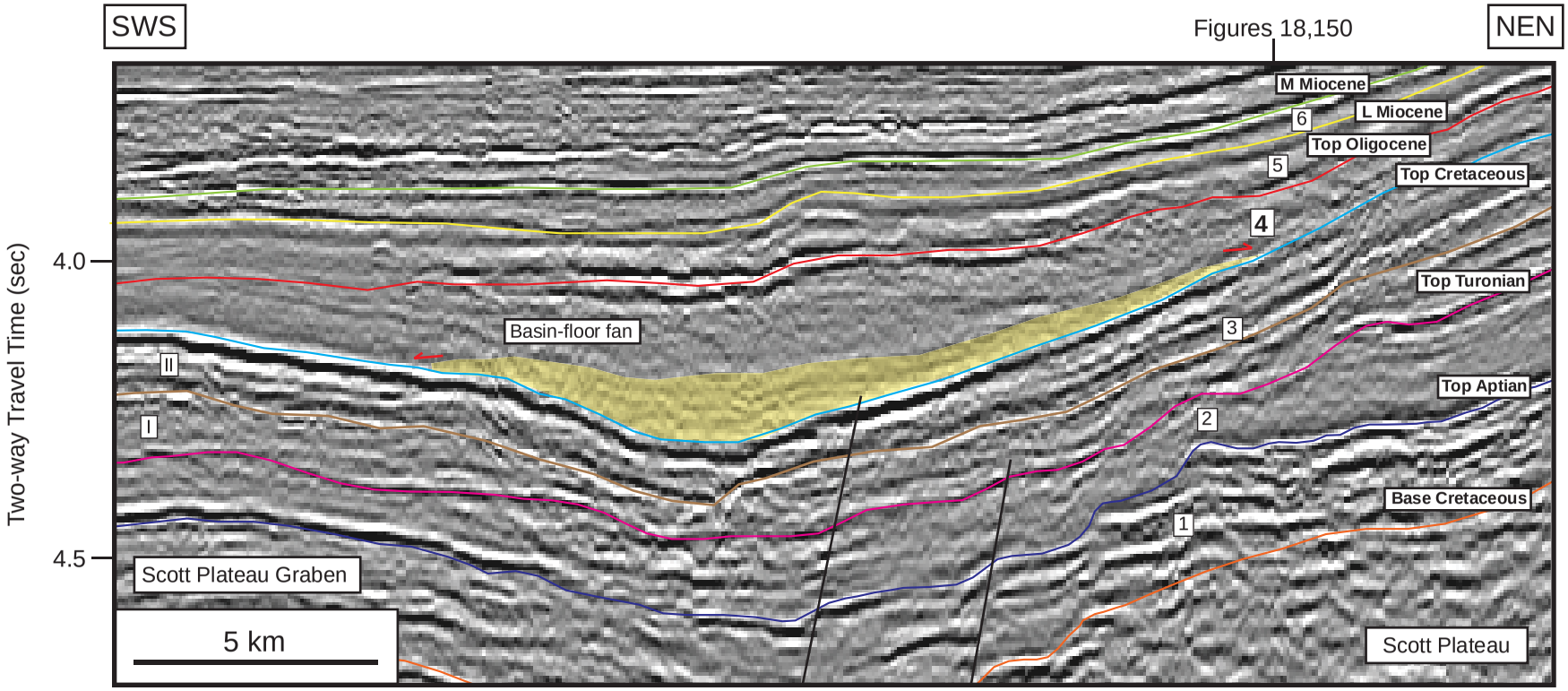

Figure 153b. Regional strike-oriented seismic profile showing all interpreted sequence boundaries from base Cretaceous to middle Miocene: A closeup view of Figure 152. The basin-floor fan is observed within the Megasequence 4 (yellow shade).

potential petroleum prospects in this area. The dip and strike oriented seismic profiles are shown in Figures 150-153.

Megasequence 5: top Oligocene to lower Miocene (23.0-19.0 Ma) interval

Megasequence 5 developed after a transgression cycle and can be recognized from the regional seismic profiles. The shelf edge moved landward at least 30 km associated with the relative sea level. The megasequence then prograded about 20 km across the pre-existing shelf. The pgogradation did not advance to the shelf edge of the underlying megasequence 4. Because of the relative thinness of the interval, the number of possible depositional sequences that are present is unknown. The lower (Top Oligocene horizon) is defined by a prominent downlap surface. The top Lower Miocene is erosional sequence boundary in certain area.

In the time structural contour map, the two-way travel time value varies between 630 to 4053 msec. The lowest relief is in the Scott Plateau Graben where as the shallowest area is on the Scott Platform (Figure 154).

The isochron map shows significant differences time thickness values between iso-thin in the Barcoo Syncline and higher time thickness of the adjacent area of the Barcoo Platform (Figure 155). The values range from 0 to 389 msec two-way travel time (TWTT).

Five seismic facies have been mapped in this sequence (Figure 160; Table 16). Seismic facies 1 and 4 correlated throughout most of the megasequence which is a

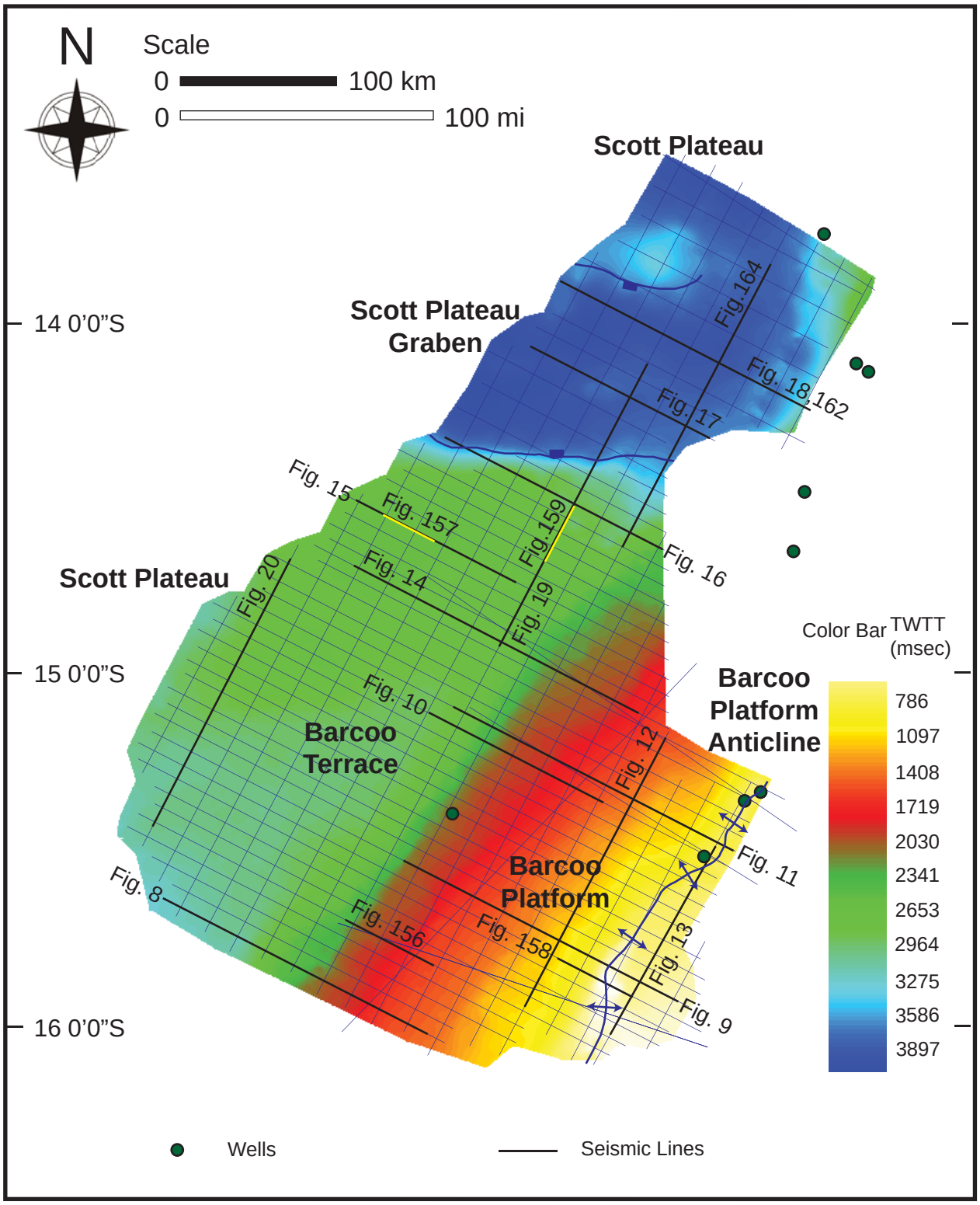

Figure 154. Time structural contour map (in TWTT msecs) of lower Miocene: 19.0 Ma (Megasequence 5). Distribution of 2D seismic profiles interpreted to generate the maps are shown by white lines, and wells are shown by green dots. Locations of Figures 8-20, 156-159, 162-165 are shown.

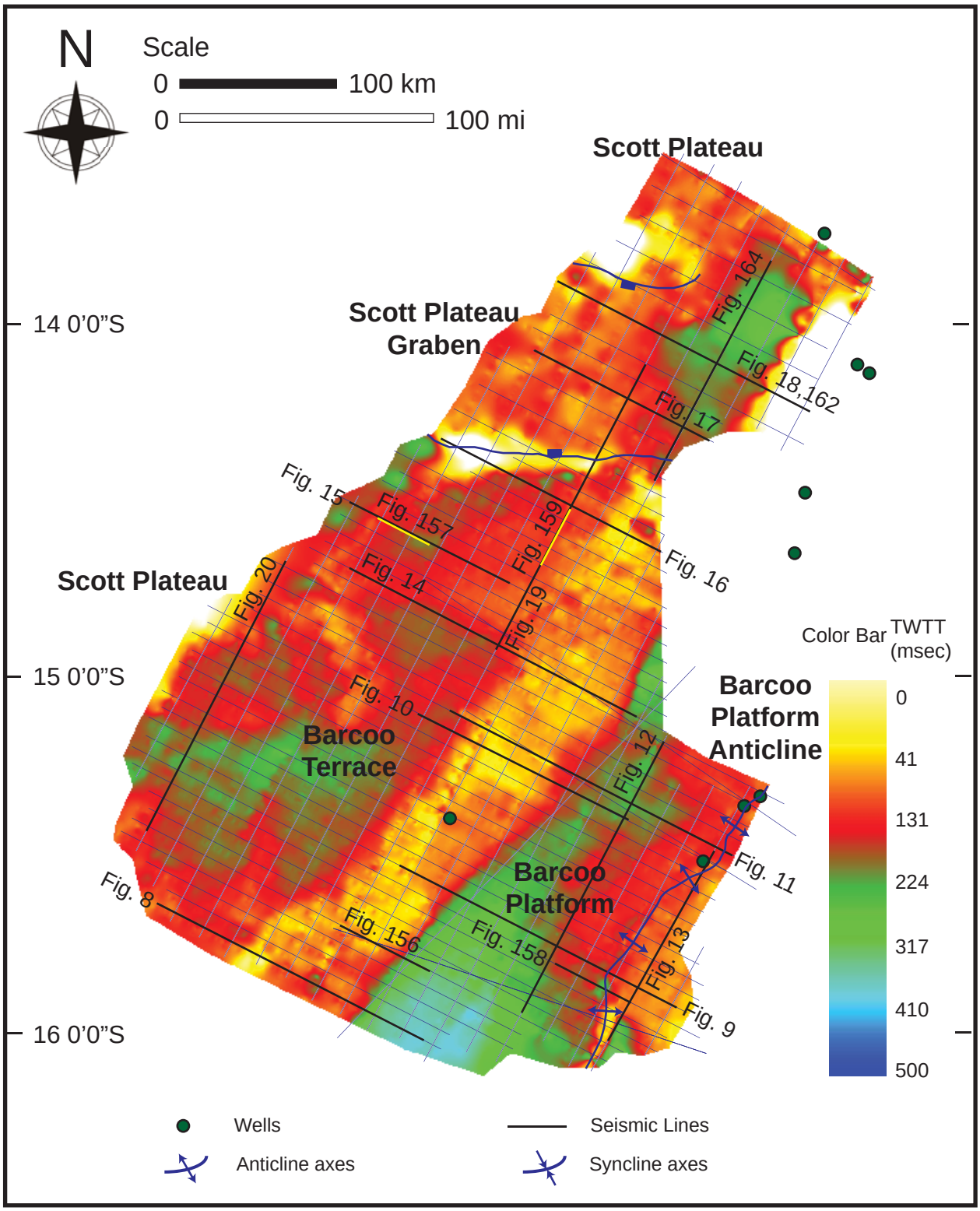

Figure 155. Isochron map (in TWTT msecs) of Megasequence 5 (top Oligocene to lower Miocene: 23.0-19.0 Ma) interval. Distribution of 2D seismic profiles interpreted to generate the maps are shown by white lines, and wells are shown by green dots. Location of Figures 8-20, 156-159, 162-165 are shown.

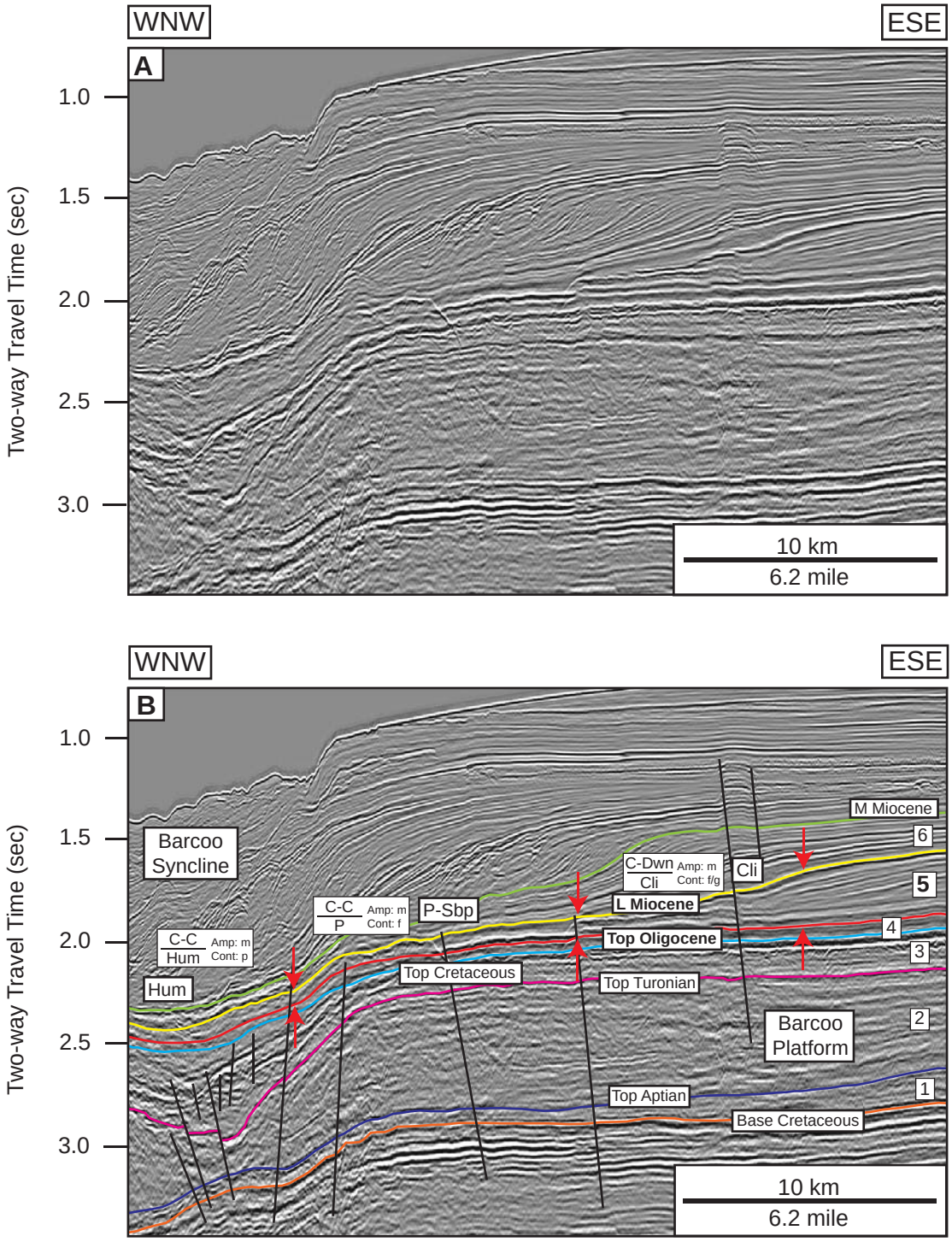

Figure 156. Dip-oriented seismic profile showing seismic facies of Megasequence 5 (top Oligocene to lower Miocene: 23.0-19.0 Ma) interval: (a) uninterpreted, (b) interpreted. The distinct prograding clinoform morphology is the major characteristic of this megasequence. See Table 2 for codes and abbreviations and Figures 154-155, 160-161 for location of the profile.

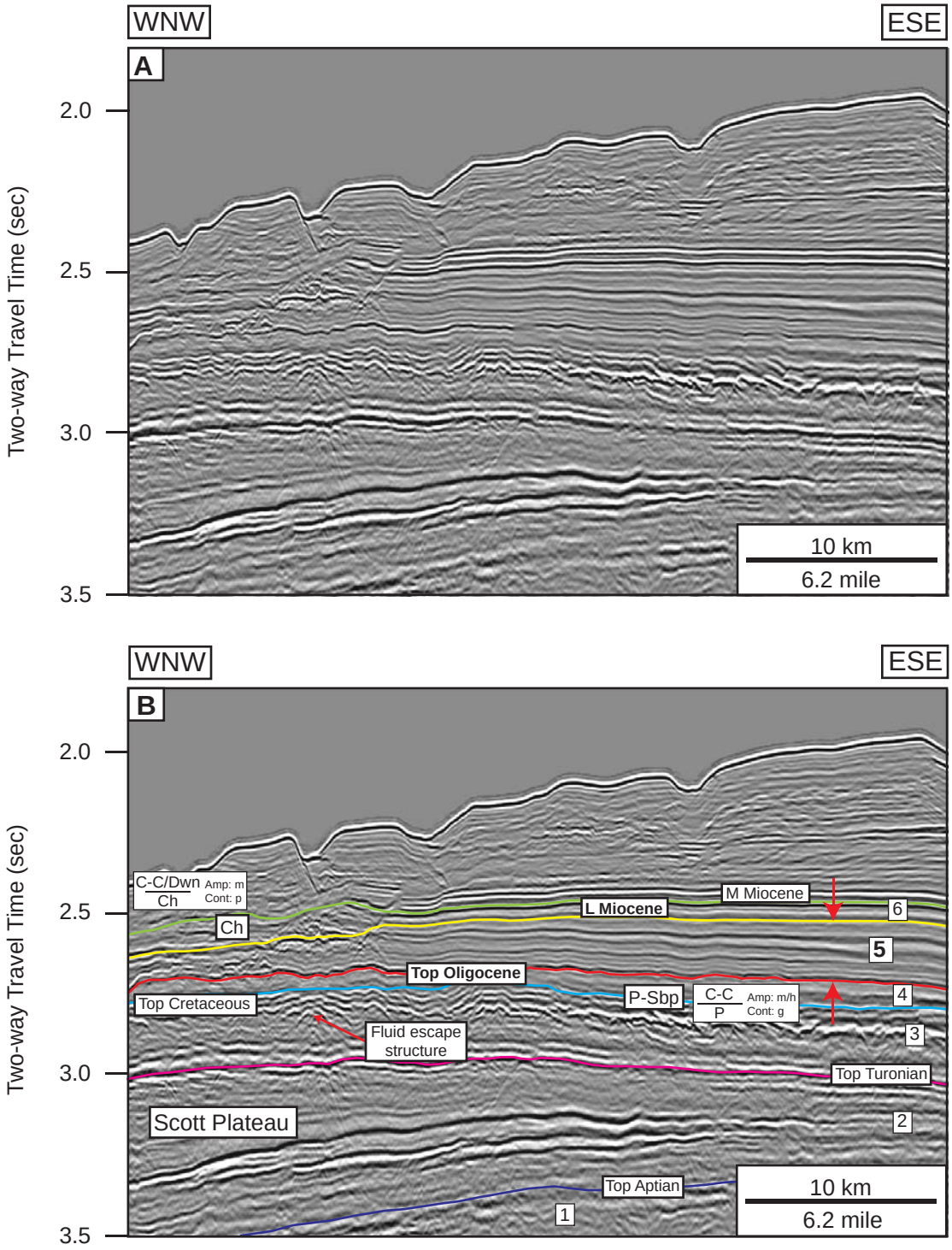

Figure 157. Dip-oriented seismic profile showing seismic facies of Megasequence 5 (top Oligocene to lower Miocene: 23.0-19.0 Ma) interval: (a) uninterpreted, (b) interpreted. This sequence shows the very good continuous and parallel seismic reflections. See Table 2 for codes and abbreviations and Figures 154-155, 160-161 for location of the profile.

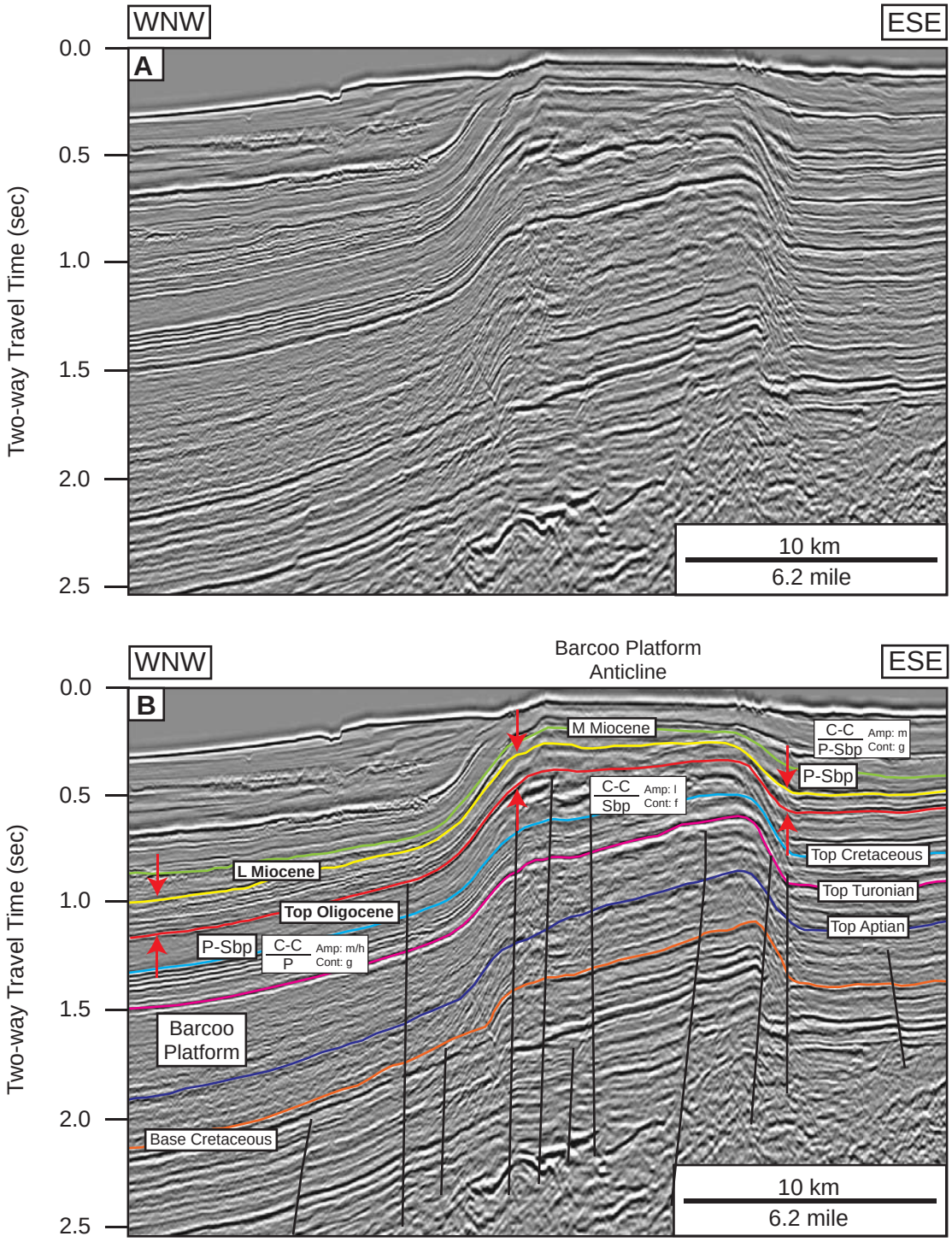

Figure 158. Dip-oriented seismic profile showing seismic facies of Mega-sequence 5 (top Oligocene to lower Miocene: 23.0-19.0 Ma) interval: (a) uninterpreted, (b) interpreted. See Table 2 for codes and abbreviations and Figures 154-155, 160-161 for location of the profile.

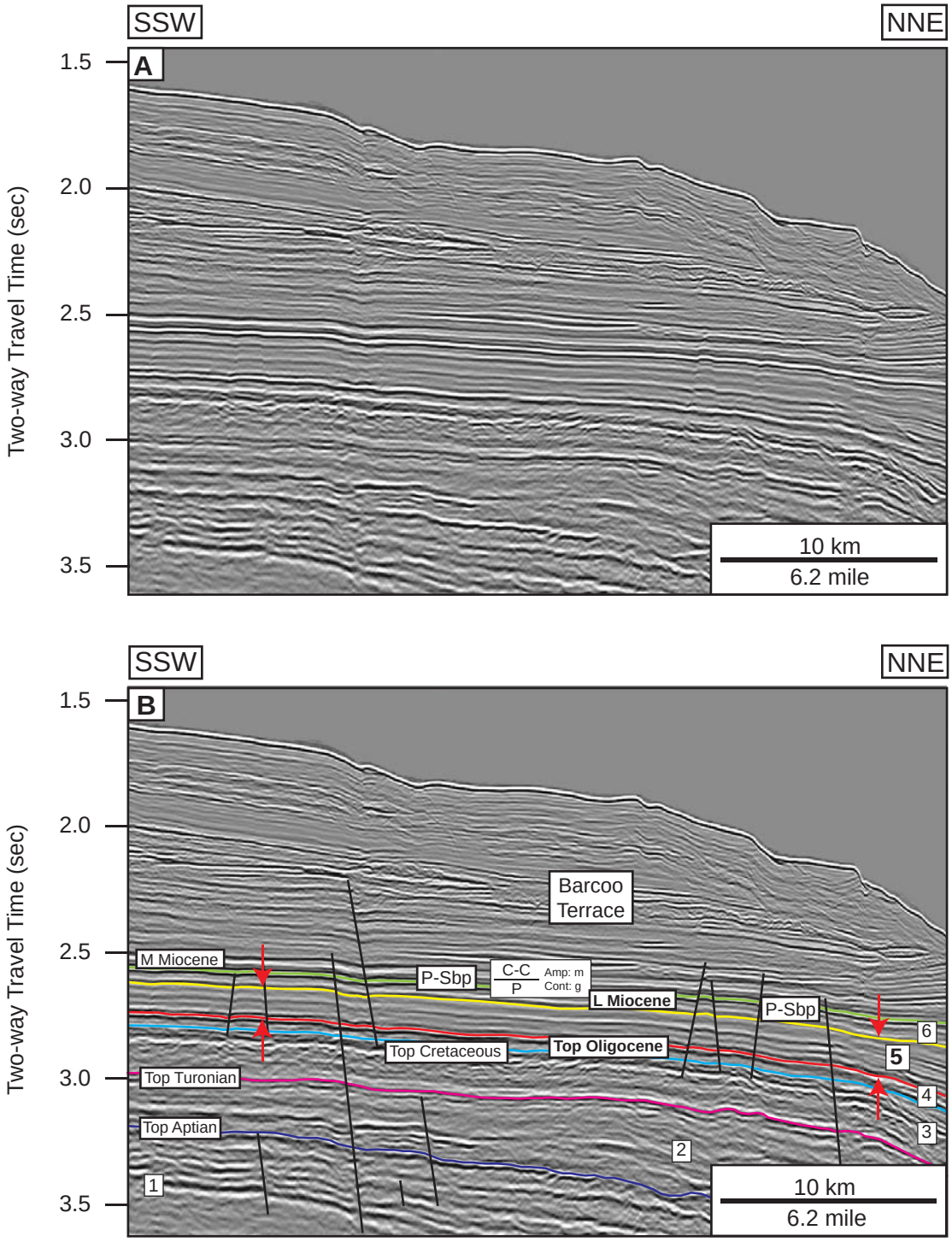

Figure 159. Strike-oriented seismic profile showing seismic facies of Mega-sequence 5 (top Oligocene to lower Miocene: 23.0-19.0 Ma) interval: (a) uninterpreted, (b) interpreted. See Table 2 for codes and abbreviations and Figures 154-155, 160-161 for location of the profile.

parallel to subparallel reflections with moderate amplitude in the middle part, and high amplitude in the upper and lower part (Figures 156-159). The seismic reflection continuity is fair to good. Lombardina-1 and Sheherazade-1 wells penetrate in seismic facies 1. Well log data shows the sand-prone interval (Figures 23, 25).

Table 16. Seismic facies and geologic interpretation of Megasequence 5: 23.0-19.0 Ma.

Seismic Facies	Upper Sequence Boundary	Lower Sequence Boundary	Internal Reflection Configuration	Amplitude	Continuity	Geologic Interpretation
1	Concordant	Concordant	Parallel to Subparallel	moderate to high	fair to good	Shelf deposits
2	Concordant	Downlap	Clinoform	moderate	fair to good	Prograding clinoform
3	Concordant	Concordant	Hummocky	moderate	poor	Inversion – related structure
4	Concordant	Concordant	Parallel to Subparallel	moderate to high	fair to good	Basinal deposits
5	Concordant	Concordant /Downlap	Chaotic	moderate	poor	Poor quality data

Facies 2 is characterized to be the clinoform facies (Figure 156). Its amplitude is moderate and continuity is fair to good. No wells penetrate in this seismic facies.

The internal configuration of seismic facies 3 (Figure 156) illustrates as hummocky with moderate amplitude and poor continuity which caused by the reactivation of Barcoo fault trend. Barcoo-1 well penetrates in facies1. The well log data shows the coarsening upward sequence of thick sandstone interval.

Seismic facies 5 is a disorganized and chaotic unit (Figure 157). The amplitude is moderate whereas the continuity is poor. No wells penetrate in seismic facies 5.

The geologic facies map of magesequence 5, Figure 161, shows main characteristic of this sequence is the distinct clinoform morphology which caused by the rate of sediment supply is higher than the rate of subsidence (Figure 156). The

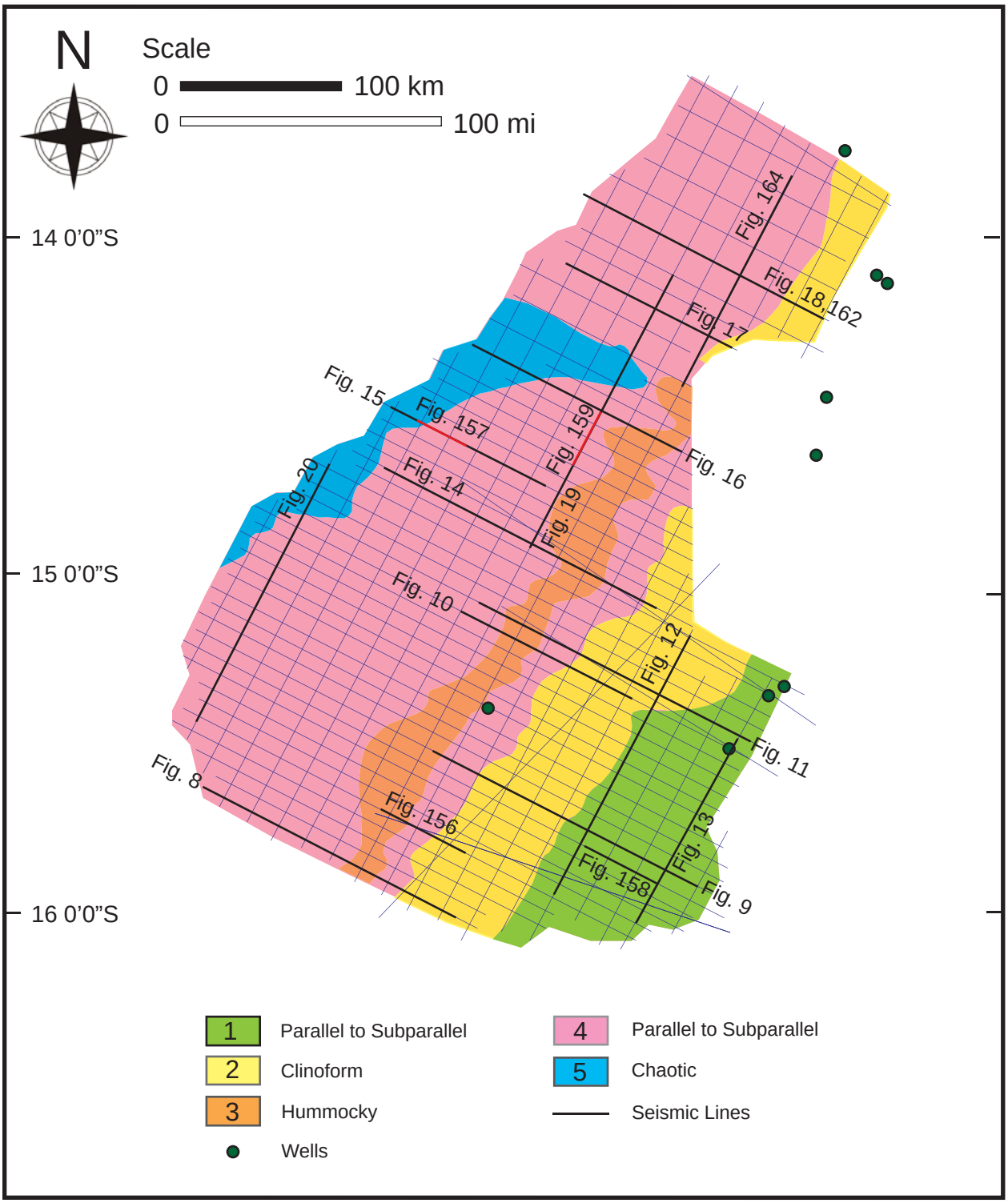

Figure 160. Seismic facies map of Megasequence 5 (top Oligocene to lower Miocene: 23.0-19.0 Ma) interval. Each facies is numbered as described in the text. See Table 2 for seismic facies coding and Table 7 for a summary of seismic facies analysis and geologic interpretation. Locations of Figures 8-20, 156-159, 162-165 (black lines) are shown, and wells are shown by green dots.

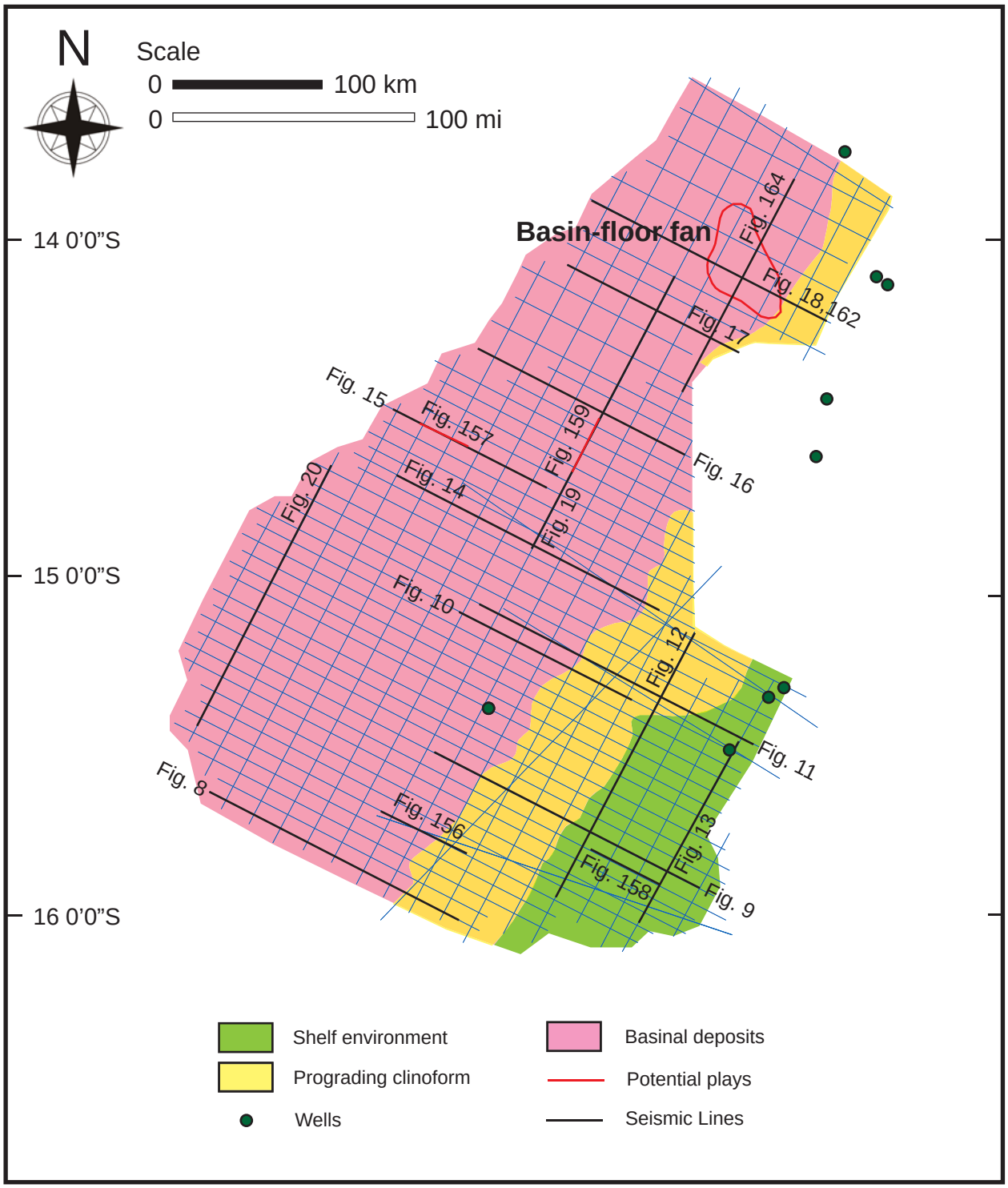

Figure 161. Geologic facies map of Megasequence 5 (top Oligocene to lower Miocene: 23.0-19.0 Ma) interval. See Table 7 for a summary of seismic facies analysis and geologic interpretation. Locations of Figures 8-20, 156-159, 162-165 (black lines) are shown, and wells are shown by green dots.

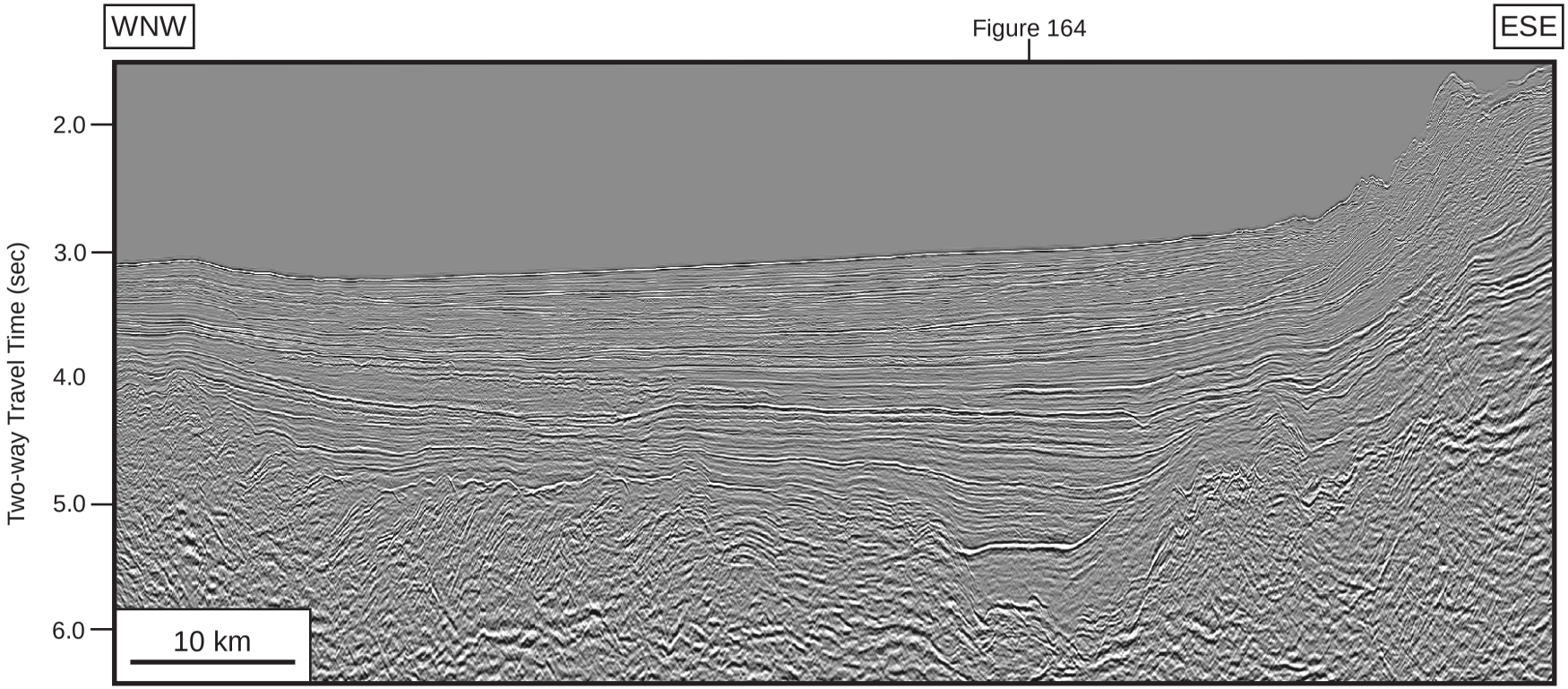

Figure 162a. Uninterpreted regional dip-oriented seismic profile (br-98:br98-057). Location of the profile is shown in Figures 154-155, 160-161 and location of where Figure 164 crosses the profile.

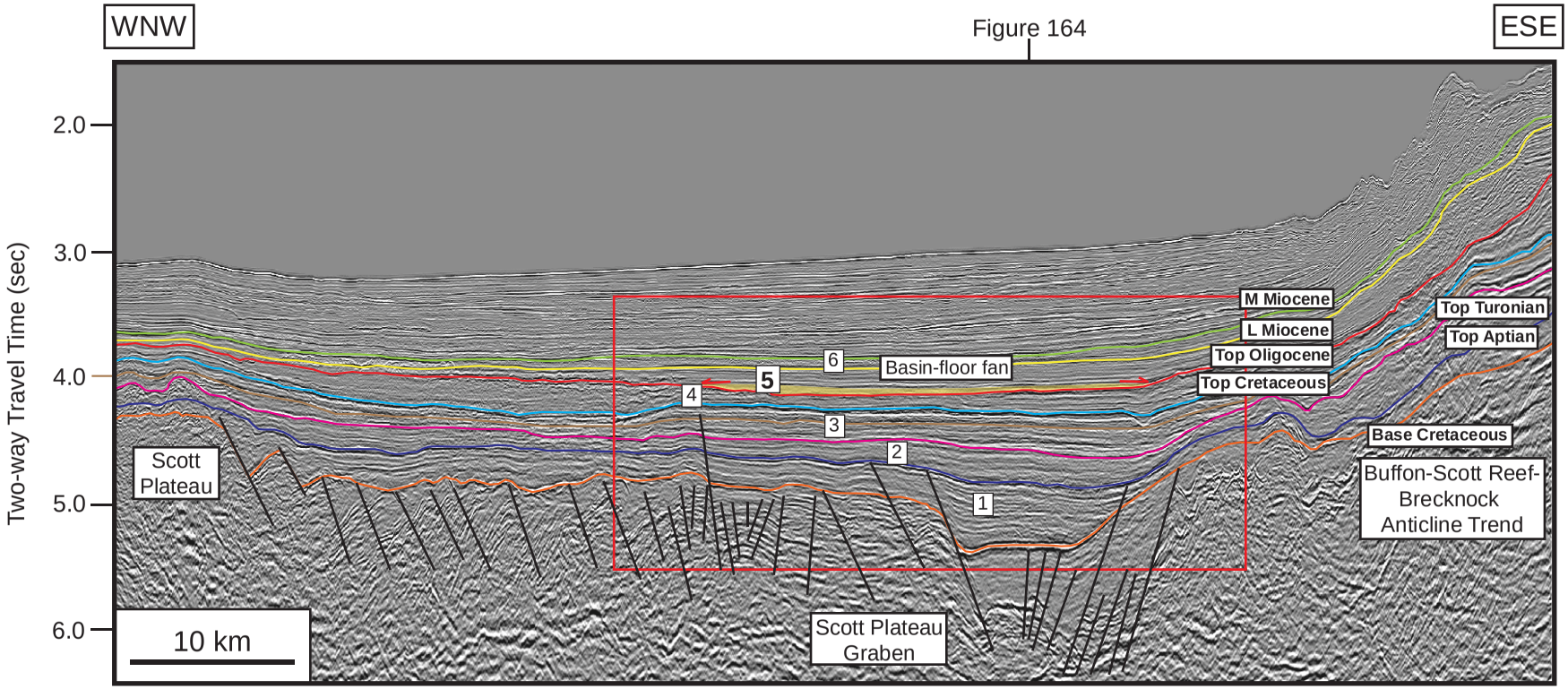

Figure 162b. Regional dip-oriented seismic profile showing all interpreted sequence boundaries from base Cretaceous to middle Miocene. This profile shows the deeper area of the Scott Plateau Graben and shallower area of the Buffon-Scott Reef-Brecknock Anticline Trend in the northern part of the study area. Series of faults in the underlying Jurassic strata caused the irregular topography. The basin-floor fan is observed within Megasequence 5 (yellow shade). Location of the profile is shown in Figures 154-155, 160-161 and location of where Figure 164 crosses the profile.

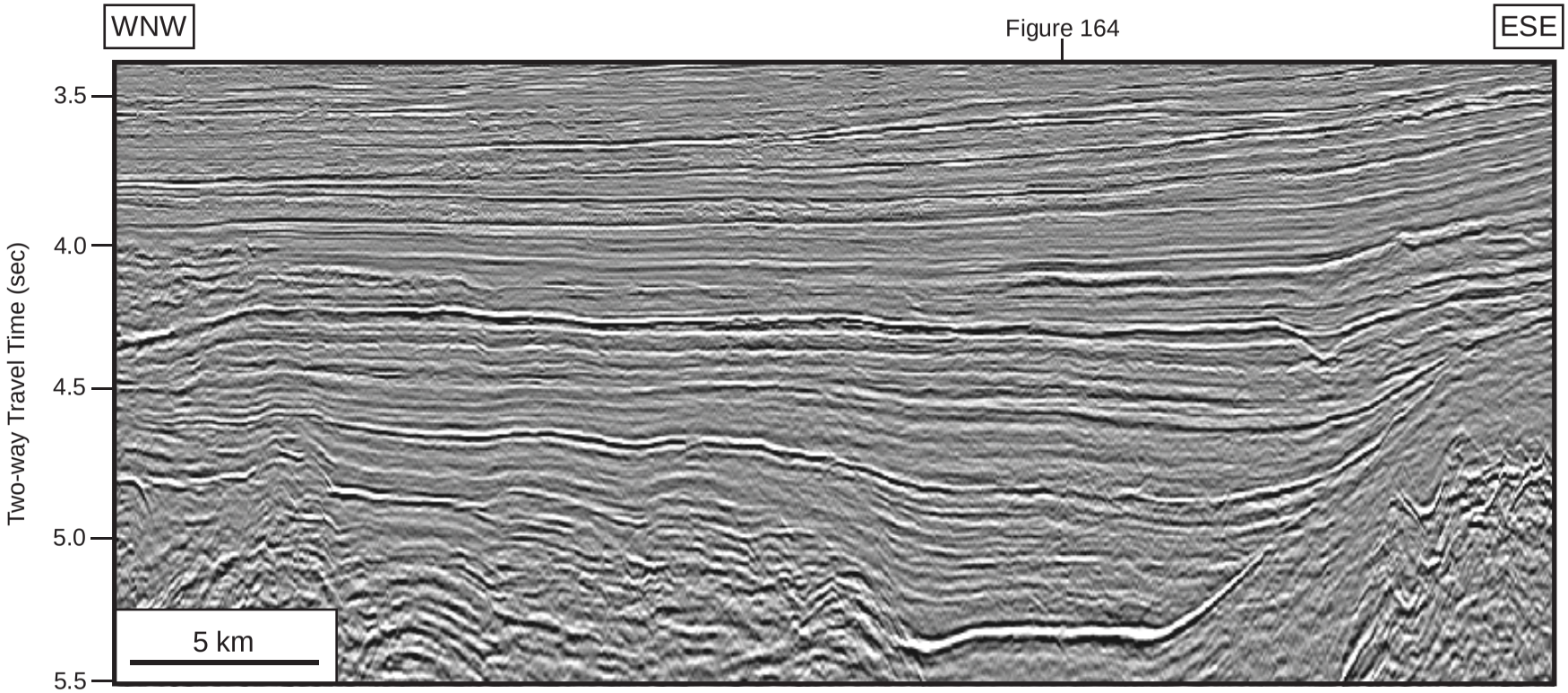

Figure 163a. Uninterpreted regional dip-oriented seismic profile (br-98:br98-057): A closeup view of Figure 162.

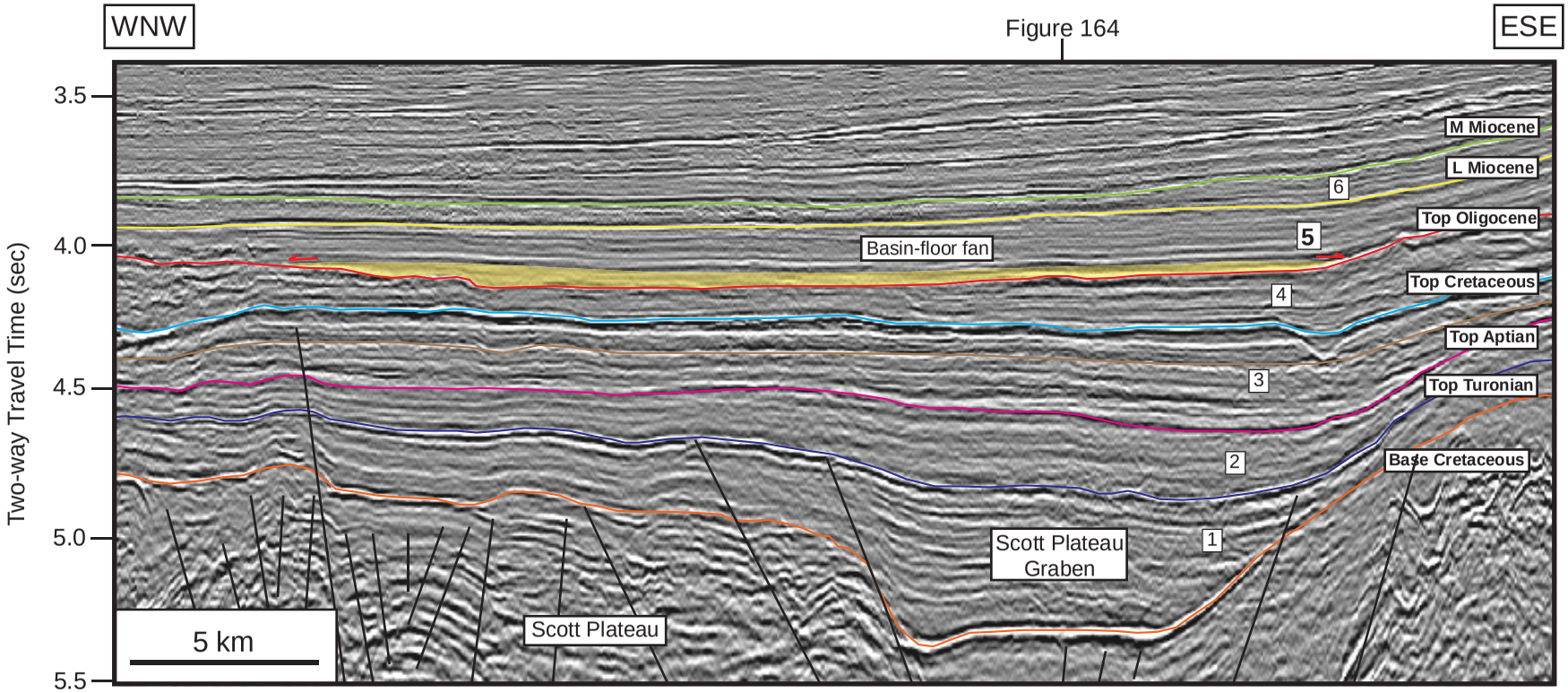

Figure 163b. Regional dip-oriented seismic profile showing all interpreted sequence boundaries from base Cretaceous to middle Miocene: A closeup view of Figure 162. The basin-floor fan is observed within Megasequence 5 (yellow shade).

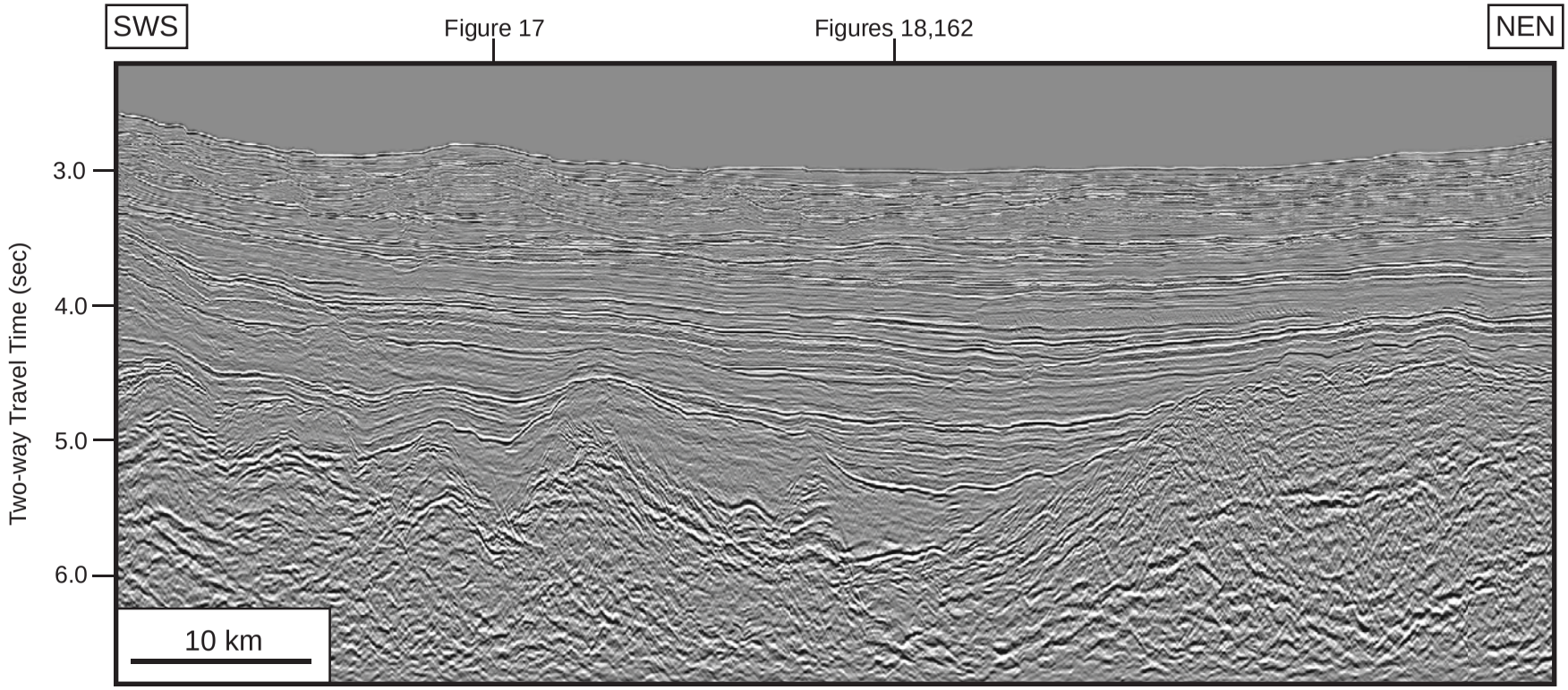

Figure 164a. Uninterpreted regional dip-oriented seismic profile (br-98:br98-080). Location of the profile is shown in Figures 154-155, 160-161 and locations of where Figures 17, 18, 162 cross the profile.

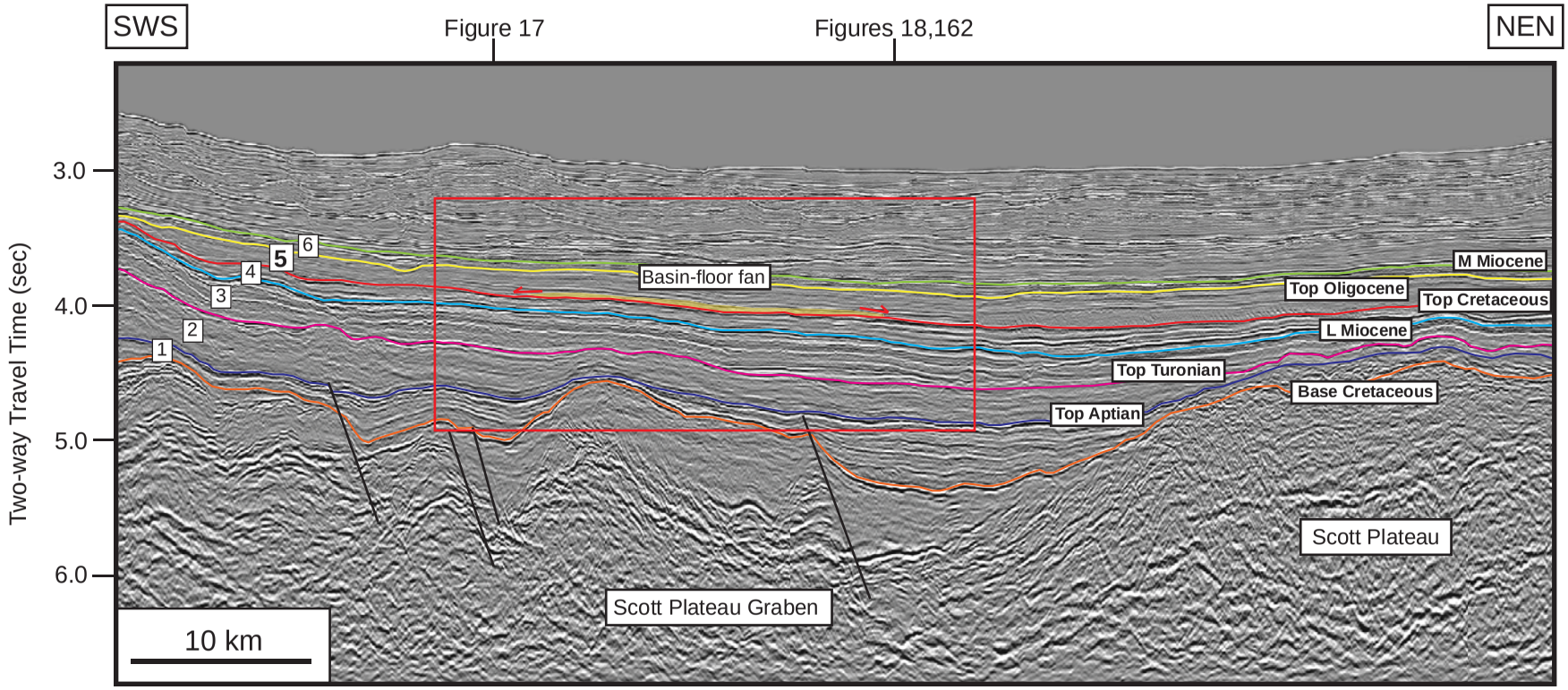

Figure 164b. Regional strike-oriented seismic profile showing all interpreted sequence boundaries from base Cretaceous to middle Miocene. This profile shows the area of the Scott Plateau Graben and the shallower area of the Scott Plateau. The basin-floor fan is observed within Megasequence 5 (yellow shade). Location of the profile is shown in Figures 154-155, 160-161 and locations of where Figures 17, 18, 162 cross the profile.

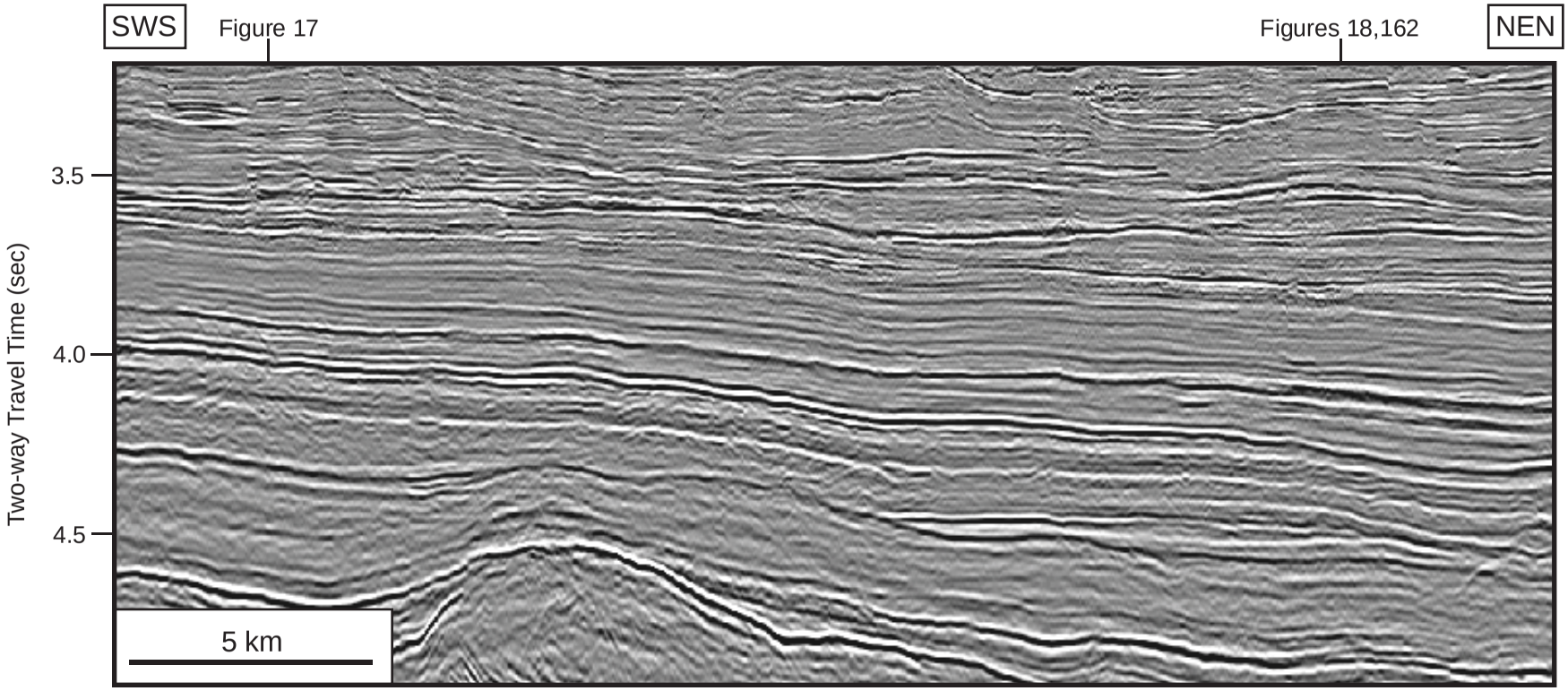

Figure 165a. Uninterpreted regional dip-oriented seismic profile (br-98:br98-080): A closeup view of Figure 164.

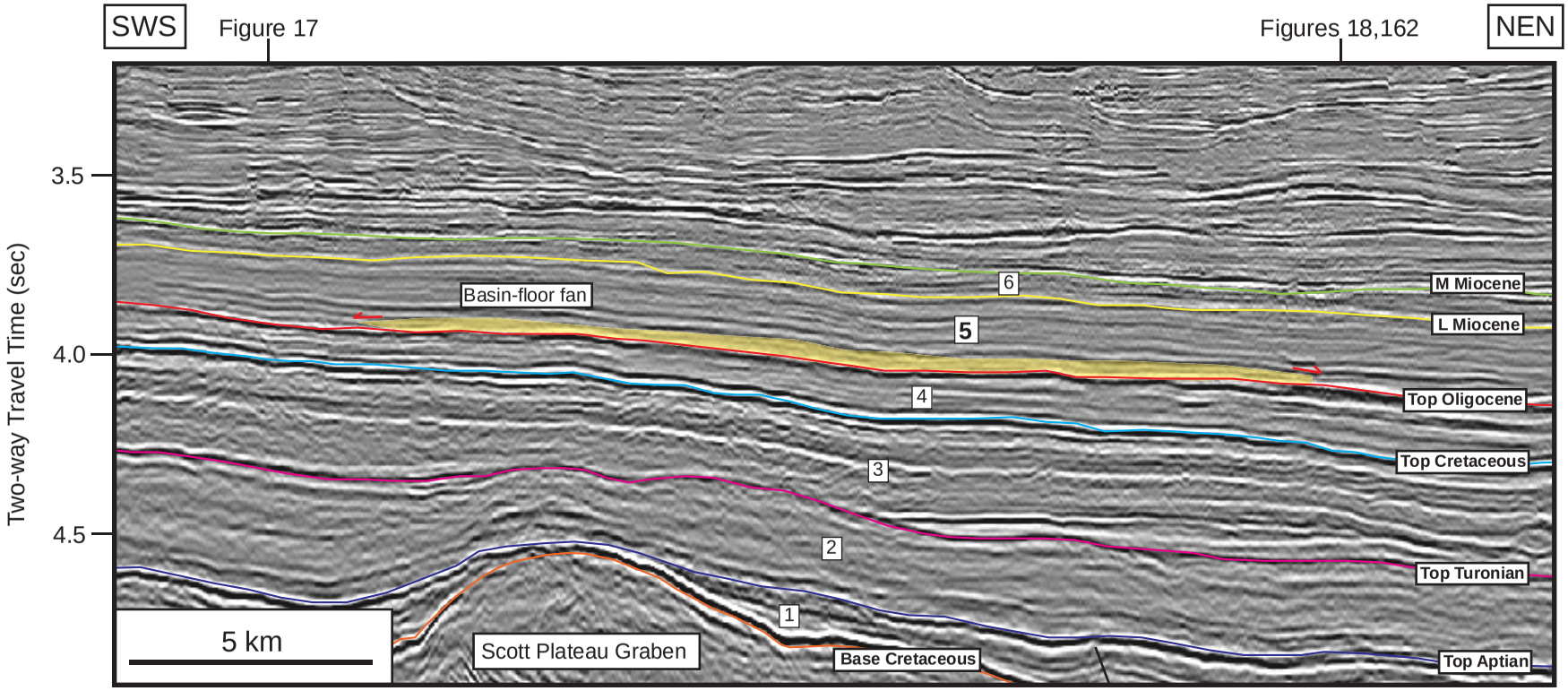

Figure 165b. Regional strike-oriented seismic profile showing all interpreted sequence boundaries from base Cretaceous to middle Miocene: A closeup view of Figure 164. The basin-floor fan is observed within Megasequence 5 (yellow shade).

Megasequence 6: lower Miocene to middle Miocene (19.0-14.2 Ma) interval

Similar to sequences 89.3-65.5, 65.5-23.0 and 23.0-19.0 Ma, three wells which are wells Barcoo-1, Lombardina-1 and Sheherzade-1, were penetrated through this stratigraphic unit. The lower Miocene and middle Miocene horizon which are the lower and upper surface boundaries of this sequence were picked from the bounding surface of the clinoform morphology. The time structural contour map (Figure 166) shows that the sediments were deposited thickening to the northwest into the basin center. The value of two-way travel time is varied from 603 to 4008 msec. At the eastern margin of the sub-basin, the Barcoo Platform anticline is observed next to the Leveque Shelf (Figures 9, 11 and 13).

The isochron map shows the constant thickness occurring along the edge between the Barcoo Platform and the Barcoo Syncline (Figure 167). The values range from 0 to 1497 msec two-way travel time (TWTT). This sequence consists of five seismic facies (Figure 172). The summarized table is demonstrated in Table 17.

Table 17. Seismic facies and geologic interpretation of Megasequence 6: 19.0-14.2 Ma.

Seismic Facies	Upper Sequence Boundary	Lower Sequence Boundary	Internal Reflection Configuration	Amplitude	Continuity	Geologic Interpretation
1	Concordant	Concordant	Parallel to Subparallel	moderate	fair	Shelf deposits
2	Concordant	Downlap /Onlap	Clinoform	moderate to high	good	Prograding clinoform
3	Concordant	Concordant	Hummocky	moderate	fair	Inversion – related structure
4	Concordant	Concordant	Parallel to Subparallel	moderate	fair	Basinal deposits
5	Concordant	Concordant	Chaotic	low to moderate	poor	Poor quality data

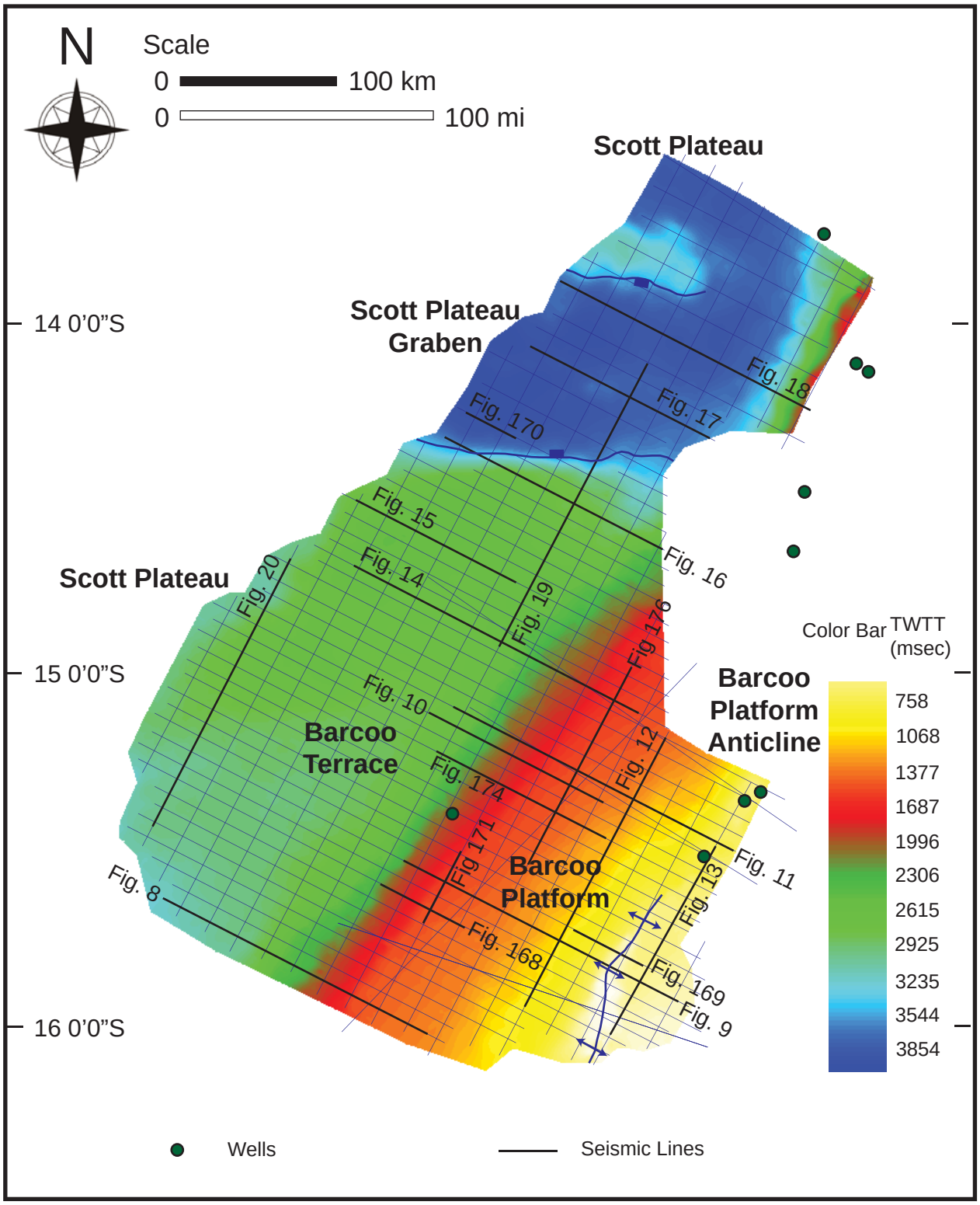

Figure 166. Time structural contour map (in TWTT msecs) of middle Miocene: 14.2 Ma (Megasequence 6). Distribution of 2D seismic profiles interpreted to generate the maps are shown by white lines, and wells are shown by green dots. Locations of Figures 8-20, 168-171, 174-177 are shown.

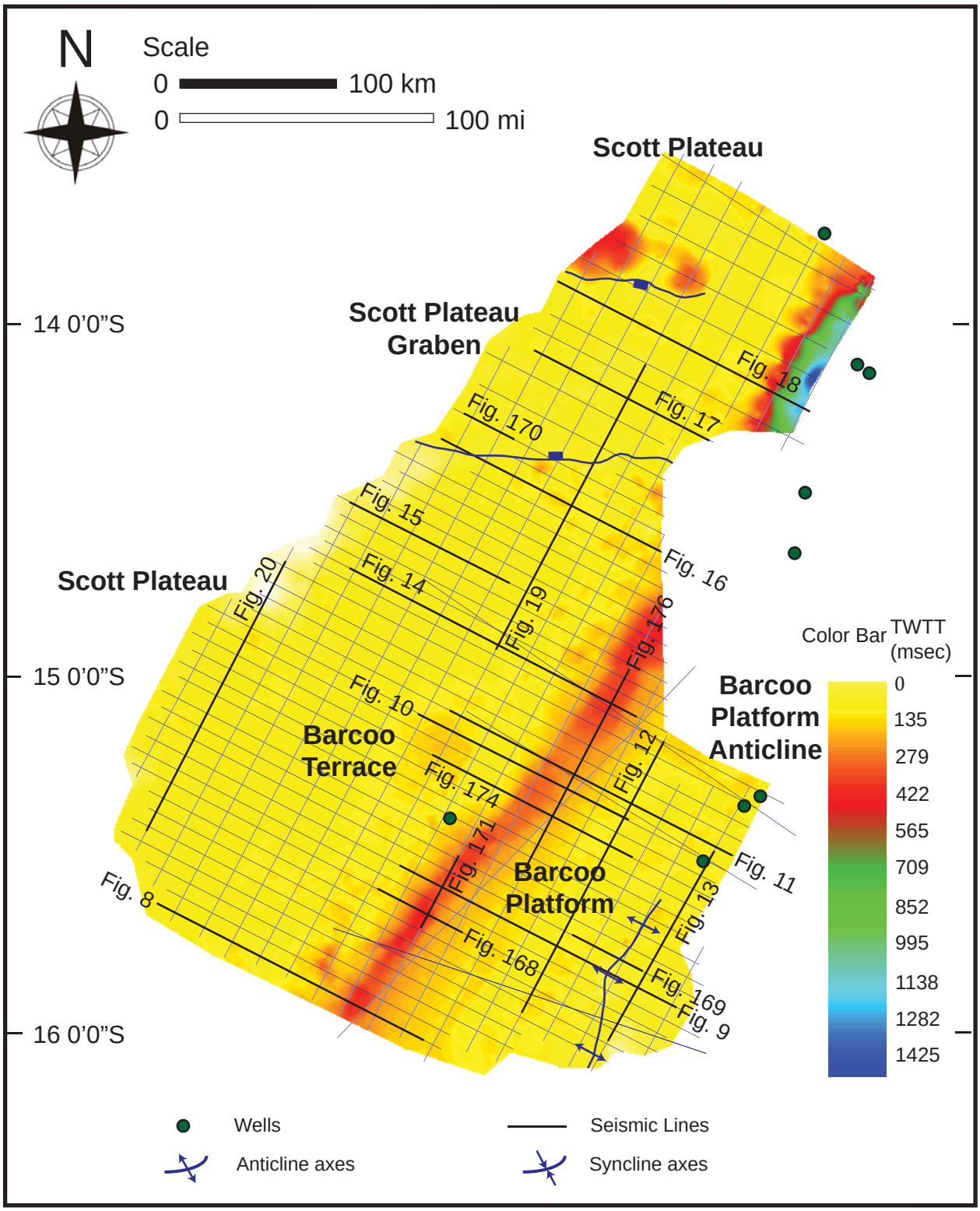

Figure 167. Isochron map (in TWTT msecs) of Megasequence 6 (lower Miocene to middle Miocene:19.0-14.2 Ma) interval. Distribution of 2D seismic profiles interpreted to generate the maps are shown by white lines, and wells are shown by green dots. Locations of Figures 8-20, 168-171, 174-177 are shown.

Facies 1 and 4 consist of parallel to subparallel internal reflection configuration with moderate amplitude and fair continuity. The seismic reflections sit concordantly on lower surface which is the middle Miocene sequence boundary (Figure 169).

The lower surface of seismic facies 2 (Figures 168, 171) is downlap/onlap onto the lower surface boundary. The internal configuration displays as clinoform with moderate amplitude and good continuity. Seismic facies 3 is characterized to be the hummocky internal reflection configuration. The seismic amplitude is moderate whereas the continuity is fair (Figure 168). Facies 5 shows chaotic internal reflection configuration. Its amplitude is low to moderate whereas the continuity is poor (Figure 170).

The geologic map of this sequence is in Figure 173. Megasequence 6 is covered by the shelf, clinoform and basin environments where channels, overbanks and deepwater deposits are recognized. Distinct prograding clinoform is the major aspect of this stratigraphic sequence due to the rate of sediment supply is higher than the rate of subsidence. The prograding sediments deposited with the external wedge shape is recognized (Figure 168). The lateral migrated channel is observed in this sequence as shown in Figure 178.

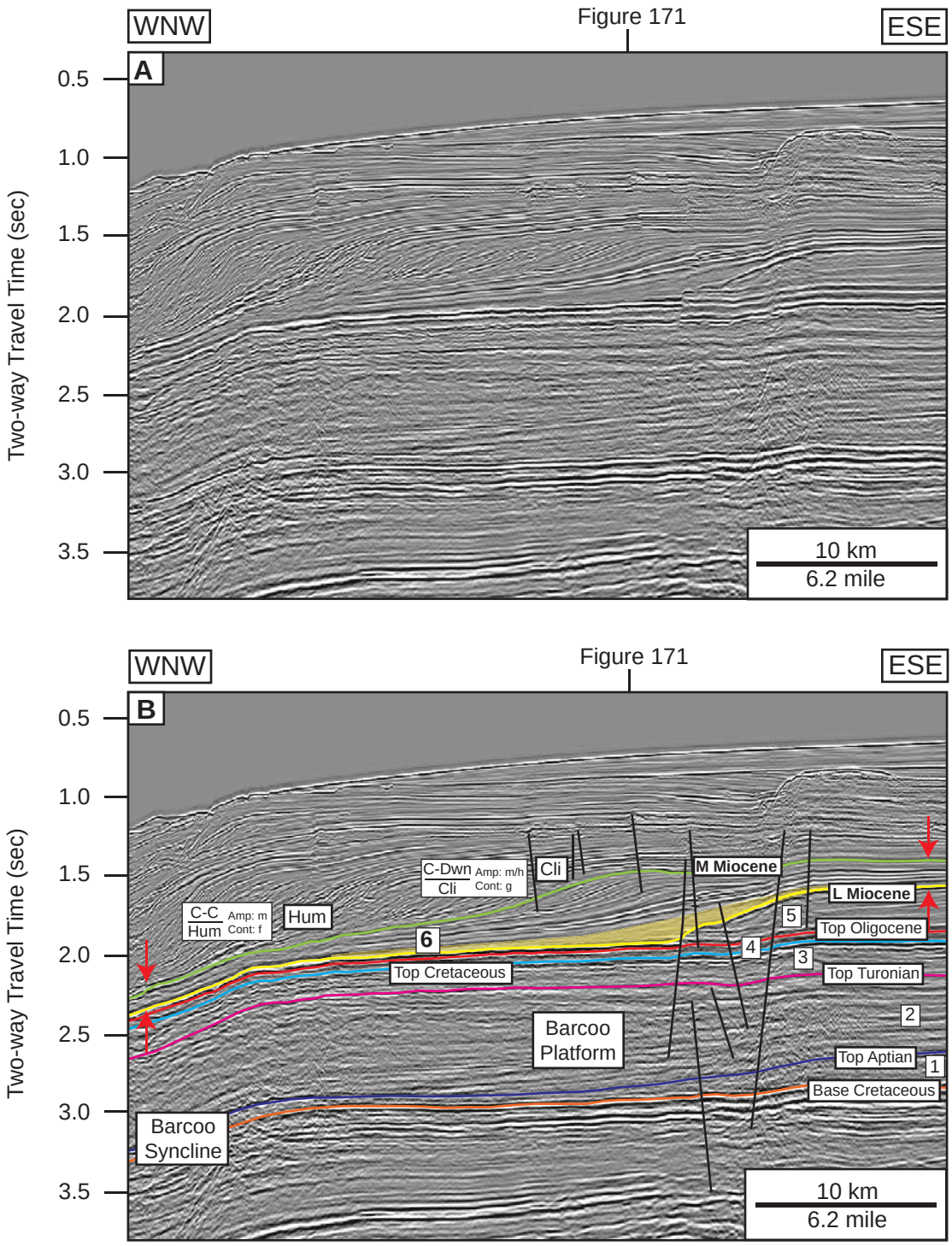

Figure 168. Dip-oriented seismic profile showing seismic facies of Megasequence 6: lower Miocene to middle Miocene (19.0-14.2 Ma) interval: (a) uninterpreted, (b) interpreted. The distinct prograding clinoform is the main characteristic of this megasequence. See Table 2 for codes and abbreviations and Figures 166-167, 172-173 for location of the profile and location of where Figure 171 crosses the profile.

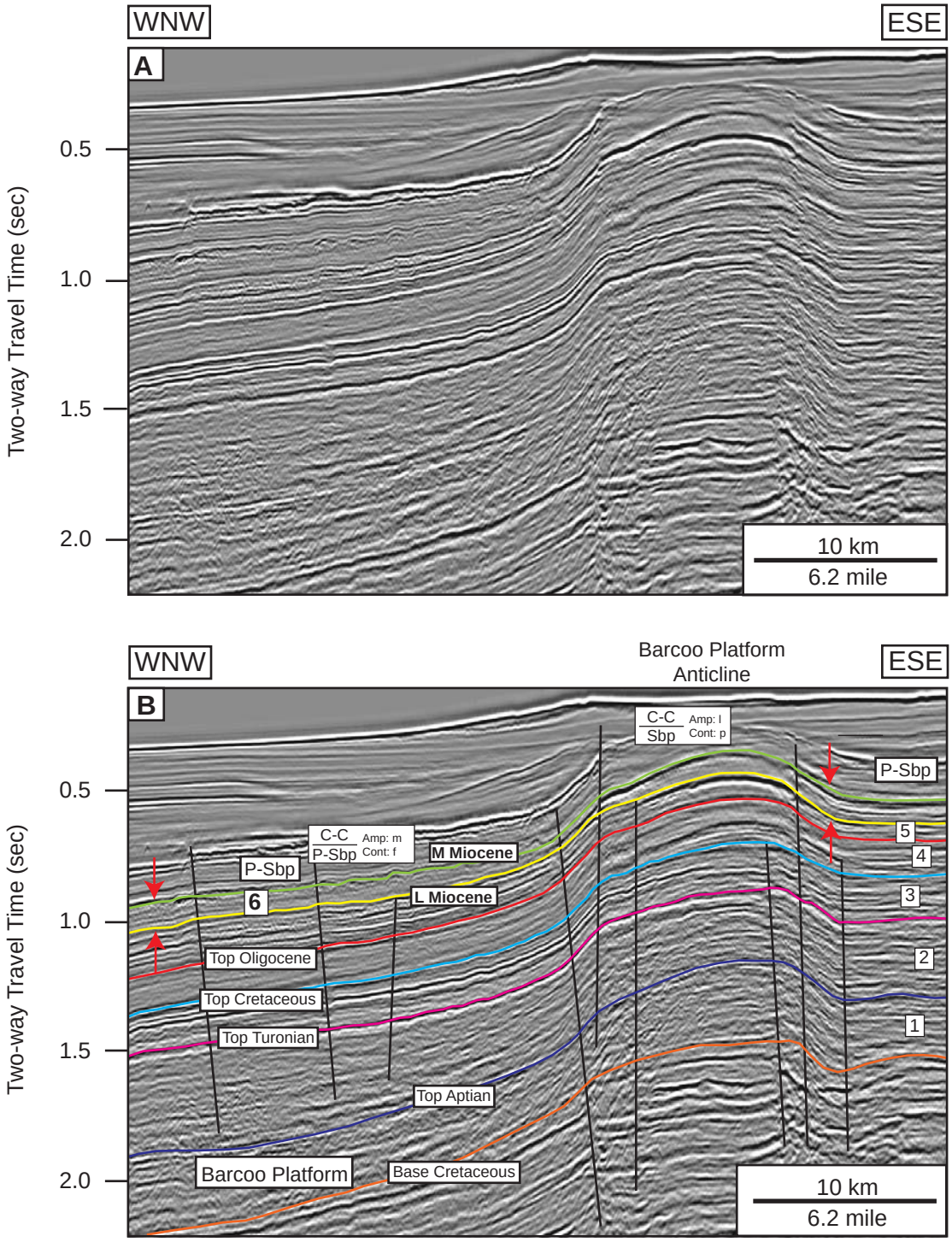

Figure 169. Dip-oriented seismic profile showing seismic facies of Mega-sequence 6 (lower Miocene to middle Miocene: 19.0-14.2 Ma) interval: (a) uninterpreted, (b) interpreted. See Table 2 for codes and abbreviations and Figures 166-167, 172-173 for location of the profile.

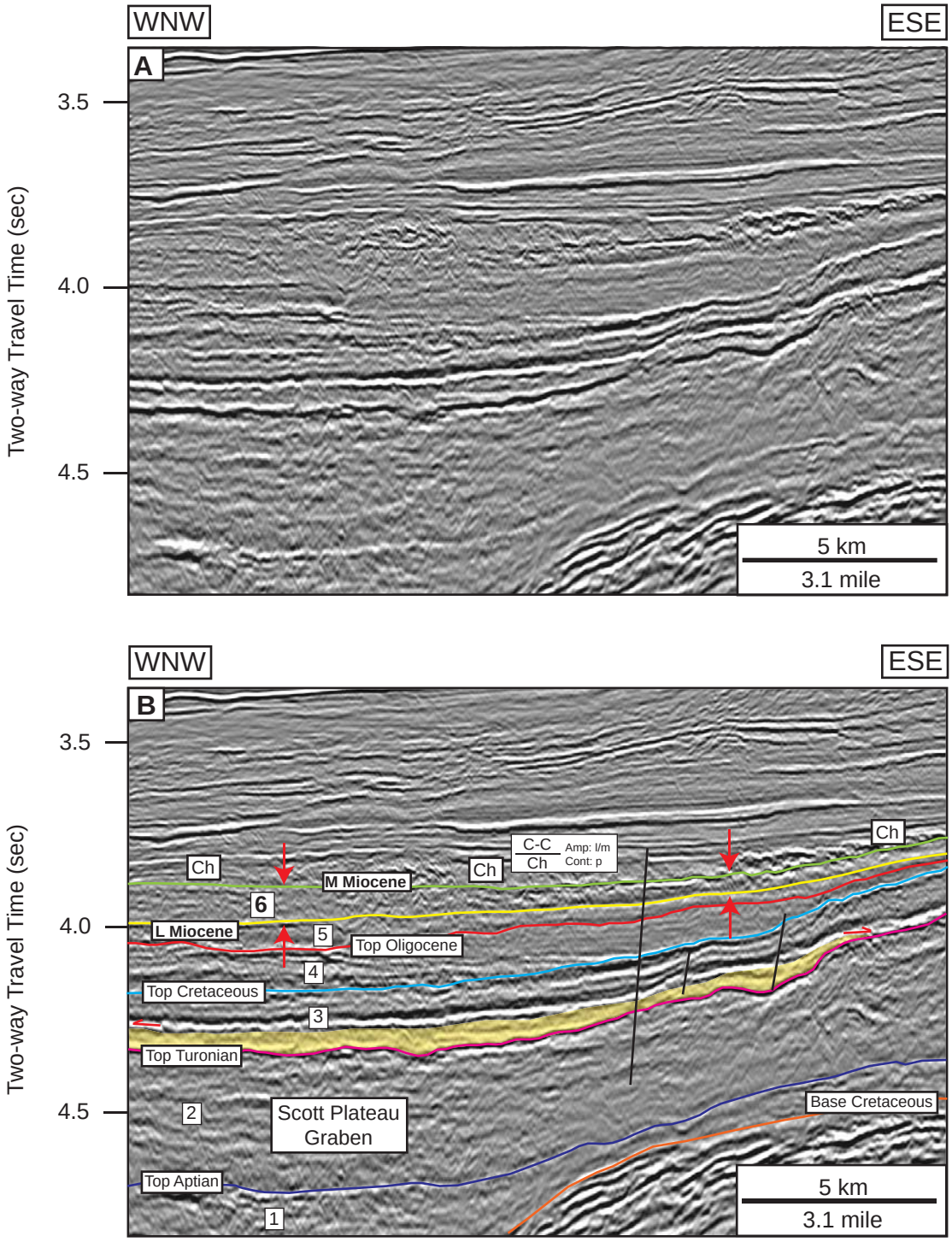

Figure 170. Dip-oriented seismic profile showing seismic facies of Megasequence 6 (lower Miocene to middle Miocene: 19.0-14.2 Ma) interval: (a) uninterpreted, (b) interpreted. The basin-floor fan is observed (yellow shade) in Megasequence 3. See Table 2 for codes and abbreviations and Figures 166-167, 172-173 for location of the profile.

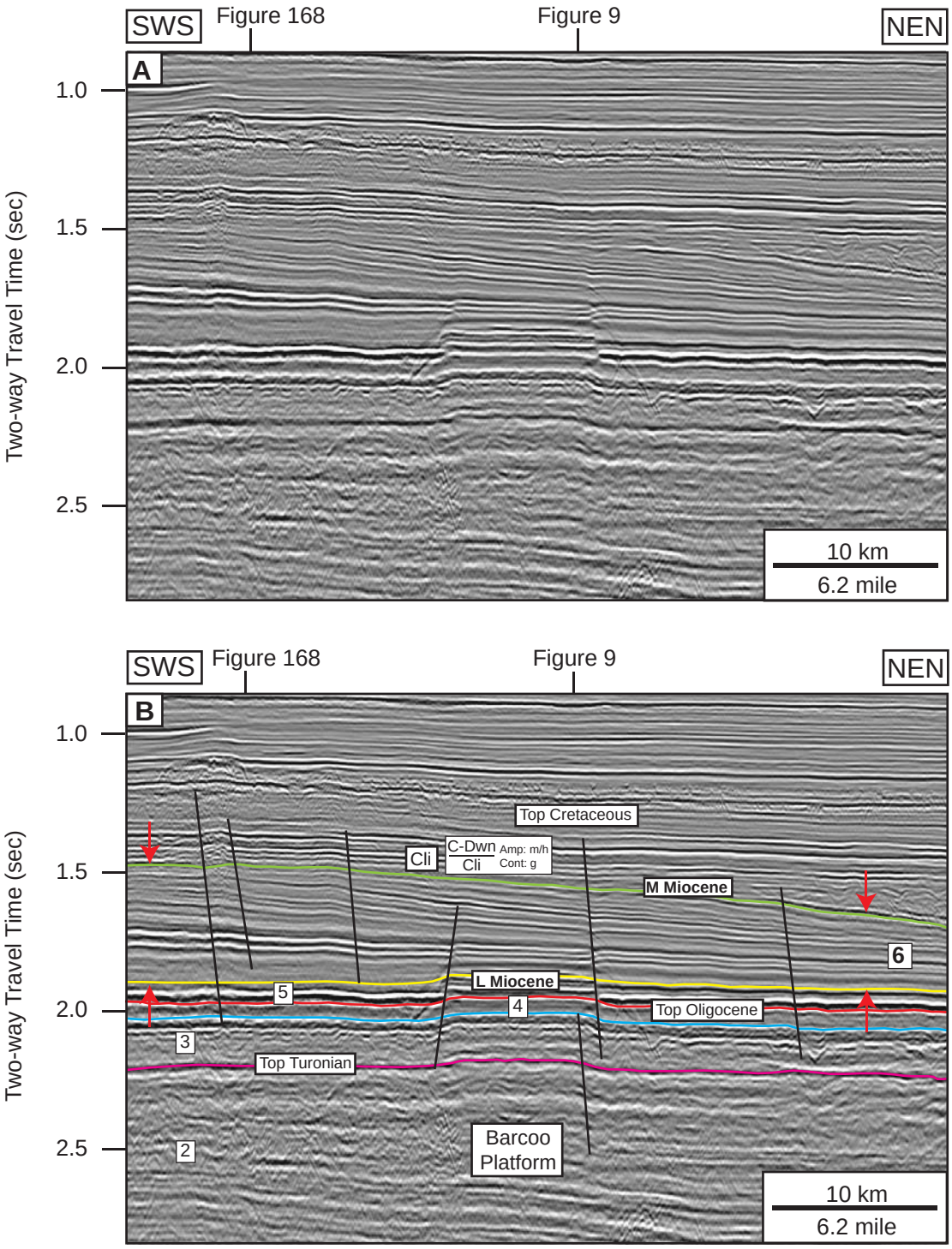

Figure 171. Strike-oriented seismic profile showing seismic facies of Mega-sequence 6 (lower Miocene to middle Miocene: 19.0-14.2 Ma) interval: (a) uninterpreted, (b) interpreted. The distinct prograding clinoform morphology is the major characteristic of megaseuence. See Table 2 for codes and abbreviations and Figures 166-167, 172-173 for location of the profile and locations of where Figures 9, 168 cross the profile.

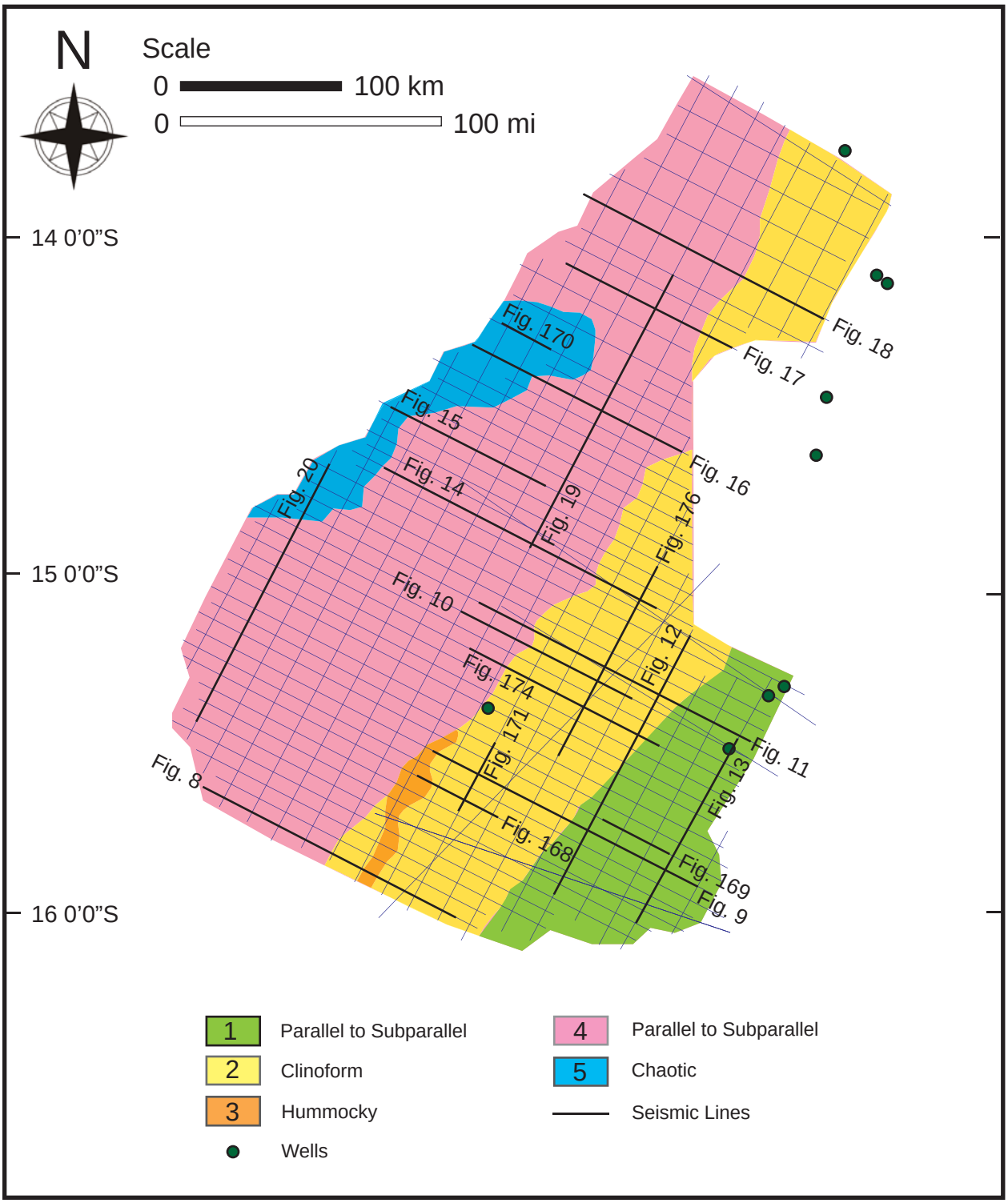

Figure 172. Seismic facies map of Megasequence 6 (lower Miocene to middle Miocene: 19.0-14.2 Ma) interval. Each facies is numbered as described in the text. See Table 2 for seismic facies coding and Table 8 for a summary of seismic facies analysis and geologic interpretation. Locations of Figures 8-20, 168-171, 174-177 (black lines) are shown, and wells are shown by green dots.

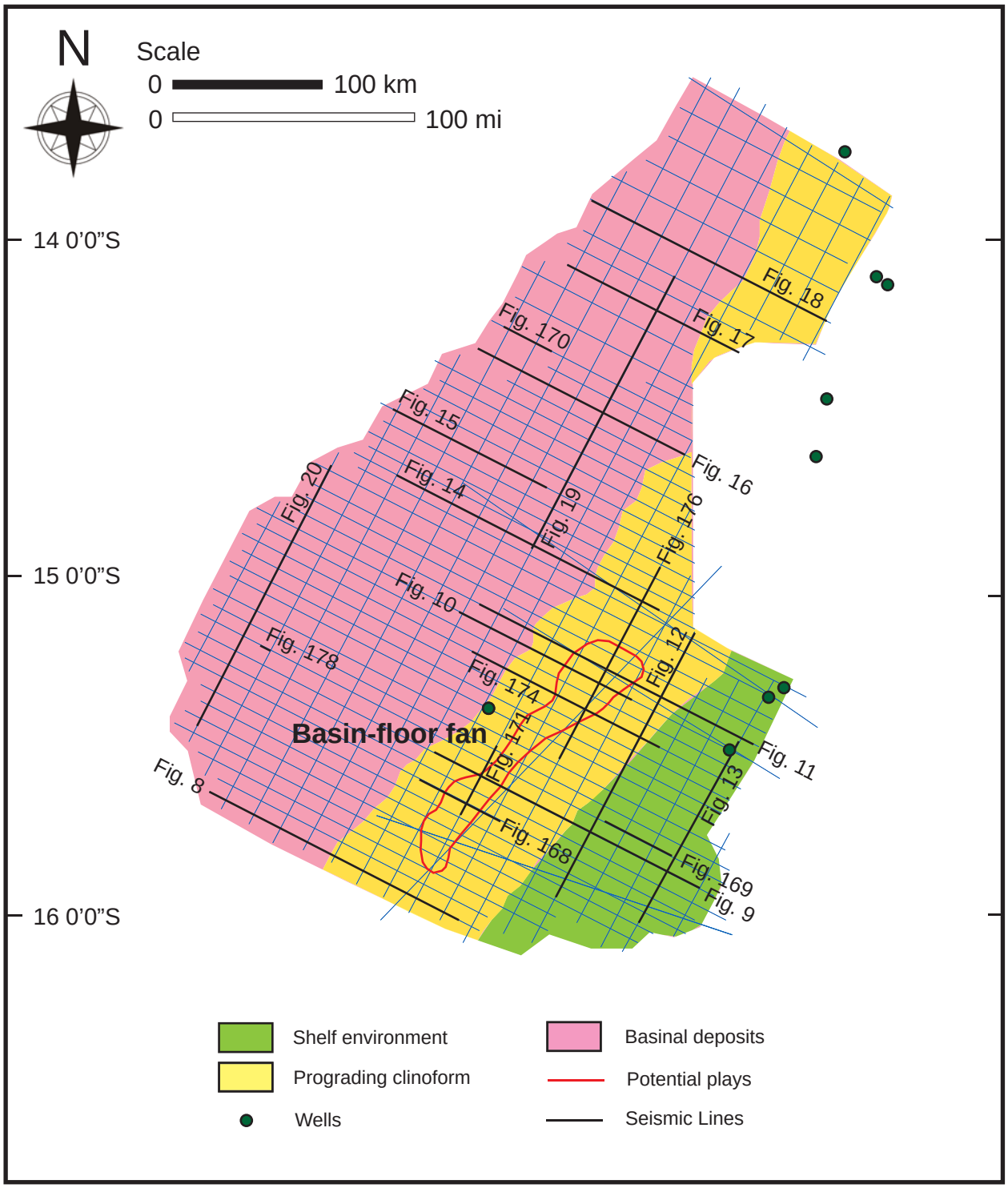

Figure 173. Geologic facies map of Megasequence 6 (lower Miocene to middle Miocene: 19.0-14.2 Ma) interval. See Table 8 for a summary of seismic facies analysis and geologic interpretation. Locations of Figures 8-20, 168-171, 174-177 (black lines) are shown, and wells are shown by green dots.

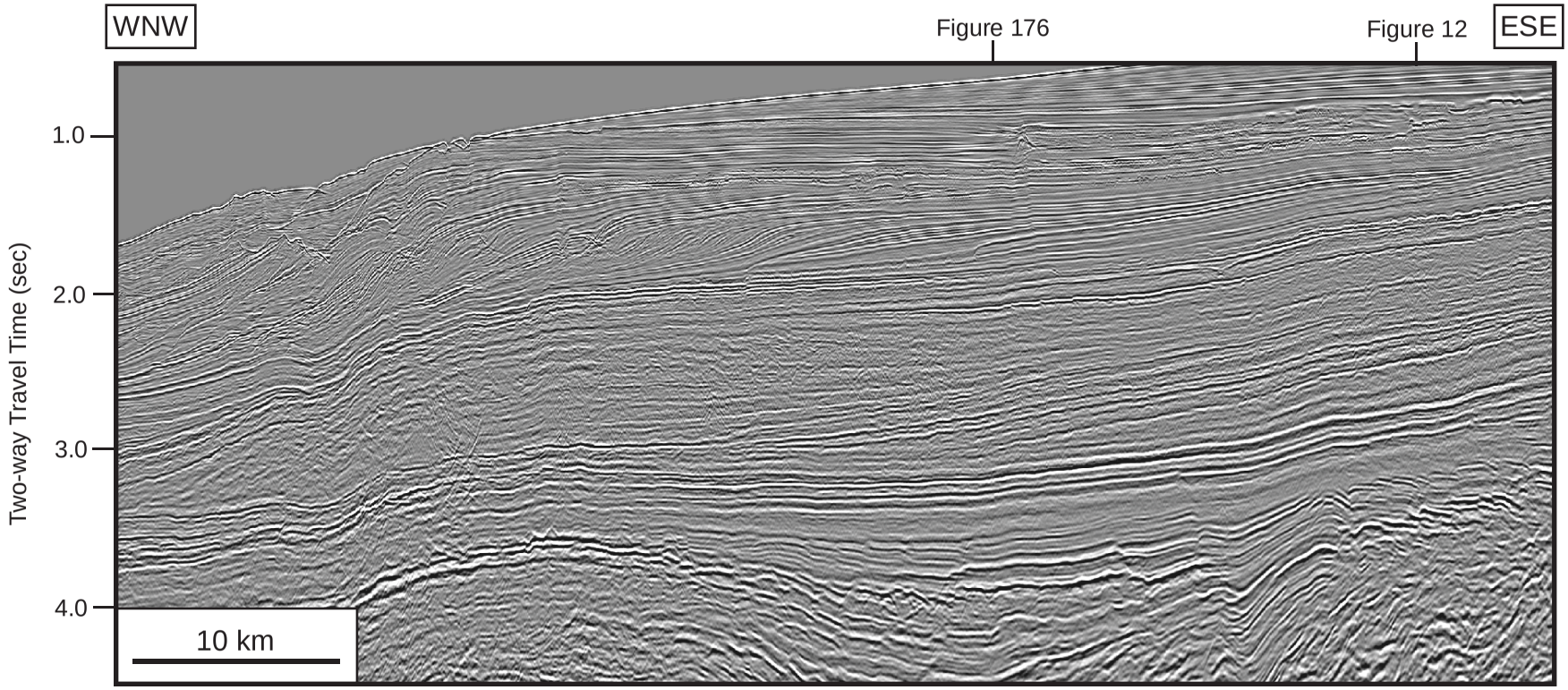

Figure 174a. Uninterpreted regional dip-oriented seismic profile (br-98:br98-017). Location of the profile is shown in Figures 166-167, 172-173 and locations of where Figures 12, 176 cross the profile.

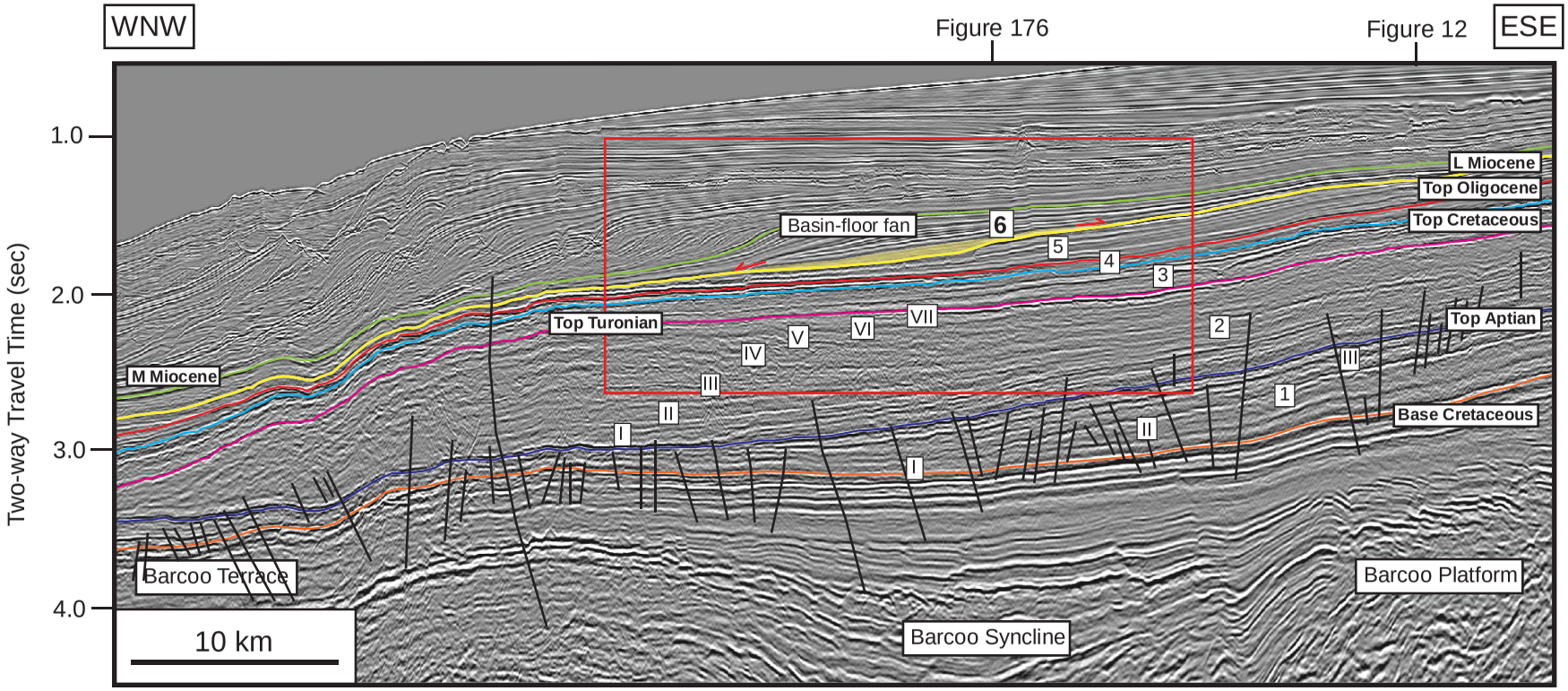

Figure 174b. Regional dip-oriented seismic profile showing all interpreted sequence boundaries from base Cretaceous to middle Miocene. This profile shows the area of the Barcoo Terrace, the Barcoo Syncline and the Barcoo Platform from west to east. The Barcoo Anticline and small faults of Barcoo fault system in the underlying Jurassic strata are observed. Megasequence 6 displays the distinct prograding clinoform which a basin-floor fan is identified (yellow shade). Location of the profile is shown in Figures 166-167, 172-173 and locations of where Figures 12, 176 cross the profile.

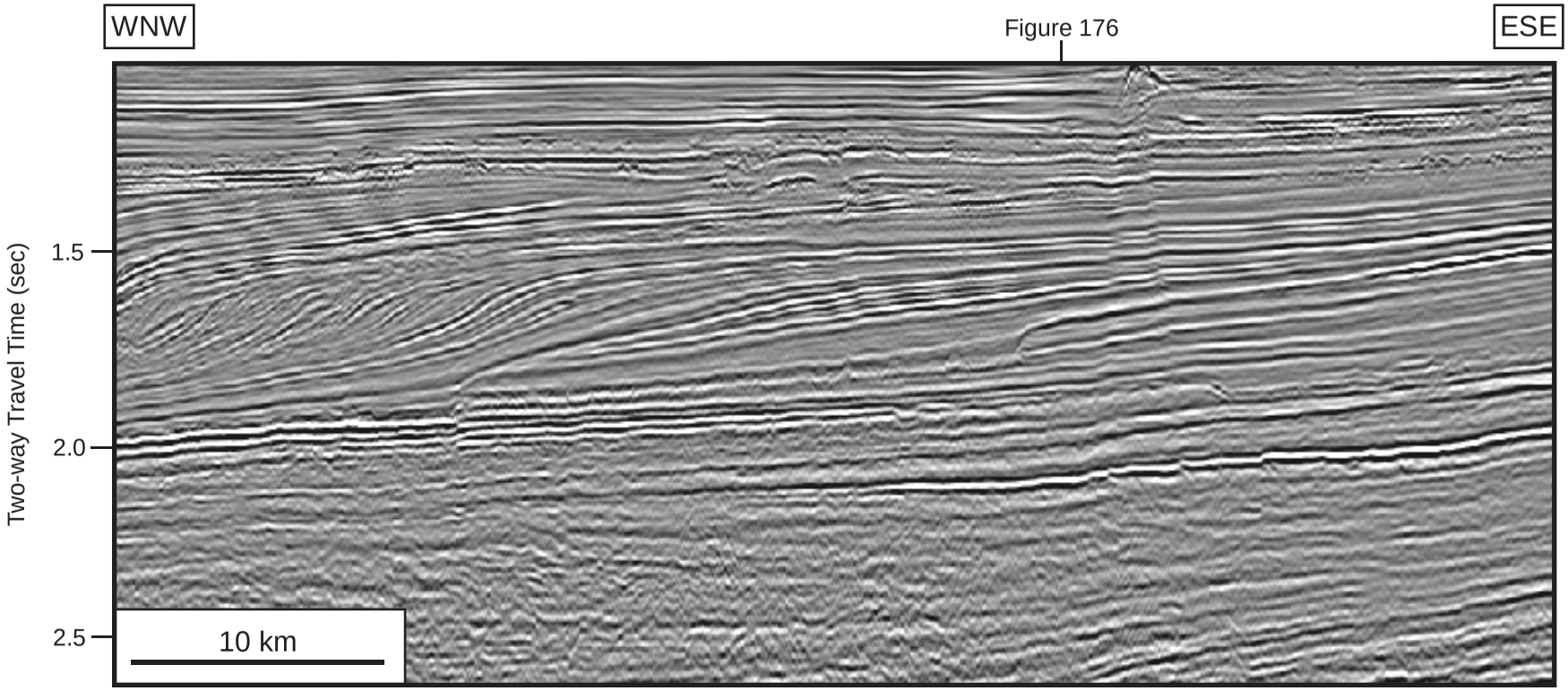

Figure 175a. Uninterpreted regional dip-oriented seismic profile (br-98:br98-017): A closeup view of Figure 174.

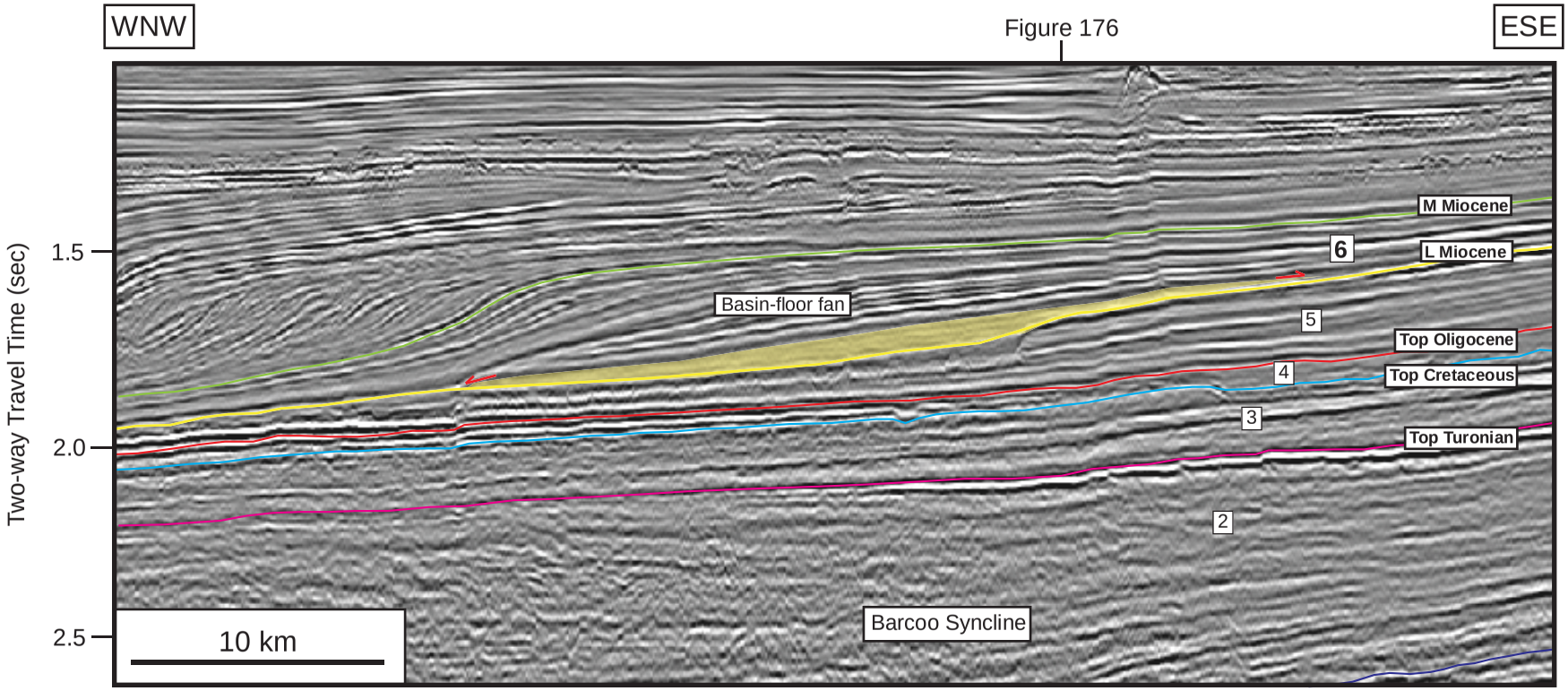

Figure 175b. Regional dip-oriented seismic profile showing all interpreted sequence boundaries from base Cretaceous to middle Miocene: A closeup view of Figure 174. Megasequence 6 displays the distinct prograding clinoform which a basin-floor fan is identified (yellow shade).

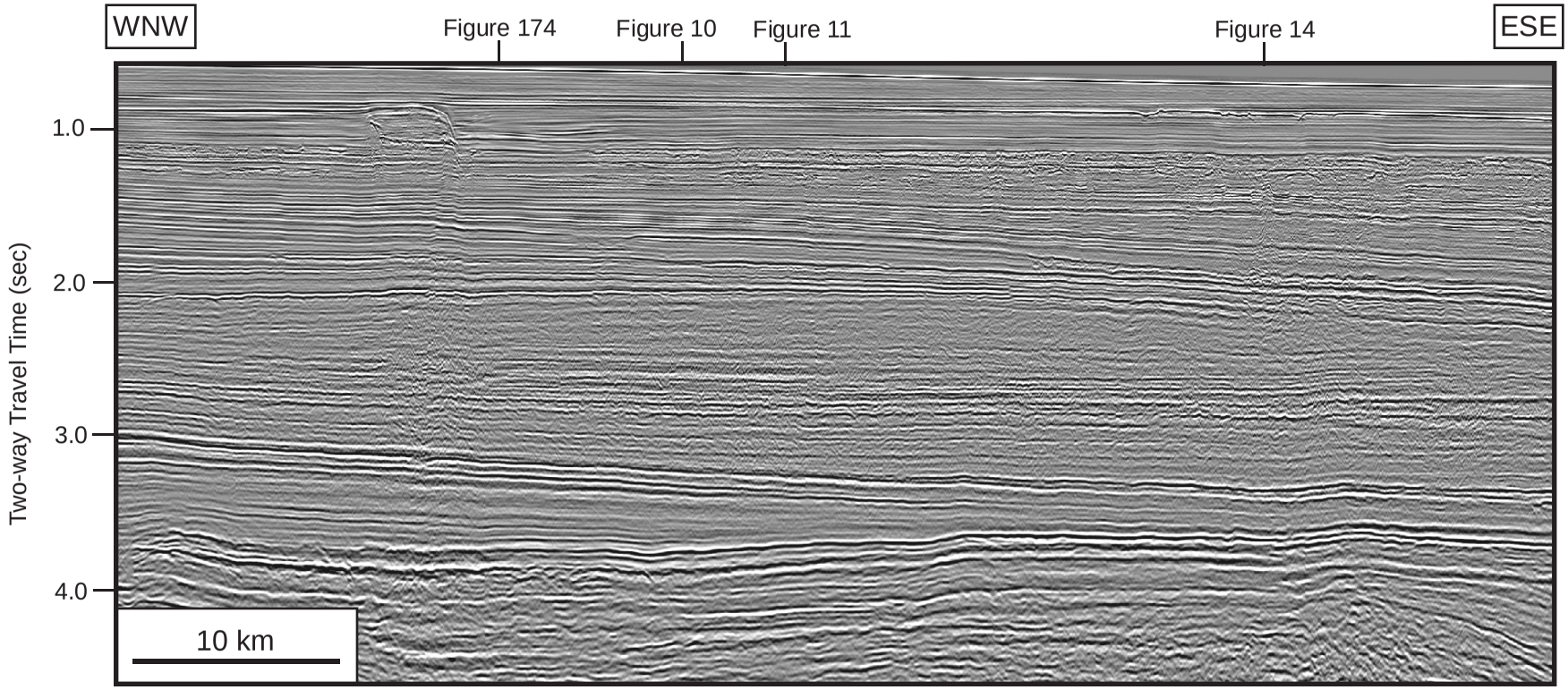

Figure 176a. Uninterpreted regional strike-oriented seismic profile (br-98:br98-075b). Location of the profile is shown in Figures 166-167, 172-173 and locations of where Figures 10, 11, 14, 174 cross the profile.

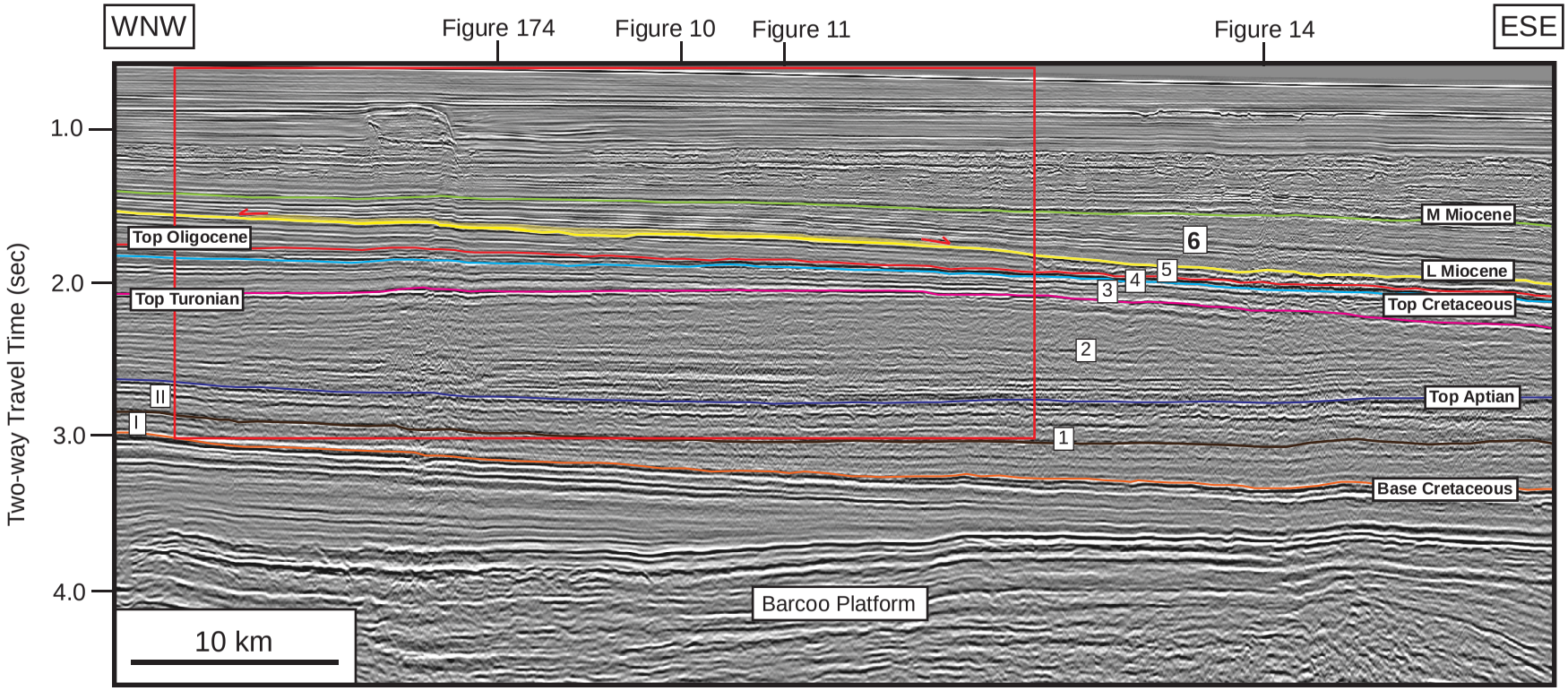

Figure 176b. Regional strike-oriented seismic profile showing all interpreted sequence boundaries from base Cretaceous to middle Miocene. The Barcoo Platform Anticline is observed at the eastern part of the profile. The low angle clinoform consists the sediment wedge (yellow shade) which is illustrated in Megasequence 1. Additionally, the aggrading slope system is demonstrated in Megasequence 2. Megasequences 5 and 6 display the distinct prograding clinoform. Location of the profile is shown in Figures 166-167, 172-173 and locations of where Figures 10, 11, 14, 174 cross the profile.

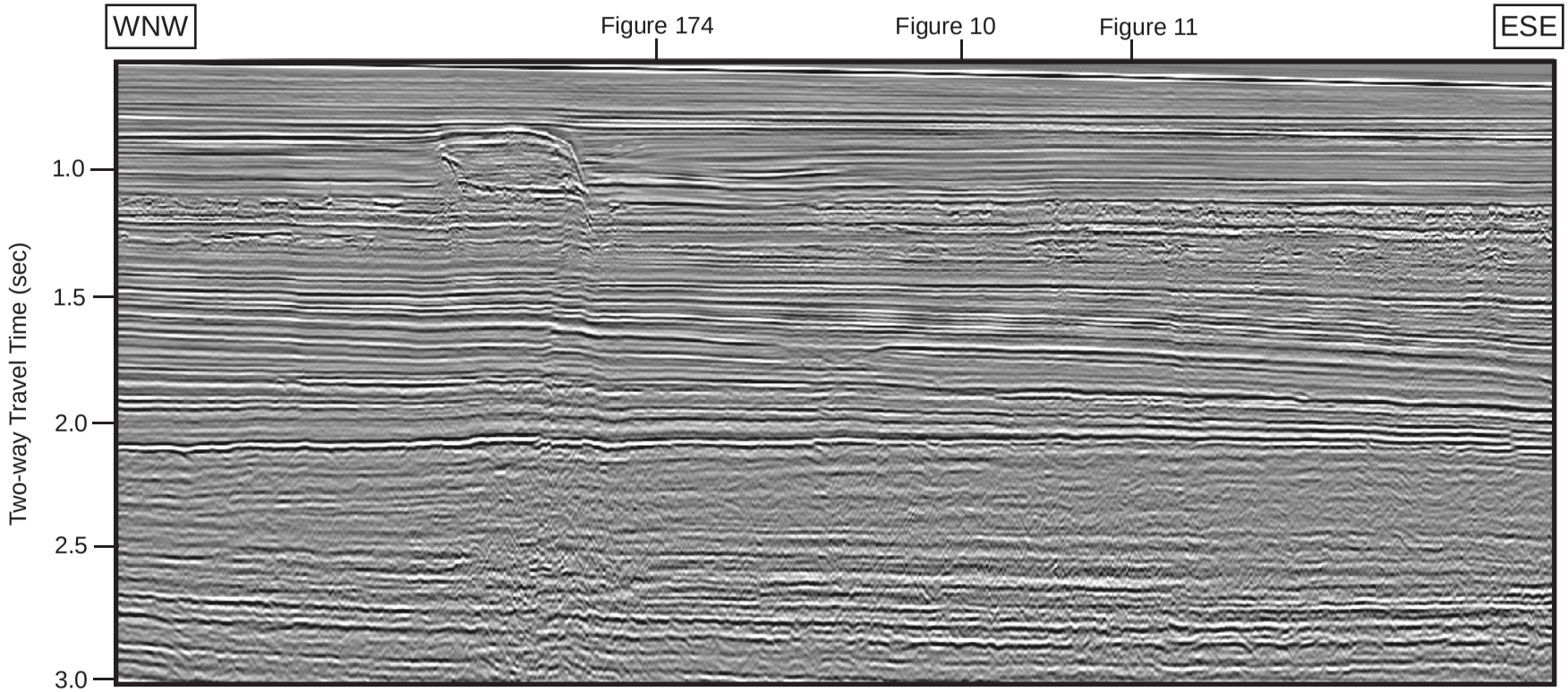

Figure 177a. Uninterpreted regional strike-oriented seismic profile (br-98:br98-075b): A closeup view of Figure 176.

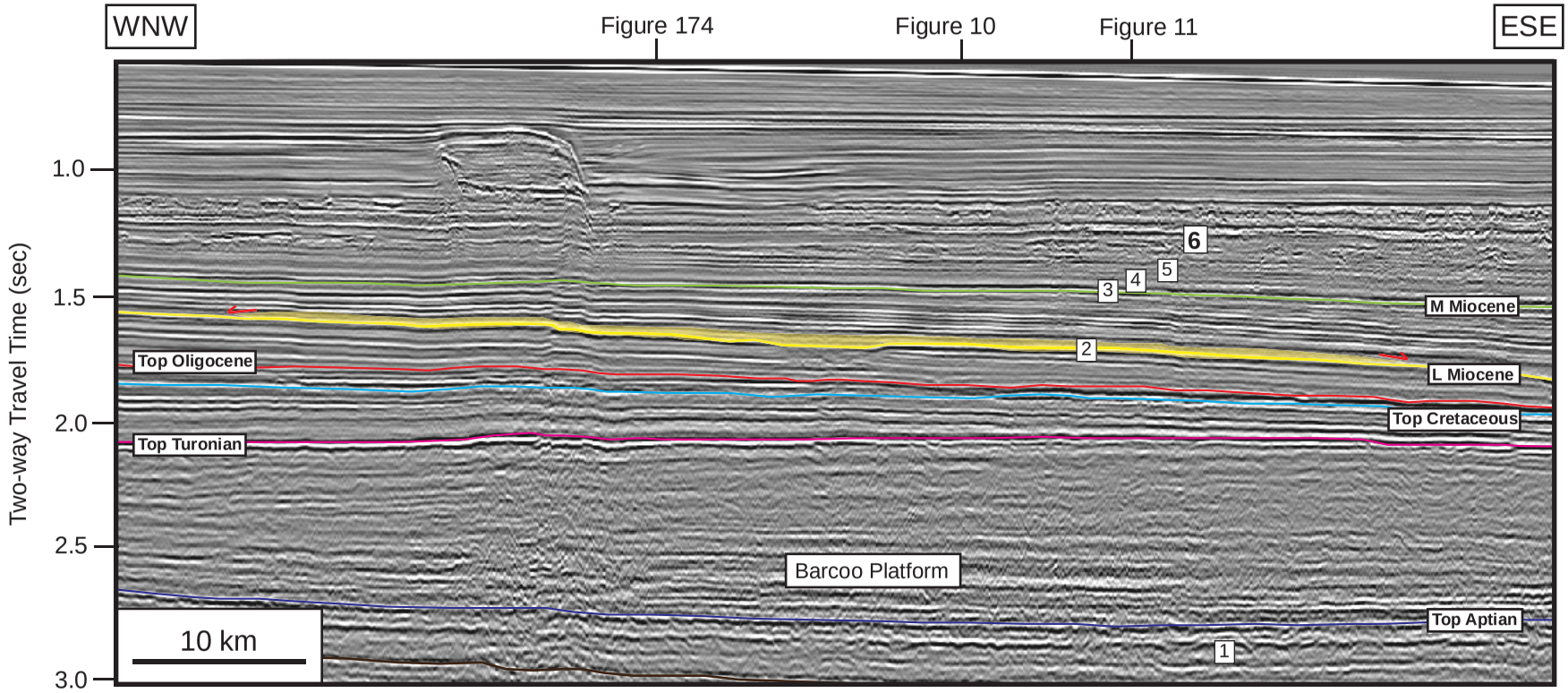

Figure 177b. Regional strike-oriented seismic profile showing all interpreted sequence boundaries from base Cretaceous to middle Miocene: A closeup view of Figure 176. The aggrading slope system is demonstrated in Megasequence 2. Megasequences 5 and 6 display the distinct prograding clinoform.

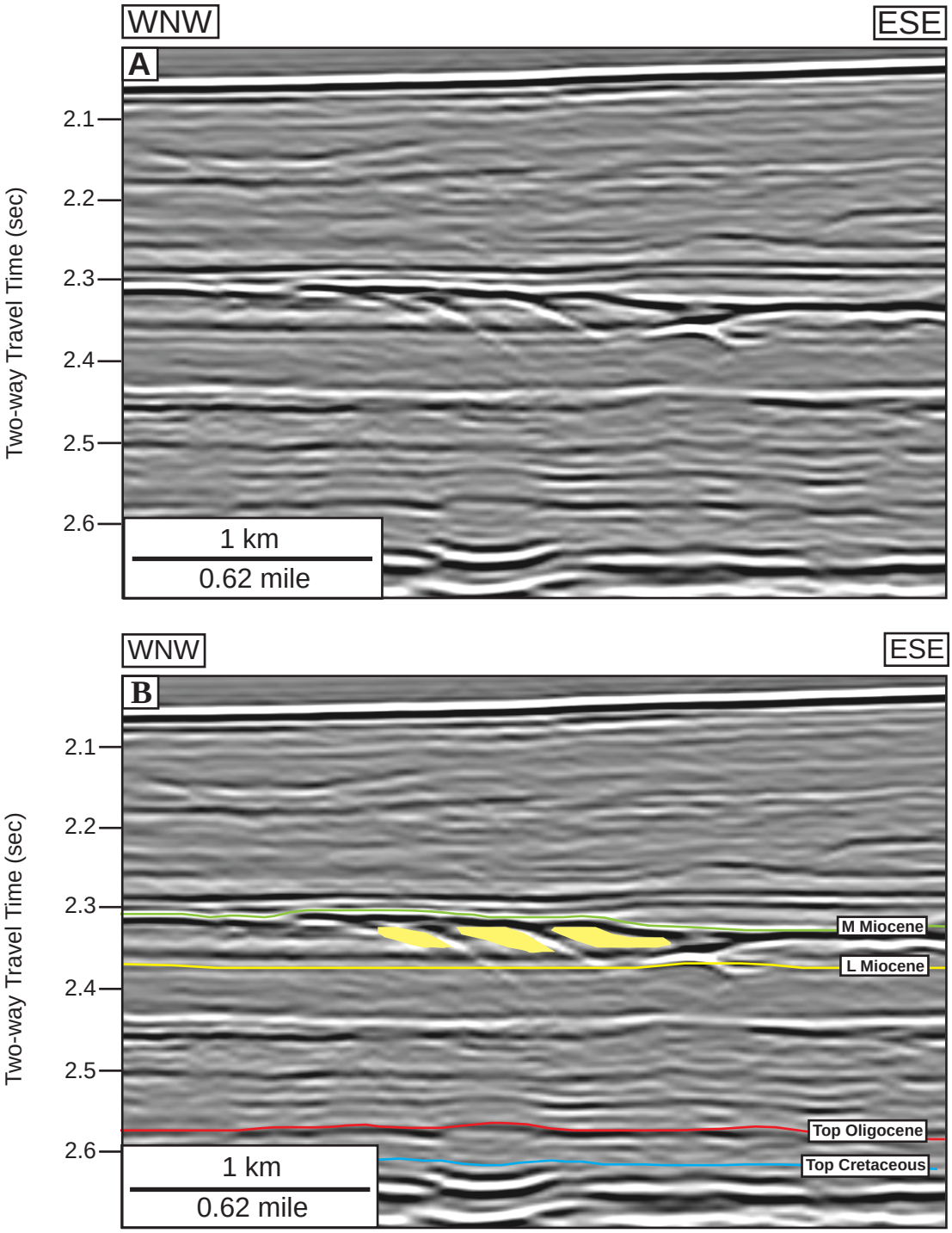

Figure 178. An uninterpreted (a) and interpreted, (b) vertical profile through channel showing lateral migration in the SE/NW direction.

V. DISCUSSION

One of the objectives of this research is to look for the potential plays for successful future exploration. Therefore, the following section will summarize the petroleum system of the study area.

1. The major petroleum accumulation in this area comprises gas/condensate reservoirs in Upper Triassic shallow marine sediments, Lower to Middle Jurassic marginal marine or fluvio-deltaic and Lower Cretaceous deepwater sandstone deposits.

2. The main reservoirs in the Browse Basin present in the fluvio-deltaic in Lower to middle Jurassic age and the submarine fans of the deepwater deposits.

3. The presence of a mature source rock and working petroleum system in the Browse Basin is proven by the fields and small discoveries. The most oil-prone source potential associated with the transgressive marine shale sequences of the Upper Jurassic to Lower Cretaceous whereas the gas-prone source is associated with the fluvio-deltaic shale of the Lower to Middle Jurassic. However, the petroleum source rock in the Barcoo Sub-basin occurs mainly in Lower to Middle Jurassic marine and fluvio-deltaic sediments which were deposited during rifting phase.

4. In this area, structures and traps are the main problem of the petroleum system. The structural elements in the basin include major anticlinal (Barcoo Platform anticline) and synclinal (Barcoo syncline and Scott Plateau syncline) features. They were classified as being early-, intermediate-, and late-formed traps, according to the amount of structural tilt in block-faulted sequences underlying each feature. The important potential traps consist of Upper Triassic faulted anticlines, Jurassic horst/tilted

fault block associated with drape anticlines and the Upper Cretaceous structure (Willis, 1988). Therefore, the stratigraphic trap is the major target.

5. Even though there are a thick marine claystones in the study area. Lack of effective base and top seals is considered a critical risk to this area. The potential intraformational sealing shales occur within the Lower to middle Jurassic and Upper Cretaceous.

6. Neogene reactivation and inversion have reactivated underlying basement structures on the Northwest Shelf. It resulted in a fault-controlled anticlinal zone which is the main cause of the petroleum accumulations in the Browse Basin as well as the Barcoo Sub-basin.

7. The significant petroleum play concept in this area is the deepwater sandstone deposits. It occurred in the different trapping style which onlapping and the structural-controlled are the major ones.

VI. CONCLUSIONS

1) Seven sequence boundaries (145.5, 112.0, 89.3, 65.5, 23.0, 19.0 and 14.2 Ma) were identified on seismic profiles throughout the study area.
2) Seismic reflection characteristics including the internal reflection configuration, seismic amplitude and seismic continuity were examined for the seismic facies analysis.
3) Seismic facies analysis combined with the well log data are the important tools in order to make an interpretation about the depositional environment and generate the geologic facies map of this study.
4) The seismic correlation, seismic facies analysis and geologic interpretation were used to generate the structural, isochron, seismic facies and geologic maps for these six megasequences.
5) The regional 2D seismic data indicated that the parallel and subparallel seismic characters are the most prominent seismic facies in this study area. However, clinoform, hummocky and chaotic seismic reflection have been recognized.
6) The sediments were transported and deposited from the coastal plain environrment east of the study area to shallow marine environment to the basin in the southeast-northwest direction. The overall depositional characteristic of this area is the shelf, slope and basinal environments.
7) The failure of the exploration wells in this area is due to the relationship between generation, timing of source rock passing through the hydrocarbon generative

window and the formation of structure. Therefore, the target of this area should be emphasized on the area which was not affected by the Neogene reactivation.

8) The main petroleum play concept of this area is the onlapping deepwater sand deposits.

VII. REFERENCES

Argo North West Shelf Study Group, 1994, Deep reflections on the North west shelf: Changing perceptions of basin formation, *in* Purcell, P. G., and Purcell, R. R., eds., The Sedimentary Basins of Western Australia: Proceedings of Petroleum Exploration Society of Australia Symposium, Perth, 1994, p. 63-76.

Baillie, P.W., C., Powell, Z.X., Li, and A.M., Ryall, 1994, The tectonic framework of western Australia's Neoproterozoic to recent sedimentary basins, *in* Purcell, P. G., and Purcell, R. R., eds., The Sedimentary Basins of Western Australia: Proceedings of Petroleum Exploration Society of Australia Symposium, Perth, 1994, p. 45-62.

Bishop, M.G., 1999, A total petroleum system of the Browse Basin, Australia: Late Jurassic, Early Cretaceous-Mesozoic. USGS Open-File Report 99-50-I, 22 p.

Bradshaw, M.T., A.N., Yeates, R.M., Beynoo, A.T., Brakel, R.P., Langford, J.M., Totterdell, and M., Yeung, 1988, Paleogeographic evolution of the North west shelf region, *in* Purcell, P. G., and Purcell, R. R., eds., The Sedimentary Basins of Western Australia: Proceedings of Petroleum Exploration Society of Australia Symposium, Perth, 1994, p. 29-54.

Bradshaw, M. T., J., Bradshaw, A.P., Murray, D.J., Needham, L., Spencer, R.E., Summons, J., Wilmot, and S., Winn, 1994, Petroleum systems in west Australian basins, *in* Purcell, P. G., and Purcell, R. R., eds., The Sedimentary Basins of Western Australia: Proceedings of Petroleum Exploration Society of Australia Symposium, Perth, 1994, p. 93-118.

Butcher, B.P., 1986, Northwest shelf of Australia, *in* Edwards, J. D., and Santogrossi, P. A., eds., Divergent/passive Margin basins: AAPG Memoir 48, p. 81-115.

Geological Survey of Western Australia 2009, Summary of petroleum prospectivity, Western Australia 2009: Bonaparte, Bight, Browse, Canning, Officer, Perth, Southern Carnarvon, and Northern Carnarvon Basins: Geological Survey of Western Australia, 39p.

Gonzalez, H., 2001, Sequence stratigraphy of Upper Miocene to Pleistocene sediments of the Central Mississippi Canyon and Northern Atwater Valley Areas, Northern Gulf of Mexico: unpublished Master's Thesis, University of Colorado, 144 p.

Iavering, I.H., and L., Pain, 1991, Australian petroleum accumulations report 7, *in* Australian Government Publishing Service Canberra 1991.

Keep, M., A., Bishop, and I., Longley, 2000, Neogene wrench reactivation of the Barcoo Sub-basin, Northwest Australia: Implications for Neogene tectonics of the northern Australia, *in* Petroleum Geosciences, v. 6, p. 211-220.

Longley, I.M., M.T., Bradshaw, and J., Hebberger, 2001, Australian petroleum provinces of the twenty-first century, *in* M.W. Downey, J.C. Threet, and W.A. Morgan, eds., Petroleum Provinces of the twenty-first century: AAPG Memoir 74, p. 287-317.

Maung, T.U., S., Cadman, and B., West, 1994, A review of the petroleum potential of the Browse Basin, *in* The sedimentary basins of western Australia, p. 333-346.

Mitchum, R.M., Jr., P.R., Vail, and S., Thompson, 1977, Seismic stratigraphy and global changes of sea level, Part 2: The depositional sequence as a basic unit for stratigraphic analysis, *in* C.E, Payton, ed., Seismic stratigraphy-Applications to hydrocarbon exploration: AAPG, Memoir 26, p. 53-62.

Mitchum, R.M., Jr., P.R., Vail, and J.B., Sangree, 1977, Seismic stratigraphy and global changes of sea level, Part 6: Stratigraphic interpretation of seismic reflection patterns in depositional sequences, *in* C.E, Payton, ed., Seismic stratigraphy-Applications to hydrocarbon exploration: AAPG, Memoir 26, p. 117-133.

Mitchum, R.M., Jr., and P.R., Vail, 1977, Seismic stratigraphy and global changes of sea level, Part 7: Seismic stratigraphic interpretation procedure, *in* C.E, Payton, ed., Seismic stratigraphy-Applications to hydrocarbon exploration: AAPG, Memoir 26, p. 135-143

Mitchum, R.M., 1977, Seismic stratigraphy and global changes of sea level, Part 11: Glossary of terms used in seismic stratigraphy, *in* C.E, Payton, ed., Seismic stratigraphy-Applications to hydrocarbon exploration: AAPG Memoir 26, p. 205-212.

Mitchum, R.M., Jr., J.B. Sangree, P.R. Vail, and W.W., Wornardt, 1993, Recognizing sequences and system tracts from well logs, seismic data, and biostratigraphy: examples from the late Cenozoic, *in* P. Weimer and H.W. Posamentier, eds., Siliciclastic sequence stratigraphy: AAPG Memoir 58, p. 163-198.

Nicoll, R. S., J.M., Kennard, A.P., Kelman, D.J., Mantle, J.R., Laurie, and D.S., Edwards, 2009, Browse Basin biozonation and stratigraphy charts 32 *in* Basin biozonation and stratigraphy charts 2009: Australian government geoscience Australia.

Ramsayer, G.R, 1979, Seismic Stratigraphy, A fundamental exploration tool *in* 11th Annual Offshore Technology Conference 1979 Proceedings, v. 3, p. 1859-1867.

Stephenson, A.E., and S.J., Cadman, 1994, Browse Basin, Northwest Australia: the evolution, paleogeography and petroleum potential of a passive continental margin, *in* Paleogeography, Paleoclimate, Paleoecology, v. 111, p. 337-366.

Symonds, P.A., C.D.N., Collins, and J., Bradshaw, 1994, Deep structure of the Browse basin: Implications for basin development and petroleum exploration, *in* The Sedimentary basins of western Australia, p. 315-331.

Vail, P.R., R.G. Todd, and J.B. Sangree, 1977, Seismic stratigraphy and global changes in sea level, part 5: Chronostratigraphic significance of reflection, *in* C.E., Payton, ed., Seismic stratigraphy-Applications to hydrocarbon exploration: AAPG Memoir 26, p. 99-116.

Van Wagoner, J.C., R.M., Mitchum, K.M., Campion, and V.D., Rahmanian, 1990, Siliciclastic sequence stratigraphy in well logs, cores, and outcrops: AAPG Methods in Exploration Series No. 7, 63 p.

Willis, I., 1988, Results of exploration, Browse Basin, North west shelf, Western Australia, *in* Proceedings of the Petroleum Exploration Society of Australia Symposium, Perth, 1988, p. 259-272.

Zabanbark, A., 2010, The structural features and petroleum resource potential of basins in the western and northwestern Australian margins, *in* Ocenaology, 2010, v. 50, no. 2, p. 268-280.